ADVANCES IN CARBOHYDRATE CHEMISTRY AND BIOCHEMISTRY

51

ACADEMIC PRESS

Advances in Carbohydrate Chemistry and Biochemistry

Volume 51

This Page Intentionally Left Blank

Advances in Carbohydrate Chemistry and Biochemistry

Editor

DEREK HORTON

The American University
Washington, DC

Volume 51

ACADEMIC PRESS
San Diego New York Boston
London Sydney Tokyo Toronto

This book is printed on acid-free paper. ♾

Academic Press, Inc.
A Division of Harcourt Brace & Company
525 B Street, Suite 1900, San Diego, California 92101-4495

United Kingdom Edition published by
Academic Press Limited
24-28 Oval Road, London NW1 7DX

International Standard Serial Number: 0065-2318

International Standard Book Number: 0-12-007251-3

PRINTED IN THE UNITED STATES OF AMERICA
95 96 97 98 99 00 BB 9 8 7 6 5 4 3 2 1

CONTENTS

Mechanisms in the Glucansucrase Synthesis of Polysaccharides and Oligosaccharides from Sucrose

JOHN F. ROBYT

The Variable Surface Glycolipids of Mycobacteria: Structures, Synthesis of Epitopes, and Biological Properties

GERALD O. ASPINALL, DELPHI CHATTERJEE, AND PATRICK J. BRENNAN

Nonconventional Methods of Modification of Starch

PIOTR TOMASIK AND MARK F. ZARANYIKA

PREFACE

Structural sugar chemistry received its key foundations in work by German, British, and American investigators during the late 19th and the first half of the 20th century. These investigators employed the classical tools of organic chemistry in conjunction with the physical technique of polarimetry and pioneering applications of X-ray crystallography. However, many complex problems of tautomerism posed by sugars and their derivatives, along with questions concerning their conformations and reactivities, resisted solution until the advent of more powerful analytical methods. It is noteworthy that development of the most significant of these techniques—NMR spectroscopy—as it rose to its prominent role as a structural tool in chemistry and biochemistry, owes much to the carbohydrate field and to the seminal work in the 1950s of R. U. Lemieux.

Considered a mature technique in all areas of science, NMR spectroscopy has passed from being used for the simple recording and interpretation of chemical shifts and spin couplings for small molecules to the domain of specialists performing a multitude of procedures designed to extract detailed NMR parameters from biomolecules of ever-increasing complexity. In this volume of *Advances,* two chapters are devoted to current aspects of NMR spectroscopy. Tvaroska and Taravel (Bratislava and Grenoble) discuss carbon–proton coupling constants from both the experimental and theoretical points of view and address the significance of these couplings in elucidating the conformational behavior of sugars and their derivatives. The extensive tabular information relating these couplings to dihedral angles in conformationally rigid molecules will constitute an important source of reference for other workers probing the three-dimensional structures of carbohydrates in solution.

A complementary article by Dais (Iraklion, Crete) addresses the theoretical principles underlying the phenomenon of carbon-13 nuclear magnetic relaxation, encompassing spin–lattice (T_1) and spin–spin (T_2) relaxation times, the nuclear Overhauser enhancement, and their relation to the motional behavior of carbohydrates in solution. With examples broadly selected from simple sugar derivatives, oligosaccharides, and polysaccharides, the author shows how qualitative treatments have provided useful interpretations of the gross mobility of molecules in solution, but demonstrates how a quantitative approach may be of greater ultimate value.

Advances has regularly featured articles focusing on specific enzymes or enzyme groups acting on carbohydrates. The article by Robyt (Ames, Iowa) in this volume is devoted to the glucansucrase enzymes and the mechanism whereby they utilize sucrose to transfer glucose to acceptors and elaborate polysaccharides of the dextran class, including the commercially important dextran from the B-512F strain of *Leuconostoc mesenteroides.*

Aspinall (York, Ontario) and Chatterjee and Brennan (Fort Collins, Colorado), in their article on the surface glycolipids of mycobacteria, focus on the chemistry and biology relating especially to an old medical problem, tuberculosis. This disease remains the leading cause of death from a single infectious agent. After years of decline in industrialized countries, TB is now showing a rapid increase that has some correlation with the incidence of HIV infection. The lipo-oligosaccharide antigens of these bacteria are of extraordinary complexity and variety posing, until recently, major problems of separation and structural characterization. This article brings together a comprehensive survey of isolation methodology and structural detail with a wealth of synthetic virtuosity that has been applied to the construction of oligosaccharide haptens of these antigens. Elaboration of such synthetic oligosaccharide derivatives into neoglycoconjugates has afforded a major tool for probing antibody–antigen interactions and for developing immunlogical procedures in general.

The final chapter by Tomasik and Zaranyika (Harare, Zimbabwe) deals with an aspect of carbohydrate technology that complements the article by Tomasik and co-workers in Volume 47 on the thermal decomposition of starch. The survey presented in this volume deals with the modifications taking place in starch when it is irradiated by various energy sources, ranging from ionizing radiation to ultrasound, and by such treatments as freeze–thaw cycles and dehydration. Such treatments may impart little visible change to native starch granules, but may profoundly affect the behavior of the material in important technological and nutritional applications.

The life and work of Horace S. Isbell, who ranked with Claude S. Hudson and Melville L. Wolfrom as one of the great American carbohydrate chemistry pioneers, are presented here by El Khadem (Washington, DC). During his long career, Isbell made important fundamental discoveries in conformational analysis and in neighboring-group reactions, advances that were not at the time properly recognized by "mainstream" chemists. These were but a part of a sustained dedication to understanding the mechanisms of reaction of sugars and their derivatives, especially through the use of isotopically labeled compounds.

The editor notes with regret the passing of Maurice Stacey, one of the great names of the British carbohydrate school, successor to W. N. Haworth at the University of Birmingham, and one long associated with *Advances in Carbohydrate Chemistry*. A detailed account of his life and work is reserved for a forthcoming volume in this serial.

Washington, DC
July 1995

DEREK HORTON

This Page Intentionally Left Blank

Horace S. Isbell

HORACE S. ISBELL*

1898–1992

Horace Smith Isbell was born in Denver, Colorado, on November 13, 1898. He was the second of four children born to Harvey Gilbert Isbell and Mary Elnora White Isbell. The other children were Sarah Rachel, born in 1896; Harvey Gilbert Jr., born in 1900; and Nathan Paul, born in 1904.

Harvey Gilbert Isbell came from a pioneer family who left Massachusetts around 1830, seeking the rich land of the Mississippi Valley; he was born on July 15, 1859, in Weeping Water, in the (then) Territory of Nebraska. He became a sign-painter and traveled to California and other parts of the western United States in search of business signs to paint. During his travels, he met a school teacher, Mary Elnora White, who he married. The couple settled in a small farm located in what is now South Denver. The winters there were so harsh and bitter that when the weather began to turn cold, their children were sewn into their longjohns, which were never removed or changed until spring returned. When the great day arrived for removing the winter underwear, the celebration included a long hot bath, followed by a tablespoon of castor-oil to "prevent the shock of disrobing from causing consumption." When the children became a little older, the family moved into Denver proper and lived in a house that is still standing. Harvey was often away from home on long business trips that lasted several months; during his absence, Mary had to take care of the children and tend to her teaching duties. With time, Harvey's visits to the family became shorter and farther between; the couple began to drift apart, and they ultimately separated. The divorce was kept secret from the children and from everyone else as well; it was a family skeleton of which very few were aware. After retiring, Harvey maintained his skill at painting; at the age of 82, he lettered copies of the family tree, which have been carefully guarded by every member of his family. He also started writing about his many travels and adventures.

Mary Elnora White was born in Mount Ayr, Iowa, on March 30, 1861. She began her teaching career in Ringold County, Iowa, and continued it in Denver, Colorado, after her marriage. She used her income to support the family and to further the

* The material gathered here is based on discussions with the late Dr. Isbell, as well as with his niece Helen Hawk, and with Dr. Harriet L. Frush and Marie Matheny.

children's education. As each child finished college: she took care of the next one's tuition and expenses. While teaching, she also managed to enroll in the University of Denver; she completed her Bachelor's and Master's degrees during the time her grown-up children received their degrees. It is interesting to note that in the early 1900's only unmarried women were allowed to teach. In order to keep her job, Mary let herself be known in the community as "Widow Isbell," and a newspaper article written on the occasion of her earning the Bachelor of Arts degree refers to her as such. She was an outstanding teacher, who was selected to represent the teachers of Colorado at the Sesquicentennial celebration of 1926 in Philadelphia, Pennsylvania.

During her fifty-year career as a school teacher, she instilled the love of learning in all those who came in contact with her. It was therefore not surprising that all her children graduated from college: her daughter Sarah Rachel majored in chemistry, received an M.A. degree, and became a teacher; Horace Smith obtained a B.A. degree from Denver University, received a Ph.D. from the University of Maryland, and became a research scientist; and Harvey Gilbert graduated from Denver University and eventually became head of the chemistry laboratory at Mare Island Navy Yard at Vallejo, California. Nathan Paul graduated with an A.B. and an M.D. from the University of Colorado and specialized in gynecology at Colorado General Hospital. During World War II he served as a Major in the Air Corps. Most of Mary Isbell's grandchildren and great grandchildren also graduated from college with M.A. or B.A. degrees.

Mary Elnora had an eye for land, always scrimping and scraping to purchase it. During the Depression, the family acquired several pieces because the owners had defaulted on taxes. One of the tax purchases she made was a magnificent place at 1205 Ogden, in Denver. It was a mansion with a ballroom, a huge music room, and a giant kitchen divided into two sections—one for cooking and one for serving. It also had a curved stairway leading to two floors of bedrooms and baths. She and Rachel turned this mansion into a boarding house which they operated to supplement their modest incomes as teachers.

Money was always in short supply for the family, and the children took advantage of every opportunity to help with expenses. Horace and Gilbert had a milk route. As they were making their rounds on bicycles early each morning, they would hold onto the rear of a streetcar and let it pull them to the next customer. Occasionally, the conductor would espy them and with great fanfare threaten them with dire consequences if he ever caught them doing it again. The twist to the story was that, later on, both of them worked as conductors on streetcars in order to pay their way through college. Needless to say, they knew all the "kid tricks," and few were successful when the Isbells were on the job.

Horace's interest in chemistry was sparked when he was seventeen. His sister Rachel asked him to escort her to an evening chemistry lecture on radioactivity given by Dr. S. C. Lind. The lecture was so stimulating that he decided then and

there to become a chemist; soon thereafter he enrolled at the University of Denver. As an undergraduate, young Horace won the Phi Lambda Epsilon medal for proficiency in analytical chemistry in two successive years. He received a B.S. degree in Chemistry in 1920, and enrolled in the M.S. program. To support himself as a graduate student, he worked successively as an analytical chemist at the American Smelting and Refining Company in Pueblo, Colorado, at the Pure Oil Co. in Glenwood Springs, Colorado, and then at the Paul S. Nice Laboratory in Denver, Colorado. In 1923 he obtained the M.S. degree in Organic Chemistry and was appointed Assistant Chemist in the Bureau of Animal Industry of the U.S. Department of Agriculture in Beltsville, Maryland. In 1925, he won a Graduate Fellowship from the U.S. Public Health Service to conduct research on the organic compounds of gold at the University of Maryland. The results he achieved under Professor M. S. Kharasch led to his receiving the Ph.D. degree in Organic Chemistry in 1926. In the following year, he joined the staff of the National Bureau of Standards in Washington, D.C., where he started his monumental work in carbohydrate chemistry. It was there that he made most of his important discoveries. He continued to work at the Bureau until his mandatory retirement at the age of seventy. In December, 1968, he joined the staff of the Chemistry Department at The American University, in Washington, D.C., as Research Professor, a position he held until his death in 1992. There he collaborated with Dr. Harriet L. Frush, producing some forty papers on the peroxidation of carbohydrates. The Isbell laboratory at The American University attracted a number of Postdoctoral Fellows who came from various countries. Several graduate students received their Ph.D. and M.S. degrees under his guidance, and numerous undergraduate and high school students worked during the summers on various NSF-funded programs. Isbell's graduate students and coauthors are listed in Tables I and II, respectively.

In 1930, Horace Isbell married May Davidson, and they bought a house east of Rock Creek Park, in Washington, D.C. Later, the couple moved to a larger house on Blagden Avenue also near the Park. The Isbells had no children and led a quiet family life. After some wise investments in the stock market, Dr. Isbell was able to accumulate substantial assets, including a 250-acre farm in Prince George's County, Maryland. Later on, in the early eighties, he decided to part with some of his fortune and make a charitable donation that would promote the advancement of science. He discussed the matter with his friend Dr. Milton Harris, who suggested that he endow a chair in the Chemistry Department at The American University. The idea appealed to him since this university had welcomed him a decade earlier when he retired from the Bureau of Standards. It had offered him a Research Professorship, an office, and the use of a chemistry laboratory to continue his research. He was indebted to the American University for allowing him to prove to himself and to others that, after retiring from the Bureau, he was not too old to produce outstanding research. Indeed he felt that the university had allowed him to add twenty productive years to his already fruitful career. Dr. Isbell made a

TABLE I

List of Postdoctoral Fellows and Graduate Students

Postdoctoral Fellows	
Linek, K.	(Slovak Academy of Science)
Orhanovic, Z.	(University of Zagreb)
Salam, M.	(University of London)
Graduate Students	
Fatiadi, A. J.	(Ph.D. University of Maryland)
Frush, H. L.	(Ph.D. University of Maryland)
Hepner, K. E., Jr.	(M.S. American University)
Moyer, J. D.	(Ph.D. University of Maryland)
Naves, R. G.	(M.S. American University)
Neglia, C. I.	(M.S. American University)
Parks, E. W.	(M.S., Ph.D. American University)
Pigman, W. W.	(Ph.D. University of Maryland)
Sniegoski, L. T.	(Ph.D. University of Maryland)
Soontracharoen, P.	(M.S. American University)
Wade, C. W. R.	(Ph.D. University of Maryland)

generous gift of stocks, bonds, and real estate to the American University, to create an endowed chair named the "Horace and May Davidson Isbell Chair for the Study of Carbohydrates and Natural Products." Additional funds were later donated for equipment, fellowships, and scholarships, bringing the total sum donated by the Isbell family to about two and a half million dollars.

When May Isbell's health began to deteriorate, and she could no longer climb stairs, the couple sold their house on Blagden Avenue and moved to an apartment. May died in 1989. Three years later, on July 1, 1992, Horace S. Isbell died at the age of 93. He had devoted 70 years of his life to research in the field of chemistry and to the advancement of this science.

THE SCIENTIFIC ACHIEVEMENTS OF HORACE S. ISBELL

Horace Isbell's first assignment at the National Bureau of Standards (NBS) was the preparation of aldonic acids by the oxidation of aldoses. His boss Dr. Claude S. Hudson, a great proponent of polarimetry, asked him to follow the course of the bromine oxidation of glucose by studying the changes in optical rotation that occur during the reaction. When he did this, he discovered that aldoses are oxidized to 1,5-lactones and not, as was believed at the time, to aldonic acids. This suggested to him that sugars must exist mainly in the 1,5-cyclic hemiacetal (pyranose) form and that they are oxidized directly without passing through the acyclic aldehydo form. The reason for this is that hydroxyaldehydes on oxidation produce carboxylic acids, which if lactonized, yield stable 1,4-lactones and not the observed 1,5-lactones. The conclusions Isbell reached contradicted Hudson's belief that sugars

TABLE II
List of Co-authors

Name	Number of publications	Name	Number of publications
Bates, F. J.	1	Matheson, H.	1
Bloomfield J. J.	2	McDonald, E. J.	1
Bruekner, B. H.	1	Moyer, J. D.	10
Brewster, J. F.	1	Naves, R. G.	3
Cerezo, A. S.	1	Orhanovic, Z.	2
Cohen, A.	3	Parks, E. W.	2
Deulofeu, V.	1	Perlin, A. S.	1
Dryden, M. R.	2	Peterson, R. A.	1
El Khadem, H. S.	3	Phelps, F. P.	1
Ellis, N. R.	2	Pigman, W. W.	15
Ennifar, S.	2	Sager, W. F.	1
Fatiadi, A. J.	8	Salam, M. A.	3
Fedoroňko, M.	1	Schaffer, R.	15
Frush, H. L.	68	Schumacher, J. N.	1
Galkowski, T. T.	1	Schwebel, A.	2
Helferich, H.	2	Shalaby, M. A.	1
Herve Du Penhoat, P.	1	Simon, H.	1
Hepner, K. E., Jr.	1	Smith, E. R.	1
Holt, N. B.	10	Smith, F. A.	1
Hudson, C. S.	2	Sniegoski, L. T.	9
Huff, N. B.	1	Snyder, C. F.	1
Humoller, F. L.	1	Sobarow, P.	1
Hunter, C. E.	1	Soontracharoen, P.	2
Jeanes, A.	1	Stewart, J. E.	2
Karabinos, J. V.	2	Tipson, R. S.	9
Keil, K. D.	1	Wade, C. W. R.	4
Kharasch, M. S.	4	Walton, W. W.	2
Kowkabany, G. N.	1	Wampler, G.	1
Linek, K.	2	Weygand, F.	1
Martin, E. T.	1	Wolfrom, M. L.	1

existed normally in the 1,4-cyclic hemiacetal (furanose) form. When he presented the results to his superior, he was severely rebuked. The incident was related in the Haworth Memorial Lecture,which he gave in England many years later. He reported that Hudson looked at him squarely in the eyes, raised his voice, and said: "Isbell, there's just one thing wrong with you. You think nobody knows a damn thing except yourself." The disagreement between the two giants lasted for several years and was resolved only when Haworth's evidence showing that six-membered rings were the common forms of aldoses, became widely accepted. It was finally espoused by Hudson, who then approved publication of two papers he had suppressed: one from the National Institute of Health (NIH) on the periodate oxidation of glycosides, and the other from NBS on Isbell's work on the bromine

oxidation. He co-authored both papers, but refused to give credit to Haworth for proposing for the first time that saccharides exist mainly in the pyranose form.

The work on pyranoses led Isbell to recognize the importance of conformation on reaction rates. He found that β-D-glucopyranose was oxidized much more rapidly than the α form, which led him to conclude that the six-membered tetrahydropyran ring could not be planar; otherwise, the two anomers would have been symmetrical and would have reacted at the same rate (see Fig. 1). Isbell's observation regarding the difference between the reactivity of anomers was the first of a series of phenomena now designated as the "anomeric effect."

In 1937 Isbell published an important paper on the conformational analysis of aldopyranoses, in which several of the forms were depicted (see Fig. 2). They comprise a $^4C_1$ chair (**I**), a $B_{0,3}$ boat (**II**), two half-chairs (**III** and **IV**), and a coplanar pyranose (**V**). He correctly favored the chair form (**I**) and predicted that, in the case of saccharides, the chair would tend to assume a somewhat flatter conformation than that of carbocycles such as cyclohexane because of the smaller bond angles of oxygen as compared to those of carbon (105° instead of 109.5°). We now know that such coplanarity is strongly avoided because of the strain that would be produced and because of the repulsive forces between the substituents.

Isbell was also ahead of his time in grasping the concept of reaction mechanisms. In collaboration with the late Ward Pigman, he proposed two important mechanisms: one for the anomerization of aldopyranoses by ring opening (see Fig. 3), and the other for the anomerization of their esters via a cyclic carbocation (see Fig. 4).

During the period between 1927 and 1940, in collaboration with Ward Pigman and Harriet Frush, Isbell recognized for the first time the important role that neighboring-group effects play in substitution reactions. The formation of methyl 3,6-anhydro-β-D-glucoside via an intermediate 2,3-anhydro-alloside was elegantly explained by the mechanism shown in Fig. 5.

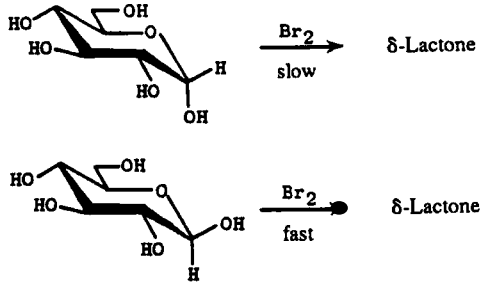

FIG. 1.—The formation of 1,5-lactones suggests that the starting aldoses exist in the 1,5-cyclic hemiacetal (pyranose) form. The difference between the rates of oxidation of the α and β anomers was taken as a proof that the ring is not planar.

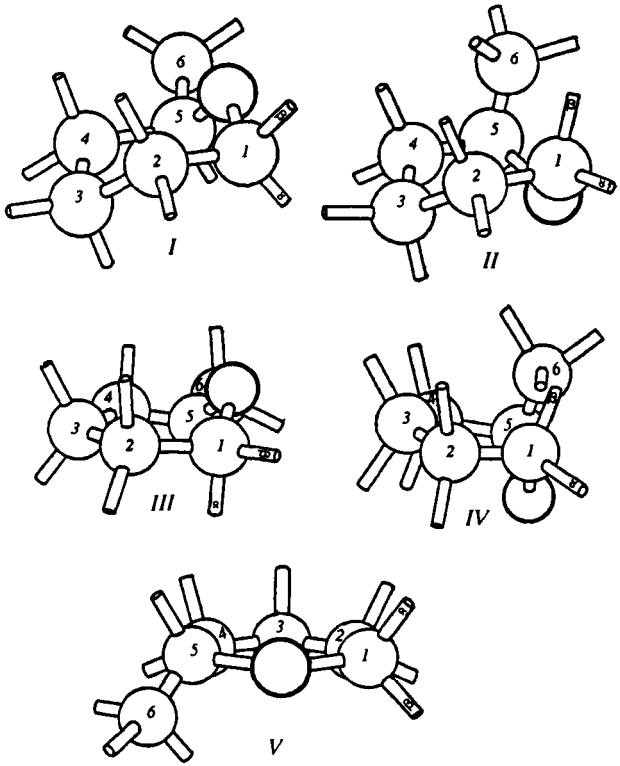

FIG. 2.—Different conformers of pyranose rings: The $^4C_1$ chair (I); the $B_{0,3}$ boat (II); two half-chairs (III and IV), and a coplanar ring (V).

In another oustanding piece of work, Isbell showed that nucleophilic attack can occur on the carbonyl group of a *trans*-oriented 2-acetate to give a cyclic orthoester (Fig. 6, reaction *1*). Such esters can undergo a second attack to afford a product having the same configuration as the starting material (Fig. 6, reaction 2). Alternatively, nucleophilic attack may occur on the anomeric carbon, by a competing reaction, to afford a product having an inverted configuration (Fig. 6, reaction *3*). He noted that, to form an orthoester, the leaving group must be *trans*-oriented with respect to the acetate group, and that attack on the orthoester always leads to a *trans* product, which is why the sequence of reactions depicted in Eqs. 1 and 2 leads to net retention of configuration.

If, on the other hand, the 2-acetate group is *cis*-oriented with respect to the leaving group, no orthoester can be formed and only an SN2 reaction can take place, which leads to inversion of configuration at C-1 (see Fig. 7). The concepts developed in this work were later assimilated into the body of organic chemistry in

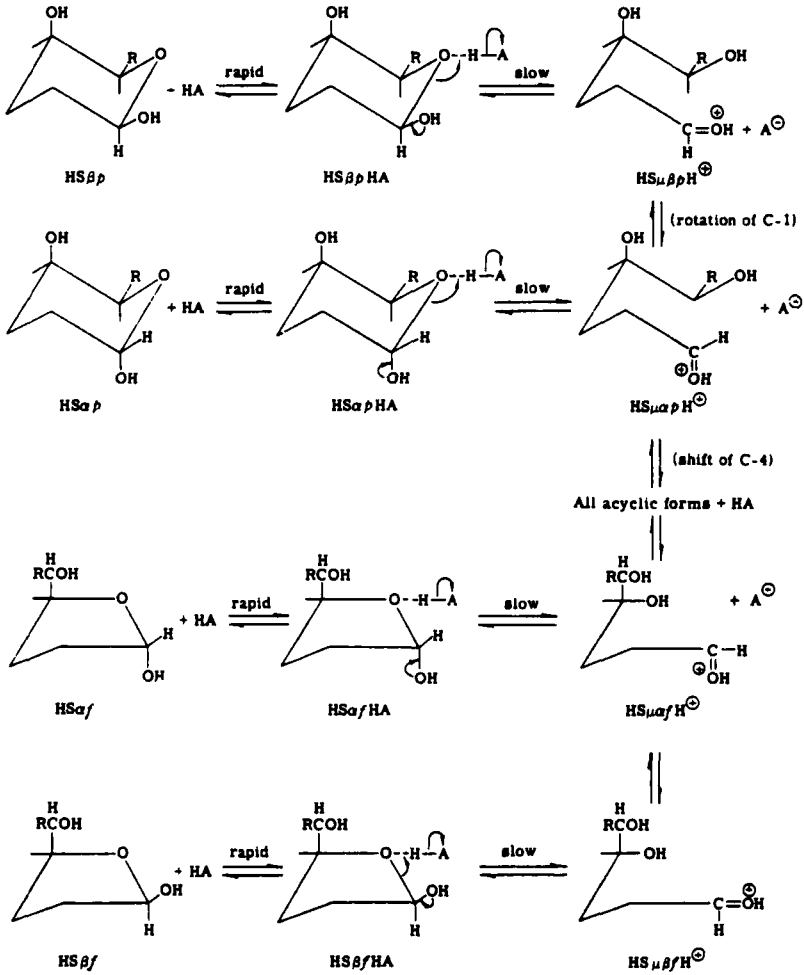

FIG. 3.—Mechanism of anomerization of aldopyranoses, by ring opening.

one of the largely unrecognized instances where a novel idea developed by a carbohydrate chemist was later adopted and used by "mainstream" organic chemists.

During World War II, Isbell worked on the synthesis of vitamin C and the use of algin, pectin, and other carbohydrates as components of dry cells. After the War, when the mildly radioactive elements ^{14}C and ^{3}H became available, chemists realized that much chemical and biological information could be obtained from

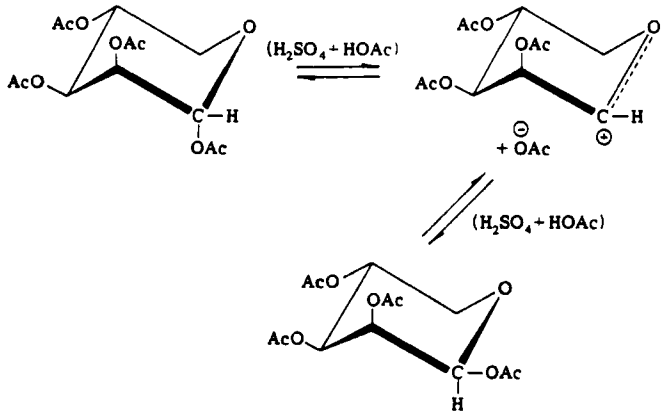

FIG. 4.—Mechanism of anomerization of aldopyranose acetates, by formation of carbocations.

carbohydrates position-labeled with either of these elements. Early attempts at the synthesis of such labeled carbohydrates met with scant success. One chemist wrote to Dr. Isbell: "Frankly, the lot of the chemist who attempts to synthesize a radioactive sugar is not a happy one." Many chemists turned to the Bureau and to Isbell's laboratory with urgent requests for help. In 1950, a project on the synthesis of position-labeled radioactive carbohydrates was funded by the (then) Atomic Energy Commission. With the increased personnel thereafter available, techniques were developed that enhanced the yields of the products. The Bureau was soon able to supply position-labeled carbohydrates to nearly every biological research laboratory in this country and to some abroad. This work was of great use in solving mechanistic problems and opened the way for the preparation of ^{13}C-labeled sugars needed for NMR work.

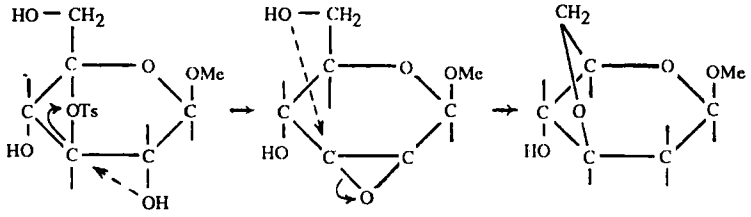

FIG. 5.—Mechanism of formation of methyl 3,6-anhydro-β-D-glucopyranoside via an intermediate 2,3-anhydro-alloside.

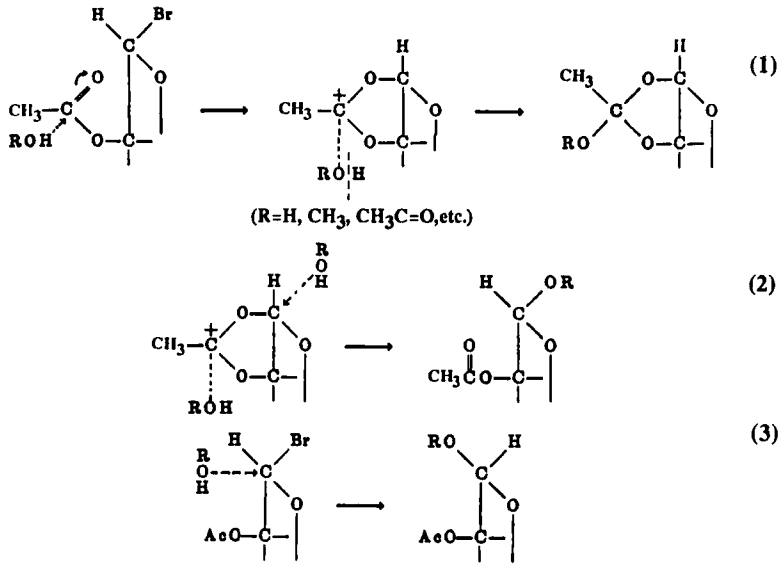

FIG. 6.—Nucleophilic attack on the carbonyl group of a *trans*-oriented 2-acetate can occur either via formation of a cyclic orthoester, which by undergoing a second attack affords a product having the same configuration as the starting material (reactions *1* and *2*), or by nucleophilic attack on the anomeric carbon to afford a product having the inverted configuration (reaction *3*).

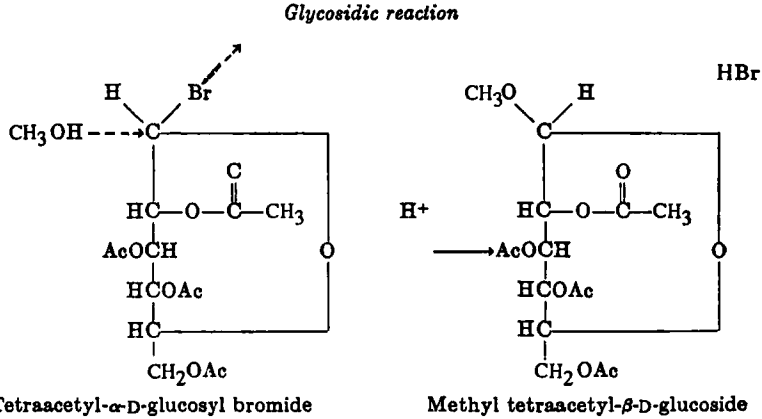

FIG. 7.—Glycosyl halides having the 2-acetyl group *cis*-oriented with respect to the leaving group cannot form orthoesters, so they undergo an SN2 reaction at C-1, which results in inversion of configuration.

At The American University, Isbell's major interest in research turned to the study of the oxidation of saccharides with hydrogen peroxide. In collaboration with Dr. Frush, he published some forty papers on the subject. A number of major discoveries were made, including that of a stepwise degradative peroxidation, which is catalyzed by base or by such metals as iron(II). It starts at the anomeric carbon of an aldose, either in the acyclic or the cyclic form, and affords the lower aldose and formic acid (see Fig. 8). Two mechanisms were recognized: an ionic one prevalent in strong alkali, and a free-radical process catalyzed by Fe(II) (see Fig. 9).

Disaccharides and polysaccharides are also oxidized by the same degradative oxidation: at first they react rapidly; then, when the point of branching is reached, they react much more slowly. When subjected to similar oxidations, ascorbic acid affords threonic acid and oxalic acid, and 2-deoxy sugars yield 2-deoxyaldonic acids and lower alditols.

In his last years, Dr. Isbell became convinced of the importance of saccharide peroxides as reaction products, and not merely as intermediates. He pointed to the structural similarity that exists between hydrazines, hydroxylamines, and peroxides and suggested that a missing group, saccharide peroxides, might be prepared by nucleophilic substitution using suitably protected glycosyl halides and aryl peroxides, as shown in the scheme below.

$$\begin{aligned} H_2N{-}NH{-}R' &\longrightarrow R{-}NH{-}NH{-}R' \\ R{-}X + H_2N{-}O{-}R' &\longrightarrow R{-}NH{-}O{-}R' \\ H{-}O{-}O{-}R' &\longrightarrow R{-}O{-}O{-}R' \end{aligned}$$

R—X = protected glycosyl halide, R′ = aryl

He was convinced that with adequate precautions peroxides could be isolated and manipulated safely. Unfortunately, he died before proving the feasibility of this reaction and left it to subsequent generations of chemists to complete his project.

Horace Isbell diligently served the American Chemical Society. He was Chairman of the Division of Carbohydrate Chemistry in 1937–1938 and Secretary of the Division's Committee on Carbohydrate Nomenclature from 1938 to 1941; he remained a member of that Committee until his death. In 1945, he was elected Chairman of the Washington Section of the A.C.S. He was recognized by the American Chemical Society as a leader in the field of chemistry, and was awarded the Hillebrand Prize by the Washington Section of the A.C.S. in 1952. In 1954, he was presented with the Merit Award (later named the Hudson Award) of the Division of Carbohydrate Chemistry in recognition of his contributions to this field of chemistry and in appreciation of his services to the Division. In 1986, the Carbohydrate Division created an award for young Carbohydrate Chemists and named it the Horace S. Isbell award. Later the Division celebrated Isbell's ninetieth birthday by organizing a symposium in his honor and by publishing "The Collected Papers of Horace S. Isbell," a three-volume series. Then after his death it organized a symposium honoring his scientific achievements.

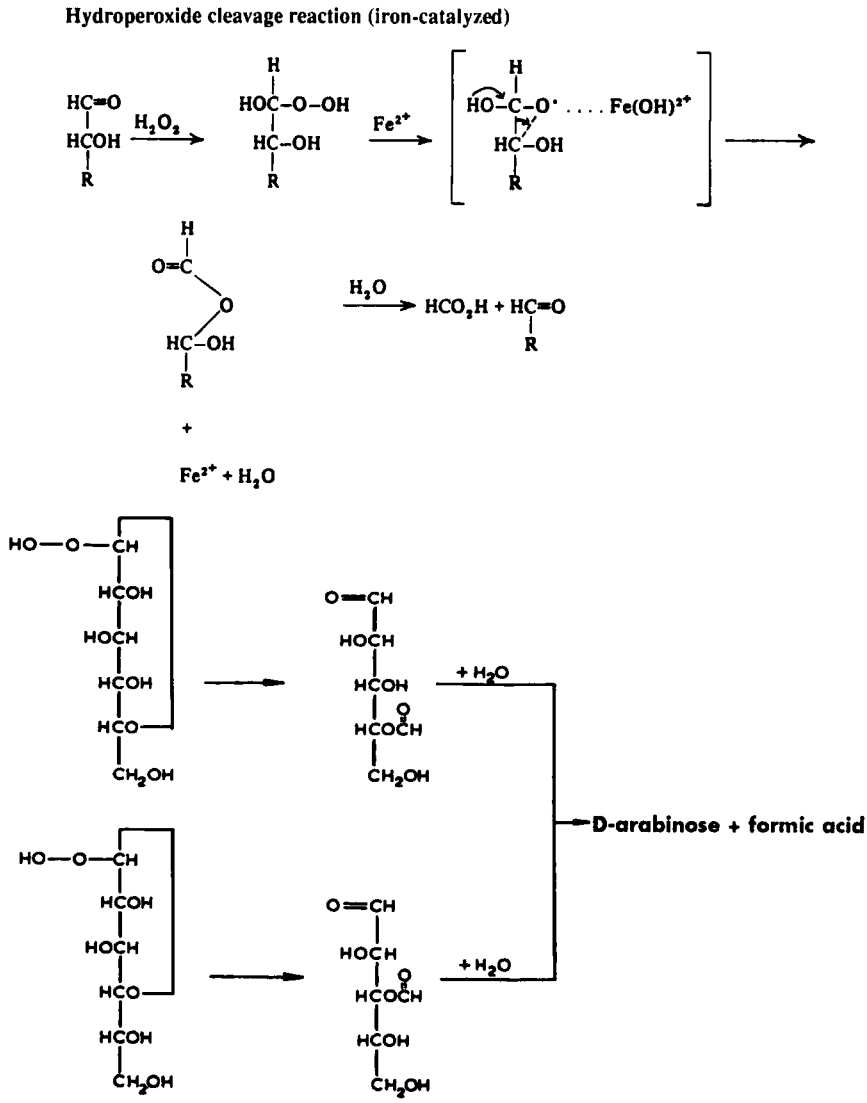

FIG. 8.—The stepwise degradative peroxidation of aldoses starts at the anomeric carbon and forms a lower aldose and formic acid.

Other honors bestowed on Horace Isbell were: The U.S. Department of Commerce Silver Medal for Meritorious Service in 1950; a Distinguished Alumni Award from the University of Denver in 1953; and in 1973, the second Sir Norman Haworth Memorial Medal of The Chemical Society (London) for his contributions

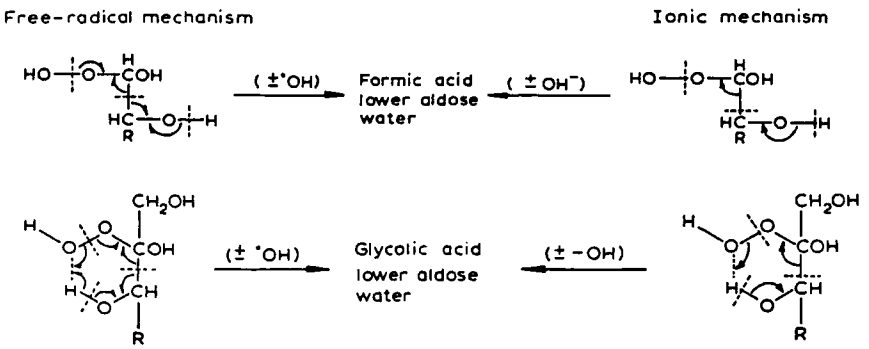

FIG. 9.—Two mechanisms compete: an ionic mechanism prevalent in strong alkaline solutions, and a free-radical mechanism catalyzed by Fe(II).

to carbohydrate chemistry. The subject of the Memorial Lecture was "The Haworth–Hudson Controversy, and the Development of Haworth's Concepts of Ring Conformation and Neighboring-Group Effects."

Horace S. Isbell is considered one of the world's greatest carbohydrate chemists and one of three American giants, along with C. S. Hudson and M. L. Wolfrom, responsible for making the United States a world leader in the field. He loved chemistry and always encouraged young chemists to achieve their goals and to succeed in their endeavors.

HASSAN S. EL KHADEM

This Page Intentionally Left Blank

ADVANCES IN CARBOHYDRATE CHEMISTRY AND BIOCHEMISTRY, VOL. 51

CARBON–PROTON COUPLING CONSTANTS IN THE CONFORMATIONAL ANALYSIS OF SUGAR MOLECULES

BY IGOR TVAROSKA

Institute of Chemistry, Slovak Academy of Sciences, 842 38 Bratislava, Slovak Republic

AND FRANÇOIS R. TARAVEL

Centre de Recherches sur les Macromolécules Végétales, CNRS, 38041 Grenoble cedex, France

I. INTRODUCTION

Nuclear magnetic resonance (NMR) has developed into one of the most powerful methods in structural chemistry for the study of organic molecules in solution. An important component of the information contained in NMR spectra resides in

the carbon–proton spin–spin coupling constants $^{n}J_{C,H}$. The potential of these coupling constants for the elucidation of conformations and configurations is well known, and a number of empirical correlations between their magnitude and stereochemical structure have been published.[1,2]

For carbohydrates, $^{n}J_{C,H}$ coupling constants in the glycosidic-bond region are of special interest as they are important for structural analysis. For several years, however, their utility has received little attention in the field of oligo- and polysaccharide molecules. Although their potential value in the conformational analysis of carbohydrate molecules was well recognized, their actual use has been limited by technical difficulties of measurements because of the low natural abundance of the ^{13}C isotope and by the lack of a relationship correlating $^{n}J_{C,H}$ values to the C—O—C—H dihedral angles of the glycosidic region in sugar molecules. Another obvious reason for this neglect is that there has been parallel access to nuclear Overhauser enhancement (NOE) values, which provide related structural information, namely on interproton distances. Unfortunately, the distances thus estimated are not precise and the set of data obtained is usually not complete. Moreover, the measured NOE is a weighted average on the NMR time-scale of all conformations accessible by the molecule. This factor means that interpretation of NOE data is very complex for flexible oligosaccharides, and any attempt to force a single, three-dimensional structure to agree with the average NOE data may generate a model in regions of conformational space that may, in fact, scarcely be populated in solution, leading thus to erroneous quantitative conclusions.[3,4] Consequently, additional experimental data are needed to permit a more accurate description of carbohydrate conformations. A complementary article[4a] by Dais in this volume treats in detail the ^{13}C relaxation parameters for carbohydrate molecules and their relation to molecular motion and conformation.

Relationships between carbon–proton coupling constants and structure have thus far largely been based on empirical rules, but the use of quantum-chemical calculations of coupling constants, in combination with measured NMR data, is becoming increasingly important. Especially in the field of conformational analysis of oligosaccharides, the comparison of measured coupling constants with calculated results for various conformations about glycosidic linkages has permitted the elucidation of angular dependences that would not otherwise have been possible.[5,6]

This article consists of three main parts. The principal objective of the first two is to introduce the experimental techniques that are used to measure carbon–proton coupling constants, and to describe the basic theory of quantum chemistry for calculating spin–spin coupling constants. The third part summarizes results that describe the angular dependences of carbon–proton coupling constants, along with concrete examples showing the utility of these dependences in the determination of conformational properties of oligosaccharides in solution.

II. General Theoretical Background

The fundamentals of NMR have been described in detail by many authors, from Abragam's *Principles of Nuclear Magnetism*[7] through textbooks on the basic theory of molecules in magnetic fields,[8-10] to a quantum description by Goldman[11] of high-resolution NMR in liquids. Besides these distinguished books, many others, including several devoted to chemists,[12-14] are also representative of the formidable development of NMR over the past decade in terms of sensitivity, quality of spectra, and computer-controllable pulse-sequences for multidimensional experiments. The reader who would like to know more about basic NMR is encouraged to consult this literature, as this article presents some simple ideas, serving as a reminder of the basic concepts rather than an exhaustive survey of the subject.

1. Resonance Condition

NMR spectroscopy is a consequence of the existence of nuclear spin, and is based on the magnetic resonance condition $\omega_0 = \gamma B_0$, which states that the precessional frequency ω_0 of nuclei having a nuclear spin is proportional to the applied magnetic field B_0. The proportionality constant γ is termed the gyromagnetic ratio and is characteristic of a given nucleus. In order to generate an excited state, an alternating electromagnetic field of frequency ω is applied perpendicular to the static field B_0. The condition for resonance is $\omega = \omega_0$. Changes in the energy states of the nucleus may be detected by a suitable coil arrangement, then amplified and recorded.

Within a molecule, a nucleus is characterized by its magnetic properties and electronic environment and by the following consequent parameters associated with the corresponding NMR signals: chemical shift, coupling constants, relaxation rates,[15] and nuclear Overhauser enhancement (NOE).[16,17] All these values may be used to extract qualitative or quantitative information about the structure, the conformation, and the behavior of molecules in solution.

2. Nuclear Spin–Spin Couplings

NMR signals are observed as singlet lines only when the corresponding nuclei are not influenced by the fields associated with the presence of other magnetically active nuclei. Theoretically, there are two mechanisms of interaction between the nuclear magnetic dipoles: a direct, through-space interaction that depends on the internuclear distances, and an interaction indirectly transmitted through the bonding electrons. The first interaction is averaged to zero in solution when the molecular motions are fast, free, and isotropic. In contrast, a fine structure remains in the spectra of liquids that results from through-bond interactions or indirect couplings.

A system containing n equivalent nuclei having spin quantum number I_X and m equivalent nuclei A having I_A is said to be of the type A_mX_n if the chemical-shift difference between X and A is large. The following multiplicity rule gives the number of lines in the NMR spectrum for each of these nuclei:

$$2n\,I_X + 1 \text{ for A, and}$$

$$2m\,I_A + 1 \text{ for X.}$$

The extent of through-bond coupling (up to four bonds) is expressed by coupling constants in hertz (J_{AX} here for an A_mX_n system). The values of coupling constants (in Hz) are usually measured directly from line spacings on the experimental spectra or extracted by calculation from experimental data. Coupling constants are independent of the strength of the applied magnetic field B_0, in contrast to the line separations attributable to nuclei having different screening constants. The absolute values of coupling constants decrease with the number of bonds that separate the nuclei A and X.

3. Origin of Spin–Spin Couplings

The indirect spin–spin coupling is independent of molecular rotation. The coupling mechanism is known to involve the electron spins of the bonding electrons and is the result of a weak electron polarization. The interaction energy E_{AX} is proportional to the scalar product of the nuclear spins I of A and X, according to the following expression:

$$E_{AX} = \hbar J_{AX} I_A \cdot I_X \qquad (1)$$

Theory indicates that the J_{AX} term is composed of several contributions that characterize the effect of orbital electronic motions, the polarization of electronic spins, and the Fermi contact term. The last contribution is the most significant, and affects mainly the s valence orbitals.

III. Experimental Techniques for Obtaining Carbon–Proton Coupling Constants

1. One-Bond Couplings

One direct way to determine $^1J_{C,H}$ is from the ^{13}C satellites of high-field ^1H-NMR spectra.[18] A proton signal has two ^{13}C satellites, each having an intensity that is 0.5% of that of the corresponding total proton resonance, and located symmetrically around that resonance. In addition to providing information about $^1H,^1H$ couplings, these satellites allow the determination of the $^1J_{C,H}$ couplings with good resolution. This determination is very often complicated by impurities or signal

overlaps, except for anomeric protons; but it may constitute, nevertheless, an easy and rapid method for determination of anomeric configuration via $^1J_{C,H}$ values.

An alternative is to use the gated technique,[19] which give proton-coupled ^{13}C spectra with full NOE, although this technique can be time-consuming. The resolution is often low, and furthermore the signals may be broadened by long-range $^{13}C,^1H$ couplings or overlapped by other signals. The technique may be combined with DEPT (Distortionless Enhancement by Polarization Transfer) or INEPT (Insensitive Nuclei Enhanced by Polarization Transfer) pulse-sequences[20,21] for enhancement of sensitivity. These sequences utilize the nonselective polarization transfer from ^1H to ^{13}C via $J_{C,H}$. They have been used routinely,[22,23] although these techniques still do not answer the problems of overlaps and signal broadening. Therefore, couplings thus measured, even after strong resolution-enhancement, may still be unreliable. To overcome these problems, Szilagyi and Gyorgydeak[24] have used selective excitation of individual multiplets using the DANTE (Delays Alternating with Nutations for Tailored Excitation) pulse-sequence.[25] This technique is very simple to perform, but requires a separate experiment for each carbon site in a molecule.

Another possibility is to separate coupling information from chemical-shift information into two dimensions, as first performed by Hall and Morris[26] for saccharides. They used ^{13}C two-dimensional J spectroscopy in which the second halves of modulated, ^{13}C spin-echoes are accumulated for a range of pulse spacings. The result gives a separate, proton-coupled, ^{13}C multiplet for each decoupled carbon resonance. Contributions of static magnetic-field inhomogeneity to multiplet linewidths are thus largely suppressed. However the practical realization of this procedure requires time-consuming accumulation of several data sets in order to obtain good resolution. Accordingly, experiments were described using special pulse-sequences[27,28] for "spin manipulations" that can selectively enhance (or suppress) $^1J_{C,H}$ versus $^nJ_{C,H}$ as $^1J_{C,H} \gg {}^nJ_{C,H}$. This technique does constitute a general approach to heteronuclear J-resolved spectroscopy, which can be used to solve specific problems with improved resolution and shorter measuring times.

Subsequently, Uhrinova *et al.*[29] reconsidered the problem using both proton- and carbon-detected experiments. For example, couplings of anomeric carbons were measured from the ^{13}C satellites in proton NMR spectra. The critical factor in these methods is the suppression of signals from protons bound to ^{12}C atoms. In the pulse-sequence proposed, these protons were selectively inverted by a BIRD (BIlinear Rotation Decoupling) pulse,[30] and the spin-echo method introduced by Bendall *et al.*[31] was used.

Values of $^1J_{C,H}$ were also determined by two-dimensional J-resolved spectroscopy using an INEPT-type pulse-sequence,[29] with a BIRD pulse for the suppression of $^nJ_{C,H}$ and folding in the F_1 dimension. Rules for the calculation of the correct values of $^1J_{C,H}$ from the reduced splittings observed were given. The $^1J_{C,H}$ values were also obtained from a set of J-modulated, one-dimensional ^{13}C spectra via the

experimental intensities of the individual lines.[29] This method, named the "constant-time method," may be suitable for polysaccharides having short T_2 relaxation times. Despite their results, the authors stressed the fact that the most sensitive and precise method for determination of $^1J_{C,H}$ values remains the measurement of ^{13}C satellite proton spectra. However, because of the very short spin–spin relaxation times of protons in polysaccharides, application of this procedure is in practice limited to oligosaccharides. In addition, overlaps of the nonanomeric protons further restrict its general use. Accordingly, the most promising techniques should be those using inverse-detected heterocorrelated methods in which quantum coherences are used for the indirect detection of magnetically weak nuclei (^{13}C) with the full sensitivity of such strong nuclei as ^1H to which they are coupled.[32–34] The factor is thus eight times greater in proton-detected C,H correlation than in conventional spectroscopy.[35]

2. Multiple-Bond Couplings

While such heteronuclear long-range couplings as $^3J_{C,H}$ are among the most valuable NMR parameters for determining conformation and configuration, their intensive use has been hindered by difficulties in measuring them. For example, the one-dimensional gated-decoupling ^{13}C experiment used for carbohydrates having natural ^{13}C abundance gives rise to complex multiplets, owing to the number of protons coupled to the same carbon[36] and to higher-order effects.[37] Isotopic ^{13}C enrichment constitutes one alternative approach,[38–41] but this is generally expensive, time-consuming, or difficult to achieve. Nevertheless, using selectively ^{13}C-enriched compounds,[42,43] long-range coupling constants were extracted directly from proton spectra[44] of peracetylated disaccharides ^{13}C-labeled at the C-1 position and having α- or β-D-(1→3) and α- or β-D-(1→4) linkages. The advantage of deuterium labeling has also been exploited for methyl β-cellobioside[45] and methyl α-maltoside.[46] This procedure resulted in simplification of the ^{13}C-NMR spectra of these compounds, thus facilitating the measurement of inter-residue couplings.

Another alternative is to use selective proton decoupling in ^{13}C-NMR spectra. This was successfully achieved by Bock and Pedersen,[47] who combined selective proton decoupling with gated noise-decoupling. They obtained selectively proton-decoupled ^{13}C-NMR spectra without population changes (in case of a weak irradiation field) and with nuclear Overhauser enhancement. This was performed using a second decoupling-frequency source. More modern versions of the technique have been used by Commenges and Rao[48] and by Seto *et al.*[49] following the pulse-programmer possibilities offered by newer spectrometers.

Using two-dimensional NMR spectroscopy, it is possible to present the individual coupling patterns in a spatially separated form. Bax and Freeman[50] were the first to propose a two-dimensional experiment specially designed for the detection and assignment of long-range carbon–proton coupling constants. Their procedure

is based on a 2D-experiment that detects carbon-13 spin-echoes modulated by heteronuclear spin–spin coupling, using a frequency-selective 180° radiofrequency pulse applied to an isolated proton resonance (Fig. 1). The resulting 2D spectra display in the F_1 dimension all of the long-range C,H couplings of each carbon resonance with the proton selected. The effectiveness for spin inversion (spin flip) is linked to the frequency range about the exact resonance condition for a chosen proton, so that the outer satellite lines due to $^1J_{C,H}$ are unaffected, whereas the inner satellites due to long-range coupling are inverted. Although the sensitivity of this method is not very high, it has been successfully used as such, or in a modified form involving, for example, a DANTE sequence.[25] The technique is essentially limited to compounds having well-resolved proton spectra and relatively long T_2 relaxation-times, such as oligo- or monosaccharides. Furthermore, care should be exercised in interpreting the observed C,H splittings when the protons are strongly coupled.

Other versions of the proton-flip experiment have been described by Bax[27, 51] as semiselective two-dimensional J spectroscopy and by Rutar[52] as manipulated polarization transfer in 2D-NMR. In each version two experiments permit the accurate determination of either (*a*) all direct C,H coupling constants by removal of the long-range splittings or (*b*) all long-range couplings while removing all of the direct C,H couplings. Wimperis and Freeman[53] have also reported an extension of this principle, using an excitation sequence that discriminates between direct and long-range C,H couplings; it is termed TANGO (Testing Adjacent Nuclei with a Gyration Operator).

The modified heteronuclear shift-correlation experiment described by Bauer *et al.*[54] has the advantage of giving 2D-spectra with proton shifts in the F_1 dimension and long-range C,H splittings. However, its overall sensitivity is low because of relaxation during relatively long delays, and the resolution obtained is only to the nearest Hertz.

Polarization transfer, and its subsequent advantage of magnetization enhancement, has also been used. Thus 2D extension of refocused INEPT, with a selective

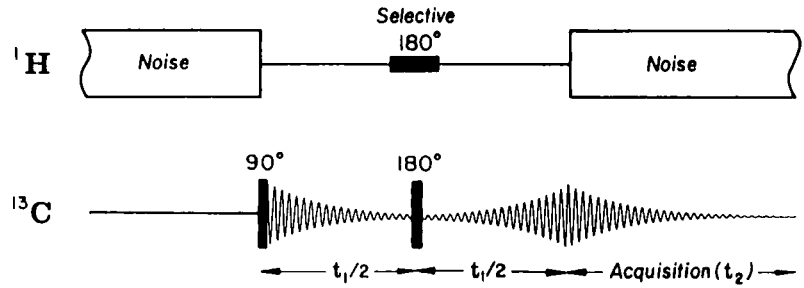

FIG. 1.—Pulse sequence used to detect long-range C,H couplings. Reprinted with permission from Ref. 50. © 1982 American Chemical Society.

180° ^{1}H-pulse/nonselective 180° ^{13}C-pulse combination, was performed by Jippo *et al.*[55] with a potential fourfold gain in sensitivity over conventional *J* spectroscopy and with the result of simple doublet patterns. Modifications to this method have been introduced for 2D and 1D spectroscopy.[56–57] Problems remain, however, despite higher sensitivity, when the T_2 relaxation times of carbons are short (< 0.2 s) or when the setting of the refocusing period is too great a compromise.

Inverse and selective detection of long-range C,H spin-coupling constants have been described by Ochs and Berger.[58] The pulse-sequence that they used (SELRESOLV), with selective ^{13}C excitation, separates $J_{H,H}$ from $J_{C,H}$ couplings. It can be understood as an inverse INEPT sequence followed by a 2D $J_{H,H}$-resolved experiment (Fig. 2). The spectrometer they used was equipped with a selective-excitation unit, and the experiment was performed with selective half-Gaussian-shaped ^{13}C pulse. Results were good, although long measurement times were sometimes necessary for adequate ^{1}H–^{12}C suppression.

With the advent of inverse detection and the corresponding gain in sensitivity, newer schemes for the measurement of long-range coupling constants have been proposed. They are based on the HMBC (Heteronuclear Multiple-Bond Correlation) derivative[59] or variants[60,61] of the HMQC (Heteronuclear Multiple-Quantum Coherence) experiment, and also on the HSQC (Heteronuclear Single-Quantum Coherence) experiment.[34] For example Poppe and van Halbeek[60] have proposed, in the case of a trisaccharide, an experiment that preserves the sensitivity advantages of inverse detection and produces pure-phase multiplets in both dimensions. The magnitudes as well as the relative signs of couplings may be obtained. The same authors[62] have also introduced into their pulse-sequences an isotropic mixing, which overcomes the spectral overlap problem.

Another very interesting method has been described by Kurz *et al.*[63] starting from a method proposed by Montelione *et al.*[64] in which an E. COSY pattern is

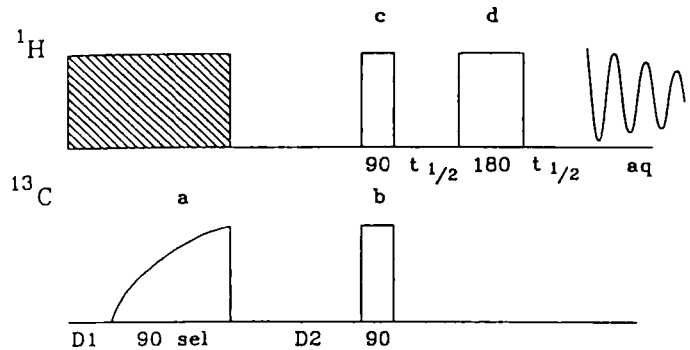

FIG. 2.—SELRESOLV sequence for inverse and selective detection of long-range C,H coupling constants. Reprinted from Ref. 58, © 1990. Reprinted by permission of John Wiley & Sons, Ltd.

obtained in the conventional TOCSY or NOESY spectra of isotopically enriched proteins. In the incremented dimension (F_1 in 2D spectra), the cross peaks show the direct, large coupling to the heteronucleus and, in the detected dimension (F_2) they reveal the desired heteronucleus through the shift of the multiplet.

In order to determine couplings to nuclei in natural abundance, it is necessary to suppress the signals of protons that are not bonded to a magnetically active heteronucleus. An ω_1 hetero half-filter that selects for such nuclei in F_1 via the phase cycle was used for this purpose. Presaturation of the protons bonded to ^{12}C by the BIRD pulse allows a rapid pulse-sequence (2 scans per second). The resulting 2D spectra are TOCSY spectra in which the cross peaks show the desired E. COSY pattern. From the results shown, the only limitation seems to be the resolution obtained, although the authors do not hesitate to use a third heteronuclear frequency domain for improvement.

IV. Theory of Nuclear Spin–Spin Coupling Constants

Such second-order molecular properties as spin–spin coupling depend upon distortion of electron clouds by additional external perturbations; that is, in the NMR experiment they depend upon the electronic motion induced by an applied magnetic field. Theories for such second-order molecular properties require a study of the change in the molecular-orbital wavefunctions, which may be found by using a perturbation method to describe the effects occurring when a magnetic field is applied.[8–10,65–67]

In this section, beginning with first principles, we write a general Hamiltonian function for a molecule in a magnetic field and illustrate formally how this term arises. With this foundation, we then construct equations for the determination of $J_{C,H}$ on the basis of perturbation theory[68–70] in terms of the electronic distribution obtained from molecular-orbital (MO) calculations.

1. The Schödinger Equation in a Magnetic Field

The general procedure to obtain the Schödinger equation for a molecule in a magnetic field[9,10] $\mathbf{B}$ consists of replacing the momentum operator $\mathbf{p}$ $(= (\hbar/i)\nabla)$ in the following way $\mathbf{p} \rightarrow \mathbf{p} + e\mathbf{A}$ with $\mathbf{A}$ the vector potential, related to the magnetic field-strength $\mathbf{B}$ via $\mathbf{A} = 0.5\ \mathbf{B} \times \mathbf{r}$, div $\mathbf{A} = 0$, $\mathbf{B} =$ curl $\mathbf{A}$. The Hamiltonian of the electronic system of any molecule considered, in the presence of a magnetic field, is then given by

$$H = \frac{1}{2m}\sum_j (\mathbf{p}_j + e\mathbf{A}_j)^2 + V = \frac{1}{2m}\sum_j \left(\frac{h}{i}\nabla j + e\mathbf{A}_j\right)^2 + V. \qquad (2)$$

There is an additional term that describes the interaction of the electron spin with the total magnetic field. This is ignored, since only systems having zero total spin are being considered.

The Hamiltonian may be written as

$$H = H_0 + H^1 + H^2 + H^3 \tag{3}$$

The corresponding Hamiltonians are given by

$$H_0 = \frac{1}{2m}\sum_j \left(\frac{\hbar}{i}\nabla_j\right)^2 + V + H_{\mathrm{LL}} + H_{\mathrm{LS}} + H_{\mathrm{SS}} \tag{4}$$

$$H^1 = \frac{e\hbar\mu_{\mathrm{B}}}{i}\sum_{k\mathrm{A}} \frac{\gamma_{\mathrm{A}}\mathbf{I}_{\mathrm{A}} \times r_{k\mathrm{A}}}{|r_{k\mathrm{A}}|^3}\nabla_k + \frac{e^2\hbar^2\mu_{\mathrm{B}}^2}{2m}\sum_{k\mathrm{AX}} \gamma_{\mathrm{A}}\gamma_{\mathrm{X}} \times \left(\mathbf{I}_{\mathrm{A}} \times \frac{\mathbf{r}_{k\mathrm{A}}}{|r_{k\mathrm{A}}|^3}\right)\left(\mathbf{I}_{\mathrm{A}} \times \frac{\mathbf{r}_{k\mathrm{X}}}{|r_{k\mathrm{X}}|^3}\right) \tag{5}$$

$$H^2 = \frac{\mu_0\mu_{\mathrm{B}}\hbar}{2\pi}\sum_{j\mathrm{A}} \gamma_{\mathrm{A}}\left\{\frac{3(\mathbf{S}_j\cdot\mathbf{r}_{j\mathrm{A}})(\mathbf{I}_{\mathrm{A}}\cdot\mathbf{I}_{\mathrm{A}})}{|r_{j\mathrm{A}}|^5} - \frac{(\mathbf{S}_j\cdot\mathbf{I}_{\mathrm{A}})}{|\mathbf{r}_{j\mathrm{A}}|^3}\right\} \tag{6}$$

$$H^3 = \frac{4\mu_0\mu_{\mathrm{B}}\hbar}{3}\sum_{j\mathrm{A}} \gamma_{\mathrm{A}}\,\delta(|\mathbf{r}_{j\mathrm{A}}|)(\mathbf{S}_j\cdot\mathbf{I}_{\mathrm{A}}). \tag{7}$$

In Eq. *4*, V is the electrostatic potential energy, which is the sum of the electrostatic interactions of electrons with the nuclei and the electrostatic repulsion energy between electrons themselves, H_{LS} is the spin–orbital interaction, H_{SS} represents the interaction between the intrinsic magnetic moments of electrons, and H_{LL} is the orbital–orbital Hamiltonian that gives the magnetic energy of interaction between the electrons as moving charged particles. I is the nuclear-spin angular momentum, S is the electron-spin angular momentum, γ is the gyromagnetic ratio, μ_0 is the permittivity of free space, μ_{B} is the Bohr magneton, and δ is the Dirac delta function.

The Hamiltonian H_0 gives the total electronic kinetic energy, and H^1 gives the magnetic interactions between electron orbital motions and nuclear magnetic moments. The Hamiltonian H^2 represents the dipole–dipole couplings between the electrons and nuclear magnetic moments, and H^3 is the Fermi contact hyperfine term, which gives the contact interaction between electron spins and nuclear spins.

2. Indirect Nuclear Spin–Spin Couplings

The effect of any indirect interaction between nuclear spins by way of the electron system may be obtained by solving the time-independent Schrödinger equation

$$H\Psi = E\Psi \tag{8}$$

using perturbation theory.[68–70] In this method, the terms in Eqs. *3–7* that depend on the coordinates of the nuclear spin system (H^1, H^2, and H^3) are selected and treated

as perturbations. Thus, the theory of the coupling is based on three types of electron-coupled interactions between the electrons and nuclei of the molecule concerned, namely (1) a contact interaction between the electron and nuclear spins; (2) a magnetic dipolar interaction between electron and nuclear spin; (3) an orbital interaction between the magnetic field produced by the orbital motion of the electrons and the nuclear magnetic dipole.

It turns out that the most significant contribution to the total nuclear spin–spin interaction in most cases is the contact term H^3. Since the first-order perturbation energy due to H^3 is zero,[9] the energy of interaction between nuclei A and X, namely E_{AX}, is represented by the second-order perturbation energy

$$E_{AX} = -\frac{16\mu_0^2\mu_B^2\hbar^2}{9}\gamma_A\gamma_X \sum_{m(\neq 0)} \sum_k \sum_j \frac{1}{E_n - E_0} \times \langle\Psi_0^0|\delta(\mathbf{r}_{kA})\mathbf{S}_k\mathbf{I}_A|\Psi_n^0\rangle$$

$$\langle\Psi_n^0|\delta\mathbf{r}_{jX})\mathbf{S}_j\mathbf{I}_X|\Psi_0^0\rangle \qquad (9)$$

where the sum is over all states of the system other than Ψ, the ground- or lowest-energy state (that is, the sum is over all excited states of the system of electrons), and E is the energy associated with state Ψ.

Comparison of Eq. *9* with Eq. *1* leads to the following expression for the contact contribution, $J^c_{A,X}$, to the spin–spin coupling constant $J_{A,X}$:

$$J^c_{A,X} = -\frac{8\mu_0^2\,\mu_B^2\hbar}{9\pi}\gamma_A\gamma_X \sum_{m(\neq 0)} \sum_k \sum_j \frac{1}{E_n - E_0} \times \langle 0|\delta(\mathbf{r}_{kA})\mathbf{S}_k|n\rangle$$

$$\langle n|\delta(\mathbf{r}_{jX})\mathbf{S}_j|0\rangle. \qquad (10)$$

It is difficult to calculate the contact contribution using the foregoing equation because we have little knowledge of the exact wavefunctions of the excited states. Therefore the average excitation energy approximation, in which $E_n - E_0$ is replaced by an average spin singlet-triplet average excitation energy E, has sometimes been applied. This greatly simplifies calculational procedures but is not necessarily justified in all situations.[9,10]

In the case of spin–spin coupling involving hydrogen nuclei, the dipolar and orbital interactions are usually neglected. However, they are very important in some examples of coupling not involving hydrogen nuclei.

A magnetic dipolar interaction between the electronic and nuclear spins is given by

$$H^2 = \frac{\mu_0\mu_B\hbar}{2\pi} \sum_A \sum_k \gamma_A\{3(\mathbf{S}_k\cdot\mathbf{r}_{kA})(\mathbf{I}_A\cdot\mathbf{r}_{kA})r_{kA}^{-5} - \mathbf{S}_k\mathbf{I}_A r_{kA}^{-5}\}. \qquad (11)$$

This interaction gives the corresponding spin–spin coupling contribution as

$$J^{\mathrm{d}}_{\mathrm{A,X}} = -\frac{\mu_0^2\,\mu_{\mathrm{B}}^2\hbar}{24\pi^3}\,\gamma_{\mathrm{A}}\gamma_{\mathrm{X}} \sum_{m(\neq 0)} \sum_k \sum_j \frac{1}{E_n - E_0}\, x\langle 0|3(\mathbf{S}_k\cdot\mathbf{r}_{k\mathrm{A}})\mathbf{r}_{k\mathrm{A}}r_{k\mathrm{A}}^{-5} - \mathbf{S}_k r_{k\mathrm{A}}^{-3}|n\rangle$$

$$\langle n|3(\mathbf{S}_j\cdot\mathbf{r}_{j\mathrm{X}})\mathbf{r}_{j\mathrm{X}}r_{j\mathrm{X}}^{-5} - \mathbf{S}_j r_{j\mathrm{X}}^{-3}|0\rangle \qquad (12)$$

where $E_n - E_0$ is the singlet–triplet excitation energy.

Finally, the orbital interaction is divided into two terms. One is an orbital contribution involving a matrix element of H_1^1 which concerns only the singlet ground state and the other is an orbital contribution involving a matrix element of H_2^1, which mixes a singlet ground state with triplet excited states:

$$H_1^1 = \frac{\mu_0^2\mu_{\mathrm{B}}^2 e\hbar}{16\pi^2} \sum_k \sum_{\mathrm{A}} \sum_{\mathrm{X}} \gamma_{\mathrm{A}}\gamma_{\mathrm{X}}(\mathbf{I}_{\mathrm{A}}\cdot\mathbf{r}_{k\mathrm{A}}/r_{k\mathrm{A}}^3)\,(\mathbf{I}_{\mathrm{X}}\mathbf{r}_{k\mathrm{X}}/r_{k\mathrm{X}}^3) \qquad (13)$$

$$H_2^1 = \frac{\mu_0\mu_{\mathrm{B}}\hbar}{2\pi i} \sum_k \sum_{\mathrm{A}} \gamma_{\mathrm{A}}(\mathbf{I}_{\mathrm{A}}\cdot\mathbf{r}_{k\mathrm{A}}/r_{k\mathrm{A}}^3) \times \nabla_k$$

$$= \frac{\mu_0\mu_{\mathrm{B}}}{\pi} \sum_k \sum_{\mathrm{A}} \gamma_{\mathrm{A}}(\mathbf{I}_{\mathrm{A}}\cdot\mathbf{m}_{k\mathrm{A}}^0/r_{k\mathrm{A}}^3) \qquad (14)$$

where $\mathbf{m}_{k\mathrm{A}}^0 = m_{xk}^0 i + m_{yk}^0 j + m_{zk}^0 k$.

Selection of the terms dependent on I_{A} and I_{X} from the second-order perturbation energy gives

$$J^0_{\mathrm{A,X}} = J^0_{\mathrm{A,X_1}} + J^0_{\mathrm{A,X_2}} \qquad (15)$$

with

$$J^0_{\mathrm{A,X_1}} = \frac{\mu_0^2\mu_{\mathrm{B}}^2\hbar}{48\pi^3 m}\,\gamma_{\mathrm{A}}\gamma_{\mathrm{X}}\langle 0|\mathbf{r}_{k\mathrm{A}}\,\mathbf{r}_{k\mathrm{X}}\,r_{k\mathrm{A}}^{-3}r_{k\mathrm{X}}^{-3}|0\rangle \qquad (16)$$

$$J^0_{\mathrm{A,X_2}} = \frac{\mu_0^2\mu_{\mathrm{B}}^2\hbar}{6\pi^3}\,\gamma_{\mathrm{A}}\gamma_{\mathrm{X}} \sum_{m(\neq 0)} \sum_k \sum_j \frac{1}{E_n - E_0} \times \langle 0|\mathbf{m}_{k\mathrm{A}}^0 r_{k\mathrm{A}}^{-3}|n\rangle\,\langle n|\mathbf{m}_{j\mathrm{X}}^0 r_{j\mathrm{X}}^{-3}|0\rangle. \qquad (17)$$

In the foregoing discussion it is necessary to consider that the coupling is represented by a scalar J_{AX} term. This is usually valid in solution where the molecule is rotating rapidly and randomly, and therefore electron-coupled interactions are isotropic. In other cases, the coupling must be treated as a second-rank tensor $\boldsymbol{J}_{\mathbf{AX}}$.

3. Finite Perturbation Theory

The calculation of spin–spin coupling constants has proven to be a difficult task for molecular-orbital theory. The state of the art of such calculations has been discussed in detail.[71–74]

The calculation of spin–spin couplings has been performed on the basis of both molecular-orbital (MO) theory and valence-bond theory. Most recent calculations of spin–spin coupling have been performed by means of MO expressions through different approaches, such as those arising from finite perturbation theory[69,70] (FPT), the Rayleigh–Schrödinger sum-over-states (SOS) theory[75], and self-consistent perturbation (SPC) theory.[76] This section is limited to one of these approaches that has been used with carbohydrate molecules, namely the FPT method.

Currently, two different lines of approach for such calculations may be distinguished. They use either very good quality *ab initio* wavefunctions or semiempirical methods to describe the ground state.[71] The obvious advantage of the former approach as compared with the second can hardly be stressed enough. However, precise *ab initio* calculations are computationally so demanding that systematic calculations for medium-sized molecules have not yet been carried out, despite striking advances in computational facilities.

On the other hand, for studying spin–spin couplings in medium-sized molecules it is common to use the intermediate neglect of differential overlap[77] (INDO) approximation, which, although it does not permit accurate calculation, still gives an adequate interpretation of many experimental trends.[74,77]

In the INDO method, a perturbation corresponding to one of the three coupling mechanisms is introduced during the calculation of the self-consistent field (SCF) wavefunction for a given molecule.

The perturbed Hamiltonian with the contact interaction as a perturbation is given by

$$H = H_0 + \frac{4\mu_0\mu_B\hbar}{3} \sum_k \sum_i \delta(r_{kA})\, S_k \cdot \mu_i, \tag{18}$$

where the first term represents the unperturbed system. Focusing attention on two interacting nuclear moments μ_A and μ_X, which both lie in the z direction, this equation may then be rewritten as

$$H = H_0 + \mu_A H_A + \mu_X H_X, \tag{19}$$

where

$$H_A = -\frac{4\mu_0\mu_B\hbar}{3} \sum_k \delta(r_{kA}) S_{kz} \tag{20}$$

$$H_X = -\frac{4\mu_0\mu_B\hbar}{3} \sum_k \delta(r_{kX}) S_{kz} \tag{21}$$

Following the same procedure as in the previous section it is possible to write, for the contact contribution to the spin–spin coupling constant,

$$J^c_{A,X} = \frac{4\mu_0^2\mu_B^2\hbar}{9\pi}\gamma_A\gamma_X \left[\frac{\partial}{\delta\mu}\langle\Psi(\mu_A)|H_X|\Psi(\mu_X)\rangle \right]_{\mu_X = 0}, \tag{22}$$

where $\Psi(\mu)$ is the wavefunction for the molecule in the presence of a perturbing spin of atom X having nuclear moment μ_X. This equation may be used to develop a method for calculating carbon–proton coupling constants within the framework of the MO theory.[69,70]

Available standard methods are of the Hartree–Fock type. This means that the wavefunction is chosen as a single determinant built up from n molecular orbitals, each double-occupied for a $2n$-electron system. In the conventional approach, the SCF equations that involve the contact interaction are defined by the matrix elements

$$F^{\beta}_{\mu\nu} = H^{\text{core}}_{\mu\nu} + \frac{2\mu_0\mu_B\hbar}{3}\int \chi^*_\mu\, \delta(r_A)\chi_\nu\, dv + \sum_\lambda \sum_\sigma \{P_{\lambda\sigma}\langle\mu\nu|\lambda\sigma\rangle - P^{\beta}_{\lambda\sigma}\langle\mu\lambda|\nu\sigma\rangle\} \tag{23}$$

$$F^{\alpha}_{\mu\nu} = H^{\text{core}}_{\mu\nu} + \frac{2\mu_0\mu_B\hbar}{3}\int \chi^*_\mu\, \delta(r_A)\chi_\nu\, dv + \sum_\lambda \sum_\sigma \{P_{\lambda\sigma}\langle\mu\nu|\lambda\sigma\rangle - P^{\alpha}_{\lambda\sigma}\langle\mu\lambda|\nu\sigma\rangle\}. \tag{24}$$

Here P is a spin-density matrix, defined as a difference of density matrices for α and β spin, the P^α, P^β. Molecular orbitals Ψ are approximated by linear combinations of atomic orbitals χ_i; the other symbols have their usual meanings.

From these SCF equations the contact contribution to the spin–spin coupling is evaluated as

$$J^{c}_{A,X} = \frac{4\mu_0^2\mu_B^2\hbar}{9\pi}\sum_\mu\sum_\nu \int \chi_\mu\, \delta(r_A)\chi_\nu\, d\nu \times \left[\frac{\partial}{\partial\mu_X} P\mu\nu\,(\mu_X)\right]_{\mu_X=0}. \tag{25}$$

Calculations of spin–spin coupling constants based on the FPT method (Eq. *25*), which have been the most successful in correlating conformational and substituent trends, have been performed in the semiempirical INDO approximation[77] of SCF MO theory. By this approach, Eq. *25* becomes

$$J^{c}_{A,X} = \frac{4\mu_0^2\mu_B^2\hbar}{9\pi}\gamma_A\gamma_X\, S_A(0)^2 S_X(0)^2 \times \left[\frac{\partial}{\partial h_X} P_{S_AS_X}(h_X)\right]_{h_X=0}, \tag{26}$$

where

$$h_X = \frac{4\mu_0\mu_B}{3}\hbar\mu_X S_X(0)^2 \tag{27}$$

and $S_X(0)^2$ is the density at the nucleus X of the valence s electrons. If either χ_{μ^*} or χ_ν are not s valence orbitals on atom X, this term vanishes.

4. Theory of the Solvent Effect on Couplings

Intermolecular solvent–solute interactions influence the charge distribution on a carbohydrate molecule. Subtle electronic changes that occur as a result of these interactions are responsible for the solvent dependence of carbon–proton coupling constants. The general aspects of solvent effects on NMR parameters have been reviewed,[78,79] and consequently, only a very brief outline of the theoretical model within FPT INDO SCF MO formalism is considered here.

In general, any satisfactory theoretical calculation of a nuclear coupling constant requires reliable calculation of the molecular wavefunction. As a consequence, a realistic approximation to the actual charge distribution in the carbohydrate molecule must presumably enter any theoretical model that attempts to provide a quantitative interpretation of solvent effects. The simplest treatments, and those that have been proposed most frequently to account for the solvent effect in the absence of specific effects, are those in which the solvent is treated as a continuum surrounding the solute molecule. Several different models where the solvent dependence of coupling interactions is related to the polarity of the medium have been proposed.[78,79] The solvation theory[80,81] has been successfully used within the FPT formalism to interpret the effect of solvent on $^1J_{C,H}$ and $^3J_{C,H}$. On the basis of this model, the Hamiltonian of a particular molecule includes the solvent–solute interaction term H_{solv}:

$$H_{solv} = \frac{\epsilon - 1}{2\epsilon}\left[\sum_i^M \sum_s^N \frac{Q_s}{r_{si}} - \sum_r^M \sum_k^N \frac{Q_s Z_k}{r_{sk}}\right], \qquad (28)$$

where Q_s is the induced solvation charge that is associated with each atom of solute, and its charge is equal in magnitude but opposite in sign to the net charge of the atom to which it is attached; r_{si} and r_{sk} are the solvation–electron and solvation–nucleus distances, respectively; and Z_k is the nuclear charge. The spin–spin coupling is calculated by the FPT method, incorporating this term into the Fock matrices given by Eqs. *23* and *24*. Details of this model are described in the original papers.

V. Conformational Dependence of Carbon–Proton Coupling Constants

The following systematic study of carbon–proton coupling constants emphasizes analysis of the dependence of carbon–proton couplings on the conformation around glycosidic linkages. One fundamental problem arises in investigating the conformational dependence of coupling constants. All theoretical relationships between the $^nJ_{C,H}$ value and the dihedral angle are defined for systems of fixed geometry. However, it is well established[3,82] that many carbohydrate molecules are

flexible and are capable of existing as an equilibrium mixture of conformers that are interconverting rapidly on the NMR time-scale. The experimental values thus reflect average values in which the form of conformational dependence is weighted with respect to the barrier that hinders internal rotation; the relationship between an observed spin–spin coupling constant and conformation is not directly obvious. If the potential surface is described by a potential energy $E(\phi_i)$, where ϕ_i is the torsion angle, that is acceptable for our purposes, it is possible to compute expected, that is, statistically averaged $\langle {}^nJ_{C,H}\rangle$ values for ${}^nJ_{C,H}$, using standard procedures[83,84] that weight each conformation of the carbohydrate molecule by the Boltzmann factor of $E(\phi_i)$, normalized by the configuration integral Z_N:

$$\langle {}^nJ_{C,H}\rangle = Z_N^{-1} \int\int\int {}^nJ_{C,H}(\phi_i)\exp[-\beta E(\phi_i)]\, d(\phi_i), \qquad (29)$$

where

$$Z_N = \int\int\int \exp[-\beta E(\phi_i)]\, d(\phi_i). \qquad (30)$$

Execution of the mathematical operations specified by Eqs. *29–30* depends on the details of the dependence of the functions ${}^nJ_{C,H}(\phi_i)$ and $E(\phi_i)$ on ϕ_i. For many purposes of interest, it is sufficient to use the summation instead of the integration in Eqs. *29–30*. The computation for carbohydrates is then straightforward, especially if the dependence of ${}^nJ_{C,H}(\phi_i)$ is known. Calculations of $\langle {}^nJ_{C,H}\rangle$ involve a process of averaging trigonometric functions, which has the effect of distorting space in a nonorthogonal way.[83,84] Therefore, it is no more correct to identify the calculated quantity $\langle {}^nJ_{C,H}\rangle$ with a value of ${}^nJ_{C,H}$ that corresponds to any real conformation. The mean conformations that would have ${}^nJ_{C,H}$ equal to $\langle {}^nJ_{C,H}\rangle$ have been called "virtual" conformations[84] and can never be identified with any actual conformation that the molecule may adopt. Conversely, any coupling constant derived from an experiment that observes the subject molecules in an ensemble of conformations should not be identified with a coupling constant that corresponds to a particular conformation of the real molecule.

Theoretically, on the other hand, a molecule is computed in a single given conformation. In the case of carbohydrate molecules, it is not usually possible to prepare a series of rigid compounds having well-defined conformations in solution for dihedral angles over the whole 360° interval and thus provide a complete source of data to estimate the angular dependence of $J_{C,H}$. However, the combined use of theoretical and experimental methods gives a unique opportunity for determining the conformational dependence of carbon–proton coupling constant in carbohydrate molecules.

1. One-Bond Couplings

Early interest in $^1J_{C,H}$ couplings focused upon an understanding of the structural terms that were intuitively considered to affect their magnitude: hybridization, changes in bond angles and bond lengths, ring strain, steric effects, substituent effects according to their electronegativity, overlap with lone pairs, and electric fields due to the substituent. For example, it was suggested[85-87] that one-bond coupling constants depend upon the amount of *s*-character in the bond joining the C and H nuclei. It has been shown[88] that this dependence may also be expressed by the following relationship in Hertz: $^1J_{C,H} = 5.7(\%s) - 18.4$, based on INDO-MO calculations of hybridization parameters, where *%s* denotes the percentage of *s*-character in the carbon hybrid orbital involved in the C—H bond. Various aspects of one-bond coupling constants have been discussed in an excellent review of the subject.[1] Molecular-orbital calculations, in general, reproduce experimental values well and are capable of predicting the effect of substituents.[1,10,85]

In the carbohydrate field, an approximately 10-Hz difference in $^1J_{C\text{-}1,H\text{-}1}$ coupling constants between the α and β anomers of glycosides was observed.[42,89-109] This promising observation encouraged further investigations, and considerable data have been accumulated during the past two decades. These observations have provided a quantitative basis for use of the $^1J_{C\text{-}1,H\text{-}1}$ constant in carbohydrates for determining the anomeric configuration or for calculating the percentage of $^1C_4$ conformation present in solution for a particular pyranose ring.

Some of the extensive experimental data on the one-bond carbon–proton coupling constants in several pyranose derivatives, as well as oligo- and polysaccharides, are summarized in Tables I–V. Several generalizations may be made from inspection of these data. The anomer that has an equatorially disposed hydrogen at C-1 has the larger coupling constant, and the $^1J_{C\text{-}1,H\text{-}1}$ value in such pyranosides is in general ~170 Hz, whereas those having axially oriented hydrogen at C-1 show $^1J_{C\text{-}1,H\text{-}1}$ couplings of ~160 Hz. The $^1J_{C\text{-}1,H\text{-}1}$ values are approximately 20 Hz larger than $^1J_{C,H}$ values involving carbon atoms of the aglycon. The difference of ~10 Hz between the equatorial and axial C-1—H-1 bonds is maintained for oligo- and polysaccharides.[100,110-114] This difference is influenced by the replacement of O-1 by other elements, and it has been shown that substituents on nonanomeric carbon atoms may alter the $^1J_{C\text{-}1,H\text{-}1}$ values to such an extent that the difference may even become negligible.[24] Solvent effects on $^1J_{C\text{-}1,H\text{-}1}$ values have also been mentioned.[5,94]

The factors that determine the magnitude of $^1J_{C\text{-}1,H\text{-}1}$ couplings have been the subject of discussion,[5,18,115-119] and various rationalizations have been offered for their origin. The relationship between *s* character and the magnitude of $^1J_{C,H}$ is supported by calculations on the model compound 2-chlorotetrahydropyran[115] in its two possible chair conformations; these calculations predicted that the equatorial C—H bond has greater *s* character than the axial one. This difference was

TABLE I
$^1J_{C,H}$ Values of the Anomeric C,H Bond in Monosaccharide Derivatives

Compound	Solvent	Anomeric C—H bond		Reference
		Axial	Equatorial	
Aldoses				
D-Arabinopyranose		160	168	93
D-Galactopyranose		160	170	19
			168.8	39
	Water	159.5	169.5	89
D-Glucopyranose		160	169	42
		160	168	38
		162	169.5	37
			169	41
			169.8	39
	Water	160	169.5	89
		161	169.2	90
			169.9	45
		161.1		91,92
		161.2		39
D-Lyxopyranose			167	93
D-Mannopyranose	Water	160	170	89
		160.7	170.4	39,93
D-Xylopyranose	Water	160	170	89
		160.5	170	93
Glycosides				
Methyl D-arabinopyranoside	Water		170	89
		160	169	93
	Acetone		170	93
Methyl 3,4-dideoxy-α-D-*erythro*-hexopyranoside	Dimethyl sulfoxide		165	94
	Water		168.5	94
	Chloroform		167.5	94
Methyl D-galactopyranoside		160	170	89
	Water	160	170	89
Methyl D-glucopyranoside	Dimethyl sulfoxide	156	167	94
	Water	160	170	94
	Water	159	170	89
Methyl D-lyxopyranoside	Water		169	89,93
Methyl D-mannopyranoside	Water		170	89
			170	19
Methyl D-xylopyranoside	Water	158		89
		159	170	89
Other Derivatives				
2-*O*-Methyl-α-D-glucopyranose			169	19
2-*O*-Methyl-β-D-mannopyranose		160		19

TABLE I—(*Continued*)

Compound	Solvent	Anomeric C—H bond		Reference
		Axial	Equatorial	
Methyl D-xylopyranoside	Water	158	170	89
phenylboronate	Dimethyl sulfoxide	159	171	93
Isopropyl 6-deoxy-L-mannoside	Water	154	166	93
Methyl 6-deoxy-L-mannoside	Water	158	170	89
Propyl 6-deoxy-L-mannoside	Water	152	166	93
Methyl 3-*O*-methyl-2,4,6-tri-*O*-acetyl-β-D-mannopyranoside	Chloroform	158.5		89

TABLE II

$^1J_{C,H}$ Values of the Anomeric C,H Bond in Carbohydrate Derivatives

Compound	Solvent	Anomeric C—H bond		Reference
		Axial	Equatorial	
2-Acetamido-2-deoxy-D-glucopyranose	Water	160	172.8	96
2-Acetamido-1,3,4,6-tetra-*O*-acetyl-2-deoxy-α-D-glucopyranose	Chloroform		177	19
2-Amino-2-deoxy-D-glucopyranose	Water	163	171	19
2-Amino-2-deoxy-D-glucopyranose · DCl	Water	161	170	95
N-*p*-Nitrophenyl-β-D-glucopyranosylamine tetraacetate	Chloroform	160		19
N-Phenyl-β-D-glucopyranosylamine tetraacetate	Chloroform	155	165	19
Tetra-*O*-acetyl-D-glucopyranosyl bromide	Chloroform		185	19
Tetra-*O*-acetyl-D-glucopyranosyl chloride	Chloroform	172	184.5	89
		171	184	19
Tetra-*O*-acetyl-α-D-glucopyranosyl fluoride	Chloroform	177.5	186	89
		178	186	19
β-D-Glucopyranosyl azide tetraacetate	Chloroform	160		19
Tetra-*O*-acetyl-β-D-glucopyranosylpyridinium bromide	Chloroform	163		19
D-Glucopyranuronic acid, sodium salt	Water	161.6	170.4	96
Ethyl 1-thio-D-glucopyranoside	Water	154	163	97
tetraacetate		155	169	97
		153		19
Methyl tetra-*O*-acetyl-1-thio-β-D-glucopyranoside	Chloroform	156		19
Methyl 5-thio-D-galactopyranoside		159	160	97
tetraacetate	Chloroform	157	160	98
Methyl 5-thio-D-glucopyranoside	Water		160	97
tetraacetate	Chloroform	153	161	97

TABLE III
$^1J_{C,H}$ Values of the Anomeric C,H Bond in Oligo- and Polysaccharide Derivatives

Compound	Solvent	Anomeric C—H bond		Reference
		Axial	Equatorial	
Maltose C-1 (OH)	Water	160	172	89
		162.5	171.5	37
C-1 (glycosidic)	Water		172	89
			172.5	37
Raffinose (Glc)	Water		170	89
(Gal)	Water		169	89
Sucrose (Glc)	Water		168.5	89
	Water		169.0	37
α,α-Trehalose	Water		172.5	5
			171.5	37
Cellobiose octaacetate	Chloroform	160	175	87
β-Gentiobiose octaacetate		162		41
α-Maltose 2,3,6,2′,3′,4′,6′-heptaacetate			174(C-1)	37
			174(C-1′)	37
β-Maltose octaacetate			174	37
Sucrose octaacetate			175	37
Methyl β-cellobioside	Water	162.1		45
Methyl β-maltoside	Water		173	37
Methyl β-cellobioside heptaacetate	Chloroform	161.8		45
Methyl β-maltoside heptaacetate			175	37
Phenyl β-maltoside heptaacetate			174	37
1,6-Anhydro-β-maltose	Water		168	37
1,6-Anhydro-β-maltose hexaacetate	Chloroform		171	37
2,3-Di-*O*-acetyl-1,6-anhydro-4-*O*-(2,3,4,6-tetra-*O*-acetyl-α-D-glucopyranosyl)-β-D-glucopyranose	Chloroform		179	5
Cyclomaltohexaose	Water		169.6	5
			168.5	37
			169.1	45
Cyclomaltoheptaose	Water		169.3	5
Cyclomaltooctaose	Water		169.4	45
Cyclomaltohexaose peracetate	Chloroform		171.8	37
Amylose triacetate			176	101
Cellulose triacetate		163		101
2,3,6-Tri-*O*-methylamylose			171	100
2,3,6-Tri-*O*-methylcellulose		151		100
2,3,4-Tri-*O*-methyldextran			168.5	100
2,4,6-Tri-*O*-methyllaminaran		163		100
2,4,6-Tri-*O*-methyllichenan		160		100
2,3,6-Tri-*O*-methylmannan		152.5		100
2,3,4-Tri-*O*-methylpustulan		160		100

TABLE III—(*Continued*)

Compound	Solvent	Anomeric C—H bond		Reference
		Axial	Equatorial	
2,3-Di-*O*-methylxylan		160		100
Permethylated glycogen			171.5	100
Chondroitin 6-sulfate residues	Water	161		96
		162		96
Chondroitin 4-sulfate residues		161		96
		160		96
Dermatan sulfate residues		162	168	96
Heparin residues			170	96
			172	96

TABLE IV

$^1J_{C,H}$ Values of the Anomeric and Aglycon C,H Bonds in Rigid Carbohydrate Derivatives

Compound	Solvent	Anomeric C—H bond	Aglycon C—H bond	Reference
1,6-Anhydro-β-D-allopyranose		187		102
1,6-Anhydro-β-D-altropyranose	Dimethyl sulfoxide	173		94,102
	Water	175		102,103
1,6-Anhydro-β-D-galactopyranose		175		102
1,6-Anhydro-β-D-glucopyranose		171		102
	1,4-Dioxane	173.2	156.5(C-5)	5
	Pyridine	172.4	155.75(C-5)	5
	Methanol	173.8	156.7(C-5)	5
	Dimethyl sulfoxide	174.1	156.7(C-5)	5
	Water	175.8	158.5(C-5)	5
	Water		152(C-6)	5
	Water		154(C-6)	5
2,3,4-Tri-*O*-acetyl-1,6-anhydro-β-D-glucopyranose	Chloroform	179		5
1,6-Anhydro-β-D-gulopyranose	Water	175		102
1,6-Anhydro-β-D-idopyranose		176		102
1,6-Anhydro-β-D-mannopyranose		175		102
4-*O*-Benzyl-1,6:2,3-dianhydro-β-D-mannopyranose	Chloroform	173.7		5
1,6-Anhydro-β-D-talopyranose	Water	174		102

TABLE V
$^1J_{C,H}$ Values of the Anomeric C,H Bond in Acetylated Monosaccharide Derivatives

Compound	Solvent	Anomeric C—H bond		Reference
		Axial	Equatorial	
D-Arabinopyranose tetraacetate	Chloroform	168	176	93
Methyl D-arabinopyranoside triacetate		159	171	93
D-Galactopyranose pentaacetate	Chloroform	161	171	19
Methyl 2,3-di-*O*-acetyl-4,6-*O*-benzylidene-α-D-galactopyranoside			172	19
Methyl D-galactopyranoside tetraacetate		161	172	89,93,103
D-Glucopyranose pentaacetate	Chloroform	161	177.5	37
		165	177	89
Methyl D-glucopyranoside tetraacetate	Water	162	173	89
	Dimethyl sulfoxide		172	19,94
	Chloroform		172	19,94
Methyl 2,3,4,6-tetra-*O*-benzyl-α-D-glucopyranoside	Chloroform		173	19
1,3,4,6-Tetra-*O*-acetyl-2-*O*-methyl-α-D-glucopyranose	Chloroform	165	175	89
Methyl 2,3-di-*O*-acetyl-4,6-*O*-benzylidene-α-D-glucopyranoside	Chloroform	162	171	19
Phenyl β-D-glucopyranoside tetraacetate		163		19
Tetra-*O*-acetyl-β-D-glucopyranosylpyridinium bromide	Chloroform	163		19
Penta-*O*-acetyl-α-D-mannopyranose	Chloroform		175	89
			176	19
Methyl α-D-mannopyranoside tetraacetate	Chloroform		171	19,89,93
Methyl 2,4,6-tri-*O*-acetyl-3-*O*-methyl-β-D-mannopyranoside	Chloroform	158.5		89
1,3,4,6-Tetra-*O*-acetyl-2-*O*-methyl-α-D-mannopyranose	Chloroform	163	176	19,89
D-Lyxopyranose tetraacetate	Chloroform	169.5	175	93
Methyl α-D-lyxopyranoside triacetate	Chloroform		170.5	93
D-Xylopyranose tetraacetate	Chloroform	166	177	93
Methyl D-xylopyranoside triacetate	Chloroform	161	171	93

considered to be a consequence of interactions of a *p*-type lone pair on the ring oxygen atom with adjacent σ bonds. In another interpretation,[18,116] the difference was discussed in terms of the proximity of the carbon–hydrogen bond relative to the lone-pair orbitals on the ring oxygen atom.

It has been suggested[108,116,119] that the difference may be due to small variations in bond lengths and angles. Based on analysis of the *ab initio*-calculated C—H bond lengths in acyclic model compounds and the experimental $^1J_{C,H}$ values, the

following correlation was proposed[119]:

$$^1J_{C,H} = -3432 + 182.2Q_CQ_H + 3889/r_{CH}, \quad (31)$$

where Q_C and Q_H are the total atomic charges on carbon and hydrogen atoms from Mulliken population analysis, and r_{CH} is the C—H bond length. The standard errors of the parameters of Eq. *31* are ~10%.

The anomeric center in carbohydrates is a very specific site as there are two electronegative atoms having lone-pair electrons linked to the anomeric carbon. The electron distribution at the anomeric center is strongly influenced by interactions between lone-pair electrons, and the consequences of these interactions are known as the anomeric and *exo*-anomeric effects.[120] The two lone pairs on oxygen are delocalized by through-bond and by through-space mechanisms. The electron transfer associated with these interactions depends on the conformation about the ring C—O bond and explains the relationship of bond lengths and bond angles to dihedral angles and hence the differences in bond lengths and bond angles observed between anomers. The difference in *s* character of the C—H bond and the energy of the highest-occupied molecular orbitals (HOMO) are both considered to be consequences of the conformational dependence of lone-pair delocalization into the antibonding orbital of the C—H and C—O bonds. As these quantities influence the magnitude of contact contribution to the coupling constant (Eq. *28*), it has been suggested[5,118] that the observed variation in $^1J_{C,H}$ is a manifestation of the anomeric and *exo*-anomeric effects.

a. Conformational Dependence of $^1J_{C,H}$.—Glycosidic-bond conformations are important for determination of the overall three-dimensional structure of oligo- and polysaccharides. Of special interest, therefore, is the question of whether or not one-bond carbon–proton coupling constants involving anomeric and aglycon carbons can be related to dihedral angles and thus provide a means of deducing values for the dihedral angles Φ and Ψ about the glycosidic linkages.

The potential of the $^1J_{C,H}$ coupling for the investigation of nucleosides, nucleotides,[121] and carbohydrates[118] has been reconsidered. Attention has been focused on the angular dependence of the $^1J_{C,H}$ value (which involves the anomeric or the aglycon carbon) on the glycosidic torsional angles Φ^H and Ψ^H. Theoretical calculations using the FPT INDO-MO method with model compounds related to glycosides,[118] and in three (1→4)-linked disaccharides,[22] have shown that the $^1J_{C\text{-}1,H\text{-}1}$ and $^1J_{C\text{-}X',H\text{-}X'}$ values vary characteristically with the torsional angles about glycosidic C—O bonds. The authors proposed a relationship in the following analytical form:

$$^1J_{C,H} = A\cos 2\phi + B\cos\phi + C\sin 2\phi + D\sin\phi + E \quad (32)$$

with different constants *A* through *E* for the α and β anomers. These investigations[22,118] also showed that, while the angular dependence of $^1J_{C,H}$ was described

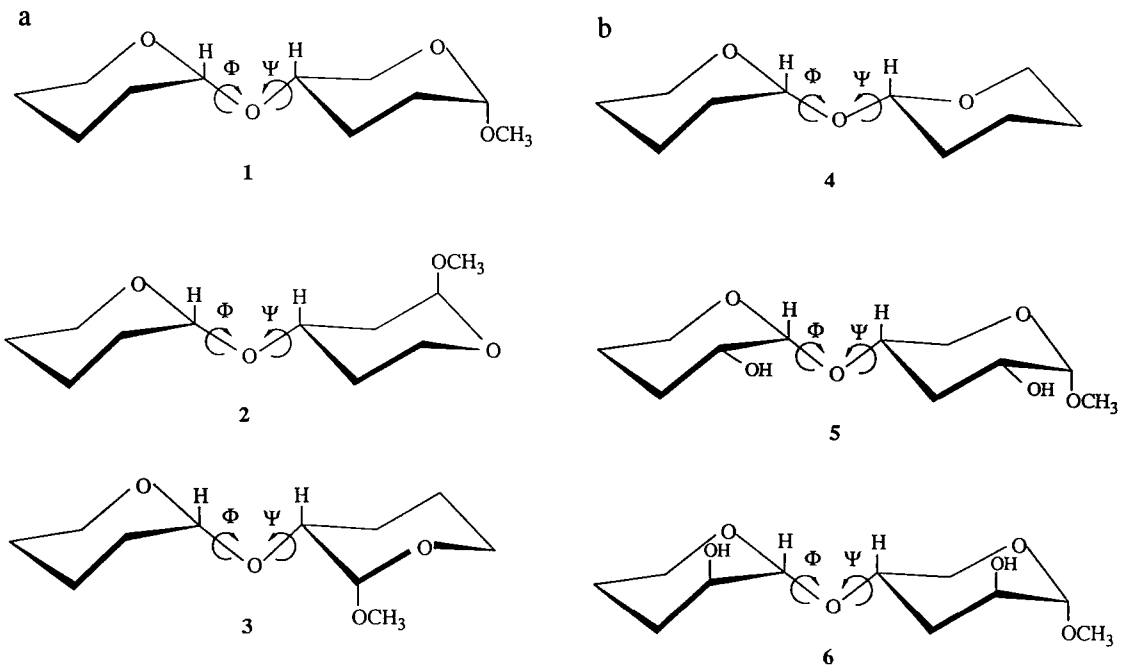

FIG. 3.—Schematic representation of the six model systems used for calculation of the angular dependences of $^1J_{C,H}$ values.

adequately, the absolute values were underestimated. A main difference was associated with the constant E, and the source of discrepancy is most likely the result of the integral parametrization and/or neglect of the effects of electron correlation in the semiempirical FPT INDO-MO description of the $^1J_{C,H}$. Therefore, a shift of all of the values by a constant amount, based on experimental data for compounds having well-defined conformations in solution, was suggested[118] as a plausible procedure. It has been shown[22,118] that the proposed angular dependences correctly reproduce experimental values for model compounds and for methyl β-xylobioside.

To clarify this behavior further, calculations were made on the angular dependence of the $^1J_{C,H}$ values for six model systems (Fig. 3) in α and β configurations.[5,6] The first four models, namely 2-methoxy-5-(tetrahydropyran-2-yloxy)tetrahydropyran (**1**), 2-methoxy-4-(tetrahydropyran-2-yloxy)tetrahydropyran (**2**), 2-methoxy-3-(tetrahydropyran-2-yloxy)tetrahydropyran (**3**), and 2-methoxy-2-(tetrahydropyran-2-yloxy)tetrahydropyran (**4**), represent α (**a**) and β disaccharides (**b**) linked by (1→4)-, (1→3)-, (1→2)-, and (1→1)-glycosidic linkages, respectively. The last two model compounds, designated as **5** and **6**, are 3-hydroxy derivatives of **1** and are thus related to (1→4)-linked disaccharides, stereochemically related to the *gluco* and *manno* configurations at C-2.

A complete description of the $^1J_{C,H}$ couplings in these molecules as a function of

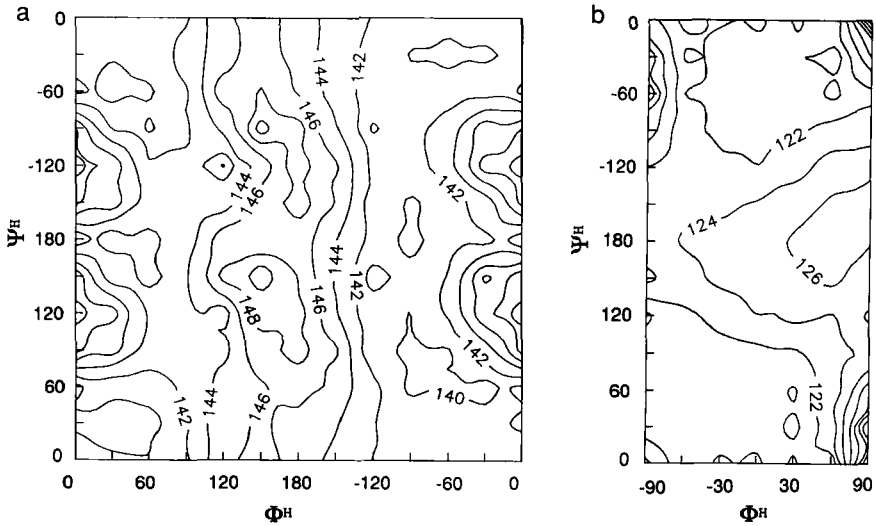

FIG. 4.—Contours of the calculated FPT-INDO results[5] for the $^nJ_{C\text{-}1,H\text{-}1}$ (a) and the $^1J_{C\text{-}4',H\text{-}4'}$ (b) values (Hz) for the α-(1→4)-linked oligosaccharide model (**1a**) as a function of Φ^H and Ψ^H.

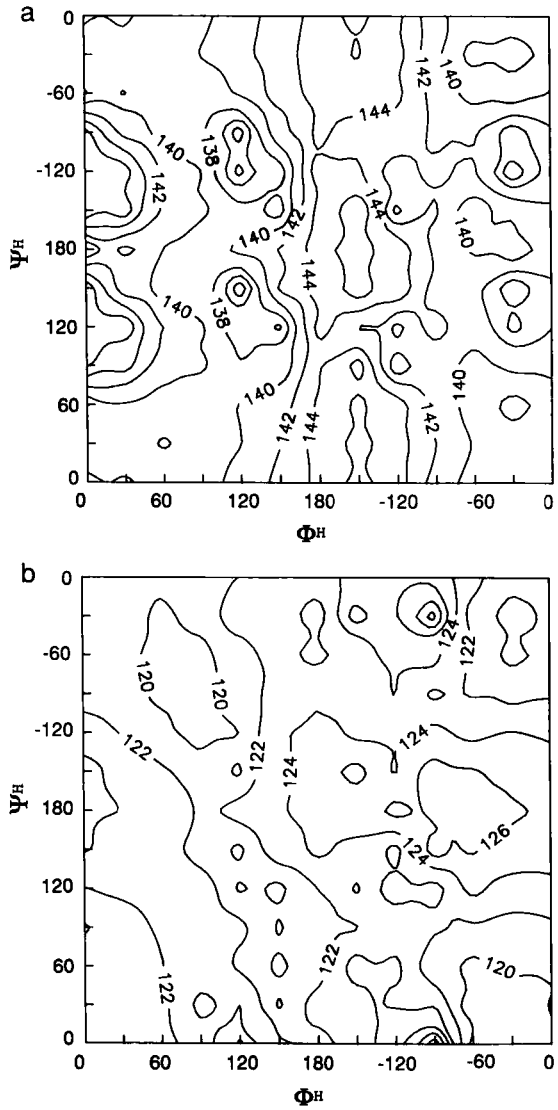

FIG. 5.—Contours of the calculated FPT-INDO results[6] for the $^1J_{C\text{-}1,H\text{-}1}$ (a) and the $^1J_{C\text{-}4',H\text{-}4'}$ (b) values (Hz) for the β-(1→4)-linked oligosaccharide model (**1b**) as a function of Φ^H and Ψ^H.

two torsion angles characterizing rotation about the glycosidic C—O bonds is given by a two-dimensional map. As examples, the FPT INDO-MO-calculated[5,6] one-bond carbon–proton coupling constant maps $^1J_{C,H}$ (Φ, Ψ) for **1a** and **1b** are

shown in Figs. 4 and 5. The calculated maps for compounds **2–6** are similar to those plotted in Figs. 4 and 5. Analysis of the results revealed that, in some conformations, steric interactions between the C—H bond and atoms on the adjacent pyranose ring strongly influence the calculated values. The $^1J_{C,H}$ values in these conformations do not correspond to any physical situation, as the energies are in excess of those required to distort the molecule. Therefore, the $^1J_{C,H}$ values calculated for such conformers are either very large or small, and influence the shape of $^1J_{C,H}$ contours of the maps. These findings were supported by investigations of the effect of the magnitude of the glycosidic-bond angle on the $^1J_{C,H}$ values. The investigations clearly showed that an increase of glycosidic-bond angle decreases the angular dependence of $^1J_{C,H}$ values on the orientation around the adjacent C—O bond.

As may be seen in the maps, the calculated values are in the range of 130–150 Hz for $^1J_{C\text{-}1,H\text{-}1}$, whereas for the $^1J_{C\text{-}x,H\text{-}x}$ values are ~20 Hz lower. Different angular dependences of $^1J_{C,H}$ were rationalized on the basis of delocalization interactions of lone pairs on oxygen atoms.[5] For a given oligosaccharide, the orientation of lone pairs on the ring oxygen with respect to the C-1—H-1 bond remains fixed. In contrast, the orientation of lone pairs on the glycosidic oxygen atom (O-1) with respect to the C-1—H-1 bond varies with rotation about C-1—O-1 bond. This orientation was suggested[5] to be the main factor that determines the conformational dependence of $^1J_{C,H}$.

The magnitude of the delocalization interactions depends on the mutual orientation of pertinent orbitals and their energies. As C-1 is linked to the ring oxygen atom (O-5), the energy of the antibonding orbital of the C-1—H-1 bond is lower than that of the aglycon C—H bond. Therefore, the delocalization of a lone pair into the aglycon region is significantly lower than at the anomeric center. Moreover, the influence of these interactions on the energy of lone pairs of O-1 is small. There are two qualitative consequences of these interactions. First, since the delocalization interactions into the C-1—H-1 bond are influenced only marginally by variation of Ψ, the $^1J_{C\text{-}1,H\text{-}1}$ values depend only slightly on Ψ. Second, since the magnitude of the delocalization interactions into the aglycon C—H bond is lower than into the C-1—H-1 bond, the angular dependence of $^1J_{C\text{-}x,H\text{-}x}$ should be smaller in comparison to that of $^1J_{C\text{-}1,H\text{-}1}$.

b. Angular Dependence of $^1J_{C,H}$.—In order to facilitate the application of $^1J_{C,H}$ values in conformational analysis of carbohydrates, it is useful to express the angular dependence on the H—C—O—C torsion angle (Φ^H or Ψ^H) in the form of Eq. *32*. Additional sine terms, in comparison with a Karplus-type equation, are necessary in order to account for the lack of symmetry about $\Phi = 180°$. Calculated $^1J_{C,H}$ values were used to derive the constants *A* through *E* in Eq. *32*. The resulting curves, based on data for **1**, are shown in Figs. 6 and 7. The same procedure was

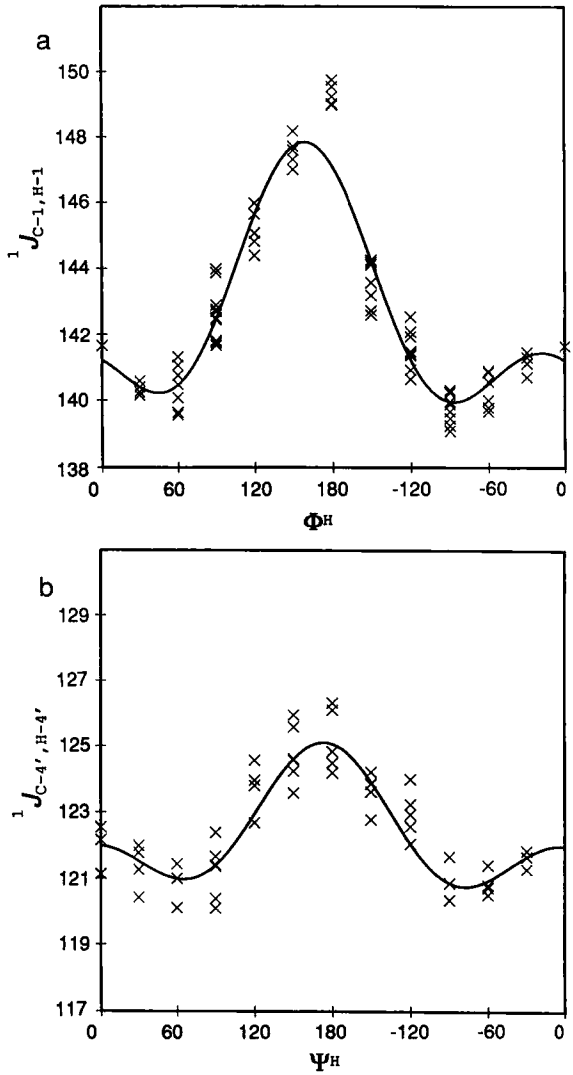

FIG. 6.—The FPT-INDO calculated[5] $^1J_{C\text{-}1,H\text{-}1}$ values (x) as a function of Φ^H (a) and the $^1J_{C\text{-}4',H\text{-}4'}$ (x) values as a function of Ψ^H (b) for the α-(1→4)-linked oligosaccharide model (**1a**). The solid curves show the best approximation to the indicated points.

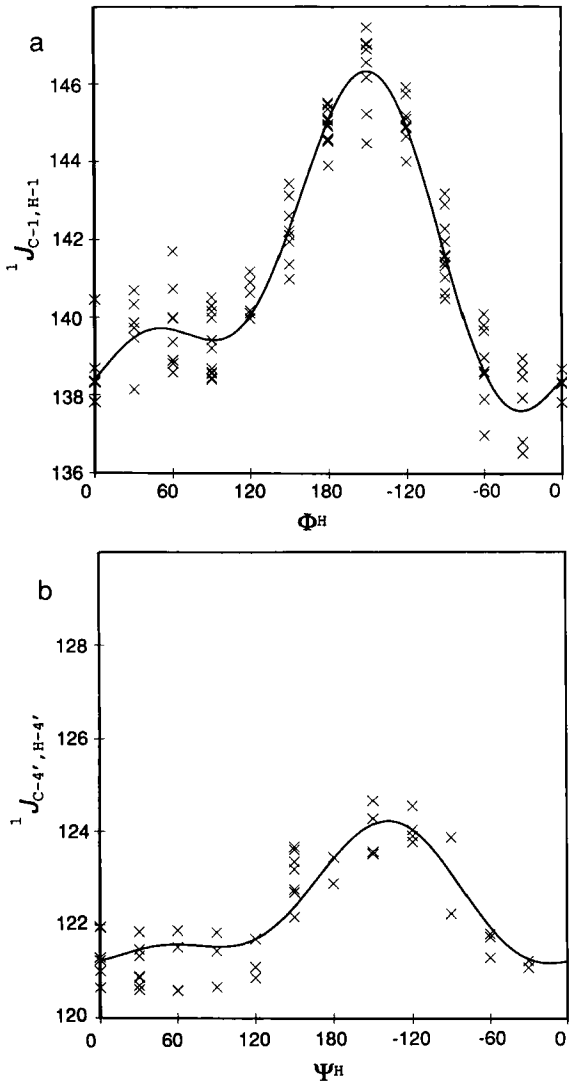

FIG. 7.—The FPT-INDO-calculated[6] $^1J_{C\text{-}1,H\text{-}1}$ values (x) as a function of Φ^H (a) and the $^1J_{C\text{-}4',H\text{-}4'}$ (x) values as a function of Ψ^H (b) for the β-(1→4)-linked oligosaccharide model (**1b**). The solid curves show the best approximation to the indicated points.

used for all molecules **1–6**, and then the mean angular dependences of $^1J_{C,H}$ were expressed in the following form:

For the α linkage

$$^1J_{C\text{-}1,H\text{-}1} = 1.32 \cos 2\Phi^H - 3.38 \cos \Phi^H - 1.05 \sin 2\Phi^H + 1.27 \sin \Phi^H + 168.9 \quad (33)$$

$$^1J_{C\text{-}x,H\text{-}x} = 1.02 \cos 2\Psi^H - 1.81 \cos\Psi^H - 0.19 \sin 2\Psi^H + 0.41 \sin \Psi^H + 145.4. \quad (34)$$

For the β linkage

$$^1J_{C\text{-}1,H\text{-}1} = 0.57 \cos \Phi^H - 3.46 \cos \Phi^H + 1.63 \sin 2\Phi^H - 1.53 \sin \Phi^H + 161.5 \quad (35)$$

$$^1J_{C\text{-}x,H\text{-}x} = 0.01 \cos 2\Psi^H - 1.08 \cos \Psi^H + 0.51 \sin 2\Psi^H - 1.01 \sin \Psi^H + 145.1. \quad (36)$$

The values of the constant E were adjusted by using the experimental $^1J_{C,H}$ values for compounds having well-defined torsion angles for the C—O—C—H segment of atoms in solution (see Table IV).

c. Solvent Effects.—In general, spin–spin coupling constants are dependent on the solvent. An investigation of the solvent effect on $^1J_{C,H}$ values was performed for 1,6-anhydro-β-D-glucopyranose. The results showed that the observed values fall on a straight line and the resulting dependences[5] are

$$^1J_{C\text{-}1,H\text{-}1} = 0.0390\epsilon + {}^1J_{C\text{-}1,H\text{-}1}(\text{isolated molecule}) \quad (37)$$

$$^1J_{C\text{-}1,H\text{-}1} = 0.0294\epsilon + {}^1J_{C\text{-}x,H\text{-}x}(\text{isolated molecule}). \quad (38)$$

The magnitudes of the constant in Eqs. *37* and *38* indicate that the solvent-induced changes are larger for the C-1—H-1 bond than for the aglycon C—H bond. Thus, the $^1J_{C,H}$ value calculated from the foregoing equations for an isolated molecule ($\epsilon = 1$) and for aqueous solution ($\epsilon = 78.5$) is 3.02 Hz for the C-1—H-1 bond and 2.28 Hz for the aglycon C—H bond.

Combination of Eqs. *33–36* with Eqs. *37* and *38* gives the following final angular dependences, which incorporate the solvent effect:

For the α linkage

$$^1J_{C\text{-}1,H\text{-}1} = 1.32 \cos 2\Phi^H - 3.38 \cos \Phi^H - 1.05 \sin 2\Phi^H + 1.27 \sin \Phi^H + 168.9 + 0.0390\epsilon \quad (39)$$

$$^1J_{C\text{-}x,H\text{-}x} = 1.02 \cos 2\Psi^H - 1.81 \cos \Psi^H - 0.19 \sin \Psi^H + 0.41 \sin \Psi^H + 145.4 + 0.0294\epsilon. \quad (40)$$

For the β linkage

$$^1J_{C\text{-}1,H\text{-}1} = 0.57 \cos 2\Phi^H - 3.46 \cos \Phi^H + 1.63 \sin 2\Phi^H - 1.53 \sin \Phi^H + 161.5 + 0.0390\epsilon \quad (41)$$

$$^1J_{C\text{-}x,H\text{-}x} = 0.01 \cos 2\Psi^H - 1.08 \cos \Psi^H + 0.51 \sin 2\Psi^H - 1.01 \sin \Psi^H + 145.1 + 0.0294\epsilon. \quad (42)$$

d. Application to Oligosaccharides.—One of the major practical advantages offered by the observed angular dependences of $^1J_{C,H}$ values is the possibility of determining the glycosidic-bond torsional angle. However, as already discussed, experimental $^1J_{C,H}$(exp) values are nonlinear ensemble averages,[84] and therefore cannot be used alone as a satisfactory means of determining torsion angles. Perhaps a more effective approach is to calculate a reliable conformational-energy surface for a given solvent and then to calculate, using Eqs. *39–42*, the ensemble average $\langle ^1J_{C,H} \rangle$. Qualitative agreement between observed values and the calculated $\langle ^1J_{C,H} \rangle$ value may be interpreted as confirming the conformational equilibrium in solution. A promising approach is molecular-dynamics simulation which, if the force field used is correct and the trajectories are long enough, should produce an ensemble-averaged $\langle ^1J_{C,H} \rangle$ value in agreement with experimental data. Six examples wherein the first method was used concerned the conformational properties of isomaltose,[5] maltose,[5] methyl β-xylobioside,[6] neoagarobiose,[6] agarobiose,[6] and mannobiose.[6]

Although the ensemble averages of $\langle ^1J_{C,H} \rangle$ were calculated using only the most stable conformers, the agreement was satisfactory. Thus, for the α linkage, the calculated $\langle ^1J_{C\text{-}1,H\text{-}1} \rangle$ was 169.8 Hz with $\langle ^1J_{C\text{-}4',H\text{-}4'} \rangle$ 147.7 Hz for maltose and $\langle ^1J_{C\text{-}1,H\text{-}1} \rangle$ 169.8 Hz for isomaltose; these values compare well with the experimental values of 172.4, 147.7, and 170.3 Hz, respectively. For the β linkage, the results obtained for methyl β-xylobioside were $\langle ^1J_{C\text{-}1,H\text{-}1} \rangle$ 162.4 Hz and $\langle ^1J_{C\text{-}4',H\text{-}4'} \rangle$ 147.6 Hz while for mannobiose $\langle ^1J_{C\text{-}1,H\text{-}1} \rangle$ was 162.4 Hz and $\langle ^1J_{C\text{-}4',H\text{-}4'} \rangle$ 147.6 Hz. Again, these values agree well with the experimental values of 162.7, 147.5, 160.4, and 147.2 Hz.

2. Two-Bond Couplings

Two-bond (geminal) carbon–proton coupling constants are much smaller than one-bond couplings, and their signs can be negative or positive. These couplings show a strong dependence on substitution, hybridization, electronegativity, bond length, and bond angle.[1] In the carbohydrate field they have been studied extensively.[36,38,39,42,44,91,92,95] It was found[38,39,42,91,92] that $^2J_{C,H}$ values depend on the conformation about the bonds through which coupling occurs and on the dihedral angles subtended by substituents on the coupled atoms. In particular, the various observed $^2J_{C,H}$ couplings were characterized in terms of the relative orientations of the coupled proton and of the oxygen atom appended to the ^{13}C nucleus; thus an oxygen *anti* to the proton appears to make a positive contribution to the $^2J_{C,H}$ value

whereas a *gauche* oxygen gives a negative contribution. This is also true when the ^{13}C atom bears two oxygen atoms and a proton is attached to a neighboring carbon. In these cases (involving the anomeric carbon), the torsion angle between the resultant vector (C-1—O-1 and C-1—O-5 bonds) and the C—H bond was considered.[92] When the dihedral angle is small, the absolute value is large and the sign negative. As the angle increases, the coupling constant increases, then passes through zero, so its sign becomes positive.

The magnitudes and signs of two-bond coupling constants in the array O—^{13}C-A—C-B—^{1}H appear to be determined by the relative orientations of the O—^{13}C-A and C-B—^{1}H bonds, as shown with a variety of carbohydrate derivatives. When C-B bears one oxygen atom, the observed $^{2}J_{C,H}$ values range from -6 to 0 Hz, whereas a range of 0 to $+8$ Hz is found when C-B bears two oxygen atoms. In contrast, for arrays in which C-B bears one oxygen atom and C-A two, the $^{2}J_{C,H}$ values vary from -6 to $+6$ Hz.

Another approach[36] was based on the assumption that the two-bond couplings have values that are determined by the orientation of the oxygen atom directly connected to the coupling path. The authors of this approach have tried to rationalize their findings by relating them to a projection of the C—O bonds onto an axis *trans* to the^{12}C—H bond (if the C—O bonds is antiperiplanar with ^{12}C—H, the projection is equal to $+1$). A projection of $+2$ corresponds to the $^{2}J_{C,H}$ value of $+9.0$ Hz, a projection of $+0.5$ to -0.5 coresponds to a value around 0 Hz, and a projection of $+1.5$ corresponds to a coupling of $+5.5$ Hz.

Geminal couplings may also furnish useful information in stereochemical studies, owing to the different values measured for α and β derivatives.[38,44,95]

Configurational assignments in *N*-acetylneuraminic acid and analogues were performed[122] by determining the signs and the magnitudes of the couplings between the protons at C-3 and the quaternary anomeric carbon C-2. The C-2, H-3*ax* coupling in the α anomers (-8 Hz) was significantly more negative than that in the β anomers (-3 to -4 Hz). It was suggested, therefore, that determination of the $^{2}J_{C,H}$ values offers a good criterion for anomeric assignment in sialic acid ketosides. These authors[122] have also discussed their results in terms of the number and orientation of the oxygen substituents.

3. Three-Bond Couplings

Since the discovery[123] that the magnitude of the three-bond (vicinal) spin–spin coupling constant $^{3}J_{H,H}$ in ethane depends on the torsion angle between the coupling nuclei, numerous investigations have exploited an analytical form of this dependence. Because of the successful application of $^{3}J_{H,H}$ and the progress of modern Fourier-transform NMR spectrometers, which made possible the measurement of coupling constants from natural-abundance ^{13}C spectra, considerable experimental effort has been expended in establishing an analogous correlation for

carbon–proton couplings. A large number of calculated FPT INDO-MO results have been given for different model compounds,[118,124–128] and Karplus-type relations for the angular dependences of $^3J_{C,H}$ have been proposed. Unfortunately, a lack of accurate experimental data has thus far prevented the development of a generalized Karplus equation such as that used in the case of proton–proton couplings.[129,139]

In the field of carbohydrates, the most important couplings for structural interpretations are those through the glycosidic linkage, involving a heteroatom X (X = oxygen, nitrogen, sulfur, carbon, . . .). They are designed as $^3J_{C,X,C,H}$. In general, vicinal coupling constants depend on several factors (substitution, hybridization, electronegativity, and bond and angle changes).[1] In this respect, a Karplus-type relationship between the magnitude of $^3J_{C,H}$ and the dihedral angle Φ for each of the C—X—C—H arrays of bonded atoms should be derived. Most of the experimental $^3J_{C,H}$ values in molecules of reasonably rigid structures have been obtained with carbohydrates[38] and nucleosides.[131]

a. C—O—C—H Arrays of Bonded Atoms.—The relationship of $^3J_{C,H}$ to the glycosidic torsion angle between ^{13}C and ^1H was explored several years ago.[45,132] In mono- and oligosaccharide derivatives, eleven values of $^3J_{C,H}$ ranging from 2.0 to 6.2 Hz were observed[45] for estimated torsion angles varying from 10° to 180°. The generated $^3J_{C,H}$ values, plotted against torsion angles, demonstrated that the coupling constant is smallest when the torsion angle is ~90° ($^3J_{C,H}$ = 0 Hz) and greatest at 180° ($^3J_{C,H}$ = 6 Hz). Over the range of torsion angles from 0 to 180°, the $^3J_{C,H}$ value approximates a Karplus-type dependence, with $^3J_{C,H}$ = 5 Hz at 0°. At the same time, a relationship $^3J_{C,H} = 11 \cos^2\phi$ was suggested.[43]

Subsequently, an angular dependence of the $^3J_{C,H}$ *vs* ϕ torsion angle in the analytical form (Eq. *43*)

$$^3J_{C,H} = A \cos^2\phi + B \cos\phi + C \qquad (43)$$

was proposed almost simultaneously by two independent groups.[133,134]

Parameters *A*, *B*, and *C* were extracted from $^3J_{C,H}$ values measured for conformationally rigid carbohydrate derivatives (Table VI) whose X-ray structures had been determined. In addition, the glycosidic linkages of cyclomaltohexaose and cyclomaltoheptaose (α- and β-cyclodextrins) were used[133] as the best available source of data for torsion angles in the range 0–20° and several C—O—C—H paths in 1,6-anhydro-β-D-glucopyranose were used[134] for angles in the range 100–170°. Moreover, all the measured carbon atoms were sp^3-hybridized, and the structures meet the condition of a constant sum of the substituent electronegativities. The resulting relationship

$$^3J_{C,H} = 5.7 \cos^2\phi - 0.6 \cos\phi + 0.5 \qquad (44)$$

is shown in Fig. 8 (curve 2). The angular dependence defined by Eq. *44* differs from

TABLE VI
Vicinal Carbon–Proton Coupling Constants Measured Using Labeled Compounds or the Gated Technique for Natural-Abundance Compounds

Compound	$^3J_{C,H}$ Anomeric	$^3J_{C,H}$ Aglycon	Reference
Methyl α-D-glucopyranoside	3.8		43
tetraacetate	4.5		44
Methyl β-D-glucopyranoside	4.4		43
tetraacetate	4.6		44
Methyl α-D-mannopyranoside	3.8		43
Methyl β-L-glucopyranoside	4.5		43
Methyl β-L-mannopyranoside	4.3		43
α-Cellobiose octaacetate	5.5		44
Methyl β-cellobioside	4.3	4.2	45
heptaacetate	5.2	4.2	45
β-Gentiobiose octaacetate	4 (H-6*R*)	3.8	41
	2 (H-6*S*)	3.8	41
β-Laminarabiose octaacetate	5.5		44
Maltose	<3.5	<3.5	37
α-Maltose 2,3,6,2′,3′,4′,6′-heptaacetate	4.0		37
α-Maltose octaacetate	3.8		44
β-Maltose octaacetate	3.5	2.0	37
Methyl β-maltoside	2.5	3.0	37
Methyl β-maltoside	4.5 (D_2O)	4.0	46
	5.1 (Me_2SO)	4.1	46
	5.3 (1,4-dioxane)	4.3	46
heptaacetate	4.0	2.0	37
Phenyl β-maltoside		2.5	37
heptaacetate	4.0		37
1,6-Anhydro-β-maltose	4.5		37
hexaacetate	4.0		37
Cyclomaltohexaose	4.8	5.2	45
	3.5	4–5	37
peracetate	<4.5	<4.0	37
β-Nigerose octaacetate	3.7		44
α,α-Trehalose	2.5		37

the previously proposed curve[45] most significantly near 180°, where the $^3J_{C,H}$ value is ~1 Hz larger, namely 6.8 Hz. The values of the *A*, *B*, *C* constants in Eq. *44* are in remarkably good agreement with the theoretical values of 6.3, 1.2, and 0.6 Hz calculated for the model compound 2-methoxytetrahydropyran,[118,135] considering substituent and hybridization variations.

Reports that have improved the data base (see Tables VI–XI), or utilized a new NMR sequence for accurate measurements of vicinal coupling constants for mono- and oligosaccharides, have been published during the past decade.[60,62,136,137,139,143–

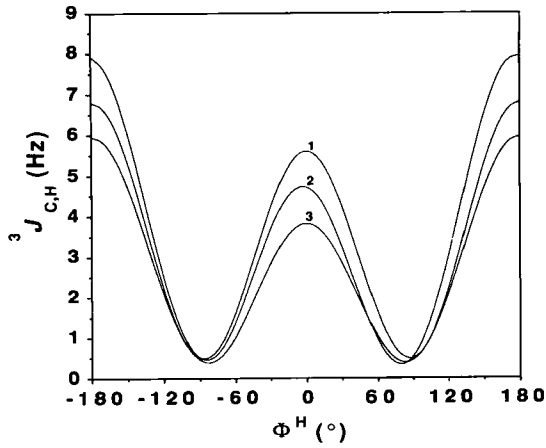

FIG. 8.—Relationship between $^3J_{C,H}$ and the C—X—C—H dihedral angle Φ^H for (1) X = O, (2) X = C, and (3) X = S.

[148] Several applications of these couplings to the conformational analysis of various mono- and oligosaccharides have also been described.[138,140,145,149,150] These applications incorporate both theoretical and experimental approaches toward determination of the conformation of saccharides in solution, a question still controversial because of the time-averaged character of the NMR data obtained (NOE and couplings) and the occurrence of conformational equilibria.[3] Variations of $^3J_{C,H}$ values for maltose according to the solvent used have been observed,[46] and

TABLE VII
Vicinal Proton–Carbon Coupling Constants for Glycosides

Compound	Coupling	Value	Reference
Methyl α-D-galactopyranoside tetraacetate	C-1, H(OMe)	4.7	137
	C(OMe), H-1	3.9	137
Methyl β-D-galactopyranoside tetraacetate	C-5, H-1	1.8	133
	C-1, H(OMe)	4.8	137
	C(OMe), H-1	4.7	137
Methyl α-D-glucopyranoside tetraacetate	C-1, H(OMe)	4.7	136
	C(OMe), H-1	3.9	137
Methyl β-D-glucopyranoside tetraacetate	C-5, H-1	2.0	133
	C-1, H(OMe)	4.8	136
	C(OMe), H-1	4.5	137
Methyl α-D-mannopyranoside tetraacetate	C-1, H(OMe)	4.7	137
	C(OMe), H-1	4.1	137
Methyl β-D-mannopyranoside tetraacetate	C-1, H(OMe)	4.8	137
	C(OMe), H-1	4.4	137

TABLE VIII

Vicinal Carbon–Proton Coupling Constants for Different Dihedral Angles of C—O—C—H Arrays of Bonded Atoms, Measured from Spectra of Rigid Compounds in Natural Abundance

Compound	Array	Angle (degrees)	$^3J_{C,H}$ (Hz)	Reference
1,4,5-Tri-*O*-acetyl-2,3-*O*-isopropylidene-β-D-fructopyranose	C-7, H-3	86	0	134
1,6-Anhydro-β-D-galactopyranose	C-1, H-6*endo*	120	3.7	36
	C-1, H-5	170	6.1	36
	C-5, H-1	180	5.0	36
	C-6, H-1	160	5.2	36
2-*O*-Acetyl-1,6-anhydro-β-D-galactopyranose				
exo-3,4-benzylidene acetal	C-7, H-4	119	2.3	134
	C-6, H-1	136	5.1	134
	C-3, H-7	127	5.2	134
	C-7, H-4	119	2.1	138
	C-6, H-1	136	5.2	138
endo-3,4-benzylidene acetal	C-7, H-3	279	0	134,138
	C-7, H-4	131	3.2	134,138
	C-6, H-1	137	5.2	134
	C-4, H-7	216	4.1	134
	C-6, H-1	137	5.3	138
1,6-Anhydro-β-D-glucopyranose	C-6, H-1	141	5.1	134
	C-5, H-1	199	5.1	134
	C-1, H-5	164	5.9	134
	C-5, H-1	163	5.2	133
	C-6, H-1	144	5.2	133
	C-1, H-5	161	6.0	133
	C-1, H-6*endo*	118	3.5	133
	C-1, H-6*exo*	107	0.2	133
1,6:2,3-Dianhydro-β-D-gulopyranose	C-1, H-6*endo*	109	1.4	134
	C-1, H-6*exo*	230	2.2	134
	C-1, H-5	154	5.6	134
2-*O*-Acetyl-1,6-anhydro-β-D-gulopyranose				
2,3-(*S*)-benzylidene acetal	C-7, H-3		3.2	138
	C-6, H-1		5.6	138
2,3-(*R*)-benzylidene acetal	C-7, H-3		6.0	138
	C-6, H-1		5.6	138
2-*O*-Acetyl-1,6-anhydro-β-D-mannopyranose				
2,3-(*S*)-benzylidene acetal	C-7, H-2	−117	2.8	138
	C-6, H-1	145	6.0	138
2,3-(*R*)-benzylidene acetal	C-7, H-2		5.7	138
	C-6, H-1		5.8	138
Tri-*O*-acetyl-1,6-anhydro-β-D-allopyranose	C-1, H-6*exo*		0.8	139
	C-1, H-6*endo*		3.7	139
	C-6, H-1		5.3	139

TABLE VIII—(*Continued*)

Compound	Array	Angle (degrees)	$^3J_{C,H}$ (Hz)	Reference
altropyranose	C-1, H-6*exo*		1.1	139
	C-1, H-6*endo*		4.0	139
	C-6, H-1		5.8	139
galactopyranose	C-1, H-6*exo*		0.8	139
	C-1, H-6*endo*			139
	C-6, H-1		5.3	139
glucopyranose	C-1, H-6*exo*		0	139
	C-1, H-6*endo*		3.9	139
	C-6, H-1		5.3	139
gulopyranose	C-1, H-6*exo*		0.8	139
	C-1, H-6*endo*		3.9	139
	C-6, H-1		5.2	139
mannopyranose	C-1, H-6*exo*		1.2	139
	C-1, H-6*endo*		3.7	139
	C-6, H-1		5.8	139
talopyranose	C-1, H-6*exo*		1.4	139
	C-1, H-6*endo*		3.8	139
	C-6, H-1		5.9	139
Cyclomaltohexaose	C-5, H-1	177	7.5	133
	C-4′, H-1	15	4.4	133
	C-1, H-4′	10	4.8	45
	C-4′, H-1	10	5.2	45
	C-5, H-1		6.2	45
Cyclomaltoheptaose	C-5, H-1	178	7.0	133
	C-4′, H-1	7	5.7	133
	C-1, H-4′	11	5.6	133

it has been found that $^3J_{C,H}$ values for methyl β-xylobioside (Table X) vary with both temperature and solvent.[145] These variations are shown to be compatible with theoretical calculations that explicitly include the solvent effect on the potential-energy surface. These observations provide significant experimental evidence for the flexible character of these oligosaccharides.

b. C—S—C—H Arrays of Bonded Atoms.—A Karplus-type equation for vicinal carbon–proton coupling constants has been presented for the C—S—C—H pathway in 1-thioglycosides[151] (see Table XII). A derivation of the angular dependence was based on measurements of the $^3J_{C,H}$ values in eight thiocarbohydrate derivatives having well-defined C—S—C—H conformations in solution, which provides 17 couplings. Values of $^3J_{C,H}$ from 0.3 to 8.1 Hz were observed for a torsion angle from 30 to −60° and were accommodated in an

TABLE IX
Vicinal Carbon–Proton Coupling Constants for Di- and Trisaccharides

Compound	Coupling	Angle	Value (Hz)	Reference
Cellobiose	C-5, H-1	56	1.9	135
Lactose	C-1′, H-4		5.1	62
	C-4, H-1′		4.0	62
Maltose	C-5, H-1	178	7.1	135
Mannobiose	C-4α, H-1′		4.1	141
	C-4β, H-1′		4.4	141
Melezitose	C-2′, H-1		3.8	133
Raffinose	C-5, H-1(Glc)	180	6.8	133
	C-5, H-1(Gal)	177	6.5	133
	C-2′, H-1		3.8	133
Stachyose	C-2′, H-1		3.8	133
Sucrose	C-5, H-1(Glc)	174	6.6	133
	C-2f, H-1g		3.8	133
	C-2f, H-1g		4.2	140
	C-2f, H-1g		4.0	51
α,α-Trehalose	C-5, H-1	177	7.0	133
β-Gentibiose octaacetate	C-6, H-1′		3.4	141
	C-1′, H-6*R*		3.9	141
	C-1′, H-6*S*		2.4	141
1,6-Anhydro-β-cellobiose hexaacetate	C-1, H-4′		3.30	110
	C-4′, H-1		4.20	110
Methyl β-cellobioside	C-1, H-4′	−38	4.3 and 4.6	45, 141
	C-1, H-5	60	2.2	45
	C-4′, H-1	25	4.2 and 4.1	45, 141
heptaacetate	C-1, H-4′	180	5.2	45
	C-1, H-5		3.0	45
	C-4′, H-1		4.2	45
Methyl β-isomaltoside	C-6, H-1′		3.6	141
	C-1′, H-6*R*		2.9	141
	C-1′, H-6*S*		2.4	141
Methyl β-maltoside	C-4, H-1′		4.3	136
Methyl β-xylobioside	C-4, H-1′		4.5	51
	C-1′, H-4		4.6	51
1-Kestose	C-2′, H-1		4.28	143
α-D-Gal*p*A-(1→4)-D-Gal*p*	C-4, H-1′		3.7	142
	C-1′, H-4		4.9	142
α-D-Gal*p*A-(1→4)-D-Gal*p*A-(1→4)-D-Gal*p*	C-4, H-1′		3.7	142
	C-1′, H-4		5.1	142
	C-4′, H-1″		3.8	142
	C-1″, H-4′		5.1	142
Me α-L-Rha*p*-(1→4)-α-L-Rha*p*-(1→2)-α-Rha*p*	C-1(A), H-4(B)		5.2	144
	C-4(B), H-1(A)		3.0	144
	C-1(B), H-2(C)		4.5	144
	C-2(C), H-1(B)		3.5	144

TABLE IX—(*Continued*)

Compound	Coupling	Angle	Value (Hz)	Reference
-NeuAc-(2→6)-β-D-Gal-(1→4)-D-Glc	C-4(Glc), H-1(Gal)		4.2	60
	C-2(Neu), H-6*R*(Gal)		2.8	60
	C-2(Neu), H-6*S*(Gal)		1.8	60
lethyl-2-*O*-(methyl 4-*O*-methyl-α-D-glucopyranosyluronate)-β-xylobioside	C-4(B), H-1(A)		4.6	51
	C-1(A), H-4(B)		5.0	51
	C-2(B), H-1(C)		3.5	51
	C-1(C), H-2(B)		5.2	51

equation of the form

$$^3J_{C,H} = 4.44 \cos^2\phi - 1.06 \cos \phi + 0.45 \qquad (45)$$

with $^3J_{C,H}(0°) = 3.83$, $^3J_{C,H}(60°) = 1.03$, and $^3J_{C,H}(180°) = 5.95$ Hz.

The vicinal couplings of Eq. *45* are plotted in Fig. 8 (curve 3) as a function of torsion angle and compared with the values from Eq. *44*. The variation of $^3J_{C,H}$ values with torsion angle in the C—S—C—H segment is smaller than in the C—O—C—H segment, 5.5 versus 6.3 Hz. On the other hand, the difference between the magnitude of $^3J_{C,H}$ for the torsion angles 180 and 0° is larger in the C—S—C—H segment than in the C—O—C—H segment (2.12 versus 1.2 Hz, respectively).

The foregoing relationship was utilized in conformational analysis of methyl 4-thio-α-maltoside in solution.[153] The $^3J_{C,H}$ values of 2.95 and 5.15 Hz measured[151] for H-4′—C-4′—S—C-1—H-1 differ from those predicted from Eq. *45*: $^3J_{C\text{-}4',H\text{-}1} = 3.1$ Hz and $^3J_{C\text{-}1,H\text{-}4'} = 3.8$ Hz for the conformation in the crystal[154] as defined by $\Phi^H = 25.6°$ and $\Psi^H = 3.6°$. The observed $^3J_{C,H}$ values were not reproduced by the calculated values for any of the stable conformations of methyl 4-thio-α-maltoside, but are in good agreement with the ensemble average $\langle ^3J_{C,H}\rangle$ values 2.67 and 5.24 Hz calculated for the compound in water solution, using PCILO-calculated potential surfaces.

c. C—C—C—H Segment of Bonded Atoms.—The three-bond carbon–proton coupling constants between atoms C-4 and H-6 provide a measure of the torsion angle ω about the C-5—C-6 bond and thus may be used to ascertain the rotamer population about the primary hydroxyl group. Orientation about this bond is one of the important variables involved in conformational analysis of (1→6)-linked oligo- and polysaccharides (Table XIII). A theoretical study of the dependence of hydroxymethyl conformation of $^3J_{C,H}$ for the C-4—C-5—C-6—H-6 segment of atoms in series of 16 hexopyranoses has been reported.[155] The results of calculations using averaged geometries[156] for hexopyranoses are shown in Fig. 8

TABLE X

Vicinal Carbon–Proton Coupling Constants for Methyl β-Xylobioside [Me β-D-Xyl*p*-(1→4)-β-D-Xyl*p*] at Various Temperatures and Different Solvents[a]

Temperature (K)	1,4-Dioxane		Methanol		Me_2SO		Water	
	Anomeric	Aglycon	Anomeric	Aglycon	Anomeric	Aglycon	Anomeric	Aglycon
238			5.0	5.8				
258			5.0	5.4				
278			5.3	5.2			4.8	5.6
298	5.6	5.2	4.5	4.7	5.7	5.6	4.7	5.1
318	5.3	5.0	4.5	4.5	5.3	5.6	4.4	4.7
338	5.5	5.2			5.3	5.3	4.3	4.4
358	5.5	5.2			5.2	5.2	4.1	4.2
378					5.1	5.0		

[a]Taken from reference 145.

TABLE XI

Interglycosidic Carbon–Proton Coupling Constants for Oligosaccharides[a]

Compound	$^3J_{C,H}$ (Hz)	
	Anomeric	Aglycon
Maltohexaose (internal residues)	4.3	5.0
Maltoheptaose (internal residues)	4.4	5.1
Amylose triacetate	2.9	4.6
Cellulose triacetate	5.6	5.7
Cyclomaltohexaose peracetate	5.6	4.0
Cyclomaltoheptaose peracetate	5.5	4.6
Cyclomaltooctaose peracetate	4.8	4.5

[a]Taken from reference 146.

TABLE XII

Calculated Torsion Angles[a] and Measured Vicinal Coupling Constants for C—S—C—H Pathways in Thio Sugars[b]

Compound	Array	Torsion angle (degrees)	$^3J_{C,H}$ (Hz)
1,6-Anhydro-6-thio-β-D-glucopyranose	C-6,H-1	143.3	3.1
	C-1,H-6A	124.3	2.3
	C-1,H-6B	−117.9	0.3
triacetate	C-6,H-1	143.3	3.0
	C-1,H-6A	124.3	2.4
	C-1,H-6B	−117.9	0.3
1,4-Anhydro-4-thio-α-D-glucopyranose	C-1,H-4	179.0	6.3
tribenzoate	C-1,H-4	179.0	6.5
triacetate	C-1,H-4	179.0	6.4
2-(3,4,6-Tri-*O*-acetyl-α-D-glucopyranosylthio)acetic 1,2′-lactone	C-7,H-1	35.6	1.7
	C-1,H-7A	−59.4	2.4
	C-1,H-7B	178.2	5.0
2-(3,4,6-Tri-*O*-acetyl-β-D-glucopyranosylthio)acetic 1,2′-lactone	C-7,H-1	−61.6	0.5
	C-1,H-7A	79.5	0.9
	C-1,H-7B	−155.8	8.1
5-Thio-α-D-glucopyranose 2,3,4,6-tetraacetate	C-5,H-1	−172.1	5.4
	C-1,H-5	−70.8	0.3
Methyl 4-thio-β-cellobioside	C-1,H-4′		5.80
	C-4′,H-1		2.95
Methyl 4-thio-α-maltoside	C-1,H-4′		5.15
	C-4′,H-1		2.95

[a]Torsion angles are calculated using PCILO quantum chemical method or Quanta.

[b]Taken from reference 151 and 152.

TABLE XIII

Vicinal $^3J_{C,H}$ Coupling Constants (Hz) for Several Methyl Tetra-*O*-Acetyl α- and β-Glycopyranosides[a]

	α-Glc		α-Man		α-Gal		β-Glc		β-Man		β-Gal	
Array	^3J	DA[b]	^3J	DA[b]	^3J	DA[b]	^3J	DA[b]	^3J	DA[b]	^3J	DA[b]
C-1—C-2—C-3—H-3	0.9	60	<1	60	0.8	60	1.0	60	<1	60	1.2	60
C-2—C-3—C-4—H-4	<1	60	1.5	60	5.5	180	<1	60	<	60	5.8	180
C-3—C-2—C-1—H-1	5.6	180	4.9	180	5.1	180	1.1	60	<1	60	1.0	60
C-3—C-4—C-5—H-5	1.9	60	2.3	60	0.9	60	2.5	60	2.5	60	1.2	60
C-4—C-3—C-2—H-2	1.0	60	5.6	180	0.9	60	1.0	60	5.9	180	<1	60
C-4—C-5—C-6—H-6*R*	1.5		1.4		1.5		1.3		1.2		1.6	
C-4—C-5—C-6—H-6*S*	3.5		3.3		4.5		3.3		3.2		4.7	
C-5—C-4—C-3—H-3	0.9	60	1.1	60	<1	60	1.0	60	1.3	60	<1	60
C-6—C-5—C-4—H-4	3.8	60	3.5	60	0.8	60	3.4	60	3.5	60	1.0	60

[a]Taken from reference 137.

[b]Approximate dihedral angle (absolute value in degrees).

(curve 2). Clearly, the familiar behavior was again found, and a mean angular dependence was established in the form

$$^3J_{C\text{-}4,H\text{-}6} = 5.80\cos^2\phi - 1.60\cos\phi + 0.28\sin 2\phi - 0.02\sin\phi + 0.52 \quad (46)$$

The resulting curve predicts maxima for $^3J_{C,H}$ at 0 and 180° (7.92 and 4.72 Hz, respectively), and minima near 90 and −90°. The sine terms reflect the small asymmetry around 180°. Further analysis of the results showed[155] that the effect of configuration at the anomeric carbon on the angular dependence of $^3J_{C\text{-}4,H\text{-}6}$ is negligible. Based on these investigations, Eq. *45* was proposed as a tool for estimating conformational properties of (1→6)-linked oligosaccharides in solution.

VI. CONCLUSIONS

From the previous discussion it is clear that the measurement of carbon–proton coupling constants constitutes a very powerful method for investigation of the three-dimensional structures of sugar molecules in solution. With the recent progress in experimental techniques, the measurement of one-bond and three-bond C,H coupling constants may be performed with good accuracy without the necessity of synthesizing ^{13}C-enriched compounds. At the same time, the combination of theoretical studies on the angular dependences of $J_{C,H}$ with experimental data for rigid carbohydrate derivatives provides Karplus-like relationships that relate the magnitude of coupling constants and corresponding glycosidic torsion angles with an accuracy of at least 10°. These relations are strictly valid only for conformationally rigid sugars. For flexible molecules, the quantitative interpretation of experimental data in terms of conformers (three-dimensional structure) requires, in general, the calculation, from the potential surfaces, of the ensemble average of the $\langle J_{C,H}\rangle$ values. The importance of this treatment is clearly demonstrated for methyl β-xylobioside[145] and methyl 4-thio-α-maltoside.[153] Although the advantages and limits of $J_{C,H}$ measurements have not yet been systematically studied, the accumulated experience provides significant knowledge concerning the usefulness and applicability of these experimental data (in combination with NOE measurements for estimation of spatial distances) to conformational analysis of sugars in solution.

REFERENCES

1. P. E. Hansen, *Prog. Nucl. Magn. Reson. Spectrosc.*, 14 (1981) 175–296.
2. J. L. Marshall, *Carbon-Carbon and Carbon-Proton NMR Couplings, Methods in Stereochemical Analysis*, Vol. 2. Verlag Chemie International, Derfield Beach, Florida, U.S.A., 1983.
3. J. P. Carver, *Curr. Opinion Struct. Biol.*, 1 (1991) 716–720.
4. A. E. Torda and W. F. van Gunsteren, *Comp. Phys. Commun.*, 62 (1991) 289–296.
4a. P. Dais, *Adv. Carbohydr. Chem. Biochem.*, 51 (1995) 63–131, this Volume.
5. I. Tvaroska and F. R. Taravel, *Carbohydr. Res.*, 221 (1991) 83–94.

6. I. Tvaroska and F. R. Taravel, *J. Biomol. NMR*, 2 (1992) 421–430.
7. A. Abragam, *The Principles of Nuclear Magnetism*, Clarendon Press, Oxford, 1961.
8. C. P. Slichter, *Principles of Magnetic Resonance*, Springer-Verlag, Berlin, 1978.
9. J. D. Memory, *Quantum Theory of Magnetic Resonance Parameters*, McGraw–Hill, New York, 1968.
10. I. Ando and G. A. Webb, *Theory of NMR Parameters*, Academic Press, London, 1983.
11. M. Goldman, *Quantum Description of High-Resolution NMR in Liquids*, Clarendon Press, Oxford, 1988.
12. E. Breitmaier and W. Voelter, *Carbon-13 NMR Spectroscopy*, 3rd revised edition, VCH, Weinheim, 1987.
13. A. E. Derome, *Modern NMR Techniques for Chemistry Research*, Pergamon, Elmsford, N.Y., 1987.
14. J. K. M. Sanders and B. K. Hunter, *Modern NMR Spectroscopy*, Oxford Univ. Press, London/New York, 1987.
15. P. Dais and A. S. Perlin, *Adv. Carbohydr. Chem. Biochem.*, 45 (1987) 125–168.
16. J. H. Noggle and R. E. Schirmer, *The Nuclear Overhauser Effect*, Academic Press, New York/London, 1971.
17. D. Neuhaus and M. Williamson, *The Nuclear Overhauser Effect in Structural and Conformational Analysis*, VCH Publishers, Weinheim, New York and Cambridge, 1989.
18. K. Bock and C. Pedersen, *Carbohydr. Res.*, 145 (1985) 135–140.
19. K. Bock and C. Pedersen, *J. Chem. Soc. Perkin II*, (1974) 293–297.
20. G. A. Morris and R. Freeman, *J. Am. Chem. Soc.*, 101 (1979) 760–762.
21. D. T. Pegg, M. R. Bendall, and D. M. Doddrell, *J. Magn. Reson.*, 44 (1981) 238–249.
22. M. Hricovini and I. Tvaroska, *Magn. Reson. Chem.*, 28 (1990) 862–866.
23. A. D. Cox and S. G. Wilkinson, *Carbohydr. Res.*, 198 (1990) 153–156.
24. L. Szilagyi and Z. Gyorgydeak, *Carbohydr. Res.*, 143 (1985) 21–41.
25. G. A. Morris and R. Freeman, *J. Magn. Reson.*, 29 (1978) 433–462.
26. L. D. Hall and G. A. Morris, *Carbohydr. Res.*, 82 (1980) 175–184.
27. A. Bax, *J. Magn. Reson.*, 52 (1983) 330–334.
28. V. Rutar, *J. Magn. Reson.*, 56 (1984) 87–100.
29. S. Uhrinova, D. Uhrin, T. Liptaj, J. Bella, and J. Hirsch, *Magn. Reson. Chem.*, 29 (1991) 912–922.
30. J. R. Garbow, D. P. Weitekamp, and D. Pines, *Chem. Phys. Lett.*, 93 (1982) 504–509.
31. M. R. Bendall, D. T. Pegg, D. M. Doddrell, and J. Field, *J. Am. Chem. Soc.*, 103 (1981) 934–936.
32. L. M. Müller, *J. Am. Chem. Soc.*, 101 (1979) 4481–4484.
33. M. F. Summers, L. G. Marzilli, and A. Bax, *J. Am. Chem. Soc.*, 108 (1985) 4285–4294.
34. G. Bodenhausen and D. J. Ruben, *Chem. Phys. Lett.*, 69 (1980) 185–189.
35. H. Kessler, M. Gehrke, and C. Griesinger, *Angew. Chem. Int. Ed.*, 27 (1988) 490–536.
36. K. Bock and C. Pedersen, *Acta Chem. Scand., Ser. B*, 31 (1977) 354–358.
37. A. Parfondry, N. Cyr, and A. S. Perlin, *Carbohydr. Res.*, 59 (1977) 299–309.
38. J. A. Schwarcz and A. S. Perlin, *Can. J. Chem.*, 50 (1972) 3667–3676.
39. T. E. Walker, R. E. London, T. W. Whaley, R. Barker, and N. A. Matwiyoff, *J. Am. Chem. Soc.*, 98 (1976) 5807–5813.
40. R. Barker and T. E. Walker, *Methods Carbohydr. Chem.*, 8 (1980) 151–165.
41. D. Y. Gagnaire, R. Nardin, F. R. Taravel, and M. R. Vignon, *New J. Chem.*, 1 (1977) 423–430.
42. A. S. Perlin and B. Casu, *Tetrahedron Lett.*, (1969) 2921–2924.
43. R. U. Lemieux, *Ann. N.Y. Acad. Sci.*, 222 (1973) 915–934.
44. G. Excoffier, D. Y. Gagnaire, and F. R. Taravel, *Carbohydr. Res.*, 56 (1977) 229–238.
45. G. K. Hamer, F. Balza, N. Cyr, and A. S. Perlin, *Can. J. Chem.*, 56 (1978) 3109–3116.
46. S. Pérez, F. Taravel, and C. Vergelati, *New J. Chem.*, 9 (1985) 561–564.
47. K. Bock and C. Pedersen, *J. Magn. Reson.*, 25 (1977) 227–230.

48. G. Commenges and R. C. Rao, *J. Magn. Reson.*, 58 (1984) 486–499.
49. H. Seto, K. Furihata, N. Otake, Y. Itoh, S. Takahashi, T. Haneishi, and M. Ohuchi, *Tetrahedron Lett.*, 25 (1984) 337–340.
50. A. Bax and R. Freeman, *J. Am. Chem. Soc.*, 104 (1982) 1099–1100.
51. A. Bax, W. Egan, and P. Kovac, *J. Carbohydr. Chem.*, 3 (1984) 593–611.
52. V. Rutar, *J. Am. Chem. Soc.*, 105 (1983) 4095–4096.
53. S. Wimperis and R. Freeman, *J. Magn. Reson.*, 58 (1984) 348–353.
54. C. Bauer, R. Freeman, and S. Wimperis, *J. Magn. Reson.*, 58 (1984) 526–532.
55. T. Jippo, O. Kamo, and K. Nagayama, *J. Magn. Reson.*, 66 (1986) 344–348.
56. M. Hricovini, I. Tvaroska, D. Uhrin, and G. Batta, *J. Carbohydr. Chem.*, 8 (1989) 389–394.
57. D. Uhrin and T. Liptaj, *J. Magn. Reson.*, 81 (1989) 82–91.
58. M. Ochs and S. Berger, *Magn. Reson. Chem.*, 28 (1990) 994–997.
59. J. J. Titman, D. Neuhas, and J. Keeler, *J. Magn. Reson.*, 85 (1989) 111–131.
60. L. Poppe and H. van Halbeek, *J. Magn. Reson.*, 92 (1991) 636–641.
61. R. C. Grouch and G. E. Martin, *J. Magn. Reson.*, 92 (1991) 189–194.
62. L. Poppe and H. van Halbeek, *J. Magn. Reson.*, 93 (1991) 214–217.
63. M. Kurz, P. Schmieder, and H. Kessler, *Angew. Chem. Int. Ed. Engl.*, 30 (1991) 1329–1331.
64. G. T. Montelione, M. E. Winkler, P. Rauenbuehler, and G. Wagner, *J. Magn. Reson.*, 82 (1989) 198–204.
65. N. F. Ramsey and E. M. Purcell, *Phys. Rev.*, 85 (1952) 143.
66. M. Bartfield and D. M. Grant, *Adv. Magn. Reson.*, 1 (1965) 149–193.
67. J. N. Murrell, *Prog. NMR Spectrosc.*, 6 (1971) 1–60.
68. N. S. Ramsey, *Phys. Rev.*, 91 (1953) 303–307.
69. J. A. Pople, J. W. McIver, Jr., and N. S. Ostlund, *J. Chem. Phys.*, 49 (1968) 2960–2964.
70. J. A. Pople, J. W. McIver, Jr., and N. S. Ostlund, *J. Chem. Phys.*, 49 (1968) 2965–2970.
71. G. A. Webb, in *Specialist Periodical Reports on Nuclear Magnetic Resonance*, Vol. 18, Chap. 3. The Royal Society of Chemistry, London, 1989.
72. G. A. Webb, *in Specialist Periodical Reports on Nuclear Magnetic Resonance*, Vol. 19, Chap. 3. The Royal Society of Chemistry, London, 1990.
73. J. Kowalewski, *Prog. NMR Spectrosc.*, 11 (1977) 1–78.
74. J. Kowalewski, in G. A. Webb (Ed.), *Annual Reports on NMR Spectroscopy*, Vol. 12, Academic Press, London, 1982, pp. 81–76.
75. J. A. Pople and D. P. Santry, *Mol. Phys.*, 8 (1964) 1–18.
76. A. C. Blizzard and D. P. Santry, *J. Chem. Phys.*, 55 (1971) 950–963.
77. J. A. Pople, D. L. Beveridge, and P. A. Dobosh, *J. Chem. Phys.*, 47 (1967) 2026–2033.
78. M. Bartfield and M. D. Johnston, Jr., *Chem. Rev.*, 73 (1973) 53–73.
79. I. Ando and G. A. Webb, *Org. Magn. Reson.*, 15 (1981) 111–130.
80. G. Klopman, *Chem. Phys. Lett.*, 1 (1967) 200–202.
81. H. A. Germer, *Theor. Chim. Acta*, 34 (1974) 145–155.
82. J. W. Brady, *Adv. Biophys. Chem.*, 1 (1990) 155–202.
83. D. A. Brant and M. D. Christ, *ACS Symp. Ser.*, 430, (1990) 42–68.
84. O. Jardetzky, *Biochim. Biophys. Acta*, 621 (1980) 227–232.
85. G. E. Maciel, J. W. McIver, Jr., N. S. Ostlund, and J. A. Pople, *J. Am. Chem. Soc.*, 92 (1970) 1–11.
86. N. Muller and D. E. Pritchard, *J. Chem. Phys.*, 31 (1959) 768–771.
87. J. N. Shoolery, *J. Chem. Phys.*, 31 (1959) 1427–1428.
88. M. D. Newton, J. M. Schulman, and M. M. Manus, *J. Am. Chem. Soc.*, 96 (1974) 17–23.
89. K. Bock, I. Lundt, and C. Pedersen, *Tetrahedron Lett.*, (1973) 1037–1040.
90. A. S. Perlin, *MTP Int. Rev. Sci., Org. Chem. Ser. Two*, 7 (1976) 1–34.
91. J. A. Schwarcz, N. Cyr, and A. S. Perlin, *Can. J. Chem.*, 53 (1975) 1872–1875.
92. N. Cyr, G. K. Hamer, and A. S. Perlin, *Can. J. Chem.*, 56 (1978) 297–301.

93. K. Bock and C. Pedersen, *Acta Chem. Scand., Ser. B* 29 (1975) 258–264.
94. K. Bock and C. Pedersen, *Carbohydr. Res.*, 71 (1979) 319–321.
95. T. E. Walker, R. E. London, R. Barker, and N. A. Matwiyoff, *Carbohydr. Res.*, 60 (1978) 9–18.
96. G. K. Hamer and A. S. Perlin, *Carbohydr. Res.*, 49 (1976) 37–48.
97. V. S. Rao and A. S. Perlin, *Carbohydr. Res.*, 92 (1981) 141–148.
98. J. E. Nam Shin and A. S. Perlin, *Carbohydr. Res.*, 76 (1979) 165–176.
99. T. McEwan, A. G. McInnes, and D. G. Smith, *Carbohydr. Res.*, 104 (1982) 161–168.
100. H. Friebolin, G. Keilich, N. Frank, U. Dabrowski, and F. Seifert, *Org. Magn. Reson.*, 12 (1979) 216–222.
101. F. R. Taravel and P. J. A. Vottero, *Tetrahedron Lett.*, (1975) 2341–2344.
102. H. Paulsen, V. Sinnwell, and W. Greve, *Carbohydr. Res.*, 49 (1976) 27–35.
103. N. G. S. Ritchie, N. Cyr, and A. S. Perlin, *Can. J. Chem.*, 54 (1976) 2301–2309.
104. J. Thiem and B. Meyer, *Tetrahedron Lett.*, (1977) 3573–3576.
105. A. S. Perlin, *Isot. Org. Chem.*, 3 (1977) 171–235.
106. P. A. J. Gorin, *Adv. Carbohydr. Chem. Biochem.*, 38 (1981) 13–104.
107. J. Thiem, B. Meyer, and H. Paulsen, *Chem. Ber.*, 111 (1978) 3325–3335.
108. G. Adiwidjaja, B. Meyer, H. Paulsen, and J. Thiem, *Tetrahedron*, 35 (1979) 373–384.
109. N. J. Cussans and T. N. Huckerby, *Tetrahedron*, 31 (1975) 2719–2726.
110. P. Dais, T. K. M. Shing, and A. S. Perlin, *J. Am. Chem. Soc.*, 106 (1984) 3082–3089.
111. P. Dais and A. S. Perlin, *Magn. Res. Chem.*, 26 (1988) 373–379.
112. R. Kasai, M. Ohikara, J. Asakawa, K. Mitzutani, and O. Tanaka, *Tetrahedron*, 35 (1979) 1427–1432.
113. H. Grasdalen, B. Larsen, and O. Smidsrod, *Carbohydr. Res.*, 56 (1977) C11–C15.
114. J. M. Berry, G. G. S. Dutton, L. D. Hall, and K. L. Mackie, *Carbohydr. Res.*, 53 (1977) C8–C10.
115. J. Augé and S. David, *Nouv. J. Chim.*, 1 (1976) 57–60.
116. K. Bock and L. Wiebe, *Acta Chem. Scan.*, 27 (1973) 2676–2678.
117. D. G. Gorenstein, *J. Am. Chem. Soc.*, 99 (1977) 2254–2258.
118. I. Tvaroska, *Carbohydr. Res.*, 206 (1990) 55–64.
119. S. Wolfe, B. M. Pinto, V. Varma, and R. Y. N. Leung, *Can. J. Chem.*, 68 (1990) 1051–1062.
120. I. Tvaroska and T. Bleha, *Adv. Carbohydr. Chem. Biochem.*, 47 (1989) 45–123.
121. D. B. Davies, M. MacCoss, and S. S. Danyluk, *J. Chem. Soc., Chem. Commun.*, (1984) 536–538.
122. S. Prytalla, J. Lambert, J. Lauterwein, M. Klessinger, and J. Thiem, *Magn. Reson. Chem.*, 28 (1990) 888–901.
123. M. Karplus, *J. Chem. Phys.*, 30 (1959) 11–15.
124. R. E. Wasylishen and T. Schaefer, *Can. J. Chem.*, 50 (1972) 2710–2712.
125. R. E. Wasylishen and T. Schaefer, *Can. J. Chem.*, 51 (1973) 961–973.
126. M. Bartfield, J. L. Marshall, and E. D. Canada, Jr., *J. Am. Chem. Soc.*, 102 (1980) 1–7.
127. M. Bartfield, J. L. Marshall, and E. D. Canada, Jr., *J. Am. Chem. Soc.*, 102 (1980) 7–12.
128. A. A. van Beuzekom, F. A. A. M. de Leeuw, and C. Altona, *Magn. Reson. Chem.*, 28 (1990) 68–74.
129. C. A. G. Haasnoot, F. A. A. M. de Leeuw, and C. Altona, *Tetrahedron*, 36 (1980) 2783–2792.
130. K. Imai and E. Osawa, *Magn. Res. Chem.*, 28 (1990) 668–674.
131. R. U. Lemieux, T. L. Nagabhushan, and B. Paul, *Can. J. Chem.*, 50 (1972) 773–776.
132. R. U. Lemieux, S. Koto, and D. Voisin, *ACS Symp. Ser.*, 87 (1979) 17–29.
133. B. Mulloy, T. A. Frenkiel, and D. B. Davies, *Carbohydr. Res.*, 184 (1988) 39–46.
134. I. Tvaroska, M. Hricovini, and E. Petrakova, *Carbohydr. Res.*, 189 (1989) 359–362.
135. I. Tvaroska, M. Hricovini, and T. Kozar, *ACS Symp. Ser.*, 430 (1990) 162–176.
136. C. Morat, F. R. Taravel, and M. R. Vignon, *Carbohydr. Res.*, 163 (1987) 265–268.
137. C. Morat, F. R. Taravel, and M. R. Vignon, *Magn. Reson. Chem.*, 26 (1988) 264–270.
138. F. H. Cano, C. Foces-Foces, J. Jimenez-Barbero, M. Bernabe, and M. Martin-Lomas, *Carbohydr. Res.*, 155 (1986) 1–10.

139. F. H. Cano, C. Foces-Foces, J. Jimenez-Barbero, A. Alemany, M. Bernabe, and M. Martin-Lomas, *J. Org. Chem.*, 52 (1987) 3367–3372.
140. C. Herve du Penhoat, A. Imberty, N. Roques, V. Michon, J. Mentech, G. Descotes, and S. Pérez, *J. Am. Chem. Soc.*, 113 (1991) 3720–3727.
141. C. Morat and F. R. Taravel, *Tetrahedron Lett.*, 29 (1988) 199–200.
142. M. Hricovini, S. Bystricky, and A. Malovikova, *Carbohydr. Res.*, 220 (1991) 23–31.
143. T. M. Calub, A. L. Waterhouse, and N. J. Chatterton, *Carbohydr. Res.*, 199 (1990) 11–17.
144. G. Batta and A. Liptak, *J. Chem. Soc., Chem. Commun.*, (1985) 368–370.
145. M. Hricovini, I. Tvaroska, and J. Hirsch, *Carbohydr. Res.*, 198 (1990) 193–203.
146. C. Morat and F. R. Taravel, *Tetrahedron Lett.*, 31 (1990) 1413–1416.
147. M. J. Gidley and S. M. Bociek, *J. Chem. Soc., Chem. Commun.*, (1985) 220–222.
148. L. Poppe and H. van Halbeek, *J. Magn. Reson.*, 29 (1991) 848–851.
149. A. S. Perlin and G. K. Hamer, *ACS Symp. Ser.*, 103 (1979) 123–141.
150. F. H. Cano, C. Foces-Foces, J. Jimenez-Barbero, A. Alemany, M. Bernabe, and M. Martin-Lomas, *Carbohydr. Res.*, 175 (1988) 119–131.
151. I. Tvaroska, K. Mazeau, M. Blanc-Muesser, S. Lavaitte, H. Driguez, and F. R. Taravel, *Carbohydr. Res.*, 229 (1992) 225–231.
152. K. Mazeau, H. Driguez, and F. R. Taravel, *Book of Abstracts VIIth European Carbohydrate Symposium*, Cracow, Poland, 1993, p. B029.
153. K. Mazeau and I. Tvaroska, *Carbohydr. Res.*, 225 (1992) 27–41.
154. S. Pérez and C. Vergelati, *Acta Crystallogr., Sect. B*, 40 (1984) 294–299.
155. I. Tvaroska and J. Gajdos, *Book of Abstracts XVth International Carbohydrate Symposium*, Yokohama, Japan, 1990, p. 327.
156. I. Tvaroska and J. Gajdos, *Chem. Papers*, 41 (1987) 485–500.

This Page Intentionally Left Blank

ADVANCES IN CARBOHYDRATE CHEMISTRY AND BIOCHEMISTRY, VOL. 51

CARBON-13 NUCLEAR MAGNETIC RELAXATION AND MOTIONAL BEHAVIOR OF CARBOHYDRATE MOLECULES IN SOLUTION*

PHOTIS DAIS

Department of Chemistry, University of Crete, 71409 Iraklion, Crete, Greece

I. INTRODUCTION

Nuclear magnetic resonance (NMR) spectroscopy is a very powerful tool for analyzing the conformation and molecular architecture of carbohydrate molecules. Both one- and two-dimensional (1D and 2D) methodologies have provided valuable information about small and large molecules, ranging from the anomeric configuration of a monosaccharide to the sequence of monosaccharide residues that constitute an oligo- or polysaccharide.

Another important application of NMR is concerned with the property of motional freedom to which many physical and biological functions of carbohydrates

* This work was supported by the Research Committee of the University of Crete. The author is grateful to Professor Arthur S. Perlin of McGill University, who read the manuscript and made very useful comments.

in solution are related. The study of the motional dynamics of these systems provides not only complementary, and sometimes unique, information about structure and conformation, but also a deeper insight into the physical behavior and biological properties of carbohydrates in living organisms.[1]

Nuclear magnetic resonance has long been employed to monitor molecular motions and has been extensively applied to dynamic problems for small and large molecules.[2-4] In particular, ^{13}C relaxation experiments can probe motion at several carbon sites simultaneously in the molecular framework. Each carbon nucleus is associated with a set of relaxation parameters that reflect the average interaction of that nucleus with the environment. Such ^{13}C relaxation parameters as spin–lattice relaxation time (T_1), spin–spin relaxation time (T_2), and nuclear Overhauser enhancement (n.O.e.) are related to the spectral density, or power spectrum, $J(\omega)$, of local magnetic fields generated by the atomic and electronic environment of the nucleus. Modulated by the tumbling motion of the molecule in solution, these local fields can promote relaxation if they have a frequency component at or near the Larmor frequency, ω_0, of the nucleus, thus providing the link between nuclear magnetic relaxation and molecular motion.

The persistence of the fluctuating local fields before being averaged out by molecular motion, and hence their effectiveness in causing relaxation, is described by a time-correlation function (TCF). Because the TCF embodies all the information about mechanisms and rates of motion, obtaining this function is the crucial point for a quantitative interpretation of relaxation data. As will be seen later, the spectral-density and time-correlation functions are Fourier-transform pairs, interrelating motional frequencies (spectral density, frequency domain) and motional rates (TCF, time domain).

Interest in the motional behavior of carbohydrate molecules in solution has grown in recent years, and measurements of ^{13}C relaxation parameters have been performed in several instances[5-8] to probe variations in overall and internal mobility. However, in the majority of these studies the relaxation data have been interpreted in a qualitative manner, and only a few researchers[9-14] have attempted to analyze the dynamics of carbohydrate molecules by employing explicit TCFs, (dynamic models). Although qualitative analysis of ^{13}C relaxation data appears to be useful for spectral assignments[5-8,15-17] and for describing the gross features of mobility, it is likely to be less valuable than the quantitative information inherent in the measured ^{13}C relaxation parameters.

The major objective of this article is threefold: to introduce some fundamental qualitative and quantitative aspects in analyzing the dynamics of carbohydrate molecules, to demonstrate the advantages and limitations of this approach, and to critically review the results that have been obtained in the field. A complementary article in this volume by Tvaroska and Taravel[17a] surveys the use of carbon–proton coupling constants in the conformational analysis of sugar molecules.

II. THEORY

Relaxation theory of nuclear spin systems is well documented in several books[18–24] and review articles.[4,25,26] Therefore, the theory presented in this chapter is limited to a summary of some of the basic concepts crucial for understanding the material in the following sections. Furthermore, the discussion will be focused on dipolar relaxation, which is known to be the dominant relaxation mechanism in most molecules of chemical interest. For a detailed treatment of other mechanisms, the reader is referred to appropriate review articles.[4,18–26]

1. Dipole–Dipole Relaxation and Time-Correlation Function

The principal source of ^{13}C relaxation is intramolecular dipole–dipole (DD) interaction between a ^{13}C nucleus and neighboring protons. A simplified picture of this mechanism is shown in Fig. 1. A ^{13}C nucleus, situated in a rigid body which is

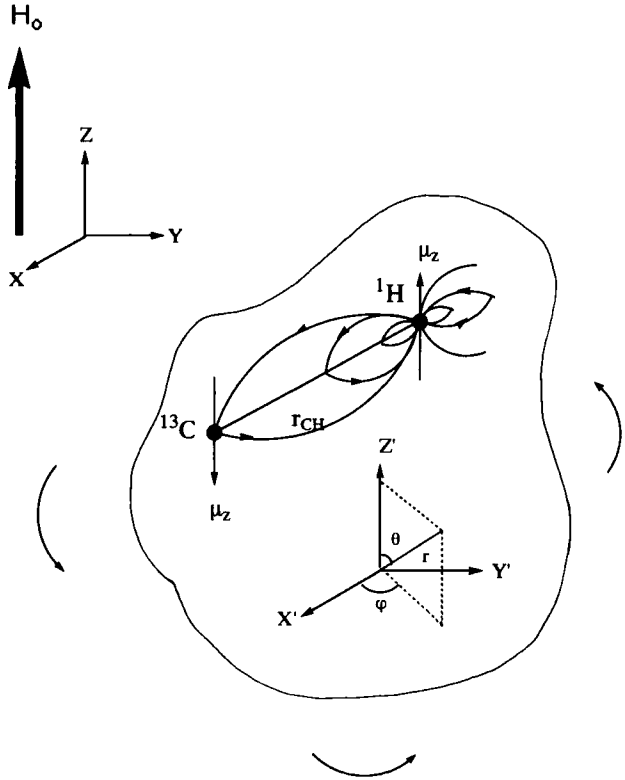

FIG. 1.—Dipole–dipole ^{13}C–^{1}H interaction mechanism. Coordinates x,y,z and x',y',z' are the laboratory and molecular coordinate systems, respectively.

undergoing complex rotational Brownian motion in solution under the influence of an external magnetic field H_o, is bonded to a proton at a distance $r_{C\text{-}H}$. The angle θ is formed between the bond vector and the direction of the external field (the z-axis of a Cartesian coordinate system fixed in the laboratory). The local magnetic field, H_{loc}, generated from the proton nucleus, or better from its magnetic moment, μ_H, at the ^{13}C nuclear site, is given by[4]

$$H_{loc} = \pm \mu_H \frac{3 \cos^2\theta - 1}{r^3_{C\text{-}H}}. \qquad (1)$$

The $\pm$ sign signifies addition or subtraction of H_{loc} from the field H_o, depending on the spin states of the proton nucleus. Owing to molecular motion, H_{loc} becomes time-dependent through the angle θ (and $r_{C\text{-}H}$ if the C—H distance is not fixed—that is, when there are intermolecular interactions or intramolecular interactions between a fixed carbon and a mobile proton), which varies continually as shown schematically in Fig. 2. In this figure, the ^{13}C nucleus is fixed at the center of a sphere, whereas the proton moves at the surface of the sphere following a kind of random-walk trajectory as the molecule tumbles.[24] The time-dependence of θ has an important consequence. If the motion is rapid enough, the average value of the local fields decays to zero because the time-average of the angular term in Eq. *1* becomes zero[23,24]; that is,

$$3 \cos^2\theta - 1 = 0 \qquad (2)$$

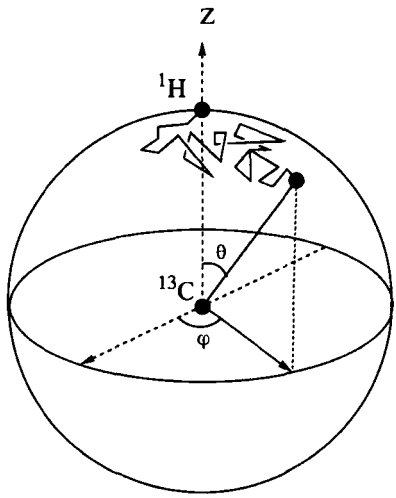

FIG. 2.—Random motion of the proton of a C–H vector. (Reproduced with permission from Fig. 11.6 of A. Carrington and A. D. McLachlan, *Introduction to Magnetic Resonance*, Harper and Row, New York, 1971.)

This phenomenon explains why resonance lines in nonviscous liquids are much narrower than those for viscous liquids or solids, where local fields are not averaged out by slower motions.

The time-dependence of the local fields is described by a TCF, which in physical terms characterizes the persistence, or correlation (or coupling), of these fields before decaying away. This persistence of the local fields is crucial for relaxation. The TCF may be written as an ensemble average of H_{loc} over all spins in the system[4,27]

$$G(t) = \langle H_{loc}(0)\, H_{loc}(t)\rangle \tag{3}$$

and characterizes the correlation of H_{loc} at the time origin, $t = 0$ (stochastic process[28]), and at a later time t. For a sufficiently short time t, the quantity in Eq. *3* has a finite value, but for a long t it becomes zero. However, the mean value of $G(t)$ is by no means zero[4,27]:

$$G(t) = \langle H^2_{loc}(t)\rangle \neq 0. \tag{4}$$

To describe the motion or the position of the two spins (such as ^{13}C and ^{1}H in Fig. 1) with respect to the external field (or the laboratory-fixed coordinate system), it is customary and useful in treating DD relaxation to introduce relevant space functions. These functions, $F^{(q)}(t)$, appear in the time-dependent Hamiltonian describing DD interactions, which can be written as a product of two second-rank tensors[25] A and F:

$$H_{DD}(t) = \sum_q (-1)^q F^{(q)}(t) A^{(-q)}, \tag{5}$$

where $A^{(-q)}$ contains spin operators and other constants defining the magnitude of interactions[25] and $F^{(q)}$ is a function of the Euler angles giving the orientation of the molecular coordinate system with respect to a set of axes fixed in the laboratory (Fig. 1). Function $F^{(q)}$ is time-dependent because of random molecular motion, and its average is expressed by a TCF analogous to that in Eq. *3*:

$$G(t) = \langle F^{(q)}(\Omega,0)\, F^{(q)}(\Omega,t)\rangle, \tag{6}$$

where the symbol Ω denotes the Euler angles specifying the orientation of the dipolar vector or the principal axis system in the molecule with respect to the external magnetic field. However, although the quantities $F^{(q)}(t)$ given in the laboratory-fixed coordinate system are not known, they can be obtained from the known quantities $F'^{(q)}$ in the molecular coordinate system by a linear transformation, as has been shown by Huntress[25]. The latter quantities are related to the second-order Legendre polynomials, the spherical harmonics.[23] These are given as follows[23,25]:

$$F'^{(0)} = \frac{1 - 3\cos^2\theta}{r^3} \tag{7a}$$

$$F'^{(1)} = \frac{\sin\theta\cos\theta}{r^3} e^{i\varphi} \tag{7b}$$

$$F'^{(2)} = \frac{\sin^2\theta}{r^3} e^{2i\varphi}, \tag{7c}$$

where r, θ, φ are the usual spherical coordinates with respect to the molecular set of axes (Fig. 1).

It can be shown[4] for the simple case of isotropic rotational diffusion that the TCF is a single exponential function of time, decaying with a time constant, τ_c, the molecular correlation time:

$$G(t) = \langle F^2(0)\rangle e^{-t/\tau_c} \tag{8}$$

The time constant τ_c is also called a phase-memory time, since it is related to the time for local fields to lose phase coherence (coupling) and decay to zero.

2. Spectral Density and Relaxation Parameters

As will be shown later, the NMR relaxation parameters are frequency-dependent quantities. Therefore, we are interested in ways to measure these frequencies associated with the nature of the rotational motion. The Fourier transform of the TCF, which evolves in the time domain, yields a spectrum of motional frequencies in which the value of the function, $J(\omega)$, at each frequency is known as the spectral density[4,23]

$$J(\omega) = \int_{-\infty}^{+\infty} G(t)e^{i\omega t}\, dt \tag{9}$$

or

$$J(\omega) = 2\int_{-\infty}^{+\infty} G(t)\cos\omega t\, dt \tag{10}$$

since we are interested in the real part of this complex Fourier transform.[29] Substituting Eq. *8* into Eq. 10 and integrating, we obtain

$$J(\omega) = \langle F^2(0)\rangle \frac{2\tau_c}{1 + \omega^2\tau_c^2}. \tag{11}$$

Equation *11* represents an important relationship because it describes the frequency-dependence of any relaxation process involving rotational correlation. Also, it provides a means of characterizing the frequency distribution and the intensity of the fluctuations in H_{loc} in the frequency domain, and hence their effectiveness in causing relaxation.

For a purely $^{13}C-^{1}H$ dipolar interaction the relaxation parameters are given by[4,23]

$$\frac{1}{NT_1} = \frac{K}{20}\{J(\omega_H - \omega_C) + 3J(\omega_C) + 6J(\omega_H + \omega_C)\} \quad (12)$$

$$\frac{1}{NT_2} = \frac{K}{40}\{4J(0) + J(\omega_H - \omega_C) + 6J(\omega_H) + 3J(\omega_C) + 6J(\omega_H + \omega_C)\} \quad (13)$$

$$\text{n.O.e.} = \frac{\gamma_H}{\gamma_C}\frac{6J(\omega_H + \omega_C) - J(\omega_H - \omega_C)}{J(\omega_H - \omega_C) + 3J(\omega_C) + 6J(\omega_H + \omega_C)} \quad (14)$$

and

$$K = \frac{\gamma_H^2\gamma_C^2\hbar^2}{r_{C\text{-}H}^6}.$$

Here, γ_H, γ_C and ω_H, ω_C are the gyromagnetic ratios and Larmor frequencies of the carbon and proton nuclei, respectively; $\hbar$ $(=h/2\pi)$ is Planck's constant; $r_{C\text{-}H}$ is the C—H bond length noted earlier; and N is the number of protons directly attached to the carbon atom under consideration. The n.O.e. value in Eq. *14* depends neither on the number of protons nor on the C—H distance, in contrast to the other two parameters. This means that the T_1 and T_2 values of the carbon nuclei are affected by neighboring intramolecular protons. The shortest distances (1.08–1.09 Å) involve directly attached protons, making them the main contributors to the relaxation of a carbon nucleus.

As the relaxation parameters described in Eqs. *12–14* are frequency-dependent quantities, their behavior is closely related to the relative magnitude of ω and τ_c in Eq. *11*. For rapid motions ($\omega \ll 1/\tau_c$), Eq. *11* becomes

$$J(\omega) = \langle F^2(0)\rangle 2\tau_c \quad (15)$$

and T_1, T_2, and n.O.e. are field-independent quantities that decrease continually as the motion becomes slower (correlation time increases). In the region of fast motions, the so-called extreme narrowing limit, Eqs. *12–14*, are simplified to

$$\frac{1}{NT_1} = \frac{1}{NT_2} = \frac{\gamma_H^2\gamma_C^2\hbar^2}{r_{C\text{-}H}^6}\tau_c \quad (16)$$

and

$$\text{n.O.e.} = \frac{\gamma_H}{2\gamma_C} = 1.988. \quad (17)$$

At the motional narrowing limit, the n.O.e. attains its maximum value of 1.988 (or 2.988 for the n.O.e. factor, $\eta = 1 +$ n.O.e.) and is determined by the gyromag-

netic ratios γ_H and γ_C. At the Larmor frequency of $\omega \approx 1/\tau_c$, relaxation is most effective; $J(\omega)$ attains its maximum value and T_1 goes to a minimum (Fig. 3a). For longer correlation times ($\omega > 1/\tau_c$) outside the extreme narrowing limit, relaxation again becomes less effective, T_1 increases and becomes, in addition, a frequency-dependent quantity (Fig. 3a). Also, T_2 becomes frequency-dependent at long correlation times; but unlike T_1, T_2 decreases continually with correlation time to the limit where motion is considered frozen (Fig. 3a). This behavior is due to the zero frequency-dependence of T_2 (compare Eqs. *12* and *13*) arising from fluctuations in the local fields along the z direction, which is equivalent in the laboratory-fixed and molecular system of coordinates (Fig. 1). Figure 3b shows variation in n.O.e. induced by molecular motions. For short τ_c values, the n.O.e. has a maximum value of ~ 2.0, in accord with the extreme narrowing condition. As motion slows down, the n.O.e. is decreased progressively to lower values toward an asymptotic value of 0.15 for long correlation times. Therefore, the n.O.e. can have values lower than 2, despite the fact that DD interaction is the dominant relaxation mechanism. This observation is extremely important for polysaccharides, as we shall see later. Finally, we note that n.O.e. is also a frequency-dependent parameter outside the extreme narrowing limit.

3. Relaxation Mechanisms

Local magnetic fields are generated not only by DD interactions, but also by such other sources as electron dipoles, electric quadrupoles, anisotropy in the chemical shielding tensor, modulation of scalar coupling, and spin rotation. Each of these interactions represents a separate relaxation mechanism, which may contribute to the measured relaxation parameters. For instance, the chemical shielding anisotropy mechanism (CSA) is significant for unsaturated quaternary ^{13}C nuclei at all resonance frequencies, and for unsaturated protonated ^{13}C nuclei it becomes increasingly so above 50 MHz. However, for saturated protonated carbons, the predominant mechanism is DD interaction with the attached protons. For small molecules or a flexible segment, such as a methyl group, appreciable competition from other mechanisms (mainly spin rotation) may arise.

In only rare instances may a substantial fraction of the observed relaxation rate be ascribed to other mechanisms.[4] Partitioning of each contributing mechanism is not an easy task and requires additional field- and temperature-dependent experiments.[4] However, separation of the DD relaxation mechanism from all other possible interactions is achieved via n.O.e. measurements by means of the equation[4]

$$\text{n.O.e.} = 1.988 \frac{1/T_1^{\text{obs}}}{1/T_1^{\text{DD}}}, \qquad (18)$$

where the observed relaxation rate, $1/T_1^{\text{obs}}$, may contain contributions from the DD ($1/T_1^{\text{DD}}$) and other ($1/T_1^0$) relaxation mechanisms according to the approximate

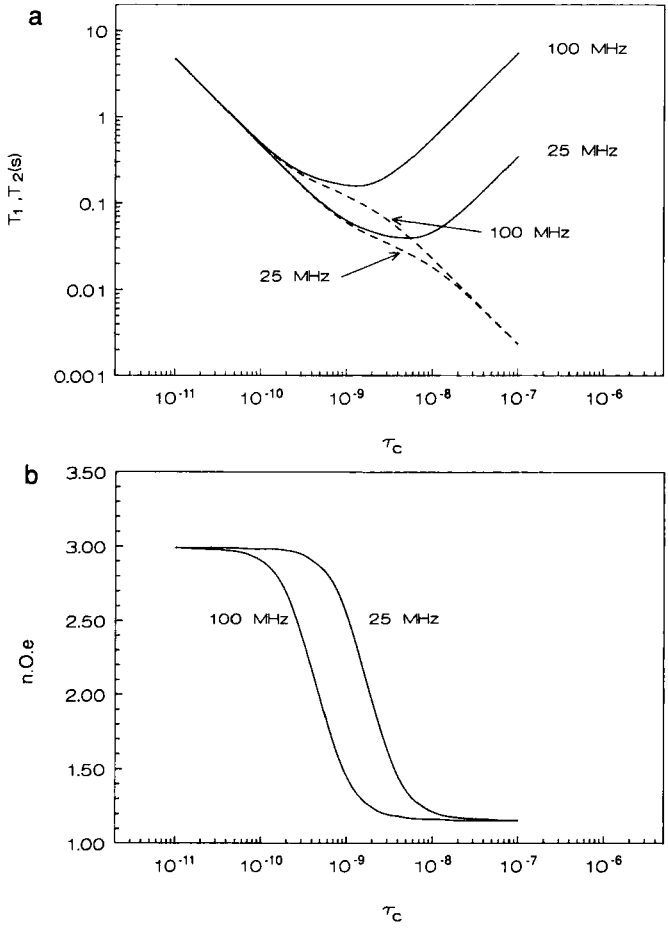

FIG. 3.—The theoretical behavior of (a) T_1 and T_2, and (b) n.O.e. as a function of correlation time and magnetic field. [Reproduced with permission from Figs. 3.2 and 3.4 of J. R. Lyerla, Jr., and G. C. Levy, *Top. Carbon-13 NMR Spectrosc.*, 2 (1974) 79–148.]

additivity relationship[4]

$$\frac{1}{T_1^{\text{obs}}} = \frac{1}{T_1^{\text{DD}}} + \frac{1}{T_1^{0}}. \tag{19}$$

4. Experimental Methods

The most commonly performed relaxation experiment is that of determining the spin–lattice relaxation time, T_1, which is relatively easily measured by a variety of methods, such as inversion recovery[30] or progressive saturation.[31] All of these

experimental methods are discussed thoroughly by Martin *et al.*,[32] while the factors affecting the accuracy in ^{13}C T_1 measurements are carefully analyzed in a review by Craik and Levy,[33] who also recommend the use of the fast version of the inversion–recovery sequence (FIRFT).[34] The optimization of the experimental design and the statistical analysis of the data are presented in a comprehensive way in a review by Weiss and Ferretti.[35] Recent modifications and extensions of the traditional pulse sequences for more demanding experimentalists are discussed in detail by Kowalewski.[36]

Measurements of spin–spin relaxation times (T_2) are much less common than T_1, mainly because the experiments are more difficult to conduct. Under ideal conditions, T_2 can be obtained from the linewidth of the NMR signal at half-height, $\Delta\nu_{1/2}$, using the relation $T_2^{-1} = \pi\Delta\nu_{1/2}$. However, ideal conditions do not usually apply (except perhaps for rapidly relaxing quadrupolar nuclei, for which high-resolution instrumentation is used), and the natural linewidth is obscured by field inhomogeneity and overlap. Field inhomogeneity can be suppressed by a spin-echo pulse sequence, the most common version of which for T_2 measurements is the Carr–Pursell–Meiboom–Gill (CPMG)[37] sequence discussed thoroughly by Martin *et al.*[32] As this pulse sequence is highly sensitive to pulse imperfections, composite refocusing pulses, designed to be less sensitive to pulse-length errors and to the spatial inhomogeneity of the radiofrequency field, have been proposed by Levitt and Freeman.[38] Bain *et al.*[39] have described an alternative method that involves measuring the signal intensity as a function of the offset of a saturating radiofrequency field. Spin–spin relaxation times T_2 can be determined by fitting the experimental curve to its theoretical form, provided that T_1 and the magnitute of the saturating field are known. Other methods and modifications, including the spin-locking experiment[32] and a two-dimensional version of the spin-echo pulse sequence[40] are reviewed by Kowalewski.[36]

Carbon-13 n.O.e. values are most easily determined by the so-called "inverse gated decoupling" method, which is based on the simple pulse sequence,[32] $(PD-90°-AT)_n$, where AT is the acquisition time and PD is the delay time between the 90° pulses. The experiment is repeated n times to obtain the desired sensitivity (signal-to-noise ratio). In this experiment, a normal spectrum is obtained with continuous wideband proton decoupling (decoupled spectrum with n.O.e.), and a second one is obtained while the decoupler is gated on only during the data-acquisition period. During the remainder of the pulse interval the decoupler is gated off (decoupled spectrum without n.O.e.). The n.O.e. factors (and from these the n.O.e. values) are obtained by dividing the peak intensities of the first experiment by those of the second experiment. For best results pulse delays should be 8–10 times the longest T_1 to ensure complete recovery of the magnetization before the next 90° pulse.

For small or medium-sized molecules undergoing rotational motion in the extreme narrowing limit, the spectral density is field-independent and the n.O.e.

attains its maximum value. Thus, T_1 measurements for several carbon sites in the molecule at one frequency suffice for extracting quantitative information for the overall motion and internal mobility. Often, T_1 measurements as a function of temperature are required to obtain activation energies (see below) and to discriminate between dynamic models that may equally well reproduce the experimental data at one temperature. For macromolecules, however, measurements at one field, even of all the relaxation parameters (T_1, T_2, n.O.e.) give insufficient information about the motional behavior of these systems. In view of the variety of macromolecular motions, ranging from frequencies as low as 10^5 Hz for the overall motion to frequencies on the order of 10^9-10^{10} Hz for segmental and other local motions in the chain, it is not surprising that a detailed quantitative examination requires the rigorous sampling of a wide variety of amplitudes and time scales. Unfortunately, magnetic relaxation measurements at a given magnetic field respond to values of $J(\omega)$ at a very limited number of frequencies. For instance, T_1 measurements sample motions at frequencies $(\omega_H - \omega_C)$ and $(\omega_H + \omega_C)$ (Eq. *12*), both of which are in the same radiofrequency region as the resonance frequencies themselves. Nevertheless, by measuring several relaxation parameters at different resonance frequencies, $J(\omega)$ can be sampled discretely at a number of frequencies, thus giving some insight into the form of the TCF.

5. Free and Diffusive Rotational Motion

This article is concerned with rotational dynamics in the liquid state, in which viscous drag and other solute–solute and solute–solvent interactions slow down the rate of rotation and cause τ_c to become longer than that of freely rotating molecules. The rotational motion of a free rotor depends only on its moment of inertia and temperature. The correlation time, τ_f, describing free rotation can be viewed as a limit approached by the actual τ_c as viscosity approaches zero.

A convenient test for determining when a particular rotational motion can be safely regarded as satisfying the diffusion assumptions is the χ-test introduced by Wallach and Huntress[41]:

$$\chi = \frac{\tau_c}{\tau_f} = \frac{5\tau_c}{3}\left(\frac{kT}{I}\right)^{1/2}, \tag{20}$$

where

$$\tau_f = \frac{3}{5}\left(\frac{I}{kT}\right)^{1/2} \tag{21}$$

denotes the period for rotation through one radian of a free gas molecule unhindered by viscous drag and I is the moment of inertia tensor of the free rotor. Three boundary regions can be distinguished, depending on the value of the τ_c/τ_f ratio:

(1) $\chi < 3$ inertial region, (2) $3 < \chi < 5$ intermediate region, and (3) $\chi > 5$ diffusion region.

In the diffusion region the reorientational motion of the molecules is impeded by a frictional force exerted by a medium considered structureless (continuum). For a spherical molecule, the rotational diffusion coefficient, D, is given by the Stokes–Einstein–Debye equation[42]

$$D = \frac{kT}{\xi}. \tag{22}$$

The rotational friction coefficient, ξ, is related to the viscosity of the medium, η, and the radius, α, of the molecule through the equation

$$\xi = 8\pi\alpha^3\eta. \tag{23}$$

In the general case, D is a tensor and the individual components of the diagonalized diffusion tensor are given by $D_i = kT/\xi_i$. Furthermore, D is related to τ_c by the simple equation

$$\tau_{c,i} = \frac{1}{6D_i}. \tag{24}$$

Although Eq. *22* appears to be valid for rigid and flexible molecules of arbitrary shape, the correlation times for small and medium-sized molecules calculated using Eqs. *22–24* were found to be 5–10 times larger than those determined from relaxation experiments. It appears that the effective viscosity at the surface of the molecule is not well represented by the bulk viscosity. However, as large molecules undergoing isotropic motion have an effective radius much larger than the radius of the solvent molecules, the medium will appear reasonably continuous to the rotating molecules, which therefore approach classical behavior. Subsequent experimental studies and theoretical calculations have impressively improved classical hydrodynamic theory.[43]

III. Dynamic Modeling

1. Overall Motion

For a rigid spherical or nearly spherical molecule undergoing diffusive rotational motion in the extreme narrowing limit, a single correlation time, given by Eq. *16*, is adequate to describe the overall motion. Equation *16* can be modified to take into account intramolecular interactions from other protons attached to other carbons in the molecule. Assuming that τ_c is the correlation time for each such

interaction, the following equation is obtained:

$$\frac{1}{T_1} = \sum_{i=1}^{n} \frac{\gamma_H^2 \gamma_C^2 \hbar^2}{r_{C\text{-}H,i}^6} \tau_c. \tag{25}$$

When the overall motion is not isotropic, the diagonal elements of the rotational diffusion tensor are no longer equivalent and rotation about the three principal axes of the diffusion tensor may be described by different diffusion coefficients or correlation times. For anisotropic motion, the correlation time in Eqs. *16* and *25* is an effective correlation time, τ_c^{eff}, containing contributions from the various modes of reorientation. Partitioning of the various components of τ_c^{eff} can be achieved through appropriate dynamic models. The simplest case of anisotropic motion is that for a symmetric-top molecule. The τ_c^{eff} of a rigid ellipsoid is expressed in terms of two parameters, $D_{\parallel}$ and $D_{\perp}$; these two parameters respectively describe the rotational diffusion about the C_3 symmetry axis (major axis) and the two perpendicular axes (minor axes), which are assumed to be equivalent[25,44] (Fig. 4):

$$\tau_c^{\text{eff}} = D_{\perp}^{-1}\left(\frac{A}{6} + \frac{B}{5+\rho} + \frac{C}{2+4\rho}\right), \qquad \rho = D_{\parallel}/D_{\perp} \tag{26}$$

$$A = \left(\frac{1}{4}\right)(3\cos^2\Delta - 1)^2$$

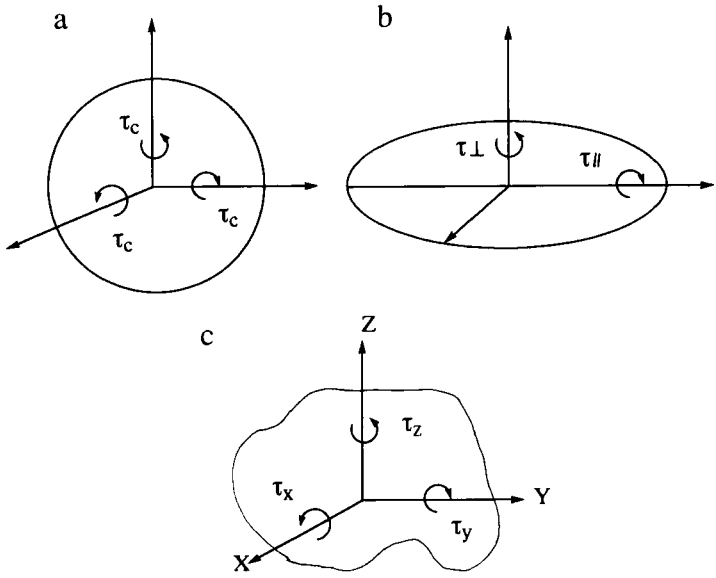

FIG. 4.—Molecular shapes and correlation times for isotropic and anisotropic motion. (a) Spherical molecule; (b) axially symmetric molecule; (c) asymmetric molecule.

$$B = 3 \sin^2\Delta \cos^2\Delta = \left(\frac{3}{4}\right) \sin^2(2\Delta), \tag{27}$$

$$C = \left(\frac{3}{4}\right) \sin^4\Delta,$$

where A, B, and C are geometric constants that are functions of the angle, Δ, formed between the C—H vector and the major axis of the ellipsoid[44] (Fig. 4). To evaluate both diffusion coefficients, either the T_1 values of two nonequivalent carbons with different angles (relative to the C_3 axis) of their respective C—H vectors must be obtained, or an independent determination of one of the parameters from other sources must be made.

For asymmetric-top molecules, all three principal values of the rotational diffusion tensor are required to describe the molecular dynamics; hence at least three different T_1 values of geometrically nonequivalent carbons are required to solve the three independent simultaneous equations derived by Woessner[45]:

$$\frac{1}{T_1} = f(D_x, D_y, D_z). \tag{28}$$

The unknown parameters in these equations are the three diffusion coefficients, D_x,D_y, and D_z, describing the diffusive rotation of the molecule about the three principal axes of the diffusion tensor (Fig. 4). The geometry of the molecule is reflected in several geometric constants, which are functions of the directional cosines of the angles formed between the C—H vectors and the three principal axes.[45]

The orientation of the diffusion tensor principal axes, relative to the moment of inertia tensor principal axes, deserves some comment. Previous equations were derived on the assumption that the principal axes of the two tensors coincide, which implies that the overall molecular symmetry is the primary factor governing diffusion. For asymmetric-top rotors with a lower symmetry, however, the two principal-axis systems need not necessarily be identical, provided that intermolecular interactions are strong enough. Thus, molecules containing such heavy atoms as Br, I, and/or polar groups, where polar interactions, hydrogen-bonding, aggregation, and the like are prominent, can cause a shift between these two axes. In this case, the orientation of the diffusion tensor principal axes with respect to the principal axes of the inertial tensor in terms of the Euler angles α, β, γ, should be determined in addition to the three diffusion coefficients:

$$\frac{1}{T_1} = f(D_x, D_y, D_z, \alpha, \beta, \gamma). \tag{29}$$

The Euler angles between both principal-axis systems may be calculated as optimizable parameters simultaneously with the rotational diffusion constants in a

optimization routine, or they may be determined by means of successive variation of the angles. In the first approach, at least six linearly independent equations, and hence six unique C—H vectors as well as their corresponding ^{13}C T_1 values, are needed for the determination of the six parameters. For the second method, however, the number of T_1 values may be less than six but not less than three. Details of this type of calculation, and of other approaches used to locate the rotational diffusion principal-axis system, are reviewed by Dolle and Bluhm.[46]

The shift in the two tensors is expected to be effective for carbohydrate molecules bearing a number of polar groups and hydrogen-bonding centers. Hence, serious difficulty for quantitative analysis may arise if the molecule does not contain three or more nonequivalent C—H vectors that relax predominantly via the overall motion. If this fact is ignored, qualitative treatment may lead to an erroneous motional description. Thus, one should be very cautious in interpreting the relaxation data for overall motion, especially when discrepancies well outside the experimental error are observed for the T_1 values. When the relaxation times are nearly similar and within the experimental error, isotropic motion may be considered as a first approximation to the problem.

2. Internal Motion

The treatment of internal motion of a flexible segment (such as a methyl or phenyl group) superposed on overall motion requires an appropriate TCF describing that motion. Assuming that these motions are independent, the total TCF, $G_t(t)$, may be written as a product of the individual TCFs[28]:

$$G_t(t) = G_o(t) \cdot G_i(t) \tag{30}$$

where $G_o(t)$ and $G_i(t)$ are the TCFs for the overall and internal motion, respectively. This factorization is exact for isotropic overall motion and represents a good approximation for the anisotropic case. The choice of $G_i(t)$ depends on the geometry of the flexible segment and the nature of the internal motion. A number of models exist in the literature describing internal mobility as a free rotation,[47] restricted rotation about a bond,[48–50] a wobbling motion in which a vector diffuses within a cone,[51–55] or jumps between equivalent[48,56–61] or nonequivalent[62] states. Other models[63–65] treat multiple internal rotations amenable to studies of a large number of molecular systems ranging from the simple *n*-alkanes to macromolecules including membranes, lipid bilayers, polysaccharides, and synthetic high-molecular-weight polymers. A number of these models are presented explicitly in the Appendix and will be discussed in subsequent sections. In this section, internal motion will be treated as an example of the free rotation of a methyl group about its C_3 symmetry axis.

The treatment of the internal rotation of a methyl group superposed on an

isotropic overall motion leads to the following equation[47]:

$$\frac{1}{T_1(CH_3)} = \frac{N\gamma_H^2\gamma_C^2\hbar^2}{r_{C\text{-}H}^6}\left(\frac{A}{6D_R} + \frac{B}{6D_R + D_i} + \frac{C}{6D_{RF} + 4D_i}\right) \qquad (31)$$

Here D_R and D_i are the diffusion coefficients for the isotropic overall and free internal motions, respectively. Equation 31 assumes a diffusional process for the methyl group. If a jumping process between three equivalent positions separated by 120° is considered,[47] the last term becomes $C/(6D_R + D_i)$. Parameters A, B, and C are geometric constants similar to those in Eq. *27*, but here the angle is that formed between the methyl C—H vectors and the axis of rotation. Assuming tetrahedral angles, for free internal motion ($D_i \gg D_R$), $1/T_1(CH_3)$ is decreased to one-ninth of the value expected for a rigidly attached CH carbon. For slow internal rotation ($D_i \rightarrow D_R$), $1/T_1(CH_3)$ becomes one-third of the value of a methine carbon in the same molecule, as predicted by Eq. *16*.

Woessner[47] has also treated the case of a methyl group attached to an axially symmetric ellipsoid, whereas Levy *et al.*[66] derived equations for the methyl internal rotation superposed on a fully anisotropic motion. The effect of anisotropic reorientation can dramatically alter the relationship between rigidly held methine, methylene, and methyl C—H vectors. Deviation from the ratio $T_1(CH)/T_1(CH_3) = 3$ can be considerable, depending on the relative orientation of C—H vectors with respect to the principal diffusion axes.

Another important factor in these studies is steric constraints imposed on methyl motion by the molecular environment. In such cases, methyl rotation is not free, but rather is subject to a potential barrier greater than kT. The potential barrier, V_i, is calculated via a conventional expression of the type

$$D_i = D_f e^{-V_i/RT} \qquad (\text{or } \tau_{c,i} = \tau_f e^{V_i/RT}). \qquad (32)$$

The pre-exponential factor D_f (or τ_f) is the diffusion constant (or correlation time) of a freely rotating methyl group and is given by an equation analogous to Eq. *21*. A rigorous approach to this problem is to calculate activation energies from variable-temperature relaxation measurements, using an Arrhenius-type plot of D_i (or $\tau_{c,i}$) versus $1/T$ (K).[67]

3. Segmental Motion

Relaxation measurements on macromolecular systems, including polysaccharides[9-11] of high molecular weight, result in frequency-dependent relaxation parameters and n.O.e. values invariably below the maximum value of ~2.00. Also, for polymers of relatively low molecular weights (MW < 10,000), T_1 values may be molecular-weight-dependent. The first two observations indicate that the spectral density of these systems is heavily weighted by slow motions occurring outside

the extreme narrowing limit, whereas the last observation is evidence for molecular-weight-dependent motions.

A deeper understanding of the motional behavior of polymer systems requires a knowledge of the types of motions in a polymer chain. There are two general types of macromolecular motions, which are assumed to be independent of each other: the reorientational motion of the polymer chain as a whole, and segmental or local motions in the polymer chain. Internal rotation of pendant groups (such as methyl, phenyl, or hydroxymethyl groups) may be classified as local motions. The overall motion is the molecular-weight-dependent motion and it represents a major source of relaxation for stiff chains and for low-molecular-weight flexible polymers. For high-molecular-weight (MW $>$ 10,000) random-coil polymers, or for natural macromolecules that do not have a rigid conformation (such as some polypeptides and polysaccharides), relaxation is controlled by segmental motions. Thus, for high-molecular-weight flexible polymers the contribution of the overall motion to the relaxation of the chain carbons is considered negligible and can be safely ignored.[11,68,69]

Factoring out the overall motion, it is necessary to consider an appropriate TCF to describe segmental motion. In view of the wide variety of segmental motions possible, as well as the multiplicity of rates and mechanisms, a single correlation time (isotropic motion) is not the right choice for a detailed quantitative examination of the relaxation data for flexible polymers.[68] Neither is an anisotropic model, such as that described by Eq. *26*, an efficient alternative. This model describes changes within a given conformation rather than genuine rotational changes from one conformation to another. The existence of a simple kinetic unit, such as an isolated monomer residue in the chain, appears highly improbable, and many possible interactions between monomer units are likely to occur. Thus, it appears more realistic to apply a TCF corresponding to a distribution of correlation times,[2,68] indicating long correlation times associated with cooperative (or correlated) interactions between monomer units, as well as correlation times within the extreme narrowing region. In this case, the appropriate TCF should contain a normalized distribution function $F(\tau,s)$, or density function with two adjustable parameters, τ and s, reflecting the distribution of correlation times and the width of the distribution, respectively:

$$G_i(t) = \int_0^\infty F(\tau,s)e^{-t/\tau}\,dt. \tag{33}$$

Density functions used earlier to interpret the relaxation data of polymers were the Cole–Cole function,[70] the Fuoss–Kirkwood function,[71] and the log (χ^2) function.[72] These functions, particularly the skewed log (χ^2) distribution, were accounted for by ^{13}C T_1 and n.O.e. data of some polymers, but the physical significance of the adjustable parameters has been questioned by some authors.[68]

Moreover, they were unsuccessful in rationalizing experimental data sets for several polymeric systems.[68]

The inadequacy of the so-called mathematical models led to a second class of distribution functions, which incorporated the specific conformational transitions available to a particular polymer system. These models, the so-called "diamond" or "tetrahedral-lattice" models, were generated by considering a three- or four-

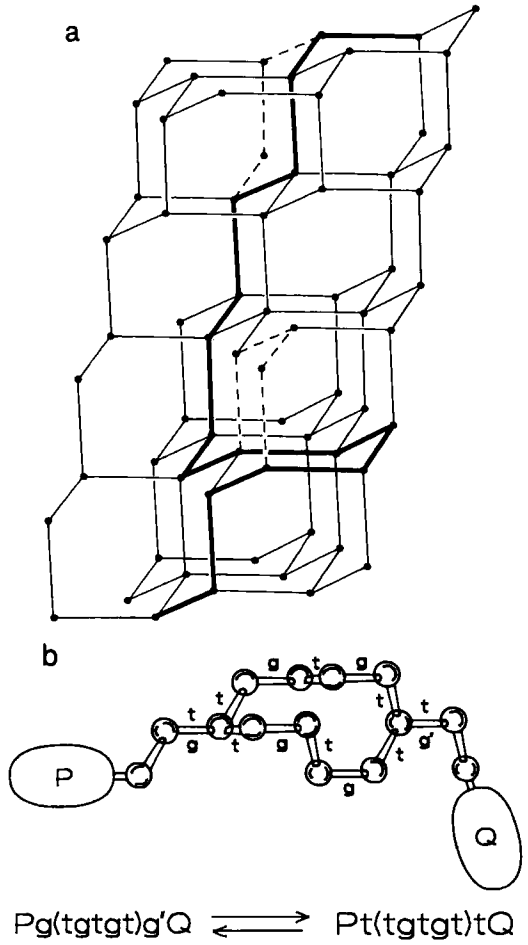

FIG. 5.—(a) Three-bond motion (top) and four-bond motion (bottom) of a hydrocarbon chain distributed on a tetrahedral (or diamond) lattice. (b) Crankshaft motion of five bonds around two collinear bonds. P and Q represent the tails of the polymer chain; t and g denote the *trans* and *gauche* conformations, respectively. [Reproduced with permission from Figs. 2 and 3 of F. Heatley, *Progr. NMR Spectrosc.*, 13 (1979) 47–85, and Elsevier Science.]

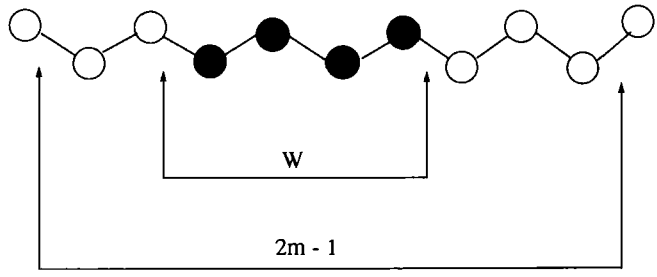

FIG. 6.—Jones–Stockmayer (JS) motional model.

bond crankshaft arrangement in a chain randomly distributed in a diamond lattice (Fig. 5a). The term *crankshaft motion* signifies concerted motion of a number of bonds in the chain about two collinear bonds, as shown in Fig. 5b. So far, several modifications of the lattice model have been suggested, depending on the boundary conditions involved in the solution of the lattice equation first derived by Hunt and Pawles[73] from a different physical picture. All of these functional forms of the diamond-lattice model and their application to flexible macromolecules have been presented in two very important reviews by Heatley.[2,68] The easiest and most effective modification for performing numerical calculations has been suggested by Jones and Stockmayer.[74] In the Jones–Stockmayer (JS) model, the time scale of the segmental motion is described by a harmonic mean correlation time, τ_h, which is equal to $(2w)^{-1}$, where w is the rate of the three-bond jump in the diamond-lattice (Fig. 6). The breadth of the distribution of correlation times is characterized by a segment of $2m - 1$ bonds embracing the three-bond kinetic (central) unit, with complete neglect of correlation outside that segment (Fig. 6). The set of the equations describing this model is given in the Appendix (Eq. *A-1*).

Another interesting approach to the simulation of polymer dynamics was pursued by Helfand and co-workers.[75–78] Their method, which was based on computer simulations[75,78] and kinetic theory analysis[77] of conformational transitions in polymethylene-type chains, supported the idea that the rate-controlling step of the chain is the surmounting of only a single-bond, internal rotational barrier, accompanied by librational fluctuations in neighboring bonds in such a way as to localize the motion (Fig. 7). These fluctuations of torsional angles, bond angles, and bond

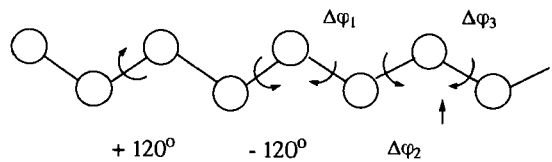

FIG. 7.—Hall–Weber–Helfand (HWH) motional model. $\Delta\varphi_1$, $\Delta\varphi_2$, and $\Delta\varphi_3$ denote angular fluctuations in neighboring bonds.

lengths prevent the unfavorable movement of the polymer tails. Corresponding analytical theories for the TCF describing conformational transitions of this type have been offered by Hall, Weber, and Helfand.[78] In the Hall–Weber–Helfand (HWH) model, the time scale for segmental motion is set by two parameters: τ_0, the correlation time for single conformational transitions, and τ_1, the correlation time for cooperative or correlated transitions. The spectral density of this model is given explicitly in the Appendix (Eq. *A-2*).

Subsequently, Dejean, Laupretre, and Monnerie[79] introduced an effective modification of the HWH model to account for different local dynamics observed experimentally at different carbon sites in the chain. Differential chain local dynamics arise because of a fast librational motion of the C—H vectors in addition to segmental motion described by the HWH model. This additional contribution developed by Howarth[53] is a type of wobbling-in-a-cone motion, in which libration is pictured as a random diffusive motion of a bond within a cone of half-angle θ with its axis oriented along the equilibrium position of the C—H vector (Fig. 8). In addition to the angle θ, the composite TCF of the Dejean–Laupretre–Monnerie (DLM) model contains the two parameters, τ_0 and τ_1, of the HWH model and a third correlation time, τ_2, describing the diffusion within the cone. The spectral density of the DLM model is given by Eq. *A-3* in the Appendix.

It should be noted that none of these dynamic models is related directly to polysaccharide structures as a basis for describing possible modes of reorientation in a carbohydrate chain. Nevertheless, some of them appear to offer a good approximation for linear polysaccharides (for instance, amylose) as seen in the following sections.

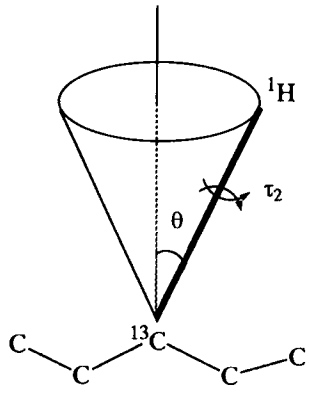

FIG. 8.—Dejean–Laupretre–Monnerie (DLM) motional model.

IV. Motional Description of Carbohydrate Molecules in Solution

Table I, which lists a number of mono-, oligo-, and polysaccharides and derivatives whose motional descriptions are available based on qualitative arguments, summarizes the experimental conditions and types of measurements used to obtain those descriptions. Table II deals specifically with those carbohydrates for which a quantitative treatment and dynamic modeling have been undertaken. In naming the compounds listed in Tables I and II, IUPAC rules are used for monosaccharide and less complex oligosaccharide molecules. However, empirical names are used for unusual oligosaccharides involving a complex aglycon substituent and polysaccharides. The gross motional features of a number of the compounds in Table I have been discussed in references 6–8, and will be mentioned here only if necessary for further clarification or for comparison with quantitative results.

1. Qualitative Motional Description

a. Monosaccharide Molecules.—Monosaccharide molecules in nonviscous media tumble in the extreme narrowing region. Therefore, n.O.e. values, assuming an asymptotic value of ~2.00, have no diagnostic utility in describing their motional characteristics. The same is true for spin–spin relaxation times because T_2 is usually equal to T_1 in this region (Eq. *16*). Moreover, T_2 values are affected preponderantly by low-frequency motions (slow motions), which are absent from these low-molecular-weight compounds. Nevertheless, spin–lattice relaxation times are affected by such intra- and intermolecular factors as molecular weight, differences in C—H bond lengths and other specific structural features, hydrogen bonding and solvent effects, and the type of the overall and internal motion.

Relaxation theory does not take explicit account of the molecular-weight dependence of the relaxation time. This factor enters indirectly into Eq. *23* in terms of the volume α^3. From this equation and Eqs. *22* and *24* it appears that, because large molecules tumble at a slower rate than small molecules of similar shape, the former are characterized by smaller T_1 values. This means that the TCF in Eq. *8* decays at a lower rate for large molecules and that the local magnetic fields are more persistent and hence more effective in causing relaxation. The effect of the molecular weight on the T_1 values for several carbohydrate molecules has been studied by Serianni and co-workers.[80–82] For example, C_5 glycosides tumble more slowly in solution than C_4 glycosides and have smaller T_1 values, as shown[80,81] by a comparison of methyl α-D-erythrofuranoside (**1**) and methyl α-D-ribofuranoside (**2**). Another example is the pair of orthoesters 3,4,6-tri-*O*-acetyl-1,2-*O*-(1-methoxyethyli-

TABLE I

Carbohydrate Molecules Whose Relaxation Behavior Has Been Treated Qualitatively

Carbohydrate	Solvent[a]	t (°C)	Field[b]	Data	Reference
A. Monosaccharides and Derivatives					
Arabinofuranose					
methyl α,β-D-glycoside	H_2O-D_2O	36	75	T_1, n.O.e.	80
3-Deoxytetrose	H_2O-D_2O	30	20	T_1, n.O.e.	81
Erythrofuranose					
α,β-D-	H_2O-D_2O	30	20	T_1, n.O.e.	81
methyl α,β-D-glycoside	H_2O-D_2O	30	20	T_1, n.O.e.	81
D-Fructose	D_2O	40	75	T_1, n.O.e.	83
	Me_2SO	40	75	T_1, n.O.e.	83
Galactopyranose					
α,β-D-	D_2O	35	20	T_1	84
2-acetamido-2-deoxy-α,β-D-	D_2O	28	25	T_1, n.O.e.	85
6-deoxy-α,β-L-	D_2O	28	25	T_1, n.O.e.	85
methyl α,β-D-glycoside	D_2O	28	25	T_1, n.O.e.	85
Glucopyranose					
α,β-D-	D_2O	5	28	T_1	86
	D_2O	35	20	T_1	84
	H_2O	45	15	T_1	87
methyl 2,3,4,6-tetra-*O*-acetyl-α,β-D-glycoside	D_2O	25	20	T_1, n.O.e.	88
methyl α,β-D-glycoside	D_2O	25	25	T_1, n.O.e.	89
	H_2O	25	25	T_1, n.O.e.	89
	D_2O	28	25	T_1, n.O.e.	85
	D_2O	25	50	T_1, n.O.e.	90
	D_2O	39	20	T_1, n.O.e.	88
	Me_2SO	25	25	T_1, n.O.e.	89
	Me_2SO	25	50	T_1, n.O.e.	90
	MeOH	25	50	T_1, n.O.e.	90
	$HCONMe_2$	25	50	T_1, n.O.e.	90
	Pyridine	25	50	T_1, n.O.e.	90
	AcOH	25	50	T_1, n.O.e.	90
	H_2O-D_2O	30	20	T_1, n.O.e.	81

DL-Glyceraldehyde	H_2O-D_2O	30	25	T_1, n.O.e.	81
Lyxofuranose					
α,β-D-	H_2O-D_2O	30	20	T_1, n.O.e.	81
methyl α-D-glycoside	H_2O-D_2O	37	75	T_1, n.O.e.	80
Mannopyranose					
2,3,4-tri-*O*-acetyl-1,6-anhydro-β-D-	C_6D_6	35	68	T_1	91
	$CDCl_3$	35	68	T_1	91
	Me_2SO	35	68	T_1	91
	Me_2SO	35	68	T_1	91
3,4,6-tri-*O*-acetyl-1,2-*O*-(1-benzyloxyethylidene)-β-D-	Me_2CO	20	50	T_1, n.O.e.	92
3,4,6-tri-*O*-acetyl-1,2-*O*-(1-methoxyethylidene)-β-D-	Me_2CO	20	50	T_1, n.O.e.	92
methyl 2,3-*O*-benzylidene-6-deoxy-α-L-	$CDCl_3$	55	25	T_1	93
Neuraminic acid					
N-acetyl-α,β-	D_2O	28	25	T_1, n.O.e.	94,95
N-acetyl-2,4,7,8,9-penta-*O*-acetyl-β-	D_2O	28	25	T_1, n.O.e.	94,95
N-acetyl-2,3-dehydro-	D_2O	28	25	T_1, n.O.e.	94,95
N-acetyl-2-*O*-methyl-α,β-	D_2O	28	25	T_1, n.O.e.	94,95
N-glycolyl-β-	D_2O	28	25	T_1, n.O.e.	94,95
Neuraminidate					
methyl *N*-acetyl-β-	D_2O	28	25	T_1, n.O.e.	94,95
methyl *N*-formyl-2-*O*-methyl-β-	D_2O	28	25	T_1, n.O.e.	94,95
Ribofuranose					
methyl α,β-D-glycoside	H_2O-D_2O	30	20	T_1, n.O.e.	81
	H_2O-D_2O	30	75	T_1, n.O.e.	80
	H_2O-D_2O	36	75	T_1, n.O.e.	82
	H_2O-D_2O	35	20	T_1, n.O.e.	81
Threofuranose					
α,β-D-	H_2O-D_2O	30	20	T_1, n.O.e.	81
methyl α,β-D-glycoside	H_2O-D_2O	30	20	T_1, n.O.e.	81
	H_2O-D_2O	36	75	T_1, n.O.e.	82
Xylofuranose					
5-deoxy-α,β-L-	H_2O-D_2O	30	20	T_1, n.O.e.	81
methyl α,β-D-glycoside	H_2O-D_2O	36	75	T_1, n.O.e.	80

continues

TABLE I—(*Continued*)

Carbohydrate	Solvent[a]	*t* (°C)	Field[b]	Data	Reference
B. Oligosaccharides, Complex Glycosides, and Derivatives					
N-Alkyl-(1-deoxylactitol-1-yl),	H_2O-D_2O		15	T_1	96
Chalcomycin	$CDCl_3$		25	T_1	97
Clindamycin · HCl	$CDCl_3$		25	T_1	98
Cyclodextrins					
cyclomaltohexaose	NaOD, D_2O	32	25	T_1	99
cyclomaltoheptaose	NaOD, D_2O	32	25	T_1	99
	NaOH, D_2O	33	25	T_1	100
Erythromycin A and B	$CDCl_3$	36	25	T_1	101
	$CDCl_3$		20	T_1, n.O.e.	102
an 11,12-cyclic carbonate	$CDCl_3$	60	25	T_1	103
Fructofuranoside					
α-D-galactopyranosyl-(1→6)-α-D-galactopyranosyl-(1→6)-α-D-glucopyranosyl-(1→2)-β-D [stachyose]	D_2O	65	15	T_1	104
	D_2O	55	50	T_1	105
α-D-glucopyranosyl-(1→2)-β-D [sucrose]	D_2O	55	50	T_1	105
	D_2O	32	68	T_1	106
Formazan					
1,5-diphenyl-3-(2,3,6-tri-*O*-acetyl-α-D-lyxofuranosyl)-	$CDCl_3$	60	25	T_1, n.O.e.	107
Glucopyranose					
β-D-galactopyranosyl-(1→4)-β-D- [lactose]	D_2O	28	20	T_1, n.O.e.	85
	D_2O	35	20	T_1	84
β-D-galactopyranosyl-(1→4)-benzyl β-D-glycoside	D_2O	25	25	T_1	108
β-D-galactopyranosyl-(1→4)-β-D-glucopyranosyl-(1→6)-benzyl β-D-glycoside	D_2O	25	25	T_1	108
β-D-galactopyranosyl-(1→4)-methyl β-D-glycoside	H_2O-D_2O	30	20	T_1, n.O.e.	81
	D_2O	35	20	T_1	84
	D_2O	35	20	T_1	85

O-α-D-glucopyranosyl-(1→4)-1,6-anhydro-β-D-, hexaacetate	Me_2CO	20	50	T_1, n.O.e.	109
O-β-D-glucopyranosyl-(1→4)-1,6-anhydro-β-D-, hexaacetate	Me_2CO	20	50	T_1, n.O.e.	110
(*N*-acetyl-α-neuraminic acid)-(2→3)-β-D-galactopyranosyl-(1→4)-α,β-D-	D_2O	35	20	T_1, n.O.e.	85
	D_2O		25	T_1	111
(*N*-acetyl-α-neuraminic acid)-(2→6)-β-D-galactopyranosyl-(1→4)-α,β-D-	D_2O		25	T_1	111
α-D-glucopyranosyl-(1→4)-β-D- [maltose]	D_2O	5	25	T_1	86
β-D-glucopyranosyl-(1→4)-β-D- [β-cellobiose]	D_2O	3, 13	50	T_1	112
methyl *O*-β-D-glucopyranosyl-(1→4)-β-D-glycoside	D_2O	35	20	T_1	84
per-*O*-acetyl-α-D-oligomers	$CDCl_3$	33	68	T_1	113
Isomaltose oligomers	D_2O	21	126	T_1	114
	D_2O	30	63	T_1, T_2	17
Lankamycin	$CDCl_3$	36	25	T_1	101
Leukomycin	$CDCl_3$		25	T_1	97
Lincomycin · HCl	D_2O		25	T_1	98
Megalomycin A and C2	$CDCl_3$		20	T_1, n.O.e.	102
Maltose oligomers	D_2O	21	126	T_1	114
	D_2O	30	63	T_1, T_2	17
Oleandomycin	$CDCl_3$	36	25	T_1	101
Paeoniflorine	Pyridine	25	25	T_1	115
Pircromycin	$CDCl_3$	36	25	T_1	101
Pullulan oligomers	D_2O	30	63	T_1, T_2	17
Rutin	Me_2SO		22.5	T_1	116
	Pyridine		22.5	T_1	116
Spiramycin	$CDCl_3$		25	T_1	97
k-Strophanthoside	Pyridine		22.5	T_1	117

continues

TABLE I—(*Continued*)

Carbohydrate	Solvent[a]	*t* (°C)	Field[b]	Data	Reference
Tylosin	$CDCl_3$		25	T_1	97
	$CDCl_3$	25	50	T_1, n.O.e.	118
Xylopyranose					
methyl β-D-glucopyranosyl-(1→4)-β-D-glycoside	D_2O	VT[c]	75	T_1	119
C. Polysaccharides					
Amylose	D_2O	VT	15	T_1, n.O.e.	9
	D_2O	21	126	T_1	114
					130
	D_2O	90	25	T_1	8
Cellulose triacetate	$CDCl_3$	33	68	T_1	113
	Me_2SO	VT	MF	T_1	120
	Me_2SO	VT	MF	T_1, T_2, n.O.e.	113
Dextrans	D_2O	90	25	T_1	121
	D_2O	21	126	T_1	114
	D_2O	34,90	25	T_1, n.O.e.	8
Glucans					
β-D-(1→3)-	Me_2SO	28	25	T_1, n.O.e.	122
	Me_2SO		15	T_1, LW[e]	123
Heparin	D_2O	70	75	T_1, LW	124
Inulin	H_2O–D_2O	30	25	T_1, n.O.e., LW	125
Klebsiella K-18 and K-41	D_2O		63	T_1	16
Mannans	D_2O	70,90	25	T_1, n.O.e.	126
Pullulan	D_2O	30	63	T_1, T_2	17
	D_2O	20	25	T_1	8
Starches	Me_2SO	80	75	T_1, n.O.e.	127

[a] Me_2CO, acetone; Me_2SO, dimethyl sulfoxide; MeOH, methanol; $HCONMe_2$, *N*, *N*-dimethylformamide; AcOH, acetic acid; $CDCl_3$, deuterated chloroform.

[b] In megahertz.

[c] VT, variable-temperature measurements.

[d] MF, multifield measurements.

[e] LW, linewidth.

dene)-β-D-mannopyranose (**3**) and 3,4,6-tri-*O*-acetyl-1,2-*O*-(1-benzyloxyethylidene)-β-D-mannopyranose (**4**).

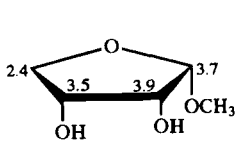

1

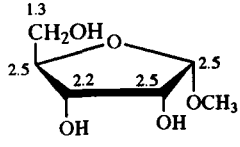

2

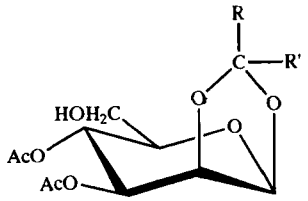

3 R = CH_3, R' = OCH_3

4 R = CH_3, R' = OCH_2Ph

In each molecule, all of the ring carbon atoms bearing a single proton show essentially the same ^{13}C T_1 values, indicating an approximately isotropic motion.[92] However, the presence of the heavier, *exo* benzyl group in **4** results in smaller T_1 values than in **3**, which has an *exo* methyl group. The effective correlation times calculated from the average of the T_1 values of the ring carbons were 18.2 ps and 26.0 ps for the methoxy and benzyloxy derivatives, respectively.

Dais and Perlin[90] have invoked the molecular-weight dependence of the T_1 values in conjunction with solvent effects in order to explain the dynamic behavior of a pair of anomeric glycosides, namely methyl α-D- (**5a**) and methyl β-D-glucopyranoside (**5b**) in a group of solvents that represent an extended range of such properties as viscosity and dielectric constants.

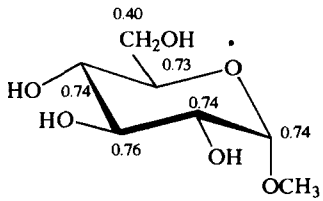

5a

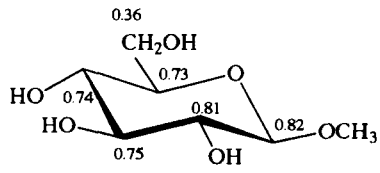

5b

TABLE II

Carbohydrate Molecules Whose Relaxation Behavior Has Been Treated Quantitatively

Carbohydrate molecules	Solvent[a]	t (°C)	Field[b]	Data	Reference
A. Monosaccharides					
Allofuranose					
1,2:5,6-di-*O*-isopropylidene-α-D-	Me_2CO	20	50	T_1, n.O.e.	12
2,3:5,6-di-*O*-isopropylidene-β-D-	Me_2CO	20	50	T_1, n.O.e.	12
Altrofuranose					
2,3:5,6-di-*O*-isopropylidene-β-D-	Me_2CO	20	50	T_1, n.O.e.	12
Apiose					
1,2:3,5-di-*O*-isopropylidene-β-L-	Me_2CO	20	50	T_1, n.O.e.	12
Glucofuranose					
2,3:5,6-di-*O*-isopropylidene-α-D-	Me_2CO	20	50	T_1, n.O.e.	12
Mannofuranose					
2,3:5,6-di-*O*-isopropylidene-α-D-	Me_2SO	VT[c]	50	T_1, n.O.e.	67
Psicose					
1,2:3,4-di-*O*-isopropylidene-β-D-	Me_2CO	20	50	T_1, n.O.e.	12
Xylofuranose					
1,2:3,5-di-*O*-isopropylidene-α-D-	Me_2CO	20	50	T_1, n.O.e.	12
Pyrone					
5-acetoxy-5,6-dihydro-6-(1,2-epoxypropyl)-2-	Me_2SO	VT	50	T_1, n.O.e.	13
B. Oligosaccharides					
Fructofuranoside					
α-D-glucopyranosyl-(1→2)-β-D- [sucrose]	D_2O	42	15	T_1, n.O.e.	14
	D_2O	VT	MF[d]	T_1, n.O.e.	128
	D_2O	VT	MF	T_1, n.O.e.	129

	Me_2SO	VT	MF	T_1, n.O.e.	129
	D_2O	VT	MF	T_1, n.O.e.	130
Glucopyranose					
β-D-galactopyranosyl-(1→4)-α-D-	D_2O	28	20	T_1, n.O.e.	85
	D_2O	35	20	T_1	84
methyl β-D-galactopyranosyl-(1→4)-β-D-glycoside	D_2O	28	20	T_1, n.O.e.	85
	D_2O	35	20	T_1	84
methyl β-D-glucopyranosyl-(1→4)-β-D-glycoside	D_2O	35	20	T_1	84
methyl 3-*O*-α-D-rhamnopyranosyl-α-D-glycoside	D_2O-Me_2SO	VT	MF	T_1, n.O.e.	129
Lacto-*N*-neotetraose	D_2O-Me_2SO	VT	MF	T_1, n.O.e.	131
C. Polysaccharides					
Amylose	D_2O	VT	15	T_1, n.O.e.	9
	Me_2SO	VT	15	T_1, n.O.e.	9
	Me_2SO	80	MF	T_1, T_2, n.O.e.	10,11,132
Bovine nasal cartilage	D_2O	37	15	T_1, n.O.e.	133
Chondroitin 4-sulfate	D_2O	37	15	T_1, n.O.e.	133
Curdlan	D_2O	28	25	T_1, n.O.e., LW[d]	134
	D_2O	60	25	T_1, n.O.e., LW	135
Dextrans	Phosphate buffer	36	20	T_1, n.O.e., LW	136
	D_2O	VT	15	T_1, n.O.e.	9
	Me_2SO	VT	15	T_1, n.O.e.	9

[a]Me_2CO, acetone; Me_2SO, dimethyl sulfoxide; MeOH, methanol; $HCONMe_2$, *N*, *N*-dimethylformamide; AcOH, acetic acid; $CDCl_3$, deuterated chloroform.

[b]In megahertz.

[c]VT, variable-temperature measurements.

[d]MF, multifield measurements.

[e]LW, linewidth.

The effective correlation times for an approximately isotropic motion, τ_R, ranged from 40.3 ps in methanol to 100.7 ps in acetic acid for **5a**, and from 61.6 ps to 180.1 ps for **5b** in the same solvents. Neither solvent viscosity nor dielectric constant bore any direct relationship to the correlation times found from the overall motion, and attempts to correlate relaxation data with parameters (other than dielectric constant) that reflect solvent polarity, such as Kosover Z-values, Winstein Y-values, and the like, were unsuccessful.[90] Based on the maximum allowed error of ± 13% in the τ_R values derived from the propagation of the experimental error in the measured T_1 values, the rate of the overall motion for either **5a** or **5b** in these solvents followed the order: methanol ≈ *N*,*N*-dimethylformamide ≈ D_2O < pyridine < dimethyl sulfoxide. This sequence appears to reflect both the solvent viscosity and the molecular weight of the solvated species. On this basis, and assuming that each hydroxyl group is hydrogen-bonded to two molecules of the solvent,[137] the molecular weights of the solvated species are as follows: in methanol 256, *N*,*N*-dimethylformamide 364, water 144, pyridine 496, and dimethyl sulfoxide 312.

Another intramolecular factor reflected in the measured relaxation times is the C—H bond length, which appears in Eqs. *12* and *16*. Nonuniformity in the bond lengths for the various C—H vectors in an isotropic tumbler may result in reproducible differences among their respective T_1 values. A 1% increase in bond length used in a relaxation calculation would overestimate the T_1 value by 6%.[138] Conversely, a correlation time deduced from the experimental value of T_1 would be overestimated by 6%. This effect should be taken into consideration in analyzing apparent differences in relaxation times, either by estimating bond lengths from other sources, such as infrared or microwave spectra, or by performing additional relaxation experiments. Deuterium spin–lattice relaxation times of selectively deuterated compounds is a consistent method of evaluating differences in bond lengths, since ^2H T_1 values are predominantly quadrupolar and essentially unaffected by bond lengths.[4,18–26]

The effect of C—H bond length on T_1 is evidenced[81] in a comparison of T_1 values for C-1 of the hydrated (**6a**) and free aldehyde (**6b**) forms of enriched DL-[1-^{13}C]glyceraldehyde. The difference in T_1 values between these forms cannot be explained by molecular-weight effects alone, whereas a shorter C-1—H-1 bond in the aldehyde form (expected when a carbon changes from sp^3 to sp^2 hybridization) would cause C-1 to relax faster and produce the small difference in relaxation times.

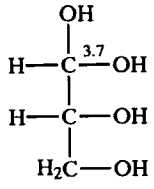

6a

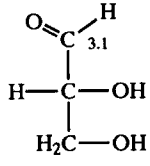

6b

Since T_1 depends on the inverse of the sixth power of the $r_{C\text{-}H}$ distance (Eqs. *12* and *16*), a directly attached proton makes the most significant contribution to the relaxation of a given carbon relative to more distant protons in the molecule. The contribution of the latter is usually as little as 2–3% and may be ignored for qualitative descriptions. However, for quantitative treatment, or in particular cases where the carbon of interest is surrounded by several nonbonded protons, Eq. *25* should be used for the analysis of the relaxation data. Such an example is offered by sucrose (**7**).[105] The substantially longer T_1 value (6.0 s) for the quaternary C-2′ carbon relative to the T_1 values of the remaining ring carbons (average 0.5 s) reflects the lack of efficient dipolar relaxation by a directly bonded proton. However, a full n.O.e. was found for this carbon, indicating that the surrounding nonbonded protons are effective contributors to its dipolar relaxation.

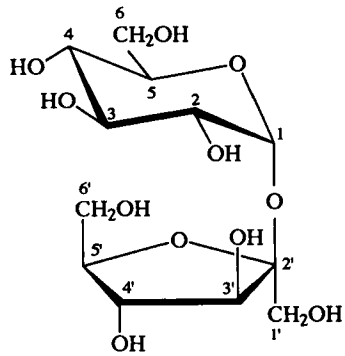

7

Specific structural features of monosaccharides are manifested in several ways, such as changes in the type of the overall motion, free or hindered internal flexibility, and intramolecular versus intermolecular hydrogen bonding. All of the pentofuranoses and pentofuranosides studied[80–83] appear to tumble isotropically in solution, as evidenced by the similarity of the T_1 values of the ring carbons. This suggests that exocyclic hydroxymethyl groups stabilize the furanosyl ring conformation, or if any puckering motion exists, it must be very slow to affect relaxation data. For the tetrofuranosyl rings, however, which lack the exocyclic hydroxymethyl group, NT_1 values for the C-4 carbons (relaxed via two directly bonded protons) are larger than the average T_1 values for the remaining ring carbons (compare compounds **1** and **2**). This observation[82] is commensurate with internal flexibility at the C-4 site for the tetrofuranosyl ring. Another observation,[82] an explanation of which is unclear, is the fact that the C-1, C-2, and C-3 carbons of

methyl α-D-erythrofuranoside (**1**) are characterized by significantly lower T_1 values than those of its β anomer (**8**).

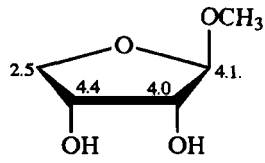

8

The motional behavior of the majority of hexopyranoses and derivatives listed in Table I has been described as isotropic, despite the fact that sizeable differences, well outside the experimental error, have been observed in the T_1 values of the ring carbons in several instances. Anisotropic motion has been observed for methyl β-D-galactopyranoside[85] (**9**), methyl β-D-glycopyranoside[85,90] (**5b**), and both anomers of the 6-deoxy sugar L-fucose[85] (α-L- **10a** and β-L- **10b**). Other examples are *exo* (**11a**) and *endo* (**11b**) methyl 2,3-*O*-benzylidene-α-L-rhamnopyranoside, which have been described[93] as isotropic tumblers, although there are large differences, as much as 26% (experimental error $\pm$ 6%) among the carbons of the pyranosyl ring, especially for the *exo* derivative. The anisotropy usually observed in the overall motion of β-hexopyranosides relative to α-hexopyranosides, which reorient nearly isotropically, has been attributed[85] to an effect of the β-anomeric substituent on the inertial axes, sufficient to cause molecular diffusion about a preferred, but undefined axis of rotation.

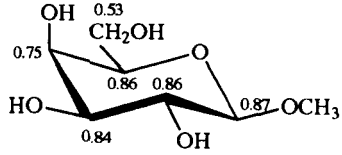

9

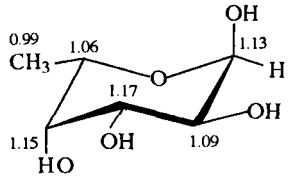

10a

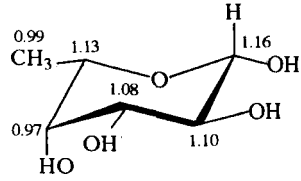

10b

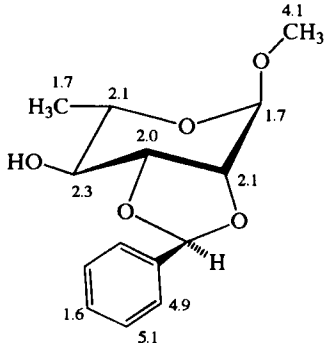

11a

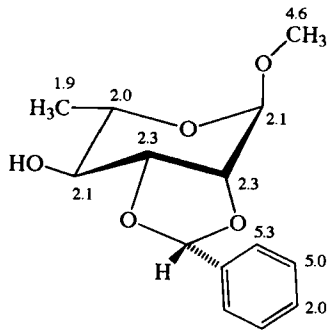

11b

Although the basic argument seems correct, it is unlikely that the anisotropic motion of, say, compound **9** can be described in terms of a preferred axis of rotation. Moreover, such solvent effects as hydrogen bonding may alter the overall shape of the solvated species, resulting not only in a further shift of the principal axes of the diffusion tensor, but also in a different type of overall motion. This phenomenon is observed for molecule **5b**, which rotates isotropically in such protonated solvents as methanol and acetic acid, whereas a slight anisotropy is detected in D_2O, *N*,*N*-dimethylformamide, pyridine, and dimethyl sulfoxide.[90] Moreover, anisotropic motion has also been observed for both anomers of compound **10**. In general, these asymmetric molecules contain several hydroxyl groups and oxygen atoms that constitute strong solvating centers. Therefore, as mentioned earlier, the assumption that the principal axes of the diffusion tensor coincide with the principal axes of the moment of inertia tensor may not be justified for these highly polar molecules. Rather, the three Euler angles defining the orientation of the diffusion tensor, in addition to the three diffusion coefficients, should be determined (Eq. *29*). As a general statement, if the relaxation data describing overall motion of hexopyranoses are not amenable to quantitative treatment, any observed anisotropy of this motion should be presented clearly.

Internal rotation occurring in pentofuranoses, hexopyranoses, and their derivatives is manifested mainly in the NT_1 values of the exocyclic hydroxymethyl carbon (moderated by two protons), which are usually larger than those of the ring carbons (see compounds **2**, **5**, and **9**). This indicates that the exocyclic carbon, apart from the overall motion, receives a relaxation contribution from internal motion about the C-4—C-5 or C-5— C-6 bond. The degree of motional freedom of the hydroxymethyl group depends mainly on structural details, as well as on the existence and strength of intramolecular hydrogen bonding. Thus, the shorter T_1 value observed[85] for the C-6 carbon in compound **5a** and **5b** relative to that in compound **9** has been attributed to a more restricted internal rotation in the former

derivatives owing to some intramolecular interaction (possibly hydrogen bonding) not present in the D-galactose derivative.

Although the hydroxymethyl groups of the α- and β anomers of methyl D-glucopyranosides exhibit the same motional freedom in D_2O,[85,90] changes of solvent are accompanied by a greater degree of motional freedom in the α than in the β anomer. As there is no obvious basis for assuming large differences in the rotational conformation and solvation pattern at C-6 for these monomers, the differing degrees of motional freedom consistent with the relaxation data can be attributed to variations in their principal diffusion axes and to effects on the T_1 data, as mentioned previously.

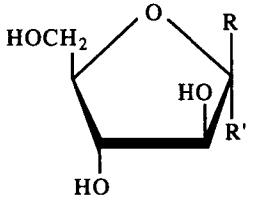

12a R = OH, R' = CH_2OH
12b R = CH_2OH, R' = OH

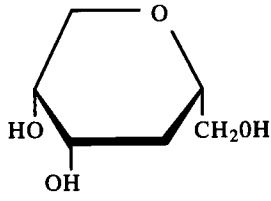

13

Another interesting example of hindered internal rotation is related to the relative stability of the β-furanose form of D-fructose (**12a**) in dimethyl sulfoxide solutions,[83,139-141] in marked contrast to the fact that the β-pyranose form (**13**) is by far the predominant tautomer in water. From the ^{13}C T_1 relaxation data[83] (see Table III) of the three major tautomers of D-fructose—α-furanose (**12b**), β-furanose (**12a**), and β-pyranose (**13**)—it can be concluded that these tautomers tumble isotropically in both D_2O and $(CD_3)_2SO$ solutions. The T_1 values[83] for the second-

TABLE III

^{13}C Spin–Lattice Relaxation Times (in Seconds) for the Protonated Carbon Atoms of the Three Major Tautomers of D-Fructose in D_2O and Me_2SO Solutions[a]

	α-f		*β-f*		*α-p*	
Carbon	**D_2O**	**Me_2SO**	**D_2O**	**Me_2SO**	**D_2O**	**Me_2SO**
C-1	0.88	0.33	0.88	0.28	0.93	0.34
C-3	1.73	0.55	1.50	0.53	1.60	0.53
C-4	1.74	0.53	1.61	0.51	1.53	0.52
C-5	1.69	0.55	1.68	0.54	1.50	0.52
C-6	0.95	0.31	0.94	0.29	0.81	0.33

[a] 1.5 *M* at 40°

ary carbons of **12a**, **12b**, and **13**, respectively, are all within 1.64 ± 0.08 s, 1.73 ± 0.07 s, and 1.55 ± 0.05 s in D_2O and 0.53 ± 0.03 s, 0.54 ± 0.04 s, and 0.52 ± 0.03 s in $(CD_3)_2SO$. In the absence of freedom of rotation about the exocyclic C—C bonds, the T_1 value of the primary carbons would be expected to be one-half that of the secondary carbon. However, these values for all isomers in D_2O are greater than the relaxation times of the overall motion.[83] This is indicative of relatively fast internal motions about the C-1—C-2 and C-5—C-6 bonds. Also, the corresponding values for **12b** and **13** in $(CD_3)_2SO$ are greater than those of the ring carbons, again indicative of fast internal rotations, as in D_2O. By contrast, the NT_1 values for the primary carbons of **12a** are only slightly greater than those of the overall motion, suggesting that there is restricted motion about the exocyclic bonds. These restricted motions have been attributed[139,140] to the presence of an intramolecular hydrogen-bonding network which, in turn, should be a major enhancement in stability for the β-furanose form in $(CD_3)_2SO$ solutions.

A final example of restricted internal motion attributable to intramolecular hydrogen bonding is offered by methyl α-*N*-acetylneuraminidic acid (**14**) and

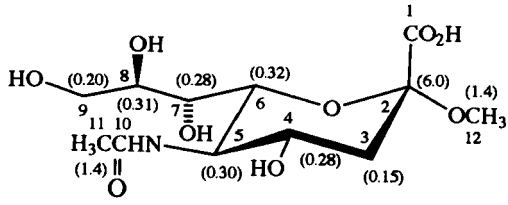

14

derivatives.[94,95] Although methyl groups experience considerable free rotation about their C_3 symmetry axis, independent of the overall molecular motion, the motions of the C-7 and C-8 carbons of the side chain are isotropic with respect to the ring, as evidenced by the near equality of their T_1 values with those of the ring carbons (C-3, C-4, C-5, C-6). The latter values, being closely similar, indicate isotropic overall motion. This evidence of hindered motion has been explained in terms of an intramolecular hydrogen-bonding network (Fig. 9), which locks the ring very strongly into its favored conformation and links the motion of C-7 and C-8 to the ring through highly favorable six-membered ring interactions. In addition, further stabilization of this conformation is possible through formation of a third intramolecular hydrogen bond, between the acetamido carbonyl oxygen and the C-4 hydroxyl group in a seven membered ring (Fig. 9).

b. Oligosaccharides, Complex Glycosides, and Derivatives.—Since the pioneering work of Allerhand and Doddrell[104] in 1971 employing relaxation measurements as an effective methodology for the assignment of resonances in proton-decoupled ^{13}C spectra of stachyose, raffinose, and sucrose, several publica-

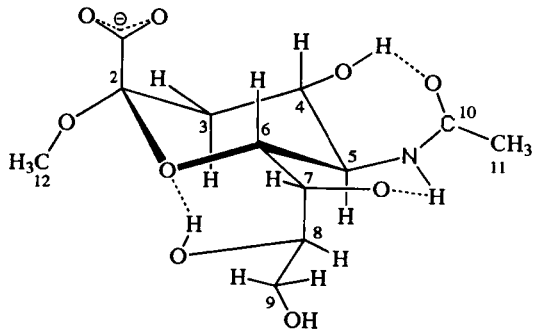

FIG. 9.—Conformational model of anion of **14** showing the proposed hydrogen-bond network and favored conformation of the glycerol side chain. [Reproduced with permission from Fig. 1 of M. F. Czarniecki and E. R. Thornton, *J. Am. Chem. Soc.*, 98 (1976) 1023–1025.]

tions have appeared in the literature adopting the same strategy. The main qualitative conclusions from these studies can be summarized as follows:

(1) The similarity of the T_1 values for all the ring carbons in a disaccharide molecule may indicate isotropic tumbling without a preferred axis of rotation.

(2) Anisotropy in the molecular reorientation of a disaccharide molecule is to be expected when a C—H bond vector of the molecule lies on or near a preferred axis of rotation. This results in a shorter T_1 value for carbons whose C—H bonds lie along the anisotropic axis than for those having other orientations.

(3) The NT_1 values of an exocyclic hydroxymethyl carbon and/or of a methyl carbon (moderated by two and three protons, respectively) are in general higher than those of the ring carbons. This indicates internal reorientation about the exocyclic bond, the rate of rotation being dependent on the molecular geometry.

(4) For tri-, tetra-, and oligosaccharides a gradation in the T_1 values of the ring carbons, from the internal monosaccharide residue to the terminal saccharide groups, is observed. This reflects an increase in internal flexibility on going from the internal residue(s) toward the end of the carbohydrate chain. The internal flexibility is more pronounced when one end of the oligosaccharide is anchored either by hydrogen bonding or some other electrostatic interaction, or by attachment through a chemical bond to a heavy anchor.

(5) Although no systematic studies have been performed to examine the effect of the types of glycosidic bonds that link the various monosaccharide units in the oligosaccharides, the nature of these bonds is expected to modify mobility along the carbohydrate chain.

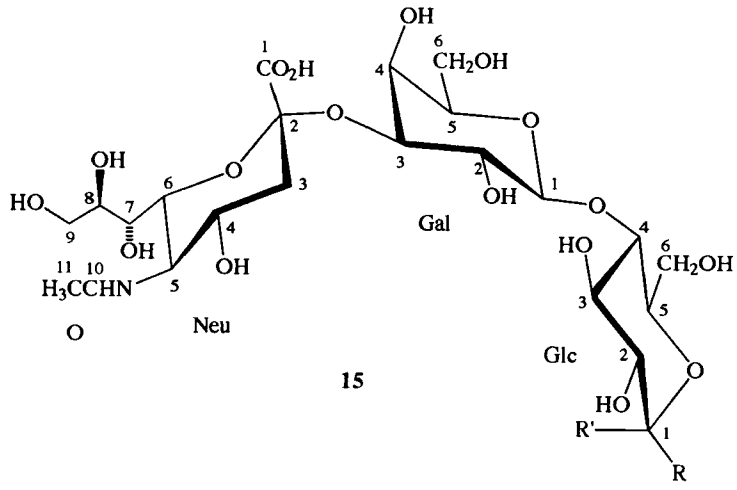

15

	R	R'
α	H	OH
β	OH	H

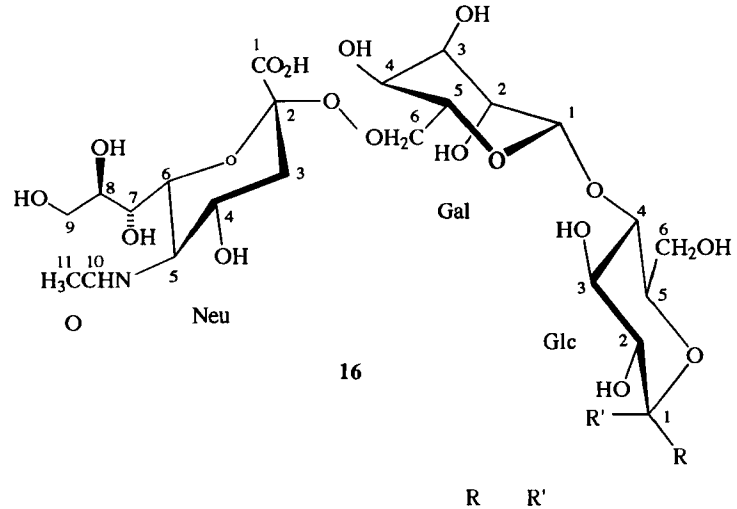

16

	R	R'
α	H	OH
β	OH	H

An example of hindered internal motion in oligosaccharides is offered by the two cell-membrane trisaccharides (*N*-acetyl-α-neuraminic acid)-(2→3)-β-D-galactopyranosyl-(1→4)-D-glucopyranose (**15**)[85] and (*N*-acetyl-α-neuraminic acid)-(2→6)-β-D-galactopyranosyl-(1→4)-D-glucopyranose (**16**),[111] which differ by the α-(2→3) and α-(2→6) glycosidic linkage between the neuraminic acid group and the D-galactopyranosyl residue. The T_1 value for the C-6 of the galactopyranosyl residue decreases from 0.145 s for the α-(2→3) isomer to 0.08 s for the α-(2→6)-linked isomer, indicating a more restricted motion of the glycosidically linked carbon in the latter.

A nuclear magnetic relaxation study[85] of lactose (**17**), which is a basic constituent disaccharide unit of all gangliosides, demonstrates that this molecule reorients anisotropically. The favored axis of molecular reorientation appears to lie along the axis of the molecule and therefore is reflected in the shorter T_1 value at C-4 of the galactose residue. The apparent differences between the relaxation times observed for the C-1 resonances of the α (**17a**) and β (**17b**) isomers may also be reflected in their differing C—H orientations relative to the anisotropic axis. Similar anisotropic motion was observed for methyl β-lactoside,[85] methyl β-cellobioside,[84] and other disaccharide derivatives in solution.

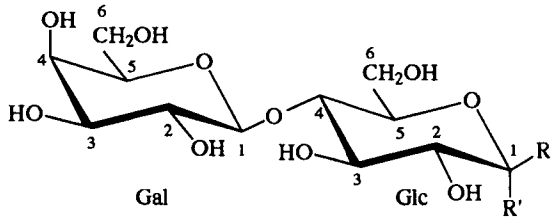

C	α-Glc	β-Glc	Gal
1	0.34	0.41	0.37
2	0.43	0.39	0.39
3	0.40	0.42	0.40
4	0.35	0.39	0.30
5	0.41	0.35	0.38
6	0.18	0.18	0.27

17a R = H, R' = OH

17b R = OH, R' = H

The presence of anisotropic motion along the molecular length is suggested for trisaccharide **15** as the anomeric carbons of the α and β anomers show different T_1 values.[85] A smaller T_1 for the C-1 carbon of the α anomer (0.11 s) relative to that of the β anomer (0.24 s) indicates a close correspondence between the equatorial C–H vector in the α-anomer and the favored axis of rotation. By contrast, relaxation studies on sucrose[14,106] (**7**) did not reveal anisotropic motion (however, see below).

As noted previously, internal mobility along a carbohydrate chain is more pronounced if one end of the chain-like molecule is fixed by chemical or physico-

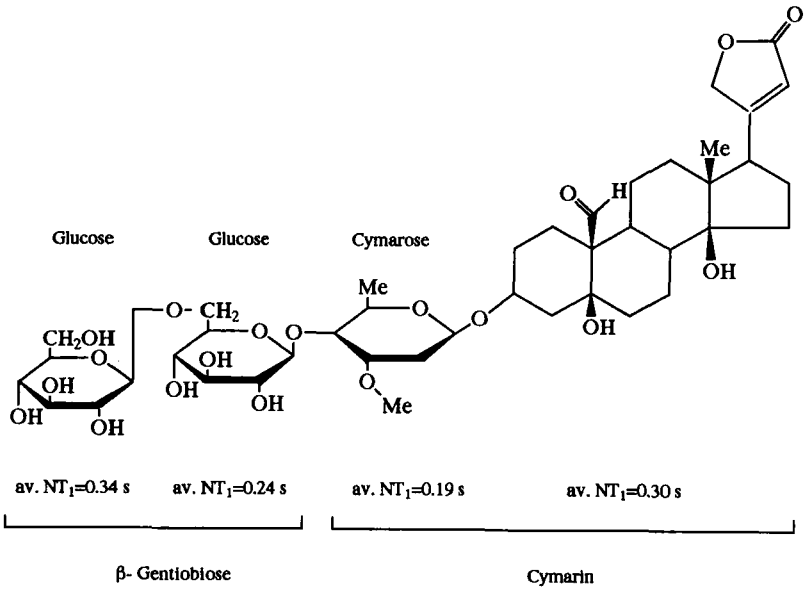

18

chemical bonding to a heavy anchor. A number of biologically important molecules are made up of a complex aglycon to which one or several sugar units may be radially attached. A representative example is κ-strophanthoside (**18**)[117]. Relaxation-time measurements allow assignment of the carbon atoms belonging either to the steroid or to the oligosaccharide component. Furthermore, the average T_1 values for the three-sugar component reflect their sequence with respect to the steroid anchor, namely T_1(terminal glycose) > T_1(central glucose) > T_1(inner sugar, cymarose). This trend in the T_1 values reflects an increase in flexibility along the oligosaccharide chain, from the sugar residue attached to the steroid toward the nonreducing end unit.

Internal flexibility along a carbohydrate chain is also reflected in T_1 data for **15** and **16**. An observed increase in T_1 values,[85,111] proceeding from the neuraminic acid residue through those of galactose and glucose, indicates increasing mobility along the same direction. However, unlike the segmental motion in stachyose,[104,108] which radiates from the central residues, the neuraminic acid component in **15** and **16** is the least mobile and appears to anchor one end of the molecule in solution.

Other interesting examples of segmental motion that clearly reflect the sequence of monosaccharide units in a given oligosaccharide are the disaccharide benzyl β-lactoside and the trisaccharide benzyl 6-*O*-(β-lactosyl)-β-D-glucopyranoside, which are attached via complexation to heptakis(2,6-di-*O*-methyl)cyclomalto-

heptaose.[108] Complex formation through the aglycon of the oligosaccharides resulted in a monotonic increase in T_1 values toward the free end of the molecules, indicating that the motional degree of freedom increases in the same direction. Similar trends were observed[97,98,101–103] in the T_1 data for a number of 14- and 16-membered macrolide antibiotics, as well as terpenoid glucosides.[115]

c. Polysaccharides.—Geometric differences within a carbohydrate chain owing to the presence of different monosaccharide residues and/or different types of glycosidic linkages result in a wide range of conformational characteristics. For instance, linear homopolysaccharides of a given hexose, such as amylose and cellulose, differing only in the glycosidic linkage position or anomeric configuration, show remarkably different solution properties owing to well known differences in their equilibrium stereochemistry.[142] The time dependence of local conformational changes in solution in the nanosecond frequency range, known as segmental motion, is described by a TCF that reflects the geometric constraints of the carbohydrate chains. These constraints, arising primarily from nonbonded interactions between the sugar residues, restrict motion about the chemical bonds of the glycosidic linkages and modulate the frequency and the strength of the local magnetic fields. Constraints around the glycosidic bonds, usually expressed in terms of torsional angles φ and ψ [and ω for (1→6) glycosidic bonds], may introduce severe restrictions on the domain of the conformational space accessible to the backbone units.

Apart from solvent effects and intramolecular hydrogen bonding, the space available to the allowed conformations depends on the type of the glycosidic linkage and the nature of the monosaccharide residues in the chain.[142] Thus, amylose, an α-(1→4)-linked glucan, is expected[11] to have a relatively smaller domain of (φ, ψ) conformational space than linear dextran, an α-(1→6)-linked glucan. In the latter the presence of three single bonds between the pyranose rings of adjacent sugar residues allows for a considerably wider range of orientations of these residues relative to each other,[114,142] and hence an increase in chain flexibility.

Support for this expectation has been obtained by Matsuo,[9] who compared the ^{13}C NMR relaxation behavior of linear dextran and amylose at ~ 15% w/v solutions in $(CD_3)_2SO$ as a function of temperature, inasmuch as dextran displayed distinctly larger T_1 values than amylose above ~ 40°C. Nevertheless the T_1 values for the two polymers were the same in $(CD_3)_2SO$, and perhaps in D_2O, in the temperature range 28–40°. This behavior suggests that in dilute aqueous solutions at room temperature viscous damping effects predominate over contributions to T_1-sensitive conformational differences in the glycosidic-linkage region. At elevated temperatures, however, the relaxation behavior of amylose and dextran is consistent with a transition to dominance of the conformational dynamics by the geometric characteristics of the glycosidic bonds. Brant *et al.*[114] observed similar relaxation behavior for the maltose and isomaltose oligosaccharides in D_2O solu-

tion. At a concentration of 3 g/dL the T_1 values of the two homooligomers were indistinguishable at 21°C.

The relative conformational freedom within a linear homopolysaccharide of hexose residues linked by two different types of glycosidic linkages has been examined with polymeric[8,17] and oligomeric[17] forms of pullulan, a fundamental fragment of which (**19**) contains two α-(1→4)- and one α-(1→6)-linked D-glucopyranosyl residues. It is to be expected that the segmental motion of the backbone is not uniform, with regions of increased segmental motion centered around

- [- α- *D* - Glc*p* -(1➤6)- α- *D* - Glc*p* - (1➤4)- α- *D* -Glc*p* - (1➤4) -] $_x$-

19

the α-(1→6)-linked residues. On this basis, the C-1 and C-4 carbons of the latter, being directly attached to the mobile α-(1→6)-linked residue, should have the larger T_1 values. Indeed, this has been observed.[8] The pullulan oligomers show a rapid leveling off in their T_1 and T_2 values after an initial sharp decrease in going from glucose to maltotetraose. This behavior indicates a progressive increase in relative motion from the stiff maltotetraose oligomer having α-(1→4) linkages to the pullulan oligomers, which contain the more flexible α-(1→6) linkages.[17]

Other measurements of dipolar ^{13}C relaxation parameters, T_1, T_2, and n.O.e. have been reported for glucose oligomers corresponding in structure to pullulan,[17] amylose, and dextran,[114] as well as to cellulose triacetate (CTA)[113] in an attempt to mimic segmental motion occurring in the high-molecular-weight analogs. Comparison of the relaxation parameters of the interior carbon resonances of the oligomers with those of the corresponding polymers gives an indication of the critical length of oligomer required to match segmental motion occurring in the polymer chain. For instance, the critical degree of polymerization of the pullulan oligomers, all of whose interior carbons have T_1, T_2, and n.O.e. values within 10% of their values for polymeric pullulan,[17] is 15. At this level, local motion must be very similar in both carbohydrate chains, despite their large molecular-weight difference. For the α-cello-oligosaccharides[113] and the maltose and isomaltose oligomers,[114] the critical degree of polymerization expected to match the segmental mobility of cellulose triacetate, amylose, and linear dextran were 7, 8, and 8, respectively.

Macroscopic and microscopic conformational changes of cellulose esters in $CDCl_3$ solution have been examined as a function of temperature and concentration.[120] The temperature dependence of the T_1 values for the carbonyl and ring carbons of CTA in $CDCl_3$ shows a remarkable change in segmental motion at ~ 53°C. This apparent transition, which is observed neither in solutions of CTA in $(CD_3)_2SO$ nor in solutions of cellulose propanoate and cellulose butanoate in

$CDCl_3$, has been attributed[120] to changes in supramolecular structure (interactions between polymer chains) rather than to changes in microscopic conformation accompanied by changes in monomer conformation, or to changes in the angle about the virtual bond connecting the monomer units. However, concentration effects on the T_1 values show a more complex pattern, which may be attributed to interrelated changes in both macroscopic and microscopic conformation.[120]

Other applications of ^{13}C NMR relaxation measurements have been concerned with determining the sequence of the monosaccharide residues in the complex biopolymer structures[8,15,113,121,125,126] and distinguishing between the sugar units in the side chain rather than the main chain, or identifying a branch-point position.[8,16,121,123–127] This approach is based primarily on differences in segmental mobility observed along the carbohydrate chain of linear polysaccharides arising from the nature of the monosaccharide units, the type of linkages, and, for branched polysaccharides, differences in segmental motion between the main and side chains.

Seymour and Knapp[8] performed a systematic study on α-D-glucans, including dextrans (**20**) and a synthetically prepared branched derivative of amylose (**21**). In these structures, *t* is a terminal group, *b* is a branch-point residue, *l* is a linear chain-extending residue (which is considered to be constant), and *m* is the carbon-atom number at the position of branching. The ^{13}C chemical-shift assignments were facilitated by comparing the T_1 values of the various carbon resonances of the monosaccharide residues in the main and side chains with those of the monosaccharide residue at the branch-point. The relative magnitudes of T_1 values associated with the various carbon-atom positions in the branched polysaccharides were reasonable indices of the relative degrees of segmental motion. These values increase in the order $T_1(b) < T_1(l) < T_1(t)$, thus reflecting increasing segmental mobility. A general summary of several other important observations based on relaxation data from linear and branched α-D-glucans can be found in references 8 and 127.

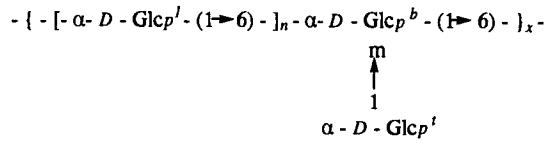

20

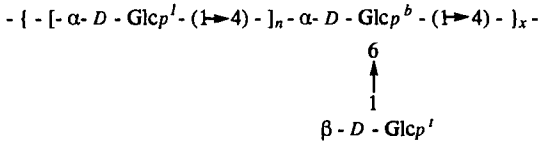

21

2. Quantitative Motional Description

a. Monosaccharide Molecules.—To obtain a full understanding of the dynamic behavior of a monosaccharide molecule in solution, the experimental relaxation data should be treated quantitatively in terms of a motional model that describes the various degrees of freedom. However, the relaxation data may not uniquely define a dynamic model, and several models may be capable of reproducing the experimental relaxation parameters. The problem of discriminating between models can be solved either by inspection of the molecular shape and existing geometric constraints or by conducting variable-temperature relaxation measurements. As to the first approach, molecular shape is important for describing overall isotropic and anisotropic molecular motion, whereas geometric constraints may restrict internal rotation of a flexible segment to within a narrow angular range (such as rotation-in-a-cone, or restricted internal diffusion). In such a case, a model based on free internal motion may not be compatible with the experimental data. The second approach is more rigorous in testing the suitability of the motional model adopted and provides, in addition, activation energies, which are useful kinetic parameters of molecular reorientation in solution.

Variable-temperature ^{13}C NMR spin–lattice relaxation time measurements have been used to probe the motional behavior of 2,3:5,6-di-*O*-isopropylidene-α-D-mannofuranose (**22**) in dimethyl sulfoxide solution.[67] This carbohydrate derivative offers structural features well suited to the study of a variety of internal motions, such as ring oscillation, ring-puckering interconversion, and methyl internal rotation, all of which are superposed on an isotropic overall reorientation. Isotropic overall motion is reflected in the T_1 values of the protonated ring carbons of the mannose ring, which are equal (within experimental error) at each temperature.[67]

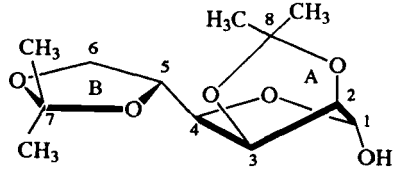

22

An Arrhenius-type plot of the correlation time of the overall motion (calculated with the use of Eq. *16*) versus reciprocal temperature yields an activation energy of 20.4 kJ/mol. Among the various models examined to evaluate internal rotations, a two-state jump model[56,143] was found satisfactory for interpreting the oscillatory and puckering motions of the flexible 5,6-*O*-isopropylidene ring. In this model the C—H vector jumps between two equivalent, stable states A and B characterized by correlation times τ_A and τ_B, respectively (Fig. 10). The angle β is defined by the

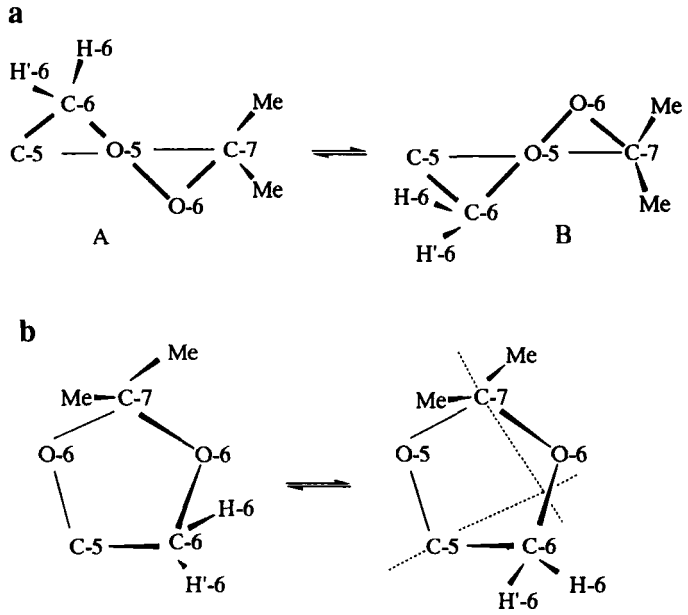

FIG. 10.—Dynamic model for the flexible 5,6-*O*-isopropylidene ring in **22**. (a) Interconversion between two antisymmetric C_2 forms; (b) same, as viewed perpendicular to the C-5—O-5—C-7 plane. The two effective internal jump axes are indicated by dotted lines. [Reproduced with permission from Fig. 3 of P. Dais and A. S. Perlin, *Can. J. Chem.*, 61 (1983) 1542–1548.]

relaxation vector and the molecular axis about which the vector jumps, and χ is one-half of the jump range; that is, the jump is between $-\chi$ and $+\chi$. The internal motion is superposed on an isotropic motion associated with correlation time, τ_R. The spectral density of this model is given explicitly by Eq. *A-4* in the Appendix. The diffusion model[44,45] (Eq. *31*), describing free rotation, was adopted for the motion of the geminal methyl groups of the rigid 2,3-*O*-isopropylidene ring. Both models were applied from 15° to 80°C. The activation energies associated with these two types of motions were 26.8 kJ/mol for the 5,6-*O*-isopropylidene ring, and 15.9 and 14.2 kJ/mol for the *exo* and *endo* methyl groups of the 2,3-*O*-isopropylidene ring, respectively. The activation energy associated with the temperature dependence of the rate of overall molecular tumbling was found[67] to agree with the hydrodynamic prediction of 19.1 kJ/mol associated with the temperature dependence of the ratio (η/T), where η is the shear viscosity of the solution.

The slight difference in the activation energy between the *exo* and *endo* methyl groups of the 2,3-*O*-isopropylidene substituent was attributed[67] to neighboring, nonbonded interactions. Owing to the twist conformation of the mannose ring ($^2T_3$) and the associated distortion of the 2,3-*O*-isopropylidene ring, nonequivalent,

nonbonded interactions occur between the *exo* methyl group and the H-2 and H-3 protons, leading to a favored conformation having the methyl group *exo*, thus increasing its activation energy relative to that of the *endo* methyl group.

A quantitative relaxation study has also been reported[13] for the sugar analog 5-acetoxy-5,6-dihydro-6-(1,2-epoxypropyl)-2-pyrone (**23**, "asperlin"), which

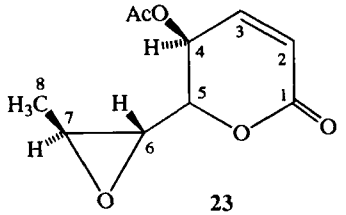

23

possesses antibiotic and antitumor activity. The rigidity of the pyrone ring and its semiplanar conformation[144–146] (shown in Fig. 11) give rise to an overall ellipsoidal shape; hence the rotational dynamics are adequately approximated by the diffusion of a prolate ellipsoid whose major axis passes through the C-2—H-2 bond (Fig. 11). Rotation about this axis is described by the rotational diffusion coefficient $D_{\parallel}$, and rotation about the minor axes is characterized by the rotational diffusion constant $D_{\perp}$. Since the C-2—H-2 vector forms an angle of 0° with the major axis, the relaxation time of C-2 is sufficient to determine $D_{\perp}$ by means of Eq. *34*:

$$\frac{1}{T_1(\text{C-2})} = \frac{N\gamma_H^2\gamma_C^2\hbar^2}{r_{\text{C-H}}^6}(6D_{\perp})^{-1} \qquad (34)$$

whereas the relaxation time for C-4 (or C-5), which forms an equal angle of 70.5° with the major axis (and characterized by nearly similar T_1 values), is used to

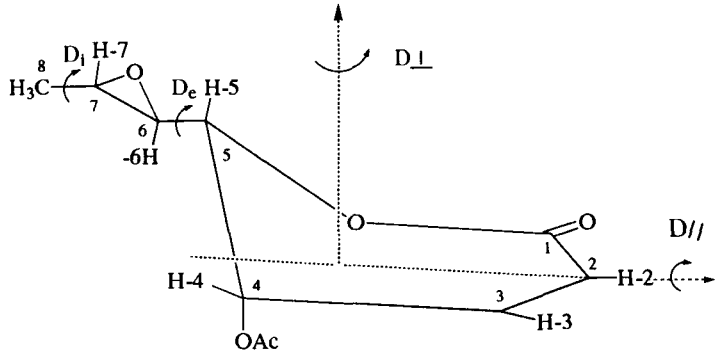

FIG. 11.—Axes of rotation in "Asperlin" (**23**) and rotational diffusion coefficients. [Reproduced with permission from Fig. 1 of P. Dais and G. Fainos, *Can. J. Chem.*, 64 (1986) 560–565.]

calculate the coefficient $D_{\|}$ (Eq. *35*)

$$\frac{1}{T_1} = \frac{N\gamma_H^2\gamma_C^2\hbar^2}{r_{C\text{-}H}^6}(D_\perp)^{-1}\left(\frac{A}{6} + \frac{B}{5+\rho} + \frac{C}{2+4\rho}\right) \qquad (35)$$

By using the diffusion coefficients calculated from Eqs. *34* and *35*, the experimental T_1 values of the C-3 carbon, which forms an angle of 60° with the major axis, were nicely reproduced over the whole temperature range studied.[13] This result gave validity to the model chosen. The ratio, ρ, of the two diffusion coefficients was constant (~ 1.5) over the whole temperature range studied, in accord with simple hydrodynamic theory. However, the anisotropy of the overall motion is not very large; and if nonbonded C–H interactions from nearby protons are taken into account in the calculations, the overall motion may be described as isotropic, especially at high temperatures.[13] This finding underscores the fact that nonbonded $^{13}C-^{1}H$ dipole–dipole interactions should be taken into consideration in quantitative analyses of relaxation data, as mentioned earlier in this article.

The description of the internal motion of the epoxypropyl ring of **23** is strongly model-dependent. This motion can be satisfactorily approximated either by free rotation about the C-5—C-6 bond or by a jumping process between two stable conformations. Discrimination between these two models from the relaxation data was not possible owing to a fortuitous similarity in the activation energies (~17 kJ/mol) of the internal and overall diffusional motions.[13] Inspection of molecular models indicates, however, that the rotation of the epoxypropyl ring is not sufficiently constrained to justify restricted rotation about the C-5—C-6 bond.

The relaxation of the methyl carbon (C-8) receives contributions from three types of molecular motions: (1) the internal rotation of the methyl group about its symmetry axis described by diffusion coefficient D_i, (2) the reorientation of the adjacent oxirane ring with diffusion coefficient D_e, and (3) the overall molecular motion characterized by diffusion coefficients $D_{\|}$ and $D_\perp$. Approximate separation of these relaxation contributions can be realized by applying the stochastic diffusion model of multiple internal rotations, developed initially by Wallach[64] and subsequently modified by Levine *et al.*[63] In the present case, two internal rotations about the C-5—C-6 and C-7—CH_3 bonds are considered to be free and independent of the overall molecular reorientation. Lack of rotation about the C-6—C-7 bond ensures that the two internal motions are independent of each other. The spectral-density function of this model is given by Eq. *A-5* in the Appendix. The temperature dependence of the calculated D_i diffusion coefficient corresponds to an activation energy of 12.2 kJ/mol. This energy value implies that some resistance to free methyl internal rotation is likely to occur in **23**. This result is not unexpected because of the geminal disposition of the methyl group and H-7 in the oxirane ring of **23**.

Through measurements of ^{13}C spin–lattice relaxation times, a number of noteworthy motional characteristics related to overall molecular tumbling, hydrogen

bonding, and internal mobility, have been detected[12] for a series of di-*O*-isopropylideneglycofuranose derivatives **24–30** (including **22**) in acetone solution. As

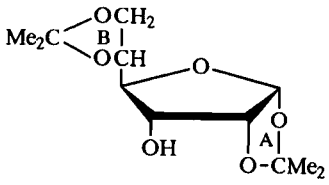

24

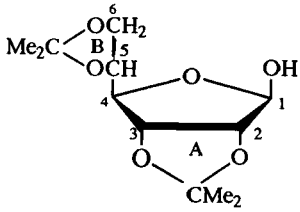

25

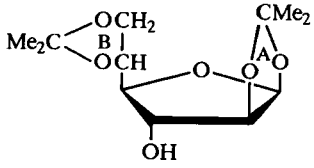

26

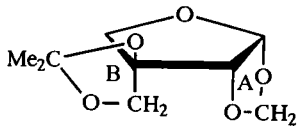

27

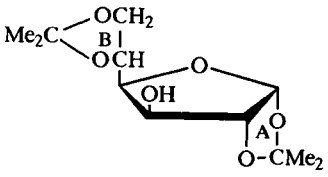

28

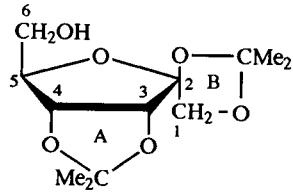

29

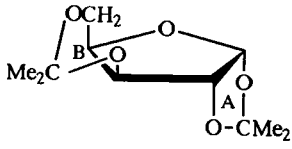

30

all of the n.O.e. values were found to approach the asymptotic value of 1.988 ± 0.15, dipole–dipole interactions constituted the preponderant relaxation mechanism.

Overall molecular motion is reflected in the T_1 values of the furanose ring. For each compound **22**, **25**, **26**, **27**, and **30**, the values for C-1 to C-4 are similar (Table IV), within experimental error (± 10%), which implies that the overall motion of

TABLE IV

^{13}C Spin–Lattice Relaxation Times (in Seconds) for Compounds 22 and 24–30[a]

Carbon	22	24	25	26	27	28	29	30
C-1	2.58	2.45	2.94	3.36	3.28	2.41	5.11	5.66
C-2	2.78	2.94	2.62	3.25	3.22		4.87	5.76
C-3	2.88	3.16	2.75	2.89	2.87	3.89	4.75	
C-4	2.73	2.82	2.82	3.23	3.14	3.77	4.17	2.76
C-5	2.98	2.98	2.97	3.23	3.28	3.35	2.52	3.69
C-6	1.90	2.14	2.00	2.06	2.21	2.07		
Me(*exo*-A)	1.38	1.46	1.37	1.45	1.88	2.01	1.96	2.72
Me(*endo*-A)	1.70	1.73	1.63	1.72	1.78		2.24	2.80
Me(*exo*-B)	1.74	1.85	1.82	1.89	1.53	1.88	2.44	2.82
Me(*endo*-B)	1.86	1.88	1.87	1.90	1.90		2.51	2.41

[a]Solution (0.5 *M*) in acetone-d_6.

these molecules is somewhat isotropic. The other compounds (**24**, **28**, and **29**) appear to reorient anisotropically because of the larger variations ($> \pm 10\%$) in T_1^{DD} values) within their sets of T_1 values. It is noteworthy that **29** and **30** relax faster, by a factor of 1.5–2.0, than the other members of the series. As there are only small differences in mass, this contrast is attributed to the fact that only **29** and **30** have no free hydroxyl group and hence, unlike **22–28**, are unable to form aggregates by hydrogen bonding. Accordingly, the smaller T_1 values for the latter group of compounds represent averages that reflect strong solute–solute and/or solute–solvent interactions. For compound **28** it is likely that rotation about the C-5—C-6 bond is restricted; in this case, the NT_1 value of C-6 (moderated by two protons) is close to the T_1 values of the ring carbons, a phenomenon that is not observed for the primary carbons of the other compounds. Although this may be due to intermolecular association, it is also consistent with the suggestion[12] that OH-6 of **28** engages in intramolecular hydrogen bonding with O-2. The calculated diffusion coefficients, $D_R = 1/6\tau_R$, describing the overall motion of compounds **22**, **25–27**, and **30** are summarized in Table V. These values were obtained from the average T_1 values of the ring carbons for each molecule by employing Eq. *16*. The D_R values in Table V indicate clearly that the rate of the overall rotational diffusion for **30** is twice that of the isotropic tumblers, which are capable of hydrogen bonding.

The relaxation time of C-5 of the B-type *O*-isopropylidene ring in each isotropic molecule **25**, **26**, and **27** is, within experimental error, similar to the T_1 values of the furanose ring carbon atoms of each (see Table IV), indicating restricted rotation about the C-4—C-5 bond, which may be regarded as a very small oscillation. However, the fact that the NT_1 values for C-6 are larger than predicted by Eq. *16*,

TABLE V

Average Relaxation Time (s) Diffusion Coefficients (s^{-1}) and Energy Barriers (kJ/mol) for Compounds Having Isotropic Motion[a]

Compound	T_1	$D_R \times 10^9$	D_f(*exo*-A) $\times 10^{10}$	D_f(*endo*-A) $\times 10^{10}$	V_i(*exo*-B)	V_i(*endo*-B)
22	2.74	9.8	4.1	6.6	14.2	13.0
25	2.78	10.0	4.0	6.5	14.2	13.0
26	3.18	11.1	3.7	5.5	14.2	13.4
27	3.13	11.2	7.0	6.2	12.5	13.4
30	5.65	20.2	7.6	8.2	12.5	12.5

[a]Estimated error ±15%.

assuming that these carbons relax only via overall molecular tumbling, suggests that the 5,6-*O*-isopropylidene rings undergo a puckering motion, which influences the relaxation of C-6. The dynamics of the flexible B-type ring in these molecules are amenable to a quantitative treatment similar to that used for compound **22**, as described earlier. The same type of motion is probably reflected as well in the NT_1 values for C-6 of **24**, C-1 of **28**, and C-5 of **29**, despite the anisotropic reorientation displayed by these compounds.

Two pairs of geminal *C*-methyl groups are attached to the molecular frameworks of molecules **25–27** and **30**. The pair of methyl groups of the B-type ring is not amenable to rigorous quantitative treatment in terms of internal motion about the C—CH_3 bond, owing to multiple internal motions of the ring itself. However, this limitation does not apply to the geminal methyl groups of the far more rigid A-type *O*-isopropylidene ring, as can be verified from the analysis of the coupling-constant data.[12] Diffusion coefficients calculated for the *exo* and *endo* methyl groups for isotropic tumblers through Eq. *31* are depicted in Table V, where D_f is given by[12] $D_f = (3/2)(KT/I)^{1/2}$ and I is the moment of inertia of the methyl group (3.258×10^{-40} kg cm^2). These barriers are recorded for C—C—H angles of 112°, as steric interactions increase[147] this angle from the normal 109.47°. It is apparent from Table V, which also includes data for compound **22**, that the barriers to rotation of the *endo* and *exo* methyl groups are similar in compounds **22**, **25**, and **26** and that the *endo* methyl groups rotate faster than the *exo* methyl groups. This trend may be accounted for by the increase in the barrier for the latter groups, owing to their selective interaction with the 1,3-quasidiaxial protons across the *O*-isopropylidene ring. By contrast, there is a reversal in the order of the barriers to internal rotation in **27**, even though the *endo* and the *exo* methyl groups in **30** have about the same rotational barrier. Coupling-constant data have shown[12] that the furanose ring of compound **27** adopts the E_3 conformation, whereas the furanose ring and the 3,5-*O*-isopropylidene ring in compound **30** are $^2T_3$ and $^0T_5$, respectively. These conformations bring the *endo* methyl group into proximity with the

C-3—H-3 bond in **27** and the C-4—H-4 bond in **30**. Consequently, these steric interactions may be expected to bring the energy barriers for the *endo* methyl groups more into line with those for the *exo* methyl groups.

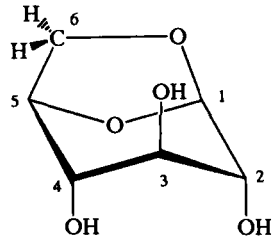

31

A more rigorous treatment of the variable-temperature ^{13}C T_1 data has been used to describe the overall molecular motion of the glucose derivative, namely 1,6-anhydro-β-D-glucopyranose (**31**) in solution.[147a] This rigid molecule contains a number of nonequivalent $^{13}C-^{1}H$ vectors and is amenable to a rigorous quantitative treatment by means of Eq. *29*. Table VI summarizes the diagonal elements of the rotational diffusion tensor, that is, the rotational diffusion constants D_x, D_y, and D_z obtained upon diagonalization of the rotational diffusion tensor with respect to

TABLE VI

Rotational Diffusion Constants ($\times 10^{10}$ s^{-1}), Euler Angles, Activation Energies (kJ/mol), D_∞ Values ($\times 10^{12}$ s^{-1}), Correlation Coefficients (R), and Quotients[a] of the Rotational Diffusion Constants for Compound 31

	$\alpha = 50°, \beta = 60°, \gamma = 40°$				
t (C°)	D_x	D_y	D_z	D_y/D_x	D_z/D_x
20	0.18	0.36	0.28	2.0	1.6
30	0.25	0.45	0.35	1.8	1.4
40	0.30	0.60	0.47	2.0	1.6
50	0.34	0.78	0.61	2.3	1.8
60	0.60	0.89	0.69	1.5	1.2
70	0.64	1.05	0.87	1.6	1.4
80	0.72	1.40	1.10	1.9	1.5
90	0.88	1.58	1.21	1.8	1.4
E_a	20	19	19		
D_∞	6.4	7.2	5.9		
R	0.98	0.99	0.99		

[a] D_i/D_x, 1.0 in all cases.

the principal-axis system of the moment of inertia tensor. The latter tensor and the principal moments of inertia ($I_{xx} = 6.24 \times 10^{-41}$, $I_{yy} = 7.46 \times 10^{-41}$, $I_{zz} = 6.97 \times 10^{-41}$ kg cm^2) were determined from the optimized geometry of **31** by employing the AM1 semiquantitative method.

The calculated Euler angles ($\alpha = 50°$, $\beta = 60°$, and $\gamma = 40°$), which determine the relative orientation between the principal-axis system of the rotational diffusion tensor and that of the moment of inertia tensor, indicate a significant shift between the two tensors. This result is expected because of the fact that molecule **31** contains a number of polar groups and hydrogen-bonding centers, leading to strong intermolecular interactions.

For the set of the Euler angles $\alpha = 50°$, $\beta = 60°$, $\gamma = 40°$, the order of the rotational diffusion constants is $D_y > D_z > D_x$. This trend is also reflected in the quotients of the rotational diffusion constants, D_y/D_x and D_z/D_x (Table VI), which describe the anisotropy of the rotational diffusion in solution. The principal axes of the rotational diffusion tensor corresponding to the aforementioned set of the Euler angles is shown graphically in Fig. 12.

In order to illustrate the anisotropy of the rotational diffusion, and hence the influence of the intermolecular interactions, the square roots of the moments of inertia $(I_{yy}/I_{xx})^{-1/2} = 0.92$, $(I_{zz}/I_{xx})^{-1/2} = 0.95$, and $(I_{xx}/I_{xx})^{-1/2} = 1.00$ are compared with the quotients of the diffusion constants in Table VI. The values of the

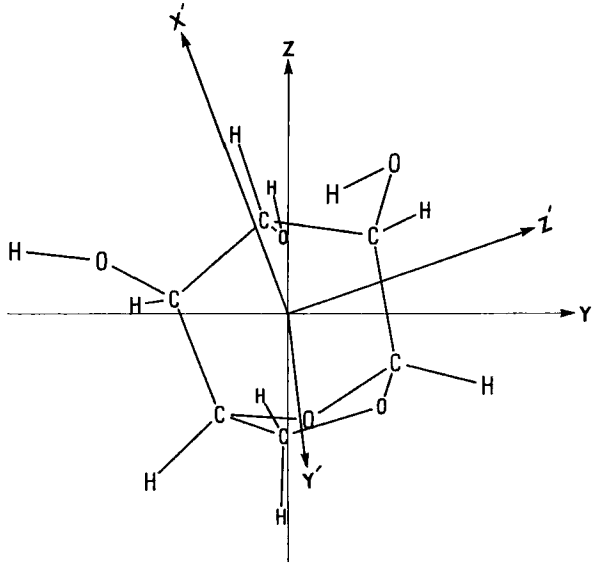

FIG. 12.—Orientation of the principal-axis system of inertia tensor (x',y',z') and that of the rotational diffusion tensor (x,y,z) for compound **31**. The principal diffusion axis x is perpendicular to the plane of the drawing. [Reproduced with permission from P. Dais, *Carbohydrate Res.*, 263 (1994) 13–24, and Elsevier Science B.V.]

quotients of the diffusion constants show clearly that the rotational motion of **31** in solution is more anisotropic than when described by the rotational diffusion tensor for which the principal axes coincide with those of the inertial tensor. Thus, it appears that the diagonalized diffusion tensor should be used for the description of the rotational motion of **31** in solution.

b. Oligosaccharides.—Information concerning the overall motion of oligosaccharide molecules in solution, and also the relative spatial rigidity of the individual sugar monomers, should be available from the spin–lattice relaxation times of the individual ring carbon nuclei. However, the dynamic modeling of these molecules based on experimental relaxation data has important limitations, which are documented here.

Partitioning of the various modes of reorientation—even for the simplest member of this class, a disaccharide molecule—is not an easy task. For instance, separation of rotatory diffusion from internal oscillations around the glycosidic bonds is not feasible because no ring carbon atom in the disaccharide moiety relaxes exclusively via the overall molecular motion. This problem becomes more serious if the internal motion of exocyclic substituents, such as a hydroxymethyl group, is considered in the process of dynamic modeling.

An approximate solution to this problem could be the simulation of the rotational correlation time associated with the overall motion through hydrodynamic or light-scattering measurements. Nevertheless, these measurements afford a single, effective correlation time, which cannot explicitly describe an anisotropic motion. Moreover, the continuum model involved in the hydrodynamic theory[42] may not be realistic for such small molecules, and thus give erroneously long correlation times. Although corrections to the hydrodynamic theory exist[43] and correlation times close to the true values can be obtained for spherical, spheroidal, and ellipsoidal molecules, a quantitative determination of the magnitude and rate of oscillatory motions around glycosidic bonds requires the elaboration of a suitable dynamic model. No such model is available, however, to describe flexibility in terms of torsional angles φ and ψ (and ω).

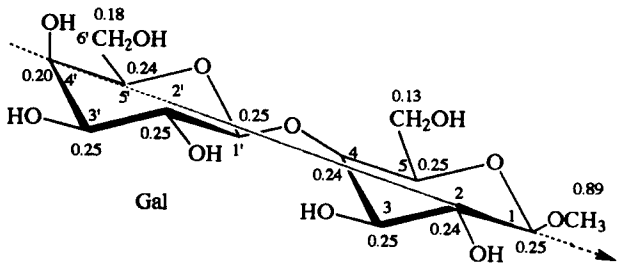

32

Most treatments assume a rigid disaccharide molecule tumbling isotropically[80,81,85,86,105,106,108–110,119] or anisotropically[84,96,128a,129] about a preferred axis of rotation. For instance, methyl β-lactoside **32** is regarded[84] as an anisotropic tumbler. Carbon atoms that bear an axially oriented proton have closely similar T_1 values, whereas C-4′, which uniquely bears an equatorially oriented proton, is characterized by a smaller T_1 value. This difference suggests that the tumbling motion is anisotropic, with a principal axis of rotation directed parallel to the C-4—H-4 vector. Assuming that this axis is perpendicular to the axial C—H vectors and lies in the general direction joining C-4′, C-1′, C-4, and C-1, the Woessner equations give $D_\perp = 6.7 \times 10^8\ s^{-1}$ and $D_{||} = 10.4 \times 10^8\ s^{-1}$ ($\rho = D_{||}/D_\perp = 1.55$), which suggests a small, but definite anisotropic overall motion.

Another example is sucrose (**7**), the dynamics of which have been studied extensively[14,105,106,128,129,130] in various solvents as a function of temperature, concentration, and magnetic field. In two studies,[14,106] this molecule was described as a rigid isotropic tumbler adopting a solution conformation similar to that in the solid, except, perhaps, for the loss of one intramolecular hydrogen bond. Very careful ^{13}C spin–lattice relaxation measurements undertaken by McCain and Markley[128a] and others[105] for sucrose in aqueous solution revealed that this molecule tumbles anisotropically. The relaxation data have been presented in terms of normalized relaxation rates, $\langle 1/T_1 \rangle$, defined as the relaxation rate for an individual ring carbon divided by the average $1/T_1$ value for all the ring carbons as measured during in a given run. This definition ensures that these values are independent of the experimental conditions and systematic errors in the relaxation measurements[128a]. On the average, two sets of ring carbons gave results well outside the experimental error. Ring carbons C-2, C-3, C-4, and C-5 of the glucose moiety were characterized by shorter $\langle 1/T_1 \rangle$ values ($\langle 1/T_1 \rangle = 0.97\ s^{-1}$) than those of carbons C-1 of glucose and C-3′, C-4′, C-5′ of the fructose residue ($\langle 1/T_1 \rangle = 1.03\ s^{-1}$). This pattern is in agreement with the different angles formed by the two sets of C—H vectors, with a preferred axis of rotation assumed[128a] to parallel the crystallographic *b* axis of sucrose in the crystal. The former set of vectors lie nearly parallel to each other and almost perpendicular to the long axis (*b* axis) of the molecule (angle 87° ± 2°), whereas the latter set of the four vectors form a cone that has its axis parallel to the long axis so that all four bonds make angles of 27° ± 10° to the *b* axis. This pattern of relaxation times is evidence that the conformation of sucrose in water is similar to that in the crystal.

The rigidity of disaccharide molecules has been questioned in two papers[128b,129] dealing with the dynamics of sucrose (**7**) and methyl 3-*O*-α-L-rhamnopyranosyl-α-D-glucopyranoside (**33**) in solution. In these instances, the experimental T_1 and n.O.e. data have been used to determine the frequency dependence and amplitude of the rotational spectral-density function, $J(\omega)$. The frequency dependence of $J(\omega)$ shows the same behavior as the theoretical spectral-density function for a rigid molecule, but it has a lower amplitude, ~ 89% of the theoretical value of a rigid

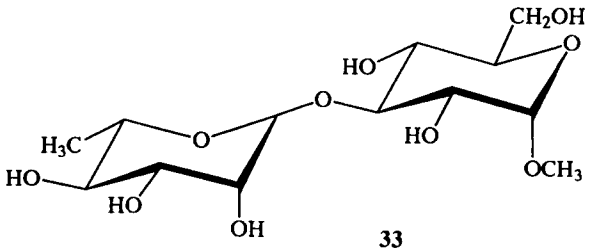

33

molecule. This behavior is attributed to a rapid initial decay of the correlation function caused by internal motions (such as vibrational and torsional oscillations), which rapidly accomplish part of the averaging of an internuclear vector over all its possible orientations. This initial decay is followed by a slower exponential decay caused by overall molecular rotation, with the usual molecular rotational correlation times.

Quantification of the relaxation data of an oligosaccharide molecule containing more than two monomer residues has been attempted[131] for the tetrasaccharide lacto-*N*-neotetraose (**34**). The relaxation parameters T_1 and n.O.e. measured as a

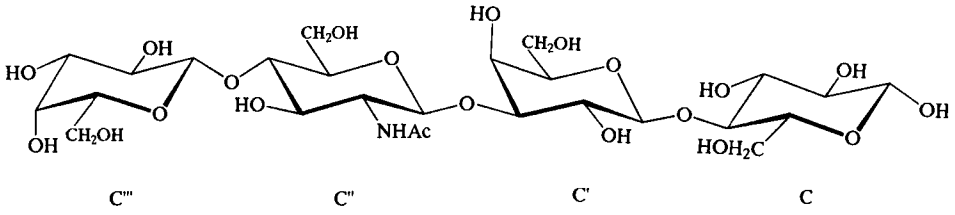

C''' C'' C' C

34

function of temperature and magnetic field, which are outside the extreme narrowing limit, are analyzed by using the "free model" approach of Lipari and Szabo.[148] The spectral density of this model (Eq. *36*) is expressed in terms of a generalized parameter, S^2, which is a measure of the spatial restriction of the local motion, and the correlation times, τ_M and τ_e, for the overall and local motion:

$$J(\omega) = \frac{2}{5}\left(\frac{S^2\tau_M}{1 + \omega^2\tau_M^2} + \frac{(1 - S^2)\tau}{1 + \omega^2\tau^2}\right) \qquad \text{where } \tau^{-1} + \tau_M^{-1} + \tau_e^{-1} \qquad (36)$$

Assuming that the overall motion for **34** is isotropic, the experimental data of the inner rings C′ and C″ and those of the two outer rings C and C‴ were fitted, using either Eq. *36*, or its truncated form, Eq. *37*, neglecting the local motion term in the spectral density:

$$J(\omega) = \frac{2}{5}\left(\frac{S^2\tau_M}{1 + \omega^2\tau_M^2}\right) \qquad (37)$$

Comparison between the different fitting procedures revealed that local motions of the inner rings are restricted (high values for the order parameter S^2), whereas this type of motion is more pronounced for the outer rings (low values for S^2). These findings are in agreement with previous qualitative interpretation that internal flexibility increases progressively along the oligomeric carbohydrate chain toward the free ends.

Equation *37* has been used in an attempt[130] to describe internal flexibility of the three hydroxymethyl groups of sucrose molecule in D_2O solutions. The experimental data showed that the contribution of the overall motion to the spectral-density function of the hydroxymethyl group is similar to that of the ring carbons of sucrose. However, the presence of rapid internal motions about the three exocyclic bonds reduces the spectral density amplitudes. On the basis of the calculated order parameters in conjunction with model calculations, it was suggested[130] that internal motions may be described as torsional librations.

c. Polysaccharides.—In modeling the dynamics of a long carbohydrate chain three general types of motion are considered: (1) the overall rotatory diffusion, (2) segmental motion, and (3) the internal motion of a pendant group (such as hydroxymethyl) exocyclic to the polymer backbone. Each of these motions is considered as an independent source of the motional modulation of dipole–dipole interactions, so that the composite TCF is a product of the correlation functions associated with each motion. The overall molecular tumbling is the molecular-weight-dependent motion, whereas the segmental motion does not depend on the length of the macromolecular chain. In addition, these two motions compete with each other in the relaxation of the ring carbons. For relatively low-molecular-weight polysaccharides, the overall motion is the dominant relaxation source. With an increase in molecular weight, this motion becomes progressively slower until the segmental contribution prevails and the relaxation parameters become molecular-weight-independent. Therefore, for sufficiently high-molecular-weight polymers, the overall rotatory diffusion is a negligible contributor to the relaxation of the backbone carbons and, as mentioned earlier, can be safely ignored. For example, the overall motion of an amylose sample (MW = 3.3×10^5) in dimethyl sulfoxide corresponds to a long correlation time of 7.0×10^{-6} s, as estimated from hydrodynamic measurements.[11]

The second independent motion requires a suitable dynamic model that reflects the geometric constraints of chain flexibility characteristic of polysaccharides. However, no model is yet available that takes polysaccharide structural details into account or describes possible modes of reorientation in the carbohydrate chain.

Several attempts have been made to interpret the relaxation data of polysaccharides by employing a variety of dynamic models suitable for local chain motions of synthetic polymers. One motional model that has been applied to polysaccharides[133,135,136] is the log(χ^2) model[72] (Eq. *A-6* in the Appendix), which assumes that isotropic reorientation is characterized by a skewed distribution of correlation times, with tails toward longer correlation times (Fig. 13). The distribution func-

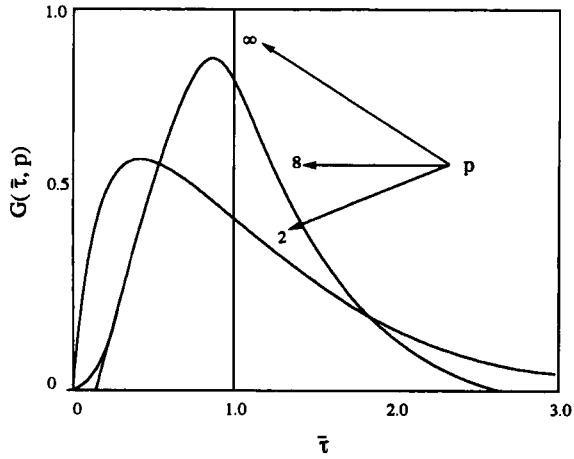

FIG. 13.—Log(χ^2) distribution of correlation times for three values of the width parameter p. For a very long p value ($p \rightarrow \infty$), the distribution approaches a δ function. [Reproduced with permission from Fig. 3 of J. Schaefer, *Macromolecules*, 6 (1973) 882–888. © 1973 American Chemical Society.]

tion of this model contains two parameters: the width, p, of the distribution, and the average correlation time, $\bar{\tau}$, characterizing the center of the distribution (Fig. 13). Here, the larger the width parameter p, the narrower is the distribution. For very large values of p, the distribution is so narrow as to be indistinguishable experimentally from a single correlation time. Correlation times and distribution widths obtained by the log(χ^2) model have also been used to explain the conformational behavior of gel-forming (1→3)-β-D-glucans, aggregation among the helical segments, and its consequences for the gelation mechanism.[135,136] In agreement with expectation, the average correlation times showed the existence of distinct differences in mobility between the glucans with a finite network ($\overline{DP}_n$ = 49 and 131) and the gels with an infinite network ($\overline{DP}_n$ = 540). Nevertheless, an increase in the width parameter was observed with increasing molecular weight, which appears to be unreasonable for the glucans having a finite network.[136] Moreover, the fitting parameters of the model could not reproduce the experimental linewidths. Thus, a truncated log(χ^2) distribution (excluding very long correlation times >500–1000 ns from the distribution) was invoked to reproduce the experimental relaxation parameters and improve the problem of the width parameters. The truncated log(χ^2) distribution function was employed as well by Torchia *et al.*[133] to compare the segmental mobility of glycosaminoglycan chains in solution and in intact tissue. However, as discussed by Torchia *et al.*,[133] truncation of the log(χ^2) distribution function may be an artifact of the fitting procedure, and thus would exclude any slow motions that are present, as shown by dipolar decoupling experiments.

The applicability of the Jones–Stockmayer (JS)[74] model to the relaxation of polysaccharides was tested first by Matsuo[9] for linear dextrans and amylose in

dimethyl sulfoxide and D_2O. However, this model appears to be limited, as shown by NMR multifield relaxation experiments on amylose in dimethyl sulfoxide.[10] The ineffectiveness of the JS model for describing the dynamics of carbohydrate molecules has been rationalized[10,11] on the basis of the specific nature of a carbohydrate chain, as compared with a hydrocarbon chain for which the model applies. Instead, it has been suggested[10,11] that local conformational changes in carbohydate chains can be expressed in terms of oscillatory or other types of motions within a disaccharide unit. These motions, the amplitude of which depends on geometric constraints within the simple kinetic unit, introduce an angular dependence of the C–H dipole–dipole interactions, a fact that may explain the observed[10] differences between the T_1 value of C-1 and those of the remaining ring carbon atoms in amylose. An examination of the nature of the internal and overall modes of reorientation in amylose has been made[11] by employing a variety of dynamic models. On the basis of multifield ^{13}C parameters T_1, T_2, and n.O.e., two models were found to be consistent with the nature of the internal motion: the internal conic diffusion model[55] and the internal two-state jump model.[57] Both internal motions are superposed on an anisotropic overall motion of helical segments within the amylose chain.

In the first model,[55] depicted schematically in Fig. 14, internal motion is described as wobbling in a cone, so that the C—H vector moves freely at a given rate, τ_w, inside the conical boundary defined by an angle θ but has zero probability of being found outside the boundary. The director of the cone makes the angle β with the z-axis, while τ_z and $\tau_x = \tau_y$ are the correlation times for rotation about the z- and

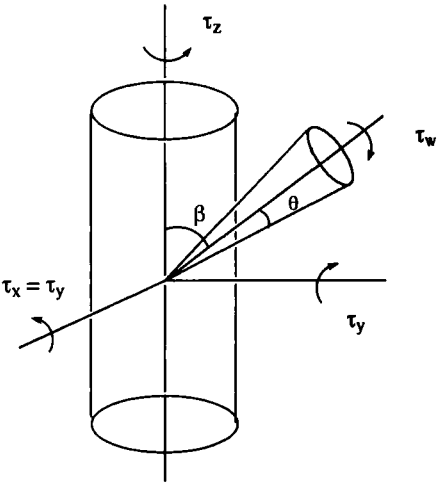

FIG. 14.—Diffusion in a cone model. [Reproduced with permission from Fig. 2 of P. Dais, *Carbohydr. Res.*, 160 (1987) 73–93, and Elsevier Science B.V.]

x-(or y-)axes of the cylinder (helical segment). The mathematical expression for this model appears in the Appendix (Eq. *A-7*). In the second model, developed by London and Phillipi,[57] the relaxation vector jumps internally between stable states A and B, with lifetimes τ_A and τ_B, respectively. The extent of the jump or the jump range is defined by angle 2θ (that is, the jump is between $-\theta$ and $+\theta$ with respect to the bisector, as shown in Fig. 15). Also, the internal motion is superposed on the anisotropic overall motion described by the τ_z and $\tau_x = \tau_y$ rotational correlation times. Here, β_1 describes the angle between the z-axis and the internal jump axis, and β_2 describes the angle between the jump axis and the C—H vectors. The orientation of the bisector relative to the z-axis is described by angle α. The form of the spectral-density function describing this model is given in the Appendix (Eq. *A-8*). Considering restricted rotations or jumps about an internal axis, it was assumed that the reference segment is the α-D-glucosyl residue defined by a rotation (or jump) axis, which coincides with the virtual bond,[11,149] that is, the vector spanning the D-glucopyranosyl residue and joined at the bridge-oxygen atom, as shown in Fig. 16. Relating these two models to the helix-like structure of amylose,[11,149] it was assumed that the reference is the helical chain segment, subject to the overall motion defined by the helix axis as in the solid state.[11,149] This assumption implies that the monomer residues within a helical segment have the same z-axis, which is aligned with the helix axis.

The experimental multifield relaxation data (T_1, T_2, n.O.e.) for amylose were nicely reproduced by using these two models.[11] However, the wobbling-in-a-cone model is favored for two reasons: first, it requires fewer adjustable parameters than the bistable jump model to fit the data; second, the jump model requires $\beta_2 = 48.9°$

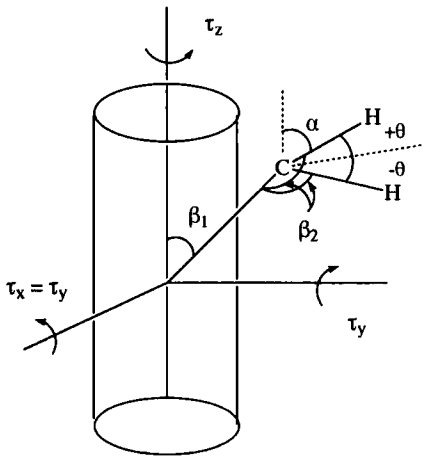

FIG. 15.—Bistable (two-state) jump model. [Reproduced with permission from Fig. 3 of P. Dais, *Carbohydr. Res.*, 160 (1987) 73–93 and Elsevier Science B.V.]

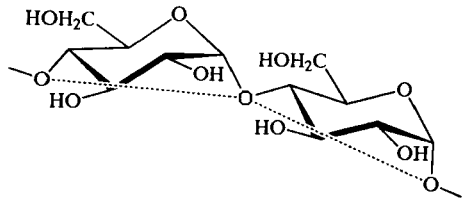

FIG. 16.—Schematic representation of a disaccharide residue of amylose showing the definition of the virtual bond (broken lines). [Reproduced with permission from Fig. 4 of P. Dais, *Carbohydr. Res.*, 160 (1987) 73–93 and Elsevier Science B.V.]

for the C-1 atom, which is very different from the angle observed (37°) in the crystal structure of amylose.[150–153] Comparison[11] of the calculated fitting parameters τ_z and $\tau_x = \tau_y$ from the two models with correlation times $\tau_\parallel$ and $\tau_\perp$ obtained from hydrodynamic measurements, as a function of the number of monomer units per helical segment, are commensurate with a helical segment comprising, on the average, 40–50 monomer residues (wobbling-in-a-cone model) and 20–60 monomer residues (bistable jump model).

Although the foregoing treatment of amylose is successful in reproducing its relaxation data—particularly the difference between the relaxation parameters of the anomeric carbons and those of the remaining ring carbons—and in accounting for its helix-like character in dimethyl sulfoxide, it cannot be generalized to include other linear or branched polysaccharides having less pronounced helical segments in solution. Morever, the complexity of the models used does not facilitate a description of the additional internal motion of the exocyclic hydroxymethyl group.

The backbone motion of amylose has been described[132] by using the Dejean–Laupretre–Monnerie (DLM) model,[79] which takes into consideration the local anisotropic motion described by fast libration of the C—H vectors in addition to segmental motion. Indeed, the DLM model was capable of reproducing the multifield relaxation data for amylose in dimethyl sulfoxide.[132] The different relaxation data for the anomeric carbon relative to those for the remaining ring carbons was explained on the basis of the simulated values of the half-angle, θ, of the cone. This angle is 21° for C-1 and 26° on the average for the remaining carbons, indicating that these two types of carbon sites do not experience the same local dynamics. The smaller θ value for the anomeric carbon is indicative of greater steric hindrance to the librational motion of the corresponding equatorial C—H vector relative to that of the axial vectors in the remaining ring sites. Shortening of the C-1—O-1 and C-1—O-5 bonds relative to the remaining C—O bonds, which is observed in the crystal structure of amylose[151–153] and other α-glucopyranosides,[154,155] appears to be a major cause for restricting the amplitude of local libration at the anomeric carbons.

Rotation of the hydroxymethyl group about the exocyclic bond is considered next. Free internal rotation about the C-5—C-6 bond superposed on segmental motion, as described by a composite TCF[132] based on the Hall–Weber–Helfand (HWH) model[75,78] and the Woessner equations[45,47] for stochastic diffusion and jump processes, could not reproduce the experimental relaxation data for the C-6 carbon. Models incorporating restricted rotation were then considered. One is the internal two-state jump model of London,[56] which has also been discussed by Jones[61] and has already been mentioned (see Section IV.2.a and Eq. *A-4* in the Appendix). In the second model *O*-6 moves continuously between two limiting values of an angle χ (that is, the amplitude of restricted motion is 2χ). Restricted diffusion about a single axis has been solved analytically[50,156] (Eq. *A-9* in the Appendix). The TCF of internal motion, as described by these two models, can be combined with the HWH correlation function to give two new composite TCFs.

HWH + two-state jump TCF:

$$G(t) = (1 - C)\exp(-t/\tau_0)\exp(-t/\tau_1)I_0(t/\tau_1) + C\exp(-t/\tau_0)\exp(-t/\tau_c)\exp(-t/\tau_1)I_0(t/\tau_1) \quad (38)$$

The parameters C and τ_c are given in Eq. *A-4* in the Appendix.

HWH + restricted internal diffusion TCF:

$$G(t) = \sum_{a=-2}^{+2}\sum_{n=0}^{\infty} |d_{a0}(\beta)|^2\,|E(a,n)|^2\exp(-t/\tau_0)\exp(-t/\tau_n)\exp(-t/\tau_1)I_0(t/\tau_1) \quad (39)$$

The parameter τ_n is given in Eq. *A-9* in the Appendix, as a function of the correlation time, τ_i, associated with internal motion. One of the input parameters is the angle β, formed between the relaxation vector (C—H bond) and the internal axis of rotation (or jump axis), namely the C-5—C-6 bond. The others are correlation times τ_0 and τ_1 of the HWH model, obtained from the fit of the data for the backbone carbons. The fitting parameters for the two-state jump model are lifetimes τ_A and τ_B, and for the restricted-diffusion model, the correlation time τ_i for internal rotation. The allowed range of motion (or the jump range) is defined by 2χ for both models (Eqs. *A-4* and *A-9*).

Both models were capable of reproducing the experimental data for the C-6 carbon of amylose,[132] although they differ somewhat in the time scale and range of restricted motion. Nevertheless, the restricted-diffusion model is inadequate, because it does not respond properly at the limit of free rotation ($2\chi = 360°$), which is an important criterion for its applicability.[50,132] Indeed, a large discrepancy was found[132] between the calculated relaxation parameters corresponding to a full range of motion, $2\chi = 360°$, and parameters derived by using the free internal

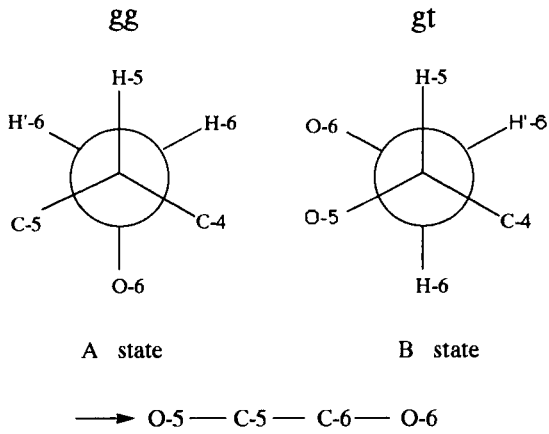

FIG. 17.—Newman-Type Projections showing the two States A and B Corresponding to the *gauche–gauche* and *gauche–*trans Conformations of the Hydroxymethyl Group of Amylose. [Reproduced with permission from Fig. 1 of P. Dais and R. H. Marchessault, *Macromolecules*, 24 (1991) 4611–4614. © 1991 American Chemical Society.]

rotation model. Furthermore, the internal two-state jump model appears to be more realistic for describing the nature of the motion of the hydroxymethyl group in its two favored conformations (Fig. 17), in accord with crystallographic data.[154,155] The longer lifetime τ_A ($\tau_A = 3\tau_B$), derived from the two-state model,[132] may be ascribed to the most stable *gauche–gauche* conformation (60%) as compared to the *gauche–trans* (40%) state for the *gluco* configuration[154,155] (Fig. 17).

Multifield, variable-temperature ^{13}C T_1, T_2, and n.O.e. parameters have been used to examine the dynamics of the α- (**35a**) and β- (**35b**) anomeric forms of

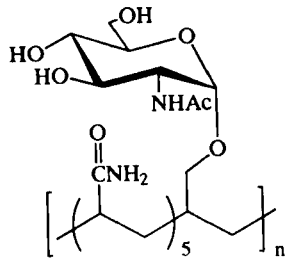

35a

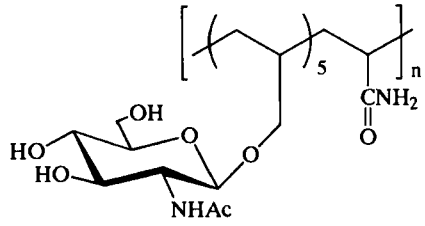

35b

poly[acrylamide-co(allyl 2-acetamido-2-deoxy-D-glucopyranoside)] glycopolymers in D_2O solution.[157] The time-scale motions and the spatial restrictions of the various modes of reorientation in the polymers were determined semiquantita-

tively by using various forms of the "model free" approach (Eqs. *36* and *37*). The overall motion is found to be anisotropic. The *N*-acetylmethyl and sugar hydroxymethyl groups exhibited internal motions, whereas no internal mobility was detected for the sugar moiety in the side chain.

On the basis of small differences ($\sim 8\%$) in T_1 values between the α- and β-anomeric forms of the sugar and conformational energy calculations, Roy *et al.*[157] suggested that the motions of the sugar rings may be different for the two systems. Although this conclusion may be correct, the use of the "model free" approach for analyzing the relaxation data of this copolymer, and especially those of the backbone carbons, is questionable, inasmuch as this approach failed to reproduce the n.O.e. values of the various carbons of the copolymer. The n.O.e. parameters are considered[158,159] to be more discriminating physical quantities than T_1 for testing model applicability.

The present analysis of the multifield relaxation data for amylose in dimethyl sulfoxide clearly shows how complex the dynamics of carbohydrate chains in solution can be. Although various models have been used successfully in reproducing relaxation data for amylose while others have been eliminated on theoretical and structural grounds, the problem of satisfactorily describing the segmental motions of even one polysaccharide in solution is far from being solved. What is primarily needed is the formulation of a TCF that can be accounted for explicitly by the geometric constraints of a carbohydrate chain in terms of torsional angles φ and ψ (and ω). The determination of amplitudes and correlation times for oscillatory motions about the glycosidic bonds should give valuable information for nonbonded interactions between monomer units in the chain, intramolecular hydrogen-bonding that may be present, and solvent effects, as well as about chain conformation in solution. Such calculations based on experimental data would also be very helpful in assessing the applicability of the various semiempirical conformational computations[142,160] for polysaccharides.

In addition to the dynamic modeling problem, further experiments are necessary to detail the shape of polysaccharides in solution from many points of view. An *a priori* knowledge of the nature of a system under investigation may assist in critically assessing the various modes of reorientation that contribute to the relaxation of the molecule.

V. APPENDIX

JS Model[74]

$$J(\omega) = 2 \sum_{k=1}^{s} G_k \frac{\tau_{k0}}{1 + \omega^2 \tau_{k0}^2}$$

$$\tau_{k0}^{-1} = \tau_k^{-1} + \tau_R^{-1}$$

$$\tau_k^{-1} = w\lambda_k \qquad s = (m + 1)/2$$
$$\lambda_k = 4 \sin^2[(2k - 1)\pi/2(m + 1)] \qquad (A\text{-}1)$$
$$\tau_h = (2w)^{-1} \qquad \gamma = \ln 9$$
$$G_k = 1/s + (2/s) \sum_{q=1}^{s-1} \exp(-\gamma q) \cos[(2k - 1)\pi q/2s)]$$

HWH Model[77,78]

$$J(\omega) = 2(\alpha^2 + (-\beta)^2)^{-1/4} \cos[(1/2) \arctan(-\beta/\alpha)$$
$$\alpha = \tau_0^{-2} + 2(\tau_0\tau_1)^{-1} \qquad \text{and} \qquad \beta = -2\omega(\tau_0^{-1} + \tau_1^{-1}) \qquad (A\text{-}2)$$

DLM Model[79]

$$J(\omega) = \text{Re}\left(\frac{1 - A}{(\alpha + i\beta)^{1/2}}\right) + \frac{A\tau_2}{1 + \omega^2\tau_2^2}$$
$$1 - A = \left(\frac{\cos\theta - \cos^3\theta}{2(1 - \cos\theta)}\right)^2 \qquad (A\text{-}3)$$

Two-State Jump Model (Isotropic Overall Motion)[56]

$$J(\omega) = \frac{(1 - C)\tau_R}{1 + \omega^2\tau_R^2} + \frac{C\tau_N}{1 + \omega^2\tau_N^2}$$
$$\tau_N^{-1} = \tau_R^{-1} + \tau_C^{-1} \qquad \tau_C^{-1} = \tau_A^{-1} + \tau_B^{-1} \qquad (A\text{-}4)$$
$$C = \frac{3\tau_A\tau_B}{(\tau_A + \tau_B)^2} [\sin^2\beta(1 - \cos2\chi)][2 - \sin^2\beta(1 - \cos2\chi)]$$

Multiple Internal Rotations Model[13]

$$J(\omega) = \sum_{\substack{m,a \\ b,c=-2}}^{+2} |d_{ma}(\beta_0)|^2 |d_{bc}(\beta_1)|^2 |d_{c0}(\beta_2)|^2 \frac{\tau}{1 + \omega^2\tau^2} \qquad (A\text{-}8)$$

$$\tau = (6D_\perp + m^2(D_{||} - D_\perp) + a^2D_e + c^2D_i \qquad (A\text{-}5)$$

Log(χ^2) Model[72]

$$J(\omega) = \int_0^\infty \frac{G(\tau_c,p)\tau_c\, d\tau_c}{1 + \omega^2\tau_c^2}$$
$$G(\tau_c,p) = \frac{p}{\Gamma(p)} (p\tau_c)^{p-1} \exp(-p\tau_c)p$$

$$G(\tau_c,p)\,d\tau_c = F(s)\,ds$$

where

$$s = \log_b[1 + (b-1)\tau_c/\tau]$$

then

$$F(s) = \frac{p}{\Gamma(p)}(ps)^{p-1}\exp(-ps)p$$

and finally

$$J(\omega) = \int_0^\infty \frac{F(s)\tau(b^s-1)}{(b-1)\{1+\omega^2\tau^2[(b^s-1)/(b-1)]^2\}}\,ds \qquad (A\text{-}6)$$

Diffusion-in-a-Cone Model[55]

$$J(\omega) = \sum_{k,m=-2}^{+2} |d_{km}(\beta)|^2 \left\{ C_m(0)\frac{\tau}{1+\omega^2\tau^2} + [C_m(0) - C_m(\infty)]\frac{\tau'}{1+\omega^2(\tau')^2}\right\} \qquad (A\text{-}7)$$

$$\tau^{-1} = 6D_x + k^2(D_z - D_x)$$

$$(\tau')^{-1} = 6D_x + k^2(D_z - D_x) + 6D_{\text{eff}}^{(m)}$$

$$D_{\text{eff}}^{(m)} = [C_m(0) - C_m(\infty)]D_m$$

Simple closed-form expressions of $C_m(0)$, $C_m(\infty)$, and $D_{\text{eff}}^{(m)}$ in terms of θ and τ_w are given in reference 55*c*.

Two-State Jump Model (Anisotropic Overall Motion)[57]

$$J(\omega) = \sum_{a,a',b,b'=-2}^{+2} A_{aa'}d_{ab}(\beta_1)\,d_{ab'}(\beta)[(A'^{(1)}_{bb'} + A'^{(2)}_{bb'})\cos(b-b')\alpha - A'^{(3)}_{b'b}\sin(b-b')\alpha]\,d_{b0}(\beta_2)\,d_{b'0}(\beta_2)$$

$$A_{aa'} = \frac{\tau}{1+\omega^2\tau^2}$$

$$\tau^{-1} = 6D_x + a^2(D_z - D_x) \qquad (A\text{-}8)$$

$$A'^{(1)}_{mm'} = (1-k)\cos(m-m')\theta + k\cos(m+m')\theta$$

$$A'^{(2)}_{mm'} = k[\cos(m-m')\theta - \cos(m+m')\theta]\frac{\tau_c}{1+\omega^2\tau_c^2}$$

$$A'^{(3)}_{mm'} = ik' \sin(m - m')\theta$$

$$\tau_c^{-1} = \tau_A^{-1} + \tau_B^{-1}$$

$$k = \frac{2\tau_A\tau_B}{(\tau_A + \tau_B)^2} \qquad k' = \frac{(\tau_A^2 - \tau_B^2)}{(\tau_A + \tau_B)^2}$$

Restricted Internal Diffusion Model[50]

$$J(\omega) = \sum_{i=2}^{+2} \sum_{n=0}^{\infty} |E(i,n)|^2 |d_{i0}(\beta)|^2 \frac{\tau_n}{1 + \omega^2\tau_n^2} \qquad (A\text{-}9)$$

$$\tau_n^{-1} = \frac{n^2\pi^2}{24\tau_i\chi^2}$$

REFERENCES

1. J. W. Finley, S. G. Schmidt, and A. S. Serianni (Eds.), *NMR Applications in Biopolymers*, Plenum, New York, 1990.
2. F. Heatley, *Annu. Rep. NMR Spectrosc.*, 17 (1986) 179–230.
3. D. A. Wright, D. A. Axelson, and G. C. Levy, *Top. Carbon-13 NMR Spectrosc.*, 3 (1979) 103–170.
4. J. R. Lyerla, Jr., and G. C. Levy, *Top. Carbon-13 NMR Spectrosc.*, 1 (1974) 79–148.
5. R. A. Komoroski, I. R. Peat, and G. C. Levy, *Top. Carbon-13 NMR Spectrosc.*, 2 (1976) 179–267.
6. A. S. Perlin and B. Casu, in G. O. Aspinall (Ed.), *The Polysaccharides*, Vol. 1, Chapter 4. Academic Press, New York, 1982.
7. P. A. J. Gorin, *Adv. Carbohydr. Chem. Biochem.*, 38 (1981) 13–104.
8. F. R. Seymour and R. D. Knapp, *Carbohydr. Res.*, 81 (1980) 67–103.
9. K. Matsuo, *Macromolecules*, 17 (1984) 449–452.
10. P. Dais, *Macromolecules*, 18 (1985) 1351–1354.
11. P. Dais, *Carbohydr. Res.*, 160 (1987) 73–93.
12. P. Dais and A. S. Perlin, *Carbohydr. Res.*, 146 (1986) 177–191.
13. P. Dais and G. Fainos, *Can. J. Chem.*, 64 (1986) 560–565.
14. A. Allerhand, D. Doddrell, and R. Komoroski, *J. Chem. Phys.*, 55 (1971) 189–198.
15. K. Dill and A. Allerhand, *J. Biol. Chem.*, 254 (1979) 4524–4531.
16. M. Vignon, F. Michon, and J.-P. Joseleau, *Macromolecules*, 16 (1983) 835–838.
17. A. J. Benesi and D. A. Brant, *Macromolecules*, 18 (1985) 1109–1116.

17a. I. Tvaroska and F. R. Taravel, *Adv. Carbohydr. Chem. Biochem.*, 51 (1995) 15–61, this Volume.

18. C. P. Poole, Jr. and H. A. Farach, *Relaxation in Magnetic Resonance*, Academic Press, London, 1971.
19. A. Abragam, *The Principles of Nuclear Magnetism*, Oxford Univ. Press, London, 1961.
20. C. P. Slichter, *Principles in Nuclear Magnetism*, Harper & Row, New York, 1963.
21. A. H. Morish, *The Physical Principles of Magnetism*, Wiley, New York, 1965.
22. N. Bloembergen, *Nuclear Magnetic Relaxation*, Benjamin, New York, 1961.
23. T. C. Farrar and E. D. Becker, *Pulse and Fourier Transform NMR*, Chap. 4. Academic Press, New York, 1971.

24. A. Carrington and A. D. McLachlan, *Introduction to Magnetic Resonance*, Chap. 11. Harper & Row, New York, 1967.
25. W. T. Huntress, Jr., *Adv. Magn. Reson.*, 4 (1970) 1–37.
26. A. G. Redfield, *Adv. Magn. Reson.*, 1 (1965) 1–32.
27. J. M. Deutch and I. Oppenheim, *Adv. Magn. Reson.*, 3 (1968) 43–78.
28. R. Lenk, *Brownian Motion and Spin Relaxation*, Chap. 2. Elsevier, Amsterdam, 1977.
29. C. F. Foskett, in P. R. Griffiths (Ed.), *Transform Techniques in Chemistry*, Chap. 2. Plenum, New York, 1978.
30. R. L. Vold, J. S. Waugh, M. P. Klein, and D. E. Phelps, *J. Chem. Phys.*, 48 (1968) 3831–3832.
31. R. Freeman and H. D. W. Hill, *J. Chem. Phys.*, 54 (1971) 3367–3377.
32. M. L. Martin, G. J. Martin, and J.-J. Delpuech, *Practical NMR Spectroscopy*, Heyden, London, 1980.
33. D. J. Craik and G. C. Levy, *Top. Carbon-13 NMR Spectrosc.* 4 (1984) 239–275.
34. D. Canet, G. C. Levy, and I. R. Peat, *J. Magn. Reson.*, 18 (1975) 199–204.
35. G. H. Weiss and J. A. Ferretti, *Progr. NMR Spectrosc.*, 20 (1988) 317–335.
36. J. Kowalewski, *Annu. Rep. NMR Spectrosc.*, 22 (1990) 307–414.
37. S. Meiboom and D. Gill, *Rev. Sci. Instrum.*, 29 (1958) 688–691.
38. M. H. Levitt and R. Freeman, *J. Magn. Reson.*, 43 (1981) 65–80.
39. A. D. Bain, W. P. Y. Ho, and J. S. Martin, *J. Magn. Reson.*, 43 (1981) 328–330.
39a. A. Bain and G. J. Duns, *J. Magn. Reson. Ser. A*, 109 (1994) 56–64.
40. K. R. Metz and R. W. Briggs, *J. Magn. Reson.*, 61 (1985) 526–535.
41. D. Wallach and W. T. Huntress, *J. Chem. Phys.*, 50 (1969) 1219–1227.
42. A. Einstein, *Investigations on the Theory of the Brownian Movement*, pp. 19–34. Dover, New York, 1956.
43. R. T. Boere and R. G. Kidd, *Annu. Rep. NMR Spectrosc.*, 13 (1982) 319–385.
44. D. E. Woessner and B. S. Snowden, Jr., *Adv. Mol. Relaxation Processes*, 3 (1977) 181–191.
45. D. E. Woessner, *J. Chem. Phys.*, 37 (1962) 647–654.
46. A. Dolle and T. Bluhm, *Progr. NMR Spectrosc.*, 21 (1989) 175–201.
47. D. E. Woessner, B. S. Snowden, and G. H. Meyer, *J. Chem. Phys.*, 50 (1969) 719–721.
48. R. J. Wittebort and A. Szabo, *J. Chem. Phys.*, 69 (1978) 1722–1736.
49. R. E. London and J. A. Avitabile, *J. Chem. Phys.*, 65 (1976) 2443–2450.
50. R. E. London and J. A. Avitabile, *J. Am. Chem. Soc.*, 100 (1978) 7159–7165.
51. C. C. Wang and R. Pecora, *J. Chem. Phys.*, 72 (1980) 5333–5340.
52. R. Richarz, K. Nagahama, and K. Wuthrich, *Biochemistry*, 19 (1980) 5189–5196.
53. O. W. Howarth, *J. Chem. Soc. Faraday Trans. 2*, 75 (1980) 1031–1041.
54. T. E. Bull, *J. Magn. Reson.*, 31 (1978) 453–458.
55. (a) G. Lipari and A. Szabo, *Biophys. J.*, 30 (1980) 489–506; (b) *Biochemistry*, 20 (1981) 6250–6256; (c) *J. Chem. Phys.*, 75 (1981) 2971–2976; (d) J. R. Brainard and A. Szabo, *Biochemistry*, 20 (1981) 4618–4628.
56. R. E. London, *J. Am. Chem. Soc.*, 100 (1978) 2678–2685.
57. R. E. London and M. A. Phillipi, *J. Magn. Reson.*, 45 (1981) 476–489.
58. R. King and O. Jardetzky, *Chem. Phys. Lett.*, 55 (1978) 15–18.
59. R. King, R. Maas, M. Gassner, R. K. Nanda, W. W. Conover, and O. Jardetzky, *Biophys. J.*, 24 (1978) 103–117.
60. A. A. Ribeiro, R. King, C. Restivo, and O. Jardetzky, *J. Am. Chem. Soc.*, 102 (1980) 4040–4051.
61. A. A. Jones, *J. Polym. Sci. Polym. Phys. Ed.*, 15 (1977) 863–872.
62. A. Tsutsumi, *Mol. Phys.*, 39 (1979) 111–127.
63. Y. K. Levine, N. J. M. Birdsall, A. G. Lee, J. C. Metcalfe, P. Partington, and G. C. K. Roberts, *J. Chem. Phys.*, 60 (1974) 2890–2899.
64. D. Wallach, *J. Chem. Phys.*, 47 (1967) 5258–5268.

65. R. E. London and J. A. Avitabile, *J. Am. Chem. Soc.*, 99 (1977) 7765–7776.
66. G. C. Levy, A. Kumar, and D. Wong, *J. Am. Chem. Soc.*, 105 (1983) 7536–7540.
67. P. Dais and A. S. Perlin, *Can. J. Chem.*, 61 (1983) 1542–1548.
68. F. Heatley, *Progr. NMR Spectrosc.*, 13 (1979) 47–85.
69. P. Dais, M. E. Nedea, F. G. Morin, and R. H. Marchessault, *Macromolecules*, 22 (1989) 4208–4212.
70. K. S. Cole and R. H. Cole, *J. Chem. Phys.*, 9 (1941) 341–353.
71. R. M. Fuoss and J. G. Kirkwood, *J. Am. Chem. Soc.*, 63 (1941) 385–394.
72. J. Schaeffer, *Macromolecules*, 6 (1973) 882–888.
73. B. I. Hunt and J. G. Pawles, *Proc. Phys. Soc. London*, 88 (1966) 513–528.
74. A. A. Jones and W. H. Stockmayer, *J. Polym. Sci. Polym. Phys. Ed.*, 15 (1977) 847–861.
75. E. Helfand, Z. R. Wasserman, and T. A. Webber, *Macromolecules*, 13 (1980) 526–533.
76. E. Helfand, *J. Chem. Phys.*, 54 (1971) 4651–4661.
77. J. Skolnick and E. Helfand, *J. Chem. Phys.*, 72 (1980) 5489–5500.
78. C. K. Hall and E. Helfand, *J. Chem. Phys.*, 77 (1982) 3275–3282; T. A. Weber and E. Helfand, *J. Phys. Chem.*, 87 (1983) 2881–2889.
79. R. Dejean de la Batie, F. Laupretre, and L. Monnerie, *Macromolecules*, 21 (1988) 2045–2052.
80. G. D. Wu, A. S. Serianni, and R. Barker, *J. Org. Chem.* 48 (1983) 1750–1757.
81. A. S. Serianni and R. Barker, *J. Magn. Reson.*, 49 (1982) 335–340.
82. A. S. Serianni and R. Barker, *J. Org. Chem.*, 49 (1984) 3292–3300.
83. P. Dais and A. S. Perlin, *Carbohydr. Res.*, 169 (1987) 159–169.
84. J. M. Berry, L. D. Hall, and K. F. Wong, *Carbohydr. Res.*, 56 (1977) C16–C20.
85. M. F. Czarniecki and E. R. Thornton, *J. Am. Chem. Soc.*, 99 (1977) 8279–8282.
86. A. Sugget, S. Ablett, and P. J. Lillford, *J. Solution Chem.*, 5 (1976) 17–31.
87. C. Williams and A. Allerhand, *Carbohydr. Res.*, 56 (1977) 173–179.
88. K. Bock and L. D. Hall, *Carbohydr. Res.*, 40 (1975) C3–C5.
89. P. A. J. Gorin, A. P. Tulloch, and M. Mazurek, *Carbohydr. Res.* 117 (1983) 279–284.
90. P. Dais and A. S. Perlin, *Carbohydr. Res.*, 194 (1989) 288–295.
91. K. Bock, L. D. Hall, and C. Pedersen, *Can. J. Chem.*, 58 (1980) 1916–1922.
92. P. Dais, T. K. Shing, and A. S. Perlin, *Carbohydr. Res.*, 122 (1983) 305–313.
93. A. Neszmelyi, A. Liptak, and P. Nanasi, *Carbohydr. Res.*, 58 (1977) C7–C9.
94. M. F. Czarniecki and E. R. Thornton, *J. Am. Chem. Soc.*, 98 (1976) 1023–1025.
95. M. F. Czarniecki and E. R. Thornton, *J. Am. Chem. Soc.*, 99 (1977) 8273–8278.
96. P. D. Hoagland, P. E. Pfeffer, and K. M. Valentine, *Carbohydr. Res.*, 74 (1979) 135–143.
97. A. Neszmelyi, S. Omura, and G. Lukacs, *Chem. Commun.*, (1976) 97–98.
98. S. Mizsak, G. Slomp, A. Neszmelyi, S. D. Gero, and G. Lukacs, *Tetrahedron Lett.*, (1977) 721–724.
99. K. Uekama, F. Hirayema, N. Matsuo, and H. Koinuma, *Chem. Lett.*, (1978) 703–706; *ibid*, (1977) 1393–1396.
100. J. P. Behr and J. M. Lehn, *J. Am. Chem. Soc.*, 98 (1976) 1743–1747.
101. A. Neszmelyi, S. Omura, T. T. Thang, and G. Lukacs, *Tetrahedron Lett.*, (1977) 725–728.
102. M. S. Puar and R. Brambilla, *J. Chem. Soc. Perkin II*, (1980) 1847–1849.
103. A. Neszmelyi and H. Bojarska-Dahling, *J. Antibiot.*, 5 (1978) 487–489.
104. A. Allerhand and D. Doddrell, *J. Am. Chem. Soc.*, 107 (1971) 2777–2779.
105. A. Allerhand and M. Dohrenwend, *J. Am. Chem. Soc.*, 107 (1985) 6684–6688.
106. K. Bock and R. U. Lemieux, *Carbohydr. Res.*, 100 (1982) 63–74.
107. A. Neszmelyi, V. Zsoldos-Mady, A. Messmer, and I. Pinter, *Acta Chim. Hung.*, 113 (1983) 423–429.
108. A. Neszmelyi, A. Liptak, P. Nanasi, and J. Szejtli, *Acta Chim. Hung.*, 113 (1983) 431–436.
109. P. Dais and A. S. Perlin, *Magn. Reson. Chem.*, 26 (1988) 373–379.

110. P. Dais, T. K. Shing, and A. S. Perlin, *J. Am. Chem. Soc.*, 106 (1984) 3082–3089.
111. L. W. Jaques, S. Glant, and W. Weltner, Jr., *Carbohydr. Res.*, 80 (1980) 207–211.
112. A. Lepri, C. Rossi, and S. Ugliati, *Magn. Reson. Chem.*, 25 (1987) 521–523.
113. C. M. Buchanan, J. A. Hyatt, S. S. Kelley, and J. L. Little, *Macromolecules*, 23 (1990) 3747–3755.
114. M. Kadkhodael, H. Wu, and D. A. Brant, *Biopolymers*, 31 (1991) 1581–1592.
115. K. Yanasaki, M. Kaneda, and O. Tanaka, *Tetrahedron Lett.*, (1976) 3965–3968.
116. Y. Takeuchi, *Heterocycles*, 15 (1981) 1147–1150.
117. A. Neszmelyi, K. Tori, and G. Lukacs, *Chem. Commun.*, (1977) 613–614.
118. C. Rossi, A. Donati, M. Pia Ricchi, M.-R. Sanson, G. Corbini, and P. Corti, *Magn. Reson. Chem.*, 30 (1992) 954–957.
119. M. Horicovini, I. Tvaroska, and J. Hirsch, *Carbohydr. Res.*, 210 (1991) 13–20.
120. C. M. Buchanan, J. A. Hyatt, and D. W. Lowman, *J. Am. Chem. Soc.*, 111 (1989) 7312–7319.
121. F. R. Seymour and R. D. Knapp, *Carbohydr. Res.*, 72 (1979) 229–234.
122. H. Saito, T. Ohki, N. Takasuka, and T. Sasaki, *Carbohydr. Res.*, 58 (1977) 293–305.
123. H. Saito, T. Ohki, Y. Yoshioka, and F. Fukuoka, *FEBS Lett.*, 68 (1976) 15–18.
124. P. Dais, Q.-J. Peng, and A. S. Perlin, *Carbohydr. Res.*, 168 (1987) 163–179.
125. H. C. Jarrell, T. F. Conway, P. Moyna, and I. C. P. Smith, *Carbohydr. Res.*, 76 (1979) 45–47.
126. P. A. J. Gorin and M. Mazurek, *Carbohydr. Res.*, 72 (1979) C1–C5.
127. Q. J. Peng and A. S. Perlin, *Carbohydr. Res.*, 160 (1987) 57–72.
128. (a) D. C. McCain and J. L. Markley, *Carbohydr. Res.*, 152 (1986) 73–80; (b) *J. Am. Chem. Soc.*, 108 (1986) 4259–4264.
129. H. Kovacs, S. Bagley, and J. Kowalewski, *J. Magn. Reson.*, 85 (1989) 530–541.
130. D. C. McCain and J. L. Markley, *J. Magn. Reson.*, 73 (1987) 244–251.
131. S. Bagley, H. Kovacs, J. Kowalewski, and G. Widmaln, *Magn. Reson. Chem.*, 30 (1992) 733–739.
132. P. Dais and R. H. Marchessault, *Macromolecules*, 24 (1991) 4611–4614.
133. D. A. Torchia, M. A. Hasson, and V. C. Hascall, *J. Biol. Chem.*, 252 (1977) 3617–3625.
134. H. Saito, T. Ohki, T. Sasaki, *Biochemistry*, 16 (1977) 908–914.
135. H. Saito, E. Miyata, and T. Sasaki, *Macromolecules*, 11 (1978) 1244–1251.
136. A. J. Benessi and J. Gerig, *Carbohydr. Res.*, 53 (1977) 278–283.
137. J. M. Harvey and M. C. R. Symons, *J. Solution Chem.*, 7 (1978) 571–586.
138. R. K. Harris and R. H. Newman, *Mol. Phys.*, 38 (1979) 1315–1327.
139. P. Dais and A. S. Perlin, *Carbohydr. Res.*, 136 (1985) 215–223.
140. A. S. Perlin, P. Herve de Penhoat, and H. S. Isbell, *Carbohydr. Res.*, 36 (1974) 111–120.
141. H. S. Isbell and W. W. Pigman, *J. Res. Natl. Bur. Stand.*, 20 (1938) 773–780.
142. D. A. Brant and M. D. Christ, in A. D. French and J. W. Brady (Eds.), *Computer Modelling of Carbohydrate Molecules*, ACS Symposium series No. 430. Washington, DC, 1990, pp. 42–68.
143. D. Ghesquiere, B. Ban, and C. Chachaty, *Macromolecules*, 10 (1977) 743–752.
144. S. Lesage and A. S. Perlin, *Can. J. Chem.*, 56 (1978) 2889–2896.
145. S. Lesage and A. S. Perlin, *Can. J. Chem.*, 56 (1978) 3117–3120.
146. P. Dais and A. S. Perlin, *Can. J. Chem.*, 63 (1985) 1009–1012.
147. J. W. Blunt and J. B. Stothers, *J. Magn. Reson.*, 27 (1977) 515–519.
147a. P. Dais, *Carbohydr. Res.*, 263 (1994) 13–24.
148. (a) G. Lipari and Szabo, *J. Am. Chem. Soc.*, 104 (1982) 4546–4559; (b) *ibid*, 104 (1982) 4559–4570.
149. D. A. Brant, *Ann. Rev. Biophys. Bioeng.*, 1 (1972) 369–408.
150. R. L. Whistler and J. R. Daniel, in R. L. Whistler, J. N. BeMiller, and E. F. Paschall (Eds.), *Starch Chemistry and Technology*, 2nd edn., Chap. VI. Academic Press, New York, 1984.
151. W. T. Winter and T. Sarko, *Biopolymers*, 13 (1974) 1461–1482.

152. W. T. Winter and T. Sarko, *Biopolymers*, 13 (1974) 1447–1460.
153. S. Arnot and W. E. Scott, *J. Chem. Soc. Perkin Trans.* 2, (1972) 324–335.
154. M. Sundaralingam, *Biopolymers*, 6 (1968) 189–213.
155. R. H. Marchessault and S. Pérez, *Biopolymers*, 18 (1979) 2369–2374.
156. W. Gronski, *Makromol. Chem.*, 180 (1979) 1119–1124.
157. R. Roy, F. D. Tropper, A. J. Williams, and J.-R. Brisson, *Can. J. Chem.*, 71 (1993) 1995–2006.
158. J. Denault and J. Prud'homme, *Macromolecules*, 22 (1989) 1307–1316.
159. A. Spyros, P. Dais, and F. Heatley, *Macromolecules*, in press.
160. D. Gagnaire and S. Pérez, *Makromol. Chem.*, 185 (1984) 829–837.

This Page Intentionally Left Blank

ADVANCES IN CARBOHYDRATE CHEMISTRY AND BIOCHEMISTRY, VOL. 51

MECHANISMS IN THE GLUCANSUCRASE SYNTHESIS OF POLYSACCHARIDES AND OLIGOSACCHARIDES FROM SUCROSE

JOHN F. ROBYT

Laboratory of Carbohydrate Chemistry and Enzymology, Department of Biochemistry and Biophysics, Iowa State University, Ames, Iowa

I. HISTORICAL BACKGROUND AND STRUCTURES OF THE POLYSACCHARIDES

In 1861, Louis Pasteur[1] reported a polysaccharide that was produced from sucrose. In 1874, Scheubler[2] determined its empirical formula and named it dextran. The formation of polysaccharide (dextran) was observed as the result of bacterial transformation of sucrose solutions into viscous solutions, gels, and/or flocculent precipitates.[3] The synthesis of dextran from sucrose by a cell-free

TABLE I

Glucans Synthesized from Sucrose by Glucansucrases from Selected *Leuconostoc* and *Streptococci*

Species and strain number[a]	Solubility class[b]	Percent of linkages					Description of the ethanol precipitate	References
		1→6	1→3	1→3 Bra[c]	1→2 Bra[c]	1→4 Bra[c]		
L.m. B-512F	L	95					translucent gel	7,13
L.m. B-742	L	87				13	heavy, opaque	10,11
L.m. B-742	S	50		50			fine[d]	10,11
L.m. B-1299	L	66		1	27		flocculent[d]	19
L.m. B-1299	S	65			35		fine[d]	10,19
L.m. B-1355	L	95		5			translucent gel	10,19
L.m. B-1355	S	54	35	11			heavy, opaque	19
L.m. B-1191	L	94		2		4	cohesive, stringy[d]	17
L.m. B-1308	L	95				5	pasty, crumbly	19
S.s. B-1526	I	83				17	fluid, stringy[d]	15
L.m. B-523	I		100				water-insoluble	17
L.m. B-1149	I		100				water-insoluble	18
S.m. 6715	S	64		36			heavy, opaque	8
S.m. 6715	I	4	96	2			water-insoluble	9,17
S.v. B-1351	S	89		11			short[d]	17,19

[a]L.m. = *Leuconostoc mesenteroides*; S.m. = *Streptococcus mutans*; S.s. = *Strep.* species; S.v. = *Strep. viridans*; the B-numbers refer to the strain number in the Northern Regional Research Laboratory Collection (NRRL) of the USDA Laboratory, Peoria, IL. [b]L = less soluble, referring to glucans precipitated by 34–37% ethanol; S = more soluble, referring to glucans precipitated by 40–44% ethanol; I = water-insoluble. [c]Bra = branch linkage. [d]Description taken from Jeanes *et al.*[5]

Adapted by permission from Table 1 in J. F. Robyt, *Developments in Carbohydrate Chemistry* (R. J. Alexander and H. F. Zobel, Eds.), Am. Assoc. Cereal Chem., St. Paul, MN, 1992, pp. 261–292.

bacterial culture filtrate was first reported by Hehre.[4] The enzyme(s) responsible for the synthesis were called dextransucrases or glucansucrases.

The genera of bacteria recognized to produce enzymes capable of synthesizing polysaccharides from sucrose are principally *Leuconostoc* and *Streptococcus*. These two genera are gram-positive, facultatively anerobic cocci that are closely related to each other. One notable difference between them is that, until recently (see Section II.1), *Leuconostoc* species required sucrose in the culture medium to induce the formation of the enzyme(s), whereas the *Streptococcus* species did not require sucrose in the culture medium for the formation of the enzymes. Thus, the *Leuconostoc* species were INDUCIBLE for the formation of glucansucrases, and the *Streptococcus* species were CONSTITUTIVE for their formation.

In 1954, Jeanes *et al.*[5] reported the formation of glucan(s) by 96 strains of bacteria that were primarily *Leuconostoc* strains. (There is a question here as to whether they are strains or species, particularly with regard to the formation of different kinds of polysaccharides. The classification of the time was to place them into one species, *mesenteroides*, that had several different strains. This classification stands today.) The polysaccharides were characterized by various properties such as optical rotation, viscosity, periodate oxidation profile, and physical appearance after alcohol precipitation. The latter were observed to have different appearances, which were described by Jeanes *et al.*[5] in various qualitative terms such as pasty, fluid, stringy, tough, long, short, flocculent, and so on. These differences in appearance provided an early suggestion of differences in structure (see Table I). Both water-soluble and water-insoluble polysaccharides were formed, and some strains seemed to form more than one kind of polysaccharide, as judged by their water solubility and by differences in the amount of alcohol needed to precipitate them.

Shortly thereafter, Wilham *et al.*[6] showed, using differential alcohol precipitation, that more than one type of polysaccharide was being formed by some of the strains. Periodate-oxidation analysis suggested differences in the amounts and types of glycosidic linkages in the polysaccharides. The actual structures of many of these polysaccharides were later determined by methylation analysis[7-10] and ^{13}C-NMR.[11-20] See Table I for a summary of the amounts and types of linkages found in various polysaccharides synthesized by glucansucrases.

Leuconostoc mesenteroides B-512F formed only one dextran, and this dextran is the only one, to date, to be commercially produced. The B-512 strain (it later was renamed B-512F) was first isolated at the USDA laboratory in Peoria, Illinois, from a contaminated sample of root beer that was described as "ropy." Methylation analysis and ^{13}C-NMR of the glucan showed that it contained 95% α-(1$\rightarrow$6) linkages and 5% α-(1$\rightarrow$3) branch linkages.[7,13] It has main chains of contiguous α-(1$\rightarrow$6) linked D-glucopyranose residues and two types of branches—single glucose units and chains of α-(1$\rightarrow$6) glucose units attached by α-(1$\rightarrow$3) branch linkages to the α-(1$\rightarrow$6)-linked chains (see Fig. 1). This B-512F dextran has

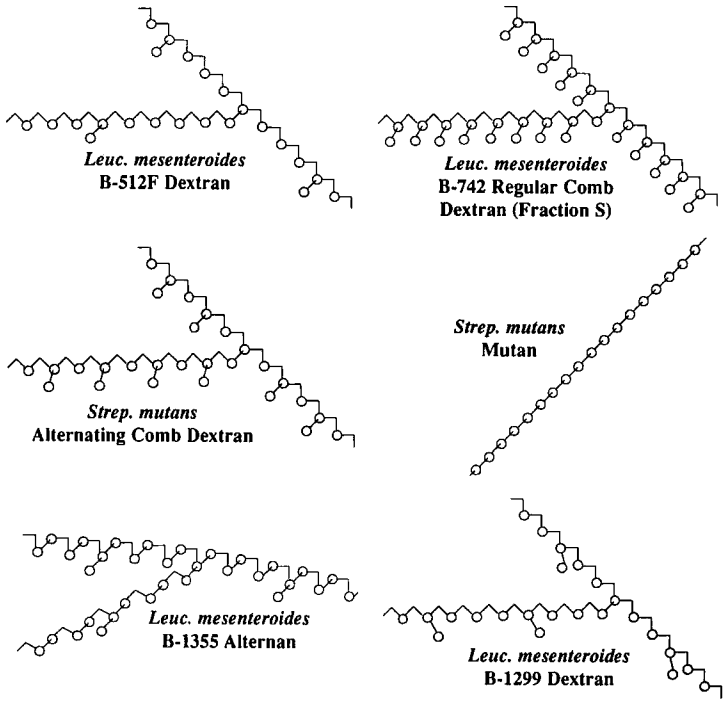

FIG. 1.—Structural representation of segments of different glucans synthesized by glucansucrases from sucrose.

represents a glucose residue linked α-(1→6) to another glucose residue;

represents a glucose residue linked α-(1→3) to another glucose residue;

represents a glucose residue linked α-(1→2) to another glucose residue.

(Adapted from Fig. 3 in ref. 42 and reprinted by permission of the American Association of Cereal Chemists.)

become the structural prototype for the dextrans. The definition now used for a dextran is that it is a glucan with contiguous α-(1→6)-linked glucose residues in the main chains.

Differences in the different dextran structures include the types, amount, length, and arrangement of the branches. The principal type of branch linkage is α-(1→3), but α-(1→2) and α-(1→4) branch linkages also have been observed (see Table I.) *Leuconostoc mesenteroides* B-742 produces two types of dextrans—fraction L dextran, which is precipitated by 38% alcohol has about 14% α-(1→4) branch linkages, and fraction S dextran, which is precipitated by 44% alcohol and has a very high degree (50%) of α-(1→3) branch linkages that primarily consist of single glucose units.[10] The high percentage of branch linkages means that there

must be one glucose residue attached to every α-(1→6)-linked glucose residue in the main chains (see Fig. 1). *Leuconostoc mesenteroides* strain B-1142 dextran has a structure similar to that of B-742 fraction S dextran. The structure is essentially a B-512F dextran structure having some α-(1→6)-linked chains attached by an α-(1→3) branch linkage, but having single glucose residues attached by α-(1→3) branch linkages to every glucose residue in the α-(1→6)-linked chains (see Fig. 1). This structure results in the most highly branched dextran possible. Polymer chemists would characterize the structure as a bifurcated comb polymer in which each of the single α-(1→3)-linked glucose branches is like a tooth of a comb while the α-(1→6)-linked chains are the backbone of the comb. A dextran of this structure would be highly resistant to hydrolysis by *endo*-dextranase, as hydrolysis requires a minimum of six or seven unsubstituted contiguously linked α-(1→6) glucose residues.[21,22]

Streptococcus mutans 6715 elaborates a dextransucrase (glucosyltransferase-soluble, GTF-S) that synthesizes a water-soluble dextran reported to have 35% α-(1→3) branch linkages,[8] composed primarily of single glucose residues. If one considers the single-branch glucose residues to be uniformly distributed along the α-(1→6) contiguously linked glucan chain, the result is an alternating, bifurcated comb polymer in which the single-branch glucose residues are attached by α-(1→3) branch linkages to every other glucose residue in the α-(1→6)-linked main chains (see Fig. 1). This structure also would be resistant to hydrolysis by *endo*-dextranase.

Streptococcus mutans dextrans, prepared under different conditions, have been reported to have varying susceptibilities toward *endo*-dextranase hydrolysis, ranging from as high[23] as 72% to as low[8] as 12%, with several values in between. For example, when the synthesis was conducted in a dialysis bag that enclosed the enzyme and the bag was immersed in a solution of sucrose, the amount of branching was increased over that of a comparable reaction conducted in a homogeneous solution, as judged by a lower degree of hydrolysis by *endo*-dextranase.[23] The amount of branching was also increased when 1.6 *M* ammonium sulfate was present.[23] The susceptibility of the synthesized dextran to hydrolysis by *endo*-dextranase was dependent on the concentration of sucrose used in the reaction, with higher concentrations giving dextrans of greater *endo*-dextranase resistance.[23]

Initially, all of the bacterial glucans synthesized from sucrose were considered to be dextrans. A so-called S-dextran produced by *Leuc. mesenteroides* B-1355 that was precipitated by 42% alcohol gave, on partial acid hydrolysis, two trisaccharides: 6^2-*O*-α-D-glucopyranosylnigerose[24] and 3^2-*O*-α-D-glucopyranosylisomaltose.[25] Using methylation analysis and ^{13}C-NMR, Seymour *et al.*[18] showed that the main chains of this glucan did not have a contiguous sequence of α-(1→6) linkages, but rather had an alternating sequence of α-(1→6)- and α-(1→3)-linked glucose residues. The glucan had 11% α-(1→3) branch linkages.[19] Because of the absence of contiguous α-(1→6) linkages, this glucan is totally resistant to hydrol-

ysis by *endo*-dextranase; it is not, therefore, a dextran and has been named *alternan* on account of its alternating α-(1→6) and α-(1→3) structure.[26]

In addition to elaborating an enzyme that synthesizes a soluble dextran, *Strep. mutans* 6715 also produces an enzyme, mutansucrase (glucosyltransferase-insoluble, GTF-I), that synthesizes a water-insoluble glucan from sucrose. This glucan has a high percentage of contiguous α-(1→3)-linked glucose residues instead of α-(1→6) linkages[15] and is obviously not a dextran; it is resistant to *endo*-dextranase hydrolysis and is called *mutan*.

II. Sources and Characteristics of the Enzymes

1. Bacterial Strains

The enzymes that catalyze the synthesis of glucans from sucrose are secreted into the culture medium. The enzymes produced by *Leuc. mesenteroides* strains are inducible by sucrose, which is absolutely required in the culture media for their production.[27] On the other hand, the enzymes produced by *Streptococcus* species are constitutive and are produced in media lacking sucrose.[28] In later work, however, Kim and Robyt[29] have obtained *Leuc. mesenteroides* mutants from strains B-512FM, B-742, B-1299, and B-1355 that are constitutive for glucansucrases. Active enzymes were produced when the mutants were grown in media containing glucose or fructose instead of sucrose.

2. Purification of the Enzymes

Both *Leuc. mesenteroides* B-512F[30-36] and *Strep.* sp.[37-41] glucansucrases have been purified from their culture supernatants. A hyperproducing *Leuc. mesenteroides* B-512F mutant (B-512FM) that produces 500 times more enzyme than the parent type has been obtained by mutagenesis using nitrosoguanidine.[36] The glucans that are formed from sucrose in the culture supernatants by the inducible *Leuc. mesenteroides* glucansucrases are difficult to remove. Much of the dextran can be removed from *Leuc. mesenteroides* B-512FM by the addition of *endo*-dextranase.[34] The addition of *endo*-dextranase, however, necessitates its subsequent removal to obtain a dextransucrase preparation that can synthesize dextran of high molecular weight.[34-36]

The removal of glucan from the glucansucrases in the culture supernatants of other strains of *Leuc. mesenteroides*, such as B-742 dextransucrase or B-1355 alternansucrase, is much more difficult, as the glucans that accompany these enzymes are quite resistant to *endo*-dextranase hydrolysis.[42] The formation of *Leuc. mesenteroides* mutants that are constitutive for the glucansucrases should alleviate these problems of glucan removal and should greatly facilitate the purification of the enzymes. In addition, many of these *Leuconostoc* strains also form more than one glucansucrase, and these synthesize glucans having different struc-

tures. Some of the *Leuc. mesenteroides* constitutive mutants form only one of the glucansucrases,[43] and this further aids in the purification process.

3. Molecular Weights and Structures of the Enzymes

The molecular sizes of the glucansucrases have been reported to range from 1.85×10^5 Da[44] to 6.4×10^4 Da.[45] Aggregates of very high molecular weight have also been observed, especially when the enzyme is elaborated in a sucrose medium and glucan is synthesized.[32,34] These aggregates often precipitate from solution, but readily dissolve again when sucrose or dextran is added. Addition of other carbohydrates, such as soluble starch, levan, or methyl α-D-glucopyranoside had no such effect. The 6.4×10^4 Da enzyme, reported by Kobayashi and Matsuda,[44] had very low enzyme activity[45]; most probably, it either was an inactive subunit that partially reassembled in the presence of substrate (sucrose) during the assay to give some active enzyme containing more than one subunit, or it contained a small amount of active, multisubunit enzyme that was not detected in the molecular-weight analysis. Miller *et al.*[35] and Fu and Robyt[36] found that the molecular size of the *Leuc. mesenteroides* B-512FM initially secreted into the culture medium was 1.77×10^5 Da; but on being kept, the enzyme exhibited a drop in molecular size to 1.58×10^5 Da without any loss in enzyme activity. Grahame and Mayer[46] made a similar observation for the dextransucrase of *Strep. sanguis*. Purified dextransucrase obtained from the constitutive mutant *Leuc. mesenteroides* B-512FMC has a molecular size of 1.85×10^5 Da and is made up[47] of three subunits—two with molecular weights of 6.3×10^4 and one with a weight of 5.9×10^4. Likewise, several constitutive mutants of *Leuc. mesenteroides* B-742 (B-742C, B-742CA, and B-742CB) also had molecular sizes of 1.84×10^5 Da.[43]

III. Mechanisms of Polysaccharide Synthesis

1. Substrates and the Activity of the Enzyme

The glucansucrases use sucrose as a high-energy glucosyl donor for polysaccharide and oligosaccharide syntheses. In addition to sucrose, α-D-glucopyranosyl α-L-sorbofuranoside,[48] β-D-galactopyranosyl-(1→4)-β-D-fructofuranosyl α-D-glucopyranoside (lactulosucrose),[49] α-D-glucopyranosyl fluoride,[50] and *p*-nitrophenyl α-D-glucopyranoside[51] also serve as glucopyranosyl donors. Of these substrates, sucrose is the best, with the lowest K_m. The substrates have glucosidic bond energies of 5.5–5.0 kcal/mol. This is of the same level of energy found in such nucleoside glucose diphosphate donors as uridine 5′-(α-D-glucopyranosyl diphosphate) (UDPGlc) and adenosine 5′-(α-D-glucopyranosyl diphosphate) (ADPGlc).

The reaction of glucansucrases with sucrose may be simply formulated by the

following:

$$n \text{ Sucrose} \longrightarrow (\text{glucose})_{n\text{-}m\text{-}w} + n-m \text{ fructose} + m \text{ leucrose} + w \text{ glucose.}$$

The reaction is essentially irreversible. The main products are a high-molecular-weight ($1 \times 10^7 - 1 \times 10^8$ Da) glucan, together with fructose, and the minor products are glucose and leucrose (where, $n >> m$ or w). Glucose arises from an acceptor reaction with water, and leucrose [5-*O*-α-D-glucopyranosyl-D-fructopyranose] arises from an acceptor reaction with the primary product, fructose. (The acceptor reactions are discussed in Section IV.)

The reaction of glucansucrases may be measured in two general ways: (1) by measuring the amount of glucan synthesized and (2) by measuring the formation of fructose. The latter can be obtained either by determining the reducing value[52-54] or by measuring the amount of fructose formed enzymatically.[55] The determination of the amount of glucan formed can be obtained by measuring the amount of ^{14}C-glucose incorporated into glucan from [U-^{14}C]sucrose, using a filter-paper assay with a liquid-scintillation spectrometer.[56] In this assay, aliquots (10–25 μL) are added to 1.5 × 1.5 cm Whatman 3MM paper which is immediately placed in 200 mL of methanol to stop the reaction and precipitate the polysaccharide onto the paper. Aliquots are taken at various times, such as 5, 10, 15, and 20 min. The paper squares are washed three times with 200 mL of methanol, dried, and counted in a liquid-scintillation spectrometer using a toluene cocktail. The amount of glucose incorporated into glucan can then be calculated.

The radioactive method has proven to be very accurate, convenient, and relatively rapid method for measuring the rate of glucan synthesis, the principal reaction catalyzed by glucansucrases. In addition, it can directly measure the effect of the presence of acceptors or inhibitors on the rate of glucan synthesis. In contrast, reducing-value methods often cannot be used in these kinds of reactions because the acceptors, or the inhibitors themselves, have reducing values that would give very high initial values, exceeding the range of the method and producing large errors owing to the small differences obtained between the blank value and the value produced by the reaction.

After the discovery that α-D-glucopyranosyl fluoride could be a glucosyl donor for glucansucrases,[50] Grier and Mayer[57] synthesized and tested a number of α-D-glucopyranosyl analogs, such as α-D-mannopyranosyl, α-D-allopyranosyl, α-D-galactopyranosyl, α-D-gulopyranosyl, 3-*O*-methyl-α-D-glucopyranosyl, 4-deoxy-α-D-*xylo*-hexopyranosyl, 6-deoxy-α-D-glucopyranosyl, α-D-xylopyranosyl, and β-D-glucopyranosyl fluoride, as possible alternative glycosyl donors for *Strep. sanguis* dextransucrase. Disappointingly, they found that none of these analogs was a substrate for glycosyl donation for the synthesis of polysaccharides or oligosaccharides. The study did show that glucansucrases were highly

specific for the binding of the glucosyl part of sucrose and that only the D-glucopyranose structure could be productively bound to give glucosyl transfer.

2. Formation of Enzyme Covalent Intermediates

For glucan synthesis, the energy of the glucose glycosidic linkage of sucrose must be conserved until the glucose is incorporated into the polysaccharide. Furthermore, the glucose moiety must be manipulated so that the enzyme can perform its catalytic function of synthesizing a glycosidic bond. This can be achieved by the transfer of the glucose moiety of sucrose to the enzyme with the formation of a covalent, high-energy-enzyme intermediate.

Using *Leuc. mesenteroides* B-512F dextransucrase and *Strep. mutans* 6715 dextransucrase and mutansucrase immobilized on Bio-Gel P-2, Robyt *et al.*[58,59] showed that both covalent glucosyl- and glucanyl-enzyme intermediates were formed during glucan synthesis by these three enzymes. They further showed that the glucosyl-intermediate was incorporated into the growing glucans. Parnaik *et al.*[60] isolated a glucosyl-enzyme intermediate for *Strep. sanguis* dextransucrase. Mooser and Iwaoka[61] also isolated a covalent glucosyl-enzyme by rapidly denaturing a *Strep. sorbrinus* dextransucrase–[^{14}C]sucrose digest. They showed that this glucose was attached to the enzyme by a β-glycosidic linkage, as had been predicted for a double-displacement mechanism.[62]

By treating the glucose-enzyme complexes with pepsin, Mooser *et al.*[63] later isolated and sequenced the active-site peptides from dextransucrase (GTF-S) and mutansucrase (GTF-I), each of which has a covalently linked glucose. The two peptides had nine amino acids and the following similar, but not identical, sequences:

GTF-S peptide	Asp-Gly-Val-Arg-Val-Asp-Ala-Val-Asp
GTF-I peptide	Asp-Ser-Ile-Arg-Val-Asp-Ala-Val-Asp

Fast-atom-bombardment mass spectrometry of a proteinase-truncated glucosyl-enzyme complex showed that the glucose was covalently linked as a β-acetal ester to the carboxyl group of the aspartic acid located at the sixth residue from the *N*-terminal of the peptide:

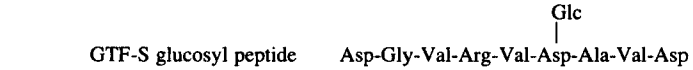

3. Primer-Dependent Synthesis of Polysaccharide from the Nonreducing End

When dextransucrase was first described in 1941,[4] Cori and Cori[64] were studying the action of muscle phosphorylase and Hanes[65] was studying potato phosphorylase. These investigators observed that phosphorylase could elongate

glycogen and starch chains by the transfer of glucose from α-D-glucopyranosyl phosphate (Glc-1-P) to the nonreducing end of the glucan chain.[66] At this time, it was believed that phosphorylase was the synthetic enzyme responsible for the synthesis of glycogen and starch. The synthesis required a pre-formed polysaccharide chain, called a *primer,* and an activated or high-energy monosaccharide donor (Glc-1-P in this case). Later it was shown that *in vivo,* phosphorylase was a degradative enzyme that catalyzed the reaction of inorganic phosphate with the nonreducing-end glucose residue of the polysaccharide chain to give Glc-1-P.[67] The so-called synthetic reaction was the reverse of the degradative reaction. It is now obvious that the reverse reaction of the degradative reaction would then require the nonreducing end of a pre-formed polysaccharide chain, as the polysaccharide chain is necessary for its own degradation. At the time, however, this requirement was neither recognized nor appreciated, and so the primer mechanism for the biosynthesis of polysaccharides was developed and accepted. For synthesis of a polysaccharide to occur by a primer-dependent mechanism, the nonreducing ends of the primer molecules (either polymer or oligomer) are *required* for the addition of new monomer units.[68]

Thus, in the 1940s and 50s, the primer mechanism was assumed for the synthesis of dextran.[52,53,69,70] This mechanism was strengthened in the 1970s when Germaine *et al.*[71–73] found that the addition of dextran to digests of *Strep. mutans* dextransucrase increased the rate of dextran synthesis. They found that the rate reached a maximum when the average size of the added dextran was 30 glucose residues.[71,72]

Kobayashi and Matsuda[44,45] also reported that the purified dextransucrases of both *Leuc. mesenteroides* B-512F and *Strep.* sp. were stimulated by dextran, although both enzymes could synthesize dextran without the addition of dextran primer. The reaction was accompanied by a lag period that could be abolished by the addition of exogenous dextran. Based on these results, Kobayashi *et al.*[74] proposed a primer-dependent mechanism for dextran synthesis, which is illustrated in Fig. 2. They proposed that the active site has two types of substrate binding sites, one for sucrose and the other for the primer dextran. The elongation of the primer was hypothesized to take place when an enzyme nucleophile (presumably a carboxylate anion) attacks C-1 of the glucose moiety of sucrose to give a glucosyl-enzyme covalent intermediate. This glucose is then transferred to the 6-hydroxyl group of the nonreducing end of the primer chain. The reaction takes place when the nonreducing-end 6-hydroxyl group of the primer chain attacks at C-1 of the glucosyl-enzyme covalent intermediate to give an α-(1→6) glycosidic linkage, thereby elongating the primer chain by one glucose residue. For synthesis to continue, the chain with the newly added glucose residue must dissociate from the primer binding site and a new primer molecule must bind in the primer binding site with its nonreducing glucose residue in position to accept the next glucose unit. The synthesis is, thus, a discontinuous process.

A problem with the primer-dependent mechanism is the synthesis of glucan by

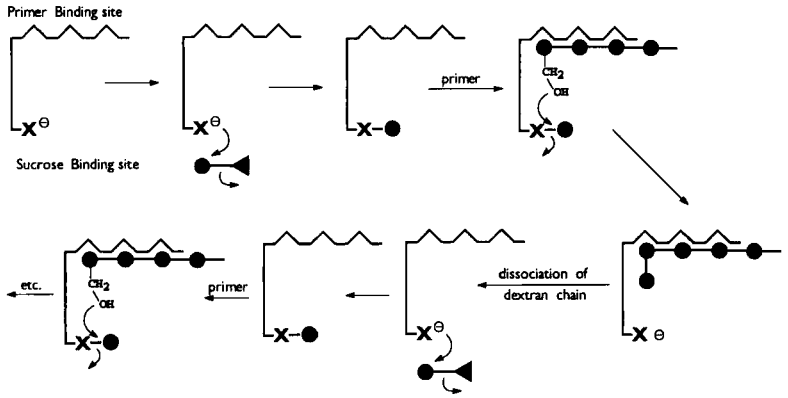

FIG. 2.—Primer-dependent mechanism for the synthesis of *Leuc. mesenteroides* B-512F dextransucrase. ●—◀ is sucrose, ● is glucose, ◀ is fructose, X^- represents an enzyme nucleophile, and ●—● represents two glucose residues linked α-(1→6).

the constitutive *Strep.* and *Leuc.* sp. glucansucrases in the absence of any primer polysaccharide. One answer to this criticism was that sucrose itself was acting as a primer[70,75]; however, no real evidence for this explanation was presented. In fact, when the first putative product of the sucrose-primed reaction—namely 6^{Glc}-*O*-α-D-glucopyranosylsucrose (theanderose)—was used as a primer, the synthesis of dextran was inhibited and only oligosaccharide acceptor products were formed.[76,77] In addition, the sucrose-primed reaction would be expected to form oligosaccharides, specifically isomalto-oligosaccharide intermediates, but these intermediates have never been observed in the sucrose digests. A third problem with the primer-dependent mechanism was how the dextran chain became branched. A branching enzyme similar to the branching enzyme involved in starch biosynthesis was postulated, but a search for this dextran-branching enzyme has not been productive. Furthermore, the energy for branch formation by a branching enzyme in which there is the transfer of an α-(1→6) linkage to an α-(1→3) branch linkage is unfavorable because the α-(1→6) linkage is of lower energy than the α-(1→3) branch linkage. There is evidence that branch linkages are synthesized by the synthesizing enzyme itself and that branching does not occur by catalysis of a distinct branching enzyme (see Section III.5).

Robyt and Corrigan[78] found that a dextran, modified by a blocking (triisopropylbenzenesulfonyl, tripsyl) group on the C-6 position of the nonreducing-end glucose residue, increased the rate of dextran synthesis by *Strep. mutans* dextransucrase equally as well as unmodified dextran. The modified dextran could not participate in a priming reaction because the requisite site for glucose transfer, the 6-hydroxyl group of the nonreducing-end, was blocked by a tripsyl group. This result showed that the added dextran was not stimulating the reaction by acting as a

primer, but by some other mechanism. Robyt and Corrigan proposed two alternative mechanisms. The first was the action of the added dextran as an acceptor that receives the transfer of single glucose groups and dextran chains from the active site to give α-(1→3) branch linkages on the added dextran. This proposal was consistent with the mechanism demonstrated for the formation of branch linkages by Robyt and Taniguchi.[79] The second mechanism was that the added dextran was stimulating the action of the enzyme by binding to an allosteric site and inducing an enzyme conformation favorable for catalysis. This mechanism has received some support by the finding of Mooser *et al.*[80,81] that *Strep. mutans* dextransucrase has a dextran-binding domain distinct from the active-site domain. Both the *Strep.* dextransucrases[82–84] and the *Leuc. mesenteroides* B-512F dextransucrase[35,47] bind to lightly crosslinked dextran (Sephadex G-200); this binding is inhibited when dextran is present, further supporting the idea of a dextran-binding domain for these enzymes. It is this dextran-binding domain that could give a positive allosteric effect on the enzymes. The allosteric effect was further suggested by the sigmoidal activity curve obtained when increasing amounts of dextran were added to *Strep. mutans* dextransucrase (GTF-S) digests.[85] Similar results were obtained for the dextransucrase produced by the constitutive mutant *Leuc. mesenteroides* B-512FMC grown on glucose.[47,85]

4. Two-Site Insertion Mechanism for the *de Novo* Synthesis of Polysaccharide by Addition of Glucose to the Reducing End

In 1967, two possible general mechanisms for the biosynthesis of linear polysaccharides were proposed.[86] The first was the primer mechanism already discussed, and the second was the sequential addition of monomer units to the reducing end by the insertion between a carrier and the growing polysaccharide chain. This latter mechanism had been shown for *Salmonella* sp. O-antigenic polysaccharide[87]; then in 1973, it was shown for the bacterial cell-wall polysaccharide murein[88] in which the carrier was a polyisoprenoid pyrophosphate.

In 1962, Ebert and Patat[89] had proposed a similar insertion mechanism for the synthesis of dextran, with the addition of glucose to the reducing end. This proposal was based on (a) the very high molecular weight of the dextran that was obtained at very low degrees of sucrose conversion, (b) the effect on the molecular weight of dextran as the concentration of acceptor was increased, and (c) the capacities of different acceptors either to increase or decrease the rate of reaction of sucrose. The carrier was postulated to be the enzyme itself. Ebert and Schenk[90] further elaborated on the mechanism in a review. No definitive experimental evidence was presented, however; and no detailed explanation of exactly how the glucose moiety of sucrose was transferred to the reducing end was offered. The mechanism thus remained a hypothesis that was not widely accepted as the mechanism for dextran synthesis.

In 1974, Robyt *et al.*[58] presented experimental evidence for the insertion mechanism and the addition of glucose to the reducing end of dextran. They used pulse and chase techniques with [U-^{14}C]sucrose and *Leuc. mesenteroides* B-512F dextransucrase immobilized on Bio-Gel P-2. The enzyme was located on the surface of the highly crosslinked Bio-Gel beads. The immobilized enzyme was pulsed with a low concentration of [U-^{14}C]sucrose. The enzyme beads were removed by centrifugation and washed with buffer several times to remove any soluble label—primarily [^{14}C]fructose. Some label remained tightly associated with the immobilized enzyme. This label could be stoichiometrically released by adjusting the pH to 2 and heating for 5 min at 55°. Chromatographic analysis showed that the released label was [^{14}C]glucose and [^{14}C]dextran. In a separate experiment, the pulsed-labeled enzyme beads were chased by incubation in nonlabeled sucrose solution for a short time. The enzyme beads were removed, washed with buffer, adjusted to pH 2, and heated for 5 min at 55°. Chromatographic analysis of the released label showed only ^{14}C-labeled dextran. These experiments showed that glucose and dextran were covalently attached to the enzyme during synthesis and that the glucose was being incorporated into the dextran.

The dextrans produced in the pulse and chase experiments were purified (separated from glucose) by chromatography on Bio-Gel P-6. They were reduced with sodium borohydride and then acid-hydrolyzed. The hydrolysates contained labeled D-glucitol and D-glucose. The ratio of labeled D-glucitol to labeled D-glucose was much higher in the pulse-dextran hydrolysate than it was in the chase dextran hydrolyzate. This experiment showed that the glucose was being transferred to the reducing end of the growing dextran chain that was covalently attached to the enzyme active site.

Robyt *et al.*[58] proposed a two-site insertion mechanism to explain the results of the pulse and chase experiments. In this mechanism, two sucrose binding sites and two nucleophiles (presumably two carboxylate anions; see references 61,63,91) attack the two sucrose molecules to give two covalent glucosyl-enzyme intermediates (see Fig. 3). The 6-hydroxyl group of one of these glucosyl intermediates nucleophilically attacks the C-1 of the other glucosyl intermediate to form an α-(1$\rightarrow$6) glycosidic linkage and an isomaltosyl-enzyme intermediate. The newly released nucleophile then attacks another sucrose molecule to give a new glucosyl-enzyme intermediate (this is shown in Fig. 3 as a concerted reaction that takes place as the nucleophile is displaced from the glucosyl unit). The 6-hydroxyl group of the new glucose intermediate then attacks the C-1 of the isomaltosyl intermediate to give a second α-(1$\rightarrow$6) linkage and the formation of an isomaltotriosyl-enzyme intermediate. The process continues in a similar fashion between the two sites, effecting the synthesis of a dextran chain by the addition of glucose to the reducing end of the chain and the apparent insertion of glucose between the enzyme and the growing chain. In this mechanism, a dextran chain can be synthesized *de novo* in a continuous manner without the presence of any pre-formed dextran.

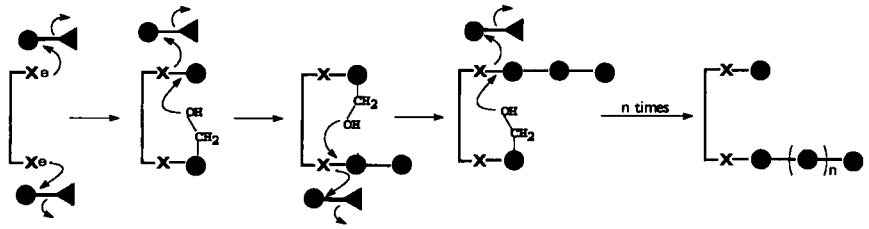

FIG. 3.—Two-site insertion mechanism for the synthesis of *Leuc. mesenteroides* B-512F dextran by dextransucrase. The symbols are the same as in Fig. 2. X orients the glucosyl units so that their 6-hydroxyl groups can attack at C-1 of the apposed glucosyl unit. (Adapted from ref. 58 and reprinted by permission of Academic Press.)

Robyt and Eklund[62] considered the stereochemistry of the reaction and concluded that the linkages of the glucosyl and dextranyl units to the enzyme must be β to retain the configuration of the glucose residue in going from sucrose to dextran. They further postulated that the 6-hydroxyl group is stereochemically apposed to the α side of C-1 of the opposite β-glucosyl unit of the dextran chain, which then assumes a planar conformation to give an axial glycosidic bond to the enzyme (see

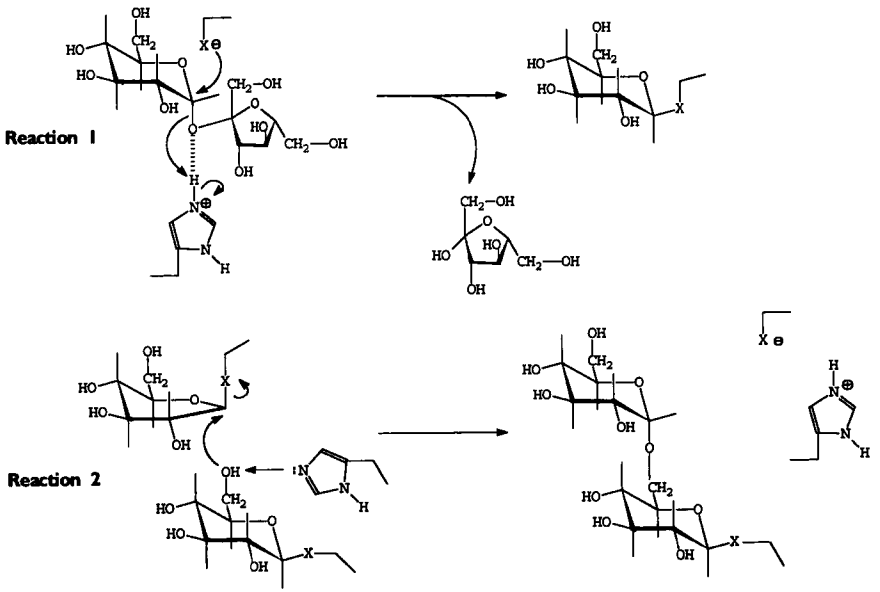

FIG. 4.—Mechanism for the cleavage of sucrose and the formation of an α-(1→6)-glycosidic bond by dextransucrase. Reaction 1: Nucleophilic displacement and protonation of the fructose moiety to form a glucosyl-enzyme intermediate. Reaction 2: Formation of an α-(1→6)-glycosidic bond by attack of a 6-hydroxyl group at C-1 of a glucosyl-enzyme complex; the attack is facilitated by abstraction of a proton from the hydroxyl group by the imidazole group. (From Ref. 92, reprinted by permission of Elsevier Science Press B.V.)

Fig. 4). The 6-hydroxyl group of the single glucosyl unit makes a nucleophilic attack at the axially bonded C-1, displacing the enzyme nucleophile and forming an α-(1→6) linkage. During synthesis, the growing dextran chain is transferred from one site to the other. The chain, however, does not have to move a great distance; only one or two of the glucosyl residues at the reducing end of the chain must move a few angstroms to effect the transfer. The chain is thus extruded from the active site as the glucose units are added to the reducing end.

An additional requirement for the reaction to take place is the transfer of a hydrogen ion to the displaced fructosyl moiety of sucrose.[62] Fu and Robyt[92] showed, by chemical modification of the enzyme with diethyl pyrocarbonate and photo-oxidation with Rose Bengal dye, that two imidazolium groups of histidine were essential for dextran synthesis. They postulated that these two imidazolium groups donate their hydrogen ions to the leaving fructose units (see Fig. 4) and that the resulting imidazole group, in a second step, becomes reprotonated by abstracting a proton from the attacking 6-hydroxyl group of the glucosyl-enzyme intermediate, thereby facilitating the nucleophilic attack and the formation of the α-(1→6) linkage. Thus the imidazole group also becomes reprotonated for the next reaction with sucrose.

In 1983, Robyt and Martin[59] conducted similar [^{14}C]sucrose pulse and chase studies with *Strep. mutans* 6715 dextransucrase (GTF-S) and mutansucrase (GTF-I). They found that these two enzymes also had an insertion mechanism in which the glucose was added to the reducing end of the growing chain. For GTF-I, which catalyzes the synthesis of α-(1→3) glycosidic linkages, the stereochemistry of the enzyme-glucosyl unit must be such that the 3-hydroxyl group is placed in a position that facilitates nucleophilic attack at the opposite glucosyl unit of the growing chain to effect the synthesis of α-(1→3) linkages (see Fig. 5). The synthesis of the dextran chain by GTF-S dextransucrase occurs in a manner similar to that of B-512F dextransucrase. In 1984, Ditson and Mayer[93] confirmed the synthesis of dextran from the reducing end by *Strep. sanguis* GTF-S dextransucrase.

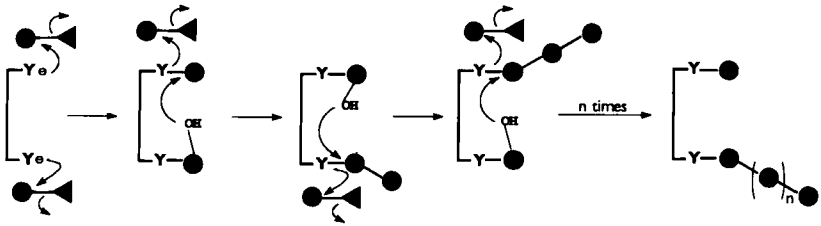

FIG. 5.—Two-site insertion mechanism for the synthesis of *Strep. mutans* mutan by mutansucrase. The symbols are the same as in Fig. 3 with the substitution of **Y** for **X** as the nucleophiles; ●— represents a glucose residue linked α-(1→3) to another glucose residue. **Y** orients the glucosyl units so that their 3-hydroxyl groups can attack at C-1 of the apposed glucosyl unit.

Mechanisms for the synthesis of other glucans, such as *Leuc. mesenteroides* B-1355 alternan and *Leuc. mesenteroides* B-742 regular comb-polymer dextran can also be formulated by a two-site insertion mechanism. For the synthesis of alternan the mechanism can be postulated to have the two glucosyl intermediates stereochemically positioned differently. On one site (the **X** site), the glucosyl intermediate is stereochemically positioned so that only its 6-hydroxyl group is in position to attack the C-1 of the opposite glucosyl-enzyme intermediate to give an α-(1→6) linkage; on the other site (the **Y** site), the glucosyl-enzyme intermediate is stereochemically positioned so that only its 3-hydroxyl group attacks the C-1 of the opposite glucosyl intermediate to give an α-(1→3) linkage. In this manner, the chain goes back and forth between the two sites, giving an alternating synthesis of α-(1→6) and α-(1→3) glycosidic linkages (see Fig. 6).

A two-site mechanism can also be postulated for the complete synthesis of the more complex, highly branched structure of the B-742 regular comb-dextran. In this mechanism (Fig. 7), when a single glucose intermediate attacks the C-1 of the opposite glucosyl intermediate, its 6-hydroxyl group is *always* in stereochemical position to make the attack. The next reaction, however, is by the 3-hydroxyl group of the same glucosyl unit that had just been added to the reducing end of the growing dextran chain. In this mechanism, it is postulated that the 3-hydroxyl group is stereospecifically placed to make the attack by virtue of the fact that its glucosyl unit has just formed an α-(1→6) linkage and been incorporated into the dextran chain. A consideration of the reactions with molecular models shows that the stereopositioning of the 3-hydroxyl group can readily be achieved by rotation of the glucosyl unit 180° around the **X** site. This reaction thus adds a single glucose residue linked by a branched α-(1→3) linkage to the growing dextran chain. Then a 6-hydroxyl group of the opposite single glucosyl intermediate attacks the C-1 of the dextranyl chain to form an α-(1→6) linkage and thus adds another glucose residue to the reducing end of the chain; the 3-hydroxyl group of this added glucose residue makes an attack at C-1 of the apposed glucosyl unit. The process then

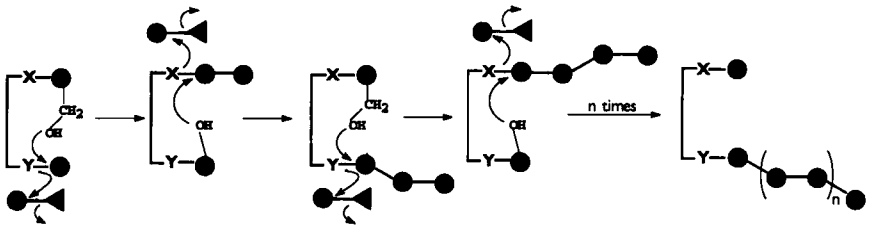

FIG. 6.—Two-site insertion mechanism for the synthesis of *Leuc. mesenteroides* B-1355 alternan by alternansucrase. The symbols are the same as in Fig. 5 with the addition that the two nucleophiles are **X** and **Y**; **X** orients its glucosyl unit so that its 6-hydroxyl group can attack at C-1 of the apposed glucosyl unit and **Y** orients its glucosyl unit so that its 3-hydroxyl group can attack at C-1 of the apposed glucosyl units.

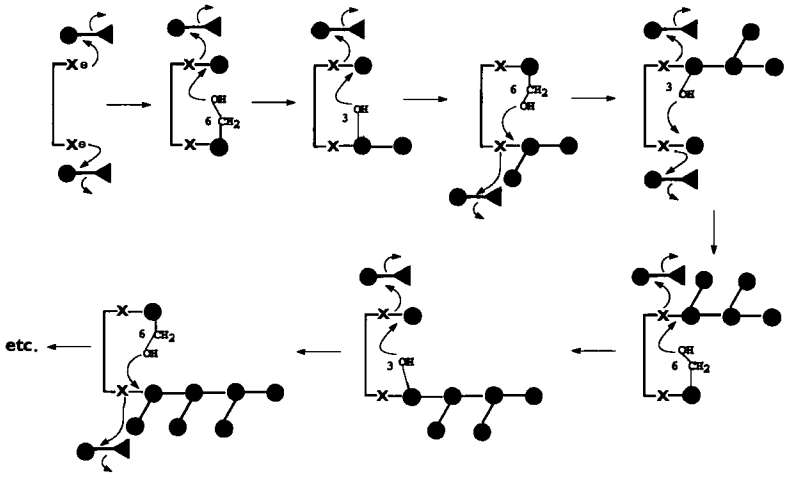

FIG. 7.—Two-site insertion mechanism for the synthesis of *Leuc. mesenteroides* B-742 regular comb dextran by dextransucrase. The symbols are the same as in Figs. 3 and 5.

continues between the two sites, giving an α-(1→6)-linked chain with single α-(1→3)-branch glucose residues attached to every glucose residue in the main chain. The mechanism differs from the B-512F dextransucrase mechanism (see Fig. 3) only by virtue of the fact that two reactions occur sequentially from the same site—the first reaction by the 6-hydroxyl group, followed by a second reaction by the 3-hydroxyl group—before the next set of two reactions takes place from the opposite site.

Su and Robyt[94] confirmed the two-site mechanism for *Leuc. mesenteroides* B-512FM dextransucrase by using equilibrium dialysis with 6-deoxysucrose, a strong competitive inhibitor for the enzyme. They showed that there are two sucrose binding-sites at the active site. They further showed that two sites were required for dextran synthesis, as shown in Fig. 3, and one site for acceptor-product synthesis, as shown in Fig. 9 (see Section IV. 3), by determining the relative decrease in the rate of dextran synthesis and the rate of acceptor-product synthesis as a function of the modification of histidine residues by diethyl pyrocarbonate. The argument was based on the hypothesis that if two sites are required for glucan synthesis and one of the sites is modified, synthesis of glucan would stop; but if only one of the two sites is required for the acceptor reaction, the acceptor reaction can still occur when only one site is modified. This modification should therefore produce a difference in the relative rates in the decrease of the synthesis of dextran and acceptor products because modification of one site stops dextran synthesis but does not stop acceptor reactions. The experimental results verified the hypothesis, as the enzyme lost the ability to synthesize dextran more rapidly than it lost the ability to synthesize acceptor products.[94]

5. Inhibition of Glucan Synthesis

A number of active-site directed inhibitors have been synthesized by chemically modifying sucrose. Two of the best competitive inhibitors are 6-deoxysucrose[95] and 6-deoxy-6-fluorosucrose.[96] Kinetic studies have shown that these inhibitors are bound 5–20 times more tightly to B-512F dextransucrase, GTF-I, and GTF-S than to sucrose.[95–99] 6-Thiosucrose was a moderate competitive inhibitor, being bound about as tightly as sucrose. Other sucrose analogs, such as 3-deoxysucrose and 3-deoxy-3-fluorosucrose were weak competitive inhibitors for GTF-I and GTF-S.[98] 3-Deoxysucrose was a very weak noncompetitive inhibitor for B-512F dextransucrase. Xylosucrose (α-D-xylopyranosyl β-D-fructofuranoside) was a good competitive inhibitor, being bound twice as strongly as sucrose.[99] Allosucrose (α-D-allopyranosyl β-D-fructofuranoside) was a very weak inhibitor that showed mixed-type inhibition.

Several amino sugars, such as methyl 6-amino-6-deoxy-α-D-glucopyranoside, 6,6′-diamino-6,6′-dideoxysucrose, and 6′-amino-6′-deoxysucrose, have been reported to be highly effective inhibitors of GTF-S.[100,101] The doubly substituted sucroses 6,6′-dideoxysucrose[100] and 6,6′-dideoxy-6,6′-difluorosucrose[99] surprisingly were not inhibitors at all for the glucansucrases, whereas the monosubstituted 6-deoxy- and the 6-deoxy-6-fluorosucroses were strong competitive inhibitors. After it had been found that α-D-glucopyranosyl fluoride and *p*-nitrophenyl α-D-glucopyranoside were glucosyl donors, it was thought that the fructose moiety played very little, if any, role in the binding to the active site. The lack of the binding of the doubly substituted sucroses in which the fructose has been substituted at C-6′ indicates that fructose does play a role in sucrose binding.

Nojirimycin (5-amino-5-deoxy-D-glucopyranose) and 1-deoxynojirimycin (reduced nojirmycin) are relatively strong inhibitors for dextran synthesis by GTF-S.[102] Their mode of inhibition was supposedly competitive for the sucrose binding site(s). They were reported to be bound 5–8 times more strongly than sucrose. Acarbose, a tetrasaccharide analog with an unsaturated cyclitol group attached to 6-deoxy-D-glucose by an α-imino nitrogen followed by an α-(1→4) linkage to maltose, effectively inhibited the synthesis of dextran by GTF-S.[102]

Most of the acceptors, such as maltose, isomaltose, and methyl α-D-glucopyranoside, were apparent competitive inhibitors for dextransucrase, as determined by Lineweaver–Burke or Hanes–Woolf plots[103]; however, when higher sucrose concentrations were used in a Michaelis–Menten plot, the inhibition was not reversed for methyl α-D-glucopyranoside as it should have been for a competitive inhibitor.[103] It was concluded that the acceptors were being bound at a site that was separate and distinct from the sucrose binding-sites.

Very early kinetic studies by Hehre[30] showed that sucrose became a substrate inhibitor above 200 m*M*, and this observation was verified by several other studies.[31,103–107] Substrate inhibition at relatively high sucrose concentrations has been interpreted to be due to the binding of sucrose at an allosteric site to effect a

conformational distortion of the active site so that dextran cannot be synthesized.[106] In fact, very high concentrations of sucrose (2 *M*) with B-512F dextransucrase did not give any dextran over a 15-h period. However, when the enzyme–sucrose solution was diluted to a sucrose concentration of 1 *M* or lower, dextran was synthesized. Thus, the very high concentrations of sucrose completely stop dextran synthesis; they do not, however, denature the enzyme because synthesis can be obtained by diluting the solution to lower the sucrose concentration, hence reversing the allosteric inhibition.

IV. Acceptor Reactions—Synthesis of Oligosaccharides and Branching of Dextrans

1. Acceptors and the Acceptor Reaction

In addition to catalyzing the synthesis of dextran from sucrose, dextransucrase also catalyzes the transfer of glucose from sucrose to other carbohydrates that are present or are added to the digest.[52,53] The added carbohydrates are called *acceptors* and the reaction is called an *acceptor reaction.* When the acceptor is a monosaccharide or disaccharide, a series of oligosaccharide acceptor-products[108] is usually produced. Figure 8 shows a chromatographic analysis of acceptor products that result when D-glucose is the added acceptor. Actually, there are two classes of acceptors: those that give a homologous series of oligosaccharides, each differing one from the other by one glucose residue, and those that form just a single acceptor product containing one glucose residue more than the acceptor.

Koepsell *et al.*[52] and Tsuchiya *et al.*[53] also observed that the presence of acceptors of low molecular weight shifted the course of the reaction from the synthesis of high-molecular-weight dextran to the synthesis of a lower-molecular-weight dextran. Robyt and Eklund[108] showed that the amount of dextran synthesized decreased as the molar ratio of maltose (the best known acceptor) to sucrose increased.

2. Structures of the Acceptor Products

When D-glucose, methyl α-D-glucopyranoside, maltose, and isomaltose are the acceptors, the glucose from sucrose is transferred either to the 6-hydroxyl group of the monosaccharide or to the 6-hydroxyl group of the nonreducing-end glucose residue of the disaccharides to give a series of isomalto-oligosaccharides of degree of polymerization (d.p.) of 2–7 attached to the acceptor.[108,109] The first product in the series with isomaltose is isomaltotriose and the first product in the series with maltose is panose [6^2-*O*-α-D-glucopyranosylmaltose].[110] The next product in the maltose series is a tetrasaccharide, 6^2-*O*-α-isomaltosylmaltose, and the other members of the series have isomalto-oligosaccharide chains of increasing degrees of polymerization linked to the 6-hydroxyl group of the nonreducing-end glucose

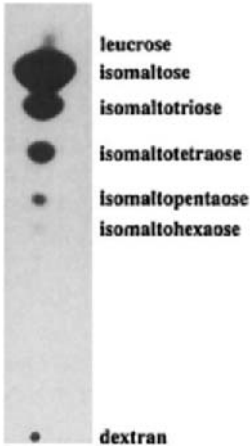

FIG. 8.—Thin-layer chromatographic autoradiogram of the acceptor products formed in the reaction of B-512FM dextransucrase with [^{14}C]sucrose and D-glucose. The first acceptor product of D-glucose is isomaltose, followed in decreasing amounts by isomaltotriose through isomaltooctaose. A small amount of leucrose results from the acceptor reaction of D-fructopyranose. Dextran remains at the origin.

residue of maltose.[109] Similar homologous series are obtained from nigerose, 1,5-anhydro-D-glucitol, and turanose.[108] The amount of each saccharide product in the series decreases as the degree of polymerization increases, usually terminating at d.p. 6 or 7.

Cellobiose gives an unusual series in which the first product is 2^1-*O*-α-D-glucopyranosylcellobiose with glucose attached to the 2-hydroxyl group of the reducing-end glucose residue.[111,112] In the succeeding products of the cellobiose series, the glucose unit of sucrose was transferred to the 6-hydroxyl group of the glucose attached to C-2 of the reducing residue of cellobiose. When the cellobiose analog lactose was the acceptor, only one acceptor product was formed, namely 2^1-*O*-D-glucopyranosyllactose.[112–114] There seems to be a pattern that when D-galactose composes part of the acceptor structure, only one acceptor product is formed; for example, raffinose [6^{Glc}-*O*-α-D-galactopyranosylsucrose] also gave only a single acceptor product, 2^{Glc}-*O*-α-D-glucopyranosylraffinose.[115] When fructose is the acceptor, two products are formed, depending on the ring form of the fructose acceptor. The major product leucrose [5-*O*-α-D-glucopyranosyl-D-fructopyranose] is formed from D-fructopyranose, and the minor product isomaltulose [4-*O*-α-D-glucopyranosyl-D-fructofuranose] is formed when D-fructofuranose is the acceptor.[116–118] Because D-fructose is a major product in the dextransucrase-catalyzed synthesis of dextran from sucrose, it acts as an acceptor to give leucrose in all dextransucrase–sucrose digests (see Fig. 8). A small amount of D-glucose is also formed when water acts as an acceptor.[108] This reaction represents the hydrol-

ysis of sucrose. One study has suggested that dextransucrase has distinct active sites for sucrose hydrolysis and dextran synthesis.[119] Luzio *et al.*,[120,121] however, showed that the three reactions catalyzed by dextransucrase—(1) sucrose hydrolysis, (2) polymerization of the glucose moiety of sucrose, and (3) glucosyl transfer to acceptors—are competitive and therefore take place at the same active site.

Other unusual acceptor products result from the reaction of D-mannose and D-galactose. D-Mannose gave a nonreducing, α,β-trehalose isomer α-D-glucopyranosyl β-D-mannopyranoside, and D-galactose gave α-D-glucopyranosyl β-D-galactofuranoside.[122]

α,β-Trehalose gave two products, β-isomaltosyl α-D-glucopyranoside and α-isomaltosyl β-D-glucopyranoside,[112] and β,β-trehalose gave one product, β-isomaltosyl β-D-glucopyranoside.[112] α,α-Trehalose, however, was not an acceptor.[108,111]

Fu and Robyt studied the structures of the malto-oligosaccharides maltotriose to maltooctaose (G3–G8), acceptor products produced by *Leuc. mesenteroides* B-512FM dextransucrase[123] and by *Strep. mutans* dextransucrase (GTF-S) and mutansucrase (GTF-I).[124] They found that B-512FM dextransucrase transfers D-glucose to the 6-hydroxyl group of both the nonreducing-end and the reducing-end residues of G3–G8. Thus, G3 gave two tetrasaccharides, 6^3-*O*-α-D-glucopyranosylmaltotriose and 6^1-*O*-α-D-glucopyranosylmaltotriose. The former acceptor product was also an acceptor, giving a homologous series of isomalto-oligosaccharides attached to the 6-hydroxyl group of the nonreducing-end glucose residue. The acceptor product with glucose attached to the reducing-end residue, however, was not an acceptor. This same pattern was observed for the other malto-oligosaccharides studied.[123] None of the glucose residues between the reducing-end glucose and the nonreducing-end glucose served as acceptor sites.

The maltose acceptor products of GTF-S and GTF-I gave panose, thus resembling the B-512FM dextransucrase. Panose, however, served as an acceptor to give two products, 6^2-*O*-α-isomaltosylmaltose and 6^2-*O*-α-nigerosylmaltose. In contrast, panose reacting with B-512FM dextransucrase as an acceptor gave only 6^2-*O*-α-isomaltosylmaltose, which served as an acceptor for all three enzymes to give a homologous series of 6^2-*O*-α-isomalto-oligosaccharidylmaltoses. Like B-512FM dextransucrase, GTF-S and GTF-I transferred glucose to the C-6 hydroxyl groups of both the nonreducing-end and the reducing-end residues; and when glucose was transferred to the nonreducing-end residues, a series of homologous oligosaccharides resulted.[124] When GTF-I reacted with G3 as an acceptor, four tetrasaccharide products resulted, with glucose transferred to the 6-hydroxyl and the 3-hydroxyl groups of both the nonreducing-end and the reducing-end glucose.[124] The acceptor product with glucose substituted on C-6 of the nonreducing-end residue of G3 served as an acceptor to give the homologous series. Only two acceptor products, however, were initially formed with G4–G7 in which glucose was substituted at C-6 on the reducing and the nonreducing residue. As

with G3, the latter acceptor products also served as acceptors to give a homologous series.

Côté and Robyt[125] studied the acceptor products catalyzed by alternansucrase. They found that alternansucrase was capable of forming both α-(1→6) and α-(1→3) glycosidic bonds with acceptors. Isomaltose gave both isomaltotriose and 3^2-α-D-glucopyranosylisomaltose. These initial acceptor products also acted as acceptors, and the structures of the products of higher degree of polymerization show that an α-(1→3) glysosidic bond is formed only when the nonreducing-end glucose residue is linked by an α-(1→6) bond to another glucose residue. Nigerose thus gave 6^2-*O*-α-glucopyranosylnigerose. Maltose gave 6^2-*O*-α-glucopyranosylmaltose; however, this saccharide gave an unusual tetrasaccharide, 6^2-*O*-α-nigerosylisomaltose, in which there are three types of glycosidic linkages in sequence from the nonreducing-end: α-(1→3), α-(1→6), and α-(1→4). Thus, alternansucrase can synthesize both α-(1→6) and α-(1→3) acceptor-product linkages. When the nonreducing residue acceptor is linked by an α-(1→6) linkage, alternansucrase can transfer glucose to either the 6-OH or 3-OH groups to give an α-(1→6) or α-(1→3)-linked glucose unit; but when the nonreducing glucose unit of the acceptor is linked by an α-(1→3) or α-(1→4) bond, alternansucrase will transfer glucose only to the 6-OH group of the nonreducing glucose residue. Another unusual feature is that nigerose proved to be a better acceptor than isomaltose.

Table II summarizes the major acceptors and their products.

3. Mechanism of Acceptor-Product Formation

Robyt and Walseth[109] studied the mechanism of the acceptor reactions of *Leuc. mesenteroides* B-512FM dextransucrase. A purified dextransucrase was incubated with sucrose, and the resulting fructose, glucose, leucrose, and unreacted sucrose were removed from the enzyme by chromatography on a Bio-Gel P-6 column. The charged enzyme was incubated with D-[^{14}C]glucose, D-[^{14}C]fructose, and [^{14}C]-reducing-end-labeled maltose acceptors. Each of the three acceptors gave two types of labeled products—a high-molecular-weight product, identified as dextran, and a low-molecular-weight product that was an oligosaccharide. It was found that all three of the acceptors were incorporated into the products at the reducing end. Similar results were obtained when the enzyme and labeled acceptors were allowed to react in the presence of sucrose, the only difference being higher yields of the labeled products and a series of homologous oligosaccharides from the glucose and the maltose acceptor reactions. Because both a labeled oligosaccharide and a labeled dextran were produced when labeled acceptor and enzyme were incubated together with and without sucrose, it was concluded that the acceptor reactions were taking place via the acceptor's nucleophilic displacement of the glucosyl and dextranyl groups from the covalent enzyme interme-

TABLE II

Acceptor Products Formed by Glucansucrases[a]

Acceptor	First acceptor product[b]	References
Maltose	Panose*	109,110
Isomaltotriose	Isomaltotriose*	109,110
Nigerose	6^2-*O*-α-D-Glucopyranosylnigerose*	108
Methyl α-D-glucopyranoside	Methyl α-isomaltoside*	107
1,5-Anhydro-D-glucitol	1,5-Anhydroisomaltitol*	108
D-Glucose	Isomaltose*	108,109
Lactose	2^{Glc}-*O*-α-D-Glucopyranosyllactose	112–114
Cellobiose	2^1-*O*-α-D-Glucopyranosylcellobiose*	111,112
D-Fructose	Leucrose (5-*O*-α-D-glucopyranosyl-D-fructose)	116–118
Raffinose	2^{Glc}-*O*-α-D-Glucopyranosylraffinose	115
Melibiose[c]	—	
D-Glucitol[c]	—	
D-Mannose	α-D-Glucopyranosyl β-D-mannopyranoside	122
D-Galactose	α-D-Glucopyranosyl β-D-galactofuranoside	122
Theanderose	6^{Glc}-*O*-α-Isomaltosylsucrose*	111
α,β-Trehalose[d]	β-Isomaltosyl α-D-glucopyranoside	112
	α-Isomaltosyl β-D-glucopyranoside	112
β,β-Trehalose	β-Isomaltosyl β-D-glucopyranoside	112
α,α-Trehalose[e]	—	108,112
Maltotriose[d]	6^3-*O*-α-D-Glucopyranosylmaltotriose*	123
	6^1-*O*-α-D-Glucopyranosylmaltotriose*	123
Maltotriose[f]	6^3-*O*-α-D-Glucopyranosylmaltotriose*	124
	6^1-*O*-α-D-Glucopyranosylmaltotriose	124
	3^3-*O*-α-D-Glucopyranosyl maltotriose	124
	3^1-*O*-α-D-Glucopyranosyl maltotriose	124
Maltotetraose[d]	6^4-*O*-α-D-Glucopyranosylmaltotetraose*	123
	6^1-*O*-α-D-Glucopyranosylmaltotetraose	123
Panose[g]	6^2-*O*-α-Nigerosylmaltose*	125

[a] The products are those produced by *Leuc. mesenteroides* B-512F dextransucrase unless otherwise indicated. [b] The starred products are also acceptors that give a homologous series with α-isomalto-oligosaccharides attached to the acceptor. [c] Structure not determined. [d] Two products are formed by *Leuc. mesenteroides* B-512F dextransucrase. [e] Not an acceptor. [f] Four products are formed by *Strep. mutans* GTF-I. [g] Product formed by alternansucrase.

diates. It was further concluded that the acceptor reactions serve to terminate polymerization of dextran by displacing the growing chain from the active site, in contrast to previous ideas[52,53,70] that acceptors were serving as primers for dextran synthesis.

With regard to the possible priming mechanism of the acceptor for dextran synthesis, it was observed that many of the acceptors give a homologous series in which the amounts of oligosaccharide products decrease as the degree of polymerization (d.p.) of the products increases.[108,126] Furthermore, as the ratio of acceptor

to sucrose increases, the *amount* of acceptor product increases but the *number* of acceptor products decreases.[126] Even with the best acceptor, maltose, a discontinuous set of products was formed: a set of low-molecular-weight oligosaccharides (d.p. 3–6 for an acceptor-to-sucrose ratio of 1 : 1) and a high-molecular-weight dextran. Intermediate-sized oligosaccharide acceptor products of d.p. 7–15 were not present. If the acceptors were acting as primers for dextran synthesis, a continuous series of oligosaccharides from d.p. 3 and upward should have been produced. Furthermore, it would have been expected that, as the concentration of the acceptor (the so-called primer) was increased, dextran synthesis should have been stimulated, rather than decreased, as the number of priming sites was increased.[108,126]

Robyt and Walseth[109] proposed the mechanism shown in Fig. 9 for the acceptor reaction. In this mechanism, the acceptor is bound at an acceptor binding site[103]; and when maltose is the acceptor, its 6-hydroxyl group at the nonreducing end attacks C-1 of the glucosyl or dextranyl groups in the enzyme complex to give an oligosaccharide or a dextran acceptor product, respectively. When glucose is the acceptor, its 6-hydroxyl group makes the attack; and when fructose is the acceptor, its 5-hydroxyl group makes the attack. For acceptors that form a homologous series, Robyt and Walseth also showed that, when the concentration of the first acceptor product becomes sufficiently high, it too can act as an acceptor to give the

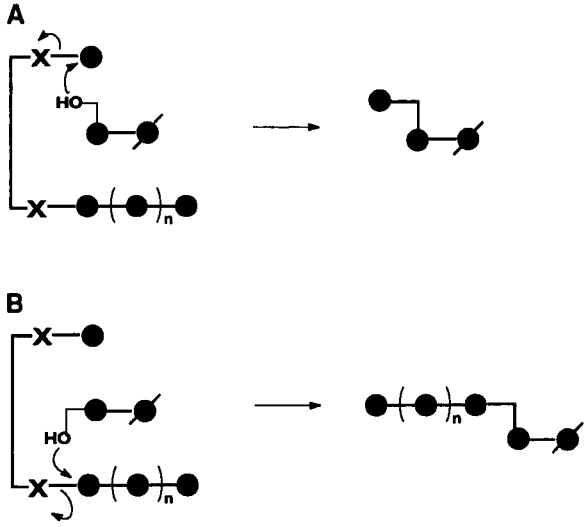

FIG. 9.—Mechanism for the acceptor reaction of *Leuc. mesenteroides* B-512F dextransucrase. A disaccharide acceptor binds in the acceptor binding site so that (A) its nonreducing 6-hydroxyl group can attack at C-1 of the glucosyl unit, releasing it from the active site to give a trisaccharide, or (B) its nonreducing 6-hydroxyl group can attack at C-1 of the glucanyl chain, releasing it from the active site.

next higher homolog, which in turn can act as an acceptor so that a series of homologous oligosaccharides is formed. This observation was later confirmed by Mayer *et al.*[127] for *Strep. sanguis* dextransucrase.

Thus, it was determined that the mechanism of action of the acceptors is one of terminating dextran synthesis by the release of the glucosyl and dextranyl units from the covalent enzyme intermediate rather than one of priming the synthesis of dextran.

Initially, it was expected that because most of the acceptors had some similarity to the glucopyranosyl moiety of sucrose, such as maltose, isomaltose, and methyl α-D-glucopyranoside, they were binding at the sucrose binding sites, competing with sucrose for the site. This behavior was also suggested by the binding of α-D-glucopyranosyl fluoride at the sucrose binding site, where it acts as a glucosyl donor for dextransucrase.[50] Hanes–Woolf plots showed, however, that methyl α-D-glucopyranoside and methyl 6-deoxy-α-D-glucopyranoside were very weak apparent competitive inhibitors, and that methyl 6-deoxy-6-fluoro-α-D-glucopyranoside was a very weak apparent noncompetitive inhibitor.[103] This finding was unexpected, as 6-deoxysucrose and 6-deoxy-6-fluorosucrose were strong competitive inhibitors.[96,98] If the acceptor analogs, methyl 6-deoxy-α-D-glucopyranoside and methyl 6-deoxy-6-fluoro-α-D-glucopyranoside, were binding at the sucrose binding sites, they too should have been strong competitive inhibitors. Most inhibitor diagnostic plots, such as Lineweaver–Burke or Hanes–Woolf plots, are made at relatively low substrate concentrations. Michaelis–Menten plots, however, can be made at much higher substrate concentrations. If the acceptors were indeed competing with sucrose for the sucrose binding sites, higher sucrose concentrations should eliminate the inhibition. Michaelis–Menten plots of the initial velocities of the incorporation of D-glucose into dextran versus sucrose concentration in the presence and absence of two inhibitors, 6-deoxysucrose (a strong competitive inhibitor) and methyl α-D-glucopyranoside (a weak apparent competitive inhibitor, but a relatively good acceptor) should show a sucrose concentration at which the inhibition is eliminated. The Michaelis–Menten plot showed that the inhibition by 6-deoxysucrose was completely eliminated when the sucrose concentration was 500 m*M*, but the inhibition by methyl α-D-glucopyranoside, a relatively good acceptor but poor apparent competitive inhibitor, was not eliminated at 600 m*M* sucrose.[103] Because methyl α-D-glucopyranoside was a weak apparent competitive inhibitor, the inhibition should have been eliminated at around 200 m*M* sucrose. From this result, it was concluded that acceptors were not binding at the sucrose binding site, and therefore were binding at a separate acceptor binding site. The number of acceptor binding sites was determined to be one for *Leuc. mesenteroides* B-512FM dextransucrase by Su and Robyt,[94] who used maltose in an equilibrium-dialysis experiment. Thus, the active site of *Leuc. mesenteroides* B-512FM dextransucrase has two sucrose binding sites (see Section III.4) and one acceptor binding site.

4. Control of the Synthesis of Dextran and Acceptor Product and the Efficiencies of Different Acceptors

A systematic study of the effects of three parameters on the acceptor reaction was made for *Leuc. mesenteroides* B-512FM dextransucrase using maltose as the acceptor.[126] The amount and distribution of acceptor products and the amount of dextran were studied as a function of (1) the ratio of maltose to sucrose, (2) the concentration of maltose and sucrose, and (3) the concentration of enzyme. The ratio of maltose to sucrose was varied from 0:1 to 100:1. As the ratio was increased, the amount of dextran steadily decreased with a concomitant increase in the amount of acceptor products. The *number* of acceptor products, however, decreased. At a constant sucrose concentration of 100 m*M*, a ratio of 1:5 gave 47.0% dextran and eight acceptor products (d.p. 3–10), a ratio of 2:1 gave 3.8% dextran and four acceptor products, and a ratio of 20:1 gave 0% dextran and one acceptor product. Keeping the ratio constant at 1:1 and increasing the concentrations of maltose and sucrose from 1.25 to 300 m*M* also gave a decrease in the amount of dextran from 49.3 to 0.6% and an increase in the amount of acceptor products. The number of acceptor products in this experiment remained relatively constant at five or six.

Using a constant 1:1 ratio of maltose to sucrose and different concentrations from 1.25 to 200 m*M*, the concentration of enzyme was varied 1000-fold from 0.12 to 120 U/mL. As the concentration of enzyme was increased, the amount of dextran formed decreased and the amount of acceptor products formed increased. The decrease in dextran was most pronounced at the lower substrate concentrations. At the highest enzyme concentration (120 U/mL), all of the substrate concentrations (1.25 to 200 m*M*) gave just 5% dextran out of the total amount of product formed.

It was concluded from the study that a high yield of four to six maltose acceptor products and a low yield of dextran could be obtained at any 1:1 maltose-to-sucrose concentration by using a high concentration of enzyme. A single acceptor product (panose in the case of maltose as an acceptor) may be obtained free of dextran by using a concentration of 100 m*M* sucrose at a maltose-to-sucrose ratio of 20:1 and an intermediate concentration of enzyme of 1 U/mL.

Not all of the acceptors react with equal efficiency. In a series of reactions with different acceptors with a 1:1 acceptor-to-sucrose ratio at 80 m*M*, the amount of dextran formed in the reaction was determined for *Leuc. mesenteroides* B-512FM dextransucrase.[108] Maltose was the most effective acceptor for decreasing the amount of dextran formed. Sixteen other acceptors were compared on a relative scale, with maltose defined as 100%. The next best acceptor was isomaltose (89%), followed by nigerose (58%), methyl α-D-glucopyranoside (52%), D-glucose (17%), turanose (13%), lactose (11%), cellobiose (9%), and D-fructose (6.4%).

The relative efficiencies of the malto-oligosaccharides, maltose to maltooctaose, as acceptors were determined for *Leuc. mesenteroides* B-512FM dextransu-

crase.[123] The relative efficiencies decreased from 100% for maltose to 6.2% for maltooctaose. The malto-oligosaccharides had higher relative efficiencies as acceptors with *Strep. mutans* GTF-S and GTF-I than they did with B-512FM dextransucrase.[124] The efficiencies of reaction of GTF-S and GTF-I with the malto-oligosaccharides also decreased as the size of these saccharides increased; but unlike the case of B-512F dextransucrase, efficiency reached a minimum with maltopentaose and then increased again with maltohexaose and maltoheptaose.[128]

5. Synthesis of Branch Linkages in *Leuconostoc mesenteroides* B-512F Dextran

In 1959, Bovey[129] attempted to study the synthesis of branch formation in B-512F dextran using light-scattering measurements. He postulated a branching enzyme similar to the branching enzyme found in the biosynthesis of starch. Such a branching enzyme, however, has never been found. In 1967, Ebert and Brosche[130] proposed a reaction for the formation of branches in which a dextran chain itself acts as an acceptor, attacking an enzyme–dextran complex so that the acceptor dextran is the main chain and the dextran chain from the enzyme is the side-branched chain. Using a ^{3}H-labeled acceptor dextran of low molecular weight and assuming an average molecular weight of 4×10^5 for the synthesized dextran, they calculated from the specific activity of the synthesized product that only one labeled acceptor dextran molecule was present in each synthesized dextran. While this finding seemed to be proof for the proposed mechanism, some doubt was cast on the mechanism owing to the assumptions and circular arguments that were made.

In 1976, Robyt and Taniguchi[79] studied the acceptor branching reaction using *Leuc. mesenteroides* B-512FM dextransucrase immobilized on Bio-Gel P-2. The immobilized enzyme was labeled by incubating it with a relatively low concentration of [^{14}C]sucrose. In a second procedure, the immobilized enzyme was first incubated with nonlabeled sucrose, washed, and then labeled with a low concentration of [^{14}C]sucrose. In both experiments, the labeled material was shown to be glucose and dextran. When either of the labeled, immobilized enzymes was incubated with a low-molecular-weight, nonlabeled dextran, all of the enzyme-bound label was released as [^{14}C]dextran. No [^{14}C]dextran was released when the labeled enzyme was incubated in buffer alone. The [^{14}C]dextran released was shown by hydrolysis with an *exo*-dextranase to be slightly branched. Acetolysis of the labeled dextran gave 7.3% of the ^{14}C in nigerose. Reduction of the labeled nigerose, followed by acid hydrolysis, gave all of the label in glucose, demonstrating that the nigerose was exclusively labeled in the nonreducing glucose residue. The results of the experiments indicated that the ^{14}C label was being released by the action of the added low-molecular-weight dextran (acceptor dextran) and that this action gave the formation of a new α-(1→3) branch linkage. The reasoning, based on the

acetolysis experiment, for the formation of an α-(1→3) branch linkage is illustrated in Fig. 10. Robyt and Taniguchi[79] proposed a mechanism for the synthesis of branch linkages by *Leuc. mesenteroides* B-512FM dextransucrase in which a 3-hydroxyl group of an interior glucose residue on an acceptor dextran makes a nucleophilic attack at C-1 of either the glucosyl-enzyme complex or C-1 of the dextranyl-enzyme complex, thereby forming an α-(1→3) branch linkage by displacing glucose and dextran from the enzyme (Fig. 11). Thus, branching can take place without a separate enzyme via the action of an acceptor dextran on the glucosyl- and dextranyl-dextransucrase complexes. It is possible, of course, that the 6-hydroxyl group of the nonreducing-end glucose residue makes the attack, giving the elongation rather than the branching of the acceptor-dextran chain. This reaction is analogous to the priming reaction: while possible, it is highly improbable, as there are thousands of 3-hydroxyl groups available along the length of the

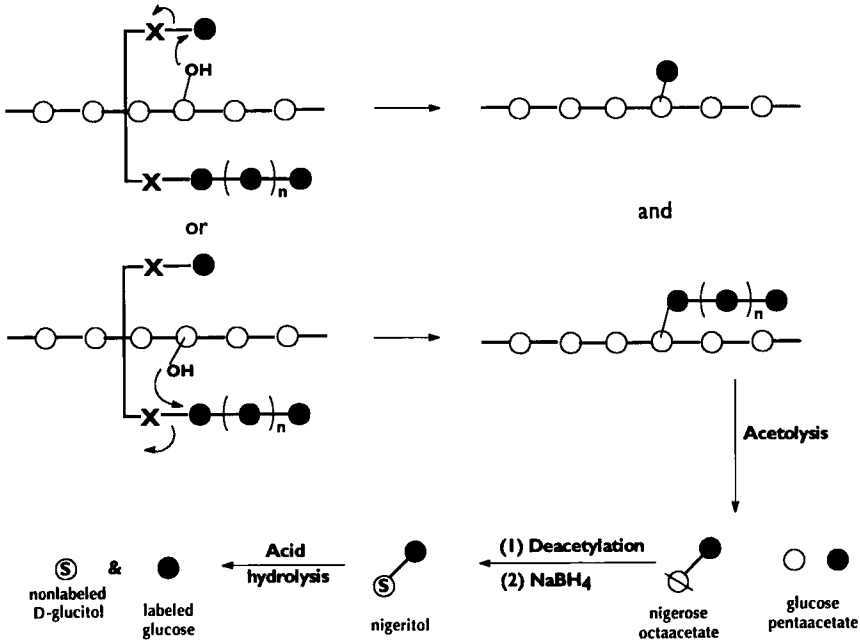

FIG. 10.—Reasoning used in the branching experiment for *Leuc. mesenteroides* B-512F dextransucrase. The immobilized enzyme is labeled with [^{14}C]sucrose (the closed circles represent ^{14}C-labeled glucosyl and glucanyl); the labeled enzyme was washed with buffer and incubated with nonlabeled dextran (open symbols). The released labeled dextran was isolated and acetolyzed, the products deacetylated, and labeled nigerose isolated. The nigerose was reduced and acid-hydrolyzed, showing that the label was exclusively located in the glucose of nigeritol, thus indicating that the release of labeled dextran and glucose from the enzyme by incubation with low-molecular-weight dextran was due to the formation of an α-(1→3) branch linkage.

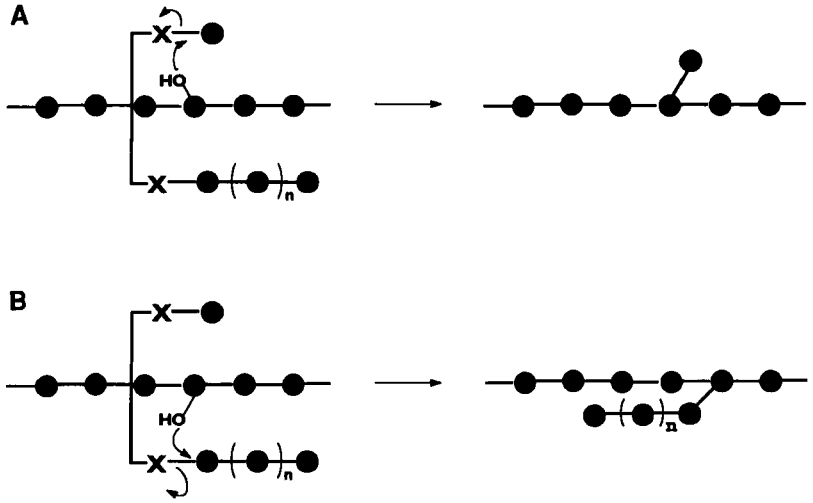

FIG. 11.—Mechanism for the synthesis of α-(1→3) branch linkages by *Leuc. mesenteroides* B-512F dextransucrase. The 3-hydroxyl group of an acceptor dextran chain makes an attack onto (A) the glucosyl unit to give a single branched glucose linked α-(1→3) or (B) the 3-hydroxyl group of the acceptor dextran attacks at C-1 of the glucosyl unit of the dextranyl chain to give a long α-(1→3)-linked branched dextran chain.

dextran acceptor chain and only *one* 6-hydroxyl group, which is located at the nonreducing-end. This reaction does occur when isomalto-oligosaccharides are the acceptors. Walker[131] has shown that the branching reaction starts to occur over that of the nonreducing-end 6-hydroxyl acceptor reaction when the size of the isomalto-oligosaccharide is 7–9 glucose residues long.

Viscosity, sedimentation, and light-scattering studies combined with theoretical considerations led Senti *et al.*[132] to conclude that, when 77% of the branch linkages of B-512F dextran are single glucose residues, the remaining branch chains have 50 or more glucose residues. Walker and Pulkownik,[133] studying the hydrolysis of B-512F dextran by dextranglucosidase, also concluded that a dextran having 85% single glucose branches must have 33 or more glucose residues in the remaining branch chains to give the yield of glucose that they observed. The long branches would not necessarily be of uniform length, but could comprise a distribution of chain lengths. Senti *et al.*[132] further concluded that, if the branches are longer than the number of glucose residues separating them along the main chain, the branch chains themselves should be branched. These observations and conclusions are consistent with the branching mechanism proposed for the synthesis of B-512F dextran by dextransucrase, namely that single glucose units and long dextran chains are transferred from the active site to an acceptor dextran chain.

To test the possibility of a separate branching enzyme, Robyt[134] incubated crude

dextransucrase and purified dextransucrase with sucrose and determined that the degree of branching for the two resulting dextrans was the same. If there had been a separate branching enzyme present in the crude enzyme, the purified dextransucrase preparation would be expected to give a dextran with a lower degree of branching, as at least some of the branching enzyme would be removed during the purification.

For the synthesis of the more highly and regularly branched dextrans, it would seem, however, that mechanisms other than dextran chain-acceptor reactions might also be involved. See Fig. 7 for a proposed two-site synthesis of *Leuc. mesenteroides* B-742 regular comb dextran in which a single glucose residue is attached by an α-(1→3) branch linkage to every glucose residue in the main α-(1→6)-linked dextran chain during the polymerization reaction.

The degree of branching in B-512F(M) dextran may be decreased or increased by running the reactions at lower or higher temperatures, respectively.[134-136] Furthermore, it has been observed that the degree of branching catalyzed by B-742 dextransucrase preparations and *Strep. mutans* GTF-S preparations may be increased by conducting the synthesis with the enzyme in a dialysis bag.[137] The addition of 1.6 *M* ammonium sulfate also caused GTF-S to synthesize a dextran with a higher degree of branching.[21]

6. Applications of the Acceptor Reactions

Reaction of *Leuc. mesenteroides* B-512F dextransucrase with sucrose and an excess of maltose has been used to prepare panose on a large scale.[110] A series of methyl α-isomalto-oligosaccharides has been prepared in a similar manner using methyl α-D-glucopyranoside as the acceptor.[107] In the latter reaction, the individual methyl α-isomaltosides (d.p. 2–5) were separated by charcoal–Celite column chromatography and crystallized. The isomalto-oligosaccharidylmaltose homologous series (d.p. 3–6) has also been prepared by using B-512F dextransucrase with maltose as an acceptor.[138] The synthesis of oligoalternans was achieved by using alteransucrase and three acceptors: maltose, isomaltose, and methyl α-D-glucopyranoside.[139] B-512F dextransucrase has been used in conjunction with *endo*-dextranase to produce a product with a high content of isomaltose and D-fructose.[140] The D-fructose can be removed by a calcium cation-exchange resin to give a high-isomaltose syrup.

The B-512F dextransucrase reaction in the presence of maltose has been reported as a means of controlling the molecular weight of dextrans.[141,142] A mathematical optimization showed that the sucrose-to-maltose ratio has an influence on the yield of oligosaccharides formed, and that their weight-average molecular weight is a linear function of the ratio. In a second-step reaction, using mixtures of different oligosaccharide acceptor products as acceptors, it was possible to obtain various molecular weights and polydispersities.[142]

Leuconostoc mesenteroides B-1299 dextransucrase has been used with maltose as an acceptor to give oligosaccharides containing α-(1→2) glycosidic linkages in addition to α-(1→6) and α-(1→4) linkages.[143]

V. Formulation and Kinetics of the Glucansucrase Reactions

As has already been discussed, glucansucrases catalyze the synthesis of glucans from sucrose and the transfer of glucose from sucrose to acceptors. The glucans themselves can serve as acceptors, giving rise to the synthesis of branch linkages. It is necessary to consider these reactions taking place together in the digests when developing kinetic equations that describe the catalytic process. The various reactions that can take place are formulated by the following reaction scheme.

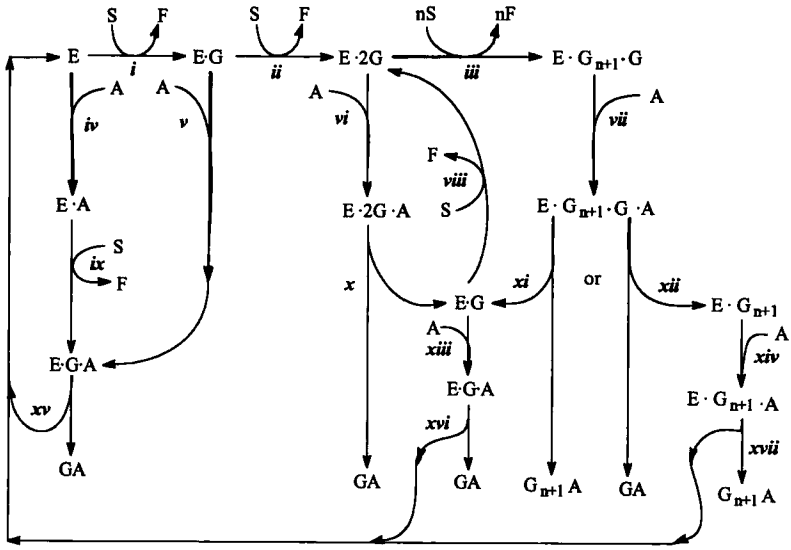

Reaction Scheme for Dextransucrase

In the scheme, E denotes enzyme, S is sucrose, F is fructose, G is glucose, and A is an acceptor. The reaction scheme presented here is for a two-site insertion mechanism that forms covalent glucosyl- and glucanyl-enzyme complexes. Reactions *i*, *ii*, and *iii* are involved in the synthesis of the glucan chain. In reactions *i* and *ii*, the two sites are glycosylated from sucrose bound in the two sucrose-binding sites. These reactions could occur simultaneously rather than sequentially as written. The two glucosylated sites interact with each other to give the synthesis (elongation) of a glucan chain as shown in reaction *iii*. The covalent glucosyl- and glucanyl-enzyme complex can form a complex with an acceptor (reaction *vii*). The

acceptor in this ternary complex can either release glucan, forming $G_{n+1}A$ (reaction *xi*) or it can release glucose, forming GA (reaction *xii*). Whether the acceptor releases glucan or glucose depends on the way the acceptor is bound at the acceptor binding site in relation to the covalent glucanyl- and glucosyl-enzyme complexes.

If the acceptor A is a low-molecular-weight carbohydrate, GA is a low-molecular-weight saccharide, and $G_{n+1}A$ is a glucan with the acceptor linked at the reducing end of the glucan. If the acceptor A is a glucan (preferably the same type of glucan being synthesized, or at least similar in structure), a branched glucan results. In this case when the glucan acceptor A attacks the glucosyl-enzyme complex, a single glucose branch attached to A results; and when glucan A attacks the glucanyl-enzyme complex, a long branch glucan chain is attached to A.

When an acceptor A is present, acceptor reactions can occur, diverting G away from incorporation into glucan. When the concentration of A is high with respect to that of S, reaction *iii* is inhibited and reactions *v*, *vi*, and *xiii* are favored to give acceptor products in reactions *x*, *xv*, and *xvi*. Some of these reactions (*xv*, *xvi*, and *xvii*) give free enzyme E that has to be glucosylated by reaction *i* before ANY products can be formed. In one instance (reaction *iv*), the acceptor forms a complex with free enzyme and this intermediate must be glucosylated by reaction *ix* before any products can be formed by reaction *xv*.

This reaction scheme does not take into account the negative allosteric effect of sucrose concentrations above 200 m*M* or the positive allosteric effect of low concentrations of glucan.

Even though the reaction scheme is complex, attempts have been made to model the reaction and develop kinetic equations. Mooser *et al.*[144] developed kinetic equations for a limited case based on the primer mechanism. Reh *et al.*[145] developed kinetic equations for the synthesis of dextran and for the maltose acceptor reaction based on the two-site insertion mechanism. Likewise, Böker *et al.*[146] developed a kinetic equation for the formation of the fructose acceptor product, leucrose, based on the two-site insertion mechanism that included an acceptor site. An equation was derived for the overall reaction rate that was a function of the consumption of sucrose by dextran formation and acceptor-product formation.

REFERENCES

1. L. Pasteur, *Bull. Soc. Chim. Paris*, (1861) 30–36.
2. C. Scheubler, *Z. Ver. Dtsch. Zuker-Ind.*, 24 (1874) 309–317.
3. M. E. Durin, *Compt. Rend.*, 83 (1876) 128–137.
4. E. J. Hehre, *Science*, 93 (1941) 237–238.
5. A. Jeanes, W. C. Haynes, C. A. Wilham, J. C. Rankin, E. H. Melvin, M. J. Austin, J. E. Cluskey, B. E. Fisher, H. M. Tsuchiya, and C. E. Rist, *J. Am. Chem. Soc.*, 76 (1954) 5041–5047.
6. C. A. Wilham, B. H. Alexander, and A. Jeanes, *Arch. Biochem. Biophys.*, 59 (1955) 61–69.
7. J. W. Van Cleve, W. C. Schaefer, and C. E. Rist, *J. Am. Chem. Soc.*, 78 (1956) 4435–4440.
8. A. Shimamura, H. Tsumori, and H. Mukasa, *Biochim. Biophys. Acta*, 702 (1982) 72–80.

9. M. D. Hare, S. Svensson, and G. J. Walker, *Carbohydr. Res.*, 66 (1978) 245–255.
10. F. R. Seymour, E. C. M. Chen, and S. H. Bishop, *Carbohydr. Res.*, 68 (1979) 113–121.
11. F. R. Seymour, R. D. Knapp, S. H. Bishop, and A. Jeanes, *Carbohydr. Res.*, 68 (1979) 123–140.
12. F. R. Seymour, R. D. Knapp, and S. H. Bishop, *Carbohydr. Res.*, 72 (1979) 229–234.
13. A. Jeanes and F. R. Seymour, *Carbohydr. Res.*, 74 (1979) 31–40.
14. F. R. Seymour, R. D. Knapp, and S. H. Bishop, *Carbohydr. Res.*, 74 (1979) 77–92.
15. F. R. Seymour, R. D. Knapp, E. C. M. Chen, A. Jeanes, and S. H. Bishop, *Carbohydr. Res.*, 75 (1979) 275–294.
16. F. R. Seymour and R. D. Knapp, *Carbohydr. Res.*, 81 (1980) 67–104.
17. F. R. Seymour and R. D. Knapp, *Carbohydr. Res.*, 81 (1980) 105–129.
18. F. R. Seymour, R. L. Julian, A. Jeanes, and B. L. Lamberts, *Carbohydr. Res.*, 86 (1980) 227–246.
19. F. R. Seymour, R. D. Knapp, E. C. M. Chen, and S. H. Bishop, *Carbohydr. Res.*, 74 (1979) 41–47.
20. F. R. Seymour, M. E. Slodki, R. D. Plattner, and A. Jeanes, *Carbohydr. Res.*, 53 (1977) 153–159.
21. E. J. Bourne, D. H. Huston, and H. Weigel, *Biochem. J.*, 85 (1962) 158–162.
22. G. N. Richards and M. Streamer, *Carbohydr. Res.*, 62 (1978) 191–196.
23. G. L. Côté and J. F. Robyt, *Carbohydr. Res.*, 127 (1984) 95–107.
24. I. J. Goldstein and W. J. Whelan, *J. Chem. Soc.*, (1962) 170–175.
25. T. Sawai, T. Tohyama, and T. Natsume, *Carbohydr. Res.*, 66 (1978) 195–205.
26. G. L. Côté and J. F. Robyt, *Carbohydr. Res.*, 101 (1982) 57–74.
27. A. Jeanes, *Methods Carbohydr. Chem.*, 5 (1965) 118–127.
28. J. E. Ciardi, A. J. Beaman, and C. L. Wittenberger, *Infect. Immun.*, 18 (1977) 237–241.
29. D. Kim and J. F. Robyt, *Enzyme Microbiol. Technol.*, 16 (1994) 659–664.
30. E. J. Hehre, *J. Biol. Chem.*, 163 (1946) 221–227.
31. A. Goodman, R. M. Weil, and K. G. Stern, *J. Biol. Chem.*, 217 (1955) 977–981.
32. K. H. Ebert and G. Schenk, *Z. Naturforsch.*, 17b (1962) 732–740.
33. F. Paul, D. Auriol, E. Oriol, and P. Monsan, *Ann. N. Y. Acad. Sci.*, 434 (1984) 267–270.
34. J. F. Robyt and T. F. Walseth, *Carbohydr. Res.*, 68 (1979) 95–111.
35. A. W. Miller, S. H. Eklund, and J. F. Robyt, *Carbohydr. Res.*, 147 (1986) 119–133.
36. D. Fu and J. F. Robyt, *Prep. Biochem.*, 20 (1990) 93–106.
37. G. J. Walker and M. D. Hare, *Carbohydr. Res.*, 58 (1977) 415–432.
38. R. R. B. Russell, *FEMS Microbiol. Lett.*, 6 (1979) 197–199.
39. W. R. Figures and J. R. Edwards, *Biochim. Biophys. Acta*, 577 (1979) 142–146.
40. T. Koga, S. Sato, T. Yakushiji, and M. Inoue, *FEMS Microbiol. Lett.*, 16 (1983) 127–130.
41. H. Tsumori, A. Shimamura, and H. Mukasa, *J. Gen. Microbiol.*, 131 (1985) 553–559.
42. J. F. Robyt, in R. J. Alexander and H. F. Zobel (Eds.), *Developments in Carbohydrate Chemistry*, Am. Assoc. Cereal Chem., St. Paul, MN, 1992, pp. 261–292.
43. D. Kim and J. F. Robyt, *Enzyme Microbiol. Technol.*, (1995) in press.
44. M. Kobayashi and K. Matsuda, *Biochim. Biophys. Acta*, 614 (1980) 46–62.
45. M. Kobayashi and K. Matsuda, *J. Biochem. (Tokyo)*, 100 (1986) 615–621.
46. D. A. Grahame and R. M. Mayer, *Biochim. Biophys. Acta*, 786 (1984) 42–48.
47. D. Kim and J. F. Robyt, *Enzyme Microbiol. Technol.*, 16 (1994) 1010–1015.
48. J. C. Mazza, A. Ackerman, and J. R. Edwards, *Carbohydr. Res.*, 40 (1975) 402–406.
49. E. J. Hehre and H. Suzuki, *Arch. Biochem. Biophys.*, 113 (1966) 675–683.
50. D. S. Genghof and E. J. Hehre, *Proc. Soc. Exp. Biol. Med.*, 140 (1972) 1298–1301.
51. T. P. Binder and J. F. Robyt, *Carbohydr. Res.*, 124 (1983) 287–299.
52. H. J. Koepsell, H. M. Tsuchiya, N. N. Hellman, A. Kazenko, C. A. Hoffman, E. S. Sharpe, and R. W. Jackson, *J. Biol. Chem.*, 200 (1953) 793–801.
53. H. M. Tsuchiya, N. N. Hellman, H. J. Koepsell, J. Corman, S. S. Stringer, S. P. Rogovin, M. O. Bogard, G. Bryant, W. H. Feger, C. A. Hoffman, F. R. Senti, and R. W. Jackson, *J. Am. Chem. Soc.*, 77 (1955) 2412–2419.

54. K. H. Ebert and G. Schenk, *Z. Naturforsch.*, 23b (1968) 788–798.
55. E. Newbrun and J. Carlsson, *Arch. Oral Biol.*, 14 (1969) 461–466.
56. G. R. Germaine, C. F. Schachtele, and A. M. Chludzinski, *J. Dent. Res.*, 53 (1974) 1355–1360.
57. T. J. Grier and R. M. Mayer, *Arch. Biochem. Biophys.*, 212 (1981) 651–659.
58. J. F. Robyt, B. K. Kimble, and T. F. Walseth, *Arch. Biochem. Biophys.*, 165 (1974) 634–640.
59. J. F. Robyt and P. J. Martin, *Carbohydr. Res.*, 113 (1983) 301–315.
60. V. K. Parnaik, G. A. Luzio, D. A. Grahame, S. L. Ditson, and R. M. Mayer, *Carbohydr. Res.*, 121 (1983) 257–268.
61. G. Mooser and K. R. Iwaoka, *Biochemistry*, 28 (1989) 443–449.
62. J. F. Robyt and S. H. Eklund, *Bioorg. Chem.*, 11 (1982) 115–132.
63. G. Mooser, S. A. Hefta, R. J. Paxton, J. E. Shively, and T. D. Lee, *J. Biol. Chem.*, 266 (1991) 8916–8922.
64. G. T. Cori and C. F. Cori, *J. Biol. Chem.*, 131 (1939) 397–398.
65. C. S. Hanes, *Proc. Roy. Soc. B*, 129 (1940) 174–208.
66. M. A. Swanson and C. F. Cori, *J. Biol. Chem.*, 172 (1948) 815–829.
67. D. Stetten, Jr. and M. R. Stetten, *Physiol. Rev.*, 40 (1960) 513–519.
68. J. F. Robyt, *Trends Biol. Sci.*, 4 (1979) 47–49.
69. E. J. Hehre, *Adv. Enzymol.*, 11 (1951) 297–337.
70. H. M. Tsuchiya, *Bull. Soc. Chim. Biol.*, 42 (1960) 1777–1788.
71. G. R. Germaine, A. M. Chludzinski, and C. F. Schachtele, *J. Bacteriol.*, 120 (1974) 287–294.
72. A. M. Chludzinski, G. R. Germaine, and C. F. Schachtele, *J. Dent. Res. Special Issue C*, 55 (1976) C75–C86.
73. G. R. Germaine, S. K. Harlander,W-L. S. Leung, and C. F. Schachtele, *Infect. Immun.*, 16 (1977) 637–648.
74. M. Kobayashi, I. Yokoyama, and K. Matsuda, *Agric. Biol. Chem.*, 50 (1986) 2585–2590.
75. W. B. Neely, *Adv. Carbohydr. Chem.*, 15 (1960) 341–369.
76. R. W. Bailey, S. A. Barker, E. J. Bourne, M. Stacey, and O. Theander, *Nature*, 179 (1957) 310.
77. S. Imai, K. Takeuchi, K. Shibata, S. Yoshikawa, S. Kilahata, S. Okada, S. Araya, and T. Nisizawa, *J. Dent. Res.*, 63 (1984) 1293–1297.
78. J. F. Robyt and A. J. Corrigan, *Arch. Biochem. Biophys.*, 183 (1977) 726–731.
79. J. F. Robyt and H. Taniguchi, *Arch. Biochem. Biophys.*, 174 (1976) 129–135.
80. G. Mooser and C. Wong, *Infect. Immun.*, 56 (1988) 880–884.
81. C. Wong, S. A. Hefta, R. J. Paxton, J. E. Shively, and G. Mooser, *Infect. Immun.*, 58 (1990) 2165–2170.
82. S. F. Kobs, *Carbohydr. Res.*, 211 (1991) 337–342.
83. R. R. B. Russell, *J. Gen. Microbiol.*, 112 (1979) 197–201.
84. R. M. Hamelik and M. M. McCabe, *Biochem. Biophys. Res. Commun.*, 106 (1982) 875–880.
85. J. F. Robyt, D. Kim, and L. Yu, *Carbohydr. Res.* 266 (1995) 293–299.
86. P. W. Robbins, D. Bray, M. Dankert, and A. Wright, *Science*, 158 (1967) 1536–1538.
87. D. Bray and P. W. Robbins, *Biochem. Biophys. Res. Commun.*, 28 (1967) 334–338.
88. J. B. Ward and H. R. Perkins, *Biochem. J.*, 135 (1973) 721–726.
89. K. H. Ebert and F. Patat, *Z. Naturforsch.*, 17b (1962) 738–745.
90. K. H. Ebert and G. Schenk, *Adv. Enzymol.*, 30 (1968) 179–221.
91. K. Funane, M. Shiraiwa, K. Hashimoto, E. Ichishima, and M. Kobayashi, *Biochemistry*, 32 (1993) 13696–13702.
92. D. Fu and J. F. Robyt, *Carbohydr. Res.*, 183 (1988) 97–109.
93. S. L. Ditson and R. M. Mayer, *Carbohydr. Res.*, 126 (1984) 170–175.
94. D. Su and J. F. Robyt, *Arch. Biochem. Biophys.*, 308 (1994) 471–476.
95. T. P. Binder and J. F. Robyt, *Carbohydr. Res.*, 132 (1984) 173–177.

96. S. H. Eklund and J. F. Robyt, *Carbohydr. Res.*, 177 (1988) 253–258.
97. T. P. Binder and J. F. Robyt, *Carbohydr. Res.*, 140 (1985) 9–20.
98. T. P. Binder and J. F. Robyt, *Carbohydr. Res.*, 154 (1986) 229–238.
99. A. Tanriseven and J. F. Robyt, *Carbohydr. Res.*, 186 (1989) 87–94.
100. W. R. Figures and J. R. Edwards, *Carbohydr. Res.*, 48 (1976) 245–253.
101. S. Thaniyavarn, S. Singh, C. M. Maynard, K. G. Taylor, and R. J. Doyle, *Carbohydr. Res.*, 96 (1981) 134–137.
102. E. Newbrun, C. I. Hoover, G. J. Walker, *Arch. Oral Biol.*, 28 (1983) 531–536.
103. A. Tanriseven and J. F. Robyt, *Carbohydr. Res.*, 225 (1992) 321–329.
104. F. Patat and H. Meyer, *Biochem. Z.*, 330 (1958) 209–214.
105. C. S. Stringer and H. M. Tsuchiya, *J. Am. Chem. Soc.*, 80 (1958) 6620–6623.
106. A. Tanriseven and J. F. Robyt, *Carbohydr. Res.*, 245 (1993) 97–104.
107. R. W. Jones, A. Jeanes, C. S. Stringer, and H. M. Tsuchiya, *J. Am. Chem. Soc.*, 78 (1956) 2499–2502.
108. J. F. Robyt and S. H. Eklund, *Carbohydr. Res.*, 121 (1983) 279–286.
109. J. F. Robyt and T. F. Walseth, *Carbohydr. Res.*, 61 (1978) 433–445.
110. M. Killey, R. J. Dimler, and J. E. Cluskey, *J. Am. Chem. Soc.*, 77 (1955) 3315–3318.
111. R. W. Bailey, S. A. Barker, E. J. Bourne, P. M. Grant, and M. Stacey, *J. Chem. Soc.*, (1958) 1895–1900.
112. F. Yamauchi and Y. Ohwada, *Agr. Biol. Chem.*, 33 (1969) 1295–1300.
113. E. J. Bourne, J. Hartigan, and H. Weigel, *J. Chem. Soc.*, (1959) 2332–2337.
114. R. W. Bailey, S. A. Barker, E. J. Bourne, and M. Stacey, *Nature*, 176 (1955) 1164–1165.
115. W. B. Neely, *Arch. Biochem. Biophys.*, 79 (1959) 154–160.
116. F. H. Stodola, H. J. Koepsell, and E. S. Sharpe, *J. Am. Chem. Soc.*, 74 (1952) 3202.
117. F. H. Stodola, E. S. Sharpe, and H. J. Koepsell, *J. Am. Chem. Soc.*, 78 (1956) 2514–2518.
118. E. S. Sharpe, F. H. Stodola, and H. J. Koepsell, *J. Org. Chem.* 25 (1960) 1062–1064.
119. Y. Yamashita, N. Hanada, M. Itoh-Andoh, and T. Takehara, *FEBS Letters*, 243 (1989) 343–346.
120. G. A. Luzio and R. M. Mayer, *Carbohydr. Res.*, 111 (1983) 311–318.
121. G. A. Luzio, V. K. Parnaik, and R. M. Mayer, *Carbohydr. Res.*, 121 (1983) 269–278.
122. Y. Iriki and E. J. Hehre, *Arch. Biochem. Biophys.*, 134 (1969) 130–136.
123. D. Fu and J. F. Robyt, *Arch. Biochem. Biophys.*, 283 (1990) 379–387.
124. D. Fu and J. F. Robyt, *Carbohydr. Res.*, 217 (1991) 201–211.
125. G. L. Côté and J. F. Robyt, *Carbohydr. Res.*, 111 (1982) 127–142.
126. D. Su and J. F. Robyt, *Carbohydr. Res.*, 248 (1993) 339–348.
127. R. M. Mayer, M. M. Matthews, C. L. Futerman, V. K. Parnaik, and S. M. Jung, *Arch. Biochem. Biophys.*, 208 (1981) 278–287.
128. J. F. Robyt, in M. A. Clarke (Ed.), *Carbohydrates in Industrial Synthesis*, Bartens, Berlin, 1992, pp. 56–67.
129. F. A. Bovey, *J. Polym. Sci.*, 35 (1959) 167–182.
130. K. H. Ebert and M. Brosche, *Biopolymers*, 5 (1967) 423–430.
131. G. J. Walker, *Carbohydr. Res.*, 82 (1980) 404–410.
132. F. R. Senti, N. N. Hellman, N. H. Ludwig, G. E. Babcock, R. Tobin, C. A. Glass, and B. L. Lamberts, *J. Polym. Sci.*, 17 (1955) 527–546.
133. G. J. Walker and A. Pulkownik, *Carbohydr. Res.*, 29 (1973) 1–14.
134. J. F. Robyt, unpublished results.
135. J. Sabatie, L. Choplin, F. Paul, and P. Monsan, *Biotech. Lett.*, 8 (1986) 425–430.
136. J. Sabatie, L. Choplin, M. Moan, J. L. Doublier, F. Paul, and P. Monsan, *Carbohydr. Polym.*, 9 (1988) 87–101.
137. G. L. Côté and J. F. Robyt, *Carbohydr. Res.*, 119 (1983) 141–156.

138. E. Oriol, F. Paul, P. Monsan, A. Heyraud, and M. Rinaudo, *Ann. N. Y. Acad. Sci.*, 501 (1989) 210–215.
139. V. Pelenc, A. Lopez-Munguia, M. Remaud, J. Biton, J. M. Michel, F. Paul, and P. Monsan, *Sci. Ailments*, 11 (1991) 465–476.
140. F. B. Paul, P. F. Monsan, M. M. C. Remaud, and V. P. Pelenc, *U.S. Patent No. 4,861,381* (1989).
141. F. Paul, E. Oriol, D. Auriol, and P. Monsan, *Carbohydr. Res.*, 149 (1986) 433–441.
142. M. Remaud, F. Paul, P. Monsan, A. Heyraud, and M. Rinaudo, *J. Carbohydr. Chem.*, 10 (1991) 861–876.
143. M. Remaud-Simeon, A. Lopez-Munguia, V. Pelenc, F. Paul, and P. Monsan, *Appl. Biochem. Biotech.*, 44 (1994) 101–117.
144. G. Mooser, D. Shur, M. Lyou, and C. Watanabe, *J. Biol. Chem.*, 260 (1985) 6907–6915.
145. K.-D. Reh, H.-J. Jördening, and K. Buchholz, *Ann. N. Y. Acad. Sci.*, 613 (1990) 723–729.
146. M. Böker, H.-J. Jördening, and K. Buchholz, *Biotechnol. Bioeng.*, 43 (1994) 856–861.

ADVANCES IN CARBOHYDRATE CHEMISTRY AND BIOCHEMISTRY, VOL. 51

THE VARIABLE SURFACE GLYCOLIPIDS OF MYCOBACTERIA: STRUCTURES, SYNTHESIS OF EPITOPES, AND BIOLOGICAL PROPERTIES

BY GERALD O. ASPINALL

Department of Chemistry, York University, North York, Ontario, M3J 1P3, Canada

DELPHI CHATTERJEE AND PATRICK J. BRENNAN

Department of Microbiology, Colorado State University, Fort Collins, Colorado

I. INTRODUCTION

Mycobacteria (members of the *Mycobacterium* genus), in the diseases they cause, remain serious problems. Tuberculosis, the magnitude of whose worldwide incidence is enormous—estimated at 2.9 million deaths and 8 million new cases

per year[1]—is the leading cause of death from a single infectious agent. Furthermore, the burden of tuberculosis in the developing world is concentrated in the economically most productive age group. In Africa and the Indian subcontinent, the absolute number of tuberculosis cases has apparently increased steadily over the years. The situation is rapidly worsening in many sub-Saharan African countries because of the human immunodeficiency virus (HIV) pandemic. In some of these countries, the number of reported TB cases has doubled in the past 4–5 years because one-third to one-half of the population in the high-risk group for HIV is already infected with the tubercle bacillus, and HIV infection is the highest risk factor thus far identified for the progression of latent tuberculosis infection to active disease. In many industrialized countries, the long-time decline in tuberculosis has stopped or been reversed; in the United States, for example, the number of cases reported in 1992 exceeded by about 30,000 cases[2] the numbers predicted on the basis of a continued decline. This increase, together with the emergence of multidrug-resistant *Mycobacterium tuberculosis*, is attributable to HIV infection and a variety of societal problems.[2]

Interest in the nontuberculous (atypical) mycobacteria, especially members of the *Mycobacterium avium*, *Mycobacterium intracellulare*, *Mycobacterium scrofulaceum* complex, has also been stimulated by AIDS. Infection with the *M. avium* complex is seen in up to 50% of patients with AIDS in some areas of the world.[3] A review of U.S. cases found an overall 5.5% incidence of *M. avium* complex in AIDS patients.[3] Leprosy, however, is clearly on the wane, although it remains a substantial problem.[4] Its prevalence has been steadily diminished to a present-day worldwide figure of about 3 million registered cases and 5.5 million estimated cases, owing in part to a most effective multiple-drug regimen. The World Health Assembly has dedicated itself to the technical elimination of leprosy (that is, a prevalence of less than 1 per 10,000 population) by the turn of the century.

Interest in glycolipids of mycobacteria dates to the historic work of R. J. Anderson[5] at Yale University in the 1940s. The Anderson group encountered most of the chemically and biologically significant mycobacterial lipids and glycolipids, such as the mycolic acids, the branched fatty acids, the mannose-containing phosphoinositides, and arabinogalactan, that have been studied since. Other glycolipids that have significant functional or biological activities, such as trehalose 6,6′-dimycolate—cord factor—and the trehalose-2-sulfate-containing sulfolipids, were subsequently described by others. Likewise, the determination of the structures of the entire spectrum of mycolic acids was completed by a consortium of French and British researchers.[6] Other investigators were collectively to describe fully the $C_{21}-C_{25}$ α-methyl-branched (mycosonoic) fatty acids, the $C_{24}-C_{28}$ α-methyl-branched β-hydroxy (mycolipanolic) fatty acids, the unsaturated versions (the mycolienic or phthionoic acids), and the multimethyl-branched series (the phthioceronic acids).[6] Almost all of these fatty acids are esterified to various glycosyl groups or other polyols comprising an array of unusual cell-wall glyco-

lipids implicated in many of the relationships between host and pathogen. Much of this early phase of mycobacterial glycolipid biochemistry has been reviewed.[6,7] Several workers have advanced chemical models of the cell wall of mycobacteria[8-10] in an effort to understand intramolecular relationships within the mycolylarabinogalactanpeptidoglycan complex that forms the framework of the cell wall, as well as the intermolecular relationships with the trans-species and species-specific glycolipids that are the subject of this article.

II. Isolation and Fractionation of Glycolipids And General Structural Approaches

1. Isolation and Fractionation of Glycolipids

a. Glycopeptidolipids and Derived Haptens as Oligoglycosyl Alditols.— Detailed procedures for the isolation and purification of the species-specific glycolipids of mycobacteria have been reviewed.[11] Typically, suspensions of harvested cells are evaporated to dryness; then the dry residue is extracted with 4 : 2 : 1 chloroform–methanol–water and allowed to form a biphase. The lower organic phase is the source of glycolipids. Large quantities of acylglycerols and phosphoglycerides are also present, and it is often impossible to isolate specific glycopeptidolipids (GPLs) in preparative amounts directly from these extracts. The relative alkaline stability of the GPLs may be exploited under conditions that result in the saponification of acyl esters when the crude lipid extract, in 2 : 1 chloroform–methanol, is treated with an equal volume of 0.2 *M* sodium hydroxide. Specific polar GPLs are purified by chromatography on silica gel, using open columns, or preferably by flash chromatography, with a final purification by high-performance liquid chromatography (HPLC). The main limitation of this overall procedure concerns those *O*-acetylated GPLs whose inadvertent *O*-deacetylation may result in loss of antigenicity. In this case, smaller quantities of the naturally *O*-acetylated GPLs may be isolated by HPLC.[12] Oligoglycosylalditols are liberated, by reductive β-elimination with alkaline sodium borohydride, from *O*-glycosidic attachment to the D-allothreonine in the peptide core,[13] and a modified procedure[14] has been developed with final desalting on a column of Bio-Gel P-2.

b. Purification of Lipo-oligosaccharide Antigens.— Lipo-oligosaccharide (LOS) and GPL antigens are apparently mutually exclusive constituents of mycobacteria; if one is present, the other is absent. The GPLs are characteristically found in the *M. avium* and associated complexes. The trehalose-containing LOSs are present in a host of other mycobacteria, such as *M. kansasii*, *M. szulgai*, *M. xenopi*, *M. malmoense*, *M. gastri*, *M. smegmatis*, and the atypical Canetti strain of *M. tuberculosis*. As these are acylated oligosaccharides and hence alkali-labile, purification is more stringent; anion-exchange chromatography is necessary to separate the phospholipids, particularly phosphoinositides, from the neutral LOS. Typ-

ical isolation procedures involve chromatography of washed lipid extracts on columns of DEAE-cellulose (acetate form) and elution with chloroform–methanol mixtures, followed by further purification by HPLC. Pure LOS is used as the source of the corresponding oligosaccharide; some clearly resolvable LOSs yield the same oligosaccharide. The saponification of an individual LOS in chloroform–methanol or reaction with sodium hydroxide in methanol is followed by desalting on a mixed-bed ion-exchange resin and futher purification on Bio-Gel P-2.

c. Purification of Phenolic Glycolipids.—In view of the biological importance of phenolic glycolipid I (PGL-I), the original protocols for isolation and purification from armadillo tissues[15] have been modified.[11] This procedure, which is described by McNeil *et* al.[11] involves a series of chromatographic separations on Florisil with chloroform–methanol mixtures followed by HPLC on a silica column.

2. General Structural Approaches

Approaches to the elucidation of glycolipid structures are no different in principle from those used for other groups of complex carbohydrates. However, with an awareness of certain recently discovered novel features, greater emphasis is placed on procedures that may not always be necessary in the examination of other classes of carbohydrates. Complete structural elucidation requires acquisition of knowledge of the following features: glycosyl composition, including the anomeric and enantiomeric configurations of glycosyl residues; the sites of linkage between the glycosyl residues; the sequences in which the residues are linked; and the identification and location of short- and long-chain *O*- and *N*-acyl and other noncarbohydrate substituents. While information on these various features has been acquired mainly from analytical chemical manipulations, increasing emphasis is now placed on nuclear magnetic resonance and mass spectroscopic (NMR and MS) data obtained from the examination of the intact molecules and their derivatives.

a. Glycosyl Composition.—Direct compositional analysis of glycolipids from mycobacteria remains the simplest and most necessary first step, in the light of the widespread occurrence of endogenously methylated glycose residues. Hydrolysis of the glycolipid, followed by identification by gas-chromatographic mass spectroscopy (GC-MS) using capillary columns of the derived alditol acetates, is most appropriate since this method allows for the location of the methyl ether substituents when these are present. In addition, it is often possible to identify provisionally the parent sugar by comparison of the unknown sugar derivatives with those derived upon random incomplete methylation of individual monosaccharides. In confirmation of this identity, *O*-demethylation of the unknown sugar

may be performed, as with boron tribromide.[16] The absolute enantiomeric configurations of glycosyl residues are determined through the formation, for GC analysis, of equilibrium mixtures of volatile derivatives of glycosides prepared from optically pure 2-butyl or 2-octyl alcohols.[17,18] It should be kept in mind that different derivatives of both enantiomers, such as D- and L-rhamnose in the GPLs from *M. avium* serovar 14 and 20, may be present in the same oligosaccharide chain.[19] In such cases, more subtle and less direct approaches are required.

It cannot be assumed, however, that all glycose constituents are liberated without decomposition during conventional hydrolysis with 2 *M* trifluoroacetic acid.[14,20] Since glycosiduronic acids are resistant to hydrolysis, uronic acids will be incompletely released, as will be the glycose units to which they are attached; other sugars may be decomposed under severe hydrolysis conditions. For uronic acids, various methods of carboxyl reduction are used in order to generate 6,6-dideuteriohexosyl residues before formation of alditol acetates.[14] The liberation of sugars with branched chains and/or acylamino substituents at C-4, which are decomposed during conventional hydrolysis, may be achieved by modified procedures; such procedures include treatment with anhydrous hydrogen fluoride, as for the amino sugars in GPLs from *M. avium* serovars 25 (ref. 14) and 14 (ref. 19) or after base-catalyzed degradation of the terminal uronic acid residue[21] in the GPL from *M. avium* serovar 19.[20]

b. Methylation-Linkage Analysis.—The standard technique of linkage analysis based on the identification of partially methylated alditol acetates by GC-MS[22] is especially appropriate for glycolipids containing endogenous methyl ether substituents when alkylation using trideuteriomethyl iodide is routinely performed. Under the strongly basic conditions used in the Hakomori[23] and Ciucanu and Kerek[24] procedures, base-catalyzed degradation of uronic acid residues by β-elimination,[14] which is a potential difficulty, has not been reported. However, base-catalyzed degradation has been carried out on previously permethylated oligosaccharides.[20] Methylation under nonbasic conditions using methyl triflate and 2,6-di-*tert*-butylpyridine[25] has been used in the location of base-labile *O*-acyl substituents (Section II).

c. Sequences of Glycosyl Residues and Detection of Noncarbohydrate Substituents by Mass Spectrometry.—Traditional GC-MS in the electron-impact and chemical-ionization modes is still widely used for mono-, di-, and triglycosyl derivatives, and many examples are to be found in cited references. The techniques are rarely adequate for higher oligosaccharides or for glycolipids. For these compounds, information on sugar sequences is mainly derived from fast-atom bombardment mass spectrometry (FAB-MS)[26] and plasma-desorption mass spectrometry (PD-MS) with californium-252,[27] especially in the positive-ion mode. Positive-ion FAB-MS is conveniently performed on permethylated derivatives and

on the original oligoglycosylalditols carrying several methyl ether substituents. Sequence information is readily derived from the characteristic mass increments in the series of glycosyloxonium ions formed on fragmentation, provided that the increments are different, either naturally or by virtue of substituents introduced during derivatization. Unusual mass increments point to the presence of sugars having substituents such as those in the acetamidodideoxy-*O*-methylhexose in *M. avium* serovar 25 (ref. 14) and the dideoxy-*C*-methyl-*O*-methylhexose in *M. avium* serovar 19 (ref. 20), which had not been detected on standard hydrolysis.

Plasma-desorption mass spectrometry is another technique that has been applied successfully to the detection of readily removable fatty acyl substituents in intact glycolipids and their acylated derivatives. The specific location of the fatty acyl substituents in the ring of the glycosyl residues, as in LOS antigens, is determined by methylation under nonbasic conditions (see Section II.1b), followed successively by *O*-deacylation, ethylation of the exposed hydroxyl groups, and GC-MS analysis of partially alkylated alditol acetates[21]; ethyl groups denote the sites of previous *O*-acylation.

d. Anomeric and Ring Configurations of Glycosyl Residues.—Nuclear magnetic resonance spectroscopy (^1H and ^{13}C) is the primary tool for determination of anomeric configurations. Chemical shifts and $J_{1,2}$ coupling constants in the ^1H spectra for the anomeric protons of glycopyranosyl residues of the more common configurations are readily recognized to be of three main types: *α-gluco* and *α-galacto*, *β-gluco* and *β-galacto*, and *manno*. In the latter instance, chemical shifts, but rarely coupling constants, serve to distinguish between α and β anomers. A useful parameter here, and in other cases of ambiguity, is the one-bond heteronuclear C–H coupling constant from C-1 of the individual glycosyl residue.[11]

At the outset of an examination of an oligosaccharide, a well resolved one-dimensional (1D) NMR spectrum provides a guide to anomeric configuration, and may also reveal unsuspected features, such as noncarbohydrate substituents. As an example (Fig. 1), the ^1H-NMR spectrum of the oligoglycosylalditol from *M. avium* serovar 25 shows characteristic anomeric protons, especially for the *β-gluco* configuration of the penultimate glucosyluronic residue.[14]

Two-dimensional (2D) NMR, both homonuclear and heteronuclear correlation spectroscopy (COSY), is also used to establish the complete ring configuration of some novel glycosyl residues. One such example is the oligoglycosylalditol from the GPL of serovar 25. The coupling constants measured in the 1D spectrum for all ring protons of the terminal acetamido sugar indicate that this residue is in the *galacto* configuration. Location of the nitrogen-carrying carbon was established by homo- and heteronuclear ($^{13}C-^1H$) COSY, Fig. 2 (A and B). Thus, the CH–NH signal was at δ 56.0, which was found to correlate with the proton resonance at δ 4.25 in the heteronuclear ($^{13}C-^1H$) spectrum.

An example of the use of NMR in the examination of intact glycolipids has been reported for one of the serine-containing GPLs from *M. xenopi*. Rivière and Puzo[28]

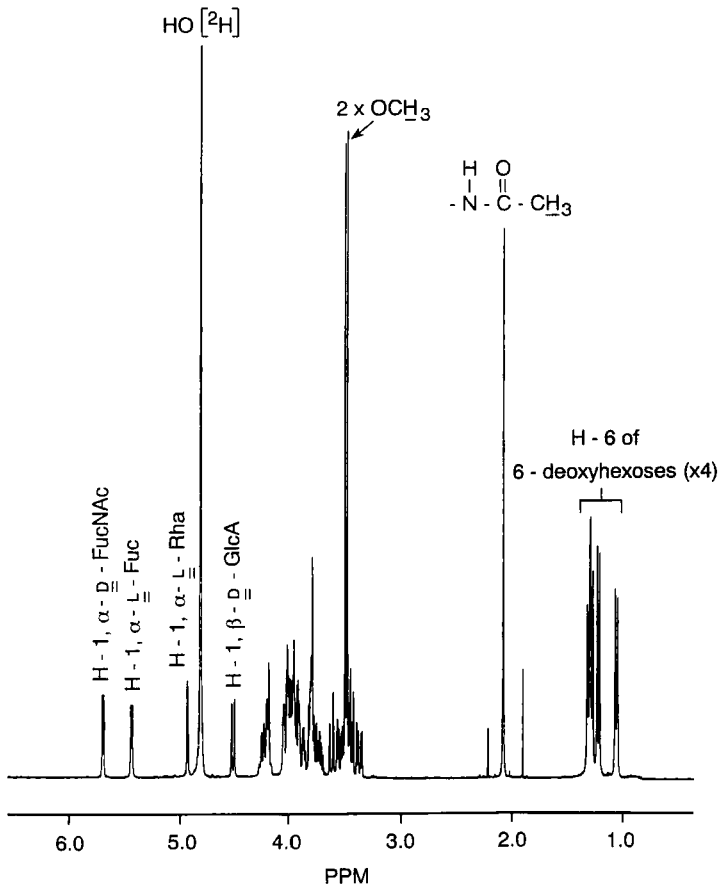

FIG. 1.—^{1}H-NMR spectrum of the oligoglycosylalditol from the GPL of *M. avium* serovar 25.

used two-dimensional ^{1}H-NMR rotating-frame nuclear Overhauser enhancement spectroscopy (ROESY) to detect n.O.e. contacts. From these experiments it was possible to establish the sequence of the tetrapeptide core, to localize the sites of glycosylation, and to define the locations of different *O*-acyl substituents.

III. STRUCTURES OF THE SPECIES- AND TYPE-SPECIFIC GLYCOLIPIDS OF MYCOBACTERIA

1. Historical Perspective

The first evidence for the presence of species- and type-specific glycolipids within members of the *Mycobacterium* genus was generated by Smith and colleagues[29–31]; they proposed the term *mycoside* for "type-specific glycolipids of

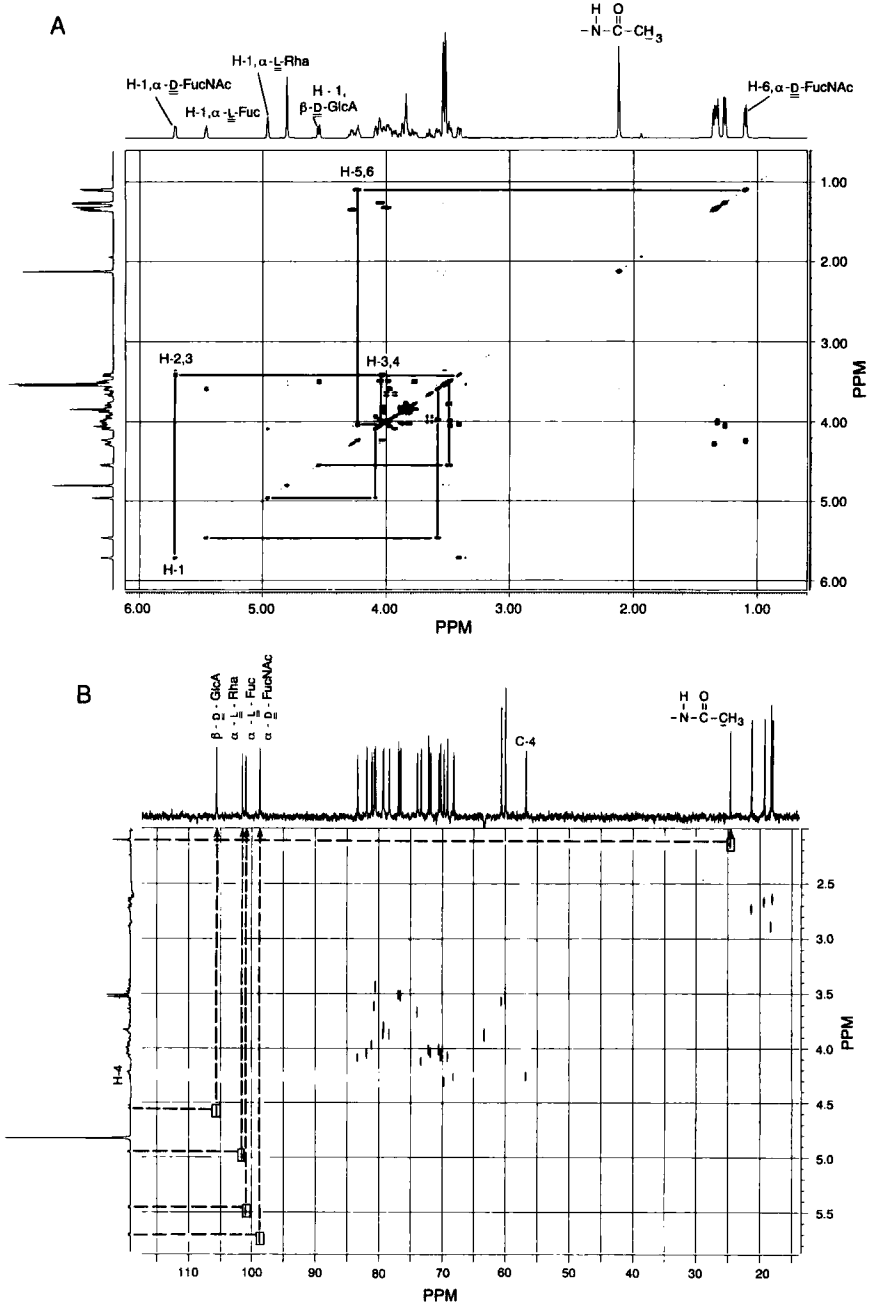

FIG. 2.—(A) Homonuclear ($^1H-^1H$) COSY spectrum of the oligoglycosylalditol from the GPL of *M. avium* serovar 25. (B) Heteronuclear ($^{13}C-^1H$) COSY spectrum of the oligoglycosylalditol from the GPL of *M. avium* serovar 25.

mycobacterial origin which had been discovered by IR spectroscopy of chromatographically fractionated ethanol–diethyl ether extracts." Originally, they had applied infrared analysis for the purposes of relating strain differences to fatty acid profiles; but, instead, distinct lipids within *M. bovis*, *M. avium*, *M. tuberculosis*, and other species were observed, thereby allowing the differentiation of these species. Chromatographic purification and chemical analyses, notably IR spectroscopy,[31–33] revealed compounds which were labeled A, B, C, and D substances; phthiocerol dimycocerosate; G substances from the photochromogenic mycobacteria and *M. bovis*; and J substances from *M. avium*. Of initial interest were the G substances, Ga and Gb. Infrared spectroscopy of Ga from the atypical photochromogenic Group I mycobacteria and Gb from *M. bovis* indicated in each case the presence of an aromatic ether and the common lipid component, diacylphthiocerol. The G substances also contained carbohydrates, as detected by paper chromatography. Whereas Ga showed the presence of three *O*-methyl-6-deoxyhexoses, Gb contained only the one.[32] The Ga and Gb substances were renamed mycoside A and mycoside B, respectively,[31] and today are classified as members of the phenolic glycolipid family. Discovery of the phenolic glycolipid I of *M. leprae*, and subsequent extensive work in its role in the immunoreactivity and pathogenesis of leprosy, raised the level of general interest in these products.

The J substances described originally by Smith *et al.* contained an unknown fatty acid moiety, and three amino acids—alanine, threonine, and phenylalanine—were detected by paper chromatography.[32] They were subgrouped as Jat, found only in scotochromogenic organisms, and Jav, found in *M. avium* and other related nonphotochromogenic mycobacteria. Sugar analysis revealed monosaccharides resembling those in the G compounds, namely *O*-methyl-6-deoxyhexoses. The Jat and the Jav compounds differed in their content of these sugars. They were later termed mycoside C (C-mycosides),[31] following the mycoside A and B nomenclature. To add to the complexity of the nomenclature of this family of compounds, Brennan and Goren[34] renamed them peptidoglycolipids, and later, more correctly, glycopeptidolipids (GPL).[13] Although the discovery of polar, multiglycosylated, highly antigenic GPLs is attributed to Brennan and Goren,[34] in retrospect, it would seem that the first evidence of the existence of both polar and apolar versions of the C-mycosides came from Smith *et al.*[32] Their so-called Jabs appear to contain the same amino acids as Jav and Jat but were lacking most of the sugar components: "The IR spectrum of Jabs resembles the IR spectrum of substances Jav and Jat from which the sugars have been removed."[33]

The structures of the apolar C-mycoside GPLs were established by several groups of French investigators in the period from 1967 to 1971. A moot question for some time was whether the internal -D-alloThr-D-Ala- unit was repeating. However, with the recognition of 2-aminopropanol (alaninol) the now-accepted structure **1** for the lipopeptide core was advanced. Further unequivocal proof of the accepted core structure was provided by field-desorption MS and by californium-

desorption MS.[27] The consensus now is that the basic tetrapeptide structure is the only one in existence in the C-mycoside GPLs.

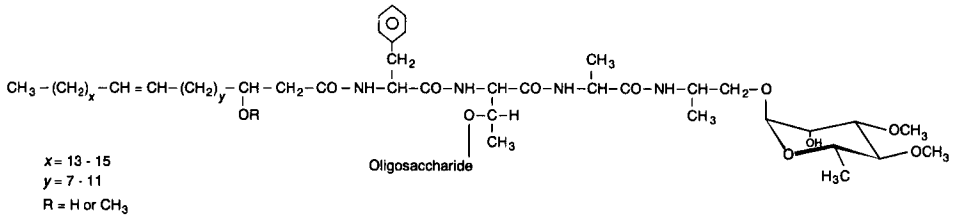

1

The recent history of the polar antigenic GPLs (**1**) has been amply documented.[35] It was born of two distinct observations, thought to be unconnected at the time. W. B. Schaefer had observed that most nontuberculosis mycobacteria are endowed with highly immunogenic species- or type-specific antigens, and was able to devise a seroagglutination assay based on these antigens for purposes of identification and classification of strains.[36] His procedure allowed recognition of at least 31 antigenically distinct serovars within the complex comprising serovars of *M. avium*, *M. intracellulare*, and *M. scrofulaceum*.[37–39] Quite independently, Marks, Jenkins, and their colleagues recognized that whole-lipid extracts derived from the *M. avium* serovars contained an individualistic array of glycolipids which, in general, could be used to identify subspecies.[40–42] In what has proved to be a key study, Brennan and Goren[34] demonstrated that the Schaefer typing antigens and the Marks–Jenkins lipids were synonymous and were in fact polar C-mycoside glycopeptidolipids in which small oligosaccharides were attached to the allothreonine substituent of the common fatty acyl–peptidyl–*O*-(3,4-di-*O*-methylrhamnoside) C-mycoside core. Discovery of the polar, multiglycosylated GPLs was the first step in the recognition of a general phenomenon, namely that most mycobacteria are endowed with large quantities of glycolipids which contain small oligosaccharides of sufficient antigenicity to evoke antibodies of such exquisite specificity as to allow unequivocal identification of species or subspecies.

The origins of the trehalose-containing lipo-oligosaccharide antigens of other mycobacterial species also lay in the seminal observations of W. B. Schaefer that the products responsible for the specific antigenicity of other atypical mycobacteria were susceptible to alkali treatment, and thus must differ from the GPLs.[37] Hunter *et al.*[43] were then able to show that the alkali-labile, highly immunoreactive glycolipids of *M. kansasii* are trehalose-containing linear oligosaccharides in which the acyl functions were invariably asymmetrically located on the trehalose unit at one end of the molecule, and specific antigenicity lay in a combination of

unique sugars at the nonreducing end. At the same time, Ballou *et al.*[44,45] while exploring the biosynthesis of bacterial glycolipids, recognized the presence of acyltrehaloses bearing *O*-pyruvated glycosyl substituents.

The structures, synthesis, and some of the biological properties of these three major classes of mycobacterial glycolipid antigens are the basis of this article.

2. Glycopeptidolipids of the *M. avium* Complex

These surface antigens provide the basis for serotyping in the *M. avium* serocomplex. As indicated previously, they were originally called C-mycoside polar glycopeptidolipids as distinct from the serologically inactive apolar glycopeptidolipids, the original "C-mycosides."[31] Their distinctive features are oligosaccharide chains in which the inner disaccharide unit, *O*-(α-L-rhamnopyranosyl)-(1→2)-6-deoxy-α-L-talopyranose, common to GPL antigens of all serovars examined to date, is *O*-glycosidically linked to the allothreonine in the *N*-fatty acyl tetrapeptide which also bears a glycosylated alaninol C-terminus (**1**). Brennan and Goren[34] furnished the first compositional data for these serologically active antigens by showing that the oligosaccharide chains were liberated on reductive β-elimination with alkaline sodium borohydride.[13] This behavior was typical of peptides carrying *O*-glycosyl substituents on serine or threonine residues, in this instance the D-allothreonine residue of the *N*-acylpeptides of C-mycosides. The oligosaccharide haptens in the parent GPLs carry *O*-acetyl substituents (see Section II), but in only one instance thus far—that of serovar 9—has an *O*-acetyl substituent been identified as part of the epitope. Liberated oligoglycosylalditols terminated by the *O*-(α-L-rhamnopyranosyl)-(1→2)-6-deoxy-L-talitol fragment contain sugars characteristic of the particular serovar.[46] Methyl ethers, especially of 6-deoxyhexoses, are constituents of all but one GPL. The first structural studies[46] were undertaken with less fully developed analytical and spectroscopic methods, and it seemed likely that partially methylated sugars were the main distinguishing features of the GPLs. Subsequently, uronic acids[14,20] were found, as were acetalically linked pyruvic acid moieties,[46,47] acylaminodideoxyhexoses,[14,19,48] and branched-chain sugars.[20] No single basis for classification of the 12 known examples is obvious, but structural similarities between otherwise unrelated GPLs may be readily recognized, as in sugar constituents or in the presence of ionizable groups. In this article, GPLs will be considered in groups showing some degree of constitutional or stereochemical homology suggestive of parallel biosynthetic pathways. Assuming that biosynthesis of the oligosaccharide chain is by stepwise transfer from glycosyl esters of nucleoside pyrophosphates to the common α-L-rhamnopyranosyl-(1→2)-6-deoxy-α-L-talopyranosyl inner unit attached to *N*-acylpeptide, chain extension with attachment of (1) 2-*O*-methyl (or 2,3-di-*O*-methyl)-α-L-fucopyranose, (2) α-L-rhamnopyranose, or (3) 3-*O*-methyl-β-D-glucopyranose residues, offers a provisional basis for structural clas-

TABLE I

Grouping of Haptens of the GPL Antigens of *M. avium* Complex, Based on Structural Similarities

Serovar number	Structure of oligosaccharide
Group 1	
2	4-*O*-Ac-2,3-di-*O*-Me-α-L-Fuc*p*-(1→3)-α-L-Rha*p*-(1→2)-6-deoxy-L-Tal
4	4-*O*-Me-α-L-Rha*p*-(1→4)-2-*O*-Me-α-L-Fuc*p*-(1→3)-α-L-Rha*p*-(1→2)-6-deoxy-L-Tal
9	4-*O*-Ac-2,3-di-*O*-Me-α-L-Fuc*p*-(1→4)-β-D-Glc*p*A-(1→4)-2,3-di-*O*-Me-α-L-Fuc*p*-(1→3)-α-L-Rha*p*-(1→2)-6-deoxy-L-Tal
14	4-formamido-4,6-dideoxy-2-*O*-Me-3-*C*-Me-α-Man*p*-(1→3)-2-*O*-Me-α-D-Rha*p*-(1→3)-2-*O*-Me-α-L-Fuc*p*-(1→3)-α-L-Rha*p*-(1→2)-6-deoxy-L-Tal
20	2-*O*-Me-α-D-Rha*p*-(1→3)-2-*O*-Me-α-L-Fuc*p*-(1→3)-α-L-Rha*p*-(1→2)-6-deoxy-L-Tal
25	2-*O*-Me-α-D-Fuc*p*4*N*Ac-(1→4)-β-D-Glc*p*A-(1→4)-2-*O*-Me-α-L-Fuc*p*-(1→3)-α-L-Rha*p*-(1→2)-6-deoxy-L-Tal
26	2,4-di-*O*-Me-α-L-Fuc*p*-(1→4)-β-D-Glc*p*A-(1→4)-2-*O*-Me-α-L-Fuc*p*-(1→3)-α-L-Rha*p*-(1→2)-6-deoxy-L-Tal
Group 2	
12	4-(2-hydroxy)propanamido-4,6-dideoxy-3-*O*-Me-β-D-Glc*p*-(1→3)-4-*O*-Me-α-L-Rha*p*-(1→3)-α-L-Rha*p*-(1→3)-α-L-Rha*p*-(1→2)-6-deoxy-L-Tal
17	3-(3-hydroxy-2-methyl)butanamido-3,6-dideoxy-β-D-Glc*p*-(1→3)-4-*O*-Me-α-L-Rha*p*-(1→3)-α-L-Rha*p*-(1→3)-α-L-Rha*p*-(1→2)-6-deoxy-L-Tal
19	3,4-di-*O*-Me-β-D-Glc*p*A-(1→3)-3-*C*-Me-2,4-di-*O*-Me-α-L-Rha*p*-(1→3)-α-L-Rha*p*-(1→3)-α-L-Rha*p*-(1→2)-6-deoxy-L-Tal
Group 3	
8	4,6-*O*-(1-carboxyethylidene)-3-*O*-Me-β-D-Glc*p*-(1→3)-α-L-Rha*p*-(1→2)-6-deoxy-L-Tal
21	4,6-*O*-(1-carboxyethylidene)-β-D-Glc*p*-(1→3)-α-L-Rha*p*-(1→2)-6-deoxy-L-Tal

sification. Table I summarizes the known structures of the oligosaccharide haptens, grouped so as to emphasize structural relationships. In this section, details of structure determinations based on (1) compositional and alkylation linkage analysis, (2) ^{1}H and ^{13}C NMR spectroscopy, and (3) FAB mass spectrometry of the parent and derivatized oligoglycosyl alditols will be cited only in support of those spectroscopic and chemically degradative procedures which were required to unravel special structural features. Attention is also given to aspects of structure relating to immunological specificity.

a. Group 1.—GPLs from serovars 2, 4, 9, 14, 20, 25, and 26 with chains emanated via 2-*O*-methyl (or 2,3-di-*O*-methyl) -α-L-fucopyranosyl residues.

***(i)* GPL from *M. avium* Serovar 2.**—The structure of the simplest glycotriosyl GPL having a single 2,3-di-*O*-methyl-α-L-fucopyranosyl residue external to the core, was established from ^{1}H and ^{13}C NMR data, from the electron-impact (EI) mass spectrum of the trideuteriomethylated derivative, and by methylation linkage analysis.[23] The parent GPL is *O*-acylated, but since *O*-deacylation does not influence interaction of the otherwise intact GPL with anti-serovar 2 murine monoclonal antibodies,[47] *O*-acetyl groups are presumably substituents of the inner two residues of the trisaccharide unit. An identical GPL had been isolated previously from strains presumed to be of *M. paratuberculosis*[49]; however, it now appears that these were strains of *M. avium* serovar 2.

***(ii)* GPL from Serovar 4.**—*Mycobacterium avium* serovar 4 is the most frequently encountered *M. avium* serovar in AIDS patients with disseminated mycobacterioses. The main structural features of the GPL were derived from compositional and linkage analyses, supported by data from FAB and EI mass spectrometry of the fully alkylated derivative, and the ^{1}H-NMR spectrum of the parent triglycosylalditol.[12] Evidence to define the ring size of the 2-*O*-methylfucosyl residue as pyranose and the linkage site at O-4 was obtained from characterization of two disaccharides formed on partial hydrolysis of the pertrideuteriomethylated oligosaccharide, followed by sequential reduction and methylation. Enantiomeric configurations were established as L after *O*-demethylation of the triglycosylalditol and conversion of sugars into trimethylsilyl ethers of (*S*)-(+)-2-butyl glycosides.

***(iii)* GPLs from Serovars 14 and 20.**—The oligosaccharide hapten from serovar 14 (ref. 19) differs from that of serovar 20 (ref. 50) in that the GPL from serovar 14 carries an additional branched-chain amino sugar residue at its nonreducing terminus. The haptens contain a 2-*O*-methyl-α-D-rhamnopyranosyl residue, contrasting with that of 4-*O*-methyl-α-L-rhamnopyranosyl in GPLs from serotypes 4, 12, and 17. The methyl ethers are all located in the outer regions of the GPLs, which also contain the L-rhamnopyranose residue in the inner region. The

structure of the triglycosylalditol from the serovar 20 GPL[50,51] was determined in a manner similar to that from serovar 4. Compositional and linkage analyses, supported by FAB-MS data for the peralkylated oligosaccharide, established the sequence of sugar residues and their linkage positions; and the ^{1}H spectrum of the parent oligosaccharide showed that all of the glycosyl residues had the α-D or α-L configuration. The formation of chiral glycosides of L-rhamnose from the original hapten, but of both D- and L-rhamnose after *O*-demethylation, showed that the 2-*O*-methylrhamnose was the D enantiomer.

Liberation of the tetraglycosylalditol from serovar 14 GPL by reductive β-elimination was accompanied by *N*-deformylation of about half of the hapten molecules. The presence of the terminal sugar as a dideoxyformamido-*C*-methyl-*O*-methylhexose was indicated by FAB-MS and ^{1}H-NMR data for the *N*-formyl-oligoglycosylalditol. *N*-Acetylation of the *N*-deformyl oligoglycosylalditol, followed by controlled hydrolysis, reduction, and acetylation, furnished an alditol acetate identical (GLC-MS) to the corresponding derivative formed by *N*-acyl exchange from the *M. kansasii* lipo-oligosaccharide constituent, *N*-[(*R*)-2-methoxypropanoyl]kansosamine {4,6-dideoxy-4-[(*R*)-2-methoxypropanamido]-3-*C*-methyl-2-*O*-methyl-L-mannopyranose}. The complete sequence was determined by glycosyl-linkage analysis and EI-MS of the pertrideuteriomethylated tetraglycosylalditol and of products of partial acid hydrolysis followed by methylation, but no monomeric kansosamine derivatives were detected. Anomeric configurations were provisionally assigned as α from ^{1}H-NMR data, and enantiomeric configurations were determined for the 6-deoxyhexoses, as for those of the serovar 20 hapten, but not for the *N*-formylkansosamine. Evidence that this latter sugar residue has the same α-L configuration as that of the sugar from *M. kansasii* lipo-oligosaccharide was obtained later from synthesis (see Section IV.2).

***(iv)* GPLs from Serovars 3, 9, 25, and 26.**—Glycopeptidolipids from these four serovars have closely related structures in that they share glucosyluronic and partially methylated fucosyl residues. From successive investigations,[14,34,46] the complete sequence of the tetraglycosylalditol from the serovar GPL was derived from ^{1}H- and ^{13}C-NMR studies, and FAB-MS of the parent and trideuteriomethylated derivatives in support of methylation analyses.

Figure 3 shows the FAB-MS of the pertrideuteriomethylated derivative[14] of the tetraglycosylalditol of the serovar 9 GPL, together with the alkylation patterns of the sugar constituents shown in methylation analysis. Supporting sequence evidence was obtained from selective base-catalyzed degradation, which resulted in loss of the penultimate uronic acid residue and the attached fucosyl residue with exposure of the 4-OH of the inner 2,3-di-*O*-methylfucopyranosyl residue to be located after *O*-ethylation of the resulting diglycosylalditol.[14]

The GPL from serovar 9 provides the only example thus far in which reductive elimination from *O*-deacetylated GPL gives rise to two oligoglycosylalditols. The

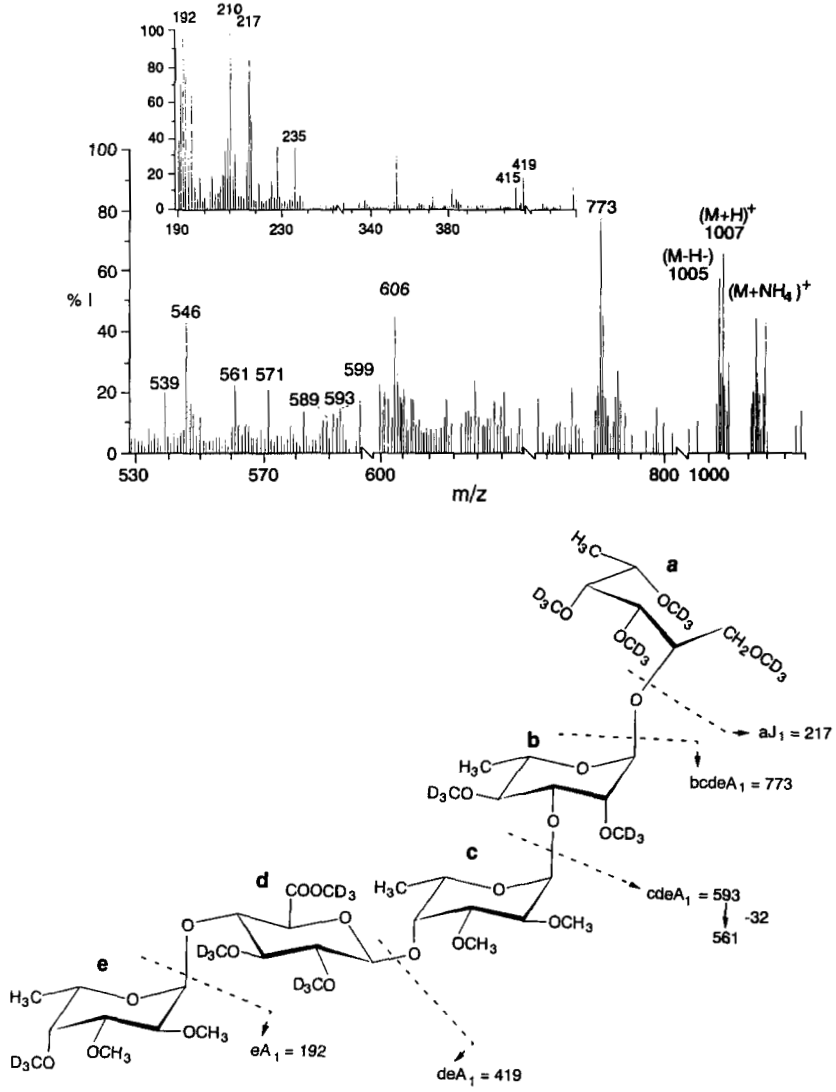

FIG. 3.—FAB-MS of the perdeuteriomethylated derivative of the oligoglycosylalditol from the GPL of *M. avium* serovar 9, and the origin of the fragment ions.

second product was shown to be identical to the first, except in its having retained the natural *O*-acetyl substituent at O-4 of the terminal 2,3-di-*O*-methyl-α-L-fucopyranosyl residue, which is recognized by antibodies to serovar 9. Further evidence for this necessary part of the epitope was obtained subsequently (see

Section IV.3). Later, the GPL from serovar 3 was examined, and determination of the molecular weight of the liberated oligoglycosylalditol by FAB-MS together with methylation analysis showed that the GPL was devoid of the *O*-acetyl substituent, but in all other respects was identical to the serovar GPL.

The same general approach to analysis of the structure of the serovar 25 GPL and FAB-MS revealed that the nonreducing, terminal-residue sugar was an acetamido-dideoxy-*O*-methylhexose.[14] Liberation of the sugar on treatment of the oligosaccharide hapten with hydrogen fluoride (to avoid *O*-deacylation), followed by reduction and acetylation, furnished an acetylated alditol whose mass spectrum showed the sugar to be a 4-acetamido-4,6-dideoxy-2-*O*-methylhexose, whose *galacto* configuration was established by NMR and confirmed by synthesis (see later). Since the susceptibility of the acylamino substituent to acid cleavage does not permit the formation of chiral glycosides, no direct determination of the absolute enantiomeric configuration was performed. It is noteworthy that the GPL from serovar 25 provided the third example, with those from serovars 9 and 26 (see later), of structural variation of substituents in outer trisaccharide units having the [α-L-fucopyranosyl-β-D-glucopyranosyluronic acid-α-L-fucopyranosyl] configurational sequence. It was assumed, therefore, on the grounds of apparent stereohomology, that the terminal sugar in the serovar 25 GPL would likewise have the α-L-fucose configuration. It was only later, when neoglycoconjugates containing the outer disaccharide units were synthesized (see Section IV.2), that evidence was obtained that this sugar is the D enantiomer.

The structure of the GPL from serovar 26 was established in a manner like that of serovar 9; it was shown to be of a generally similar type, but with the nonreducing terminal sugar as 2,4-di-*O*-methyl-α-L-fucopyranose.

b. Group 2.—This group comprises GPLs from serovars 12, 17, and 19 with chains emanating via a further 3-linked α-L-rhamnopyranose residue.

***(i)* GPLs from Serovars 12 and 17.**—The terminal sugar residue of the GPL from serovar 12 (ref. 48) is a derivative of viosamine (4-amino-4,6-dideoxyglucose), the previously unknown 4-(2-hydroxy)propanamido-4,6-dideoxy-3-*O*-methylglucopyranose, and was liberated on hydrolysis with retention of the *N*-acyl substituent. The structure was established by GLC-MS of the derived alditol acetate, and from one-dimensional and COSY two-dimensional ^{1}H-NMR spectra of α- and β-glycosyl acetates. Compositional and methylation linkage analyses, supported by FAB-MS of the pertrideuteriomethylated oligoglycosylalditol, established the sequence and linkage types of the sugar residues in the pentasaccharide hapten. The ^{1}H-NMR spectrum of the parent tetraglycosylalditol permitted assignment of anomeric configurations of the four outermost glycosidic linkages, and the formation of chiral glycosides from the hydrolysate of the purified GPL before β-elimination confirmed the absolute configurations for the four innermost

sugar residues, including the 6-deoxy-L-talopyranose unit, leaving only that of the amino sugar and the chiral *N*-acyl substituent to be determined.

From the isolation of the *O*-deacylated but otherwise unmodified GPL from serovar 12, it was also shown that the structure of the lipopeptide core was identical to that accepted for glycolipids of this group with respect to D-amino acid configurations, but not of the alaninol unit, and of the mono-unsaturated monohydroxy fatty acid.[48]

The GPL from serovar 17 has an inner tetrasaccharide segment identical to that of serovar 12. The enantiomeric configuration of the 3-(3-hydroxy-2-methyl)-butanamido-3,6-dideoxy-β-glucopyranose residue and the absolute configuration of the *N*-acyl substituent remain to be determined.[11]

(*ii*) **GPL from Serovar 19.**—Fast-atom bombardment MS of the tetraglycosylalditol and the trideuteromethylated derivative established the sequence of glycose residues and, in conjunction with NMR data, pointed to the presence of terminal 3,4-di-*O*-methyl-β-glucuronic acid and subterminal 6-deoxy-3-*C*-methyl-2,4-di-*O*-methylmannose residues.[20] A branched-chain sugar having a tertiary hydroxyl substituent would be susceptible to degradation during the acid hydrolysis required to cleave the glycosiduronic acid linkage of the terminal unit, and was not detected. Removal of the uronic acid residue from the peralkylated oligosaccharide by base-catalyzed degradation afforded the attenuated triglycosylalditol, from which the branched-chain sugar was liberated without decomposition on controlled hydrolysis. Absolute configurations were established for the D-glucuronic acid and L-rhamnose residues, but not for the branched-chain sugar constituent.[20]

c. Group 3.—This group comprises GPLs from serovars 8 and 21 with 3-*O*-methyl-β-D-glucopyranose residues attached to the inner core.

(*i*) **GPLs from Serovars 8 and 21.**—The oligosaccharide hapten from serovar 8 GPL was the first for which a complete structure for the glycobiosylalditol with location of the pyruvate acetal was proposed on the basis of glycosyl-linkage analysis with supporting spectroscopic data.[46] Similar data obtained for the glycobiosylalditol from the serovar 21 GPL showed that it was identical to that from serovar 8, except for the absence of the methyl ether substituent.[47]

(*ii*) **GPLs from Serovars 5,7,10,11,13,15,16,18,22,23,24, and 28 (ref. 52).**—The dominant serovar-specific GPLs from each of these serovars were purified and the sugar composition studied. In most cases, the oligoglycosylalditol was not liberated and sequenced. However, based on compositional analysis, it appears that all are terminated by the →3-(-α-L-rhamnopyranosyl-(1→2)-6-deoxy-L-talitol fragment, with the exception of serovars 5, 10, and 11, which

are distinguished by the →4)-3-*O*-methyl-α-L-rhamnopyranosyl-(1→2)-6-deoxy-L-talitol component. Moreover, it was established that the GPLs of serovars 10 and 11 were identical, as were 23 and 24, supporting other evidence that the organisms themselves were similar. The oligosaccharide chain of the GPL from serovar 5 was also distinguished by the presence of glucose and galactose—those of serovars 7,13,16, and 28 by new, incompletely characterized amino sugars, that from serovar 15 by 4,6-dideoxy-4-dodecanamido-3-*O*-methylglucopyranose, that from serovar 11 by glucose and 2,3-di-*O*-methylgalactose, that from serovar 18 by 6-*O*-methylglucose, and that from serovar 22 by arabinose.

***(iii)* Other GPLs from Other Mycobacteria, Including Those Not Based on C-Mycoside (Table II).**—In addition to those of the *M. avium* serocomplex, the C-mycoside GPLs are also found among some other mycobacterial species. That from *M. chelonae* subsp. *chelonae* and subsp. *abcessus* was identified with an oligosaccharide unit of the apparent structure (incomplete), (3,4-di-*O*-methyl-rhamnose)→(rhamnose)→(6-deoxytalose).[53] *Mycobacterium simiae* is known to consist of a two-member serocomplex, based on heretofore undefined GPLs. The GPL from *M. fortuitum* biovar *peregrinum* is worthy of mention in that Tsang *et al.*[53] had noted that it was of the C-mycoside class, but had not deemed it special. However, Lopez-Marin *et al.*[54] demonstrated the presence of a disaccharide, either 3,4-di-*O*-methyl-α-L-rhamnopyranosyl-(1→2)-α-L-rhamnopyranose or 3-*O*-methyl-α-L-rhamnopyranosyl-(1→2)-3,4-di-*O*-methyl-α-L-rhamnopyranose linked to the alaninol, and a single sugar, 3-*O*-methyl-α-L-rhamnopyranose, attached to the threonine. Subsequently, Rivière and Puzo[55] reported on a novel GPL apparently confined to *M. xenopi* isolates and named X-1, which differs markedly from those of the *M. avium* complex and therefore is classified as a non-C-mycoside GPL. As in the case of the conventional GPLs, allothreonine and

TABLE II

Structures of the Oligosaccharide Haptens from Glycopeptidolipid Antigens from Other *Mycobacteria*

Species	Structure of oligosaccharide	Reference
M. fortuitum biovar *peregrinum*	3,4-di-*O*-Me-α-L-Rha*p*-(1→2)-3,4-di-*O*-Me-α-L-Rha*p* or 3-*O*-Me-α-L-Rha*p*-(1→2)-3,4-di-*O*-Me-α-L-Rha*p*	53,54
M. senegalense M263	3,4-di-*O*-Me-α-L-Rha*p*-(1→2)-3,4-di-*O*-Me-α-L-Rha*p* or 3-*O*-Me-α-L-Rha*p*-(1→2)-3,4-di-*O*-Me-α-L-Rha*p*	54a
M. xenopi CIPT 140 35004	2,3,4-tri-*O*-Me-α-L-Rha*p*-(1→3)-α-L-Rha*p*-(1→3)-α-L-Rha*p*-(1→3)-α-L-6-deoxy-Glc*p*	55
M. xenopi ATCC 19250	α-L-Rha*p*-(1→3)-α-L-Rha*p*	56
M. paratuberculosis	4-*O*-Ac-2,3-di-*O*-Me-α-L-Fuc*p*-(1→3)-α-L-Rha*p*-(1→2)-6-deoxy-L-Tal	49

phenylalanine were present, but serine was also present in the form of the tetrapeptide structure -Ser-Ser-Phe-aThr-OCH_3. With an oligosaccharide chain *O*-glycosidically attached to the carboxy-terminal allothreonine residue, present as a methyl ester in the lipopeptide core, base-catalyzed β-elimination of the haptenic oligosaccharide occurs with ease. Such a method of chemical degradation to furnish the oligosaccharide was of limited value because, in addition, further degradation ensued from the 3-*O*-substituted glycose terminus, and *O*-acetyl and *O*-fatty acyl substituents were readily removed. The major structural features of the oligosaccharide, including the sites of attachment of *O*-acyl substituents, were established largely from a combination of pyrolysis electron-impact (EI) MS to give sequence information, and nondegradative NMR spectroscopy, including $^1H-^1H$ COSY experiments performed on the native and peracetylated GPL for linkage and configurational assignments. The *N*-C_{12} fatty acyl (dodecanoyl) substituent in the lipopeptide core contrasts with the $C_{32}-C_{35}$ acyl substituents in the *M. avium* GPLs, and *O*-acyl (acetyl and dodecanoyl) substituents in the oligoglycosyl chain were arbitarily assigned in the proposed structure **2**. In addition to the unusual glycosyl constituents shown in the oligoglycosyl chain, a single 3-*O*-methyl-6-deoxy-α-L-talopyranosyl substituent was attached to the *N*-terminal serine residue.

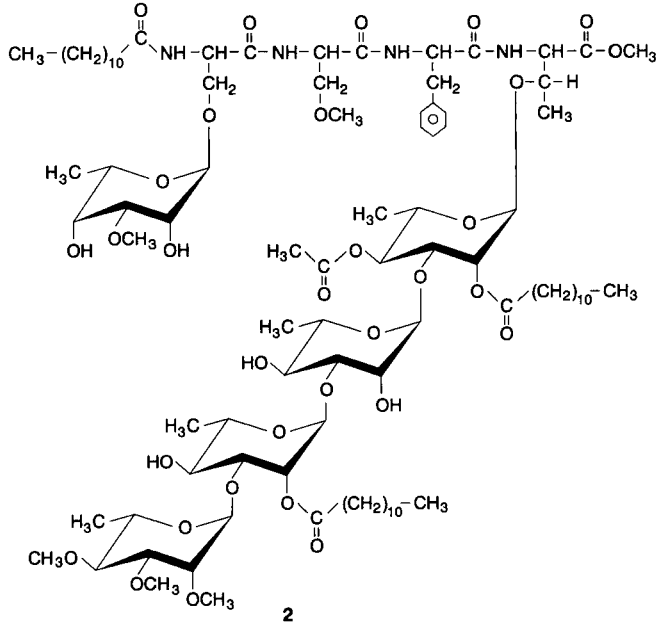

2

Later, Besra *et al.*[56] completed an independent study of the new GPLs of another strain of *M. xenopi* and concluded that the one described by Rivière and Puzo was

not a major component. Instead, the penultimate serine was glycosylated by a single 2-*O*-acetyl-6-deoxy-3-*O*-methyl-α-L-talopyranosyl group and the *C*-terminal allothreonine-*O*-methyl ester by a diglycosyl group, 4-*O*-(octanoyl or decanoyl)-α-L-rhamnopyranosyl-(1→3)-2-*O*-dodecanoyl-α-L-rhamnopyranosyl (structure **3**).

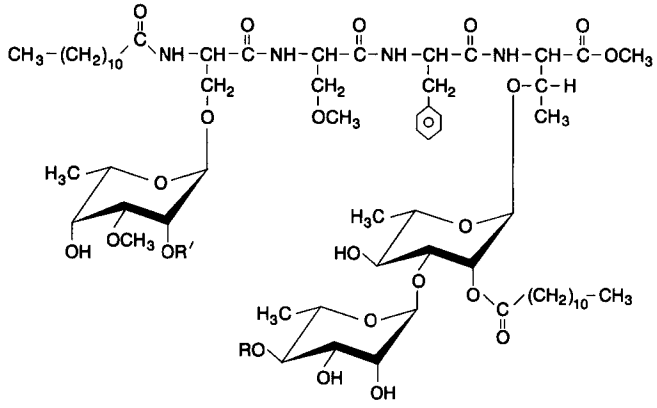

GPL-I:	R = H;	R′ = H
GPL-II:	R = H;	R′ = Acetyl
GPL-III:	R = C_8 or C_{10} Acyl;	R′ = H
GPL-IV:	R = C_8 or C_{10} Acyl;	R′ = Acetyl

3

3. The Trehalose-Containing Lipo-oligosaccharides

The newest glycolipids from *Mycobacterium* spp., and the most surprising in terms of novel structural principles, are the trehalose-containing lipo-oligosaccharides (LOS). The structures of all of those described thus far are summarized in Table III.

a. ***Mycobacterium kansasii.***—Schaefer[37] and Brennan *et al.*[57] had observed that the serologically active lipid extracts of *M. kansasii* and *M. szulgai* and several other mycobacteria, unlike those from members of the *M. avium* serocomplex, were alkali-labile, suggesting an entirely different structural arrangement from the C-mycoside GPLs. These glycolipids are based on α,α-trehalose units in which one α-D-glucopyranose residue carries two or three fatty acyl substituents (structure (**4**) and, sometimes, an *O*-methyl group. The other α-D-glucopyranose residue carries one of several oligoglycosyl groups showing variations in sugar composition and linkage types. The glycolipids are referred to as alkali-labile, since even

TABLE III

Structures of Major Trehalose-Containing Lipo-oligosaccharides of *Mycobacterium*

Species	Trivial name	Structure of oligosaccharide	Positions of acyl residues	Reference
M. smegmatis	(Acidic oligosaccharide A)	4,6-*O*-(1-carboxyethylidene)-3-*O*-Me-β-D-Glc*p*-(1→3)-4,6-*O*-(1-carboxyethylidene)-β-D-Glc*p*-(1→4)-β-D-Glc*p*-(1→6)-α-D-Glc*p*-(1↔1)-α-D-Glc*p*	4 and 6-hydroxyls of terminal trehalose	44
M. smegmatis	(Acidic oligosaccharide B_1)	4,6-*O*-(1-carboxyethylidene)-β-D-Glc*p*-(1→4)-β-D-Glc*p*-(1→6)-α-D-Glc*p*-(1↔1)-α-D-Glc*p*	ND[a]	
M. smegmatis	(Acidic oligosaccharide B_2)	4,6-*O*-(1-carboxyethylidene)-3-*O*-Me-β-D-Glc*p*-(1→3)-β-D-Glc*p*-(1→4)-β-D-Glc*p*-(1→6)-α-D-Glc*p*-(1→1)-α-D-Glc*p*	ND	
M. kansasii	LOS I′	3-*O*-Me-α-L-Rha*p*-(1→3)-β-D-Glc*p*-(1→3)-β-D-Glc*p*-(1→4)-α-D-Glc*p*-(1↔1)-α-D-Glc*p*	ND	
M. kansasii	LOS I	β-D-Xyl*p*-(1→4)-3-*O*-Me-α-L-Rha*p*-(1→3)-β-D-Glc*p*-(1→3)-β-D-Glc*p*-(1→4)-α-D-Glc*p*-(1↔1)-α-D-Glc*p*	ND	
M. kansasii	LOS II, III	$(\beta\text{-D-Xyl}p)_2$-(1→4)-3-*O*-Me-α-L-Rha*p*-(1→3)-β-D-Glc*p*-(1→3)-β-D-Glc*p*-(1→4)-α-D-Glc*p*-(1↔1)-α-D-Glc*p*	ND	
M. kansasii	LOS IV, V, VI	Kan*N*acyl-(1→3)-Fuc-(1→4)-$(\beta\text{-D-Xyl}p)_4$-3-*O*-Me-α-L-Rha*p*-(1→3)-β-D-Glc*p*-(1→3)-β-D-Glc*p*-(1→4)-α-D-Glc*p*-(1↔1)-α-D-Glc*p*[b]	ND	
M. kansasii	LOS VII, VIII	Kan*N*acyl-(1→3)-Fuc*p*-(1→4)-$[\beta\text{-D-Xyl}p\text{-}(1\rightarrow4)]_6$-3-*O*-Me-α-L-Rha*p*-(1→3)-β-D-Glc*p*-(1→3)-β-D-Glc*p*-(1→4)-α-D-Glc*p*-(1↔1)-α-D-Glc*p*[b]	3-, 4-, and 6-hydroxyls of terminal Glc*p* unit of terminal trehalose	43,58,59
M. malmoense	LOS II	α-D-Man*p*-(1→3)-α-D-Man*p*-(1→2)-α-L-Rha*p*-(1→2)-$[3\text{-}O\text{-Me-}\alpha\text{-L-Rha}p\text{-}(1\rightarrow2)]_2$-α-L-Rha*p*-(1→3)-α-D-Glc*p*-(1→1)-α-D-Glc*p*	3-, 4-, and 6-hydroxyls of terminal Glc*p* unit of terminal trehalose	61

continues

TABLE III—(*Continued*)

Species	Trivial name	Structure of oligosaccharide	Positions of acyl residues	Reference
M. szulgai	LOS I	2-*O*-Me-α-L-Fuc*p*-(1→3)-α-L-Rha*p*-(1→3)-β-L-Rha*p*-(1→3)-β-D-Glc*p*-(1→6)-α-D-Glc*p*-(1↔1)-2-*O*-Me-α-D-Glc*p*	3-, 4-, and 6-hydroxyls of terminal 2-*O*-Me-Glc*p* unit of terminal mono-*O*-Me-trehalose	62
M. "linda"	LOS	β-D-Glc*p*-(1→3)-α-L-Rha*p*-(1→3)-α-D-Glc*p*-(1↔1)-α-D-Glc*p*	3-, 4-, and 6-hydroxyls of terminal Glc*p* unit of terminal trehalose	63
M. butyricum	LOS I	4,6-*O*-(methyl 1-carboxyethylidene)-3-*O*-Me-β-D-Glc*p*-(1→3)-4,6-*O*-(methyl 1-carboxyethylidene)-β-D-Glc*p*-(1→4)-β-D-Glc*p*-(1→6)-α-D-Glc*p*-(1↔1)-α-D-Glc*p*	2′ and 3,4-hydroxyls of terminal trehalose	70a
M. tuberculosis Canetti	LOS I	4-Acylamino-4,6-dideoxy-Gal*p*-(1→4)-2-*O*-Me-α-L-Fuc*p*-(1→3)-β-D-Glc*p*-(1→3)-2-*O*-Me-α-L-Rha*p*-(1→3)-2-*O*-Me-α-L-Rha*p*-(1→3)-β-D-Glc*p*-(1→3)-4-*O*-Me-α-L-Rha*p*-(1→3)-6-*O*-Me-α-D-Glc*p*-(1↔1)-α-D-Glc*p*	2,3,6- and 3,4,6-hydroxyls of terminal trehalose in the proportions of 2 : 3	66

M. gordonae 989	LOS I	4-Acylamino-4,6-dideoxy-2,3-*O*-Me-α-Gal*p*-(1→3)-4-*O*-Ac-2-*O*-Me-α-L-Fuc*p*-(1→3)-β-D-Glc*p*-(1→3)-2-*O*-Me-α-L-Rha*p*-(1→3)-[β-D-Xyl*p*-(1→2)]-α-L-Rha*p*-(1→3)-β-D-Glc*p*-(1→3)-α-L-Rha*p*-(1→3)-6-*O*-Me-α-D-Glc*p*-(1↔1)-α-D-Glc*p*	2,3,4- and 6-hydroxyls of terminal trehalose	65
M. gordonae 990	LOS I	α-L-Rha*p*-(1→2)-3-*O*-Me-α-L-Rha*p*-(1→3)-[β-D-Xyl*p*-(1→2)]-α-L-Rha*p*-(1→3)-β-D-Glc*p*-(1→3)-β-D-Glc*p*-(1→3)-α-L-Rha*p*-(1→3)-6-*O*-Me-α-D-Glc*p*-(1↔1)-α-D-Glc*p*	2,3,4- and 6-hydroxyls of terminal trehalose	65
M. fortuitum biovar *fortuitum*		β-D-Glc*p*-(1→6)-α-D-Glc*p*-(1↔1)-α-D-Glc*p*	2′- and 2,3,6-hydroxyls of terminal trehalose	64
M. tuberculosis H37Rv	DAT_1, DAT_2	α-D-Glc*p*-(1→1)-α-D-Glc*p*	2- and 3-hydroxyls of terminal trehalose	68

[a] ND = Not determined.

[b] Kan = 4-amino-4,6-dideoxy-3-*C*-methyl-2-*O*-methyl-L-mannose, kansosamine.

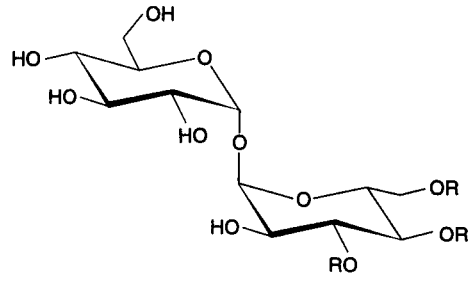

4

mild treatment of lipid extracts with alkali, as in the isolation of GPLs, results in partial or complete removal of *O*-acyl substituents with consequent loss of antigenicity. The major structural principles of the alkali-labile LOSs were revealed using *M. kansasii* as the prototype strain. Also in this instance, a very unusual sugar constituent was detected and then shown to be required for antigenicity.[43] Eight such glycolipids (LOS-I through LOS-VIII) were isolated from *M. kansasii,* each was purified, the inherent oligosaccharides were obtained, and the relevant features of their unique structures were determined by acetolysis, partial acid cleavage, ^{1}H- and ^{13}C-NMR spectroscopy, and chemical-ionization and electron-impact MS of permethylated derivatives.[43,58] They all had in common a glucotetraose core terminated by a glycosidically linked α,α-trehalose component that was first revealed by its distinctive anomeric signals in the ^{1}H-NMR spectrum. Variable residues of xylose, 3-*O*-methylrhamnose, fucose, and a novel *N*-acylamido sugar were linked in turn to this glucotetraose, and the resulting oligosaccharides were acylated by 2,4-dimethyltetradecanoyl functions to present a familial arrangement.

The structure of the *N*-acylamido sugar was established by Hunter *et al.*[59] and turned out to be the first of a group of novel amino sugars present in the GPLs, LOSs, and PGLs of mycobacteria. The reducing sugar, its *O*-acetylated alditol, and the *N*-deacylated, *N*- and *O*-acetylated alditol were all examined by ^{1}H- and ^{13}C-NMR spectroscopy and by mass spectrometry. The sugar was shown to be an aminodideoxyhexose having *C*-and *O*-methyl substituents that was present as an *N*-(2-methoxypropanoyl) derivative. The NMR data established the ring configuration as *manno*, the enantiomeric configuration was tentatively assigned as L, the structure was proposed as 4,6-dideoxy-(2-methoxypropanamido)-3-*C*-methyl-2-*O*-methyl-L-*manno*-hexopyranose, and the trivial name *N*-acylkansosamine (Kan-*N*Acyl) was proposed. Later, chemical synthesis by Yoshimura *et al.*[60] confirmed the absolute configuration of the sugar, including that of the *N*-(*R*)-2-methoxypropanoyl substituent.

The complete structures of the oligosaccharides from these antigens were elucidated by using FAB-MS, NMR, acetolysis, and methylation analysis. Further key experiments performed by Hunter *et al.*[58] involved partial acid hydrolyses of

permethylated oligosaccharides, followed by further sequence analysis of the lower oligosaccharides. The structures are shown in Table III. Only those LOSs containing the nonreducing terminal *N*-acylkansosaminyl-(1→3)-L-fucopyranose disaccharide group (**5**) were antigenic and displayed precise anti-*M. kansasii*

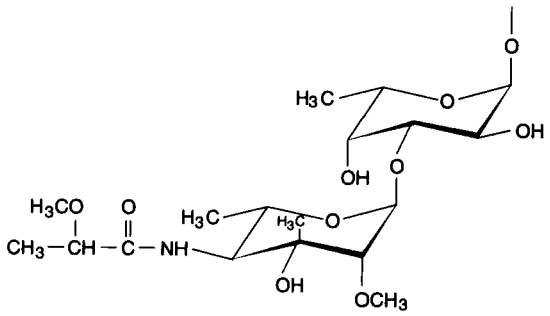

5

specificity.[58] Thus, the unit is the unique antigenic epitope of *M. kansasii*, and the amino sugar *N*-acylkansosamine is the single most characteristic feature of the organism.

The question of the number and location of the acyl functions on the oligosaccharides to form the native, immunogenic lipo-oligosaccharide was addressed, initially through use of ^{252}Cf plasma-desorption (^{252}Cf-PD) MS.[27] The positive-ion ^{252}Cf-PD spectra of several of the intact LOSs revealed clusters of molecular ions in high abundance. For example, that for LOS-V showed a cluster of ions centering at *m/z* 2499. Considering that the M_r value of the component oligosaccharide of LOS-V, Kan*N*Acyl-Fuc-Xyl_4-3-MeRha-Glc_4 is 1761, incorporation of three 2,4-dimethyltetradecanoyl groups will give an M_r of 2476. The ion at *m/z* 2499 was therefore interpreted as being the $[M + Na]^+$ ion. In addition, the most intense ions in every molecular cluster for each LOS examined (*m/z* 1697 for LOS-I, *m/z* 2499 for LOS-V, and *m/z* 2763 for LOS-VII) may be similarly interpreted as being the $[M + Na]^+$ ion of a lipo-oligosaccharide of known carbohydrate structure containing three 2,4-dimethyltetradecanoyl groups. The positive-ion ^{252}Cf-PD-MS clearly demonstrated that each LOS was heterogeneous with respect to acyl substituents. In addition, an intense ion generally appeared 28 mass units above the most intense ion assigned as the species containing three 2,4-dimethyltetradecanoyl groups. This ion was thought to be a formyl residue at an unknown location.

b. *Mycobacterium malmoense.* —A partial definition of the trehalose-containing LOSs from *M. malmoense*, again a group of atypical mycobacteria implicated in pulmonary infections, has been reported.[61] *O*-Deacylation of the primary,

highly antigenic LOS, followed by partial acidic cleavage to release the glycosidically linked trehalose, α-mannosidase digestion to demonstrate the presence of a mannobiose unit at the nonreducing terminus, perdeuteriomethylation, partial acid hydrolysis, reduction, and *O*-ethylation, combined with ^{1}H-NMR and EI- and FAB-MS, revealed the structure α-D-mannopyranosyl-(1→3)-α-D-mannopyranosyl-[(1→2)-α-L-rhamnopyranosyl)]$_4$-(1→3)-α-D-glucopyranosyl-(1↔1)-α-D-glucopyranoside, in which two of the 2-linked α-L-rhamnopyranosyl residues are *O*-methylated at C-3 (Table III). The structures of the oligosaccharides from several of the minor LOSs were also established. In addition, the characteristic chromatographic mobility of the major LOSs allowed *M. malmoense* to be distinguished, *sensu stricto*, from other closely related, clinically significant mycobacteria.

c. *Mycobacterium szulgai.* —The species-specific glycolipid of *M. szulgai* was one of the first to be recognized as a member of the alkali-labile LOS class. However, its structure defied definition until more vigorous hydrolysis conditions, coupled with capillary gas–liquid chromatography (GLC) of derivatives, revealed the presence of a terminal 2-*O*-methyl-α-D-glucopyranosyl residue originating from the nonglycosylated residue of a 2-*O*-methyltrehalose component in place of trehalose itself.[62] In fact, all six LOSs of *M. szulgai* are based on a novel core containing a 2-*O*-methyltrehalose component, and the complete structure of the oligosaccharide from the simplest of the LOSs in *M. szulgai* has been elucidated.[62] This oligosaccharide, like those in *M. kansasii*, is tri-*O*-acylated, with a mixture of 2,4,6-trimethyldocosanoic acid, 2,4-dimethylicosanoic, 2-methyltetracosanoic acid, and a 3-hydroxy, methyl-branched fatty acid. These also occupy the 3, 4, and 6 hydroxyl functions of the terminal glycosyl group (Table III).

d. An Unknown *Mycobacterium* sp. —A smooth variant of a *Mycobacterium* sp. originating in patients with Crohn's disease provided a simpler version of the trehalose-containing LOS. Using a combination of high-resolution of ^{1}H-NMR and FAB-MS and methylation and ethylation, the structure of the oligosaccharide component in the one major LOS in this organism was identified as β-D-glucopyranosyl-(1→3)-α-L-rhamnopyranosyl-(1→3)-α-D-glucopyranosyl-(1↔1)-α-D-glucopyranosyl; and GC-EI-MS allowed identification of the fatty acyl esters as primarily 2,4-dimethyltetradecanoate.[63] The relative simplicity of the oligosaccharide and the attached acyl residues, combined with methyl triflate-catalyzed permethylation techniques, allowed the ready location of three such acyl residues on the C-3, C-4 and C-6 positions of the terminal glucosyl group of the trehalose component. Thus, the native LOS was decidedly amphipathic. With the development of such acyl-locating procedures allowing the unequivocal location of acyl groups, it was further established that other LOS antigens are similarly substituted. Thus, in the LOS from *M. szulgai*, the acyl groups are also located on

the 3-, 4-, and 6-hydroxyl groups of the terminal glucose residue of the trehalose unit, as shown in formula **6**.

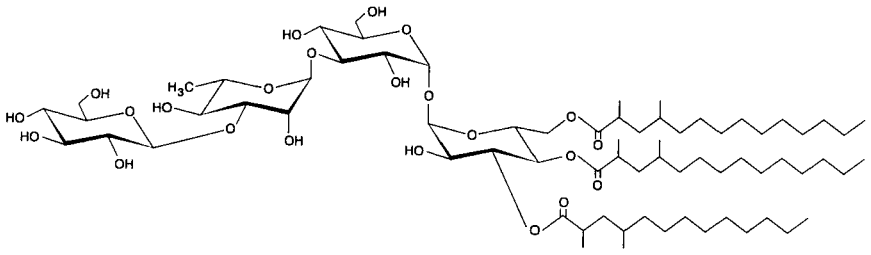

6

e. *Mycobacterium fortuitum.* —Tsang *et al.*[61] had reported that *M. fortuitum*, biovar *fortuitum*, the cause of serious skin and soft-tissue infections, can be distinguished from *M. fortuitum*, biovar *peregrinum*, and other rapidly growing opportunistic mycobacteria by the presence of a unique antigenic glycolipid. This turned out to be also among the simplest of the known LOSs. The application of ^{1}H- and ^{13}C-NMR, methylation analysis, FAB-MS, and other procedures demonstrated the structure β-D-glucopyranosyl-(1→6)-(2-*O*-acyl-α-D-glucopyranosyl)-(1↔1)-3,4,6-tri-*O*-acyl-α-D-glucopyranoside[64] (**7**).

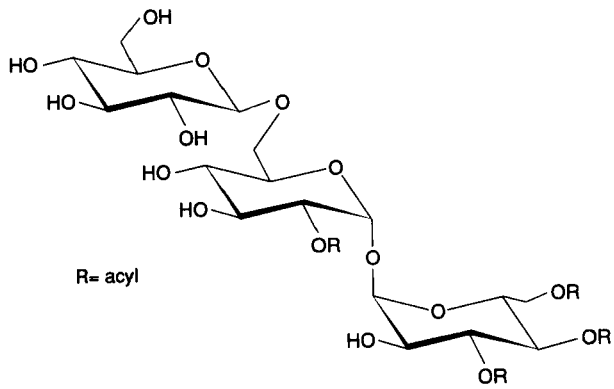

7

f. *Mycobacterium gordonae.* —*Mycobacterium gordonae*, formerly called *Mycobacterium aquae*, the tap-water bacillus, a slow-growing, sometimes opportunistic pathogen, is characterized by the presence of yet further novel variations on the theme of trehalose-containing lipo-oligosaccharides.[65] The structure of the major lipo-oligosaccharide, LOS-I from *M. gordonae* strain 989, was defined as 4-*O*-acetyl-2-*O*-methyl-α-L-fucopyranosyl-(1→3)-β-D-glucopyrano-

syl-(1→3)-2-*O*-methyl-α-L-rhamnopyranosyl-(1→3)-[β-D-xylopyranosyl-(1→2)]-α-L-rhamnopyranosyl-(1→3)-β-D-glucopyranosyl-(1→3)-α-L-rhamnopyranosyl-(1→3)-6-*O*-methyl-α-D-glucopyranosyl-(1↔1)-2,3,4,6-tetra-*O*-acyl-α-D-glucopyranoside, which was further glycosylated at C-3 of the 4-*O*-acetyl-2-*O*-methyl-α-L-fucopyranosyl group by an incompletely defined *N*-acyl derivative of a 4-amino-4,6-dideoxy-2,3-*O*-methylgalactopyranose group (Table III). On the other hand, the structure of the major lipo-oligosaccharide, LOS-I of *M. gordonae* strain 990, was defined as follows: α-L-rhamnopyranosyl-(1→2)-3-*O*-methyl-α-L-rhamnopyranosyl-(1→3)-[β-D-xylopyranosyl-(1→2)]-α-L-rhamnopyranosyl-(1→3)-β-D-glucopyranosyl-(1→3)-α-L-rhamnopyranosyl-(1→3)-6-*O*-methyl-α-D-glucopyranosyl-(1↔1)-2,3,4,6-tetra-*O*-acyl-α-D-glucopyranoside. Both LOS families contain a novel mono-6′-*O*-methyl-2,3,4,6-tetra-*O*-acyltrehalose unit, constituting the first example of such a unit in the LOS family of products isolated from mycobacteria. Also, the more polar antigenic glycolipids, LOS-I, -II′, -II″ and -III (*M. gordonae* 989), and LOS-I, -II, and -II′ (*M. gordonae* 990), were characterized by novel branching of the oligosaccharide backbone. In the case of LOS-I and -III, the branching involved a terminal β-D-xylopyranosyl group, whereas, in LOS-II′ and II″, these groups are terminal 3-*O*-methyl-β-D-xylopyranose and terminal α-D-arabinofuranose, respectively, from *M. gordonae* 989. Similarly, the more polar antigenic glycolipids of *M. gordonae* 990 are also characterized by branching in the oligosaccharide backbone, a single terminal β-D-Xyl*p* residue in the case of LOS-I and LOS-II′ and an α-D-Ara*f* unit in LOS-II″. These characteristic glycolipids of *M. gordonae* strains 989 and 990 were found to react with anti-*M. gordonae* serum in an enzyme-linked immunosorbent assay and showed only weak cross-reactivity against *M. gordonae* 989 and 990, respectively, indicating that *M. gordonae* is a serocomplex based on the LOS surface antigens, analogous to the *M. avium* serocomplex, based as it is on the GPL antigens.

g. *Mycobacterium tuberculosis.* —The highly attenuated, laboratory Canetti strain of *M. tuberculosis* contains two major members of the LOS class. The structure of the simpler of the two (LOS-I) has been fully elucidated[66] (Table III). It is unique in that the tri-*O*-acyltrehalose unit is *O*-methylated at the 6′ position. Further glycosylation of the octaglycosyl unit of LOS-I (which is nonantigenic) with an incompletely defined *N*-acyl derivative of a 4-amino-4,6-dideoxygalactopyranose results in a second, highly antigenic, nonasaccharide-containing glycolipid.[66]

However, a search for similar products in field isolates of *M. tuberculosis* proved fruitless. The work instead focused on a family of simple acylated trehaloses first reported by Minnikin *et al.*[67] The structures of these acylated trehaloses were elucidated by a combination of GC-MS and $^{1}H-^{13}C$-NMR spectrometry.[68]

The fatty acyl substituents were mainly of three types: saturated straight-chain $C_{16}-C_{19}$ acids; $C_{21}-C_{25}$ "mycosanoic acids"; and $C_{24}-C_{28}$ "mycolipanolic acids." Analysis of one of the major 2,3-di-*O*-acyltrehaloses by two-dimensional ^{1}H-chemical-shift-correlated and ^{1}H-detected heteronuclear multiple-bond correlation spectroscopy established that the C_{18} saturated straight-chain acyl group was located at the O-2 position and that the C_{24} mycosanoyl substituent was at the O-3 position of the same nonglycosylated terminus (structure **8**). At least six molecular

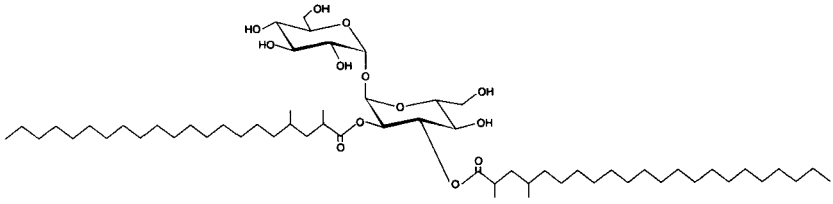

8

species, different only in their fatty acid content, comprised this family of di-*O*-acylated trehaloses. This observation of the presence of an extensively glycosylated LOS in an aberrant strain (Canetti) of *M. tuberculosis* and its absence in virulent field isolates (which, instead, contained simple forms) suggested that these acyltrehaloses were elementary forms of the multiglycosylated acyltrehaloses (the LOS), arising perhaps because of an inability of the majority of isolates of virulent tubercle bacilli to glycosylate core acyltrehaloses.

h. ***Mycobacterium smegmatis.***—The presence in mycobacteria of glycosylated *O*-acyltrehalose was first recognized by Ballou *et al.*[44,45] during a search for biosynthetic precursors for the 6-*O*-methylglucose-containing lipopolysaccharide elaborated by *M. smegmatis*.[69] In looking for acidic lipids containing glyceric acid, Saadat and Ballou[44] isolated substances in which the acidic character was due to acetalically linked pyruvic acid units. The sugar residues were those of 4,6-*O*-(1-carboxyethylidene)-β-D-glucopyranose and its 3-methyl ether; and the structures of the di-*O*-pyruvated pentasaccharide and a related mono-*O*-pyruvated tetrasaccharide, a probable biosynthetic precursor, are those of triglycosyl- and diglycosyltrehaloses. It is noteworthy that these pyruvated glycose residues are those that occur individually as constituents of the type-specific GPL antigens of *M. avium* complex serovariants 8 and 21 (Section III,2). The structures of the *O*-deacylated oligosaccharides were established from methylation analysis, Smith degradation, and NMR and MS data. Subsequently, Ballou and co-workers[45] showed the presence of a mixed population of *O*-acyl, tetradecanoyl, hexadecanoyl, and 2,4-dimethyleicos-2-enoyl substituents. Fast-atom bombardment MS examination of the

parent glycolipids provided evidence that the *O*-acyl substituents were present only on the two glucose residues of the trehalose moiety, a conclusion supported by the results of Smith degradation and methylation analysis. However, a more precise location of the *O*-acyl substituents could not be achieved, since even under mild conditions methylation was either incomplete or resulted in appreciable *O*-deacylation. Besra *et al*[70] have encountered similar substances in *M. butyricum*,

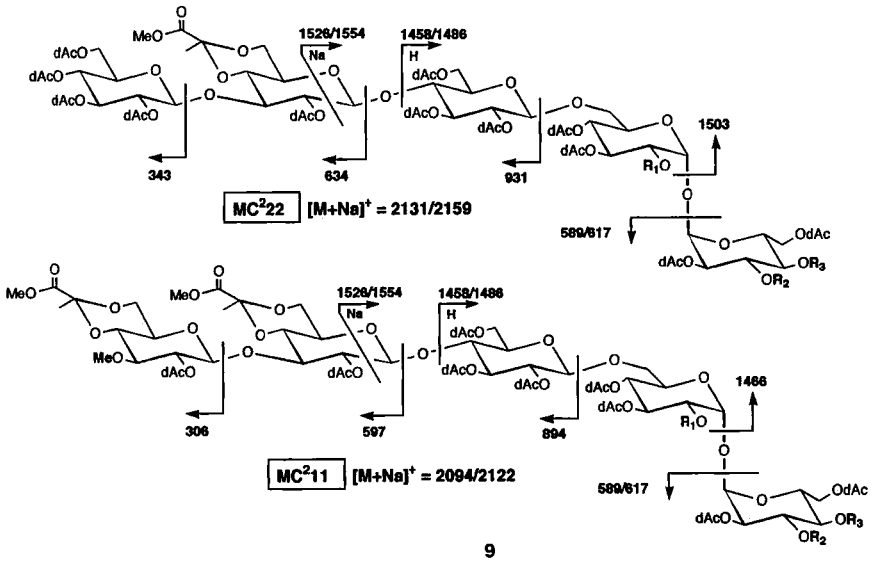

9

and in two phage-resistant strains of *M. smegmatis* (strains mc²ll and mc²22) (**9**); but in these cases, FAB-MS of **9** established that both of the pyruvate substituents were present as their methyl esters and that the 2-′, 3-, and 4-hydroxyl groups, rather than the 4′ and 6-hydroxyl groups,[45] were acylated. Nevertheless, such minor structural modifications were implicated in the emergence of resistance of the mycobacteria to mycobacteriophage absorption.

4. General Approach toward Location of Acyl Substituents

Considerable effort has been expended in defining precisely the location of the acyl substituents on the oligosaccharide backbone. The first efforts to achieve this in the context of the simple acylated tetrasaccharide from an unclassified *Mycobacterium* sp. have already been mentioned. In general, glycolipids were purified to homogeneity and then methylated with methyl trifluoromethanesulfonate in trimethyl phosphate in the presence of a hindered base.[25] The per-*O*-methylated lipo-oligosaccharides were then purified and treated with methylsulfinyl carbanion and ethyl iodide, thus replacing the *O*-acyl functions with *O*-ethyl groups. The

resulting *O*-ethylated, *O*-methylated oligosaccharides were further converted into alditol acetates. As an example, when the native LOS from the unclassified *Mycobacterium* sp. was subjected to such analysis, formation of a 1,5-di-*O*-acetyl-3,4,6-tri-*O*-ethyl-2-*O*-methylglucitol unequivocally established that the reducing-end terminal Glc of the α,α-trehalose unit was substituted with fatty acyl functions.[63] The other alditol acetates—1,3,5-tri-*O*-acetyl-2,4-di-*O*-methyl-rhamnitol, 1,5-di-*O*-acetyl-2,3,4,6-tetra-*O*-methylglucitol, and 1,3,5-tri-*O*-acetyl-2,4,6-tri-*O*-methylglucitol–did not contain any ethyl substituents and hence were not acylated. Using the same acyl-locating approach, it was determined that, in the *M. szulgai* product, the acyl groups were located on the C-3, C-4, and C-6 hydroxyl groups of the terminal glucose of the trehalose unit.[62] Daffé *et al.*[66] also used ^{1}H-NMR (1D and 2D COSY) to establish the location of acyl functions in LOS from *M. tuberculosis* (Canetti). Since resonances of the ring protons attached to carbon atoms bearing esterified hydroxyl groups were shifted downfield (δ 4.8–5.6), a region where otherwise only the anomeric protons resonate, it was possible to observe scalar connectivities between protons and thereby determine the position of acyl functions. In this case, well resolved triplets at δ 5.41 and 5.50 (H-3 of glucosyl units) were the starting points. Cross-peaks showing connectivity to H-2, H-4, and H-5 were readily recognized; in this way, it was established that one of the major LOSs consisted of a mixture of 3,4,6- and 2,3,6-tri-*O*-acylated terminal glucosyl residues.

Plasma-desorption mass spectrometry (PDMS) also allowed location of the acyl functions. Thus, ^{252}Cf-PDMS of LOS V in *M. kansasii* gave[27] molecular-weight-associated ions at *m/z* 2499. The major acylating function of the intact LOS was determined to be a 2,4-dimethyltetradecanoate. Addition of three of these fatty acyl residues to the oligosaccharide portion gave a mass of 2476 daltons. Thus, the ion at *m/z* 2499 must be equivalent to $[M + Na]^+$, and therefore LOS V must be a tri-*O*-acyl-undecasaccharide. However, exact location of the acyl functions was not obtained in this way.

Such analysis was also extended to *M. malmoense*.[27] Native LOS gave a molecular mass of $[M + Na]^+$ at *m/z* 2276, corresponding to a mass 126 amu higher than the expected molecular weight. This was due to the presence of a C_8 fatty acyl residue in addition to C_{21} and C_{26} functions. A combination of these three fatty acids on the oligosaccharide provided a molecular weight of 2253. Peracetylation of the LOS followed by PDMS analysis showed a molecular ion at *m/z* 3074, an increase of 798, equivalent to 19 acetyl groups. Sequence ions at *m/z* 331, 620, 850, 1052, 1254, 1484, 1715, and 2003 unambiguously confirmed the sugar sequence and confirmed that all three fatty acids were located at the terminal glucose residue of the trehalose unit.

Plasma-desorption MS analysis on the LOS from the unknown *Mycobacterium* sp. and from *M. szulgai*, however, allowed elucidation of complete structures for these molecules, including location of fatty acid positions. Thus, in *M. szulgai*,

PDMS of native LOS-I showed a $[M + Na]^+$ ion at *m/z* 1823, confirming the presence of one of each of C_{15}, C_{15}:OH, and C_{25} fatty acids per molecule of LOS; and fragment ions of *m/z* 245.6, 477.3, 706.9, 993.9, and 1282.4 supported the evidence for the structure of LOS-I, showing that the fatty acids are present on the terminal 2-*O*-methyl-glucose of the trehalose unit. Similarly, for the LOS from the unknown *Mycobacterium*, the location of the acyl functions was confirmed by using PDMS. Thus, a combination of alkylation and degradation techniques and PDMS may be used simultaneously to establish the nature and position of the acyl functions on the lipo-oligosaccharides.

5. Phenolic Glycolipids Containing Phenolphthiocerols

Smith *et al.*[31] had described glycolipids that are devoid of amino acids, terming them glycosides of phenolphthiocerol dimycocerostate. These were renamed as phenolic glycolipids (**10**) by Hunter and Brennan[71,74] when they discovered the

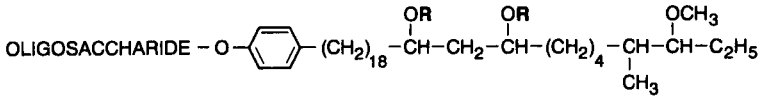

10

glycoside of phenolphthiocerol from *M. leprae*. To date, phenolic glycolipids have been described in many mycobacterial species: *M. leprae, M. tuberculosis* strain Canetti, *M. kansasii, M. bovis, M. gastri, M. marium, M. ulcerans, M. haemophilum,* and *M. gastri* (Table IV). The aglycon structures are quite similar, usually formed by the dimycocerosate of phenolphthiocerol, with the oligosaccharide units contributing to the overall antigenicity of each species and largely responsible for the specificity of the antibody response.

a. *Mycobacterium leprae.* — A species-specific, highly immunogenic glycolipid discovered by Hunter and Brennan[71] and independently by Tarelli *et al.*[72] was termed PGL-I.This glycolipid was isolated in large quantities from infected armadillo liver freed of *M. leprae* itself. The carbohydrate composition consisted of 3,6-di-*O*-methyl-β-D-glucopyranose, 2,3-di-*O*-methyl-α-L-rhamnopyranose, and 3-*O*-methyl-α-L-rhamnopyranose[71] and these components were shown to exist as the trisaccharide 3,6-di-*O*-methyl-α-D-glucopyranosyl-(1→4)-2,3-di-*O*-methyl-α-L-rhamnopyranosyl-(1→2)-3-*O*-methyl-α-L-rhamnopyranosyl[73] (**11**). Independently, NMR studies by Tarelli *et al.*[72] established the anomeric configurations of the glycosyl residues of PGL-I. The acyl residues of PGL-I of *M. leprae* were all tetramethyl-branched C_{30}, C_{32}, and C_{34} mycocerosic acids.[71,32] Fractionation of

TABLE IV

Structures of Major Phenolic Glycolipids from *Mycobacterium*

Species	Trivial name	Structure of oligosaccharide	Reference
M. bovis	Mycoside B	2-*O*-Me-α-L-Rha*p*-(1→dimycocerosyl phenolphthiocerol)	32,33,78
M. bovis	Mycoside B′	α-L-Rha*p*-(1→dimycocerosyl phenolphthiocerol)	33
M. bovis	Mycoside B″	2-*O*-Me-α-L-Rha*p*-(1→phenolphthiocerol)	33
M. leprae	PGL-I	3,6-di-*O*-Me-β-D-Glc*p*-(1→4)-2,3-di-*O*-Me-α-L-Rha*p*-(1→4)-3-*O*-Me-α-L-Rha*p*-(1→dimycocerosyl phenolphthiocerol)	9,71,72.73
M. kansasii	PGL-KI (Mycoside A)	2,6-dideoxy-4-*O*-Me-α-*arabino*-Hex*p*-(1→3)-4-*O*-Ac-2-*O*-Me-α-L-Fuc*p*-(1→3)-2-*O*-Me-α-L-Rha*p*-(1→3)-2,4-di-*O*-Me-α-L-Rha*p*-(1→dimycocerosyl phenolphthiocerol)	9,81,82
M. tuberculosis Canetti	PGL-TbI	2,3,4-tri-*O*-Me-α-L-Fuc*p*-(1→3)-α-L-Rha*p*-(1→3)-2-*O*-Me-α-L-Rha*p*-(1→dimycocerosyl phenolphthiocerol)	77
M. haemophilum	—	2,3-di-*O*-Me-α-L-Rha*p*-(1→2)-3-*O*-Me-α-L-Rha*p*-(1→4)-2,3-di-*O*-Me-α-L-Rha*p*-(1→dimycocerosyl phenolphthiocerol)	90,91
M. ulcerans	—	3-*O*-Me-α-L-Rha*p*-(1→dimycocerosyl phenolphthiocerol)	88,89
M. marinum	Mycoside G	3-*O*-Me-α-L-Rha*p*-(1→dimycocerosyl phenolphthiocerol)	85,86
M. gastri	PGL-GI	2,6-dideoxy-4-*O*-Me-α-*arabino*-Hex*p*-(1→3)-4-*O*-Ac-2-*O*-Me-α-L-Fuc*p*-(1→3)-2-*O*-Me-α-L-Rha*p*-(1→3)-2,4-di-*O*-Me-α-L-Rha*p*-(1→dimycocerosyl phenolphthiocerol)	92,93

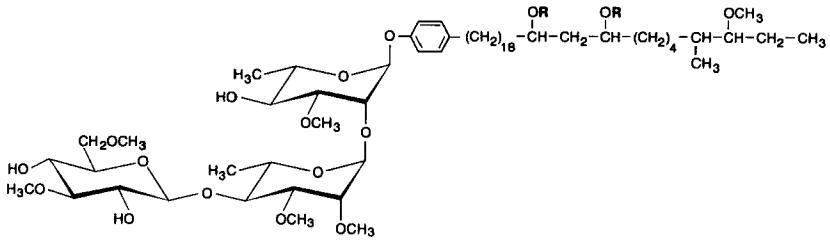

11

PGL-I, homogeneous by thin-layer chromatography, through reverse-phase HPLC showed heterogeneity based on fatty acid content, and PD-MS analysis demonstrated the existence of the C_{30},C_{30} mycocerosate glycolipid, the C_{32},C_{32} species, and the C_{34},C_{34} species.[27] Two other minor phenolic glycolipids isolated from *M. leprae*, known as PGL-II and PGL-III, show minor variations in the methylation of the glycosyl residues.[74] These proved of considerable importance in defining the basis of the antigenicity of PGL-I.

b. *Mycobacterium bovis* BCG (Mycoside B).—The phenolic glycolipid (mycoside B) from *M. bovis*, discovered by Smith *et al.*[32,33] and Noll and Jackim,[75] was reported to contain a 2-*O*-methylrhamnose residue. The structure was later investigated by Demarteau-Ginsberg and Lederer[76] and assigned as 2-*O*-methyl-β-D-rhamnose linked to a phenolphthiocerol. The esterified fatty acids were assigned as hexadecanoic acid and a C_{29} mycocerosic acid. However, reexamination of the structure of mycoside B by three independent investigators[77-79] established the glycosyl residue as 2-*O*-methyl-α-L-rhamnopyranose, and the acyl substituents were all identified as of the methyl-branched, mycocerosic acid type. Other minor "metabolic" derivatives of mycoside B have been observed (Table IV), and Vercellone and Puzo[79] reported the presence of a minor diglycosylated phenolic glycolipid in *M. bovis* BCG having the structure α-D-rhamnopyranosyl-(1→3)-2-*O*-methyl-α-L-rhamnopyranosyl.

c. *Mycobacterium kansasii.*—This bacterium contains two distinct classes of surface glycolipid antigens, the lipo-oligosaccharides and several phenolic glycolipids once termed mycoside A.[80] Puzo and colleagues[81-84] refractionated old mycoside A preparations and fully defined the structures of several new homogeneous entities. The major component of mycoside A is now called phenolic glycolipid K-I. This is the only glycolipid described thus far having a tetrasaccharide unit; the entire structure is 2,6-dideoxy-4-*O*-methyl-α-*arabino*-hexopyranosyl-(1→3)-4-*O*-acetyl-2-*O*-methyl-α-fucopyranosyl-(1→3)-2-*O*-methyl-α-rhamnopyranosyl-(1→3)-2,4-di-*O*-methyl-α-rhamnopyranosyl (Table IV). A minor phenolic glycolipid, Phe-GL-K-II, has been described in which the terminal dideoxyhexose of PGL-K-I is replaced by a 2,4-di-*O*-methyl-α-D-mannopyranosyl residue.

d. *Mycobacterium tuberculosis* (Canetti).—Lanéelle's group reported that, among many strains of *M. tuberculosis*, only the Canetti strain contained a major phenolic glycolipid having the trisaccharide: 2,3,4-tri-*O*-methyl-α-L-fucopyranosyl-(1→3)-α-L-rhamnopyranosyl-(1→3)-2-*O*-methyl-α-L-rhamnopyranosyl.[77]

e. *Mycobacterium marinum* and *ulcerans*.—The product in *M. marinum* was first described by Demarteau-Ginsburg as mycoside G and shown to contain one glycosyl unit, 3-*O*-methylrhamnopyranosyl,[85] which was later confirmed by Daffé *et al.*[86] Dobson *et al.*[87] used the *M. marinum* product to examine extensively the nature of the fatty acids and phenolphthiocerol unit through ^{1}H-NMR and GC-MS of derivatized products. They observed unprecedented heterogeneity in the phenolphthiocerol sustituents, with the presence of phenolphthiocerol A and B (differing in the position of the methoxyl group), phenolphthiotriol A (in which the methoxyl is replaced by hydroxyl), and phenolphthiodiolone A (a keto group

instead of methoxyl). The main fatty acids were C_{26} dimethyl- and C_{27} and C_{29} trimethyl-branched fatty acids. Thus the products described by these and other workers[88,89] in *M. marinum* and *M. ulcerans* are the same, and the two species are apparently identical.

f. *Mycobacterium haemophilum.* —The lipid portion of the glycolipid from *M. haemophilum* showed similarities to the PGL-I from *M. leprae*.[90] However, the structure of the oligosaccharide portion is 2,3-di-*O*-methyl-α-L-rhamnopyranosyl-(1→2)-3-*O*-methyl-α-L-rhamnopyranosyl-(1→4)-2,3-di-*O*-methyl-α-L-rhamnopyranose.[91]

g. *Mycobacterium gastri.* —Although it was thought[92] that the LOS from *M. kansasii* was identical to the product from *M. gastri*, a subsequent analysis[93] has shown otherwise. The most antigenic LOS from *M. gastri* (LOS-III) contains a novel terminal sugar, 3,6-dideoxy-4-(2,3-dimethoxypropyl)-α-hexopyranose, thus differing from the antigenic determinant of LOS from *M. kansasii*. Whereas the xylopyranosyl units in the *M. kansasii* product are in the D configuration, in *M. gastri* they are in the L form. The LOSs from *M. gastri* contain β-Gal*p*, as distinct from the LOS from *M. kansasii*, which contains fucopyranosyl residues. One interesting feature that arose from this later study was that the LOS-III from *M. gastri* was present in all strains examined, namely strains W471, HB 4362, and HB 4389; however, the latter two strains also contained the LOSs of *M. kansasii*.

IV. SYNTHESIS AND ANTIGENICITY OF GLYCOLIPID-BASED NEOGLYCOCONJUGATES

The synthesis of oligosaccharide haptens related to the glycolipids of the different classes was undertaken to prepare substances for immunological examination in order to define the structural requirements for antigenic determinants interacting with antibodies to the particular bacterial species or serotype. The approach, which was examined first and developed most extensively in relation to the phenolic glycolipid antigen (PGL I) from *M. leprae*, was to synthesize sequentially oligoglycosyl units from the terminal, and presumably most exposed, region of the glycolipid and to use these in immunoassays to define the minimum size for the epitope. Reducing oligosaccharides were examined first, as competitive inhibitors of the interaction between native PGLs and homologous antibodies.[94] Attention was then turned to haptens as glycosides of the correct anomeric configuration and with linker-arms attached for conjugation to protein (or potentially any other macromolecular carrier having limited antigenicity). In this section the emphasis is on the synthesis of neoglycoconjugates (NGCs), and specifically on neoglycopro-

teins (NGPs). However, attention is given to improved methods for the synthesis of the oligosaccharides themselves that have not yet been extended to NGC assembly. A more detailed consideration of synthetic strategy is given later in Section IV.2.

1. Synthesis of Leprosy-Specific Neoglycoconjugates

The first syntheses of oligosaccharides related to the leprosy PGL I were performed simultaneously in two laboratories to determine which sugar residues in the trisaccharide hapten of the natural glycolipid were required as the antigenic determinant.[94,95] As the biosynthetically incomplete glycolipid PGL-III, lacking the methyl ether group at O-6 of the 3,6-di-*O*-methyl-β-D-glucopyranose residue, and deglycosylated glycolipids, lacking the sugar, were markedly less active toward human lepromatous leprosy sera than PGL I,[94] the terminal 3,6-di-*O*-methyl-β-D-glucopyranose residue was indicated as the primary antigenic determinant. In support of this contention, Fujiwara *et al.*[94,96,97] synthesized di- and trisaccharides, 3,6-di-*O*-methyl-β-D-glucopyranosyl-(1→4)-2,3-di-*O*-methyl-L-rhamnopyranose (**12**) and *O*-(3,6-di-*O*-methyl-β-D-glucopyranosyl)-(1→4)-*O*-(2,3-di-*O*-methyl-α-L-rhamnopyranosyl)-(1→2)-3-*O*-methyl-L-rhamnose (**13**), together with less fully methylated analogs. The structurally complete haptens were more effective in inhibition assays, and this result confirmed that the terminal 3,6-di-*O*-methyl-β-D-glucopyranose residue was the primary antigenic determinant. Gigg *et al.*[95] reached the same conclusion through the synthesis of the disaccharide and its propyl α-glycoside (**12**), the latter as the first oligosaccharide hapten with both sugar residues in correct defined anomeric configuration. Fujiwara *et al.*[94] prepared the first NGC capable of interacting with human lepromatous leprosy sera. Conjugation of disaccharide **12** to ε-amino groups of lysine residues in bovine serum albumin, by reductive amination[98] with sodium cyanoborohydride, furnished a product that was qualitatively similar in its immunoreactivity to the natural PGL I. This type of synthesis (Table V, method 1a), however, is wasteful in that structural information carried by the reducing residue of the disaccharide is lost on conversion into the acyclic 1-amino-1-deoxyalditol, which is furthermore an unnecessarily complex spacer-arm. For other NGPs, glycosyl residues have been assembled as glycosides of a bifunctional alcohol to serve as the linker-arm for covalent attachment to protein (Table V).

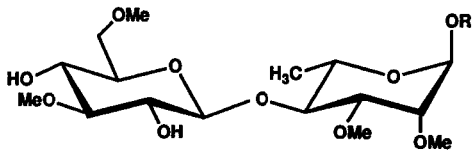

12a R= H
12b R= $CH_2CH_2CH_3$
12c R= MCO*
12d R= DEE*

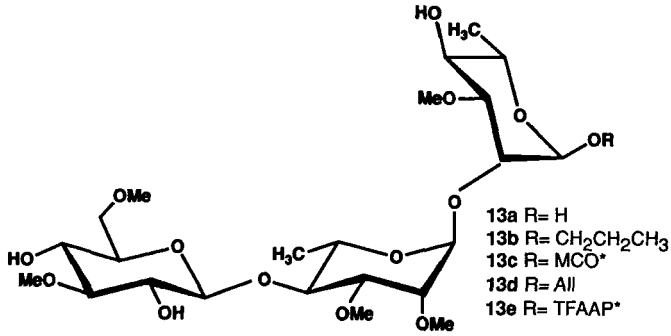

* DEE = 1,3-dioxolan-2-yloxyethyloxyethyl
MCO = methoxycarbonyloctyl
TFAAP = 4-N-trifluoroacetylaminophenyl

TABLE V

Methods for Conjugation of Glycosyl Units to Protein

1. ***Reductive amination to ϵ-amino groups of lysine residues in proteins***
   (a) *N*-glycitol-1-yl derivatives from reducing groups (hemiacetals)

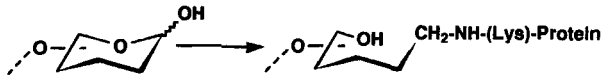

   (b) *N*-glycosyloxyethyl derivatives from formylmethyl glycosides

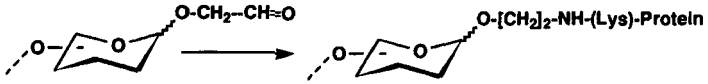

   (c) from glycosides of 8-hydroxy-3,6-dioxaoctanal (protected as dioxolane acetal)

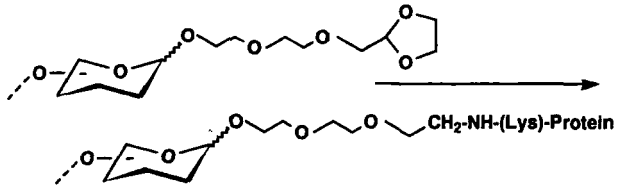

2. ***Linker-arm acylation of ϵ-amino groups of lysine residues in protein***
   (a) glycosyloxynonanoyl derivatives from alkoxycarbonyloctyl glycosides

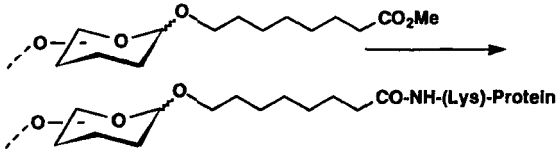

continues

TABLE V—(*Continued*)

(b) 3-(4-glycosyloxy)phenylpropanoyl derivatives from 4-(2-methoxycarbonylethyl)phenyl glycosides

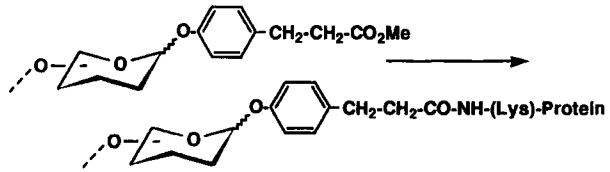

3. *Copolymerization of allyl glycosides and acrylamide*

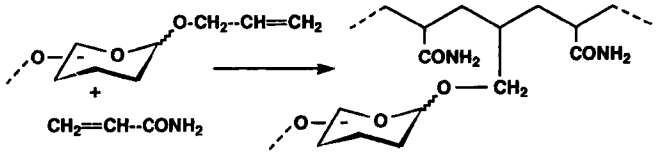

4. *Formation of thiourea linkages from isothiocyanates and ϵ-amino groups of lysine residues in proteins*

(a) from 4-aminophenyl glycosides via 4-glycosyloxyphenyl isothiocyanates

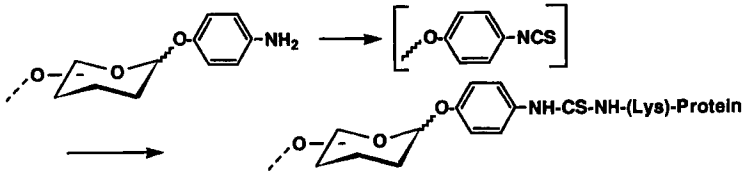

(b) from ω-aminoalkyl glycosides via ω-glycosyloxyalkylisothiocyanates

For leprosy-specific NGCs, most syntheses of di- and trisaccharides, discussed next, have been achieved by stepwise glycosylation from the innermost residue with a glycosidically attached linker-arm in configurationally correct form. For conjugation to protein, two basic strategies have been used for covalently linking to ϵ-amino groups of lysine residues. In the first approach (Table V, method 2), the linker-arm method of Lemieux *et al.*,[99,100] the innermost glycosyl residue is assembled as a glycoside bearing an alkoxycarbonyl group for conversion, via the acyl hydrazide, to an acyl azide for coupling to lysine residues. The commonest version of this procedure with the 8-methoxycarbonyloctyl glycoside as a lipophilic spacer (method 2a) has been used in a series of studies by Chatterjee *et al.*[101-103] The same principle was adopted by Fujiwara and co-workers,[104,105] who prepared glycosides

having a methyl 3-(4-hydroxyphenyl)propanoate linker-arm (method 2b) to simulate the natural antigen for the evocation of and binding to anti-glycolipid antibodies. In the second approach, Gigg and co-workers prepared allyl glycosides for conversion into formylmethyl glycosides[106] (method 1b) for reductive amination to ϵ-amino groups of lysine residues in the carrier protein. Disaccharide synthesis as a protected allyl glycoside was followed by epoxidation and basic epoxide opening, then removal of benzyl ether substituents by hydrogenolysis. The resulting glycerol-1-yl glycoside was then converted into the formylmethyl glycoside by oxidation with sodium metaperiodate.[106] This conjugation procedure would be limited to compounds containing glycosyl residues that are not susceptible to glycol cleavage with periodate, or conceivably to those in which rates of endocyclic diol cleavage were markedly lower than those of exocyclic diols, and where selective reaction might be achieved with limited quantities of oxidant. In Section IV.2, examples are given of the use of allyl glycosides as precursors of formylmethyl linker-arms, where direct conversion is by ozonolysis. This simple conversion method is limited only by restrictions in the use of protecting groups during allyl glycoside synthesis [see Section IV.3], such that removal of benzyl ethers by hydrogenolysis would not be compatible. An alternative procedure[107] employs glycosides of 8-hydroxy-3,6-dioxaoctanal to function as the spacer-arm for attachment to protein by reductive amination (method 1c). Glycosides, such as that (**21**) of the terminal disaccharide hapten from PGL I, are synthesized in protected form as the ethylene glycol (dioxolane) acetal in reactions which permit the use of benzyl ether protecting groups. After removal of other protecting groups, *O*-deacetalation under mildly acidic conditions affords glycosides of 3,6-dioxaoctanal for conjugation.

One of the first general procedures for the preparation of NGCs bearing oligosaccharide antigenic determinants from bacterial capsular polysaccharides, or the O chains of lipopolysaccharides,[108] is that based on 4-aminophenyl glycosides (Table V, method 4a). Reaction of these glycosides with thiophosgene introduce 4-iso-thiocyanatophenyl groups for reaction with ϵ-amino groups of lysine in the carrier protein.[109] The 4-aminophenyl glycosides are conveniently formed from 4-nitrophenyl glycosides, often concurrently with removal of *O*-benzyl groups by catalytic hydrogenolysis, and may be stored until required as their *N*-trifluoroacetyl derivatives. The procedure was subsequently applied to the synthesis of spacer-armed oligosaccharide derivatives related to mycobacterial glycolipids. The same principle of coupling based on ω-aminoalkyl glycosides, which are conveniently formed as benzyloxycarbonyl derivatives, has also been reported (Table V, method 4b) and examples are given later.

Copolymerization of allyl glycosides with acrylamide is a simple, direct method for the synthesis of non–protein-based NGCs,[110] and has been used by Verez-Bencomo and co-workers[111] to prepare leprosy-related conjugates. The same limitations as before apply to the preparation and use of allyl glycosidic substituents.

Syntheses[95,102–106,111–113] of derivatives of **12** and **13** have used 2,4-di-*O*-acetyl-

3,6-di-*O*-methyl-α-D-glucopyranosyl chloride (**14**) or bromide (**15**) as the glycosyl donor for creation of the β-D-glycosidic linkage. Direct, high-yielding syntheses of the previously inaccessible 3,6-di-*O*-methyl-D-glucose have been described by Liav and Goren[114] and by Sen *et al.*[115] For syntheses of derivatives of disaccharide **12**, alkyl 2,3-*O*-isopropylidene-α-L-rhamnopyranosides have been used for introduction of the 4-linked distal rhamnose residue. Glycosylation may be followed by *O*-deacetalation and methylation. Alternatively, protection at O-4, *O*-deacetalation, and subsequent methylation and deprotection at O-4 furnishes the 2,3-di-*O*-methyl-α-L-rhamnopyranose residue for glycosylation. The first oligosaccharide hapten synthesis was that of the propyl glycoside (**12**) of **1** (ref 95). In the absence of evidence for the enantiomeric configuration of the rhamnose residue, Gigg *et al.*[116] also synthesized the diastereomeric 3,6-di-*O*-methyl-β-D-glucopyranosyl-(1→4)-2,3-di-*O*-methyl-α-D-rhamnose as the propyl glycoside **16**. Both glycobiosides were effective as inhibitors of the natural antigen–antibody interaction, in confirmation of the role of the 3,6-di-*O*-methyl-β-D-glucopyranose residue as the main antigenic determinant.[117] In the first preparation of the glycobiosyl NGP with the correct anomeric configuration for both glycosyl residues, disaccharide **12** with attached linker-arm was synthesized from 8-methoxycarbonyloctyl 2,3-di-*O*-methyl-α-L-rhamnopyranoside. (**17**).[102] For the as-

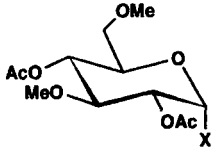

14 X = Cl
15 X = Br

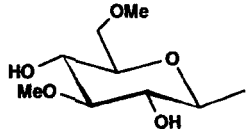

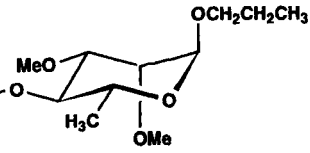

16

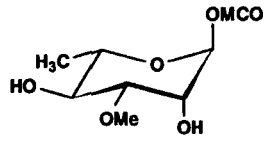

17

sembly of trisaccharide **13**, various 4-*O*-allyl(benzoyl or benzyl)-α-L-rhamnopyranosides have been used for the proximal glycosyl residue. However, the requirement for a participating group at O-2 in a glycosyl donor for the formation of an α-L-rhamnopyranosyl linkage at the distal residue may conflict with the introduction of a methyl ether substituent. In the first trisaccharide synthesis, a glycosyl donor having a methyl ether substituent at O-2 gave mixtures of α- and β-L-rhamnopyranosyl linkages.[94,97] This difficulty was overcome in three syntheses. In two syntheses, glycosyl donors **18** with participating *O*-acetyl groups at O-2 in condensation with **19** led variously to rhamnobiose derivatives **20**, **21**, and **22**. The

requisite manipulations of substituents in different sequences led to the introduction of the desired *O*-methyl groups and to glycosylation at O-4 of the distal rhamnose residue, ultimately yielding[103,106] trisaccharide hapten glycosides **13**. The 8-methoxycarbonyloctyl glycoside **13** afforded the corresponding NGP. In contrast, stereoselective α-L-glycosylation with a nonparticipating group at O-2 was achieved by Marino-Albernas *et al.*[111] With Lewis acid catalysis by boron trifluoride etherate, 1,4-di-*O*-acetyl-2,3-di-*O*-methyl-α-L-rhamnopyranose (**18**) reacted as donor with allyl 4-*O*-benzoyl-3-*O*-methyl-α-L-rhamnopyranoside (**19**) and thence by selective *O*-deacetylation to give the rhamnobioside. Glycosylation of **19** with **5** followed by *O*-deacylation gave the trisaccharide hapten as allyl glycoside **13** for preparation of NGC by copolymerization with acrylamide.[118]

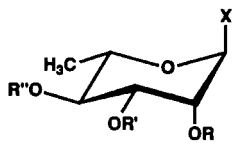

18a X = Cl, R = R' = R" = Ac
18b X = Cl, R = Ac, R' = Me, R" = All
18c X = OAc, R = R' = Me,R" = Ac

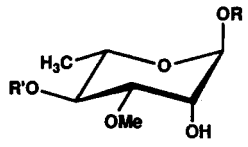

19a R = All, R' = Bn
19b R = MCO, R' = Bn
19c R = All, R' = Bz

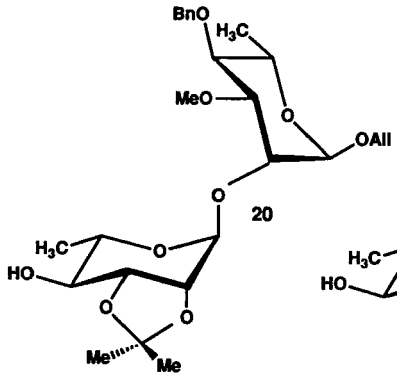

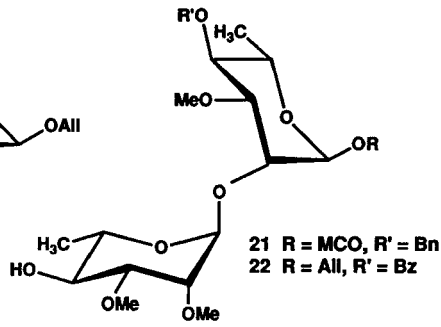

21 R = MCO, R' = Bn
22 R = All, R' = Bz

MCO= 8-methoxycarbonyloctyl

In an alternative route employing fewer overall steps, Borbas and Lipták[119] synthesized the trisaccharide hapten as a 4-aminophenyl glycoside protected as the *N*-trifluoroacetyl derivative **13** for potential conjugation to protein.[108] Ethyl 1-thio-α-L-rhamnopyranoside as the 2,3-*O*-diphenylmethylene acetal **23** was the precursor for both rhamnosyl residues. Condensation of **23** with glycosyl bromide **24** with silver triflate as promoter, followed by *O*-deacetylation and *O*-benzyliden-

ation, gave **25**, which was converted successively into **26** by hydride opening of the acetal rings and *O*-methylation to give **27**. Compound **23** was also transformed by *O*-benzylation, acetal removal, regioselective *O*-methylation, and glycosylation to yield the 4-nitrophenyl glycoside **28**. Glycosylation of acceptor **28** with glycobiosyl donor **27** gave a fully protected 4-nitrophenyl trisaccharide glycoside **29**. Reduction of the nitrophenyl glycoside using Adams' catalyst and subsequent trifluoroacetylation of the amino group was followed by *O*-debenzylation to give the protected trisaccharide hapten **22**.

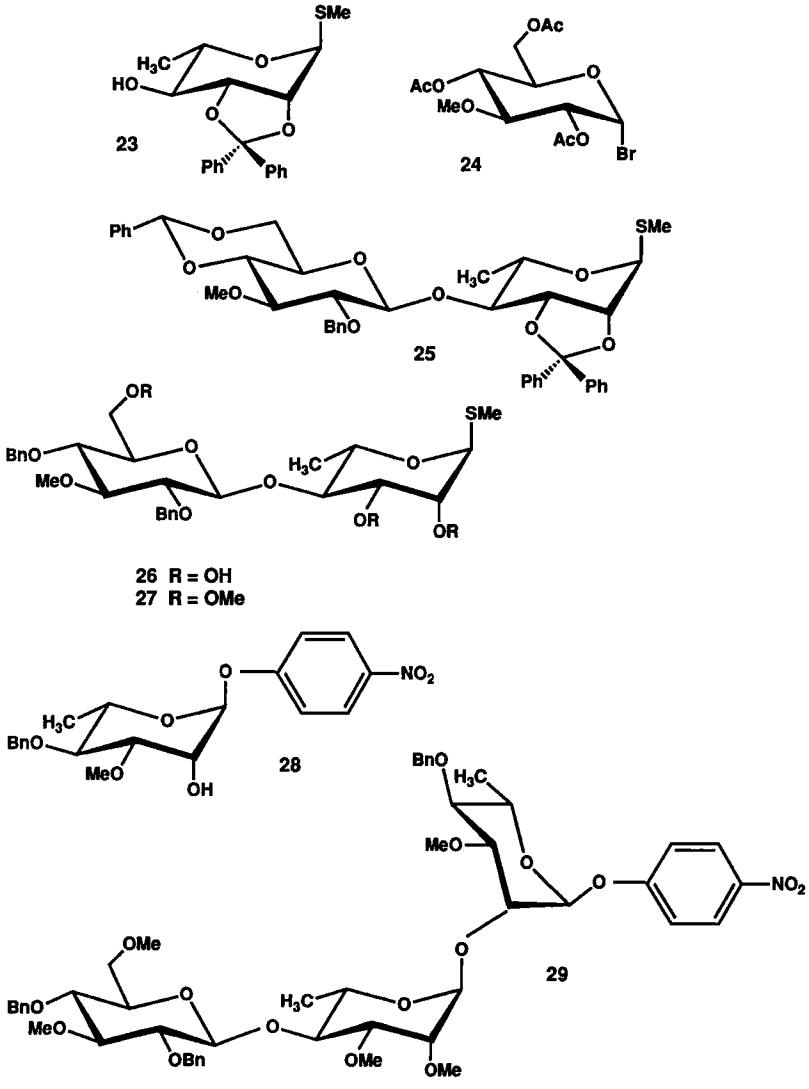

2. Synthesis and Antigenicity of Neoglycoconjugates Related to the Glycopeptidolipids of the *M. avium* Complex

Glycopeptidolipids from serovars of the *M. avium* complex differ from one another in the distinctive outer regions of the oligosaccharide chains external to the (1→3)-(α-L-rhamnopyranosyl)-(1→2)-6-deoxy-α-L-talopyranose core unit. Aspinall, Brennan, and co-workers have emphasized the construction of these outer regions for incorporation into NGPs carrying the minimum number of these sugar residues necessary for specific interaction with homologous antibodies. It had already been observed in parallel studies that neoglycoproteins (NGPs) related to the phenolic glycolipid from *M. leprae* bearing the outer two sugar residues or only the terminal residue interact with antibodies to *M. leprae* (Section IV.1). In this section attention is directed first (Section IV.2a) to the synthesis of GPL-related NGPs in relation to antigenicity. From the standpoint of synthetic strategy and methodology, the assembly of complete oligosaccharide haptens from GPLs presents interesting challenges. Progress toward these objectives is discussed in Section IV.2b (see also ref. 119a). Thus far, no reports have been published of conjugation to protein of these more complete oligosaccharides or of their immunoreactivity. There is little doubt that studies of the longer oligosaccharides will yield a new generation of NGPs for the study of immunological specificity.

a. Neoglycoconjugates Based on Serovar-Specific Outer Regions.—The widely used conjugation strategy of Lemieux and associates[99,100] (Table V, method 2) is incompatible with the retention of base-sensitive *O*-acyl substituents, since the first step in the conversion of 8-methoxycarbonyloctyl glycosides into acyl azides involves treatment with hydrazine. However, the conjugation procedure of Bernstein and Hall,[120] with reductive amination of formylmethyl glycosides (from ozonolysis of allyl glycosides; Table I, method 1b) to lysine residues with sodium cyanoborohydride at pH 7.8. takes place with retention of the *O*-acetyl substituent when allyl 4-*O*-acetyl-2,3-di-*O*-methyl-α-L-fucopyranoside is the substrate.[121,122] The potential value of monoglycosyl NGPs from allyl glycosides in probing the structural requirements for epitopes of mycobacterial glycolipids was shown (1) by the interaction of a neoantigen bearing only the 3,6-di-*O*-methyl-β-D-glucopyranose residue with antibodies to *M. leprae*[122] and (2) by specific interactions[47] of neoantigens with 2,3-di-*O*-methyl-α-L-fucopyranose and 4-*O*-acetyl-2,3-di-*O*-methyl-α-L-fucopyranose residues, respectively, with monoclonal antibodies to *M. avium* serovars 2 and 9. In several cases, however, monoglycosyl conjugates fail to interact with homologous antibodies, but all glycobiosyl conjugates examined thus far have proven effective. The observation that NGPs bearing the glycobiosyl [(4-*O*-methyl-α-L-rhamnopyranosyl)-(1→4)-2-*O*-methyl-α-L-fucopyranosyl] epitope of the serovar 4 GPL with *N*-glycosyloxyethyllysine (Table V, method 1b) and *N*-glycosyloxynonanoyllysine (Table V, method 2a) spacers interacted indistinguishably with MAb 32B8 raised against whole cells of *M. avium*

serovar 4 indicated that epitope recognition was independent of the linker-arm.[122] Since residues of the same sugar may be found in terminal and nonterminal positions in GPLs, allyl glycosides have the added advantages of being simple to prepare and suitable for conversion into glycosyl donors as well as acceptors. However, retention of the integrity of the allyl glycosidic substituent does place restrictions on the protecting groups (such as benzyl ethers requiring removal by hydrogenolysis) used elsewhere in oligosaccharide synthesis.

Synthetic strategy for the assembly of oligoglycosyl NGPs is dictated by balancing the competing requirements for

(1) the introduction and retention of spacer-arm functionality required for conjugation;
(2) the correct placing of stable (for example, methyl ether) substituents;
(3) the propensity of substituents at O-2 of glycosyl donors to influence the creation of glycosidic bonds of specific anomeric configuration, such as 2-*O*-acyl substitutents which serve as participating groups in the synthesis of 1,2-*trans* glycosides;
(4) the introduction and retention during subsequent operations of permanent but potentially removable substituents, such as acetal or *O*-acyl groups;
(5) the modification for later alteration, as by reduction or oxidation, of precursor substituents introduced at an early stage.

If particular glycosyl units are not directly available so that synthesis requires functional and/or configurational modification of more accessible precursors, the sequence in which operations are performed, that is, before or after incorporation of the glycosyl residue into the oligosaccharide chain, may be an important consideration. Neoglycoprotein synthesis from reducing termini of the epitope with allyl, 8-methoxycarbonyloctyl, or other glyosides ensures definition of the anomeric configuration of the proximal residue. This advantage is becoming less important as improved methods for glycosylation in block synthesis are developed, so that complete oligoglycosyl units may be transferred to the linker-arm with high stereoselectivity from such donors as thioglycosides.[123]

A synthesis of a monoglycosyl neoantigen related to *M. avium* serovar 8 involving temporary protection of the allyl glycosidic substituent (Fig. 4) has been described.[124] Epoxidation gave diastereomeric epoxypropyl glycosides from which the allyl glycoside was regenerated later by reaction with 3-methylbenzothiazole-2-selone.[125] Protection was required during the synthesis of a stereochemically defined pyruvate acetal **31**[124] in a reaction involving oxidation[126] by ruthenium tetraoxide of a 3,4-dimethoxyphenylethylidene acetal[127] (**30**) derivative. More direct methods for pyruvation with satisfactory diastereoselectivity are described in Section IV.2b.

For the synthesis of oligosaccharide units containing residues of configurationally accessible 6-deoxyhexoses, standard protecting-groups methodology has

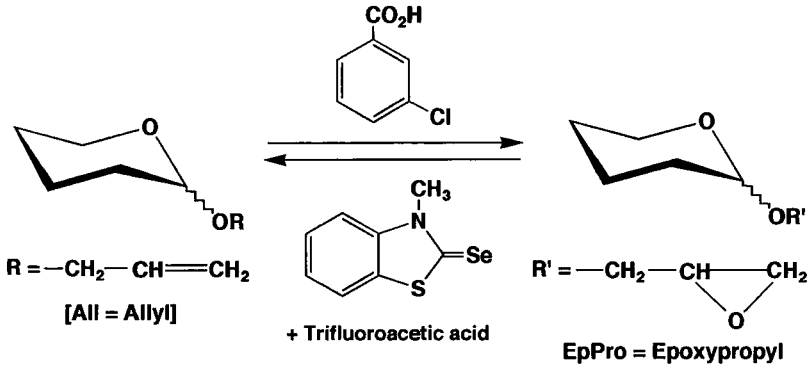

FIG. 4.—Protection and Regeneration of Allyl Glycosidic Substituent.

been employed for the introduction of methyl ether substituents and in the preparation of suitably protected glycosyl acceptors. Here, attention is directed only to chemically selective processes for the introduction and subsequent removal of common protecting groups. Syntheses of allyl glycosides of the distal glycobiosyl units of the GPLs from serovars 4 (ref. 122) and 20 (ref. 50) utilized complementary reactions for regioselective substitutions of the vicinal *cis*-3,4-diol of allyl 2-*O*-methyl-α-L-fucopyranoside (**32**) in preparations of glycosyl acceptors (**33** or **34**, and **35**). For the assembly of the inner unit of the serovar 4 disaccharide[122] (**36**), regioselective alkylation of the equatorial 3-hydroxyl group (pathway *a*) was effected by reaction of the dibutylstannylene derivative[128] with 4-methoxybenzyl or 2-nitrobenzyl halides. After glycosylation with trichloroacetimidate **37**, temporary protecting groups in the fully substituted disaccharides (**38** and **39**) were removed without effect on the allyl glycosidic substituent by oxidative[129] or photolytic cleavage,[130] respectively. For the 2-*O*-methyl-α-L-fucopyranose unit of the serovar 20 GPL, regioselective acylation of the axial 4-hydroxyl group (pathway *b*) to give **35** was achieved through acid-catalyzed opening of the cyclic orthobenzoate.[131] Regioselective 4-methoxybenzylation of the 2,3-dibutylstannylene de-

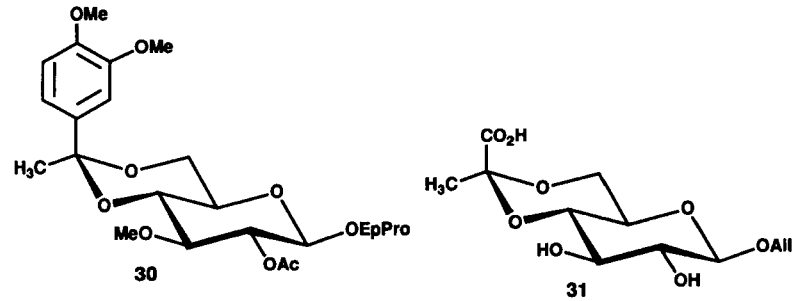

rivative of allyl 4-*O*-benzoyl-α-D-rhamnopyranoside (**40**) was used as the first step in the preparation (via **41** and **42**) of glycosyl donor **43** having the required substitution pattern for the terminal 2-*O*-methyl-α-D-rhamnopyranose residue. In the fully substituted disaccharide glycoside (**44**), the selective removal of *O*-acetyl in the presence of *O*-benzoyl groups on treatment with cold methanolic hydrogen chloride afforded a disaccharide acceptor (**45**) used for the chain extension required in the synthesis of the homologous distal trisaccharide unit (**46**) of the serovar 14 GPL.

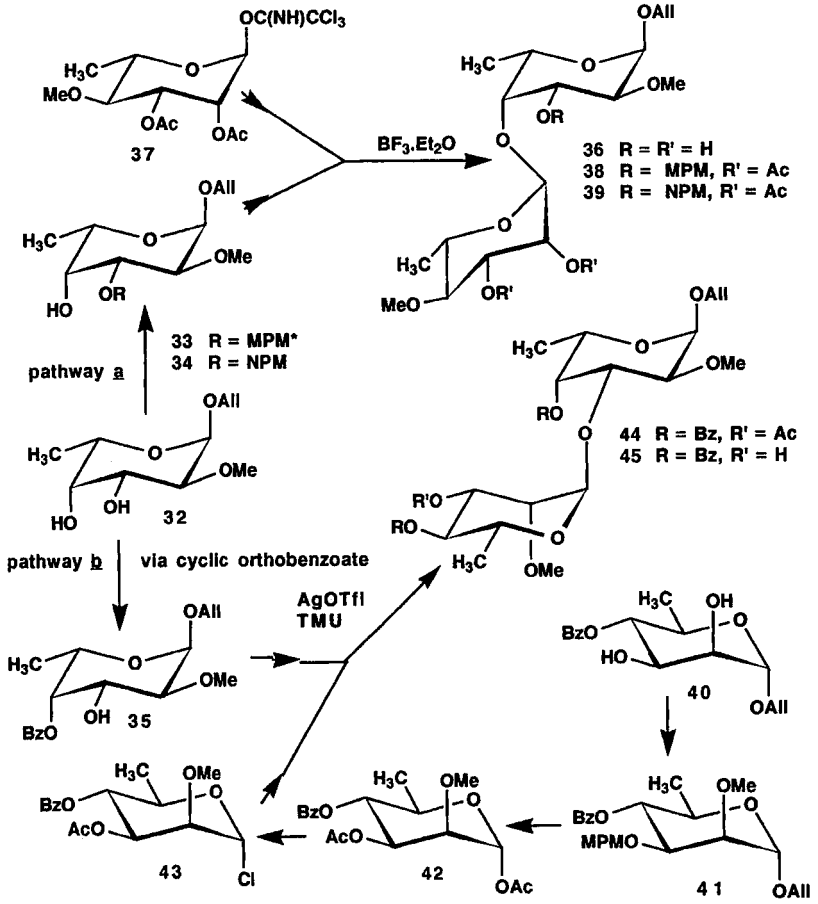

SCHEME.—Syntheses of allyl glycosides of distal disaccharide units of GPLs from *M. avium* serovars 4 and 20 involving regioselective substitutions in the preparations of glycosyl acceptors. MPM = 4-methoxyphenylmethyl [*p*-methoxybenzyl]; NPM = 2-nitrophenylmethyl [*o*-nitrobenzyl].

For the assembly of NGPs related to GPLs containing unusual or hard-to-obtain individual glycosyl or oligoglycosyl units, synthesis may require or be best achieved through structural modification of more readily available sugars. These modifications may be performed before or after insertion into the oligoglycosyl unit. In two of the following examples, the synthesis of the correct enantiomer in conjunction with immunological assay of the NGP was necessary in order to confirm the absolute configurations of the sugar in the natural epitope.

The absolute configuration of the branched-chain sugar kansosamine (4-amino-4,6-dideoxy-3-*C*-methyl-L-mannopyranose) as the *N*-(*R*)-2-methoxypropanoyl derivative having the terminal residue of the lipo-oligosaccharide from *M. kansasii* was established by synthesis. The synthesis by Yoshimura *et al.*[132] involved reductive amination of a pyranosid-4-ulose and gave an epimeric mixture of 4-amino-4-deoxy derivatives. Bajza and Lipták[133] adopted a similar route in the preparation of a thioglycoside donor for the terminal Kan4NFo residue of assumed α-L configuration in the synthesis of the hapten of the serovar 14 GPL. In a different approach, Aspinall and co-workers[50] took advantage of the elegant stereoselective syntheses by Giuliano and Kasperowicz[134] of derivatives of the related branched-chain sugars, sibirosamine, vinelose, and kansosamine. Entry into the 6-deoxy-3-*C*-methyl-L-mannopyranose series as allyl α-L-glycoside **47** was gained by stereoselective reduction of allyl 6-deoxy-3-*C*-methyl-α-L-*lyxo*-hexopyranosid-4-ulose[135] (**48**) with tetramethylammonium triacetoxyborohydride.[136] Methanesulfonylation of the 2,3-*O*-isopropylidene derivative (**49**), followed by *O*-deisopropylidenation and treatment with base, afforded the 3,4-*talo*-epoxide (**50**). Subsequent *O*-methylation and stereoselective introduction of the 4-azido substituent, followed by conversion into a glycosyl trichloroacetimidate[137] furnished a glycosyl donor (**51**) which, despite the absence of a participating substituent at O-2, reacted with the acceptor **45** to give the desired α-L-glycosidic linkage in the trisaccharide. For the conversion of the fully substituted trisaccharide derivative into the allyl glycoside (**46**) of the distal segment of the serotype 14 GPL, removal of protecting groups, delayed reduction of the azido substituent, and subsequent *N*-formylation were the final stages of the synthesis.[50] The interaction of the derived NGPs with antibodies to whole cells of serovar 14 provided effective confirmation of the assumption concerning the absolute configuration of the *N*-formyl-α-L-kansosamine residue in the GPL.

Of the four GPLs with glycobiosyluronic acid units as distal disaccharide segments, that from serovar 9 is the only case for which an NGP bearing only the terminal sugar residue interacts with antibodies against whole cells of the serovar.[121] Aspinall and co-workers[138] used similar strategies for the synthesis of glycobiosyl NGPs related to GPLs from serovars 25 and 26. Since differential substitution of β-D-glucopyranose residues is readily achieved, suitable intermediates leading to the required 4-linked β-D-glucopyranosyluronic acid residues were first prepared for glycosylation at O-4 with a selectively removable protect-

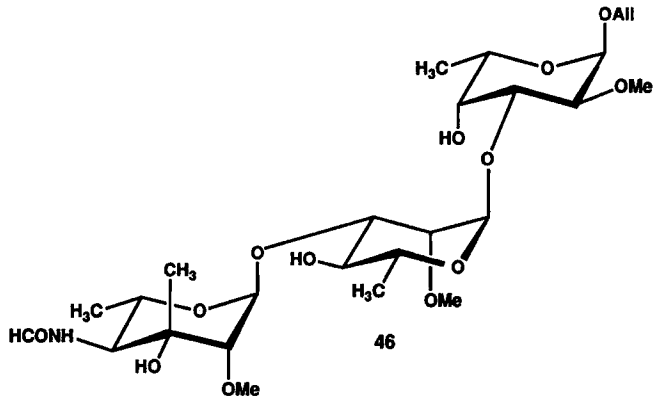

46

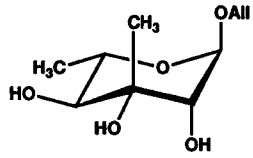

47

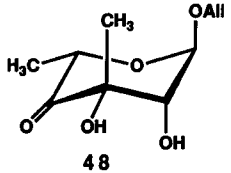

48

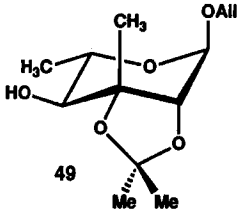

49

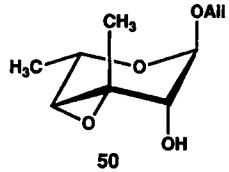

50

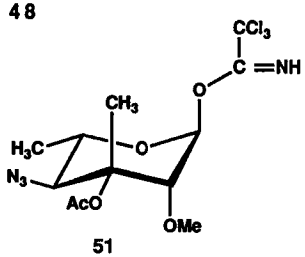

51

ing group at O-6 for subsequent oxidation to the glycosyluronic acid. For the synthesis of the neoantigen related to serovar 26 bearing a glycobiosyluronic acid unit, allyl 2,3-di-*O*-benzoyl-6-*O*-(4-methoxybenzyl)-β-D-glucopyranoside (**52**) was prepared by regioselective hydride opening of the corresponding 4,6-*O*-alkylidene acetal with acidified sodium cyanoborohydride,[129] and glycosylation was effected with 3-*O*-acetyl-2,4-di-*O*-methyl-α-L-fucopyranosyl chloride (**53**) in the presence of silver triflate. Selective deprotection at O-6 with ceric ammonium nitrate was followed by oxidation of the resulting disaccharide (**54**) with Jones' reagent (CrO_3 in acetic acid), which took place without effect on the allyl glycoside substituent; and removal of the remaining protecting groups gave the desired allyl glycoside of the glycobiosyluronic acid (**55**) for conversion into the NGP.

In the absence of evidence for the absolute configuration of the terminal 4-acet-

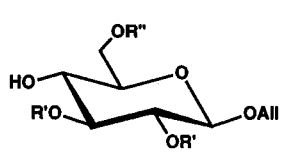

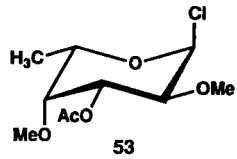

53

52 R' = Bz; R" - MPM
60 R' = Ac; R" = MP*

* MP = 4-methoxyphenyl
[p-anisyl]

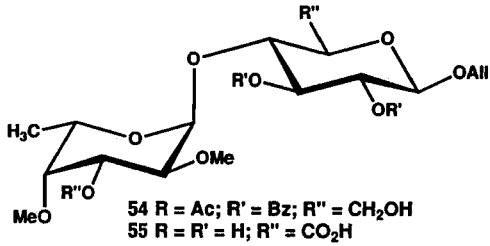

54 R = Ac; R' = Bz; R" = CH_2OH
55 R = R' = H; R" = CO_2H

amido-4-deoxy-2-*O*-methyl-α-fucopyranose residue, synthesis of the glycobiosyluronic acid unit of the serovar 25 GPL was undertaken first with the amino sugar as the L enantiomer in light of the apparent stereohomology of the oligosaccharide haptens of the three acidic serovars in which other fucose derivatives were of the L configuration. At the outset there was also uncertainty as to the relative configuration of the amino sugar residue in the tetraglycosylalditol, which showed a coupling constant, $J_{1,2}$ = 3.6 Hz, indicative of an α-*galacto* or α-*gluco* configuration. The uncertainty was resolved later from NMR data and by synthesis.[138] Synthesis of the sugar as a suitable glycosyl donor led to derivatives of both C-4 epimers, whose configurations were readily established from their NMR spectra. Regioselective oxidation of the dibutylstannylene derivative of methyl 2-*O*-methyl-α-L-fucopyranoside with bromine[139] gave the pyranosid-4-ulose **56**, from which catalytic reduction of oximes, followed by acetylation afforded both *galacto* (**57**) and *gluco* (**58**) isomers. Subjection of the derived alditol acetates to GLC-MS showed that the contituent of the hapten was the 6-deoxy-*galacto* (fucose) isomer. The methyl glycoside **57** was converted into the corresponding glycosyl acetate and thence, into the 2′-pyridyl thioglycoside[140] **59** as glycosyl donor for activation with methyl iodide. Allyl 2,3-di-*O*-6-*O*-(4-methoxyphenyl)-β-D-glucopyranoside (**60**) was synthesized as an acceptor bearing at O-6 a protecting group less susceptible than the 4-methoxybenzyl group to premature removal with traces of acid, and glycosylation gave a disaccharide.

Oxidative removal of the 4-methoxyphenyl group in **61**, followed by oxidation and deprotection as for the synthesis of **55**, gave the allyl glycoside (**62**) of the

glycobiosyluronic acid for conversion into neoantigen **63** bearing the 4-acetamido-4-deoxy-2-*O*-methyl-α-L-fucopyranosyl-(1→4)-β-D-glucopyranosyluronic acid epitope. Unexpectedly, the NGP failed to interact with the antibodies to serovar 25. In a parallel synthetic sequence, the allyl glycoside (**67**) of the diastereomeric glycobiosyluronic acid was prepared using an anomeric mixture of thioglycosides (**64, 65**) formed from the D enantiomer (**66**) of **57** as glycosyl donor for reaction with the same acceptor (**60**). The NGP bearing the 4-acetamido-4-deoxy-2-*O*-methyl-α-D-fucopyranosyl-(1→4)-β-D-glucopyranosyluronic acid epitope (**68**) showed a positive interaction with antibodies to serovar 25. These observations provided a striking illustration of immunochemical stereoselectivity for an assignment of absolute configuration that could not be achieved by other means.

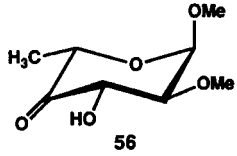

56

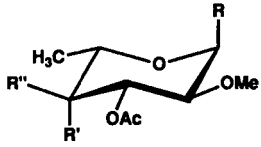

57 R = Me; R' = AcNH; R" = H
58 R = Me; R' = H; R" = AcNH
59 R = S-2-Pyr; R' = AcNH; R" = H

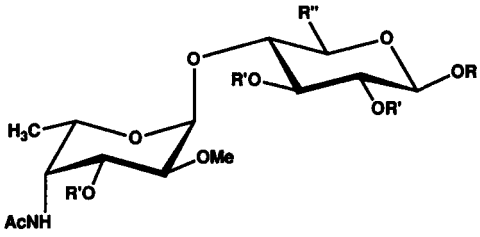

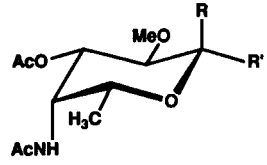

64 R = S-(2-Pyridyl), R' = H
65 R = H, R', = S-(2-Pyridyl)
66 R = OMe, R' = H

61 R = All; R' = Ac; R" = CH_2OMP
62 R = All; R' = H; R" = CO_2H
63 R = O-$[CH_2]_2$-NH-(Lys)-Protein; R' = H; R" = CO_2H

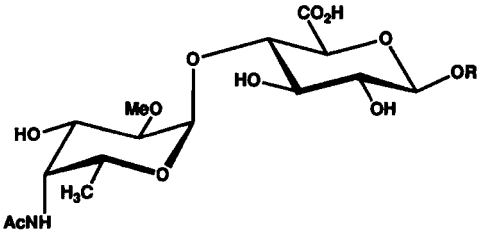

67 R = All
68 R = O-$[CH_2]_2$-NH-(Lys)-Protein

Studies of the immunoreactivities of NGPs with homologous antibodies (Abs) have been mainly directed to qualitative conclusions, some of which have already been mentioned. Table VI shows the structures of the outer regions of the hapten moieties of the *M. avium* serocomplex, followed by the structures of the glycosyl units in the synthetic NGPs, and the reactivity or lack thereof with the relevant specific antibodies. Antibodies were of two types, polyclonal rabbit antisera and

TABLE VI

Haptens of GPLs from *M. avium* Serovars and Related NGPs

Serovar number	Hapten structure[a] [NGPs prepared with 1,2, or 3 residues]	Structurally related NGP[b] [reaction with homologous Abs]
2	**2,3-Me_2-α-L-Fuc*p*[c]-[(1→3)-α-L-Rha*p*-(1→2)-6-deoxy-L-Tal]**[d]	
	2,3-Me_2-α-L-Fuc*p*	neo 2-1 [+]
	2,3-Me_2-α-L-Fuc*p*-(1→3)-α-L-Rha*p*[b]	neo 2-2 [+]
	4-Ac-2,3-Me_2-α-L-Fuc*p*	neo 9-1 [−]
4	**4-Me-α-L-Rha*p*-(1→4)-2-Me-α-L-Fuc*p***	
	4-Me-α-L-Rha*p*	neo 4-1 [−]
	4-Me-α-L-Rha*p*-(1→4)-2-Me-α-L-Fuc*p*	neo 4-2 [+]
	4-Me-α-L-Rha*p*-(1→3)-2-Me-α-L-Fuc*p*	neo 4-2* [−]
8	**3-Me-4,6-Pyr-β-D-Glc*p***	
	3-Me-4,6-Pyr-β-D-Glc*p*	neo 8-1 [+]
9	**4-Ac-2,3-Me_2-α-L-Fuc*p***-(1→4)-β-D-Glc*p*A-(1→4)-2,3-Me_2-α-L-Fuc*p*	
	4-Ac-2,3-Me_2-α-L-Fuc*p*	neo 9-1 [+]
	2,3-Me_2-α-L-Fuc*p*	neo 2-1 [−]
14	**α-L-Kan*p*4NFo-(1→3)-2-Me-α-D-Rha*p***-(1→3)-2-Me-α-L-Fuc*p*	
	α-L-Kan*p*4NFo-(1→3)-2-Me-α-D-Rha*p*	neo 14-2 [+]
	α-L-Kan*p*4NFo-(1→3)-2-Me-α-D-Rha*p*-(1→3)-2-Me-α-L-Fuc*p*	neo 14-3 [+]
20	**2-Me-α-D-Rha*p*-(1→3)-2-Me-α-L-Fuc*p***	
	2-Me-α-D-Rha*p*	neo 20-1 [−]
	2-Me-α-D-Rha*p*-(1→3)-2-Me-α-L-Fuc*p*	neo 20-2 [+]
25	**2-Me-α-D-Fuc*p*4NAc-(1→4)-β-D-Glc*p*A**-(1→4)-2-Me-α-L-Fuc*p*	
	2-Me-α-L-Fuc*p*4NAc	neo 25-1 (L) [−]
	2-Me-α-L-Fuc*p*4NAc-(1→4)-β-D-Glc*p*A	neo 25-2 (L) [−]
	2-Me-α-D-Fuc*p*4NAc-(1→4)-β-D-Glc*p*A	neo 25-2 (D) [+]
26	**2,4-Me_2-α-L-Fuc*p*-(1→4)-β-D-Glc*p*A**-(1→4)-2-Me-α-L-Fuc*p*	
	2,4-Me_2-α-L-Fuc*p*	neo 26-1 [+]
	4-Ac-2,4-Me_2-α-L-Fuc*p*	neo 26-1 (O-acetyl) [−]
	2,4-Me_2-α-L-Fuc*p*-(1→4)-β-D-Glc*p*A	neo 26-2 [+]

[a] Kan4N = kansosamine (4-amino-4-deoxy-3-*C*-methyl-2-*O*-methylrhamnose); Ac = acetyl; Fo = formyl; Me = *O*-methyl; Pyr = pyruvic acetal [4,6-*O*-(1-carboxyethylidene)].

[b] NGP bearing the glycobiosyl unit of the GPL from serovar 2 is designated neo 2-2; [+] or [−] indicates interaction with homologous antibodies.

[c] Bold type is used to define recognized epitopes to specific antibodies.

[d] All internal chains are terminated by this sequence in attachment to allothreonine residues in the peptide moiety.

murine monoclonal antibodies (MAbs), raised in most cases against whole cells of the particular serovar, whole lipids, or intact GPLs. All polyclonal Abs were consistently serovar-specific[121,122] in interacting with the terminal sugar residue in the homologous monoglycosyl and/or glycobiosyl NGCs (Table V). The minimum requirements were for the constitutionally defined terminal sugar inclusive of methyl ether and *O*-acetyl substituents to be of the correct enantiomeric, and presumably also anomeric, configuration. The synthetic NGPs may play a dual role in defining the structural requirements for antigen–antibody interactions. On the one hand, the interactions, or lack thereof, provide supportive or even definitive evidence in confirmation of molecular structure. On the other hand, they also define the specificities of antibodies, especially MAbs, where several such may be directed to different regions of complex structures. At this time, definitions of the specificities of some MAbs toward related structures appear to be rather unpredictable.

Table VI summarizes observations of the interactions of Abs that relate to the dual role of NGPs. The absence of cross-reactions between GPLs of serovars 2 and 9 could be explained when monoglycosyl NGPs with a 2,3-di-*O*-methyl-α-L-fucopyranose residue (neo 2-1) and a 4-*O*-acetyl-2,3-di-*O*-methyl-α-L-fucopyranose residue (neo 9-1) were made available; they interacted specifically with the homologous polyclonal Abs, and thereby gave confirmatory evidence[121] for the presence of the latter residue as the terminal unit in the GPL from serovar 9. Conversely, the reactivity of monoglycosyl NGP (neo 26-1) toward homologous anti-serovar 26 rabbit antisera is eliminated on introduction of the 3-*O*-acetyl group. The unpredictable specificity of monoclonal as opposed to polyclonal Abs is illustrated by the interaction of both monoglycosyl neo 2-1 and glycobiosyl neo 2-2 with polyclonal Abs, but of the former only with MAb.[122] A related observation concerning the more precise requirements of MAbs was shown by the recognition of both monoglycosyl NGP 4-1 and glycobiosyl NGP 4-2 by anti-serovar 4 antiserum, but only of the glycobiosyl NGP by anti-GPL 4 MAbs.[121,122]

Two of three MAbs recognizing the GPL of serovar 8 show an absolute specificity to the 3-*O*-methyl substituent of the terminal 4,6-*O*-(1-carboxyethylidene)-3-*O*-methyl-β-D-glucopyranose residue. For one of these MAbs, the monoglycosyl NGP 8-1 provided definitive evidence for the structural identity of the epitope.[121] A third MAb also interacts with the GPL of serovar 21, later examination of which showed the presence of the related nonmethylated, pyruvated terminal sugar.

Another example of the unpredictable nature of the monoclonal antibodies raised to the GPL of serovar 14 was observed in some of their reactions. Whereas both polyclonal Abs and MAbs clearly discriminated between the terminal disaccharide units of GPLs from serovars 14 and 20, some of the MAbs to serovar 14 recognized the terminal glycobiosyl units of NGP neo 14-2 but not the more extended glycotriosyl unit in 14-3 (ref. 50).

b. Synthesis of Complete Oligosaccharide Haptens. — Syntheses have been reported of four complete oligoglycosyl haptens from GPLs with attached linker-arms bearing latent functionality for prospective use in conjugation to protein.[119a] In addition to the previously outlined strategic considerations, these syntheses have taken advantage of developments in glycosylation methods. The concept of "armed" and "disarmed" reagents was first introduced by Fraser-Reid and colleagues[141] in connection with *n*-pentenyl glycosides, but applies equally to thioglycosides.[141–143] Changes in protecting groups, especially at O-2, not only influence the stereochemical consequences at the newly formed anomeric center by participation or nonparticipation, but also markedly affect reactivity.

Gurjar and Viswanadham[144] reported the first synthesis of the complete *M. avium* serovar 4 tetraglycosyl hapten as the methyl glycoside **69**. These researchers used the 2 + 2 block approach in conjugation with the previously demonstrated high degree of α-selectivity in glycosylation with glycosyl acetates in the presence of boron trifluoride etherate.[111,145] Thus, reaction of **70** with **71** proceeded with the desired stereoselectivity, and deprotection afforded the tetrasaccharide **69**.

Zuurmond and co-workers[146] have carried out a synthesis of the same haptenic oligosaccharide with linker-arm (**72**) using the four key synthons: **73**, **74**, **76**, and **77**. The "disarmed" L-rhamnose thioglycoside **74** provides an excellent example

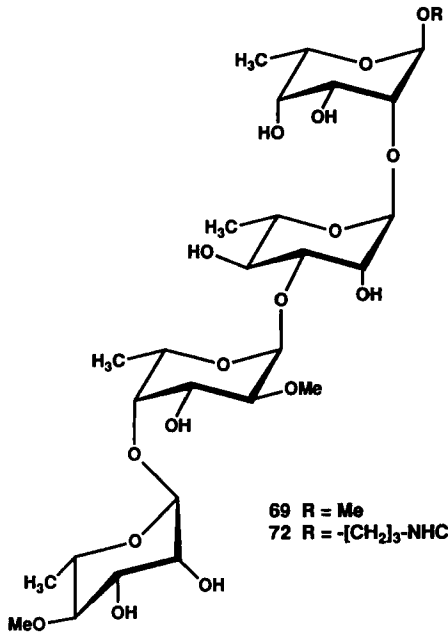

69 R = Me
72 R = -[CH_2]$_3$-NHCbz [Cbz = *N*-benzyloxycarbonyl]

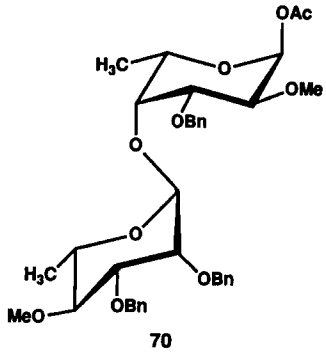

70

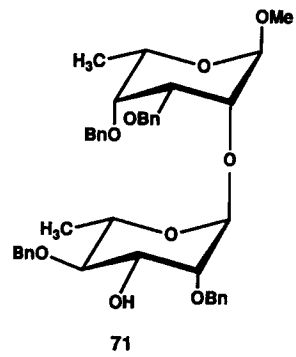

71

of a synthon having the potential to serve as glycosyl acceptor in reaction with **73** as glycosyl donor with an iodonium di-*sym*-collidine perchlorate-assisted reaction to give the disaccharide derivative **75**, with no evidence for intrusive self-condensation as a competing reaction. The disaccharide **75** with the same functionality, but using *N*-iodosuccinimide and triflic acid as a catalyst, was able to serve as a glycosyl donor in reaction with **76** as synthon for the 6-deoxy-L-talose terminus bearing the linker-arm. The final stage in the assembly of the complete tetrasaccharide **72** was achieved with selective removal of the chloroacetyl substituent from the 2-*O*-methyl-L-fucose residue and glycosylation with the 4-*O*-methyl-L-rhamnose synthon **77**, followed by removal of protecting groups.

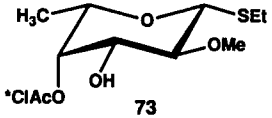

73

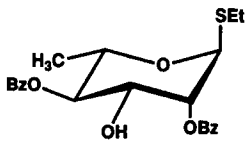

74

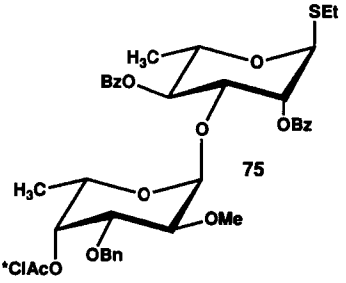

75

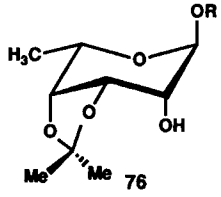

76

* ClAc = chloroacetyl

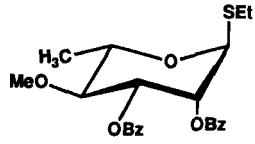

77

Lipták and collaborators[147] have applied thioglycoside methodology[123] as the principal approach in the synthesis of the complete tetraglycosyl hapten for the *M. avium* serovar 20 GPL. Synthons **78–81** were prepared for each of the glycosyl residues to serve directly, or after minor modification, as donors or acceptors. Stereoselective preparations of dioxolane benzylidene acetals (as in **81**), and their subsequent regioselective cleavage in the formation of **79** and **80a**, were key steps in the synthesis of these building blocks. In the overall strategy, both stepwise and 2 + 1 partial block approaches were used to assemble the inner trisaccharide segment (**82**). Removal of the *O*-acetyl group at O-3″ followed sequentially by glycosylation with **78**, simultaneous debenzylation, and reduction of the nitro group; trifluoroacetylation led to the complete *N*-protected tetraglycosyl hapten with spacer-arm **83** for potential conjugation to protein. The availability of the D-rhamnose synthon (**78**) in a form suitable for selective deprotection at O-3, as shown independently in the syntheses of neo 14-2 and neo 14-3 (ref. 50), and of a thioglycoside donor for the kansosamine unit[133] will allow for future chain extension in the synthesis of the pentaglycosyl hapten of serovar 14.

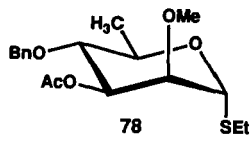

78 SEt

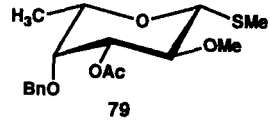

79

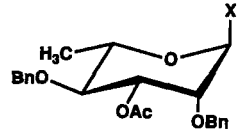

80a X = SEt
80b X = O-C(=NH)-CCl3

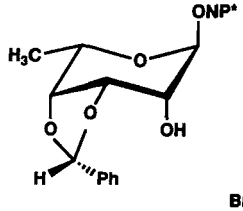

81

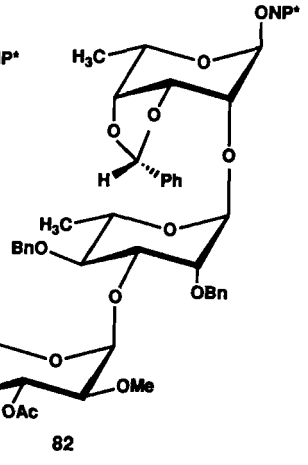

82

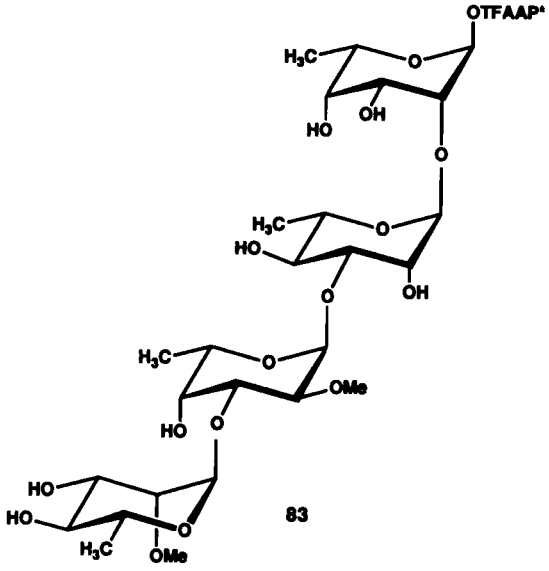

83

The inner disaccharide unit of the trisaccharide hapten of the *M. avium* serovar 8 GPL[148] was assembled in a manner similar to that of the serovar 20, but with reaction of the rhamnosyl trichloroacetimidate (**80b**) with the benzylidene acetal (**81**). *O*-Deacetylation of the product yielded the disaccharide acceptor (**84**) for the next glycosylation. Incorporation of the pyruvate acetal moiety into the terminal 3-*O*-methyl-D-glucose residue of **85** was achieved by transacetalation with methyl pyruvate diethyl dithioacetal, with sulfuryl chloride–triflic acid as catalyst. From the mixture of products the desired diastereomer was separated and converted by successive *O*-debenzylation, acetylation, selective 1-*O*-deacetylation, and reaction with trichloroacetonitrile into the trichloroacetimidate **86**. Reaction of glycosyl donor **86** with acceptor **84**, with trimethylsilyl triflate as promoter, afforded fully

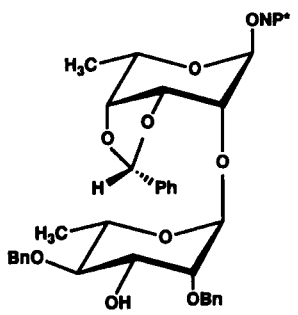

84

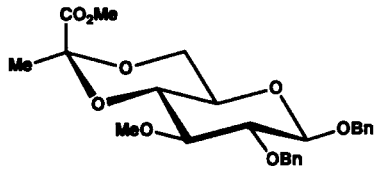

85

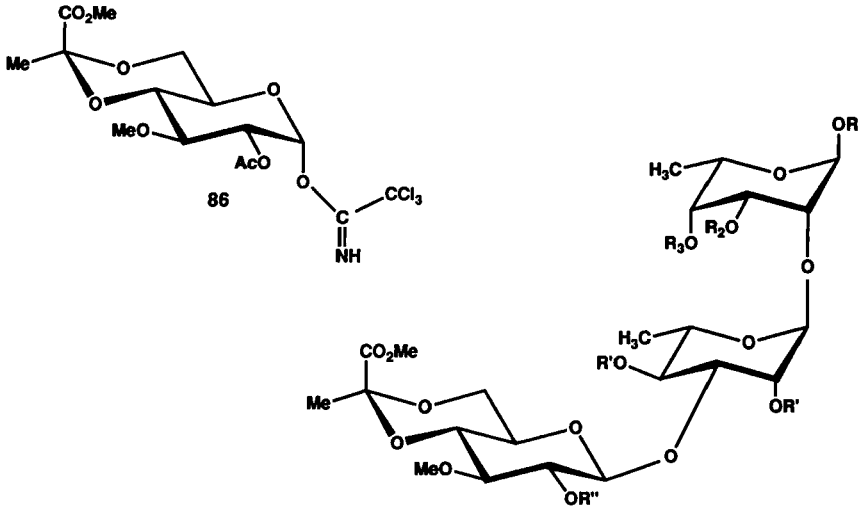

87 R = NP*; R_2,R_3 = =CH-Ph; R' = Bn; R" = Ac
88 R = TFAAP*; R_2 = R_3 = H; R' = R" = H

blocked trisaccharide **87** from which the suitably protected trisaccharide with spacer-arm **88** was derived by successive *O*-deacetylation, catalytic *O*-debenzylation, reduction of the nitrophenyl glycosidic substituent, and *N*-trifluoroacetylation.

Ziegler[149] has reported a highly efficient synthesis of the very similar *M. avium* serovar 21 trisaccharide hapten with attached linker-arm (**89**). The blockwise construction minimizes the manipulation of protecting groups and hence the number of steps in the overall synthesis. The synthesis featured two key operations: (1) the kinetically controlled diastereoselective preparation from D-glucose of the

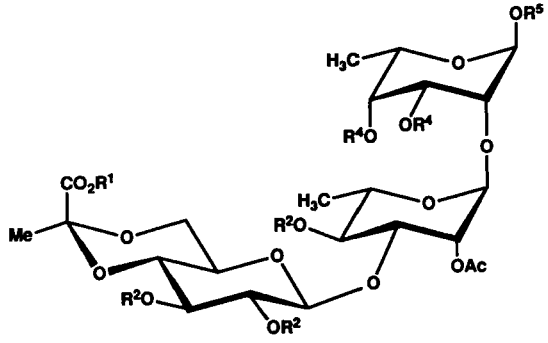

89 R^1 = R^2 = R^3 = R^4 = H, R^5 = $[CH_2]_5$-NH_2
96 R^1 = Me, R^2 = Bz, R^3 = Ac, R^4 = Bn, R^5 = $[CH_2]_5$-NHCbz

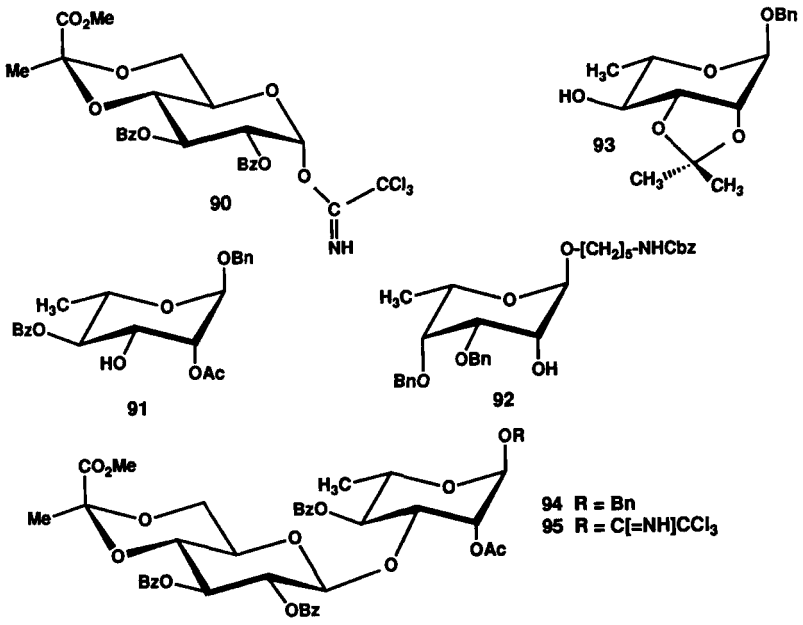

pyruvated glycosyl donor[150] as the trichloroacetimidate **90**; and (2) the preparation of L-rhamnose (**91**) and 6-deoxy-L-talose (**92**) synthons from a common precursor **93**. The outer glycobiosyl unit **94** was assembled from **90** and **91** and then converted into the corresponding glycobiosyl donor **95** for condensation with **92** to give fully protected trisaccharide hapten (**89**) which, after deprotection, gave a water-soluble NGP on reductive crosslinking with protein in the presence of glutardialdehyde. Subsequently, Ziegler[150a] reported a strategically similar synthesis of the *M. avium* serovar 8 trisaccharide hapten with attached linker-arm.

As the harbinger of a new approach to the creation of NGCs that lies beyond the scope of this article, Gurjar and Saha[151] have reported the chemical synthesis of the C-mycoside group. The synthetic derivative **97** carries an *N*-acetyl in place of the

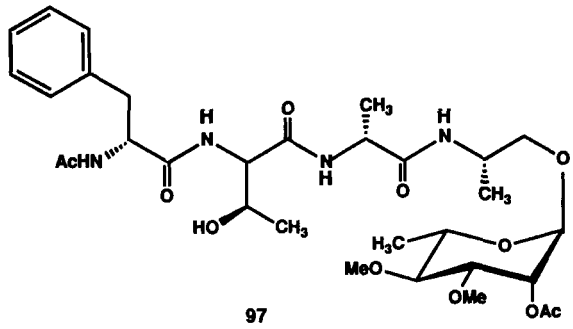

natural *N*-fatty acyl substituent on the terminal D-phenylalanine unit and, with the hydroxyl group of the D-allothreonine residue, would serve as glycosyl acceptor in the synthesis of NGCs that would more closely resemble the natural GPLs.

3. Synthesis and Immunoreactivity of Other Neoglycoconjugates

Three syntheses[145,152,153] have been reported for the complete trisaccharide hapten moiety of the phenolphthiocerol glycoside from the Canetti strain of *M. tuberculosis*.[77] In one of these syntheses, Fujiwara[152] prepared a derivative (**98**) of the trisaccharide with the methyl 3-(4-hydroxyphenyl)propanoate linker-arm (Table V, method 2b) previously reported for the synthesis of leprosy-related NGPs.[104,105] The key step in the synthesis of **98** was the condensation of 2,3,4-tri-*O*-methyl-α-L-fucopyranosyl chloride (**99**) and linker-arm-attached 2,4-di-*O*-benzyl-α-L-rhamnopyranosyl-(1→3)-4-*O*-benzyl-2-*O*-methyl-α-L-rhamnopyranoside (**100**) in the presence of silver triflate. Gurjar and Viswanadham[145] used a similar approach in the synthesis of trisaccharide as methyl glycoside (**103**) with glycosyl α-acetate (**101**) as the donor in reaction with methyl rhamnobioside (**88**) as acceptor in the presence of boron trifluoride etherate. The third trisaccharide synthesis by Veeneman *et al.*[153] yielded the 3-aminopropyl glycoside **102** as spacer-arm for conjugation to protein. The key feature was an iodonium-ion-promoted glycosidation approach using ethyl 1-thioglycosides with suitably chosen substituents in glycosyl donors and acceptors to achieve fast chemoselective and highly stereoselective glycoside-bond formation.[142,143] Derivatives of ethyl 2,3-di-*O*-acetyl-4-*O*-benzyl-1-thio-α-L-rhamnopyranoside (**91**) served in two capacities: (1) to furnish **105** as glycosyl donor for attachment of the protected spacer in reaction with 3-(benzyloxycarbonylamino)-1-propanol, with subsequent conversion into the glycosyl acceptor **106**; and (2) for conversion into acceptor **107** for glycosylation by the more reactive donor **108** without obvious self-condensation. The resulting disaccharide thioglycoside **109**, in its role as glycosyl donor with **106** as acceptor, acted as a powerful promoter in the presence of *N*-iodosuccinimide–triflic acid to give the fully protected trisaccharide **110**, and thence the desired antigenic trisaccharide **104** with attached spacer-arm.

Preliminary studies on the seroreactivity of the NGP prepared from the trisaccharide with the methyl 3-(4-hydroxyphenyl)propanoate linker-arm (**98**) showed relatively high activity and specificity against human tuberculosis sera.[152] The wider significance of this observation must be assessed in the light of observations by Daffé *et al.*[86] with the corresponding glycobiosyl neoantigen. These workers synthesized the terminal disaccharide unit of the Cannetti strain glycolipid with the glycosyloxynonanoyl linker-arm (**111**) (Table V, method 2a) for conjugation to protein. This synthetic antigen and the native glycolipid were strongly correlated, but the seroreactivity rate of tuberculosis sera was disappointing; only a small proportion of tuberculosis patients showed evidence of anti-glycolipid antibodies.

Serodiagnosis using this NGC would not therefore seem to be a general procedure for the detection of tuberculosis infection.

The seroreactivity of a synthetic monoglycosyl NGC related to the major phenolic glycolipid of *M. bovis* BCG has provided strong confirmatory evidence for revision of the enantiomeric configuration of the glycosyl residue in the so-called "mycoside B"[78] to that of 2-*O*-methyl-α-L-rhamnopyranose. The NGC with the glycosyloxynonanoyl linker-arm was suitable for the serodiagnosis of bovine tuberculosis.

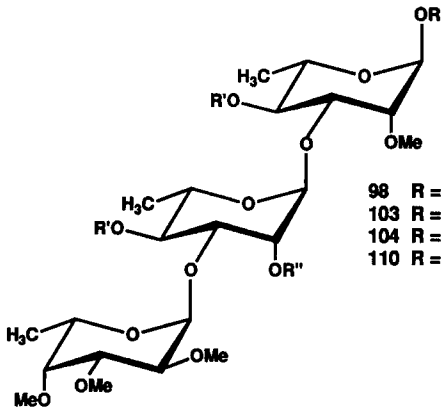

98 R = C_6H_4-$[CH_2]_2$-CO_2Me; R' = R'' = H
103 R = Me; R' = R'' = H
104 R = $[CH_2]_3$-NH_2
110 R = $[CH_2]_3$-NHCbz; R' = Bn; R'' = Ac

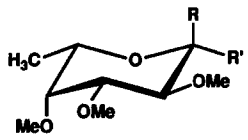

99 R = Cl; R' = H
101 R = Ac; R' = H
108 R = H; R' = SEt

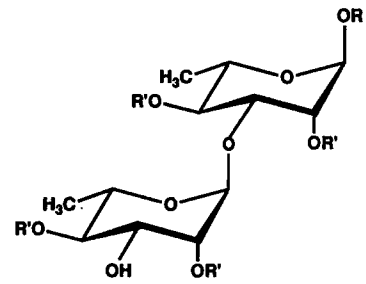

100 R = C_6H_4-$[CH_2]_2$-CO_2Me; R' = Bn
102 R = Me; R' = Bn

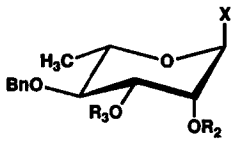

105 X = SEt; R_2 = R_3 = Ac
106 X = O-$[CH_2]_3$-NHCbz; R_2 = Me; R_3 = H
107 X = SEt; R_2 = Ac; R_3 = H

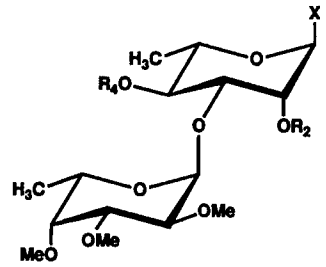

109 X = SEt; R_2 = Ac; R_4 = Bn
111 X = OMCO; R_2 = R_4 = H

Other syntheses directed toward NGPs related to other mycobacterial glycolipids include those of the common inner-core trisaccharide fragment of the phenolic glycolipids of *M. kansasii*.[154,155] In one of these syntheses,[155] the tyramine moiety in the spacer-arm is suitable for conjugation to protein, and the trisaccharide segment in **112** has been prepared for the subsequent attachment of strain-specific terminal sugar residues.[156–158]

The subsequently discovered different glycopeptidolipid core structures in *M. xenopi*[55,56] and *M. fortuitum*[54] have attracted attention as feasible synthetic targets.[159–161] Gurjar and Saha[159] have reported the assembly of an *N*-acetyltetrapeptide (**113**) bearing the 3-*O*-methyl-6-deoxy-α-L-talopyranosyl substituent at the outer serine residue but lacking the *O*-fatty acylated tetrasaccharide moiety that adorns the threonine residue in the natural GPL.

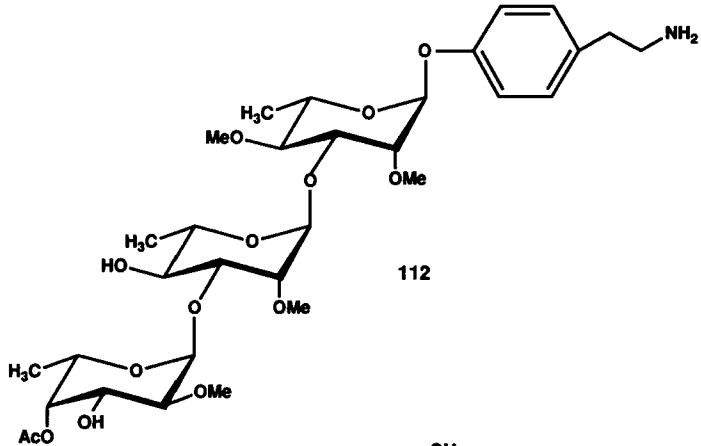

V. Other Biological Features of the Glycolipids of Mycobacteria

1. Antigenicity of the Native Glycolipids and Their Neoglycoproteins

Members of the *M. avium* complex, as opportunistic pathogens, cause disseminated infections in the majority of patients with AIDS.[3,162] The source of infection is undoubtedly the environment,[163] since the organisms are commonly isolated

from soil, water, and house dust,[164] although infection might also be acquired from contact with fowl or domestic and wild animals.[165] Despite their ubiquity, no serious study of the serology of *M. avium* infections has been undertaken. There is evidence for elevated antibodies to the GPLs of the *M. avium* complex in populations at risk of developing *M. avium* infections.[166] Nevertheless, neither the GPLs themselves nor the GPL-related NGCs have, as yet, had any practical application in the diagnosis of *M. avium* infections. This is partially explained by the poor status of humoral immunity in patients with advanced AIDS, together with doubt as to whether treatment of secondary *M. avium* infections, and consequently diagnosis of these infections, helps the patient. Thus, it is unlikely that the large array of *M. avium*-based NGCs will have practical use in serodiagnosis. However, antigenicity of the various NGCs, particularly those based on the GPLs, has been successfully exploited in synthetic strategies, in that the reactivity of the synthetic product against murine monoclonal or rabbit polyclonal antibodies has proved to be an excellent test of structural authenticity. This point was best demonstrated in the case of the first generation of NGCs generated—those based on PGL-I rather than the GPLs—in which both the anomeric and absolute configuration of sugars were in doubt.[94] Also, Western blot analysis (that is, resolution of NGCs on polyacrylamide gels and reaction with the appropriate antibody) is an excellent gauge of purity of NGCs, as in those, for example, containing the triglycosyl unit of PGL-I[103] and the terminal mono- and disaccharides of the GPL of serovar 4.[121] The power of a combination of monoclonal and polyclonal antibodies, as applied to NGCs in order to define the molecular dimensions of the epitopes of individual GPLs,[121] is well documented in Section IV.

Nevertheless, the discovery that PGL-I is biochemically unique[71] led first to the demonstration that it is immunologically specific for *M. leprae*,[167,168] and then to reawakened interest in the serodiagnosis of subclinical leprosy. The majority of human antibody to PGL-I is of the immunoglobulin M subclass, and virtually all monoclonal antibodies generated against PGL-I in mice are IgM.[167] Enzyme-linked immunosorbent assay (ELISA) procedures, using the highly hydrophobic native PGL-I have been worked out by many investigators, and attempts have been made to standardize and simplify the procedures.[169] However, the ready availability of a range of NGCs and their application in simple kit form[170] has resulted in their widespread application such that the native glycolipid is now seldom used. Anti-PGL-I antibody is found in virtually all multibacillary, lepromatous leprosy patients.[171] However, although the number of false-positive responses is about 4% in a nonendemic population, the response of pauci-bacillary tuberculoid leprosy patients and contacts is also disappointingly low, thus limiting the use of this test for epidemiological purposes or for identification of patients with subclinical infection.[172–174] There is evidence of a correlation between decreased bacillary load and anti-PGL-I antibody levels after chemotherapy in lepromatous leprosy patients.[175] However, because PGL-I is a major component of *M. leprae* and is

present in abundance in the tissue and blood of lepromatous leprosy patients,[176,177] sensitive detection of the antigen, rather than the antibody, through antigen-capture procedures or sensitive physical methods, could identify infected individuals. Although this challenge has been addressed,[178,179] the sensitivity and ease of assays do not yet allow for meaningful epidemiological use.

Clearly, serology based on the PGL-I-related NGCs has a place in the control of leprosy, although it does not meet pressing needs in terms of measuring incidence and reservoirs of infection, chains of disease transmission, and early diagnosis.

The presence in at least some strains of *M. tuberculosis* of an analogous phenolic glycolipid with its own unique triglycosyl unit[77] offered similar promise for the serodiagnosis of tuberculosis. However, the information to date is contradictory. Preliminary results from one study showed that antibodies reacting with the native glycolipid occurred in the serum of most tuberculosis patients and were seldom encountered in healthy persons.[180] Another preliminary study reported a very high sensitivity and specificity of 96.8% for anti-glycolipid antibodies and concluded that this antigen had potential "for case finding in tuberculosis epidemiology,"[181] a contention that has never been substantiated. For example, Daffé *et al.*,[182] employing the NGC that emulates the terminal diglycosyl unit of the phenolic glycolipid, observed that only 24 of 119 sera from tuberculosis patients showed evidence of anti-glycolipid antibodies, even though the serological correlation between the native PGL and the NGC against the few positive sera was excellent. Moreover, this study demonstrated that only one of eleven isolates of *M. tuberculosis* from tuberculosis patients contained the glycolipid, which information is in accord with poor results from serology. Also, a thorough study by competent serologists concluded that, while the phenolic glycolipid from the peculiar Canetti strain of *M. tuberculosis* and such glycolipids as the simpler diacyltrehaloses[68,183] from a more conventional strain (H37Rv) could react readily with rabbit sera raised against the homologous strain, none was able to discriminate between patient and control sera at a level suitable for a serodiagnostic test.[184] Thus it would seem that none of the glycolipids of *M. tuberculosis* or their corresponding NGCs offer promise for the serodiagnosis of tuberculosis in clinical situations where such diagnosis would be of practical benefit.

2. Other Biological Properties Including Biosynthesis of the Glycolipids of Mycobacteria

It is obvious from the work of Papa *et al.*[185] and Belisle and Brennan[186] that the LOSs of *M. kansasii* are antigenic in the laboratory sense. Belisle and Brennan used this property to demonstrate that rough strains of *M. kansasii* were devoid of the LOSs, an observation that may be important in the context of the infectivity and persistence of some strains of *M. kansasii* in some hosts.[186] *M. tuberculosis*, *M. leprae*, and *M. avium* are intracellular parasites able to proliferate inside macro-

phages, in spite of the antimicrobial activity of the phagocytic cell.[187] Fibrillar, capsule-like structures (the electron-transparent zone, ETZ), often observed in electron micrographs and long considered to be glycolipid in nature, have been implicated in the intracellular survival and persistence of mycobacteria. Draper[188] and later Barrow *et al.*[198] clearly demonstrated that the fibrillar filamentous material comprised mostly GPLs. Application of freeze-fracture electron microscopy to *M. avium* growing within mouse liver macrophages demonstrated progressive accumulation of GPLs around intramacrophagic bacteria, especially in long-term infections.[190]

Besides serotypic differences, the *M. avium* complex also shows highly characteristic morphological variations, most vividly seen when organisms are grown on solid medium,[191] which are described as smooth-domed (SmD), smooth-transparent (SmT), and rough (Rg). Although the molecular basis of the SmD and SmT phenotype switch is not known, the SmT variants have generally been considered the more virulent form, in that fresh clinical isolates from AIDS patients with disseminated *M. avium* disease are predominantly of the SmT morphotype[192–194]; there is also a distinct difference in the types of cytokines produced by monocytes infected with isogeneic morphotypes of *M. avium*.[195,195a] Also, the SmT variants are more resistant to antibiotics.[196] Since the GPL composition of both the SmD and SmT variants seems to be identical, it is unlikely that their surface antigens are implicated in the greater propensity of the SmT form to survive *in vivo* and cause disease. Nevertheless, it has clearly been demonstrated that the GPLs, the L1 layer of Barksdale,[189] do survive within the intraphagosomal environment where they are resistant to degradation by lysosomal enzymes,[197] lending further support for a role in intracellular survival.

It was known from early studies that the stable rough (Rg) morphological forms of *M. avium* are devoid of the GPLs.[198] However, the biological consequences were not known. In an extensive study, Belisle *et al.*[199,200] determined the molecular basis of this deficiency. Two types of spontaneous (Rg) mutants were shown to exist in nature. One class (such as Rg-3 and Rg-4) is completely devoid of any semblance of the GPL structure.[198] However, the other (for instance Rg-0 and Rg-1) contained two novel lipopeptides, both devoid of any of the characteristic sugars of the GPLs.[199] The application of GC, FAB-MS, and ^{1}H-NMR demonstrated the structure of one of these as $C_{32:2}$-β-hydroxyfatty acyl-D-phenylalanine-D-allothreonine-D-alanine-L-alaninol, whereas the other was a minor variation on this structure: $C_{32:1}$-β-hydroxyfatty acyl-D-phenylalanine-D-allothreonine-D-alanine-L-alaninol.[189] Thus, these two were considered to be "deep-rough" mutants of *M. avium*. Separately, these investigators reported that these rough mutants of *M. avium* differ genetically from the smooth forms because of major deletions of portions of the genes responsible for GPL synthesis.[200] Specifically, the defect in the Rg-0 and RG-1 mutants, namely, those devoid of sugars but retaining the lipopeptide portion, was attributed to the deletion of approximately 28 kilobases;

and this particular deletion was thought to be mediated by recombination between repetitive sequences that flank both sides of the 28-kilobase excised region.

Little is known about the biosynthesis of the GPLs. The recognition of two nonglycosylated lipopeptides, obvious core or elemental forms of the GPL antigens, was the culmination of a search begun several years earlier for mutants defective in features of the GPL molecule, particularly glycosyl appendages. Based on the lipopolysaccharide paradigm, it had been suggested that formation of a lipopeptide core was the first phase in the biosynthesis of the GPLs.[7,201] Two separate means exist in prokaryotes for nonribosomal peptide biosynthesis, the principles of either of which may apply to the short tripeptide-amino alcohol core of the GPLs. The first possibility involves a form of direct synthesis in which the amino acids are added directly to an acceptor through the intervention of adenosine triphosphate (ATP). The muramyl-tetrapeptide unit of the peptidoglycan is synthesized in this way.[202] In the case of the peptide antibiotics, the amino acids are attached through thiol groups to a polyenzyme complex, and the peptide bond is subsequently formed through successive pantetheine-aided transpeptidation–transthiolation steps.[203] If this latter mechanism were to apply to GPL biosynthesis, it is likely that the final step in lipopeptide synthesis would involve transfer of the full peptide unit to the fatty acyl function. David *et al.*[204] demonstrated that the addition of *m*-fluorophenylalanine to cultures of *M. avium* inhibited GPL biosynthesis and, specifically, the incorporation of radiolabeled amino acids into lipid. They also showed that D-cycloserine inhibited L-Ala racemization to D-Ala, resulting in a 20% inhibition of Ala incorporation into lipid without affecting the incorporation of allothreonine or Phe. Even though these results do favor the direct synthesis route, additional lipopeptide intermediates of this pathway need to be isolated for definitive proof. From the earlier work of Belisle *et al.*,[205] who actually cloned the genes responsible for the biosynthesis of the oligosaccharide segment of the *M. avium* serovar 2-specific GPL and expressed them in *M. smegmatis* (which naturally contains only the apolar GPLs), it was obvious that the singly glycosylated GPLs are intermediates of the multiglycosylated serovar-specific GPLs. However, further work is required to determine whether the oligosaccharide hapten of the antigenic GPLs is formed on a lipid carrier and then transferred to the simpler GPL or whether the sugars are added singly and sequentially to the growing *O*-linked oligosaccharide chain of the GPLs.

Clearly, the isolation and characterization of a variety of deep rough mutants of *M. avium* represent a major development in the goal of elucidating the biosynthetic pathway of the GPLs. They also provide the means to examine the roles of GPLs in the disease processes induced by *M. avium*, specifically in eliciting an immunosuppressive response.[206]

A strong case has also been made for the PGL-I and related dimycocerosyl phthiocerol in the intracellular survival of *M. leprae*. Early investigators of the microscopic properties of *M. leprae* noted material (capsular matrices, transparent

halos, sheaths, electron-transparent zones) that bound the organism into clumps or globi. In a series of elegant ultrastructural analyses, Fukunishi *et al.*[207] and others redefined the electron-transparent zone and concluded that the materials described in the older literature as "peribacillary substance," "small spherical droplets," "foamy structures," and "capsular materials" were synonymous with substances surrounding *M. leprae* within the phagolysosomes of cells from patients with lepromatous leprosy, macrophages of nude mice, or *M. leprae*-infected armadillos. They further inferred that the electron-transparent zones of individual bacilli coalesced with one another to form distinct intracytoplasmic foamy structures when the lesions became old, and that these were mycobacterial in origin.

For a time, the question of the bacterial origin of these bodies was hotly debated. Hanks,[208] from cytological evidence and the fact that such materials were confined to the leprosy bacillus and disappeared during sulfone therapy, persuasively reasoned that they originated in *M. leprae*. Moreover, since chloroform in aqueous systems declumped and dispersed *M. leprae*, he concluded that mycobacterial lipids were the major bonding substances in the electron-transparent material. Since the material of the capsule can be stained with Sudan Black B, Fisher and Barksdale[209] and Nishiura *et al.*[210] had concluded that the electron-transparent zone which surrounds *M. leprae in vivo* is lipid.

Little doubt remains that the phthiocerol-containing lipids of *M. leprae* are extracellular and comprise the capsular electron-transparent zone. That they are extracellular was obvious from the time of their early discovery; most of them were found in supernatants of homogenized leprosy-infected tissue after the bacteria had been centrifuged down. Further evidence that the capsular material of *M. leprae* is composed in large measure of the phthiocerol-containing lipids is persuasive. The quantities of diacylphthiocerol and phenolic glycolipid recovered from infected tissue is far in excess of that to be expected from the bacillary load.[211] Immunogold labeling of ultrathin sections has been used most effectively to demonstrate "many PGL-I sites" on cell walls of *M. leprae* in human lepromatous skin.[212] Also, capsules were discernible around isolated *M. leprae* cells which displayed heavy PGL-I labeling and which was sometimes confined to an area distinct from the cell wall.[213,214] Also, much extrabacterial PGL-I was encountered by this method.[212–214]

In one effort to address the exact roles of the phthiocerol lipids in the intracellular environment, Neil and Klebanoff[215] examined the ability of PGL-I to scavenge toxic oxygen metabolites, thereby allowing the organisms to survive and replicate. Owing to the failure of *M. leprae* to grow *in vitro*, thus making measurement of viability difficult, *Staphylococcus aureus* was used instead. The staphylococci were exposed to the cell-free myeloperoxidase and xanthine oxidase systems and to human monocyte-derived macrophages, either untreated or activated by γ-interferon, and the effect of added PGL-I on viability was determined. PGL-I proved to be an effective scavenger of the toxic products of the peroxidase–hydrogen peroxide–halide system and also prevented bacterial killing by hydroxyl radicals

generated by the xanthine oxidase system and by γ-interferon-activated macrophages. These conclusions were reinforced by a second study in which electron-spin resonance and spin-trapping was used to demonstrate that PGL-I is especially effective in scavenging hydroxyl radicals and superoxide anions.[216] In addition to its scavenging ability, PGL-I can also apparently inhibit the normal production of superoxide anion by stimulated monocytes,[217] a property that shows surprising specificity in that the phenolic glycolipid K-I from *M. kansasii* or that from *M. bovis* did not show the same effect. In addition, PGL-I of *M. leprae* is also implicated in phagocytosis of bacteria into mononuclear phagocytes. The lipid itself and 3,6-di-*O*-methylglucopyranosyl-containing NGCs bind selectively to complement component 3 in serum, which in turn binds to complement receptors CR1 and CR3 of human mononuclear phagocytes, comprising a three-component receptor–ligand–acceptor complex for mediating phagocytosis of *M. leprae*.[218,219]

Information on the biosynthesis of the phenolic glycolipids is very limited.[220] The carbon atoms in the methyl-branched structures in mycocerosic acids are derived from propanoate.[221,222] So also are those in phthiocerol.[223,224] The aromatic ring can be derived from tyrosine.[224] The methoxyl residue in phenolphthiocerol presumably comes from methionine, by analogy with the known source in the related lipid phthiocerol.[225,226] Rainwater and Kolatukuddy[226] demonstrated two steps in the biosynthesis of mycocerosic acids, and isolated the enzymes involved, but the biosynthetic steps leading to phenolphthiocerol itself are not known.

Draper *et al.*[220] have isolated two lipids from *M. microti* which became labeled when the cells were grown in the presence of [2-^{14}C] propanoate. They were purified by thin-layer chromatography and studied by chemical degradation and mass spectrometry. The lipids were identified as phenolphthiocerol dimycocerosate and phenolphthiodiolone dimycocerosate, the aglycosyl derivatives of mycoside B, the phenolic glycolipid produced by *M. microti*. Cell-free extracts of the organism were able to glycosylate the lipids to form mycoside B *in vitro*. The authors concluded that the lipids are intermediates in the biosynthesis of phenolic glycolipids by mycobacteria. A chapter can now be closed on the discovery, chemical elucidation, and synthesis of the highly unusual glycolipids of *Mycobacterium* spp. The challenges for the future lie in explaining the roles of these copious products in the intracellular life and infectivity of mycobacteria, particularly from a biogenesis and genetic basis. Future research will emphasize the creation of conditional mutants defective in these materials which, in turn, will greatly aid elucidation of their roles in bacterial physiology and pathogenesis.

ACKNOWLEDGMENTS

Research conducted by the authors was supported by a grant (AI-18357) and contract (AI-05074) from the National Institute of Allergy and Infectious Diseases, National Institutes of Health (to PJB), and by operating and strategic research grants from the Natural Sciences and Engineering Research Council of Canada (to GOA).

REFERENCES

1. WHO, Proposed Tuberculosis Control Programme Work Plan and Budget: 1992–1993, November 1991.
2. Centers for Disease Control, *Morbid. Mortal. Wkly. Rep.*, 40 (1992) 1–23.
3. F. M. Collins, *Microbiol. Rev.*, 2 (1989) 360–377.
4. S. K. Noordeen, L. Lopez-Bravo, and T. K. Sundaresan, *Bull. WHO*, 70 (1992) 7–10.
5. R. J. Anderson, *The Harvey Lectures Series*, 35 (1940) 271.
6. D. E. Minnikin, in C. Ratledge and J. Stanford (Eds.), *The Biology of the Mycobacteria*, Vol. 1, Academic Press, New York, 1982, pp. 95–184.
7. M. Goren and P. J. Brennan, in G. P. Youmans (Ed.), *Tuberculosis*, Saunders, Philadelphia, 1979, pp. 63–193.
8. D. E. Minniken, *Res. Microbiol.*, 142 (1991) 423–427.
9. H. L. David, N. Rastogi, S. Clavel-Seres, F. Clement, and M. F. Thorel, *Zbl. Bakt. Hyg.*, A264 (1987a) 49–66.
10. M. R. McNeil and P J. Brennan, *Res. Microbiol.*, 142 (1991) 355–486.
11. M. McNeil, D. Chatterjee, S. W. Hunter, and P. J. Brennan, in V. Ginsburg (Ed.), *Methods in Enzymology*, Vol. 179, Academic Press, San Diego, 1989, pp. 215–242.
12. M. McNeil, A. Y. Tsang, and P. J. Brennan, *J. Biol. Chem.*, 262 (1987) 2630–2635.
13. P. J. Brennan, H. Mayer, G. O. Aspinall, and J. E. Nam Shin, *Eur. J. Biochem.*, 115 (1981) 7–15.
14. D. Chatterjee, G. O. Aspinall, and P. J. Brennan, *J. Biol. Chem.*, 262 (1987) 3528–3533.
15. S. W. Hunter, C. Stewart, and P. J. Brennan, *Int. J. Lepr.*, 53 (1985) 484–486.
16. S. Allen, T. G. Bonner, E. J. Bourne, and N. M. Saville, *Chem. Ind.* (1958) 630.
17. G. J. Gerwig, J. P. Kamerling, and J. F. G. Vliegenthart, *Carbohydr. Res.*, 62 (1978) 349–357.
18. K. Leontein, B. Lindberg, and J. Lönngren, *Carbohydr. Res.*, 62 (1978) 359–362.
19. M. McNeil, H. Gaylord, and P. J. Brennan, *Carbohydr. Res.*, 177 (1988) 185–198.
20. D. Chatterjee, C. Bozic, G. O. Aspinall, and P. J. Brennan, *J. Biol. Chem.*, 263 (1988) 4092–4097.
21. B. Lindberg, J. Lönngren, and J. L. Thompson, *Carbohydr. Res.*, 28 (1973) 351–357.
22. B. Lindberg, *Methods Enzymol.*, 28 (1972) 178–195.
23. S. Hakomori, *J. Biochem. (Tokyo)*, 55 (1964) 205–208.
24. I. Ciucanu and F. Kerek, *Carbohydr. Res.*, 131 (1984) 209–217.
25. P. Prehm, *Carbohydr. Res.*, 78 (1980) 372–374.
26. A. Dell, *Adv. Carbohydr. Chem. Biochem.*, 45 (1986) 19–72.
27. I. Jardine, G. Scanlan, M. McNeil, and P. J. Brennan, *Anal. Chem.*, 61 (1989) 416–422.
28. M. Rivière and G. Puzo, *Biochemistry*, 31 (1992) 3575–3580.
29. D. W. Smith, W. K. Harrell, and H. M. Randall, *Am. Rev. Tuberc.*, 69 (1954) 505–510.
30. D. W. Smith, H. M. Randall, M. M. Gastambide-Odier, and A. L. Koevoet, *Ann. N.Y. Acad. Sci.*, 69 (1957) 145–157.
31. D. W. Smith, H. M. Randall, A. P. MacLennan, and E. Lederer, *Nature (London)*, 186 (1960) 887–888.
32. D. W. Smith, H. M. Randall, A. P. MacLennan, R. K. Putney, and S. V. Rao, *J. Bacteriol.*, 79 (1960) 217–229.
33. G. B. Fregnan, D. W. Smith, and H. M. Randall, *J. Bacteriol.*, 83 (1962) 828–836.
34. P. J. Brennan and M. B. Goren, *J. Biol. Chem.*, 254 (1979) 4205–4211.
35. M. B. Goren, *Am. Rev. Respir. Dis.*, 125 (1982) 50–69.
36. W. B. Schaefer, *Am. Rev. Respir. Dis.*, 92 (Suppl.) (1965) 85–93.
37. W. B. Schaefer, in T. Bergan and J. R. Norris (Eds.), *Methods in Microbiology*, Vol. 13, Academic Press, London 1979, pp. 323–344.
38. E. Wolinsky and W. B. Schaefer, *Int. J. Syst. Bacteriol.*, 23 (1973) 182–183.
39. E. Wolinsky, *Am. Rev. Respir. Dis.*, 119 (1979) 107–159.

40. P. A. Jenkins, *Rev. Infect Dis.*, 3 (1981) 862–866.
41. P. A. Jenkins, J. Marks, and W. B. Schaefer, *Tubercle*, 53 (1972) 118–127.
42. T. Marks, P. A. Jenkins, and M. Tsukamura, *Tubercle*, 53 (1972) 210–214.
43. S. W. Hunter, R. C. Murphy, K. Clay, M. B. Goren, and P. J. Brennan, *J. Biol. Chem.*, 258 (1983) 10481–10487.
44. S. Saadat and C. E. Ballou, *J. Biol. Chem.*, 258 (1983) 1813–1818.
45. K-I. Kamisango, S. Saadat, A. Dell, and C. E. Ballou, *J. Biol. Chem.*, 260 (1985) 4117–4121.
46. P. J. Brennan, G. O. Aspinall, and J. E. Nam Shin, *J. Biol. Chem.*, 256 (1981) 6817–6822.
47. P. J. Brennan, in C. Ratledge and S. G. Wilkinson (Eds.), *Microbial Lipids*, Vol. I, Academic Press, London 1988, pp. 203–298.
48. C. M. Bozic, M. McNeil, D. Chatterjee, I. Jardine, and P. J. Brennan, *J. Biol. Chem.*, 263 (1988) 14984–14991.
49. R. T. Camphausen, R. L. Jones, and P. J. Brennan, *Proc. Natl. Acad Sci. U.S.A.*, 82 (1985) 3068–3072.
50. G. O. Aspinall, N. K. Khare, R. K. Sood, D. Chatterjee, B. Rivoire, and P. J. Brennan, *Carbohydr. Res.*, 216 (1991) 357–373.
51. W. W. Barrow, B. P. Ullom, and P. J. Brennan, *J. Bacteriol.*, 144 (1980) 814–822.
52. J. C. Denner (1991) M.S. Thesis, Colorado State University.
53. A. Y. Tsang, V. L. Barr, J. K. McClatchy, M. Goldberg, I. Drupa, and P. J. Brennan, *Int. J. Syst. Bacteriol.*, 34 (1984) 35–44.
54. L. M. Lopez-Marin, M.-A. Lanéelle, D. Prome, M. Daffé, G. Lanéelle, and J. C. Prome, *Biochemistry*, 30 (1991) 10536–10542.
54a. G. S. Besra, S. S. Gurcha, K.-H. Khoo, H. R. Morris, A. Dell, M. H. Hamid, D. E. Minnikin, M. Goodfellow, and P. J. Brennan, *Zbl. Bakt.*, 281 (1994) 415–432.
55. M. Rivière and G. Puzo, *J. Biol. Chem.*, 266 (1991) 9057–9063.
56. G. S. Besra, M. R. McNeil, B. Rivoire, K-H. Khoo, H. R. Morris, A. Dell, and P. J. Brennan, *Biochemistry*, 32 (1993) 347–355.
57. P. J. Brennan, M. Souhrada, B. Ullom, J. K. McClatchy, and M. B. Goren, *J. Clin. Microbiol.*, 8 (1978) 374–379.
58. S. W. Hunter, I. Jardine, D. L. Yanagihara, and P. J. Brennan, *Biochemistry*, 24 (1985) 2798–2805.
59. S. W. Hunter, T. Fujiwara, R. C. Murphy, and P. J. Brennan, *J. Biol. Chem.*, 259 (1984) 9729–9734.
60. J. Yoshimura, A. Agael, K.-I. Sato, R. B. Singh, and H. Hashimoto, *Carbohydr. Res.*, 166 (1987) 253–262.
61. M. McNeil, A. Y. Tsang, J. K. McClatchy, C. Stewart, I. Jardine, and P. J. Brennan, *J. Bacteriol.*, 169 (1987) 3312–3320.
62. S. W. Hunter, V. L. Barr, M. McNeil, I. Jardine, and P. J. Brennan, *Biochemistry*, 27 (1988) 1549–1556.
63. R. T. Camphausen, M. McNeil, I. Jardine, and P. J. Brennan, *J. Bacteriol.*, 169 (1987) 5473–5480.
64. G. S. Besra, M. R. McNeil, and P. J. Brennan, *Biochemistry*, 31 (1992) 6504–6509.
65. G. S. Besra, M. R. McNeil, A. Dell, K.-H. Khoo, and P. J. Brennan, *Biochemistry*, 32 (1993) 12705–12714.
66. M. Daffe, M. McNeil, and P. J. Brennan, *Biochemistry*, 30 (1991) 378–388.
67. D. E. Minnikin, G. Dobson, D. Sesardic, and M. Ridell, *J. Gen. Microbiol.*, 131 (1985) 1369–1374.
68. G. S. Besra, R. C. Bolton, M. McNeil, M. Ridell, K. E. Simpson, J. Glushka, H. van Halbeck, P. J. Brennan, and D. E. Minnikin, *Biochemistry*, 31 (1992) 9832–9837.

69. C. E. Ballou, *Pure Appl. Chem.*, 53 (1981) 107–112.
70. G. S. Besra, K.-H. Khoo, J. T. Belisle, M. R. McNeil, H. R. Morris, A. Dell, and P. J. Brennan, *Carbohydr. Res.*, 251 (1994) 99–114.
70a. K.-H. Khoo, R. Susuki, H. R. Morris, A. Dell, P. J. Brennan, and G. S. Besra, *Carbohydr. Res.*, in press.
71. S. W. Hunter and P. J. Brennan, *J. Bacteriol.*, 147 (1981) 728–735.
72. E. Tarelli, P. Draper, and S. N. Payne, *Carbohydr. Res.*, 131 (1984) 346–352.
73. S. W. Hunter, T. Fujiwara, and P. J. Brennan, *J. Biol. Chem.*, 257 (1982) 15072–15078.
74. S. W. Hunter and P. J. Brennan, *J. Biol. Chem.*, 258 (1983) 7556–7562.
75. H. Noll and E. Jackim, *J. Biol. Chem.*, 232 (1958) 903–917.
76. H. Demarteau-Ginsburg, E. Lederer, and C. R. Seances, *Acad. Sci. Ser. C*, 240 (1955) 815–817.
77. M. Daffé, C. Lacave, M.-A. Lanéelle, and G. Lanéelle, *Eur. J. Biochem.* 167 (1987) 155–160.
78. D. Chatterjee, C. M. Bozic, C. Knisley, S.-N. Cho, and P. J. Brennan, *Infect. Immun.*, 57 (1989) 322–330.
79. A. Vercellone and G. Puzo, *J. Biol. Chem.*, 264 (1989) 7447–7454.
80. M. Gastambide-Odier and P. Sarda, *Pneumonologie*, 142 (1970) 241–255.
81. J. J. Fournié, M. Rivière, and G. Puzo, *J. Biol. Chem.*, 262 (1987) 3174–3179.
82. J. J. Fournié, M. Rivière, and G. Puzo, *J. Biol. Chem.*, 262 (1987) 3180–3184.
83. J. J. Fournié, M. Rivière, and G. Puzo, *Eur. J. Biochem.*, 168 (1987) 181–183.
84. G. Puzo, *Rev. Microbiol.*, 17 (1990) 305–327.
85. H. Demarteau-Ginsburg and E. Lederer, *Biochim. Biophys. Acta*, 70 (1963) 442–451.
86. M. Daffé, A. Varnerot, and V. V. Levy-Frebault, *J. Gen. Microbiol.*, 133 (1992) 131–137.
87. G. Dobson, D. E. Minnikin, G. S. Besra, A. I. Mallet, and M. Magnusson, *Biochim. Biophys. Acta*, 1042 (1990) 176–181.
88. R. G. Navalkar, E. Wiegeshaus, E. Kando, H. K. Kim, and D. W. Smith, *J. Bacteriol.*, 90 (1965) 262–265.
89. P. Sarda and M. Gastambide-Odier, *Chem. Phys. Lipids*, 1 (1967) 434–444.
90. G. S. Besra, D. E. Minnikin, L. Rigouts, F. Portaels, and M. Ridell, *Letters Appl. Microbiol.*, 11 (1990) 202–204.
91. G. S. Besra, M. McNeil, D. Minnikin, F. Portaels, M. Ridell, and P. J. Brennan, *Biochemistry*, 30 (1991) 7772–7777.
92. A. Vercellone, M. Rivière, J. J. Fournié, and G. Puzo, *Chem. Phys. Lipids*, 48 (1988) 129–131.
93. M. Gilleron, J. Vercauteren, and G. Puzo, *J. Biol. Chem.*, 268 (1993) 3168–3179.
94. T. Fujiwara, S. W. Hunter, S.-N. Cho, G. O. Aspinall, and P. J. Brennan, *Infect Immun.*, 43 (1984) 245–252.
95. R. Gigg, S. Payne, and R. Conant, *J. Carbohydr. Chem.*, 2 (1983) 207–223.
96. T. Fujiwara, S. W. Hunter, and P. J. Brennan, *Carbohydr. Res.*, 148 (1986) 287–298.
97. T. Fujiwara, G. O. Aspinall, S. W. Hunter, and P. J. Brennan, *Carbohydr. Res.*, 163 (1987) 41–52.
98. G. R. Gray, *Methods Enzymol.*, 50 (1978) 155–160.
99. R. U. Lemieux, D. R. Bundle, and D. A. Baker, *J. Am. Chem. Soc.*, 97 (1975) 4076–4086.
100. R. U. Lemieux, D. A. Baker, and D. R. Bundle, *Can. J. Biochem.*, 55 (1977) 507–512.
101. D. Chatterjee, J. T. Douglas, S.-N. Cho, T. H. Rea, R. H. Gelber, G. O. Aspinall, and P. J. Brennan, *Glycoconjugate J.*, 2 (1985) 187–208.
102. D. Chatterjee, S.-N. Cho, P. J. Brennan, and G. O. Aspinall, *Carbohydr. Res.*, 156 (1986) 39–56.
103. D. Chatterjee, S.-N. Cho, C. Stewart, J. T. Douglas, T. Fujiwara, and P. J. Brennan, *Carbohydr. Res.*, 183 (1988) 241–260.
104. T. Fujiwara, S. Izumi, and P. J. Brennan, *Agric. Biol. Chem.*, 49 (1985) 2301–2308.
105. T. Fujiwara and S. Izumi, *Agric. Biol. Chem.*, 51 (1987) 2539–2547.
106. J. Gigg, R. Gigg, S. Payne, and R. Conant, *J. Chem. Soc. Perkin Trans. I*, (1987) 1165–1170.
107. V. Verez-Bencomo, M. T. Campos-Valdes, J. R. Marino-Albernas, V. Fernandex-Santana, M. Hernandez-Rensoli, and C. S. Perez-Martinez, *Carbohydr. Res.*, 217 (1991) 263–267.

108. P. J. Garegg and B. Gotthammer, *Carbohydr. Res.*, 58 (1977) 345–352.
109. C. R. McBroom, C. H. Samanen, and I. J. Goldstein, *Methods Enzymol.*, 28B (1972) 212–219.
110. N. K. Kochetov, B. A. Dmitriev, A. Ya. Chernyak, and A. B. Levinsky, *Carbohydr. Res.*, 110 (1982) C16–C20.
111. J. Marino-Albernas, V. Verex Bencomo, L. Gonzalez-Rodriguez, C. S. Perez-Martinez, E. Gonzalez-Abreu Castell, and A. Gonzalez-Segredo, *Carbohydr. Res.*, 183 (1988) 175–182.
112. J. R. Marino-Albernas, V. Vincente-Bencomo, L. Gonzalez, and E. S. Perez, *Carbohydr. Res.*, 165 (1987) 197–206.
113. J. Gigg, R. Gigg, S. Payne, and R. Conant, *Chem. Phys. Lipids*, 38 (1985) 299–307.
114. A. Liav and M. B. Goren, *Carbohydr. Res.*, 149 (1986) C13–C16.
115. A. K. Sen, K. S. Sarkar, and N. Banerji, *J. Carbohydr. Chem.*, 7 (1988) 645–654.
116. J. Gigg, R. Gigg, S. Payne, and R. Conant, *Carbohydr. Res.*, 141 (1985) 91–97.
117. S. J. Brett, S. N. Payne, P. Draper, and R. Gigg, *Clin. Exp. Immunol.*, 56 (1984) 89–96.
118. J. Marino-Albernas, V. Verez-Bencomo, L. Gonzalez, C. S. Perez, E. Gonzalez-Abreu Castell, and A. Gonzalez-Segredo, *Interferon Y. Biotecnologia*, 4 (1987) 65–68.
119. A. Borbas and A. Lipták, *Carbohydr. Res.*, 241 (1993) 99–116.
119a. A. Lipták, A. Borbás, and I. Bajza, *Rev. Med. Res.*, 14 (1994) 307–352.
120. M. A. Bernstein and L. D. Hall, *Carbohydr. Res.*, 78 (1980) C1–C3.
121. B. Rivoire, B. J. Ranchoff, D. Chatterjee, H. Gaylord, A. Y. Tsang, A. H. J. Kolk, G. O. Aspinall, and P. J. Brennan, *Infect. Immun.*, 57 (1989) 3147–3158.
122. G. O. Aspinall, A. M. Crane, D. W. Gammon, I. H. Ibrahim, N. K. Khare, D. Chatterjee, B. Rivoire, and P. J. Brennan, *Carbohydr. Res.*, 216 (1991) 337–355.
123. P. Fügedi, P. J. Gareff, H. Lönn, and T. Norberg, *Glycoconjugate J.*, 4 (1987) 97–108.
124. G. O. Aspinall, I. H. Ibrahim, and N. K. Khare, *Carbohydr. Res.*, 200 (1990) 247–256.
125. H. Paulsen, F. R. Jeiker, J. Feldmann, and K. Heyns, *Synthesis*, (1980) 636–638.
126. P. H. J. Carlsen, T. Katsuki, V. S. Martin, and K. B. Sharpless, *J. Org. Chem.*, 46 (1981) 3936–3938.
127. A. Lipták and P. Fügedi, *Angew. Chem. Int. Ed. Engl.*, 22 (1982) 255–261.
128. S. David, A. Thieffry, and A. Veyrières, *J. Chem. Soc. Perkin Trans.* 1, (1981) 1796–1801.
129. R. Johansson and B. Samuelsson, *J. Chem. Soc. Perkin Trans.* 1, (1984) 2371–2374.
130. D. G. Bartholomew and A. D. Broom, *J. Chem. Soc. Commun.*, (1974) 38.
131. S. Josephson and D. R. Bundle, *J. Chem. Soc. Perkin Trans.*, 1, (1980) 297–301.
132. J. Yoshimura, A. Aqell, K. I. Sato, R. B. Singh, and H. Hashimoto, *Carbohydr. Res.*, 166 (1987) 253–262.
133. I. Bajza and A. Lipták, *Carbohydr. Res.*, 205 (1990) 435–439.
134. R. M. Giuliano and S. Kasperowicz, *Carbohydr. Res.*, 183 (1988) 277–285.
135. A. Klemer, A. Prahst, H. Stegt, and J. Thiem, *J. Carbohydr. Chem.*, 5 (1986) 67–86.
136. D. A. Evans, K. T. Chapman, and E. M. Carreira, *J. Am. Chem. Soc.*, 110 (1988) 3560-3578.
137. R. R. Schmidt, *Angew. Chem. Int. Ed. Engl.*, 25 (1986) 212–235.
138. G. O. Aspinall, D. W. Gammon, R. K. Sood, D. Chatterjee, B. Riviore, and P. J. Brennan, *Carbohydr. Res.*, 237 (1992) 57–77.
139. S. David and A. Thieffry, *J. Chem. Soc. Perkin Trans.*, 1 (1979) 1568–1572.
140. G. V. Reddy, V. R. Kulkarni, and H. B. Mereyala, *Tetrahedron Lett.*, 30 (1989) 4283–4286.
141. B. Fraser-Reid, U. E. Udodong, Z.Wu, H. Ottosson, J. R. Merritt, C. S. Rao, C. Roberts, and R. Madsen, *Synlett*, (1992) 927–942.
142. G. H. Veeneman and J. H. van Boom, *Tetrahedron Lett.*, 31 (1990) 275–278.
143. G. H. Veeneman, S. H. van Leeuwen, and J. H. van Boom, *Tetrahedron Lett.*, 31 (1990) 1331–1334.
144. M. K. Gurjar and G. Viswanadham, *Tetrahedron Lett.*, 32 (1991) 6191–6194.
145. M. K. Gurjar and G. Viswanadham, *J. Carbohydr. Chem.*, 10 (1991) 481–485.

146. H. M. Zuurmond, G. H. Veeneman, G. A. van der Marel, and J. H. van Boom, *Carbohydr. Res.*, 241 (1993) 153–164.
147. J. Kerékgyártó, Z. Szurmai, and A. Lipták, *Carbohydr. Res.*, 245 (1993) 65–80.
148. I. Bajza, J. Kerékgyártó, J. Hajkó, and A. Lipták, *Carbohydr. Res.*, 245 (1993) 65–80.
149. T. Ziegler, *Angew. Chem. Int. Ed. Engl.*, 31 (1992) 1358–1360.
150. T. Ziegler, E. Eckhardt, and G. Herold, *Liebigs Ann. Chem.* (1992) 441–451.
150a. T. Ziegler, *Carbohydr. Res.*, 253 (1994) 151–166.
151. M. K. Gurjar and U. K. Saha, *Tetrahedron Lett.*, 32 (1991) 6621–6624.
152. T. Fujiwara, *Agric. Biol. Chem.*, 55 (1991) 2123–2128.
153. G. H. Veeneman, S. H. van Leeuwen, H. Zuurmond, and J. H. van Boom, *J. Carbohydr. Chem.*, 9 (1990) 783–796.
154. M. K. Gurjar, K. R. Reddy, *Carbohydr. Res.*, 226 (1992) 233–238.
155. K. Zegelaar-Jaarsveld, G. A. van der Marel, and J. H. van Boom, *Tetrahedron Lett.*, 46 (1992) 10133–10148.
156. M. Gilleron, A. Venisse, J. J. Fournié, M. Rivière, N. Gas, and G. Puzo, *Eur. J. Biochem.*, 189 (1990) 167–173.
157. M. Rivière, J. J. Fournié, and G. Puzo, *J. Biol. Chem.*, 262 (1987) 14879–14884.
158. M. Gilleron, A. Venisse, M. Rivière, P. Servin, and G. Puzo, *Eur. J. Biochem.*, 193 (1990) 449–456.
159. M. K. Gurjar and U. K. Saha, *Tetrahedron Lett.*, 34 (1992) 4979–4982.
160. M. K. Gurjar and A. S. Mainkar, *Tetrahedron*, 48 (1992) 6729–6738.
161. M. K. Gurjar and U. K. Saha, *Tetrahedron*, 48 (1992) 4039–4044.
162. C. C. Hawkins, J. W. M. Gold, E. Whimbey, T. E. Kiehn, P. Brannon, R. Commarata, A. E. Brown, and D. Armstrong, *Ann. Int. Med.*, 105 (1986) 184–188.
163. R. C. Good, *Annu. Rev. Microbiol.*, 39 (1985) 347–369.
164. M. A. Yarus and R. C. Good, *J. Clin. Microbiol.*, 28 (1990) 926–929.
165. G. Meissner and W. Anz, *Am. Rev. Respir. Dis.*, 92 (1965) 85–93.
166. B. Y. Lee, D. Chatterjee, C. M. Bozic, P. J. Brennan, D. L. Cohn, J. D. Bales, S. M. Harrison, L. A. Andron, and I. M. Orme, *J. Clin. Microbiol.*, 29 (1991) 1026–1029.
167. S.-N. Cho, D. L. Yanagihara, S. W. Hunter, R. H. Gelber, and P. J. Brennan, *Infect. Immun.*, 41 (1983) 1077–1083.
168. S. J. Brett, P. Draper, S. N. Payne, and R. J. W. Rees, *Clin. Exp. Immunol.*, 52 (1983) 221–279.
169. P. J. Brennan, D. Chatterjee, T. Fujiwara, and S.-N. Cho, *Methods Enzymol.*, 242 (1994) 27–37.
170. S. Izumi, T. Fujiwara, M. Ikeda, Y. Nishimura, K. Sugiyama, and K. Kawatsu, *J. Clin. Microbiol.*, 28 (1990) 525–529.
171. D. B. Young and T. M. Buchanan, *Science*, 221 (1983) 1057–1059.
172. R. C. Hastings, T. P. Gillis, J. L. Krahenbuhl, and S. G. Franzblau, *Clin. Microbiol. Rev.*, 1 (1988) 330–348.
173. S. Chanteau, J. L. Cartel, C. Guidi, R. Pichart, and M.-A. Bach, *Int. J. Lepr.*, 55 (1987) 626–632.
174. A. F. Bagshawe, R. J. Garsia, K. Baumgart, and L. Astbury, *Int. J. Lepr.*, 58 (1990) 25–30.
175. J. T. Douglas, R. V. Celona, M. G. Madarang, and T. Fajardo, *Int. J. Lepr.*, 55 (1987) 718–721.
176. H. Gaylord and P. J. Brennan, *Ann. Rev. Microbiol.*, 41 (1987) 645–675.
177. S.-N. Cho, S. W. Hunter, R. H. Gelber, T. H. Rea, and P. J. Brennan, *J. Infect. Dis.*, 153 (1986) 560–569.
178. D. B. Young, M. J. Fohn, and T. M. Buchanan, *J. Immunol. Methods*, 79 (1985) 205–211.
179. S.-N. Cho, R. V. Cellona, T. T. Fajardo, Jr., R. M. Abalos, E. C. de la Cruz, G. P. Walsh, J.-D. Kim, and P. J. Brennan, *Int. J. Lepr.*, 59 (1991) 25–31.
180. N. M. Casabona, T. G. Fuente, L. A. Arce, J. O. Entraigas, and R. V. Pla, *Acta Leprologica*, 7 (1989) 89–93.
181. J. Torgal-Garcia, F. Papa, and H. L. David, *Acta Leprologica*, 7 (1989) 102–106.

182. M. Daffé, S.-N. Cho, D. Chatterjee, and P. J. Brennan, *J. Infect. Dis.*, 163 (1991) 161–168.
183. D. E. Minnikin, G. Dobson, D. Sesardic, and M. Ridell, *J. Gen. Microbiol.*, 131 (1985) 1369–1374.
184. M. Ridell, G. Wallerstrom, D. E. Minnikin, R. C. Bolton, and M. Magnusson, *Tubercle Lung Dis.*, 73 (1992) 101–105.
185. F. Papa, M. Rivière, J. J. Fournié, G. Puzo, and H. David, *J. Clin. Microbiol.*, 25 (1987) 2270–2273.
186. J. T. Belisle and P. J. Brennan, *J. Bacteriol.*, 171 (1989) 3465–3470.
187. R. W. Stokes and F. M. Collins, *Infect. Immun.*, 56 (1988) 2250–2254.
188. P. Draper, *J. Gen Microbiol.*, 83 (1974) 431–433.
189. L. Barksdale, *Bacteriol. Rev.*, 41 (1977) 217–372.
190. S. Rulong, A. P. Aguas, P. P. Silva, and M. T. Silva, *Infect. Immun.*, 59 (1991) 3895–3902.
191. G. Meissner, *Rev. Infect. Dis.*, 3 (1981) 953–959.
192. P. R. Meylan, D. D. Richman, and R. S. Kornbluth, *Infect. Immun.*, 58 (1990) 2564–2568.
193. T. E. Kiehn, F. F. Edwards, P. Brannon, A. Y. Tsang, M. Maio, J. W. Gold, E. Whimbey, B. Wong, J. K. McClatchy, and D. Armstrong, *J. Clin. Microbiol.*, 21 (1985) 168–172.
194. J. T. Crawford and J. H. Bates, *Am. Rev. Respir. Dis.*, 134 (1986) 659-664.
195. H. Shiratsuchi, Z. Toossi, M. A. Mettler, and J. J. Ellner, *J. Immunol.*, 150 (1993) 2945–2954.
195a. S. K. Furney, P. S. Skinner, A. D. Roberts, R. Appelberg, and I. M. Orme, *Infect. Immun.*, 60 (1992) 4410–4413.
196. N. Rastogi, C. Frehl, A. Ryter, H. Ohanyon, M. Lesourd, and H. L. David, *Antimicrob. Agents Chemother.*, 20 (1981) 666–667.
197. M. J. Tereletsky and W. W. Barrow, *Infect. Immun.*, 41 (1983) 1312–1321.
198. W. W. Barrow and P. J. Brennan, *J. Bacteriol.*, 150 (1982) 381–384.
199. J. T. Belisle, M. R. McNeil, D. Chatterjee, J. M. Inamine, and P. J. Brennan, *J. Biol. Chem.*, 268 (1993) 10510–10516.
200. J. T. Belisle, K. Klaczkiewicz, P. J. Brennan, W. R. Jacobs, and J. M. Inamine, *J. Biol. Chem.*, 268 (1993) 10517–10523.
201. P. J. Brennan, in L. Leive and D. Schlessinger (Eds.), *Microbiology*, American Society for Microbiology, Washington, D.C., 1984, pp. 366–375.
202. J. M. Ghuysen, in G. Poste and G. L. Nicolson (Eds.), *Cell Surface Reviews Vol. 4: The Synthesis, Assembly, and Turnover of Cell Surface Components*, North–Holland, Amsterdam, 1977, pp. 463–595.
203. D. Perlman and M. Bodanszky, *Annu. Rev. Biochem.*, 40 (1971) 449–464.
204. H. L. David, N. Rastogi, S. Clavel-Seres, and F. Clement, *Curr. Microbiol.*, 17 (1988) 61–68.
205. J. T. Belisle, L. Pascopella, J. M. Inamine, P. J. Brennan, and W. R. Jacobs, Jr., *J. Bacteriol.*, 173 (1991) 6991–6997.
206. S. K. Tassel, M. Pourshafie, E. L. Wright, M. G. Richmond, and W. W. Barrow, *Infect. Immun.*, 60 (1992) 706–711.
207. Y. Fukunishi, S. Okada, M. Nishiura, and K. Kohsada, *Int. J. Lepr.*, 50 (1982) 68–75.
208. J. H. Hanks, *Int. J. Lepr.*, 29 (1961) 172–178.
209. C. A. Fisher and L. Barksdale, *J. Bacteriol.*, 106 (1971) 707–713.
210. M. Nishiura, Y. Fukunishi, S. Ohada, M. Ane, K. Kohsaka, K. Yoneda, T. Mori, T. Ito, A. Bretana, J. Convin, G. P. Walsh, W. M. Meyers, and C. H. Binford, *Int. J. Lepr.*, 48 (1980) 493–494.
211. P. J. Brennan, *J. Biosci.*, 6 (1984) 685–689.
212. J. Boddingius and H. Dijkman, *J. Gen. Microbiol.*, 136 (1990) 2001–2012.
213. J. Boddingius and H. P. Dijkman, *J. Biochem. Cytochem.*, 37 (1989) 455–462.
214. J. Boddingius and H. Dijkman, *Acta Leprologica*, 7 (1989) 107–112.
215. M. A. Neill and S. J. Klebanoff, *J. Exp. Med.*, 167 (1988) 30–42.

216. J. Chan, T. Fujiwara, P. Brennan, M. McNeil, S. J. Turco, J.-C. Sibille, M. Snapper, P. Aisen, and B. R. Bloom, *Proc. Natl. Acad. Sci. U.S.A.*, 86 (1989) 2453–2457.
217. M. Vachula, T. J. Holzer, and B. R. Andersen, *J. Immunol.*, 142 (1989) 1696–1701.
218. L. S. Schlessinger and M. A. Horwitz, *J. Exp. Med.*, 174 (1991) 1031–1038.
219. L. S. Schlessinger and M. A. Horwitz, *J. Clin. Invest.*, 85 (1990) 1304–1314.
220. P. F. Thurman, W. Chai, J. R. Rosankiewica, H. J. Rogers, A. M. Lawson, and P. Draper, *Eur. J. Biochem.*, 212 (1993) 705–711.
221. M. Gastambide-Odier, J.-M. Delaumény, and E. Lederer, *Biochem. Biophys. Acta*, 70 (1963) 670–678.
222. I. Yano and M. Kusunose, *Biochem. Biophys. Acta*, 116 (1966) 593–596.
223. M. Gastambide-Odier, P. Sarda, and E. Lederer, *Bull. Soc. Chim. Biol.*, 49 (1967) 849–864.
224. M. Gastambide-Odier and P. Sarda, *Pneumonologie*, 142 (1970) 241–255.
225. M. Gastambide-Odier, J.-M. Delaumény, and E. Lederer, *Chem. Ind.*, (1963) 1285–1286.
226. D. L. Rainwater and P. E. Kolattukudy, *J. Biol. Chem.*, 260 (1985) 616–623.

ADVANCES IN CARBOHYDRATE CHEMISTRY AND BIOCHEMISTRY, VOL. 51

NONCONVENTIONAL METHODS OF MODIFICATION OF STARCH

BY PIOTR TOMASIK AND MARK F. ZARANYIKA

Chemistry Department, Faculty of Science, University of Zimbabwe, Harare, Zimbabwe

I. INTRODUCTION

Starch is the most readily available and abundant pure carbohydrate. As a continuously renewable resource it has provided a source of energy for human beings and organisms from bacteria to mammalia. The first utilization of modified starch may even precede the discovery of fire. The same may be assumed for the enzymic transformation of starch into alcohol.

The first scientific report on modification of starch was published by Roard[1] in 1804 and concerned the dry thermolysis of starch to dextrins. Since that time, starch has sustained significant interest as the source of such materials as the pure amylose and amylopectin components of starch, along with soluble starch, dextrins, chemically modified starches, oligosaccharides, and glucose. Depolymerization of starch is the most frequently utilized procedure for manufacture of nutritional products as well as nonnutritional materials (glues, sizing agents for

textiles and paper, thickeners, additives in cosmetics, and so on). Polymerization of starch has been less frequently studied, although it has more recently become employed, generally through chemical grafting and crosslinking.

Depolymerizing modification of starch usually involves the use of enzymes, acid- (and less frequently base-) catalyzed hydrolysis, and thermolysis alone and thermolysis combined with acid-catalyzed hydrolysis (see a recent survey in this Series[2]). Despite several studies, the physical treatment of starch has not yet resulted in major practical applications. The aim of this Chapter is to review physical methods as tools for the treatment of starch which deliver amounts of energy suitable for depolymerizing starch to target products. It should be noted that the duration of such processes does not need to exceed that for conventional, namely enzymic, chemical, and thermal modifications. Moreover, a potential advantage of nonconventional physical treatments is the fact that they generate no waste products.

Nonconventional modifications of starch involving desiccation; treatment with solvents; high pressure; freezing; irradiation by neutrons, electrons, X-rays, γ-rays, infrared, ultraviolet, and microwave radiation; and also ultrasonication lead, as a rule, to destruction of starch. The energies imparted by these various means, and the mechanism of destruction, may be very different. Any comparison of results of treatment based solely on the energy delivered to starch may be rather meaningless. Thus far, suitably extensive comparative studies that would point to which methods are more destructive and which are less are lacking. Some comparisons have been published by Samec,[3] who performed studies on starch of nine different origins. He irradiated them with γ-rays, a beam of electrons, and ultrasound. The results, some of which are presented in Table I, show that γ-rays and ultrasound affect starch to quite different extents. At the outset, it is essential to specify whether solid starch, gelatinized starch, or its sols are modified. Starch sols are not affected by ultrasound.[4] With gelatinized starch, both γ-radiation and sonication decrease the viscosity and molecular mass of the gel to a similar extent. There is a decrease in the relative content of amylopectin and in the iodine uptake, with ultrasound giving the more pronounced effect. The permeability of the modified starch through collodion membranes increases, and the effect is much greater in the case of γ-irradiated products. The beta-amylolytic index and the pH vary irregularly. The effects of irradiation by electrons and by γ-rays differ only slightly. The author[3] suggests that both of these methods may be used to distinguish between starches of different origin. The same author has also[5] compared the effect of sonication, irradiation with UV light, X-rays, and γ-rays on potato starch. Both sonication and UV radiation degraded starch in a similar manner, although UV irradiation also caused some hydrolysis and oxidation. Both X- and γ-rays produce similar effects, and these are different from those obtained upon sonication and UV irradiation. Thus while ultrasound and UV irradiation do not split phosphoric acid esters, X- and γ-rays do cause their cleavage. Nevertheless (see Table II) comparative studies on modification of corn (maize) starch by acid

TABLE I

Properties of Starch of Various Origins Modified by Ultrasound and γ-Rays[a]

Property	Origin[a]	Characterized form				
		Gel			Sol	
		Original[b]	γ-Rays (2×10^6 rad)	Ultrasound (14 kHz, 5 h)	Original[b]	γ-Rays (2×10^6 rad)
Appearance	C	Little d	Quite d	cl	Quite d	cl, y-sh
	S	w d	w d	Little d	w d sed	w d
	M	d	d-sh	d-sh	d	Quite cl
	T	d-sh	d-sh	Quite d	Quite d y-sh	d y-sh
	WM	d y-sh	y op	Quite d, fl	d-sh y-sh	Quite cl, ppt
	HAM	ppt	d, partly sed	w d, ppt	w d, ppt	w d
	WS	w d	oq, y op	d-sh	d y	dsh
Viscosity ($t/t1$)	C	1.97	1.34	1.07	3.06	1.83
	S	1.74	1.11	1.07	1.62	1.32
	M	3.53	1.16	1.07	1.65	1.13 –
	T	3.13	1.2	1.07	1.62	1.07
	WM	5.86	1.17	1.16	2.11	1.07
	HAM	1.04	1.21	1.15	1.23	1.21
	WS	5.32	1.41	1.04	2.37	1.07
Reducing value (% of maltose)	C	0.4	1.46	0.81	0.15	1.78
	S	0.29	1.92	0.75	0.36	2.57
	M	0.24	1.60	0.81	0.30	2.14
	T	0.16	1.59	0.61	0.19	2.19
	WM	0.16	1.66	0.48	0.21	2.24
	HAM	0.63	1.87	1.12	0.67	2.30
	WS	0.17	1.67	0.59	0.25	2.33
pH	C	6.84	4.91	6.91	6.87	4.04
	S	4.0	3.9	6.1	4.16	3.77
	M	5.38	3.51	6.7	5.37	4.10

continues

TABLE I—(*Continued*)

Property	Origin[a]	Characterized form				
		Gel			Sol	
		Original[b]	γ-Rays (2×10^6 rad)	Ultrasound (14 kHz, 5 h)	Original[b]	γ-Rays (2×10^6 rad)
	T	4.2	3.9	6.5	5.1	3.8
	WM	4.76	3.56	4.35	4.48	3.36
	HAM	6.0	4.22	6.1	5.78	3.82 –
	WS	4.9	3.95			
Iodine uptake (%)	C	4.73	4.86	4.77	4.95	4.78
	S	3.22	3.05	5.55	3.56	2.64
	M	3.88	3.79	3.99	3.83	3.68
	T	3.01	2.8	4.37	2.98	2.62
	WM	0.34	0.43	0.53	0.59	0.63
	HAM	5.04	5.41	6.18	4.39	6.74
	WS	0.68	0.55	0.68	0.68	0.74
Beta-Amylolytic index	C	54.47	55.59	69.65	55.63	59.50
	S	61.11	57.59	63.84	62.05	59.70
	M	53.94	52.11	68.02	51.38	62.37
	T	54.67	59.82	66.11	53.12	63.68
	WM	51.52	54.93	51.32	52.41	55.80
	HAM	28.81	35.75	75.02	36.34	46.75
	WS	59.06	57.32	61.04	59.91	59.86

[a]C, Canna; S, sorghum; M, marantha; T, tapioca (cassava); WM, waxy maize; HAM, high amylose maize; WS, waxy sorghum. [b]d, dull; d-sh, dullish; y, yellow; y-sh, yellowish; ppt, precipitate; w, white; op, opalescence; oq, opaque; fl, floccules; sed, sediment; cl, clear.

TABLE II

Properties of 2% Gel of Potato Starch Modified by Ultrasound, X-Rays, γ-Rays, and Ultraviolet Radiation[5]

Source	Viscosity[a]	Alkali number	Iodine uptake by sol (%)	P_2O_5 (%)	
				Gel	Sol
	Unmodified				
Solid	150	5.2	19	0.189	0.203
	Sonicated				
Original gelatinized					
Gel					
900 s	4.8	7.8	13.3	0.155	0.061
2700 s	4.5	10	13	0.173	0.065
	UV-irradiated				
Solid irradiated then gelatinized					
Gel					
11 h	30	9.2	16.5	0.152	0.07
24 h	21	10.3	14	0.181	0.08
	X-rays, 50,000 V, 8 mA				
Gel					
900 s	170	5.3	19	0.162	0
2700 s	165	6.0	19	0.155	0
	X-rays, 140,000 V, 12 mA				
Solid irradiated then gelatinized	196	—	19	0.108	0
Gel					
900 s	160	5.2	19	0.159	0
2700 s	150	5.6	19	0.103	0
	γ-Rays (^{60}Co)				
Solid irradiated for 72 h and then gelatinized	130	—	19	0.063	0
Gel					
45 h	150	5.0	19	0.143	0
72 h	155	4.8	—	0.119	0

[a]Viscosity is given as time(s) of flow from a 15-ml pipette at 20°C. Time of flow of 15 ml of water is 4.5 s under the conditions of experiment.

TABLE III
Periodate Oxidation of Nonmodified, Dextrinized, and γ-Irradiated Starch[6]

Sample	Chain length[a]	Moles of $NaIO_4$/glucose unit
Nonmodified	30.0	0.97
Dextrinized in acid	5.4	1.17
Irradiated		
700 kRa	28.8	0.78
70 kRa	7.6	1.04

[a]Defined as moles of glucose units per one nonreducing end.

treatment and γ-irradiation demonstrate that, even if a similar decrease of the chain length of starch molecules is achieved by both methods, the γ-irradiated dextrins are contaminated by aldehydes and other products. The degree of decomposition of starch is dependent on the radiation dose. Low doses are seemingly more damaging, as shown in Table III. Comparison of data in this Table suggests that the lesser effect obtained with high-dose irradiation may be due to recombination of free radicals formed in high concentration during the preliminary stage of irradiation.[6]

II. SOLVENT EFFECTS

Native starch forms a complex matrix, and water plays an important role in its construction. It is widely accepted that water fills capillaries of the matrix as well as participates in the strengthening of the amylose helices in the granules.[7-16] Studies by Malfitano and Moschkoff[17] indicate that the amylaceus material of water-insoluble starch has a micellar character with the structure $\{[(C_6H_{10}O \cdot OH)H]_n$-$[C_6H_{10}O_5 \cdot OH]_nH_{n-1}\}H$. In every case the removal of water from starch must elicit at least some modification of the structure of the original matrix. However, the damage to the macrostructure is not the sole result of the removal of water. The aforementioned authors[17] have shown that desiccation of starch over phosphorus pentaoxide results in dextrinization. Tomasik *et al.*[18] have shown that removal of water by azeotropic removal from native potato starch by use of benzene damages starch to an extent that may be demonstrated by thermal analysis (Table IV).

This type of dehydration seems to be irreversible, whereas the sorption–desorption process at 40°C proceeds along a hysteresis-loop pattern (Fig. 1).[19]

The properties of anhydrous starch resulting from desiccation not only depend on the temperature employed but also on the method of desiccation (Fig. 2).[9,19]

The use of benzene for azeotropic removal of water illustrates one of several features of the solvent effect upon starch and the starch matrix. Studies by Baczko-

TABLE IV

Results of Thermal Analysis of Native and Dried Potato Starch[a]

Sample	DTA[b]		TG[c]	DTG[d]
Air-dried	100(730)	En	− 19%(30–156)	96(57.5)
	258(89)	En	− 34%(239–300)	256(27.5)
	269(30)	En		282(300)
	277s	En		344(70)
	283(<30)	En		
	300s	Ex		
Oven-dried (130°C)	245(30)	En	− 30%(236–280)	246(20)
	260s	En		254s(60)
	280s	En		270(165)
Azeotropically dried (benzene)	249(40)	En	− 30%(234–276)	249(22.5)
	261s	Ex		253s(55)
	265(30)	En		267(125)
	276s	Ex		
	289(20)	En		

[a]Experiments run in the air. [b]Data in parentheses give area in mm^2 under peak recalculated on 100.00-mg samples. Shoulders are denoted by "s". En and Ex denote endothermic and exothermic effects, respectively. [c]The range of temperature in which mass indicated is lost is given in parentheses. [d]The height of peak ($\times 10^{-2}$ mg) is given in parentheses. Shoulders are denoted by "s".

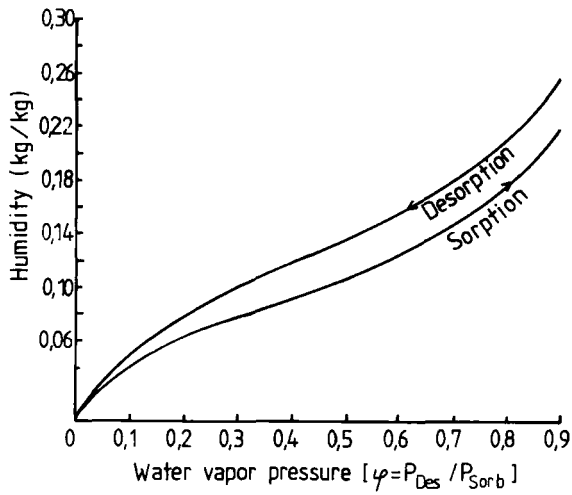

FIG. 1.—Water-vapor sorption–desorption hysteresis for maize starch at 40°C (from Ref. 19).

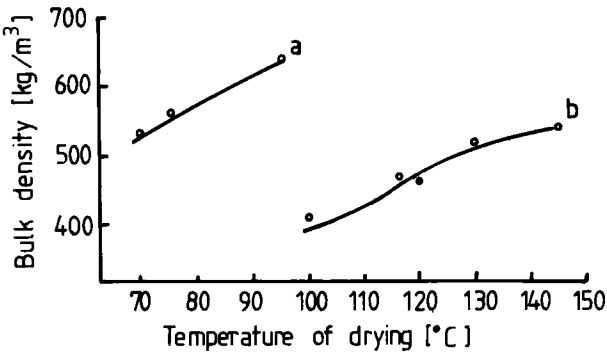

FIG. 2.—Bulk density of dried maize starch depending on the temperature applied. (a) Slow drying, (b) fast drying (from Ref. 19).

wicz and Tomasik[20] have revealed that the solvent effect on starch may be influenced also by changes of acidity of the suspension in which starch is heated (pyridine, *N,N*-dimethylformamide) as well as by penetration of the granules to swell them (by lower alcohols, water), oxidation (by nitrobenzene), or by mild proton-catalyzed hydrolysis (and/or the Henry reaction) (by nitrobenzene). The solvent effect generally causes small changes to starch when native starch is treated and quite negligible effects on oven-dried (130°C, 2 h) material. Considering the aforementioned solvents which may influence starch, the mediating role of water is obvious. It must be noted, however, that even small changes may considerably affect one of the most essential properties of starch, namely its characteristic of gelation (Fig. 3). Following treatment of starch with various solvents and then drying in air, only a few of the solvents are retained in the starch matrix in amounts that can be recognized by derivatographic techniques.[21]

Microscopic observations by polarized light of nonaqueous solvent-treated starch granules confirm that there is moderate damage to the amylopectin shell of granules (Table V). Thus, such treatment may be useful for pretreating starches prior to their reaction with weakly penetrating reagents. Such a possibility was nicely demonstrated by the reaction of starch with phosphorus pentaoxide in either pyridine or benzene suspension (Table VI).[22] Water is the solvent that has the most powerful and well known effect on starch (see, for instance, papers by Heininger[23,24] and the Chapter by BeMiller[25]). Hence the steaming of starch is frequently used for its modification.[26,27] Elevation of both temperature and pressure decreases the pH of water, which then acts as a weak acid that hydrolyzes particular components of starch quite selectively. Thus, for instance, amyloamylose hydrolyzes faster than erythroamylose. This selectivity depends on the branched structure of the latter.[28] The outcome of hydrolysis of starch with water (3% starch slurry in a sealed tube) is dependent on the pressure. The average pH shifts from

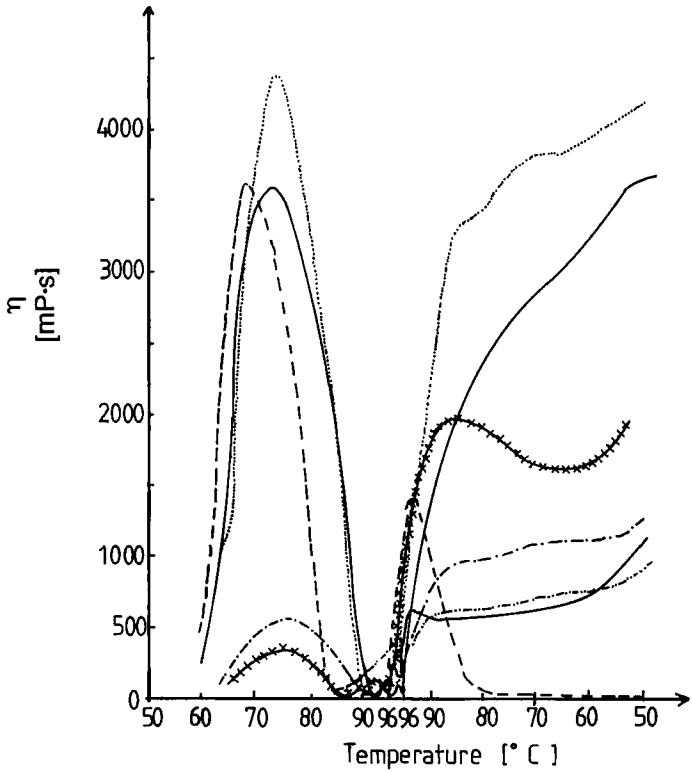

FIG. 3.—Characteristics of gelation of potato starch.[20] (· · ·) Air dried, (—) oven dried, (- - -) refluxed in benzene, (-·-·-) conditioned in nitrobenzene (100°C, 3 h), (XXX) refluxed in acetonitrile, (-· · -) conditioned in pyridine.

neutral up to 2.98 as the pressure and temperature increase. The products characterized included *(a)* alcohols (methanol, ethanol, 1-propanol, 2-propanol, 1-butanol, and 2-methylbutanol) and were characterized with yields of up to 2.8%; *(b)* carbonyl compounds (methanal, ethanal, propanal, butanal, 2-methylbutanal, pentanal, 2-methylpentanal, hexanal, propanone, butanone, 2-pentanone, 2-hexanone, butanedione, 2-furaldehyde and (5-hydroxymethyl)-2-furaldehyde) with yields up to 10% (the yield of ketones slightly exceeds the yield of aldehydes); *(c)* alkanoic acids (methanoic, ethanoic, propanoic, butanoic, 2-methylbutanoic, pentanoic, 2-methylpentanoic, hexanoic, and 2-methylhexanoic). In addition, glucose and small amounts of mannose, xylose, and arabinose were also formed. Their overall yield is 8.8%, based on starch.[29]

The process known as mashing is an alternative route for degradation of starch.[30,31] It was shown that mashing of aqueous suspensions of sweet potato

TABLE V

Microscopic Observation of Modified Air-Dried Starch in Normal and Polarized Light[a,b,20]

Solvent used in modification of starch	Temperature of observation (°C)		
	60	Increasing	245
None	yO − + (yO −,bs)	nch (nch)	nch (nch)
Benzene	y −,bOs(y +,ci)	nch (pbs at 235)	nch (y +,pbs)
Toluene	yO − + (yO − +)	nch (nch)	nch (nch)
Nitrobenzene	yO − (yO −)	nch (bO,bs at 180)	nch (yO −,bs)
Pyridine	y −,bs (y −,pbs)	nch (nch)	nch (nch)
Chloroform	y − + (y − +)	gm,sc − at 230 (sc at 230)	nch (nch)
Acetonitrile	y − +,bs (y − +,bs)	turn O,turn − (yO −,bs)	yO,bs(yO,bs)
Ethanol	y − + (yO,bs)	ps − at 185 (nch −)	yO − (yO −)
1-Propanol	y −,bs (y −,bs)	turn O at 130 (nch −)	yO − (yO −)
DMF[c]	y − (y −,ps)	y − at 190 (y −,bs at 190)	nch (nch)
Butanone	y − (y −,bs)	nch (sc at 225)	nch (y −)
Nitromethane	y −,bs (y −,bs)	nch (nch)	nch (yO,pbs)

[a]Characteristics are related to observation under normal light; the observation under polarized light is given in parentheses. [b]The notation is as follows: O, points; −, dashes; +, crosses; b, blue; ci, edges of grains illuminated; gm, grains melt; iy, illuminated yellow; p, pale; s, spot; sc, shining ceases; sv, spot vanishes; y, yellow. [c]*N*,*N*-Dimethylformamide.

starch at pH 4.5–8.0 for 1 h did not cause any appreciable hydrolysis when carried out at 100°C, and the viscosity becomes constant. However, at pH 4.0, changes of viscosity are noted, even after only 30 min. Raising the temperature of mashing to 133°C decreases the viscosity[33] of the mash by 6 min even when the pH was maintained at 5.4–8.0. A very unusual result was reported by Sair,[33] who heated potato starch of 20% moisture content in an autoclave to 125°C. The properties of this starch were found to be similar to those characteristic of corn starch, namely, a B-pattern X-ray instead of the A-pattern characteristic of potato starch, and the gelatinization temperature was raised by 8–10°C. Furthermore, the Brabender characteristics of gelation, swelling, and solubility, as well as the equilibrium moisture of dry starch were characteristic of those of corn starch. This phenomenon was interpreted as resulting from formation of hydrogen bonds.

It should be mentioned that a solventless method of hydrolytic modification of starch has recently been developed. The method employs solid superacids, perfluorinated resin-sulfonic acids, which successfully catalyze hydrolysis of starch (and other polysaccharides) and offer the possibility of continuous-process applications in plug-flow reactors.[34]

TABLE VI

Phosphorus Content in Starch Phosphates and Degree of Substitution with Phosphoric Acid Moieties[22]

Starch–P_4O_{10} (Reaction mixture)	Phosphorus content		Reaction conditions	Number of phosphorus moieties on 1 glucose unit
	Organic (mg %)	Inorganic (mg %)		
10:0.5	374.6	13.7	Benzene, 80°C	0.060
10:1	1394	205.2	As above	0.224
10:1	172.7	44.30	Benzene, <60°C	0.028
10:2	1942	132.1	Benzene, 80°C	0.313
10:2	675.0	1170	Benzene, <60°C	0.109
10:3	1070	20.17	As above	0.172
10:5	1835	423.2	As above	0.295
10:5	4268	863.2	Benzene, 80°C	0.687
10:5	570.0	279.1	Pyridine, <60°C	0.09
10:5	1273	220.3	Pyridine, 80°C	0.205
10:10	2061	1843	Benzene, 60°C	0.33
10:20	6452	2162	As above	1.04
Native starch	73.43	0.81		

III. MECHANICAL MODIFICATION OF STARCH

It is well known that, in certain macromolecules, the sum of energies of all van der Waals forces or interchain hydrogen bonds exceeds the energies of covalent bonds. In consequence, the mechanical stress on such polymers cleaves covalent bonds to give free radicals instead of disrupting interchain interactions. This behavior is observed with starch granules which are subjected to either shear on compression. The extent of damage is similar in both cases. Both the surface and the interior of the granules are affected.[35] It has been proved[36] that free radicals are generated in starch by shaking and grinding, as well as by increased pressure. When more mechanical energy is applied, a higher concentration of free radicals is observed. This suggests that drugs tabletted by use of starch may undergo unwanted changes as a result of interactions between the drug and free radicals arising from the starch. Table VII shows the number of free radicals (spins) generated in potato starch as a function of both time of shaking and pressure applied at constant time (300 s).

The first compressional characteristics of a solid starch comes from work of Bridgman,[37] who compressed starch up to 2.5×10^9 Pa (25,000 atm). For a range of organic compounds, including fructose, glucose, dextrin, starch, menthol, naphthalene, anthracene, triphenylmethane, thymol, succinic acid, anthraquinone, benzophenone, and three isomeric aminobenzoic acids, the compressibility (the volume decrement) was plotted against density of these compounds. All of them except starch and dextrin exhibit curvilinear relationships up to a constant value of approximately 3×10^{-6}. Starch has abnormally high compressibility, and dextrin exhibits abnormally low compressibility. These results may be ascribed to the properties of the matrix in the first instance and to the rigidness of molecular structure rich in intermolecular hydrogen bonds in the second.

Subsequently a small, but defined effect of compression up to 8×10^7 Pa on the viscosity of starch pastes was reported.[38] Paronen and Justin[39] investigated this

TABLE VII

The Effect of Shaking Duration and Compressive Stress on the Number of Spins/g in Potato Starch[38]

Shaking duration (s)	Spins/g $\times 10^{14}$	Compressive stress (10^5 Pa)	Spins/g $\times 10^{14}$
300	<0.01	1	<0.01
900	<0.01	10	0.01
1800	0.01	50	0.02
3600	0.02	100	0.08
5400	0.03	250	0.21
7200	0.06	500	0.39
14400	0.13	—	—

aspect in more detail by taking into account the sizes and shapes of starch granules. They compared compressional characteristics of starch of four different origins. Corn starch has had the finest granules, whereas potato starch had the largest. Wheat starch had the widest differentiation between sizes of granules, whereas barley granules have the most irregular shape. All of these factors influence the plastic flow of starches when they are compressed up to 3×10^8 Pa.

Tomasik and Kudła[40] have investigated the effect of humidity, and of pressure and its duration, on potato starch (up to 1.2×10^9 Pa for 360 s). The results are presented in Fig. 4. It may be seen that water favors a decrease of the volume of compressed sample. This effect is observed only up to a certain amount of water. Addition of water in an amount that exceeds the natural capacity of the starch matrix makes the volume of the pellet larger. This observation indicates that water cooperates with high pressure in causing deterioration of the starch matrix. Simultaneously, the ascending portions of the compressibility curves show that the resistance of the starch matrix toward compression decreases as the volume of added water increases.

The energy applied to the starch material is a function of force times the area of action of that force. Therefore the storage of grains or flour in silos, their transport, and also as excess of milling or grinding may present an opportunity for individual starch particles to suffer damage from the high energy applied. Indeed damage of

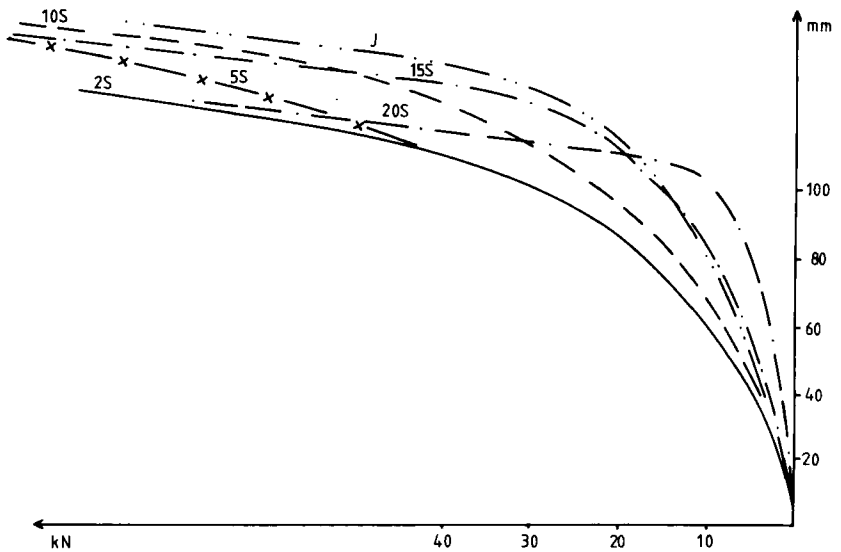

FIG. 4.—Compressibility of starch (in mm move of the plunger) as a function of applied pressure (in kN). Curves denoted as 2S, 5S, 10S, 15S, 20S, and J correspond to starch containing 2, 5, 10, 15, and 20% (w/w) of water and iodine, respectively (from Ref. 40).

starch has been observed in such situations.[41-52] The damage in the first stage of grinding of starch is due to destruction of granules, followed by depolymerization, as demonstrated by standard analytical techniques (solubility in water, reducing power, gelation characteristics, reaction with iodine, X-ray powder diffractograms, polarized-light microscopy, and enzymic reactivity). The extent of the effects evoked is obviously a function of the duration of grinding. Atmospheric oxygen has a small effect on ground starch, as shown by the alkali number of the products (Fig. 5).[45]

For some types of starch, organoleptic changes may occur. For instance, wheat starch turns gray and takes on an earthy odor.[41] Grinding gives a product which may be roughly separated into cold-water- and hot-water-soluble fractions, which differ from one another in their viscosities. Prolonged grinding reduces the amount of the second fraction in favor of the first. It was suggested by Sutra[43] that these are the amylopectin and amylose fractions, respectively. In the potato starch that he investigated, the ratio of the fractions varied from 100:37 to 100:87. This ratio influenced gelation, retrogradation, and other properties of these starch pastes. Decomposition of amylopectin to afford totally cold-water-soluble starch may be achieved. The water present in the starch causes normal hydrolysis, which is affected neither by oxygen nor by temperature.[45,46,51,52] The degree of polymeriza-

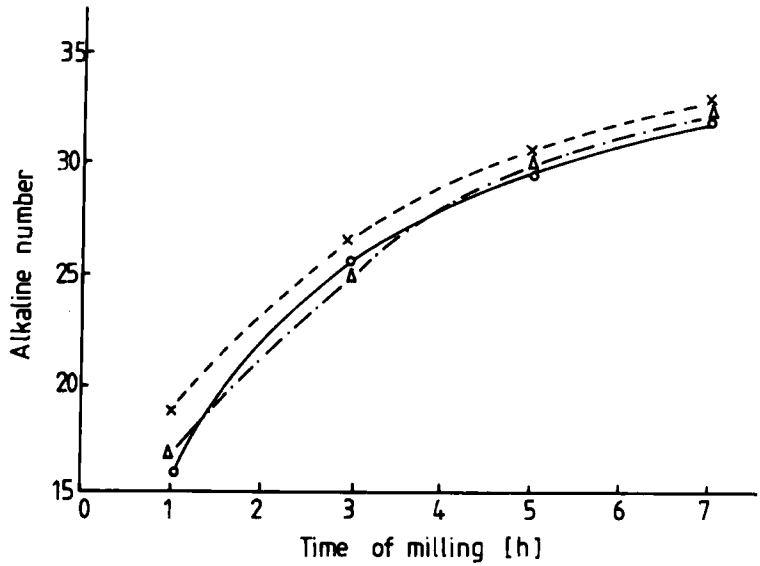

FIG. 5.—Variation of alkali number of potato starch as a function of duration of milling (—) under nitrogen, (- - -) under oxygen, and (-·-) in air (from Ref. 45).

tion of starch (DP) may be presented[47] as a function of time using the Augustat equation,

$$(DP)_t = (DP)_0(t/t_H + 1), \quad (1)$$

where t_H is the time required for the DP to decrease by half of its original value and $(DP)_t$ and $(DP)_0$ are degrees of depolymerization at the time t and zero time, respectively. Changes of DP in both amylose and amylopectin of potato starch are presented in Fig. 6.

The process of grinding starch after preconditioning with water containing SO_2 gives starch granules of high purity.[50] The shearing of starch is much more effective in causing its destruction when accompanied by increased temperature.[53-55] In this case, degradation products of starch are obtained within a period of seconds to minutes. The preconditioning of starch with some chemicals, such as ammonium carbonate, gives[56] a product having desired properties within 80 s at 130°C. Hydrochloric acid[57] may also be used for such preconditioning.

The results of grinding and milling of starch have prompted some workers to study high-pressure modifications in more detail. Two ways have been investigated. The first of these was based on the compression of starch pastes,[58] where 0.4% aqueous sols of potato starch were compressed up to 10^8 Pa (1000 atm), followed by heating until gelatinization showed the upward curvilinear increase of the gelatinization temperature as the pressure increases (Fig. 7). In the initial stage, this increase is by $3-5 \times 10^8$ Pa to reach a maximum at 1.5×10^8 Pa. This phenomenon agrees with the effect of high pressure on the viscosities of starch gels previously reported.[38] Thevelein *et al.*[58] have calculated apparent activation volumes ($\Delta V \neq$) of starch pastes. The $\Delta V \neq$ value is given by Eq. *(2)*

$$-\Delta V \neq = \frac{d(\ln G)}{dP \cdot RT}, \quad (2)$$

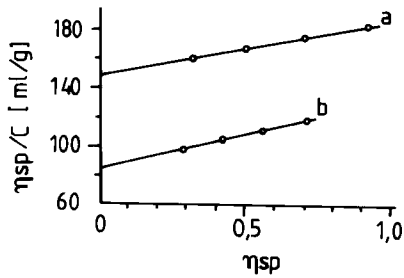

FIG. 6.—Variation of Staudinger index [η] of potato amylose (a) and amylopectin (b) as a function of specific viscosity (from Ref. 46).

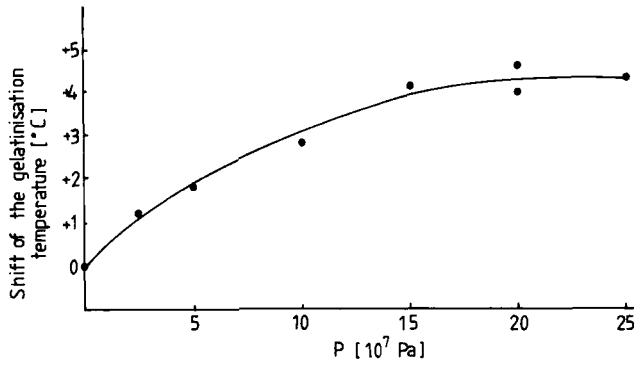

FIG. 7.—Upward shift of the gelation temperature of starch granules under the influence of high pressure (from Ref. 58).

where G is the percentage of gelatinized granules after 2400 s heating and R = 82.06 $cm^3 \cdot atm/K \cdot mol$. The value of $-V\neq$ decreases from 31.7 through 21.9 to 17.6 cm^3/mol as the temperature increases from 60 to 62°C. The apparent enthalpy of activation, $\Delta H\neq$,

$$\Delta H\neq = -R[d(\ln G)/d(1/T)] - RT \qquad (3)$$

reaches 312 kJ/mol at 333.8 K, with R = 8.314 J/K · mol. The same authors also observed the effect of 1-propanol on gelatinization.[58,59] This effect was qualitatively confirmed by Bączkowicz and Tomasik[20] in their study of solvent effects on starch. All of these effects support earlier statements that high pressure favors the formation of hydrogen bonds.[60] It means that the high pressure at least influences molecules of starch and water, but there is no evidence for any change of the original stereochemical of the amylose and amylopectin components. Thus gelation is assumed to occur with conservation of the original covalent starch structure.[58]

Another group of authors applied high pressure to solid starch of various origins. Muhr and Blanchard[61] applied 4.5×10^8 Pa, Mercier *et al.*[62] up to 6×10^8 Pa, and Tomasik and Kudła[40,63,64] up to 1.2×10^9 Pa. In the third instance the energy exerted on starch samples was of the order of the energy of C–C and C–O covalent bonds. All authors concluded that there is essential damage to the granules as the pressure increases. The extent of damage is a nonlinear function of the time of compression. There is also a lack of linearity between gelation temperature and the pressure applied. Opposite effects were observed in the case of potato starch (a decrease) and wheat starch (an increase).[61] Higher pressure produces material soluble in cold water. This is accompanied by a relatively significant (up to 100% of the original value) decrease in the reducing power of compressed starch, but this

value is still very low, suggesting negligible hydrolytic scission of the glucosidic bonds of starch. Tomasik and Kudła[40] observed additional thermal effects in derivatograms of compressed starch, and these were attributed to a repolymerization of starch at 1.0×10^9 Pa after its degradation at 0.8×10^8 Pa (Fig. 8).

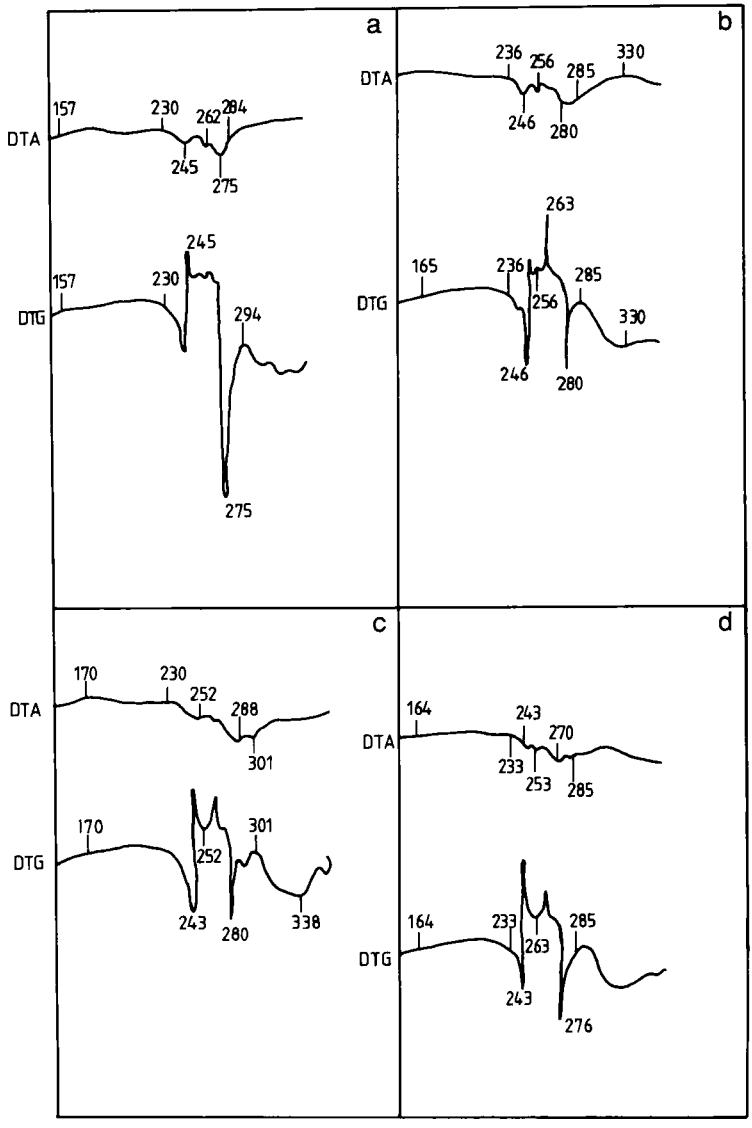

FIG. 8.—DTA and DTG curves of starch before compression (a), after compression to 0.8×10^9 Pa (b), to 1.0×10^9 Pa (c), and to 1.2×10^9 Pa (d) (from Ref. 40).

In view of the possibility of random free-radical scission of some covalent bonds, despite a great deal of dissipation of energy in the same sample, this repolymerization may be the likely interpretation, as the effect could result from recombination (or rather free-radical condensation) in the compressed material.

The result of compression depends obviously on the water content in the compressed starch. The water content, which reaches and exceeds the natural capacity of the starch matrix being compressed, produces a solid gel in the form of very hard pellets. Potato starch predried in an oven suffers either minor or no changes on compression up to 10^9 Pa. A deformation of the capillary structure of the starch matrix, accompanied by minor deformation of starch granules, are the sole effects of compression. Obviously there is no change of reducing power and solubility of such samples. The powder X-ray diagrams show changes toward a higher state of order in solid starch gels. Again this tendency is nonlinear with respect to pressure, and it is also dependent on the duration of compression (Fig. 9).

In contrast to this observation, Lelievre[65] has suggested that milling of starch turns it into a more-amorphous form. The nonlinearities observed between the pressure applied and the various properties studied is evidence of the complex character of the changes involved. Hydrolytic scission of the glucosidic bonds is certainly induced by the energy delivered in the form of heat and, simultaneously, in the form of work. On compression of gels, the effect of heat can be neglected[58] but on compression of solids it has to be taken into account.

The compression of starch in the presence of some mineral salts ($CoCl_2$ and $FeCl_3$) and of elemental iodine leads to the formation of starch–additive inclusion complexes. Among many salts tested, some form only physical mixtures, as proved by thermal analysis.[63,64] *(See Appendix for additional text.)*

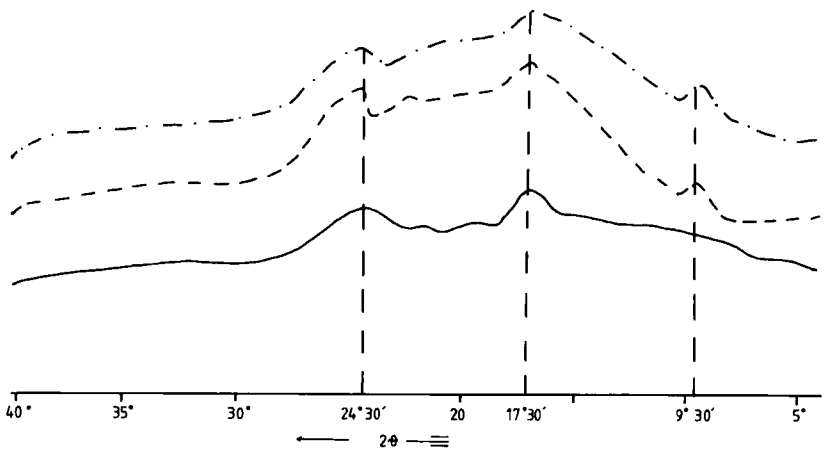

FIG. 9.—Change of powder difractogram of noncompressed starch (—) after compression at 1.2×10^9 Pa for 60 s (- · -) and for 600 s (- - -) (from Ref. 40).

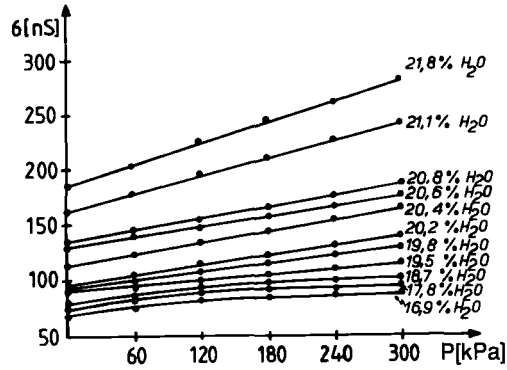

FIG. 10.—*Effect of pressure on the conductivity of starch of various humidity contents (from* Ref. 66).

It has been shown by Boruch *et al.*[66,67] that solid starch changes its electrical conductivity on compression. At constant temperature and humidity there is a positive correlation between the tamping of starch layers in cylinders, containers, and silos and their electrical conductivity.[67] Figure 10 shows how the electrical conductivity varies for potato starch as a function of the humidity and pressure applied.

Likewise the same properties as the function of degree of tamping (k) are presented in Fig. 11, where $k = (h_o - h_n)/h_o$, with h_o and h_n being the heights of the original and tamped layer of starch, respectively. The dielectric constant (ϵ) of starch varies nonlinearly with the pressure at a given humidity (Fig. 12). The relationship between ϵ and the humidity of the sample is also nonlinear (Fig. 13).

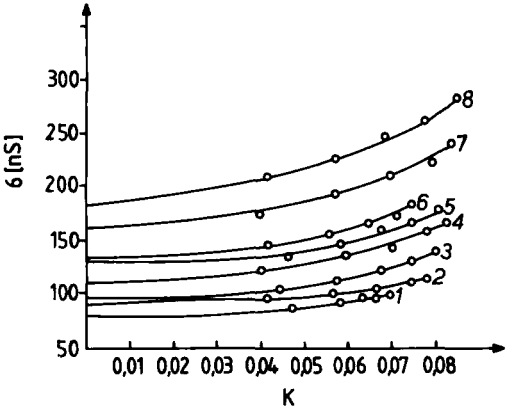

FIG. 11.—Conductivity of starch as the function of tamping, K (from Ref. 66). The water content in starch is: 1, 18.7%; 2, 19.5%; 3, 20.2%; 4, 20.4%; 5, 20.6%; 6, 20.8%; 7, 21.1%; and 8, 21.6%.

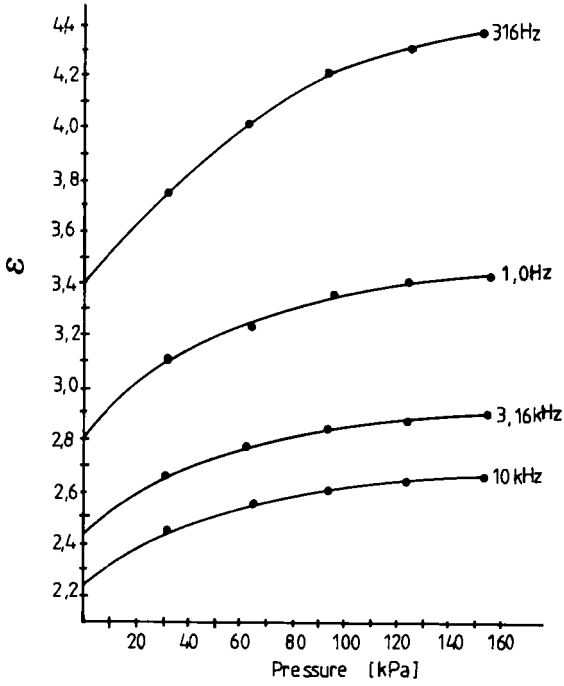

FIG. 12.—Effect of pressure, P, on dielectric constant, ϵ, of starch of 20.05% humidity (from Ref. 67).

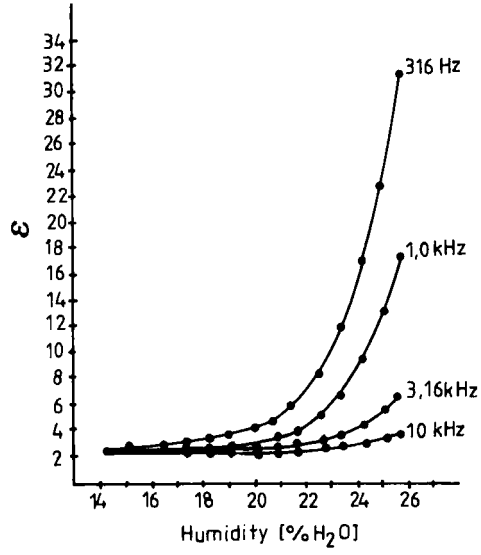

FIG. 13.—Effect of humidity content on dielectric constant, ϵ (from Ref. 67).

IV. Irradiation of Starch with Neutrons, X-Rays, High-Energy Electrons, and γ-Rays

Several reviews of this subject had been published until 1974.[68-72] Free-radical reactions of saccharides have also been reviewed.[73] Comparative studies involving X-ray, β (electron)-, and γ-irradiation of starch show that the results of such procedures are similar, but not identical. All of them lead to destruction of starch.[3,74-76]

1. Irradiation with Neutrons

Potato, corn, and wheat starch was irradiated with 9×10^{14} neutrons/cm^2. Neutrons cause only a weak peptonizing effect in comparison with γ-rays (2×10^6 rep) (see Table VIII). In the first case, starch becomes radioactive. Radioactive nuclei in starch are mostly phosphate isotopes and only to a very minor extent ^{14}C. The behavior of starch of all three origins in respect to both types of irradiation is nonuniform. Generally neutron radiation does not eliminate phosphoric moieties from starch and is less destructive.[77]

2. Irradiation with X-Rays

Very few reports have been published on the use of X-rays for modification of starch, although the formation of deoxy compounds on irradiation of solid potato starch with 5×10^6 rads under nitrogen has been described. The amount of deoxy compounds formed is related almost linearly to the irradiation dose, and formation of 2-deoxy-D-*arabino*-hexose is the major process; there are almost no side-processes. Similar qualitative, but not quantitative, behavior is shown by 1% aqueous solutions of D-glucose, D-xylose, L-arabinose, D-ribose, sucrose, and cellulose powder (Fig. 14). Starch is the most resistant to irradiation among carbohydrates tested.[74]

Starch pastes irradiated with 130,000 V, 15 mA X-rays lost their viscosity, and there was concurrent decrease of iodine-binding ability and pH. Other properties measured after such treatment point to dextrinization and oxidation of starch.[78,79] Other results of such irradiation is the cleavage of phosphoric acid esters from glucose units of potato starch. This effect is observed at 50,000 V and 8 mA as well as at 150,000 V and 12 mA. The effect of X-ray irradiation is similar in this respect to irradiation with γ-rays, whereas neither sonication with ultrasound nor exposure to UV light evoke such effects.[5] Starch irradiated by X-rays, contains free radicals, and thus the presence of free radicals in starch provides evidence of previous irradiation.

3. Irradiation with High-Energy Electrons

Irradiation of potato starch granules with high-energy electrons in doses up to 10^7 rads does not affect the material to any significant extent. The microscopic appearance and gelatinization temperature do not change. However, both solid

TABLE VIII

Comparison of Effects of Irradiation of Starch[a] of Various Origin with Neutrons and γ-Rays[77]

	Origin of starch[a] and type of modification								
	None			Neutrons[b]			γ-Rays[c]		
Property	**P**	**M**	**W**	**P**	**M**	**W**	**P**	**M**	**W**
Concentration (%)	1.75	1.91	1.89	1.66	1.88	1.94	1.88	1.92	1.89
Viscosity ($t/t1$)	2.46	1.30	1.40	1.37	1.21	1.03	1.10	1.11	1.06
Reducing value (% of maltose)	0.13	0.37	0.36	0.39	0.69	0.73	2.16	2.50	2.31
Iodine binding (%)	4.04	3.57	4.08	3.36	3.57	3.53	3.93	3.23	3.69
pH	6.2	4.0	5.75	5.0	3.9	5.6	4.00	4.9	3.3
Beta-amylolytic index	77.93	76.98	70.70	75.99	75.02	71.72	76.81	86.17	75.75
Av. molecular weight	166000	1037770	1042979	151446	476637	503119	79467	275589	261750
Sol pH	5.2	4.1	4.4	3.8	5.2	5.6	3.6	5.6	4.6
Gel pH	2.8	3.8	3.7	3.2	4.5	3.9	3.2	4.7	3.3
Gel P_2O_5	0.101	0.071	0.023	0.124	0.098	0.067	0.042	0.144	0.058

[a]P, potato; M, maize; W, wheat. [b]In 9×10^{14} n/cm^2. [c]In 2×10^6 rep.

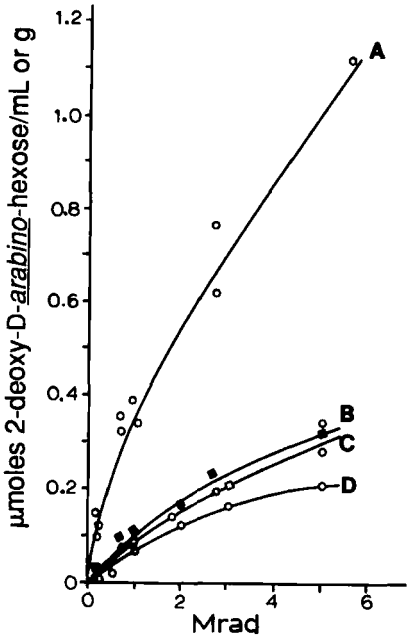

FIG. 14.—Dose dependence of the formation of deoxy compounds expressed as μmol of 2-deoxy-D-*arabino*-hexose/ml for 1% glucose and 1% sucrose solutions and as μmol of 2-deoxy-D-*arabino*-hexose/g for potato starch and cellulose powder. A, sucrose; B, glucose; C, cellulose; and D, potato starch (from Ref. 74).

amylose and solid amylopectin suffer degradation and other structural changes at a dose of 5×10^4 rad.[80] Changes in granular starch, amylose, and amylopectin that are dependent on the dose of irradiation are presented in Table IX. The results point to the importance of the macrostructure of the polysaccharide, as this affects the penetration of the material by electrons and their diffraction within the material.

The behavior of starch pastes on irradiation with 1×10^7-eV and even 3×10^7-eV electrons resembles that obtained on exposure to X-rays.[74,79] Free-radical formation in irradiated starch is observed after irradiation with even 4×10^5-eV electrons. It should be noted that, despite common opinion (see a review[2] and references therein), purporting to the high stability of free radicals generated from starch, such radicals exhibit sensitivity to atmospheric oxygen. Figure 15 shows that the concentration of free radicals decreases much faster in air than under nitrogen. The same Figure also shows that 4×10^5-eV electrons at a dose of 10 Mrad produce almost the same concentration of free radicals as 150-kV X-rays with a dose of 3 Mrad. The sensitivity of the radicals to air and their lifetime under nitrogen are the same in both cases.[81] As shown by Radley,[82] irradiation of starch up to 0.5×10^6 rads does not degrade starch to any considerable extent and may be

TABLE IX

Properties of Granular Potato Starch, Amylose, and Amylopectin after Irradiation with High-Energy Electrons[81]

	Granular Starch			
Irradiation dose (10^6 rads)	**Acidity (eq/10^6 g)**	**Gelation temp. (°C)**	**Iodine affinity (mg of I_2/100 g)**	**Amylose content (%)**
0	4.4	68–69	4.5	23
0.05	6.0		4.4	22.5
0.1	7.4	67–69	4.3	22
0.2	8.5		4.1	21
0.5	10.3	67–69	3.6	18.5
1	12.7		3.4	17.5
2	17.9	64–65	3.1	16
5	29.0		2.4	12
10	40.0	60–61	1.1	6
	Amylose			
	Beta-amylolytic index		**Intrinsic viscosity, [z]**	**DP[a]**
0	83		230	1700
0.05	86		220	1650
0.1	88		150	1100
0.2	88		110	800
0.5	87		95	700
1	86		80	600
2	84		50	350
5	83		40	300
10	83		35	250
	Amylopectin			
	Beta-amylolytic index		**Average chain length**	**Length of internal chain[b]**
0	58		24	8
0.05	57		23	7
0.1	55		23	7
0.2	54		21	7
0.5	51		18	6
1	49		16	6
2	49		15	5
5	48		14	5
10	46		13	5

[a]The average degree of polymerization calculated from DP = 7.4[z]. [b]Calculated from {A. chain length − [chain length × beta-amylolytic index + 25]}.

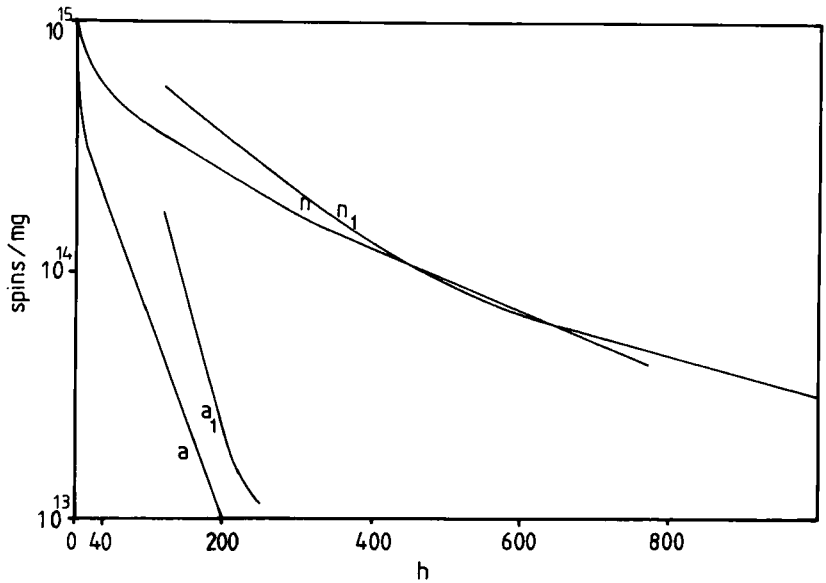

FIG. 15.—ESR signals of irradiated potato starch as a function of time of the process.[81] (a) Measurements in air, 150-kV X-rays, 3-Mrad dose; (a_1) measurements in air, 400-keV electrons, 10-Mrad dose; (n) measurements under nitrogen, 150-kV X-ray, 3-Mrad dose; (n_1) measurements under nitrogen, 400-keV electrons, 10-Mrad dose.

safely used for sterilization. However, irradiation by 10^8/rads causes a total breakdown of the starch structure.

4. Irradiation with γ-Rays

a. Irradiation of Starch.—By far the most studies have been carried out on potato and maize starch. There are, however, single reports on the radiolysis of rice,[83] pea (180–1870 rad),[84] barley (up to 450 kGy),[85] tapioca (up to 10^6 rad),[86] red gram (*Cajanus cajan*) (up to 10^6 rad),[87] Egyptian sweet potato starch (up to 10^6 rad),[88] and wheat (2×10^6 rad)[4,89–91] starches, *Cana edulis, Marantha,* and sorghum starches[4] as well as amylose and amylopectin ($0.02–4 \times 10^6$ rad).[92–95] In addition to papers by Samec[3,89,90,96] there is also a series of excellent reports by Raffi *et al.*[97–103] which present comparative studies on the conditions of γ-irradiation of maize, amylomaize, waxy maize, manioc, potato, rice, and haricot-bean starch, and bread wheat. These studies correct an early hypothesis of Guilbot *et al.*[104] that, from the qualitative point of view, the behavior of starch is practically the same irrespective of its origin. The just-cited papers of Samec and of Raffi *et al.* state that the products of decomposition (except radiodextrins) are the same, but the course of decomposition as well as the yield of particular products are dependent on the origin of the starch.

The quantity of water-soluble "radiodextrins" is linearly dependent on both the irradiation dose and the starch origin and decreases in the following order: waxy maize > maize > haricot bean > rice > manioc > bread > wheat > amylomaize > potato, as shown in Fig. 16.

Comparing starches from potato, wheat, and maize, the first is the most readily degraded by 2×10^6 rad, as demonstrated by reducing power, iodine binding, and beta-amylolytic index.[89,96] The alkali lability of starch thus irradiated increases in the following order: potato > maize > wheat.[90] In terms of the yield of organic acids (radioinduced acidity), there is a large difference between the sensitivity of starch of particular origin and the irradiation dose,[99,105] as shown in Fig. 17.

Most later studies carried out by Raffi *et al.*[99,101,102] on γ-irradiation of starch of various origins at 0.60 and 6.2 kGy/h under either air or nitrogen show that differences in total composition and yield of carbonyl compounds, acidity, hydrogen peroxide, and observed ESR spectra may be extrapolated from one starch to another, despite the fact that particular relationships are nonlinear (Figs. 18–21). The dispersibility of starch plays an important role in this kind of sensitivity, as

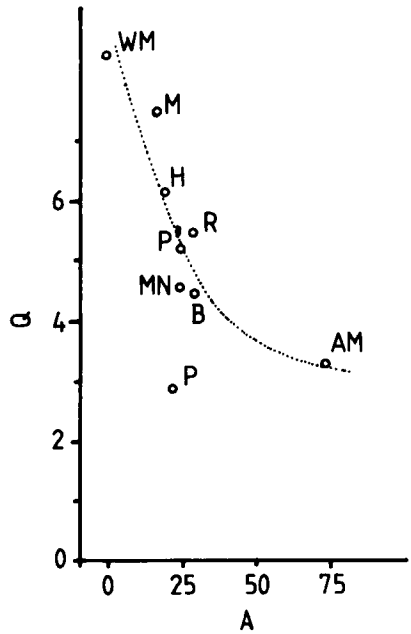

FIG. 16.—Mass, Q (mg/mL), of water-soluble products as a function of the content of amylose in starch. Variety of starch: P, potato; AM, amylomaize; M, maize; R, rice; H, haricot bean; MN, manioc; WM, waxy maize; B, bread wheat. Point P' relates to potato starch after correction of the result attributable to high water content in that source (from Ref. 102).

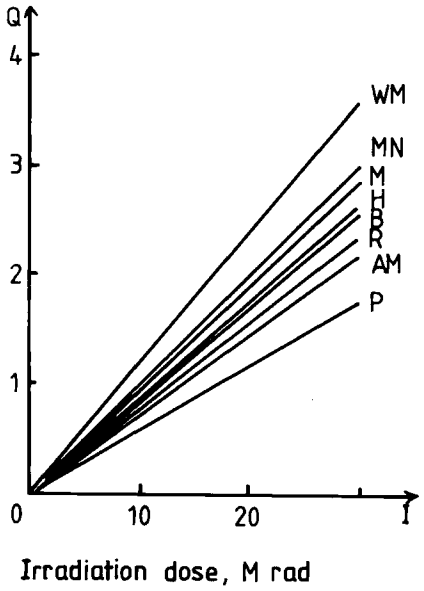

FIG. 17.—Total quantity, Q (absorbance), of carbonyl compounds as the function of irradiation dose, I (kGy). See Fig. 16 for notation of points (from Ref. 98).

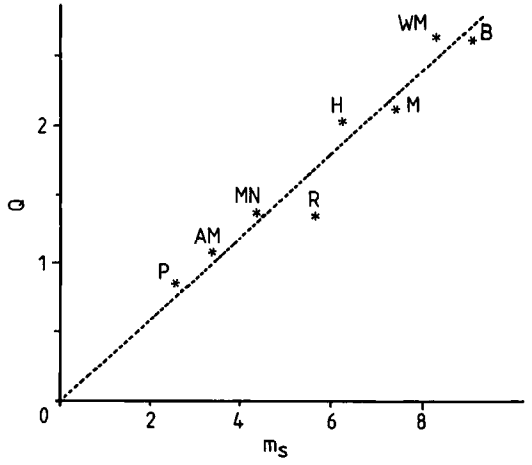

FIG. 18.—The total radioinduced acidity Q (μequiv/mL]–mass (mg/ml) relationship for dextrins produced on irradiation of starch with 10 kGy (from Ref. 102). See Fig. 16 for notations.

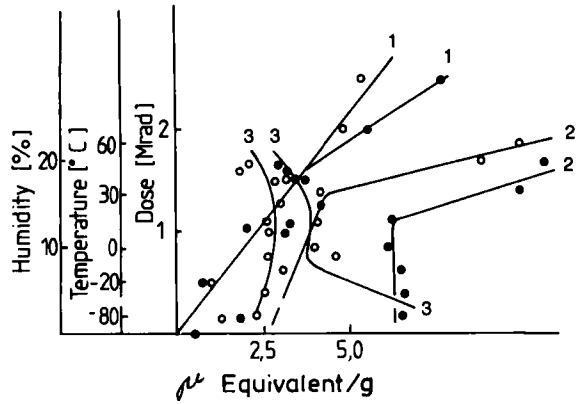

FIG. 19.—Yield of formic acid (○) and total acidity (●) as a function of the irradiation dose (1), temperature (2), and humidity (3).[169]

demonstrated by Thollier and Guilbot,[106] who studied the action of alpha and beta amylases on irradiated starches.

For the irradiation of amylose it has been shown that the solvent may stabilize the irradiated matrix. Thus the scission of amylose in dimethyl sulfoxide is almost 15 times lower than that in water.[92] Irradiation of the solution simultaneously containing amylose and amylopectin separated resulted in their grafting.[93] Thus the results of irradiation depend on whether starch is radiolyzed in the solid, paste,

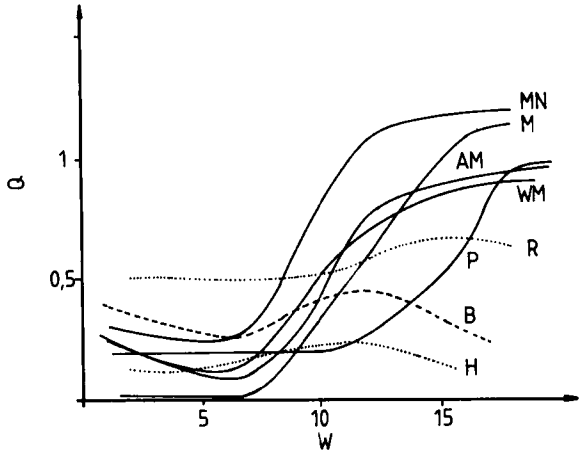

FIG. 20.—Quantity, Q (absorbance), of radioinduced hydrogen peroxide as a function of the water content (%) for starches of various origins. (from Ref. 102). See Fig. 16 for notations.

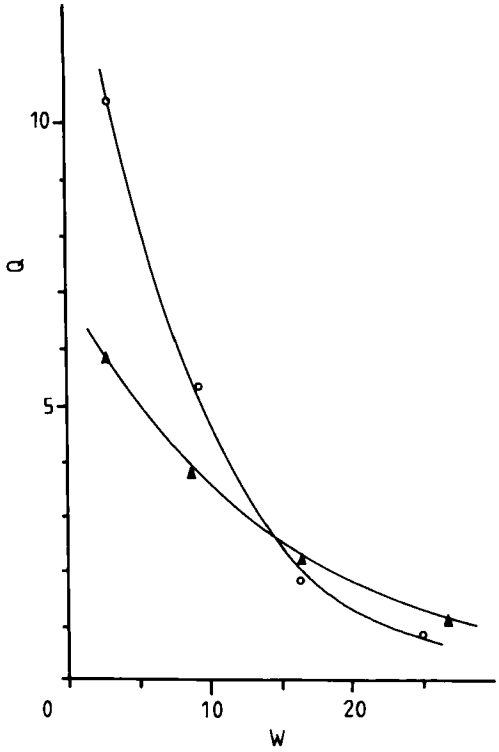

FIG. 21.—Quantities (Q) [mg/mL] of water-soluble dextrins as a function of water content (W) in potato starch (○, irradiation under oxygen; ▲, irradiation under nitrogen) (from Ref. 101).

suspended, or dissolved state. In all cases the effects of the process are dependent not only on dose, but also on temperature, atmosphere, composition, water content, and nature of any additives present. Irradiation of solid starch granules causes the granules to weaken, and their heterogenicity increases with applied dose.[95,107-111] At doses of $1.5-2.0 \times 10^6$ rad these changes are quite small.[112] Irradiated corn starch ($1-3 \times 10^6$ rad at 2000 rad/min) gives gels that have increased plastic strength. It is assumed that this is due to changes in the number of hydroxyl groups promoting hydrogen-bond formation. In the preliminary stages of irradiation, the number of hydroxyl groups increases because of bond rupture.[113,114] Again, such changes are less pronounced in the case of maize starch granules.[115] Native water has a protective effect on granules.[116]

The structure of starch granules is of essential importance. Amorphous zones of irradiated granules undergo hydrolysis prior to hydrolysis in their crystalline areas.[104] Irradiation of granules of maize starch causes them to break along radial and concentric lines. An increase of dose makes the granules more crunchy. These

effects depend on the size of the granules. Irradiated small granules swell much faster and to a much higher extent than large granules.[117]

Maize starch may be separated after irradiation into several fractions, based on solubility in alcohol and aqueous alcohol. The size of the fractions and their composition depends on the radiation dose, as shown in Table X which also shows the distribution of organic products of destruction (aldehydes and carboxylic acids) in particular fractions.[118] The relations presented in this Table are S-shaped. Under irradiation with increasing doses, the destruction of starch obviously increases. The nature of the increase of acidity in corn starch has also been studied by Athanassiades and Berger.[119] Thollier and Guilbot[120] have conducted similar studies on potato starch, and Raffi *et al.*[99] have extended their studies to more varieties of starch. The results expressed as free and total acidities, as well as the quantity of formic acid at equilibrium water content, are given in Table XI. These data vary rather nonlinearly with increase of the irradiation dose and water content.

Weak irradiation ($0.94-28.2 \times 10^6$ rad) gives swelling products, whereas stronger irradiation (up to 100×10^6 rad) causes profound destruction of starch to give water-soluble starch.[121-123] The $4-8 \times 10^8$-rad irradiation turns starch into a resinous mass.[124] Radiation with $9-18.6 \times 10^5$ rad affects mainly the secondary structure of amylose and amylopectin, although some random scission of (1 → 4) glucosidic bonds also occurs.[125-127] Samec[111] has stated that their cleavage is favored over the cleavage of isomaltose (1 → 6) bonds. An ESR study[128,129] shows that radicals formed in the primary stage of irradiation result from cleavage of the C–H, C–OH, and CO–H bonds without any particular selectivity between 1-CH and 4-CH bonds. This stage is followed by transformations of radicals through elimination of water and cleavage of C–C and C–O bonds in glucose residues, as well as glucosidic bonds. This second step is favored by further irradiation and by thermal effects. Maltose that is irradiated in the same manner decomposes solely by cleavage of 5-CH and 5-CO bonds.

The dose range $47-56 \times 10^6$ rad is the most suitable for production of carbonyl compounds.[108,128,130] Oreshko and Korotchenko[131] have given an excellent picture of the changes of several properties of native potato starch of 16.6% of humidity as the dose of γ-radiation increased up to 18.2×10^6 rad. Figure 22 shows that molecular weight and pH proportionally decreased as the dose of radiation increased. The yield of reducing sugars and gaseous products increase with the dose applied.

Raffi *et al.*[102,132] have extended a theoretical treatment of the processes taking place on irradiation of starch. This treatment provides essential predictive power and permits manipulation of certain parameters of the radiation, depending on the properties of source and the properties desired for the products. This treatment was later proved experimentally.[96] The fundamental relation between the dose of radiation and the reciprocal of degree of depolymerization (DP) is linear. Likewise, the reciprocal of intrinsic viscosity is linear in the radiation dose (that is, also in DP)

TABLE X

Some Physicochemical Properties of Fractions Isolated from γ-Irradiated Maize Starch Soluble in Aqueous Alcohol of Various Concentrations[118]

No. of soluble fraction	Concentration of ethanol (%)	Yield (%)	Average molecular weight	Aldehydes (mg/g)	pH	Carboxylic acids (mg/g)
			Dose: 15 Mrad			
1	20	1.15	5460	13.4	6.2	2.7
2	35	10.94	5460	13.4	6.2	2.7
3	45	39.61	5460	13.4	6.3	2.7
4	55	10.92	3670	19.2	5.6	4.3
5	65	3.75	2812	20.5	5.6	4.3
6	75	2.07	2530	22.8	5.4	4.3
7	80	1.83	2090	30.4	5.4	4.3
8	96	3.66	1161	56.8	4.4	14.7
Insoluble	—	20.50	8130	8.4	5.7	7.0
			Dose: 30 Mrad			
1	20	—	—	—	—	—
2	35	2.23	5460	13.4	5.7	2.7
3	45	14.84	3670	19.2	5.7	2.7
4	55	33.43	3000	23.8	5.7	2.7
5	65	9.22	2090	30.4	5.2	4.3
6	75	7.07	1714	37.6	5.2	4.3
7	80	4.45	1680	39.3	4.8	5.4
8	96	5.36	1017	64.8	4.2	18.4
Insoluble	—	17.57	4400	16.1	6.0	7.56
			Dose: 50 Mrad			
1	20	—	—	—	—	—
2	35	2.87	1760	36.6	4.3	5.4
3	45	2.12	1760	36.6	4.4	5.4

continues

TABLE X—(*Continued*)

No. of soluble fraction	Concentration of ethanol (%)	Yield (%)	Average molecular weight	Aldehydes (mg/g)	pH	Carboxylic acids (mg/g)
4	55	32.10	1760	36.6	5.1	4.1
5	65	14.60	1760	36.6	4.5	4.4
6	75	7.10	1670	40.0	4.3	5.4
7	80	6.10	1170	43.0	4.4	6.5
8	96	14.26	878	88.0	3.3	41.8
Insoluble	—	15.20	1630	42.9	4.6	14.0
			Dose: 100 Mrad			
1	20	—	—	—	—	—
2	35	—	—	—	—	—
3	45	10.42	1011	77.0	4.3	9.6
4	55	32.87	1011	77.0	4.3	9.6
5	65	16.07	1011	77.0	3.9	11.9
6	75	9.02	1011	77.0	3.8	13.5
7	80	6.74	865	83.0	3.8	14.0
8	96	22.78	675	102.0	3.1	49.6

TABLE XI

Quantities of Radioinduced Acids in Starch of Various Origin after Irradiation with 10 kGy in Air[101]

Starch variety	Acidity[a]			Equilibrium water content[a]
	Free	Total	Formic acid	
Maize	0.63	1.37	0.65	12.2
Waxy maize	1.45	<2.67	0.86	12.5
Amylomaize	0.49	1.08	0.55	14.4
Manioc	1.16	2.10	0.89	13.9
Bread wheat	<1.71	2.62	<1.35	11.4
Potato	0.15	>0.84	0.62	18.4
Rice	>0.13	1.30	0.75	12.1
Haricot bean	0.16	2.06	0.53	11.8

[a]Quantities in microequivalents per 1 g of starch.

and in the number of reducing end-groups. Further relationships were established between DP and the water content of starch and DP and the mass of water-soluble products. The relationship between the percentage of soluble products and water content (W) of starch is nonlinear only in the region of $W \leq 5\%$. The water-soluble fraction is composed, among others, of glucose (0.22%), and other sugars (0.01%). The total yield[97] of this fraction is 0.30%.

Dextrins are major products of irradiation in every case.[133–135]

The amount of water influences the color of the dextrins. A low concentration of

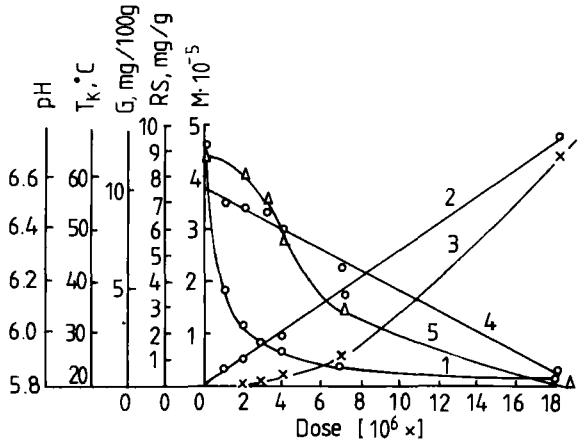

FIG. 22.—Variation of molecular mass (1), reducing sugars (2), yield of gaseous products (3), temperature of gelation (4), and pH (5) with the dose of radiation.[131]

water gives yellow dextrins, whereas higher concentrations (starch pastes) provide white dextrins. Irradiation with $4-5 \times 10^6$ rad seems to be the most suitable for production of dextrins.[133] There are some suggestions that irradiation of granules of native starch may cause crosslinking and grafting in their interior.[115,121] Such behavior of starch has been definitely negated,[136] at least in corn starch irradiated with $3-6 \times 10^6$ rad.

Nitrogen-containing components of starch reside mainly in the insoluble fraction of irradiated starch, where they undergo concentration from those parts of starch that have been damaged by irradiation.[137] The infrared (IR) spectra of particles of this fraction closely resemble those of albumin, γ-globulin, and in particular cells of *Escherichia coli*, suggesting a glycoprotein structure.[138] The same is suggested from studies on the solubility of starch fractions.[139] Powder X-ray patterns of the irradiated starch were interpreted similarly.[78] This macromolecular fraction consists of a significant number of modified glucoside chains of 3–60 glucose residues per chain. The modifications are mainly because of formation of glucose residues having predominantly α-(1 $\rightarrow$ 6) and α-(1 $\rightarrow$ 4) linkages.[140] As with the results of thermolysis of starch,[141,142] the results of γ-irradiation are dependent to a certain extent on atmospheric oxygen.[80,143-145] The destruction of starch with a dose of 28.2×10^6 rad (306 rad/s) is much lower under nitrogen, argon, and CO_2 than under oxygen. Under vacuum (4 mm Hg), extensive destruction is due to the cooperative effects of γ-irradiation and dehydration.

Water protects starch against destruction on radiolysis. The energy necessary for splitting the polymer bond (E_d) is given by

$$E_d = MD/\Delta N_o, \tag{4}$$

where M is molecular mass of glucose, D is the irradiation dose in eV/g, Δ is an increase in reducing power, and N_o is the Avogadro number. The value of E_d is a linear function of the water content [Eq. (5)],

$$E_d = 6.5 + 1.45\,W, \tag{5}$$

where W is the percentage water content. The value of E_d for $W = 0$ exceeds by two the energy of the glycosidic bond.[146]

Gaseous products from irradiation of starch are composed of molecular hydrogen, carbon monoxide, and carbon dioxide.[147,148] On irradiation with $12-20 \times 10^6$ rad, hydrogen and carbon dioxide are formed in 1 : 1 ratio. Thus it may be assumed that both gases are the products of decomposition of formic acid resulting from pentoses abstracted from starch.[148] However, Yershov and Isakova[129] have estimated the $H_2 : CO_2 : CO$ ratio as 4.5 : 5.5 : 1. The total amount of gaseous products is decreased as the amount of water in starch increases.[149] However, as shown by Phillips *et al.*[150] CO and CO_2 may also result from irradiation of D-glucose in aqueous solution.

Hydrogen peroxide is also a product. It is formed independently of other compounds, and its level is dependent on pH (inhibition by high and low pH under

nitrogen) and oxygen increases the yield.[151–153] However, the yield of hydrogen peroxide is dependent on the irradiation dose, and starches of different origin give different yields. These differences seem to be related to the structure of starch matrix rather than the water content, as may be seen[100] from Table XII. Studies on the mechanism for formation of H_2O_2 have assumed the involvement of O_2^- as an intermediate.[154] Berger *et al.*[153] have proposed an alternative mechanism involving the neutral oxygen molecule. Thus either C-5–O–C-1 or C-4–O–C-1 linkages of starch, that is, within the glucose unit or the glucosidic bond, are ruptured to give two radicals capable of reaction with oxygen molecules.

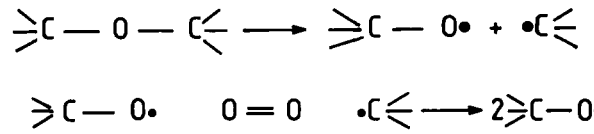

The resulting radicals can react with water ultimately to give hydrogen peroxide.

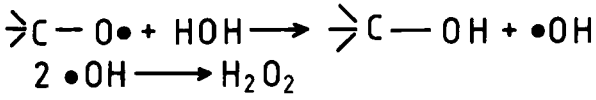

It is possible that the reaction leading to hydrogen peroxide is not so simple and involves the formation of hydrogen atoms and hydroxyl radicals in the intermediary step.

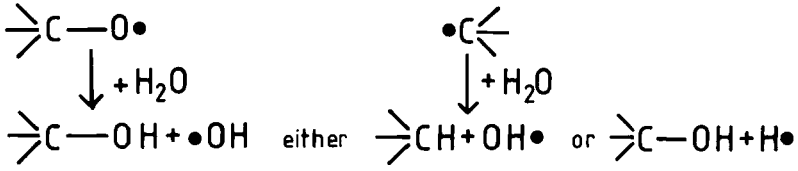

TABLE XII

Quantities of Radioinduced Hydrogen Peroxide from Starch of Various Origin[102]

Starch	Equilibrium water content	Yield of H_2O_2[a]
Maize	12.2	0.59
Waxy maize	12.5	0.37
Amylomaize	14.4	0.41
Manioc	13.9	0.58
Bread wheat	11.4	>0.17
Potato	18.4	<0.75
Rice	12.1	0.27

[a]In μmol/g of starch.

These radicals may react with molecular oxygen to give hydrogen peroxide.

$$H\bullet + O=O \longrightarrow HO_2\bullet$$
$$2\,HO_2\bullet \longrightarrow H_2O_2 + O_2$$

The low-molecular weight fraction resulting after radiolysis is composed of compounds listed in Table XIII. These include mono- and disaccharides, alcohols, aldehydes, ketones, carboxylic acids, their esters, and even oxygenated heterocycles. D-Glucose is the most obvious product of the splitting of starch. Its oxidation with atmospheric oxygen may give both D-gluconic and D-glucuronic acids. D-Arabinose results from the breakdown of D-gluconic acid. Equally obvious is also the formation of maltose. Berger *et al.*[155] have suggested the following mechanism for the formation of D-glucose, 5-deoxy-D-*xylo*-hexose (one of the deoxy sugars formed), and D-glucitol. This mechanism also accounts for the formation of maltose and of mannitol from maltose. The mechanism assumes free-radical cleavage of glucosidic bonds as well as the O–C-5 and O–C-1 bonds of glucose residues, and these products react with water.

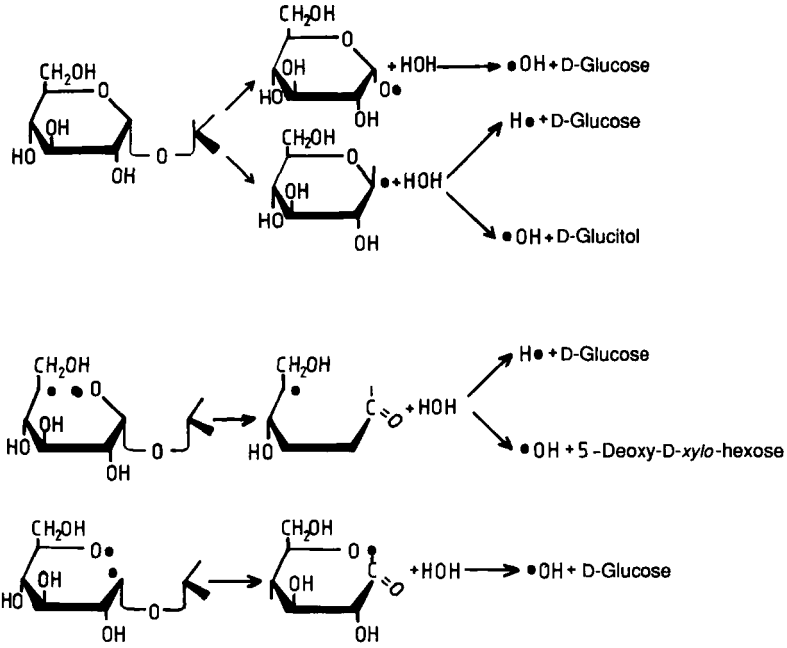

Contrary to mechanisms proposed by other authors[131,147] this mechanism rejects the possibility of the involvement of hydroxyl radicals in the cleavage of glucosidic

TABLE XIII

Products of Radiodecomposition of Starch[a]

Product	References
Saccharides	
D-Arabinose	153,155,158
2-Deoxy-D-*arabino*-hexose	72
Deoxy sugars	155,160
D-Erythrose	153,155,158
D-Fructose	153,158
D-Galactose	155,158
D-Glucose	108,130,147,154–159
Maltose	94,108,130,147,153,155–158
Mannose	94,153,155,158
D-Ribose	153,155,158
D-Xylose	153,155,158
Alcohols	
Ethanol	161
Methanol	155,161
Aldehydes	
Ethanal	98,103,145,154,155,159,164,166,167
Glyceraldehyde	145,155
Glycoaldehyde	145,155,165,166
Glyoxal	145,155,165
Malonaldehyde	98,102,103,145,152,153,155,163,168
Methanal	98,103,108,125,130,145,148,152, 153,155,159,161,162,164,166,167
Ketones	
1,3-Dihydroxy-2-propanone	108,130,131,148,155,159,164,165
Propanone	155,158,159,164
Acids	
Acetic	99
Citric	105
3-Deoxy-*glycero*-tetronic	155
5-Deoxy-*cyclo*-hexuronic	155
Formic	99,102,153,155,169
Fumaric	105
D-Gluconic	147
D-Glucuronic	147,159,164
Glycolic	99
Glyoxalic	99
Malic	99,105
Malonic	105
Oxalic	98
Pyruvic	99,159,164
Tartaric	105
Esters	
Esters (generally)	153
Methyl formate	155,161
Heterocycles	
Hydroxymaltol	160,170
(5-Hydroxymethyl)-2-furaldehyde	108,120,130,134,165

[a]Apart from dextrins.

bonds. According to Sosedov and Shabolenko,[171] water does not participate in such cleavage, even in the irradiation of starch sols and gels. D-Erythrose, which is also formed, gives glycolic aldehyde whereas glyceraldehyde is transformed into 1,3-dihydroxy-2-propanone.[150] According to Khenokh *et al.*,[172] 1,3-dihydroxy-2-propanone arises from mannitol. The yield of glycolaldehyde is linearly related to the dose of radiation, curvilinearly related to temperature with a maximum set at about 25°C and being constant up to over 60°C, and curvilinearly related to water content in starch with a maximum yield at about 12% (Fig. 23). Formaldehyde, acetaldehyde, malonaldehyde, and glyoxal are simple aldehydes formed on irradiation whereas simple ketones are represented solely by 1,3-dihydroxy-2-propanone and acetone (see Table XIII).

The levels of glyoxal and 1,3-dihydroxy-2-propanone are dose-dependent and the increase of total carbonyl compounds is a linear function of dose[167] up to 2×10^{21} eV/g. Although Tollier and Guilbot[120] found that malonaldehyde, glycolaldehyde, and (5-hydroxymethyl)-2-furaldehyde are formed with yields that depend on the radiation dose, other authors[116,168,173] have stated that the concentrations of these compounds are independent of the dose of irradiation (the latter two at least between 1.5×10^6 and 4.5×10^6 rad). Berger *et al.*[155] have proposed the following mechanism for the formation of particular aldehydes.

Malonaldehyde and glycolaldehyde are formed by the rupture of glucosidic bonds, followed by formation of the aldehyde group from the C-5 atom.

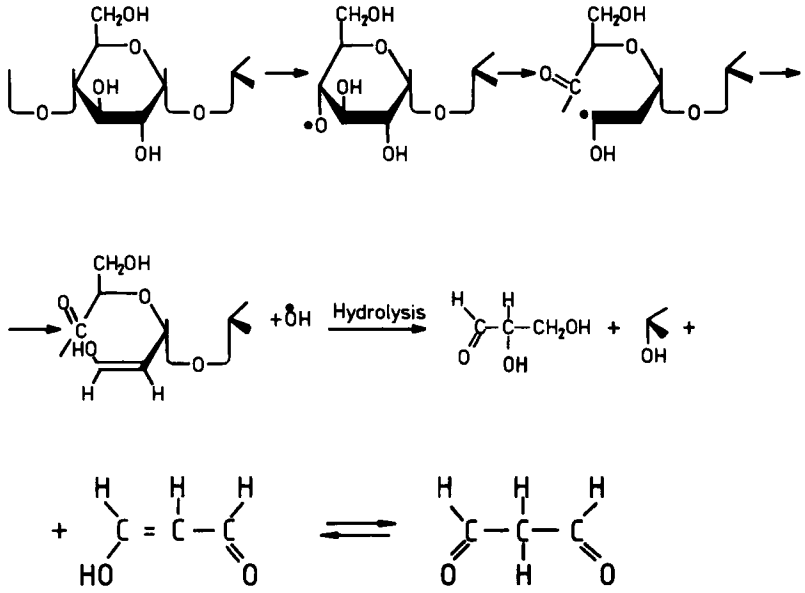

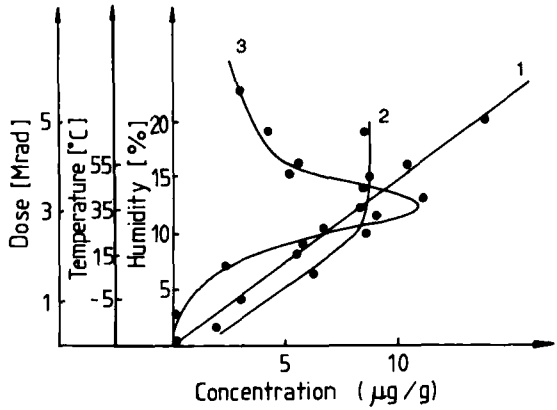

FIG. 23.—Concentration of glycolaldehyde [μg/g] as a function of the radiation dose (1), temperature (2), and humidity (3).[168]

If the aldehyde group is formed from C-4, the resulting radical can give both glycolaldehyde and acetaldehyde.

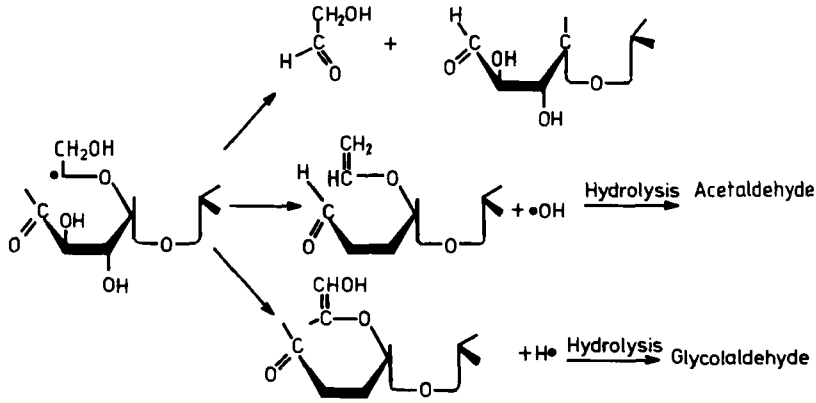

Analytical methods for the determination of malonaldehyde are particularly well developed. 2-Thiobarbituric acid in the presence of trifluoroacetic acid reacts with malonaldehyde to give a product whose absorption at 530 nm is proportional to the irradiation dose up to 400 rads. This reaction is proposed as a test for determining the absorbed dose, provided that the humidity of the sample, date of irradiation, and the temperature of storage are known.[152,168,173] An alternative method is the reaction of malonaldehyde with 2-methylindole.[174] The same reaction has also been used for the determination of deoxy sugars, but this requires oxidation with periodate to give malonaldehyde.[175,176]

Formaldehyde seems to be the obvious product of depolymerization of monosaccharides. According to Berger *et al.*[155] details of the process are as follows.

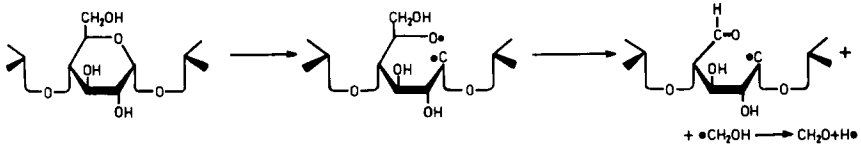

The $\cdot CH_2OH$ radical may also give methanol on reaction with water.

$$\bullet CH_2OH + HOH \longrightarrow CH_3OH + HO\bullet$$

Formic acid seems to arise from oxidation of formaldehyde. On the other hand, Berger *et al.*[154,169] have suggested the formation of formic acid from a glucose residue cleaved with participation of the hydroxyl group of the 6-CH_2OH moiety.

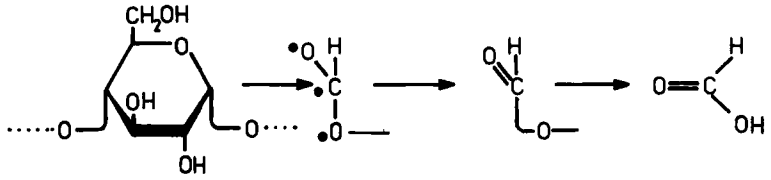

Esters are formed similarly. Formic acid contributes to the total acidity of irradiated starch, as displayed in Fig. 22. This Figure also presents the effect of the dose of radiation, temperature, and humidity.[169] Other radiation-specific products are also formed[177] (see Table XVI).

As with starch, mono- and oligosaccharides exhibit peculiar behavior in their formation of free radicals on irradiation. Stable free radicals are present, even if their formation proceeds in air and at low moisture content. Water at higher concentrations, and also methanol and ethanol, behave as free-radical scavengers, with ethanol being less effective than the other compounds. The character of the radicals from irradiated dry starch and from starch containing these solvents is different.[178] Their concentration is irradiation-dose dependent, with the maximum of their concentration at 60 Mrad being perhaps attributable to an increase in the volume of gaseous products evolved when higher doses of radiation are applied.[179–181] According to Tikhomirov *et al.*,[182,183] the increase in concentration, N, of free radicals on radiolysis is given by

$$N = N_0(1 - e^{-kD}), \qquad (6)$$

where N_0 is the original concentration of radicals, k is the rate constant of the process, and D is the radiation dose. This curvilinear plot may also result from accelerated decay of radicals in the late stages, when their concentration is high

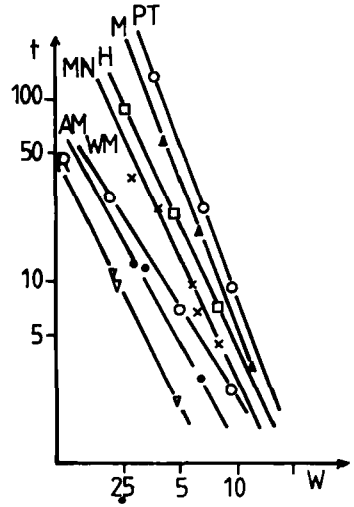

FIG. 24.—Water content, W (%), in starch as a function of time (days) of transformation of free radicals from the AA′ to the BB′ form. See Fig. 16 for notation of symbols (from Ref. 103).

enough for easy collisions. Varying conditions of permeability of gases may also be a factor.[92,184] The second-order specific rate constant of the free-radical decay, determined for periods up to 137 days, was of the order of 10^{-3} liter/mol/s.[185] The character of free radicals from irradiated starch is also dependent on the physical structure of the material. Henderson *et al.*[178] have distinguished between four different radicals. Raffi *et al.*[102,103] have distinguished between two major types, or rather groups, of radicals regardless of either the origin of the sample or the water content, although the kinetics of changes depended on the water content. There are two fundamental shapes of the ESR spectra (Fig. 24). The initial spectrum turns into a simpler one as a function of time. The authors assumed that the initial spectrum corresponds to the radical (**1**)

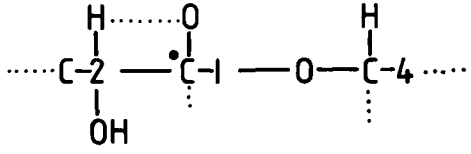

1

with the spin localized at C-1. Contact with atmospheric oxygen turns these radicals into peroxy radicals (**2**).

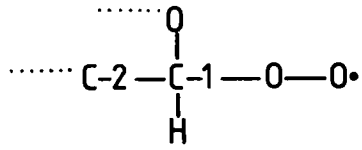

2

The kinetics of evolution of the first-type spectrum into the second type is dependent on the starch origin, and in every case is linearly dependent on the water content. Table XIV summarizes these data, together with corresponding peak-to-peak widths [H (G)] of lines constituting the changes in the spectra under consideration.

Figure 25 shows the effect of water content on the change of one type of spectrum to the other for starch of a particular origin. Adamic and Blinc[186] have suggested division of free radicals into three classes. All of them show a triplet at about 77 K and a doublet and singlet at room temperature. Yershov and Isakova[129] have ascribed the following structures (**3–5**) to these three types of radicals.

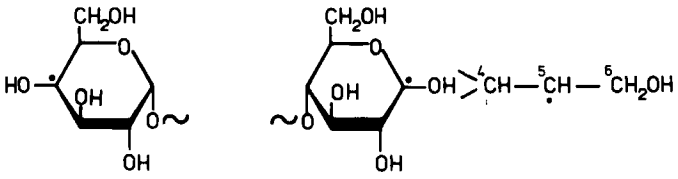

3 4 5

TABLE XIV

Average Values of g Factors and Peak-to-Peak Widths, ΔH(G) of Lines AA′ and BB′[a,104]

Starch origin	Line AA′		Line BB′	
	g	ΔH	g	ΔH
Maize	2.0044	26.1	2.0054	8.51
Amylomaize	2.0049	25.9	2.0048	9.28
Waxy maize	2.0050	25.3	2.0050	8.44
Rice	2.0049	24.9	2.0051	9.10
Potato	2.0050	26.0	2.0051	8.45
Manioc	2.0048	26.1	2.0061	8.54
Bread wheat	2.0047	26.1	2.0055	8.64
Haricot bean	2.0048	25.5	2.0053	8.56

[a]See Fig. 20 for notations.

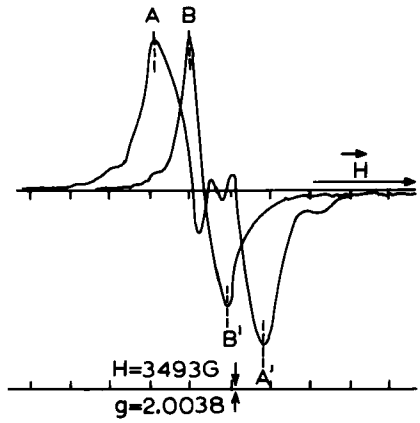

FIG. 25. — ESR spectra of irradiated starch (20 kGy).[103] Line AA', initial shape; line BB', final shape after 95 days.

That is, one of the radicals results from cleavage of the glucose unit on heating up to 200 K. Abagyan *et al.*[187] have found that the shapes of ESR spectra change not only under the influence of atmospheric oxygen but also as a function of temperature in the region above − 40°C. In the case of maize starch at − 196°C there is observed a quadruplet with splitting $\alpha_H = 19 \pm 1$, which turns on heating over the range − 20 to + 30°C into a doublet without any decrease of the overall concentration of free spins. The authors[188] identified the radicals resulting from radiolysis and mechanical treatment of starch. Raffi *et al.*[189] have noted a very close similarity of the ESR spectra of radicals from starch, maltopentaose, and maltotriose. They have proposed these oligomers, therefore, as convenient models for elucidation of the mechanism of the radiolysis of starch.

The irradiation of starch in aqueous gels, sols, and solutions leads to somewhat different results because of the operation of different mechanisms. Although all reactions in the solid state involve free-radical processes, those in aqueous solutions may involve hydrated electrons, which with oxygen give O_2^- ions. Kochetkov *et al.*[190] have assumed that deoxy sugars result from the involvement of O_2^- ions alone, whereas the formation of deoxy ketoses is assisted by hydroxyl radicals. Stockhausen *et al.*[191] have proposed the following sequences of reactions. Ionization of water leads to solvated electrons and further radicals.

$$H_2O \rightsquigarrow H_2O^+ + e^-_{aq} \xrightarrow{+H_2O} H^\bullet + OH^-$$
$$\downarrow +H_2O$$
$$H_3O^+ + OH^-$$

Hydroxyl radicals are also available by decomposition of excited water molecules.

$$H_2O \rightsquigarrow H_2O^* \longrightarrow H\bullet + \bullet OH$$

Hydrated electrons react with oxygen

$$e^-_{aq} + O_2 \longrightarrow O_2^-$$

as well as with C–H bonds.

$$e^-_{aq} + RH \longrightarrow RH^-$$

Both OH and H radicals also rupture these bonds.

$$\bullet OH + RH \longrightarrow R\bullet + H_2O$$
$$H\bullet + RH \longrightarrow R\bullet + H_2$$

Radicals formed in this manner accept oxygen molecules to form peroxide radicals, which react either with the $\cdot O_2H$ radical or are transformed into carbonyl compounds according to the following scheme.

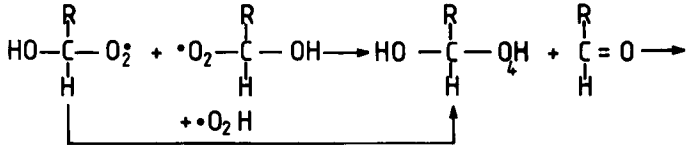

$$\longrightarrow RCH(OH)\text{-}O\text{-}O\text{-}CH(OH)R \rightleftharpoons RCHO + H_2O_2 + RCHO$$

For starch in solution, all portions of the molecule can become reaction sites.

The effect of γ-radiation at doses 10^2–10^6 rad on starch sols is negligible at the outset of the irradiation. Sedimentation then becomes slower and progressive turbidity is observed. Both phenomena are dose-related for corn[192] and potato[193] starch. According to Khenokh,[193,194] neither the increase of reducing power of 0.3% potato starch sols nor the decrease of its pH and relative viscosity are linear with respect to time of exposure at constant γ-irradiation intensity (Fig. 26).

The effect of irradiation on starch gels is generally monitored by changes in viscosity, reducing power, and reaction with iodine. It has been confirmed that the viscosity of starch gels decreases with the irradiation dose.[79] The reducing power of gels increases almost linearly with the time of irradiation.[193] Oreshko *et al.*[113] studied the plastic strength of irradiated gels. They interpreted the observed nonlinear change of this parameter with the dose (Fig. 27) as being the result of changes of the number of hydroxyl groups capable of forming hydrogen bonds attributable to depolymerization and deformation of original gel network. Low doses (up to 4×10^6 rad) change the gel network in a manner such that hydroxyl

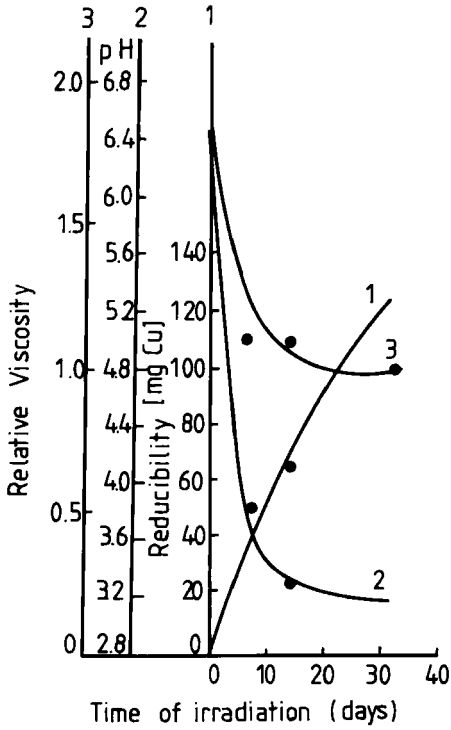

FIG. 26.—The effect of radiation on reducing power (1), pH (2), and viscosity (3) of starch sols (from Ref. 194).

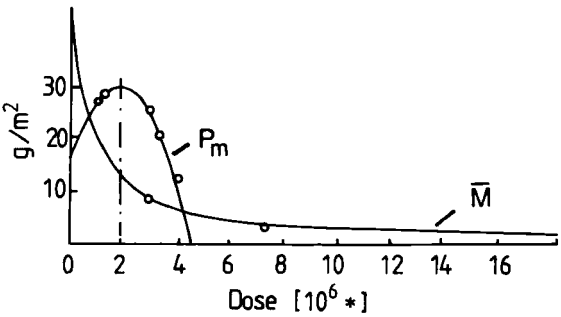

FIG. 27.—Variation of the shear, P_m, and mean molecular weight of starch gel with irradiation dose.[113]

groups of starch, normally hidden inside the network and not participating, become exposed and able to participate in the formation of starch bonds. At $4-5 \times 10^6$ rad, the average molecular weight decreases 10-fold. The plastic strength of gels at this stage is retained because of interactions of terminal groups of the macromolecules. At doses of 18.2×10^6 rad, depolymerizing breakdown produces molecules of such low molecular weight that they can no longer form gels. Water plays an essentially stabilizing role in gels of irradiated starch, in contrast to gels of nonirradiated starch.[195] It also participates in the transformation of primary radicals resulting from C–H, C–OH, and CO–H bond scission.[155] Figure 28 shows the variation of plastic strength of gels according to their concentration.

Irradiated gels show strengthening during aging, and this effect roughly parallels the increasing dose applied. Slits are formed in the same number, independently of the radiation dose, but their dimensions increase. They are filled with increasing volumes of syneretic liquid (up to 23.4% at 6.4×10^6 rad), and this accelerates aging. Simultaneously, starch depolymerizes significantly and this is accompanied by a change in the color of the iodine–saccharide complex to red-brown. The retrogradation of starch after irradiation with 10^6 rad increases[196] by almost 6%. The content of reducing compounds reaches 17.2%. These compounds are sustained in gels, and only a very low concentration of them enters the syneretic liquid.[197,198] In contrast to nonirradiated gels, there is no relation in irradiated gels between liquid formed and the concentration of starch in the gel. There is also no correlation between the content of reducing compounds and the extent of aging of the gel.[199]

Radiolysis of starch solutions gives carbonyl compounds, including malonaldehyde and peroxy compounds,[191] as well as deoxy sugars and deoxy ketoses. The

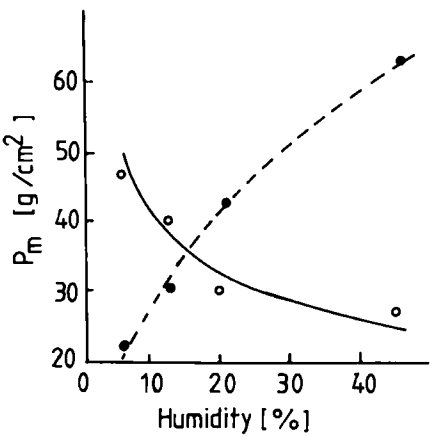

FIG. 28.—The shear–humidity relationships of original (○) and irradiated (●) starch gels (from Ref. 195).

yield, G, in molecules/100 eV of deoxy sugars from radiolysis under nitrogen reaches[200] 0.22 and of deoxy ketoses only 0.01 g. Kochetkov *et al.*[190] gave values of 0.35 and 0.08, respectively. In starch irradiated with a dose of 10^6 rad, the acidity increases[196] by 52%.

The yield of carbonyl and peroxy compounds (Table XV) is dose-dependent up to a limiting value of G (the number of reacting molecules), which is 12.6 and 3.5 per 100 eV of radiation energy absorbed, respectively. Estimation of total carbonyl compounds and peroxides may provide an appropriate indicator for irradiation control in the sterilization of foods and drugs containing starch.

The decomposition of starch in gel form is supposed to proceed by the intermediacy of the products of radiolysis of water.[92,197,199] A mechanism that involves scission of the C–O–C linkages, rearrangement of the radicals, and their reaction with oxygen and water was proposed by Berger *et al.*[155] Mechanisms proposed previously also make similar assumptions. Thus Samec[201] and others[202] have pointed to favored splitting of (1 → 4)-α-D-glucosidic bonds over the (1 → 6) (isomaltose) bonds. Khenokh[203] has proposed different pathways of radiolytic destruction by different doses of radiation. Studies on the combined action of protons and γ-radiation on depolymerization of starch have been carried out by Raffi *et al.*[204]

Interesting results published by Hofreiter[92] point to the possible involvement of a solvent effect on radiative polymerization of starch. The G(scission) values for amylose in dimethyl sulfoxide–water mixtures of various ratios vary by approximately 6 times. The G(scission) value is also dependent on atmospheric oxygen and the temperature of the irradiated gel as shown in Table XVI. The observed effect may arise from the scavenging action of solvent on the free radicals formed. Such an effect is also exerted by water itself, as well as by methanol and ethanol. Based on the shapes of ESR spectra, Henderson and Rudin[178] have distinguished four types of such radicals. One type arises by abstraction of a hydrogen atom from C-1 of the terminal glucose unit of starch, and this results in a doublet with a

TABLE XV

Yields of Radioproducts (G-values) from Radiolysis of Starch Solutions in the Presence of Oxygen[193]

Dose × 10^{18}eV/mL	$G1$ for carbonyl compounds molecules/1000eV	$G2$ for peroxides molecules/1000eV	$G1/G2$
0.75	12.35	4.01	3.08 : 1
1.45	12.50	4.10	3.05 : 1
2.46	12.32	3.91	3.15 : 1
5.07	12.35	3.20	3.86 : 1
8.92	12.30	2.09	5.88 : 1

TABLE XVI

Effect of Solvent Composition on Radiative Depolymerization of Maize Starch and Amylose[a,b,93]

Solvent composition	Solution temp. (°C)	*G*(scission) breaks/eV[c]	Sparging gas
Water	55	5.1	O_2
		32.0	None
	60	38.4	N_2
	25	30.4	N_2
Me_2SO—water 25:75	22	12.3	N_2
50:50	22	10.2	N_2
80:20	22	6.9	N_2
99.8:0.2	22	2.3	N_2

[a] The irradiation dose was 12 Mrad/h from a source of total activity of 8000 Ci. [b] The gels were prepared from 5% starch suspensions. [c]Calculated from intrinsic-viscosity data determined in 90% aq. Me_2SO.

coupling constant of 15.0 gauss. The second type of radical originates by abstraction of the hydrogen atom from the C-2, C-3, or C-4 atoms, followed by β-interaction with two adjacent protons. This radical is manifested by a triplet with a coupling constant of 13.0 gauss. The third type of radical, displaying a doublet of coupling constant 256.0 gauss, results from cleavage of either the C-5–C-6 or C-4–O bonds. Finally, the fourth type of radical is suggested to result from abstraction of the hydroxyl group from C-6. The observed solvent effect associated with the irradiation of starch may arise from the different extents of solvent interaction with individual glucose units of starch. These interactions could block certain positions of glucose units prior to irradiation and to influence radical formation.

b. Irradiation of Cereals.—Cereals are more resistant to irradiation than is the starch produced from them.[205]

Changes that occur in starch on irradiation may influence the organoleptic and technological properties of flour. Several properties of cereals following irradiation have been studied, mainly on wheat. Generally the same compounds could be identified in irradiated cereals as in starch, but the presence of lipids, proteins, and other compounds present in cereals usually obscure estimations. Thus, for instance, the test for irradiation based on the reaction of malonaldehyde and thiobarbituric acid is unsuitable.[206]

Flour has lower mechanical resistance after irradiation. The starchy component of cereal undergoes obvious changes, disulfide bonds also undergo cleavage, and albumins and globulins are degraded to polypeptides. There is, however, a fraction of gluten resistant to irradiation up to 60 krad. The amylolytic activity of flours remains unchanged. The content of reducing sugars increases and that of starch

decreases, and these changes were sustained during 13 months of storage. The changes may be on account of increased acidity of the irradiated flour. Vitamin B_1 is also partially decomposed.[207-213] Another report states, however, that amylase activity decreases by half on irradiation with a 700-krad dose while the protein fraction remains unaffected.[6] Starch protects proteins to a certain extent against degradation. Carotenoids and xanthophylls are also degraded, giving conjugated trienes and dienes.[214] The darkening of irradiated flour seems to be caused by the Maillard reaction.[215] Lipids undergo peroxidation. The dose necessary for extermination of insects is only $2-5 \times 10^4$ rads and this level changes neither the organoleptic properties nor the nutritive value of flours.[216] The effect of irradiation increases with increase of the humidity of grains and flour.[210] Heating of flour after irradiation obviously changes its composition. The content of ω-hydroxymaltol may be increased. The storage of irradiated flour also increases the content of this compound.[160]

The result of irradiation clearly depends on the nature of the flour. The amylose component of starch suffers the least change. Overall changes in polysaccharide fraction are linear with the radiation dose.[212,217,218]

The irradiation of flour decreases its technical value. Rice irradiated with 100 krads develops impaired organoleptic and cooking properties.[219] Irradiated wheat flours provide bread showing increasing deterioration of loaf volume and crumb grain. The quality of bread flour decreases linearly with increasing damage by radiation.[215] Bread from irradiated wet wheat bakes too firmly, giving a clay and loam-like texture. Bread from irradiated dry wheat baked poorly because of low rising properties.[220] This behavior may be attributed partly to an enhanced rate of retrogradation of the amylose fraction, as observed by El Saadany *et al.*[221] Doguchi *et al.*[91] have estimated that radiation doses up to 2.5×10^4 rad do not influence the properties of the dough. There are, however, reports suggesting that the effects of irradiation on wheat[222] and wheat flour[223] are opposite. According to these reports, irradiation has positive effects on the quality of bakery products.

5. Biological Studies of Irradiated Starch and Cereals

There have been several studies on the sterilization of food and its components by means of ionizing radiation. These have established the innocuity of foodstuffs irradiated at doses below 10 kGy, and doses at this level were recommended by FAO/IAEA/WHO as being safe.[224]

Because of the free-radical character of the radiative decomposition of starch, the biological studies have given major concern to the mutagenicity of the products. Several studies have revealed that free-radical content of γ-irradiated starch does not cause detectable perturbations in the physiological functions of experimental mice and rats through several subsequent populations. Starch samples tested were irradiated at doses between 20 and 600 krads.[122,225] At these dose levels

some lethality to *E. coli*, is observed, but not to *Bacillus subtilis* and *Saccharomyces cerevisiae;* the lethal effect is caused by hydrogen peroxide, one of the by-products of γ-irradiation. The lethal effect to *E. coli* is inhibited by yeast extracts or peptone.[226,227] Hydroxyalkyl peroxides may also be responsible for the observed lethality.[228] Secondary toxic action may be caused by formaldehyde, another product of irradiation.[227]

The digestibility of irradiated starch and cereals was also studied. The reports confirmed an increase of digestibility with increasing radiation dose up to 10^7 rads. Prolonged feeding of experimental rats with irradiated starch resulted in decreased excretion of calcium from the cunniculs (9.7, 5.5, and 3.5% for nonirradiated, 5-Mrad, and 10-Mrad irradiated starch, respectively).[229]

Multicomponent starchy foods such as cereals also become more digestible after irradiation, but noncarbohydrate components, particularly vitamins, undergo decomposition.[230] However, another report shows that the *in vivo* digestibility of starch in irradiated food is decreased, along with some other side effects (such as reduced digestibility of lipids and proteins), after 8 months of feeding.[231]

6. Applications of Irradiated Starch

The preparation of water-soluble starch is the major practical aim of higher-level irradiations of starch. If starch alone is irradiated the effect of irradiation is dose-dependent, but the dose should not exceed $20-30 \times 10^6$ rad, otherwise dextrins are produced.[232,233] The irradiation of starch in aqueous solution after pretreatment with hypochlorous acid is a patented procedure.[234] Irradiation with a similar dose in the presence of vanadium pentaoxide has also been patented.[235]

Water-soluble starch has found applications in the production of film-forming compositions,[236] and as sizing for paper.[89,237,238] In such cases starch acts as a dispersant for fines and fillers in repulped paper.

Disintegration of starch by radiation enhances the access of enzymes into the interior of granules. Moreover, significant amounts of mono-, di-, and oligosaccharides are formed. Thus irradiation with 5×10^7 rad allows the elimination of a precooking stage for corn starch before its fermentation into alcohol.[239] Lower doses of radiation can be used to produce animal feed of increased nutrient efficiency.[85] Irradiation of red gram *(Cajanus cajan)* starch with a 10^6 rad dose eliminates the flatulence factor in legumes and enhances their textural properties.[87] Potato and corn starches irradiated with a dose of about 10^7 rad are recommended as corrosion inhibitors for steel.[240,241] It has also been found that starch irradiated under certain defined conditions may be used for the separation of organic acids.[242] The effect of irradiation on mechanical properties of tablet granulates and tablets is inconclusive.[243]

V. Visible and Ultraviolet Irradiation

Visible light is capable of decomposing starch, especially when air is concurrently passed through it and sensitizers are present. Zinc oxide is an effective

promoter of oxidation.[244,245] Initially such depolymerizing action was suggested specifically for the case of polarized visible light. The putative depolymerizing action of moonlight on starch was assumed to be due to the fact that moonlight is polarized.[246] This type of depolymerization is in fact an enzymic reaction that is catalyzed by light. Further elegant studies carried out by Navez and Rubenstein[247] have revealed that for such enzymic hydrolysis it is practically unimportant whether the light is either nonpolarized or polarized. Light of very low intensity at 460 nm produces a photochemical oscillating reaction having sine-wave character.[248]

Ultraviolet irradiation of starch leads to its depolymerization.[5,249–252] Depending on the intensity of the irradiation conditions, the process may afford either dextrins, mono- and oligosaccharides, or even water and carbon dioxide. With amylose alone, light of 366 nm produces carbon dioxide, formaldehyde, and formic acid, either in the presence of ZnO or without this sensitizer. The process is clearly aerobic. In air the decomposition is very fast, whereas under nitrogen it is very slow and neither formic acid nor carbon dioxide are formed.[253] The photooxidation in air is followed by light-sensitized hydrolysis and, subsequently by further oxidation of hydrolysis products to the three end-products, namely carbon dioxide, formaldehyde, and formic acid. Whelan and Peat[254] proposed that the initial step of this oxidation resembles oxidation by periodate ion; that is, the C-2–C-3 bond of the glucopyranose residue is cleaved to give "starch dialdehyde." However, on the basis of EPR studies of free radicals, the formation of peroxide groups at C-1 is assumed to be responsible for the chain scission between the glucose residues.[255] The role of sensitization in the case of amylose and amylopectin is presented in Fig. 29. It may be seen that unsensitized photodegradation favors decomposition of amylopectin, whereas the sensitized process favors amylose, albeit with a higher

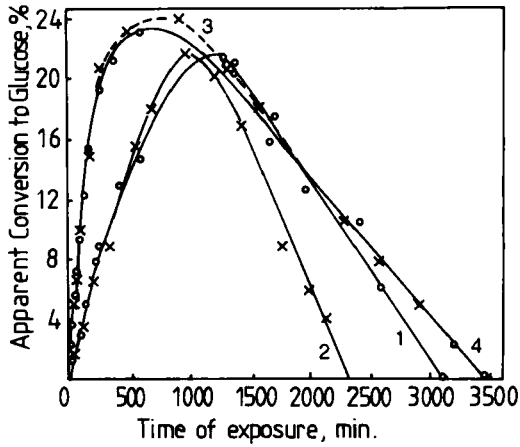

FIG. 29.—The unsensitized (lines 1 and 2) and sensitized (lines 3 and 4) photodegradation of amylose (O) and amylopectin (X).[254]

conversion into glucose in case of amylopectin. The overall degradation of starch to water and carbon dioxide is at least a five-step process. Most of the steps require oxygen to proceed. Scheme 1 depicts the first, third, and fourth steps. The second and fifth steps are purely anerobic and constitute photohydrolysis and simple decomposition, respectively. Although both terminal glucose groups, as well as

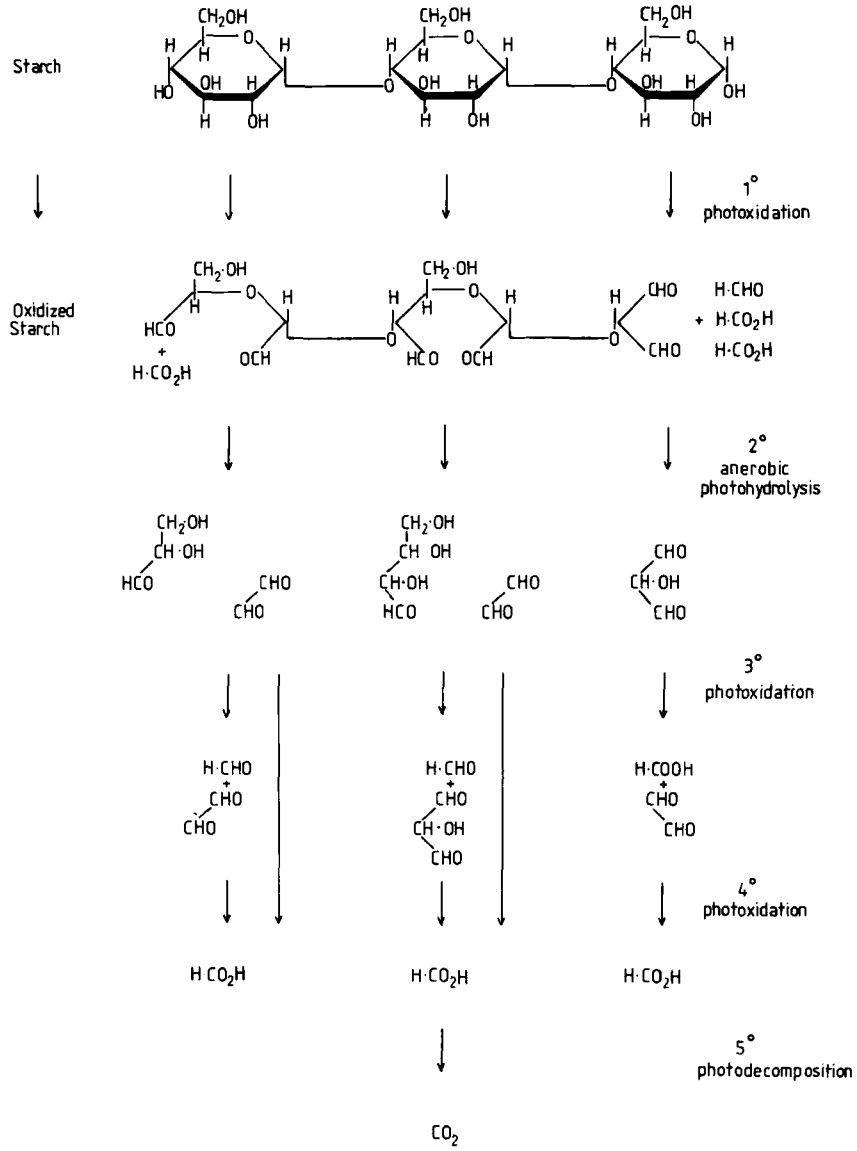

those residues within the chain, give the same final products (water and carbon dioxide), there are three different pathways of decomposition.

In addition to zinc oxide, other sensitizers of photoxidation may be employed. The addition of sodium nitrite in the presence of moisture turns starch into lower dextrins when the material is irradiated with 355-nm light.[256] Ruthenium(IV) and titanium(IV) oxides as well as platinum oxide, all in conjunction with aqueous solutions of starch, eventually produce (in the presence of alkali) hydrogen, carbon dioxide, and photoxidation products.[257] The use of Methylene Blue has also been reported. These studies provide evidence that only the sensitizer, and not the starch, is sensitized.[258]

Water plays an essential role in this photoxidation. Its presence is necessary for, among other effects, the photodecomposition taking place in the natural environment, in conjunction with microbial and enzymic degradation of organic matter.[259]

The first studies of the action of ultraviolet light on starch were performed[260–264] during the period of 1911–1913. Attention was focused on the possibility of converting starch into such useful products as dextrins and lower sugars. The process used involved simple irradiation with a mercury-vapor lamp in the presence of a mineral acid as catalyst. Photolysis of starch under carefully prescribed conditions allows observation of the hydrolysis of amylose phosphoric ester.[265] Both amylose and amylopectin produce mainly maltose and glucose, along with small proportions of other reducing sugars, including pentoses (but not fructose) and traces of trioses,[260,261,263] and also lactic acid.[266] However, ultraviolet irradiation may be a suitable tool for producing dextrins.[250,264,265] Takahashi and Kiharo[267] used a 253.7-nm lamp for 15–60 h. The pretreatment of starch with ferric chloride sensitized starch to photodextrinization.

The character and properties of free radicals produced by ultraviolet radiation appear to be identical to those produced thermally: they are stable and their EPR patterns are the same. Their concentration increases with duration of irradiation within the first 5 h of irradiation. Irradiation during an initial 5 h is slightly more effective[268] than irradiation over the next 20 h. At a given temperature, the yield of radicals generated thermally is much less time-dependent. A comparison of the generation of free radicals by temperature and by ultraviolet irradiation in solid starch is shown in Table XVII.

Free radicals originating from starch, amylose, and amylopectin form well-distinguished 1 : 3 : 1 or 1 : 4 : 1 triplets showing hyperfine splitting of ~ 30 gauss. These triplets are attributed to the derivatives of alkyl radicals produced by abstraction of hydrogen atoms from the 2-, 3-, and/or 4-positions of glucose residues.[269]

Degradation of starch by a carbon dioxide laser beam causes bond cleavage and dextrinizes the starch. The products, which exhibit negligible reducing power have the 1,6-anhydro-β-D-glucopyranose structure at their "reducing" residues[269a] thus resembling the "British gums" (pyrodextrins).[270] *(See Appendix for additional text.)*

TABLE XVII
Number of Spins/g in Potato Starch either Thermolyzed on UV-Irradiated[270]

	Heating (UV-irradiation[a]) time (h)					
Temp. (°C)	**0.25**	**0.5**	**1**	**3**	**5**	**20**
25	(3.5)	(7.0)	(14)	(35)	(56)	(128)
70			0.8			
100	0.9	1.8	3.4	7.9	8.5	10
120			48			
150			914			
170			7910			

[a]The number of spins/g after UV-irradiation is given in parentheses.

VI. THERMAL EFFECTS

The effects of increased temperature (thermolysis) of starch by conventional heating have been reviewed.[2] In the present article, the effects of freezing, as well as heating by infrared and microwave radiations, are described.

1. Modification of Starch by Freezing

The well known property wherein water reaches its maximum density around + 4°C and increases its volume on freezing offers another method for disruption of the macro- and subsequently the microstructure of starch. This potential seems to be confirmed by differential scanning calorimetry of freeze-dried wheat starch; this material exhibits lower gelatinization enthalpy than normal starch.[271] For potato starch, this expectation is again confirmed by measurements of the temperature of gelatinization. As shown in Table XVIII, normal potato starch and that frozen with an excess of water gelatinize at the same temperature. Again freeze-dried native starch and oven-dried (135°C, 3 h) starch gelatinize at a lower tem-

TABLE XVIII
Gelatinization Temperatures of Potato Starch Dried by Various Methods[275]

Starch/drying method	Gelatinization temp. (°C)
Native	66
Freeze-dried	60
Frozen with water (starch : water = 1.5)	66
Native, frozen	66
Dried at 135°C for 3 h	61

perature. The enthalpy of gelatinization is also dependent on the water content, as shown in Table XIX. It increases with water content and is lower by 1.0 to 1.3 cal/g for freeze-dried starch. This difference reflects the fact that a lesser amount of water penetrates the starch granule on gelatinization of freeze-dried starch. It is not necessarily because of damage of starch granules but on account of alteration of their structure.[272] The crystallinity of starch after freeze-drying is lower than that of air-dried starch,[273] and freeze-dried flour exhibits increased water absorption.[274]

Another possibility for the application of freezing is found in the case of starch sols and gels. In starch gels only a small amount of water (0.84–4.24 kg per 1 kg of starch, depending on the nature of the starch) is specifically bonded. This water component may be distinguished into two fractions. One fraction is strongly bonded, with a binding energy of 0.155–0.655 Mjoule/kg. It freezes in starch at 0 to − 30°C. The other fraction is very strongly bonded (binding energy of 0.655 Mjoule/kg and higher) and does not freeze, even at − 30°C. This fraction forms the main matrix of crystals.[275] Freezing of starch sols results in their coacervation. The samples take on a sponge-like appearance. Retrogradation is significantly increased in such starch. Pregelatinized starch is less sensitive to retrogradation and stays smooth after freezing and thawing.[276] It is the result of dehydration by ice formation. In order to achieve coacervation, starch has to form a colloid. This colloid separates on freezing into two sol fractions. One of them is richer in dispersed colloid (coacervate) than the other.

Gels of low concentration (0.1–1.0%) give separated droplets and myelin. At concentrations above 4.5% the gels turn into a sponge-like continuous network of sheets and stands with small amounts of droplets and myelin. Amylose and amylopectin also undergo coacervation.[277]

The results of freeze-drying, expressed in terms of the temperature of the loss of structure (T_c), depend on the rate of drying, according to

$$T_c = T_B - (t_c/45)(10°F), \tag{7}$$

where T_c is defined as the temperature above which starch turns into glass-like

TABLE XIX

Gelatinization Enthalpy of Native and Freeze-Dried Potato Starch and Effect of Water Content on It[275]

	ΔH (cal/g) of starch		
Water : starch ratio	**Native starch**	**Freeze-dried starch**	**ΔΔH**
1 : 1	2.3	0.8	1.5
1.2 : 1	3.3	2.3	1.0
2 : 1	5.2	3.3	1.3

material, T_B is the temperature of the cooling bath, and t_c is the time necessary to achieve a change at T_B after transfer from a bath of temperature T_B-10°F.[278]

2. Modification by Infrared Radiation

It has been mentioned by Baly[279] that, although carbohydrates do not selectively absorb ultraviolet and visible light, they do show selective absorption of infrared radiation in the wavelength range of 1.5–6 μm. This observation prompted Semmens[280,281] to examine the action of polarized infrared radiation upon starch. She realized that mild hydrolysis takes place in starch subjected to such treatment, as well as to irradiation by nonpolarized infrared radiation. The effects of such radiation are observed in samples both *in vitro* and *in vivo* (namely in plants).

The first result of applying infrared radiation to native starch is degradation. Schierbaum *et al.*[11] observed the sequence of dehydration, in which nonbonded water is driven off prior to capillary water (Fig. 30). The shape of the diagram suggests that the effects of heating are very mild. Thus infrared heating has the potential for subtle modifications of starch. The amounts of particular portions of water are obviously different for potato starch, cereal starches, and soaked starches.

Dohnalek and Cap[282] observed detectable changes in barley and other starches: irradiation products were observed after only a 10–60 s of irradiation. The degree of degradation was dependent on the moisture content in these starches. Dry barley was degraded to the extent of ~ 20%, whereas barley containing 12.3–22% moisture gave 40–60% of degradation. Soybean, wheat, and pea starches containing 9.5, 12, and 10.4% of moisture, respectively, were degraded by 15–20, 10–20, and 5–10%, respectively.

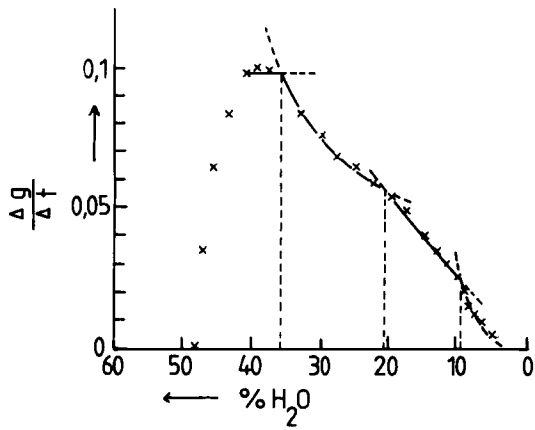

FIG. 30.—Diagram of dehydration (the loss of mass, μg, as a function of time, Δt) of potato starch by infrared irradiation (from Ref. 11).

3. Modification by Microwave Radiation

Molecules subjected to microwave radiation may undergo excitation by specific frequencies of that radiation. Such dielectric coupling causes reorientation of molecules, molecular frictions, changes in hydration, and so on. All of these factors lead to absorption of microwave energy, which is transformed into heat. The dielectric constant and moisture content of the sample are important factors for targeted heating by microwaves.

The first applications of 3.5- to 21-m microwave radiation to starch did not yield promising results. The small effects observed were attributed solely to the effect of heat.[283] The results were dependent on the type of starch, possibly resulting from their varying contents of moisture and mineral salts. The increase of temperature of irradiated starch was nonlinear in time, and showed a downward tendency. The kinetics of heating is presented in Fig. 31. It may be seen that the course of the change of temperature (in ΔT) as a function of time is not proportional to the water content. This trend is observed in all soluble starches, in amylose, and in native potato starch, as well as in gelatinized potato starch. However, a regularity is noted when changes in ΔT after the 20-min period of heating are taken into consideration. There is an essential increase in ΔT in the interval between a water content of 12–16% (by 26–28°C) and 50–55% (by even up to 42°C) (Fig. 32). This phenomenon is interpreted as the result of differences in thermal conductivity, in particular of the moisture, of the materials under study.[284] The differences in thermal capacity of the samples do not seem to be involved, as shown by Skuratov[285] in the case of native and gelatinized starch. Both samples had the same thermal capacity, c, which was proportional to and slightly dependent on the humidity content, u, as given by

$$c = 0.290 + 0.0071u. \tag{8}$$

The kinetics of heating is obviously dependent on the microwave frequency used, as shown by Goebel *et al.*[286] Comparative studies on microwave and conventionally heated starch[286–288] have shown that the kinetics of heating are not comparable (Figs. 33 and 34). In consequence, the properties of dextrins produced by microwaves and those formed by conventional heating are different, although none of these properties can be ascribed directly to the method employed. The results of both modes of heating are also different, as shown in Fig. 35. It may be seen that the heated samples are mostly nonuniform. They separate into gelled, chalky, and watery regions. No single method may be recommended as being universal in terms of uniformity of heated samples. The power of the generator is of minor importance, at least over a narrow range of radiation. In a wider range of frequencies (between 6 and 40 m) the differences are more apparent.[289] The viscosity of the samples seem to play some role. Van Everdinge[290] has reported that colloidal solutions of starch, treated with 3000-MHz microwave radiation lose their optical

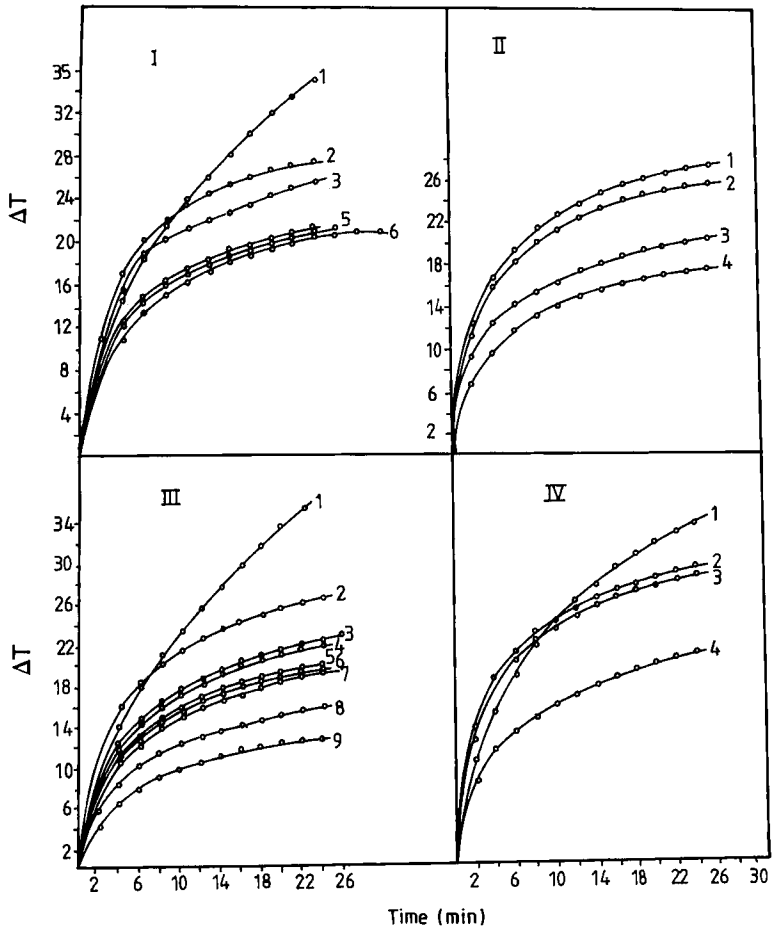

FIG. 31.—Kinetics of heating starch in a microwave field (I) Soluble starch with: 1, 55%; 2, 8.4%; 3, 33.3%; 4, 26.1%; 5, 15.75%; and 6, 0.38% water content. (II) Potato amylose with: 1, 17.9%; 2, 15.8%; 3, 22.8%; and 4, 0% water content. (III) Native potato starch with: 1, 55%; 2, 10.05%, 3, 3.05%; 4, 2.15%; 5, 37.2%; 6, 16.8%; 7, 27.9%; 8, 26.1%; and 9, 0% water content. (IV) Gelatinized potato starch with 1, 17.9%; 2, 15.8%; 3, 22.8%; and 4, 0% water content (from Ref. 284).

activity, even if diluted with glycerol instead of water. This change is related to a change of the viscosity of solution.

Six stages may be distinguished in the microwave heating of starch, based on swelling of the granules. The granules retain their shape and birefringency in the first stage. In the second stage, small granules clump and larger ones start swelling and become slightly plastic. The birefrigency is maintained. In the next, third step, small granules become folded. Nevertheless, even in this stage, they remain bire-

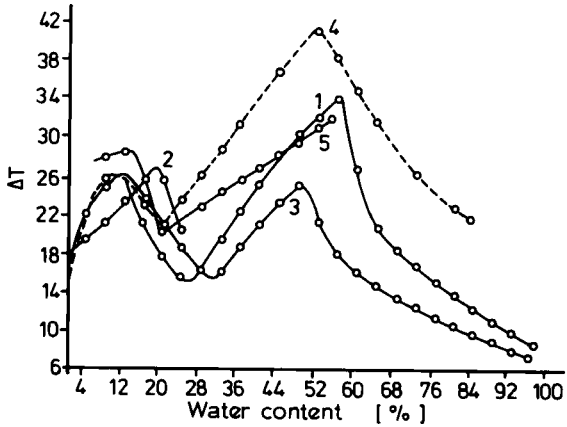

FIG. 32.—Change of temperature in the 20th min of heating of potato starch in a microwave field. 1, Native starch; 2, amylose; 3, amylopectin; 4, dispersed starch; and 5, gelatinized starch (from Ref. 284).

fringent. In the fourth stage, the change in appearance of small granules becomes pronounced and large granules fold to such an extent that the matrix is still present. Single granules still exhibit birefringency. Two remaining stages bring all granules together, finally into a fibrous matrix with large granules being barely recognizable.[286,288]

Microwave heating has not evoked a great deal of attention in the area of starch modification. Effective starch modification is achieved when the microwave energy is coupled with hydrolytic activity originating from added mineral acid. The

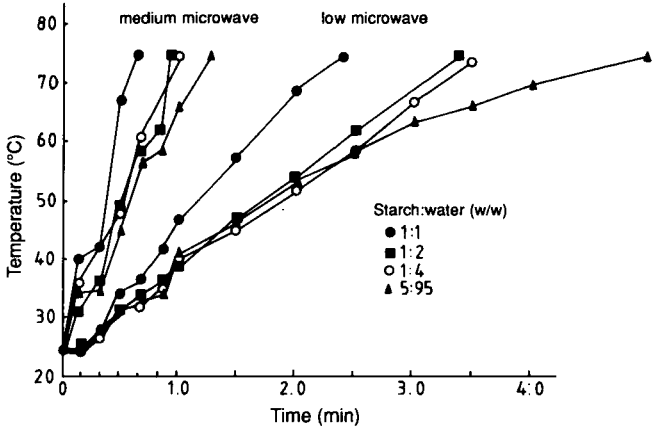

FIG. 33.—Time–temperature curves for wheat starch–water systems heated to 85°C by microwaves (from Ref. 286).

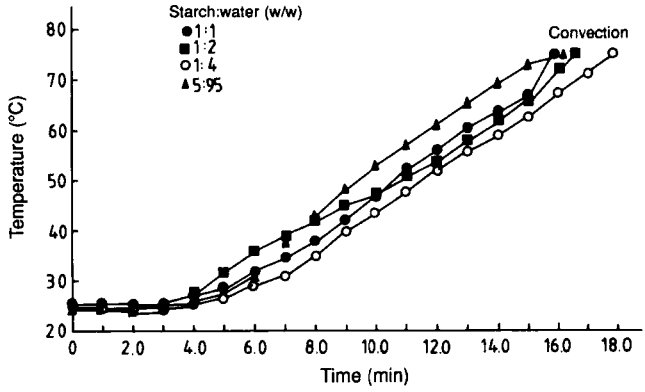

FIG. 34.—Time–temperature curves for wheat starch–water systems heated by conduction (from Ref. 286).

acidity of irradiated starch suspensions that were neutral at the outset increases as a function of the concentration of starch and period of heating. A starch solution that was originally neutral was 93.25% hydrolyzed, whereas acidified solutions were hydrolyzed faster but with approximately the same yield. This type of irradiation has been recommended for fast and efficient saccharification of starch to sugar syrups of high dextrose equivalent.[291] Two patents describe the production of dextrins using 2450-MHz microwaves. Thus a mixture of potato starch containing up to 20% (w/w) of water, 0.1% (w/w) of colloidal SiO_2, and 1 *M* hydrochloric acid fluidized in air and heated at 100–300 mA gives a dextrin of 27.1 cPs Oswald viscosity.[292] Another type of fully amorphous dextrin has been produced from maize starch of 4–60% moisture content using 300 W power at 90°C for 40 s.[293] Saccharification of starch also takes place on heating of a starch slurry by microwaves at 190–240°C in a pressure-resistant vessel.[294] This is a very effective method which may even lead to caramelization. The temperature increases, of course, faster when the concentration of the slurry is higher. The acidity of samples increases with the duration of heating and the concentration of sample. The content of sugars varies in a similar manner. The corresponding data are given in Table XX.[295] *(See Appendix for additional text.)*

VII. ULTRASONIC IRRADIATION

Ultrasonic waves cause depolymerization of starch although they show no effect on many other organic compounds. This depolymerization, using waves of frequencies of 1000–15,000 and even 722,000 Hz produce little dextrin and reducing sugars.[296,297] The decrease in granule size is comparable to that achieved thermally (IR) at about 150°C. The result is dependent on the external pressure and is related to the effect of the gaseous products penetrating the interior of granules. These

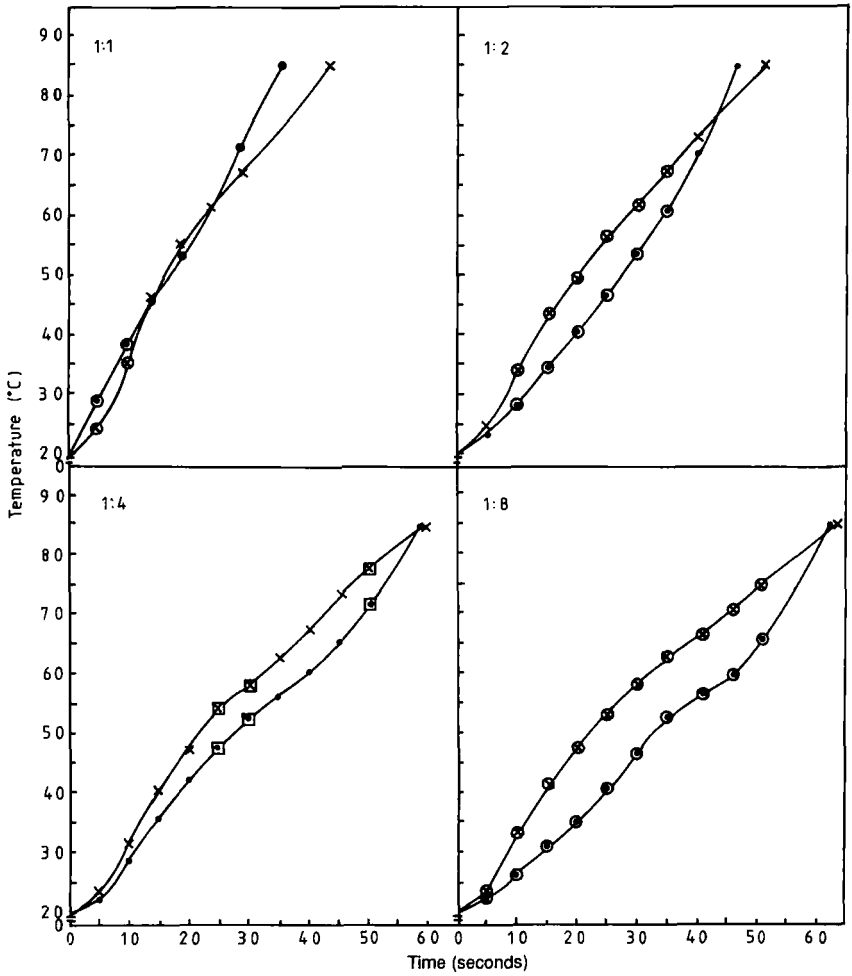

FIG. 35.—Time–temperature relationships using low and medium microwave heating for four starch-to-water ratios (from Ref. 288).

gases undergo pulsation in resonance with the ultrasonic waves. As a result, cavities appear in the granules. The yield of eroded granules is favored by a low concentration of starch in suspension, in the range of 0.1–5%. Atmospheric oxygen, and oxygen alone, increase the disintegration, but an atmosphere of hydrogen has the opposite effect. Change in temperature over the range of 15–60°C has a negligible effect on depolymerization.[298] These observations were confirmed and extended[299,300] to demonstrate the effect of vacuum and of a CO_2 atmosphere, both of which inhibit sonically induced changes at 280 and 960 KHz with ~ 15 W/cm^2.

TABLE XX

Variation of Some Parameters of the Degradation of Wheat Starch by Microwave Radiation in a Sealed Tube[297]

Concentration of Starch Suspension (%)	Time of Radiation (s)	Temp. (°C)	Pressure (kPa)	pH	Total acidity (meq/5mL)	Sugar/Starch (%)		
						Total soluble	Reducing	Glucose
10	960	<170	793	4.5	0.003	47.3	3.1	0.6
	1080	170–173	793–848	5.2	0.006	60.2	5.5	1.5
	1200	173–177	848–938	3.9	0.010	79.8	10.3	3.4
20	960	173–177	848–938	3.8	0.014	62.1	7.9	0.8
	1080	177–184	938–1096	3.6	0.027	79.8	18.0	3.4
	1200	184–191	1096–1286	3.4	0.042	88.7	33.4	11.1
30	960	177–184	1096–1286	3.8	0.028	74.3	19.3	1.8
	1080	184–191	1096–1286	3.2	0.071	93.3	41.7	15.1
	1200	191–198	1286–1489	3.1	0.084	90.4	53.4	23.9

Hence Guilbot *et al.*[299] concluded that the formation of bubbles of gases is an important factor. Their formation is a function of the solubility of gases in the suspension medium, and size of the bubbles, which have to bombard starch granules before they collapse by turning into vapor. The formation of gaseous bubbles results from the acoustic compression–decompression phenomenon in the sonicated sample. The disruption of starch granules increases inversely with the solubility of gases in the medium, with the frequency applied, and the concentration of the starch undergoing sonication. The damage of granules increases with the duration of treatment.[300] At low frequencies (100 KHz), starch granules undergo mainly radial rupture[301] and there is also a lack of separation of granules into concentric tangential lamellae on sonication with frequencies ranging from 14 to 960 KHz. Hence the same authors[299] have supported the view of Sterling and Pangborn[302] that potato starch granules are composed of radial units that probably are fibrillar. The parameters describing the properties of sonicated systems are the ultrasonic velocity, V (dependent on the temperature), adiabatic compressibility, β, acoustic impedance, Z (dependent on concentration), and relative association, RA. These parameters are given by the relations[303]

$$\beta = 1/V^2\rho, \tag{9}$$

$$\mathrm{RA} = \rho/\rho_o\,(V/V_o)^{1/3}, \tag{10}$$

$$Z = \rho V, \tag{11}$$

where ρ is the density of the solution at a given concentration, and V_o and ρ_o are the ultrasonic velocity and the density of pure solvent (water), respectively, at 0°C. Studies by Reddy[304] on aqueous solutions of starch and gelatin show that the behavior of these parameters is the same as in case of solutions of electrolytes and suspensions.

Studies by Khenokh and Zhukov[305] have shown a dramatic increase of reducing power of starch from 0.0 to 198.7 after sonication for 10 h; the electrical conductivity increased from 4.25×10^{-5} to 303×10^{-5} after this time, and the pH changed during the 10 h from an initial 6.15 to 2.37. These changes were accompanied by a change of color from white to light brown. The authors suggested that sonication causes not only hydrolysis but also oxidation. Oxidation under such conditions has already been observed for compounds of low molecular weight (Table XXI).[306] Japanese workers[307,308] have characterized small amounts of glucose and other reducing sugars in the products of sonication-induced hydrolysis of starch. This proceeds on sonification with an energy density of 166–277 ergs/cm^2 independently of the temperature, at least over the range 23–45°C. However, the disruption of cohesive forces between starch chains without decrease of the length of these chains seems to be the initial effect.[309] In addition to glucose Khenokh[310] has also characterized aldehydes and carboxylic acids among the products of sonication. He found no products resulting from decomposition of free glucose. The action of 14.3-KHz waves caused[5] significant changes of starch pastes within

TABLE XXI

Influence of Ultrasound on Starch[307]

Solution of starch	Reducibility	pH	Electrical conductivity (10^{-5} dm^{-3})	Color with iodine
Nonsonicated	0.0	6.15	4.25	Blue
Sonicated				
5 h	57.19	2.98	75.75	Dark violet
10 h	120.40	2.64	166.67	Light orange
15 h	198.66	2.37	303.03	Light brown

minutes. Evidently water plays an important role. Ultrasound of 1 MHz causes[304] gelation of starch pastes at 30°C.

Comparative spectral studies of sonicated starch pastes, inulin, and some mono- and disaccharides show that decomposition of starch is rather slow. Carbonyl compounds are formed in small amounts, as shown in Fig. 36 in which the concentration of such compounds is manifested by an absorption maximum in the region of 280–300 nm. This formation is, however, not paralleled by the formation of sonication products toxic toward paramecia. The first 8 h of sonication of

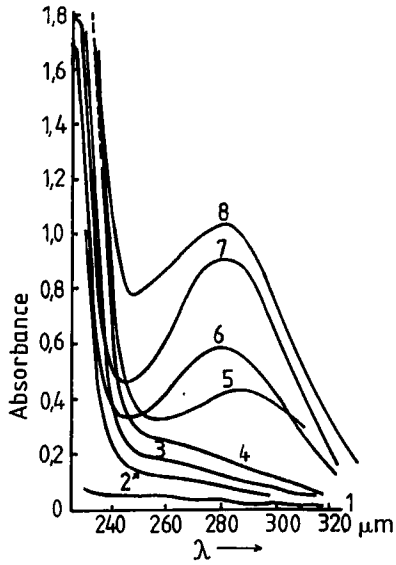

FIG. 36.—Absorption curves of starch solutions. 1, Nonsonicated; 2, sonicated for 5 h; 3, sonicated for 10 h; 4, sonicated for 15 h; 5, inulin sonicated for 15 h; 6, D-glucose sonicated for 15 h; 7, D-fructose sonicated for 15 h; and 8, sucrose sonicated for 15 h.[310]

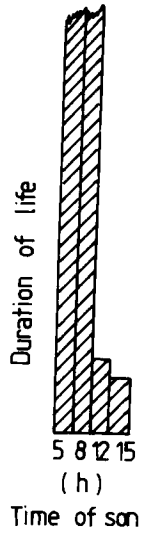

FIG. 37.—Lethality of sonicated starch to paramecia.[311]

starch does not cause any noticeable toxicity, although solutions of maltose, D-glucose, and D-galactose are quite lethal to paramecia. Starch gels sonicated by 12 h are more lethal than solutions of the aforementioned sugars sonicated for the same period (see Fig. 37).[311]

Samec[3,5] has conducted comparative studies on the effects of various types of radiation on the properties of the dextrins produced and found notable differences. The origin of the starch seems to be a factor of minor importance, at least upon sonication with 995 kc/s and 120 W. Potato and arrowroot starch gave similar results.[309] The action of ultrasound on starch gels produces complex changes.[312,313] The mechanism of disintegration has been discussed by Sozaburo.[314]

The use of sonication in combination with γ-rays and ultraviolet light has been proposed.[315] Ultrasound of 14 kHz affects starch by peptization. The use of such ultrasound in combination with acid promotes the saccharification of amylose and inhibits the process leading to amylopectin.[316]

VIII. ELECTRICAL PHENOMENA

The application of potential gradients for starch modification may be utilized in various ways. In the beginning of this century Loeb[317,318] observed that static, silent discharges are capable of deteriorating starch. Within a few hours of exposure to such discharges the starch–iodine complex no longer forms, although there is some evidence that the breakdown of starch is not the sole result. The precipitation

of floccules from starch that was originally soluble, as well as the formation of hexamethylenetetramine from ammonia in another experiment pointed to the fact that silent discharges cause also some aggregation. The floccules were not characterized by modern techniques. They give a positive blue reaction with iodine and the pH of the treated solution remains neutral. Ozone was not detected in the reaction product, but small quantities of hydrogen peroxide could be identified.

Electrodialysis of solutions of starch actually leads to the separation of amylose from amylopectin. However, this is accompanied by disintegration of amylopectin of original 130,000–140,000 molecular weight into a lower-molecular-weight, dialyzable product and a colloidal residue of molecular weight 57,000. This phenomenon is an indirect result of the potential gradient. The electrodialyzed solutions become gradually more acidic, suggesting the involvement of an oxidation process, possibly of terminal glucose groups to give carboxylic acids. Neutralized solutions show no splitting of amylopectin because acid-catalyzed hydrolysis does not occur.[319] Electrodecantation and pH-controlled electrodialysis may be useful for purification of lyophilic sols of dextrin and soluble starch. In this manner it is also possible to hydrolyze amylose phosphoric acid to afford phosphorus-free fractions.[320]

The electrolysis of "glucose syrup" from the acidic hydrolysis of starch yields pure D-glucose. Syrup is placed in a chamber with a lead cathode surrounded by diaphragm.[321] Starch was similarly electrolyzed, with an energy consumption of 0.05–0.1 kWh/kg of starch. The degradation of starch in alkali is less selective and faster than in acidic medium, as shown in Fig. 38.

The glow electrolysis technique (electrolysis with an anode immersed in the solution and the cathode above the surface) at 600–800 V dc and 300–500 mA converts a solution of starch into ethylene, methane, hydrogen, and both carbon mono- and dioxides.[323] Electrochemical methods for converting polysaccharides and other biomass-derived materials have been reviewed briefly by Baizer.[324] These methods are mainly oxidations along a potential gradient, which decreases the activation energy of the reactants. Starch in 5 *M* NaOH solution is oxidized on platinum electrodes to carboxylic acids with an activation energy of about 10 kcal/mol. In acidic media oxidation takes place at C-1 followed by decarboxylation and oxidation at the C-2 and C-6 atoms.[325]

Fig. 39 compares results of the anodic oxidation of starch in acidic and alkaline solution, the former showing the lower reactivity. D-Glucuronic acid is also available by oxidation in an electrolyzer in which chlorine is electrochemically generated from a solution of sodium chloride.[326]

The oxidation of starch to "starch dialdehyde" is the most frequently studied process, with periodate being the most commonly used oxidant. An electrolytic method provides for continuous regeneration of the oxidant.[327,328] The anode is usually made of lead[328] or lead(IV) oxide.[329,330] Cathodes are made of steel. A 99:1 Pb–Ag alloy anode and a steel cathode were used for preparation of starch

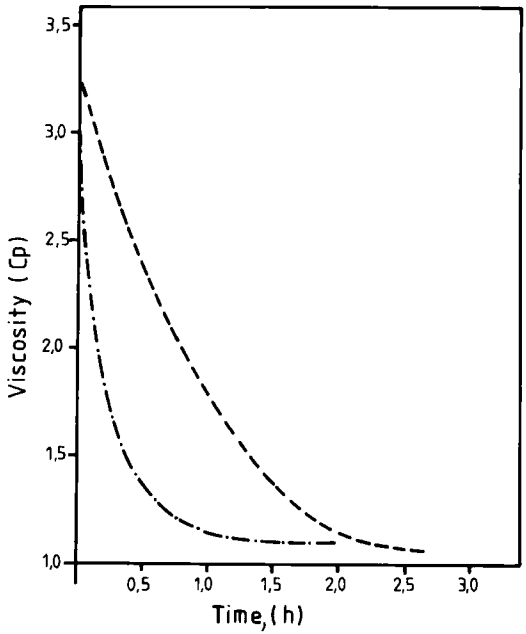

FIG. 38.—Disruption of potato starch in an electrolyzer (50°C) under acidic (- - -) and alkaline (- · -) conditions (from Ref. 322).

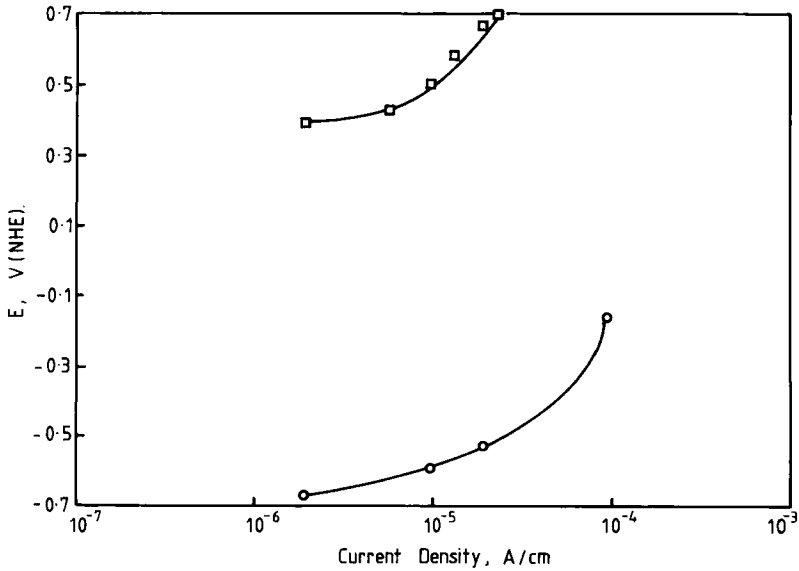

FIG. 39.—Comparison of the rate of anodic oxidation of starch in 40% phosphoric acid (○) and in 1 *M* sodium hydroxide (□) solutions at 80°C (from Ref. 325).

dialdehyde could be achieved.[331] The overall process is a combination of electrolytic oxidation of iodic to periodic acid and the chemical oxidation of starch to starch dialdehyde by periodic acid, which is thereby reduced to iodic acid. The carriers of oxygen are oxidants comprising ions of elements in higher valence states (for instance sodium dichromate).[332] *(See Appendix for additional text.)*

REFERENCES

1. J. L. Roard, *Ann. Chim. Phys.*, [1] 50 (1804) 220–224.
2. P. Tomasik, S. Wiejak, and M. Pałasiński, *Adv. Carbohydr. Chem. Biochem.*, 47 (1989) 279–343.
3. M. Samec, *Staerke*, 13 (1961) 283–291.
4. M. Samec, *Staerke*, 12 (1960) 165–169.
5. M. Samec, I. Kosovinc, and H. Reuschl, *J. Polym. Sci.*, 30 (1958) 545–550.
6. Y. Ghali, S. Gabr, N. Ibrahim, and H. Aziz, *Staerke*, 31 (1979) 372–374.
7. F. Schierbaum, *Staerke*, 12 (1960) 237–242.
8. F. Schierbaum, *Staerke*, 12 (1960) 257–264.
9. F. Schierbaum and K. Taeufel, *Staerke*, 14 (1962) 233–238.
10. F. Schierbaum and K. Taeufel, *Staerke*, 14 (1962) 274–275.
11. F. Schierbaum, K. Taeufel, and M. Ulmann, *Staerke*, 14 (1962) 161–167.
12. F. Schierbaum and K. Taeufel, *Staerke*, 14 (1962) 411–415.
13. F. Schierbaum and K. Taeufel, *Staerke*, 15 (1963) 52–56.
14. H. Lechert, W. Maiwald, R. Koethe, and W. D. Basler, *J. Food Process. Preserv.*, 3 (1979) 275–299.
15. J. A. Blackwell, J. A. Sarko, and R. H. Marchessault, *J. Mol. Biol.*, 42 (1969) 379–383.
16. H. Lechert and J. Schwier, *Staerke*, 34 (1982) 6–11.
17. G. Malfitano and A. Moschkoff, *C. R. Acad. Sci.*, 154 (1912) 443–446.
18. M. Bączkowicz, P. Tomasik, and S. Wiejak, *Staerke*, 38 (1986) 339–341.
19. F. Baunack, *Staerke*, 15 (1963) 299–304.
20. M. Bączkowicz and P. Tomasik, *Staerke*, 41 (1989) 449–452.
21. M. Bączkowicz and P. Tomasik, *Acta Aliment. Pol.*, 41 (1991) 269–271.
22. K. Marusza and P. Tomasik, *Staerke*, 43 (1990) 66–69.
23. R. Heininger, *Kolloid-Beih.*, 35 (1932) 1–48.
24. R. Heininger, *Kolloid-Beih.*, 35 (1932) 331–371.
25. J. N. BeMiller, in *Starch Chemistry and Technology*, R. L. Whistler and E. F. Paschall (Eds.), Vol. 1, Academic Press, New York, 1965.
26. Corn Products Refining Co., Brit. Pat. 531 267 (1941); *Chem. Abstr.*, 36 (1942) 1518.
27. K. Kawai, T. Arima, and K. Ueyama, *Hakko Kogaku Zasshi*, 36 (1958) 1–4; *Chem. Abstr.*, 52 (1958) 16770.
28. S. Masior, *Rocz. Chem.*, 23 (1949) 43–62.
29. K. Lorenz and J. A. Johnson, *Cereal Chem.*, 49 (1972) 616–628.
30. P. Kolbach, *Wochschr. Brau.*, 53 (1936) 369–373, 377–381.
31. M. A. Pozen, *Wallerstein Labs. Commun.*, 3 (1940) 199–206.
32. J. Kobayashi, C. Kobayashi, and T. Fukinbara, *Nippon Nogei Kagaku Kaishi*, 33 (1959) 1123–1127; *Chem. Abstr.*, 58 (1963) 1622.
33. L. Sair, *Cereal Chem.*, 44 (1967) 8–26.
34. Hahn-Haegerdal, K. Skoog, and B. Mattiasson, *Eur. J. Appl. Microbiol. Biotechnol.*, 17 (1983) 344–348.
35. C. R. Jones, *Cereal Chem.*, 17 (1940) 133–169.

36. H. Kashiwagi and S. Enomoto, *Chem. Pharm. Bull. (Tokyo)*, 30 (1982) 17–23.
37. P. W. Bridgman, *Proc. Am. Acad. Arts Sci.*, 76 (1945) 9–24.
38. U. Ebbecke and R. Haubrich, *Arch. Gesamte Physiol.*, 238 (1936) 429–430.
39. P. Paronen and M. Juslin, *J. Pharm. Pharmacol.*, 35 (1983) 627–635.
40. E. Kudła and P. Tomasik, *Staerke*, 44 (1992) 253–260.
41. L. H. Lampitt, C. H. F. Fuller, and N. Goldenberg, *J. Soc. Chem. Ind.*, 60 (1941) 1–6.
42. L. H. Lampitt, C. H. F. Fuller, and N. Goldenberg, *J. Soc. Chem. Ind.*, 67 (1948) 41–44.
43. R. Sutra, *Bull. Soc. Chim. Fr.*, (1947) 738–741.
44. L. H. Lampitt, C. H. F. Fuller, and N. Goldenberg, *J. Soc. Chem. Ind.*, 66 (1947) 417–421.
45. S. Augustat, *Ernaehrungsforsch.*, 3 (1958) 81–90.
46. H. Grohn and S. Augustat, *J. Polym. Sci.*, 29 (1958) 647–661.
47. S. Augustat and H. Grohn, *Staerke*, 14 (1962) 39–49.
48. J. W. Knight, French Pat. 2,015,683; *Chem. Abstr.*, 77 (1972) 36747c.
49. K. Vorwerck, *Ber. Getreidechem.-Tag. Detmold*, (1977) 51–64; *Chem. Abstr.*, 89 (1978) 4785v.
50. D. W. Dowie and H. D. Martin, U.S. Pat. 3,029,169 (1962); *Chem. Abstr.*, 57 (1962) 3684.
51. K. Hess and E. Steurer, *Z. Physik. Chem.*, 193 (1944) 234–247.
52. E. Steurer and K. Hess, *Z. Physik. Chem.*, 193 (1944) 248–257.
53. B. Vergues, J. P. Villemaire, P. Colonna, and J. Tayeb, *Colloq. INRA 1986*, 41(Cuisson-Extrusion) (1987) 141–149; *Chem. Abstr.*, 109 (1988) 192495d.
54. N. N. Tregubov, O. E. Pavlovskaya, and U. Tobisch, *Izv. Vyssh. Uchebn. Zaved. Sakh. Prom.*, 7 (1984) 56–59.
55. L. L. Diosady, D. Paton, N. Rosen, L. J. Rubin, and C. Athanassoulias, *J. Food Sci.*, 50 (1985) 1697–1699, 1706.
56. A. I. Zhushman, E. K. Kopteleva, T. E. Kholmanskaya, and Yu. V. Baranovskii, *Izv. Vyssh. Uchebn. Zaved. Sakh. Prom.* (6) (1974) 60–63.
57. K. Kim and M. K. Hamdy, *J. Food Sci.*, 52 (1987) 1387–1390.
58. J. M. Thevellin, J. A. van Asche, K. Heremans, and S. Y. Gerlsma, *Carbohydr. Res.*, 93 (1981) 304–307.
59. S. Y. Gerlsma, *Staerke*, 22(1970) 3–9.
60. K. Suzuki and Y. Taniguchi, in *The Effects of Pressure on Organisms*, M. A. Sleigh and A. G. MacDonald (Eds.), pp. 103–124, Cambridge Univ. Press, Cambridge, (1972).
61. A. H. Muhr and J. M. V. Blanshard, *Carbohydr. Polym.*, 2 (1982) 61–74.
62. C. Mercier, R. Charbonniere, and H. Guilbot, *Staerke*, 20 (1968) 6–10.
63. E. Kudła and P. Tomasik, *Staerke*, 44 (1991) 167–173.
64. E. Kudła and P. Tomasik, *Acta Aliment. Pol.*, 41 (1991) 285–290.
65. J. Lelievre, *Staerke*, 26 (1974) 85–88.
66. M. Boruch, S. Brzeziński, and A. Pałka, *Zesz. Nauk. Politech. Łódż.*, 343, Ser Chem. Spóż., 34 (1980) 17–28.
67. M. Boruch, S. Brzeziński, and L. Pałka, *Zesz. Nauk. Politech. Łódż.*, 361, Ser. Chem. Spóż., 35 (1980) 81–90.
68. V. F. Oreshko, L. F. Gorin, K. A. Korotchenko, G. M. Maslova, L. E. Chernenko, and N. G. Shakhova, *Izv. Vyssh. Uchebn. Zaved. Pishch. Tekhnol.*, (5) (1962) 32–37.
69. R. L. Whistler and T. R. Ingle, in *Starch Chemistry and Technology*, R. L. Whistler and E. F. Paschall (Eds.), Vol. 1, pp. 409–419, Academic Press, New York, 1965.
70. K. A. Korotchenko, in *Radiatsionnaya obrabotka pishchevykh produktov, Dokl. Vses. Nauch. Tekh. Konf.*, V. I. Rogachev, (Ed.), pp. 153–163, 1968 Atomizdat, Moskva, (1971).
71. H. Scherz, *Improv. Food Qual. Irradiat. Proc. Panel*, 1973 (1974) 39–50.
72. G. O. Phillips, *Adv. Carbohydr. Chem.*, 16 (1961) 15–38.
73. C. von Sonntag, *Adv. Carbohydr. Chem. Biochem.*, 37 (1980) 7–77.
74. H. Scherz, *Nature*, 219 (1968) 611–612.

75. L. Ehrenberg, M. Jaarma, and K. G. Zimmer, *Acta Chem. Scand.*, 11 (1957) 950–956.
76. A. Brash, W. Huber, and A. Waly, *Arch. Biochem. Biophys.*, 39 (1952) 245–247.
77. M. Samec, *Staerke*, 15 (1963) 83–85.
78. H. A. Colwell and S. Russ, *Radium*, 9 (1912) 230–232.
79. M. Samec, *Staerke*, 10 (1958) 76–79.
80. C. T. Greenwood and S. MacKenzie, *Staerke.*, 15 (1963) 444–448.
81. G. Fritsch and J. P. Bouldoires, *Mitt. Geb. Lebensmittelunters. Hyg.* 60 (1969) 245–251.
82. J. A. Radley, *Staerke*, 12 (1960) 201–203.
83. K. Takaoka, S. Kawazu, AS. Nishimura, and A. Mishina, *Hakko Kagaku Zasshi*, 33 (1960) 88–91; *Chem. Abstr.*, 55 (1961) 4019.
84. I. F. Kryuk and S. V. Markevich, *Uch. Zap. Beloruss. Inst. Narodn. Khoz.*, 5 (1959) 45–49.
85. E. P. Petryaev, S. L. Kilchitskaya, A. V. Pavlov, Zh. V. Savchenko, and L. A. Avreitsevich, *Vestsi Akad. Navuk BSSR Ser. Fiz. Energ. Navuk*, 2 (1985) 111–114.
86. M. A. Raouf El Saadany, M. Farag El Saadany, and Y. H. Foda, *Staerke*, 28 (1976) 169–172.
87. S. P. Nene, U. K. Vakil, and A. Sreenivasan, *J. Food Sci.*, 40 (1975) 943–947.
88. M. A. Raouf El Saadany, A. El Fatah, A. Safti, and M. Farag El Saadany, *Staerke*, 26 (1974) 190–192.
89. M. Samec, *J. Appl. Polym. Sci.*, 3 (1960) 224–226.
90. S. Jencic and M. Samec., *Z. Physiol. Chem.*, 322 (1960) 1–3.
91. M. Doguchi, Y. Yokoyama, and I. Okada, *Kogyo Kagaku Zasshi*, 64 (1961) 2001–2005.
92. B. T. Hofreiter, *J. Polym. Sci. Polym. Chem. Ed.*, 12 (1974) 2755–2766.
93. B. T. Hofreiter, *Diss. Abstr. Int.*, B 35 (1974) 773–774.
94. E. J. Bourne, M. Stacey, and G. Vaughan, *Chem. Ind. (London)*, (1956) 573–574.
95. Z. I. Kertesz, E. R. Schulz, G. Fox, and M. Gibson, *Food Res.*, 24 (1959) 609–617.
96. M. Samec, *Staerke*, 12 (1960) 99–102.
97. J. P. Michel, J. Raffi, and L. Saint-Lebe, *Staerke*, 32 (1980) 295–298.
98. J. Raffi, J. P. Agnel, B. Dauberte, M. d'Urbal, and L. Saint-Lebe, *Staerke*, 33 (1981) 188–192.
99. J. Raffi, C. Frejaville, J. F. Dauphin, B. Dauberte, M. d'Urbal, and L. Saint-Lebe, *Staerke*, 33 (1981) 235–240.
100. J. Raffi, J. P. Agnel, B. Dauberte, and L. Saint-Lebe, *Staerke*, 33 (1981) 269–271.
101. J. Raffi, B. Dauberte, M. d'Urbal, C. Pollin, and L. Saint-Lebe, *Staerke*, 33 (1981) 301–306.
102. J. J. Raffi, J. P. L. Agnel, C. J. Thierry, C. M. Frejaville, and L. R. Saint-Lebe, *J. Agric. Food Chem.*, 29 (1981) 1227–1232.
103. J. J. Raffi and J. P. L. Agnel, *J. Phys. Chem.*, 87 (1983) 2369–2373.
104. J. P. Robin, M. T. Tollier, and A. Guilbot, *Food Preserv. Irradiat., Proc. Int. Symp. 1977*, 1 (1978) 529–538.
105. K. A. Korotchenko, S. G. Stanimirovich, and D. L. Stanimirovich, *Prikl. Biokhim. Mikrobiol.*, 4 (1968) 721–724.
106. M. T. Tollier and A. Guilbot, *Staerke*, 18 (1966) 305–310.
107. G. M. Maslova and I. N. Putilova, *Izv. Vyssh. Uchebn. Zaved. Pishch. Tekhnol.*, 3 (1963) 28–35.
108. S. E. Traubenberg, K. A. Korotchenko, and I. N. Putilova, *Izv. Vyssh. Uchebn. Zaved. Pishch Tekhnol.*, 6 (1965) 24–28.
109. M. A. Raouf El Saadany, M. Farag El Saadany, and Y. H. Foda, *Staerke*, 28 (1976) 208–211.
110. S. Dilli and J. L. Garnett, *Chem. Ind. (London)*, (1963) 409–410.
111. M. Samec, *Staerke*, 11 (1959) 285–288.
112. K. Horitsu, *Hirosaki Daigaku Nogakubu Gakujutsu Hokoku*, 14 (1968) 7–8; *Chem. Abstr.*, 70 (1969) 44657u.
113. V. F. Oreshko, L. E. Chernenko, and N. G. Shakhova, *Dokl. Akad. Nauk SSSR*, 134 (1960) 636–638.

114. V. F. Oreshko, L. F. Gorin, and G. M. Maslova, *Izv. Vyssh. Uchebn. Zaved. Pishch. Tekhnol.*, 4 (1961) 35–38.
115. K. A. Korotchenko and A. I. Semyenov, *Izv. Vyssh. Uchebn. Zaved. Pishch. Tekhnol.*, 5 (1966) 25–30.
116. M. T. Tollier and A. Guilbot, *Staerke*, 22 (1970) 296–304.
117. I. N. Putilova, I. S. Akulova, Yu. N. Krutova, and G. M. Maslova, in *Radiatsyonnaya obrabotka pishchevykh produktov, Dokl. Vses. Nauch.-Tekh. Konf., 1968*, V. I. Rogachev (Ed.), pp. 163–169, Atomizdat, Moskva (1971).
118. I. S. Akulova, I. N. Putilova, and N. N. Tregubov, *Izv. Vyssh. Uchebn. Zaved. Pishch. Tekhnol.*, 5 (1969) 30–34.
119. M. Athanassiadis and G. Berger, *Staerke*, 25 (1973) 362–367.
120. M. T. Tollier and A. Guilbot, *Staerke*, 24 (1972) 285–290.
121. I. N. Putilova, S. E. Traubenberg, and G. M. Maslova, *Izv. Vyssh. Uchebn. Zaved. Sakh. Prom.*, 41 (1967) 49–55.
122. U. K. Vakil, M. Aravindakshan, H. Srinivas, P. S. Chauhan, and A. Sreenivasan, *Radiat. Preserv. Food, Proc. Symp., 1972*, (1973) 673–702.
123. V. Kh. Shavratskii, I. N. Shablovskaya, and I. N. Putilova, *Izv. Vyssh. Uchebn. Zaved. Pishch. Tekhnol.*, 1 (1976) 170–171.
124. K. A. Korotchenko, T. I. Dorozhkina, and E. A. Sochneva, *Izv. Vyssh. Uchebn. Zaved. Pishch. Tekhnol.*, 3 (1972) 27–30.
125. A. P. Pisanskii and N. V. Romenskii, *Izv. Vyssh. Uchebn. Zaved. Pishch. Tekhnol.*, 6 (1964) 49–53.
126. A. P. Pisanskii and N. V. Romenskii, *Izv. Vyssh. Uchebn. Zaved. Pishch. Tekhnol.*, 5 (1969) 24–29.
127. N. V. Romenskii and A. P. Pisanskii, *Izv. Vyssh. Uchebn. Zaved. Pishch. Tekhnol.*, 4 (1965) 138–140.
128. M. N. Sultankhodzhaeva, K. A. Korotchenko, M. A. Yakubova, V. A. Sharpatyi, and P. K. Khabibullaev, *Proc. Tihany Symp. Radiat. Chem., 1982*, 5 (1983) 1079–1084.
129. B. G. Ershov, and O. V. Isakova, *Izv. Akad. Nauk SSSR Ser. Khim.*, 10 (1987) 2337–2340.
130. I. N. Putilova, S. A. Traubenberg, K. A. Korotchenko, V. P. Komar, and R. G. Zhbankov, *Prikl. Biokh. Mikrobiol.*, 2 (1966) 133–138.
131. V. F. Oreshko and K. A. Korotchenko, *Dokl. Akad. Nauk SSSR*, 133 (1960) 1219–1222.
132. J. Raffi, J. P. Michel, and L. Saint-Lebe, *Staerke*, 32 (1980) 227–229.
133. V. F. Oreshko and K. A. Korotchenko, *Izv. Vyssh. Uchebn. Zaved. Pishch. Tekhnol.*, 5 (1959) 29–34.
134. K. A. Korotchenko, I. N. Putilova, and S. E. Traubenberg, *Tekhnol. Pishch. Rast. Proizkhozhd.*, (1966) 58–60.
135. I. S. Shablovskaya, K. A. Korotchenko, and I. N. Putilova, *Izv. Vyssh. Uchebn. Zaved., Pishch. Tekhnol.*, 3 (1974) 25–28.
136. V. Saini, *J. Food Sci.*, 33 (1968) 136–138.
137. K. A. Korotchenko, R. G. Zhbankov, and V. P. Komar, *Izv. Vyssh. Uchebn. Zaved. Pishch. Tekhnol.*, 5 (1972) 40–43.
138. R. G. Zhbankov, V. P. Komar, and K. A. Korotchenko, *Zh. Prikl. Spektrosk.*, 12 (1970) 149–150.
139. V. A. Yarovenko, N. V. Romenskii, and L. V. Masenko, *Izv. Vyssh. Uchebn. Zaved. Pishch. Tekhnol.*, 3 (1968) 42–44.
140. M. T. Tollier and A. Guilbot, *EURATOM [Rep.] 1974*, EUR 5126 d/e/f/i/n 181–190; *Chem. Abstr.*, 83 (1975) 41693k.
141. M. Pałasiński, P. Tomasik, and S. Wiejak, *Staerke*, 38 (1986) 221–224.
142. P. Tomasik, M. Bączkowicz, and S. Wiejak, *Staerke*, 38 (1986) 410–413.

143. I. N. Putilova, S. E. Traubenberg, and K. A. Korotchenko, *Izv. Vyssh. Uchebn. Zaved. Pishch. Tekhnol.*, 1 (1966) 48–52.
144. G. M. Maslova and I. N. Putilova, *Izv. Vyssh. Uchebn. Zaved. Pishch. Tekhnol.*, 3 (1963) 28–32.
145. J. P. Michel, M. Rigouard, G. Berger, and L. Saint-Lebe, *Staerke*, 29 (1977) 254–260.
146. V. F. Oreshko, *Zh. Fiz. Khim.*, 34 (1960) 2369.
147. A. Mishina and Z. Nikuni, *Nature*, 184, Suppl. 24 (1959) 1867.
148. V. F. Oreshko, L. F. Gorin, and N. V. Rudenko, *Zh. Fiz. Khim.*, 36 (1962) 1084–1085.
149. G. A. Fedorova, A. A. Ivko, N. T. Bondarenko, and V. A. Sharpatyi, *Dokl. Akad. Nauk SSSR*, 297 (1987) 902–906.
150. G. O. Phillips, G. J. Moody, and G. L. Mattok, *J. Chem. Soc.*, (1958) 3522–3534.
151. G. Berger and L. Saint-Lebe, *C. R. Acad. Sci. Ser. D*, 272 (1971) 1455–1458.
152. L. Saint-Lebe and G. Berger, *Report EUR-4695* (1970) 131–139; *Chem. Abstr.*, 78 (1973) 93245q.
153. G. Berger, J. F. Dauphin, H. Athanassiadis, and L. Saint-Lebe, *Report CEA-CONF-2603* (1973); *Chem. Abstr.*, 82 (1975) 121006h.
154. J. Raffi and L. Saint-Lebe, *C. R. Acad. Sci., Ser. D*, 287 (1978) 745–747.
155. G. Berger, J. F. Dauphin, J. P. Michel, G. Enrico, J. P. Agnel, F. Seguin, and L. Saint-Lebe, *Staerke*, 29 (1977) 80–90.
156. H. Scherz, *Staerke*, 23 (1971) 259–267.
157. H. N. Ananthaswamy, U. K. Vakil, and A. Sreenivasan, *J. Food Sci.*, 35 (1970) 792–794, 795–798.
158. G. Berger, J. P. Agnel, and L. Saint-Lebe, *Staerke*, 25 (1973) 203–210.
159. A. Bigler, S. Vaibel, Yu. N. Krutova, I. N. Putilova, and A. Jart, *Prikl. Biokhim. Mikrobiol.*, 5 (1969) 329–334.
160. H. Scherz, *Staerke*, 27 (1975) 46–51.
161. G. Berger, J. P. Agnel, and L. Saint-Lebe, *Staerke*, 26 (1974) 185–189.
162. G. Berger and L. Saint-Lebe, *C. R. Acad. Sci., Ser. D*, 271 (1970) 552–554.
163. G. Berger, D. R. Woodhouse, and L. Saint-Lebe, *C. R. Acad. Sci., Ser. D*, 273 (1971) 1064–1067.
164. Yu. N. Krutova, *Sb. Nauch. Tr. Mosk. Tekhnol. Inst. Pishch. Prom.*, 20 (1969) 72–74.
165. J. P. Michel, M. Rigouard, G. Berger, and L. Saint-Lebe, *Staerke*, 27 (1975) 363–368.
166. E. Hamidi and J. F. Dauphin, *Staerke*, 28 (1976) 333–336.
167. Kim Chul and Ohm Young Ran, *Wonjaryok Hakhoeji*, 4 (1972) 35–38; *Chem. Abstr.*, 76 (1972) 160741q.
168. G. Berger and L. Saint-Lebe, *Staerke*, 21 (1969) 205–211.
169. J. F. Dauphin, H. Athanassiadis, G. Berger, and L. Saint-Lebe, *Staerke*, 26 (1974) 14–17.
170. H. Scherz, *Z. Naturforsch.*, C 28 (1973) 14–20.
171. N. I. Sosedov and V. P. Shabolenko, *Biokhim. Zerna Khlebopech.*, 7 (1964) 195–201.
172. M. A. Khenokh, E. A. Kuzicheva, and V. F. Evdokimov, *Dokl. Akad. Nauk SSSR*, 135 (1960) 471–474.
173. R. V. Winchester, *Staerke*, 26 (1974) 278–281.
174. H. Scherz, G. Stehlik, E. Baucher, and K. Kaindl, *Mikrochim. Acta.*, (1967) 915–919.
175. W. S. Waravdekar and L. D. Saslaw, *J. Biol. Chem.*, 234 (1959) 1945–1950.
176. W. S. Waravdekar and L. D. Saslaw, *Biochem. Biophys. Acta*, 24 (1957) 439.
177. H. Scherz, *EURATOM [Rep.], (1974)*, EUR 5126 d/e/f/i/n, 169–180; *Chem. Abstr.*, 82 (1975) 137879f.
178. A. M. Henderson and A. Rudin, *J. Polym. Sci. Polym. Chem. Ed.*, 19 (1981) 1721–1732.
179. R. Blinc and M. Samec, *Staerke*, 15 (1963) 245–246.
180. K. Adamic, P. Cevc, and K. A. Korotchenko, *Staerke*, 19 (1967) 336–337.

181. K. A. Korotchenko, K. Adamic, M. Schara, and P. Cevc, *Izv. Vyssh. Uchebn. Zaved. Pishch. Tekhnol.*, 5 (1968) 31–33.
182. L. A. Tikhomirov and N. Ya. Buben, *Kinet. Katal.*, 6 (1965) 329–331.
183. L. A. Tikhomirov, V. A. Belayeva, and M. Ya. Buben, *Izv. Akad. Nauk SSSR Ser. Khim*, (4) (1965) 594–598.
184. Z. Kuri, Y. Fujiwara, H. Ueda, and S. Shida, *J. Chem. Phys.*, 33 (1960) 1884–1885.
185. C. C. Lee and Ching-Hong Chen, *Cereal Chem.*, 42 (1965) 573–576.
186. K. Adamic and R. Blinc, *Proc. Colloq. AMPERE, 1966*, 14 (1967) 780–785; *Chem. Abstr.*, 69 (1968) 112030r.
187. G. V. Abagyan, Yu. N. Krutova, I. N. Putilova, and P. Yu. Butyagin, *Biofizika*, 12 (1967) 820–825.
188. G. V. Abagyan and P. Yu. Butyagin, *Vysokomol. Soedin.*, 7 (1965) 1410–1414.
189. J. Raffi, J. P. Agnell, C. Boizot, C. Thierry, and P. Vincent, *Staerke*, 37 (1985) 228–231.
190. N. K. Kochetkov, L. I. Kudryashov, S. M. Yarovaya, and S. V. Voznesenskaya, *Izv. Akad. Nauk SSSR Ser. Khim.*, 1 (1970) 201–202.
191. S. Stockhausen, W. Boegl, M. Jahn, and H.-P. Weise, *Staerke*, 30 (1978) 1–4.
192. B. S. Tyler, F. J. Munno, and T. W. Cadman, *Environ. Sci. Tekhnol.*, 2 (1968) 628–632.
193. M. A. Khenokh, *Zh. Obshch. Khim.*, 17 (1947) 1024–1029.
194. M. A. Khenokh, *Zh. Obshch. Khim.*, 20 (1950) 1560–1567.
195. K. A. Korotchenko, *Izv. Vyssh. Uchebn. Zaved. Pishch. Tekhnol.*, 4 (1960) 29–31.
196. M. A. Raouf El Saadany, M. Farag El Saadany, and Y. H. Foda, *Staerke*, 29 (1977) 157–160.
197. V. F. Oreshko and K. A. Korotchenko, *Nauchn. Dokl. Vyssh. Shkoly Khim. Khim. Tekhnol.*, 3 (1958) 455–459.
198. K. A. Korotchenko, Yu. N. Krutova, I. N. Putilova, and N. N. Tregubov, *Prikl. Khim. Mikrobiol.*, 2 (1966) 338–340.
199. V. F. Oreshko and K. A. Korotchenko, *Izv. Vyssh. Uchebn. Zaved. Pishch. Tekhnol.*, 4 (1959) 51–54.
200. L. I. Kudryashov, S. M. Yarovaya, S. V. Voznesenskaya, and N. K. Kochetkov, *Zh. Obshch. Khim.*, 41 (1971) 449–455.
201. M. Samec, *Staerke*, 11 (1959) 285–288.
202. J. Pruzinec and O. Hola, *J. Radioanal. Nucl. Chem.*, 118 (1987) 427–431.
203. M. A. Khenokh, *Dokl. Akad. Nauk SSSR*, 104 (1955) 746–749.
204. J. P. Michel, J. Raffi, and L. Saint-Lebe, *Staerke*, 32 (1980) 340–394.
205. Y. Ghali, N. Ibrahim, S. Gabr, and H. Aziz, *Staerke*, 31 (1979) 325–328.
206. H. Scherz, *Rep. EUR-4695*, (1970) 27–36; *Chem. Abstr.*, 78 (1973) 28068n.
207. S. Bachman, Z. Gasyna, T. Swiercz, and H. Zegota, *Bul. Centr. Lab. Technol. Przetw. Przechow. Zboz. Warszawa*, 15 (1971) 52–57.
208. G. Egizarov, *Makromol. Elevator. Prom.*, 24(2) (1958) 17–18.
209. M. Doguchi, Y. Yokoyama, and I. Okada, *Kogyo Kagaku Zasshi*, 62 (1959) 562–566; *Chem. Abstr.*, 57 (1963) 10300g.
210. H. N. Anathaswamy, U. K. Vakil, and A. Sreenivasan, *J. Food Sci.*, 35 (1970) 792–794.
211. A. R. Deschreider, *Staerke*, 12 (1960) 197–201.
212. A. R. Deschreider, *Fermentatio*, (1963) 125–136.
213. B. S. Miller, V. L. Koenig, H. Trimbo, and A. Ogrins, *J. Sci. Food Agr.*, 15 (1964) 701–711.
214. A. R. Deschreider, *Fermentatio*, (1963) 125–136.
215. Sing-Ping Lai, K. F. Finney, and M. Milner, *Cereal Chem.*, 36 (1959) 401–411.
216. J. Bure, *Getreide Mehl*, 9 (1959) 133–135.
217. M. Shiroishi, K. Okumura, A. Hayakawa, and K. Umeda, *Shokoryo Kenkyusho Kenkyu Hokoku*, 18 (1964) 209–213; *Chem. Abstr.*, 67 (1967) 2168t.

218. M. A. Chaudhry and G. Glew, *J. Food Technol.*, 8 (1973) 295–303.
219. G. Fritsch and J. P. Bouldoires, *Mitt. Geb. Lebensmittelunters. Hyg.*, 60 (1969) 252–256.
220. N. I. Sosedov, A. B. Vakar, Z. B. Drozdeva, E. I Arkhipova, E. S. Tolchinskaya, and E. S. Pertsovskii, *Tr. Vses. Inst. Zerna Prod. Pererab.*, 36 (1959) 42–83.
221. M. A. Abd Allah, Y. H. Foda, and E. El Saadany, *Staerke*, 26 (1974) 89–93.
222. H. N. Ananthaswamy, U. K. Vakil, and A. Sreenivasan, *Basic Mech. Radiat. Biol. Med. Proc. Symp.*, (1971) 347–371; *Chem. Abstr.*, 72 (1972) 3929k.
223. T. I. Darchiashvili, R. T. Chkhaidze, U. D. Bregvadze, and N. V. Gongadze, *Radiatsyonnaya obrabotka pishchevykh produktow, Dokl. Vses. Nuchn.-Tekh. Konf., 1968*, in V. I. Rogachev, (Ed.), pp. 148–153, Atomizdat, Moskva, (1971).
224. Joint FAO/IAEA/WHO Expert Committee, *Technical Report Series*, p. 659, WHO, Geneva, (1981).
225. R. Truhaut, B. Coquet, D. Guyot, J. L. Rouaud, and L. Saint-Lebe, *J. Toxicol. Environ. Hyg.*, 9 (1976) 347–356.
226. A. Mucchielli, R. Fretton, and L. Saint-Lebe. *C. R. Acad. Sci., Ser. D*, 285 (1977) 595–598.
227. A. Mucchielli, J. Fretton, J. Nicoli, and R. Fretton, *Ann. Microbiol. (Paris)*, 128A (1977) 311–321.
228. L. Saint-Lebe, G. Berger, A. Mucchielli, and B. Coquet, *Rep. CEA-CONF-2279*, (1972); *Chem. Abstr.*, 81 (1974) 134734y.
229. K. Umeda, S. Hayakawa, A. Hayakawa, H. Toyoshima, and H. Miyazaki, *Shokuryo Kenkyujo Kenkyu Hokoku*, 25 (1970) 11–16; *Chem. Abstr.*, 73 (1970) 42264b.
230. V. P. Bychkov, M. I. Kozar, V. I. Popov, N. N. Boiko, A. G. Kasatkina, E. V. Kolchina, and V. V. Yurgov, *Kosm. Biol. Med.*, 4(5) (1970) 42–46.
231. R. O. Moore, *U. S. Dept. Co., Office Tech. Serv.*, (1961) AD 262,978; *Chem. Abstr.*, 58 (1963) 4969e.
232. M. A. Raouf El Saadany, M. Farag El Saadany, and Y. H. Foda, *Staerke*, 26 (1974) 422–425.
233. K. A. Korotchenko, *Izv. Vyssh. Uchebn. Zaved. Pishch. Tekhnol.*, 2 (1963) 74–76.
234. L. Saint-Lebe, G. Berger, J. P. Michel, M. Huchette, and F. S. A. Roquette, Fr. Pat. 2,329,749 (1977); *Chem. Abstr.*, 88 (1978) 52250t.
235. S. L. Rudin, Ger. Pat. 1,093,300 (1960); *Chem. Abstr.*, 55 (1961) 26488i.
236. K. A. Korotchenko, I. N. Putilova, S. E. Traubenberg, and Yu. N. Krutova, USSR Pat. 192,685 (1967); *Chem. Abstr.*, 68 (1968) 60731c.
237. B. T. Hofreiter and C. R. Russell, *Staerke*, 26 (1974) 18–23.
238. J. A. Restaino, Ger. Pat. 2,038,636 (1971); *Chem. Abstr.*, 75 (1971) 78378x.
239. Y. W. Chan, Y. K. Cho, and A. Ciegler, *Biotechnol. Bioeng.*, 25 (1983) 2631–2640.
240. K. A. Korotchenko and I. N. Putilova, *Ferment. Spirt. Promst.* 30(8) (1964) 16–19.
241. I. N. Putilova, K. A. Korotchenko, and L. F. Gorin, *Zh. Prikl. Khim.*, 37 (1964) 2612–2615.
242. K. A. Korotchenko, I. N. Putilova, I. S. Akulova, and N. N. Chernobayeva, *Radiatsionnaya obrabotka pishchevykh produktov, Dokl. Vses. Nauch.-Tekh., 1968*, in V. I. Rogachev (Ed.), pp. 169–173, Atomizdat, Moskva, (1971).
243. G. Schwenker and H. Poehland-Heuser, *Pharm. Ind.*, 33 (1971) 200–202.
244. C. C. Palit and N. R. Dhar, *J. Phys. Chem.*, 32 (1928) 1263–1268.
245. C. C. Palit and N. R. Dhar, *J. Phys. Chem.*, 34 (1930) 993–1005.
246. E. E. Semmens, *Nature*, 159 (1947) 613.
247. A. E. Navez and B. B. Rubenstein, *J. Biol. Chem.*, 80 (1928) 503–513.
248. H. Weigel and P. J. Plath, *Z. Phys. Chem. (Leipzig)*, 267 (1986) 225–240.
249. P. Moeckel, *Naturwissenschaften*, 64 (1977) 224.
250. E. Rousseau, *C. R. Soc. Biol.*, 93 (1925) 1482–1483.
251. C. Zucca, *Atti Ist. Bot Univ. Lab. Crittogam. Pavia*, [5] 10 (1953) 85–88; *Chem. Abstr.*, 48 (1954) 2399.

252. V. G. Soyer and A. D. Semenov, *Gidrokhim Inst. Gidrokhim. Mater.*, 57 (1973) 195–201.
253. S. Peat, E. J. Bourne, and W. J. Whelan, *Nature*, 161 (1948) 762–763.
254. W. J. Whelan and S. Peat, *J. Soc. Dyers Colourist*, 65 (1950) 748–757.
255. A. Merlin and J. P. Fouassier, *Macromol. Chem.*, 182 (1981) 3053–3068.
256. A. M. Schwartz and C. A. Rader, U.S. Pat. 3,352,773 (1967); *Chem. Abstr.*, 68 (1968) 41292u.
257. T. Kawai and T. Sakata, *Nature (London)*, 286 (1980) 474–476.
258. W. K. Subczyński and T. Sarna, *Stud. Biophys.*, 46 (1974) 233–238.
259. K. Knoevenagel and R. Himmelreich, *Arch. Environ. Contam. Toxicol.*, 4 (1976) 324–333.
260. L. Massol, *C. R. Acad. Sci.*, 152 (1911) 902–904.
261. J. Bielecki and R. Wurmser, *C. R. Acad. Sci.*, 154 (1912) 1429–1432.
262. L. Massol, *C. R. Acad. Sci.*, 154 (1912) 1645–1646.
263. J. Bielecki and R. Wurmser, *Biochem. Z.*, 43 (1912) 154–164.
264. L. Massol, *Ann. Sci. Agron.*, [4] 1 (1913) 217–218.
265. T. Isemura, *J. Chem. Soc. Jpn.*, 56 (1935) 772–778.
266. F. Lieben, L. Loewe, and B. Bauminger, *Biochem. Z.*, 271 (1934) 209–212.
267. S. Takahashi and Y. Kihara, *Nippon Nogei Kagaku Kaishi*, 34 (1960) 88–94; *Chem Abstr.*, 62 (1965) 9389.
268. H. Kashiwagi and S. Enomoto, *Chem. Pharm. Bull. (Tokyo)*, 29 (1981) 913–917.
269. K. Kuwata, T. Ichikawa, and K. Hirota, *Nippon Kagaku Zasshi*, 83 (1962) 652–655; *Chem. Abstr.*, 58 (1963) 9773.
269a. J. Azuma, T. Hosobuchi, and T. Katada, *Jpn. Kokai Tokkyo Koho* JP 01 224 386 (1989); *Chem. Abstr.*, 112 (1990) 119341h.
270. D. Horton, in *Starch Chemistry and Technology*, R. L. Whistler and E. F. Paschall (Eds.), Vol. 1, pp. 421–437, Academic Press, New York (1965).
271. D. J. Stevens and G. A. H. Elton, *Staerke*, 23 (1971) 8–11.
272. A.-C. Eliasson, K. Larson, and Y. Miezis, *Staerke*, 33 (1981) 231–235.
273. M. Ahmed and J. Lelievre, *Staerke*, 30 (1978) 78–79.
274. P. C. Williams and I. Hlynka, *Cereal Chem.*, 45 (1968) 280–289.
275. G. E. Oleneva and G. B. Chizhov, *Kholod. Tekh.*, 5 (1973) 32–36.
276. J. J. Albrecht, *Diss. Abstr. Int.*, 19 (1958) 1049–1050.
277. W. E. Schulze, D. T. Yu, and M. M. MacMasters, *Staerke*, 16 (1964) 41–44.
278. S. Tsourouflis, J. M. Flink, and M. Karel, *J. Sci. Food Agric.*, 27 (1976) 509–519.
279. E. E. C. Baly and E. S. Semmens, *Proc. R. Soc. B*, 97 (1924) 250–253.
280. E. S. Semmens, *Nature*, 144 (1939) 379–380.
281. E. S. Semmens, *Nature*, 163 (1949) 371.
282. R. Dohnalek and M. Cap, *Krimivarstvi Sluzby*, 13 (1977) 213–215.
283. E. Hasche and H. Leunig, *Strahlentherapie*, 52 (1935) 179–186.
284. M. S. Shulman, *Kolloid Zh.*, 14 (1952) 215–218.
285. S. M. Skuratov, *Kolloid Zh.*, 9 (1947) 133–137.
286. N. K. Goebel, J. Grider, E. A. Davis, and J. Gordon, *Food Microstr.*, 3 (1984) 73–81.
287. R. Collison and W. G. Chilton, *J. Food Technol.*, 9 (1974) 309–315.
288. B. J. Zylema, J. A. Grider, J. Gordon, and E. A. Davis, *Cereal Chem.*, 62 (1985) 447–453.
289. L. I. Belenkii, *Khlopchatobumazhnaya Prom.*, 12 (1940) 58–60; *Ref. Zh., Khim.*, 9 (1940) 95.
290. W. A. G. van Everdingen, *Tijdschr. Geneeskd.*, 85 (1941) 3094–3104; *Chem. Zentr.*, I (1942) 725.
291. A. R. Khan, *Diss. Abstr. Int. B*, 36 (1975) 2143.
292. P. Verberne and T. Vlot, Brit. Pat. 1,425,624 (1976); *Chem. Abstr.*, 85 (1976) 34947j.
293. G. H. A. Marquette, M. Gouze, and C. Lane, Eur. Pat. Appl. EP 59,050 (1982); *Chem. Abstr.*, 97 (1982) 184309q.

294. J. Azuma, T. Tomiya, and T. Katada, *Jpn. Kokai Tokkyo Koho*, JP 01 225 601 (1989); *Chem. Abstr.*, 112 (1990) 8947r.
295. A. R. Khan, J. A. Johnson, and R. J. Robinson, *Cereal Chem.*, 56 (1979) 303–304.
296. A. Szalay, *Z. Physik. Chem.*, A 164 (1933) 234–240.
297. E. W. Flosdorf and L. A. Chambers, *J. Am. Chem. Soc.*, 55 (1933) 3051–3052.
298. O. Sozaburo, *Rev. Phys. Chem. Jpn.*, 14 (1940) 25–41.
299. D. Gallant, M. Degrois, C. Sterling, and A. Guilbot, *Staerke*, 24 (1972) 116–123.
300. M. Degrois, D. Gallant, P. Baldo, and A. Guilbot, *Ultrasonics*, 12 (1974) 129–131.
301. U. Ohm and P. Metzner, *Naturwissenschaften*, 45 (1958) 56–57.
302. C. Sterling and J. Pangborn, *Am. J. Bot.*, 47 (1960) 577–582.
303. S. Suryanarayana, *J. Sci. Ind. Res.*, 21B (1962) 57–60.
304. M. A. Reddy, *J. Acoust. Soc. India*, 8 (1980) 24–31.
305. I. I. Zhukov and M. A. Khenokh, *Dokl. Akad. Nauk SSSR*, 68 (1949) 333–336.
306. L. P. Solovev, *Zh. Fiz. Khim.*, 9 (1937) 77–81.
307. S. Akiya and S. Okui, *J. Pharm. Soc. Jpn.*, 71 (1951) 182–184.
308. H. Sobue and K. Ishikawa, *J. Chem. Soc. Jpn., Pure Chem. Sect.*, 71 (1950) 25–27.
309. R. Sutra, *C. R. Acad. Sci.*, 232 (1951) 1490–1492.
310. M. A. Khenokh, *Dokl. Akad. Nauk SSSR*, 97 (1954) 871–874.
311. L. K. Lozina-Lozinskii and M. A. Khenokh, *Dokl. Akad. Nauk SSSR*, 76 (1951) 317–320.
312. Y. Miyahara, K. Ito, and H. Shiio, *J. Chem. Soc. Jpn., Pure Chem. Sect.*, 72 (1951) 904–905.
313. O. Sozaburo, *Rev. Phys. Chem. Jpn.*, 14 (1940) 101.
314. O. Sozaburo, *J. Chem. Soc. Jpn.*, 61 (1940) 997–1004.
315. M. Samec, *Staerke*, 15 (1963) 243–245.
316. S. Fujita, T. Ishigaki, S. Sakuma, and N. Miyata, *Nippon Igaku Hoshasen Gakkai Zasshi*, 36 (1976) 737–743; *Chem. Abstr.*, 86 (1977) 152114d.
317. W. Loeb, *Biochem. Z.*, 46 (1913) 121–124.
318. W. Loeb, *Biochem. Z.*, 60 (1914) 286–296.
319. M. Samec and A. Mayer, *Kolloidchem. Beihf.*, 13 (1921) 272–288.
320. W. Pauli, J. Szper, and S. Szper, *Kolloid-Z.*, 82 (1938) 335–344.
321. J. Mizuguchi, *J. Pharm. Soc. Jpn.*, 70 (1950) 506–510.
322. H. Kurz, *Staerke*, 4 (1952) 156–159.
323. A. Klemenc and G. Ofner, *Z. Elektrochem.*, 57 (1953) 615–617.
324. M. M. Baizer, *Proc. BIOEXPO 86*, (1986) 341–349; *Chem. Abstr.*, 106 (1986) 121756s.
325. J. O'M Bockris, B. J. Piersma, and E. Gileadi, *Electrochim. Acta*, 9 (1964) 1329–1332.
326. F. F. Farley and R. M. Hixon, *Ind. Eng. Chem.*, 34 (1942) 677–681.
327. W. Dvonch and C. L. Mehltretter, *J. Am. Chem. Soc.*, 74 (1952) 5522–5523.
328. Z. Ratajewicz, K. Stelmach, and J. Sawa, Pol. Pat. 93,031 (1977); *Chem. Abstr.*, 89 (1978) 7961k.
329. C. L. Mehltretter, U.S. Pat. 2,713,553 (1955); *Chem. Abstr.*, 49 (1955) 13806b.
330. H. V. K. Udupa, Ind. Pat. 79,075 (1964); *Chem. Abstr.*, 63 (1965) 1980g.
331. H. F. Convay and V. E. Sohns, *Ind. Eng. Chem.*, 51 (1959) 637–638.
332. I. Feher, Hung. Pat. 147,762 (1960); *Chem. Abstr.*, 58 (1963) 1658g.

APPENDIX.

The following text was added at the proof stage.

This excerpt follows the paragraph "The compression of starch in the presence of . . . " in Section III.

Starch can readily be modified by concurrent heat, application of moisture, and pressure. Such modifications may be conducted in extruders. Low moisture content favors formation of water-soluble starch with increased water-binding capacity.[65a-65e] The solubility, water binding-capacity, and viscosity of gels prepared from extruded starch do not show linear relationships against either the moisture content in starch or the extrusion temperature.[65c-65f] Such extruder variables as the type of screw (either single or twin), pattern of the barrel and die heating, screw velocity, and geometry of the screw thread are also essential factors.[65g]

In starch chemistry and technology, extrusion is used for cooking as well as for preparation of starch complexes with such guest molecules as gluten[65h] and lipids.[65i] Acylation of starch with cyclic anhydrides of dioic acids on extrusion has been demonstrated; the reaction provides anionic starches.[65j]

This excerpt follows the last paragraph of Section V.

Solid corn and cassava starches have been irradiated with 337.8-nm pulsing ultraviolet light (2.6 ns with a peak power of 100 kW) emitted by an atmospheric-pressure nitrogen laser.[270a] Small changes could be observed in the water solubility of the irradiated starches, their water-binding capacity, and the iodine uptake, provided that promoters (1% w/w) were introduced. The activity of three promoters tested—ZnO, TiO_2, and MgO—and the susceptibility of both starch varieties to the irradiation were approximately the same.

This excerpt follows the last paragraph of Section VI.

The effect of microwave radiation on maize, potato, and cassava starch (all either air-dried, in slurry, or pregelatinized) has been studied by Muzimbaranda and Tomasik.[295a] Starch readily dextrinized under such treatment. The sensitivity to microwaves increased in the order corn > cassava >> potato starch. Microwave radiation also allowed facile cross-linking of starch with formaldehyde. The reaction took place for 5–15 min. and did not require any catalyst. Extended periods of reaction led to dextrins. In the presence of hydrogen peroxide, starch could be cross-linked with acetylene.[295a]

This excerpt follows the last paragraph of Section VIII.

A novel method for oxidation of starch to "starch dialdehyde" has been presented. The oxidant (periodate) could be continuously recovered by electro-oxidation and the product was isolated on ion exchangers. The procedure permits full conversion (degree of oxidation = 1) of starch to "starch dialdehyde".[333,334]

REFERENCES

65a. M. H. Gomez and J. M. Aguilera, *J. Food Sci.*, 48 (1983) 378–381.
65b. M. H. Gomez and J. M., Aguilera, *J. Food Sci.*, 49 (1984) 40–43, 63.
65c. P. Colonna, J. L. Doubler, J. P. Melcion, F. de Monredon, and C. Mercier, *Cereal Chem.*, 61 (1984) 538–543.
65d. J. L. Doubler, P. Colonna, and C. Mercier, *Cereal Chem.*, 63 (1986) 240–246.
65e. C. Mercier and P. Feillet, *Cereal Chem.*, 52 (1975) 283–297.
65f. B. Launay and J. M. Lisch, *J. Food Eng.*, 2 (1983) 259–280.
65g. B. T. Lawton, G. A. Henderson, and E. J. Derlatka, *Can. J. Chem. Eng.*, 50 (1972) 168–172.
65h. D. Paton and W. A. Spratt, *J. Food Sci.*, 49 (1984) 1380–1385.
65i. F. Meuser, R. van Lengerich, and J. Stender, *Getreide, Mehl, Brot*, 39 (1985), 205–211, 309–314.
65j. P. Tomasik, Y. J. Wang, and Jay-lin Jane, *Staerke*, 47 (1995) 96–99.
270a. A. V. Gholap, L. H. Marondeze, and P. Tomasik, *Staerke*, 45 (1993) 430–432.
295a. C. Muzimbaranda and P. Tomasik, *Staerke*, 46 (1994) 469–474.
333. S. Veelaert, D. de Wit, and H. Tournois, *Polymer*, 35 (1994) 5091–5098.
334. S. Veelaert, D. de Wit, and H. Tournis, *Staerke*, 47, in press.

AUTHOR INDEX

Numbers in parentheses are footnote reference numbers and indicate that an author's work is referred to although the name is not cited in the text.

C

D

E

F

G

H

I

L

M

N

O

P

R

T

Y

Z

SUBJECT INDEX

D

M

N

O

P

This Page Intentionally Left Blank

ISBN 0-12-007251-3